Topics in Current Chemistry 340

Volker Schurig *Editor*

Differentiation of Enantiomers I

Springer

340
Topics in Current Chemistry

For further volumes:
http://www.springer.com/series/128

Aims and Scope

The series Topics in Current Chemistry presents critical reviews of the present and future trends in modern chemical research. The scope of coverage includes all areas of chemical science including the interfaces with related disciplines such as biology, medicine and materials science.

The goal of each thematic volume is to give the non-specialist reader, whether at the university or in industry, a comprehensive overview of an area where new insights are emerging that are of interest to larger scientific audience.

Thus each review within the volume critically surveys one aspect of that topic and places it within the context of the volume as a whole. The most significant developments of the last 5 to 10 years should be presented. A description of the laboratory procedures involved is often useful to the reader. The coverage should not be exhaustive in data, but should rather be conceptual, concentrating on the methodological thinking that will allow the non-specialist reader to understand the information presented.

Discussion of possible future research directions in the area is welcome.

Review articles for the individual volumes are invited by the volume editors.

Readership: research chemists at universities or in industry, graduate students.

Volker Schurig
Editor

Differentiation of Enantiomers I

With contributions by

A. Ciogli · J. Gal · F. Gasparrini · H. Iida · D. Kotoni · Y. Okamoto · M. Pierini · C. Roussel · V. Schurig · G.K.E. Scriba · N. Vanthuyne · C. Villani · E. Yashima

Springer

Editor
Volker Schurig
Institute of Organic Chemistry
University of Tübingen
Tübingen
Germany

ISSN 0340-1022 ISSN 1436-5049 (electronic)
ISBN 978-3-319-03238-2 ISBN 978-3-319-03239-9 (eBook)
DOI 10.1007/978-3-319-03239-9
Springer Heidelberg New York Dordrecht London

Library of Congress Control Number: 2013956811

Printed on acid-free paper

Springer is part of Springer Science+Business Media (www.springer.com)

Preface

In the wake of enantioselective syntheses and chiral technologies, efficient analytical methods for the differentiation of enantiomers have become essential.

Earlier compendia in this area [1–5] need updating due to important recent advances made in the realm of enantiomeric differentiation. Precise analytical tools for the determination of enantiomeric proportions are important in many contemporary fields associated with various aspects of chirality.

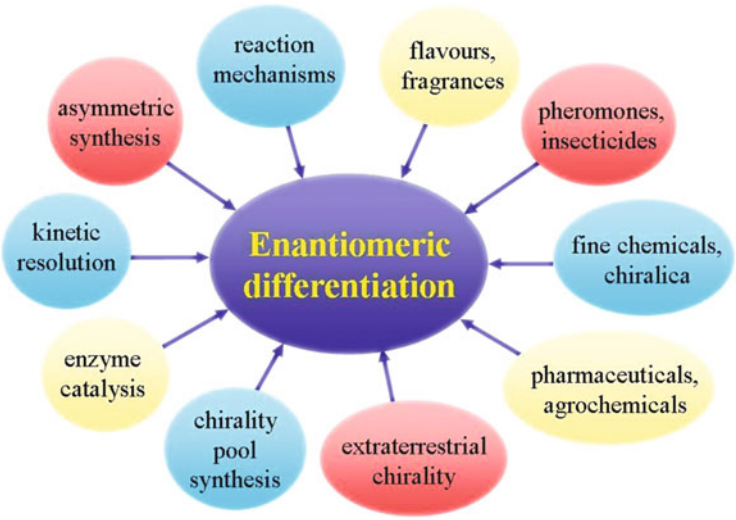

The distribution of enantioselective methods for the determination of enantiomeric proportions utilized in 319 published articles of Tetrahedron Asymmetry 2003, i.e., polarimetry [α], gas chromatography (GC), high performance liquid chromatography (HPLC), and nuclear magnetic resonance spectroscopy (NMR), has been compiled previously [6].

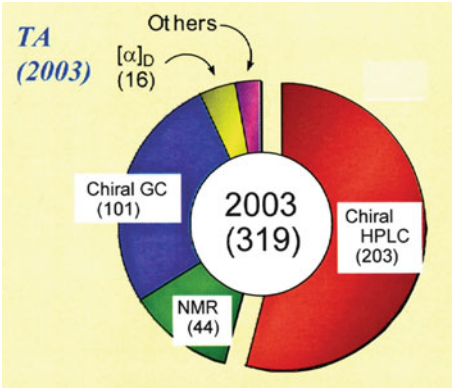

These two volumes of Topics in Current Chemistry review various modern methods and techniques of enantiomeric differentiation. Individual chapters have been written by pioneers in the field and emerge from renowned laboratories which have contributed significantly to recent research. In each chapter emphasis has been given to an extended reference format including the titles of related original work which will enable readers to appreciate and consult the important secondary literature.

The first volume begins with an introduction to historic and fundamental aspects of chirality followed by recommendations on how to quantify mixtures of stereoisomers. Enantiomeric differentiation by chiral liquid chromatography utilizing supramolecular chiral recognition systems and various chiroptic approaches is described. Enantiomeric differentiation by gas chromatography and capillary electrophoresis concludes the first volume. The second volume begins with enantiomeric differentiation by NMR spectroscopy and sensor devices followed by chiral recognition phenomena in supramolecular chemistry, chromatographic studies of stereolabile interconverting enantiomers, and anisotropy spectroscopy as a novel extension of circular dichroism. The second volume is concluded with the self-disproportionation of enantiomers due to nonlinear effects.

We hope that these volumes on the differentiation of enantiomers will provide inspiration and impetus to further advances in the ever-growing area of stereochemistry. The editor is grateful to all the colleagues who have helped to create this survey on modern tools for the differentiation of enantiomers.

Tübingen, Germany Volker Schurig

References

1. Raban M, Mislow K (1967) Modern methods for the determination of optical purity. Top Stereochem 2:199–230
2. Morrison JD (ed) (1983) Asymmetric synthesis, vol 1: analytical methods. Academic Press, Inc., New York
3. Schurig V (1985/1986) Current methods for the determination of enantiomeric compositions. Part 1: definitions, polarimetry. Part 2: NMR spectroscopy with chiral lanthanide shift reagents. Part 3: gas chromatography on chiral stationary phases. Kontakte Merck (Darmstadt) 1985(1):54–60; 1985(2):22–40; 1986(1):3–22
4. Schurig V, Lindner W (1995) Determination of enantiomeric purity. In: Helmchen G, Hoffmann RW, Mulzer J, Schaumann E (eds) Stereoselective synthesis, methods of organic chemistry (Houben-Weyl), vol E 21a. Thieme, Stuttgart, New York, pp 147–192; 193–252
5. Schreier P, Bernreuther A, Huffer M (1995) Analysis of chiral organic molecules, methodology and applications. Walter de Gruyter, Berlin, New York
6. Chen X, Yamamoto C, Okamoto Y (2007) Polysaccharide derivatives as useful chiral stationary phases in high-performance liquid chromatography. Pure Appl Chem 79(9):1561–1573

Contents

Top Curr Chem (2013) 340: 1–20
DOI: 10.1007/128_2013_435

Published online: 11 May 2013

Molecular Chirality: Language, History, and Significance

Joseph Gal

Abstract In this chapter some background material concerning molecular chirality and enantiomerism is presented. First some basic chemical-molecular aspects of chirality are reviewed, after which certain relevant terminology whose use in the literature has been problematic is discussed. Then an overview is provided of some of the early discoveries that laid the foundations of the science of molecular chirality in chemistry and biology, including the discovery of the phenomenon of molecular chirality by L. Pasteur, the proposals for the asymmetric carbon atom by J.H. van 't Hoff and J.A. Lebel, Pasteur's discovery of biological enantioselectivity, the discovery of enantioselectivity at biological receptors by A. Piutti, the studies of enzymatic stereoselectivity by E. Fischer, and the work on enantioselectivity in pharmacology by A. Cushny. Finally, the role of molecular chirality in pharmacotherapy and new-drug development, arguably one of the main driving forces for the current intense interest in the phenomenon of molecular chirality, is discussed.

Keywords Biological stereoselectivity · Drugs · Enantiomerism · History of chemistry · Language of stereochemistry · Molecular chirality · Molecular recognition · Pharmacology

Contents

J. Gal (✉)
Departments of Medicine and Pathology, School of Medicine, University of Colorado, Denver, USA
e-mail: Joe.Gal@ucdenver.edu

1 Introduction

In this opening chapter to the compendium, some background material concerning molecular chirality and enantiomerism is presented. Specifically, after a brief review of some basic aspects of these chemical phenomena, relevant terminology whose usage has been problematic is discussed, followed by an overview of some of the early discoveries that laid the foundations of the science of molecular chirality in chemistry and biology. Finally, a discussion of the role of molecular chirality in pharmacotherapy and new-drug development, arguably one of the main driving forces for the current intense interest in the phenomenon, will be provided. It should be emphasized here that molecular chirality is a vast domain of multidisciplinary scientific knowledge and it is not possible in an introductory chapter such as this to provide a full treatment of even just the basic aspects; it was, therefore, necessary to make choices concerning the material to be included in the chapter (among the many fundamental topics regretfully left out are, for example, the analysis of molecular chirality in terms of symmetry considerations, and the Cahn–Ingold–Prelog (CIP) system of stereochemical descriptors). To a significant extent the resulting article reflects, of course, the bias of the author, but it is also believed that the topics covered provide a pertinent and useful background to the subject matter of the compendium.

Two molecules are related as stereoisomers if they have the same elemental composition and order of connection of the atoms but differ in the arrangement of the atoms in space. A variety of types of stereoisomers exist, and chirality is the basis for the stereoisomerism of many molecules. Basically, molecular chirality is a relatively simple phenomenon. *Chiral* was defined in one leading monograph on stereochemistry as follows: "Not superposable. . .with its mirror image, as applied to molecules, conformations, as well as macroscopic objects, such as crystals" [1]. Mislow has provided the following definition: "An object is chiral. . .if and only if it cannot be superposed on its mirror image by a proper congruence, otherwise it is achiral" [2]. Thus, it is clear that *chirality* refers, in the molecular realm, to a spatial property that renders a molecule incongruent with (i.e., non-superposable upon) its mirror image. We are dealing here with "geometrical chirality," although chirality also has other aspects [2].

A variety of structural features can produce chirality in molecules, and some examples are shown in Fig. 1. Thus, an sp^3-hybridized carbon atom carrying four different ligands may be such an element; among the many others are suitably substituted allenes, certain substituted biaryls with hindered rotation around the aryl–aryl single bond, helical structures, etc. (Fig. 1).

The two nonsuperposable-mirror-image molecules corresponding to a chiral chemical structure are the two *enantiomers*. "Enantiomer" has been defined as follows [3]: "One of a pair of molecular species that are mirror images of each other and not superposable." Thus, the term inevitably implies a relationship between two molecules that are chiral and related as object and mirror image. Moreover, as seen in the definition, "enantiomer" refers to molecules and not to

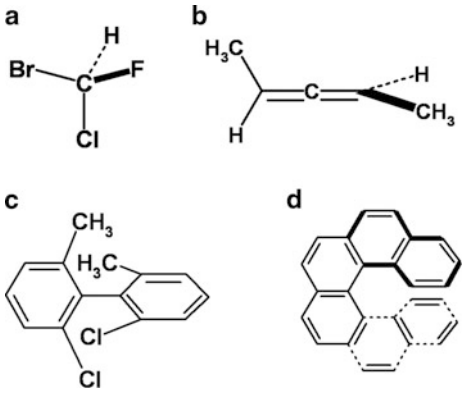

Fig. 1 Some chiral molecules. (**a**) The molecule has an sp^3-hybridized carbon atom carrying four different ligands. (**b**) A chiral allene. (**c**) A biaryl chiral by virtue of hindered rotation around the aryl–aryl bond resulting from the substituents in the *ortho* positions. (**d**) Hexahelicene, whose chirality is due to the helical conformation resulting from the steric crowding at the terminal aromatic rings; in an attempt to convey the helical form of the molecule, bonds in *bold* are used to indicate that the corresponding benzene rings are above the plane of the illustration while the bonds in *dotted lines* indicate that the rings are below the plane of the illustration

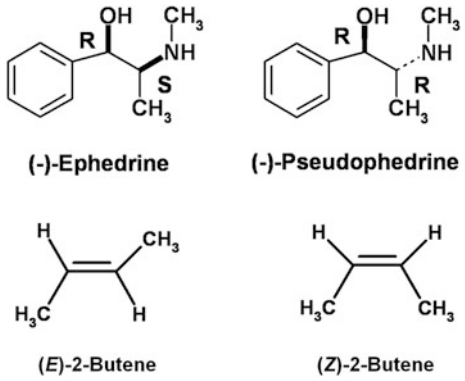

Fig. 2 (−)-Ephedrine and (−)-pseudoephedrine are chiral diastereoisomers differing in configuration at the carbon center carrying the methylamino group; (*E*)- and (*Z*)-2-butene are achiral diastereoisomers

macroscopic (chiral) objects. For the latter, "enantiomorph" is recommended [4]; however, such distinction is often blurred in the literature.

Any two stereoisomeric molecules that are *not* mirror-image forms of each other are related as *diastereoisomers*. Diastereoisomers may be chiral or achiral. For example, (−)-ephedrine and (−)-pseudoephedrine are related as chiral diastereoisomers, and (*E*)- and (*Z*)-2-butene as achiral diastereoisomers (Fig. 2).

Anslyn and Dougherty have argued in their discussion of stereochemistry [5] that during the development of the field a number of concepts and terms evolved that today are no longer considered useful and have been replaced by more modern views. For example, in molecule *a* of Fig. 1 the carbon atom has been traditionally referred to as a "chiral center." "Chiral center" (or center of chirality), "chiral axis," and "chiral plane" are "chirality elements" frequently used in the literature, but the concept of chirality elements is deemed by some to be without value [6, 7]. A more modern view of structure in stereochemistry is based on the concept of *stereogenicity*. An atom or grouping of atoms is a stereogenic center (or, more generally, a stereogenic unit) if the interchange of two ligands attached to it can result in a new stereoisomer [8]. Not all interchanges at a stereogenic center have to produce a new stereoisomer, but if one such exchange does result in a new stereoisomer, the unit is stereogenic. Note that "stereogenicity" says nothing about the chirality – or lack thereof – of the molecule, i.e., it is applicable to both chiral and achiral structures. Thus, in Fig. 1, the carbon of the chiral molecule *a* is a stereogenic unit, as is C═C in the achiral 2-butene (Fig. 2). The concept of stereogenicity is highly useful in stereochemistry, but it must be pointed out that many have not abandoned the notion and terminology of "chirality elements" [9].

The above presentation of some of the basic aspects of the phenomena of molecular chirality and enantiomerism is necessarily a brief and selective treatment; the interested reader is referred to the many textbooks, monographs, and articles on the subject, only of a few of which can be cited here [2, 7, 9–13].

2 Language

Stereochemistry, a complex and rich science, has a language that is also rich and complex. The need to use accurate language in scientific discourse is obvious: accuracy in concepts requires accuracy in language. However, it is clear that the use of stereochemical language has been fraught with problems and inaccuracies and even some of the simplest of terms are often misused [9, 14–18]. It therefore seems reasonable to provide here a brief discussion of some of the troubled uses of basic stereochemical terminology.

As discussed above, it is clear that *chiral* refers to a spatial property of objects, including molecules, i.e., that nature which makes such an object or molecule *non-superposable* on its mirror image. Importantly, therefore, the term *does not refer to the stereochemical composition of bulk material,* i.e*., compounds, substances,* etc. Thus, "chiral compound" does not tell us whether the substance is racemic, a single enantiomer, or some other mixture of the stereoisomers. Thus, "chiral drug," "chiral substance," etc., indicate that the compound in question is composed of chiral molecules, but the stereoisomer composition is not specified by this terminology. This point needs to be emphasized because the literature contains other, often troubling, uses of the term [17], e.g., to indicate that a *substance* consists of only

one of the two enantiomers. Such statements ignore the fact that the racemic mixture is also composed of chiral molecules. Therefore, such usage of the term should be avoided.

The term *homochiral* has also had a troubled history [19]. This term, coined by Lord Kelvin in 1894, indicates the same sense of chirality among chiral objects, molecules, stereogenic centers, etc., i.e., that their chirality is of the same direction or configuration. Thus, D-alanine and D-serine are homochiral, i.e., they have the same sense of chirality (configuration). Unfortunately, the usage of *homochiral* (and *homochirality*) in the literature is fraught with inconsistencies and contradictions. Above all, *homochiral* has often been incorrectly used as a synonym for *enantiomerically pure*. Such usage should be avoided and the term should be reserved to indicate the same sense of chirality when comparing similar or related molecules [19].

Enantiomer is a simple term that is nevertheless often misused [20]. Moreover, there are many terms derived from *enantiomer*, and several of them are extensively misused. *Enantiomeric*, for example, means "of the opposite handedness," and the following sentence illustrates the correct usage in that meaning: "(−)-Morphine was obtained commercially but the enantiomeric form [i.e., (+)-morphine] had to be synthesized." In the literature, however, *enantiomeric* often appears in ambiguous or confusing usage. For example, the title of one article was "The cost benefit ratio of enantiomeric drugs" [21]. What is the meaning of "enantiomeric" intended by the authors of the article? Is it the comparison of the two enantiomers of chiral drugs for cost effectiveness? (This would be the interpretation from the correct usage of the term). However, a careful reading of the article reveals that the term was used *not* to convey the comparison of the two enantiomers of chiral drugs but to compare *drugs consisting of a single chiral stereoisomer* with the corresponding racemates, a different meaning indeed.

Furthermore, *enantiomeric* is often misused in other connotations. A common usage of the term seen in the literature is in the context of chromatography using chiral stationary phases (CSPs). Thus, "enantiomeric separation," "enantiomeric chromatography," etc., are often encountered [20]. But what does "enantiomeric chromatography" mean? Based on the correct interpretation of the term, this phrase would convey that the CSP *of the opposite configuration to that first examined was used* (not a far-fetched interpretation, since some CSPs are available in both of the mirror-image configurations, and switching from one to the other is often practiced). However, examination of the uses of "enantiomeric chromatography" or related phrases in the literature reveals that the intended meaning in most such cases is "chromatography that separates the two enantiomers of a chiral substance." Thus, "enantiomeric chromatography" is ambiguous; the correct term for the intended meaning is *enantioselective chromatography* or *chromatographic enantioseparation*.

Enantiomerism and *chirality* are not synonymous: *enantiomerism* refers to the *relationship between two nonsuperposable mirror-image molecules* while *chirality* is *the phenomenon* that imparts to certain objects (or molecules) the property of not being superposable on their mirror image. This subtle but significant

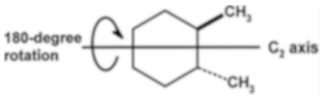

Fig. 3 *trans*-1,2-Dimethylcyclohexane and its C_2 axis of symmetry

distinction results in different applications of the terms; for example, the stereoisomers (−)-ephedrine and (−)-pseudoephedrine – differing in the configuration at one of the two stereogenic centers (Fig. 2) – have *chirality*, but there is no *enantiomeric* relationship between the two, i.e., they are not related as non-superposable-mirror-image molecules (they are *diastereoisomers*). This difference between the two terms is not always appreciated. For example, the four (!) chiral stereoisomers of 2,3-diaminobutanoic acid have been stated to be "[t]he four enantiomers of 2,3-diaminobutanoic acid" [22]. "Enantiomer," however, refers to the relationship between a chiral molecule and its nonsuperposable mirror image, and since an object can have only one mirror image, it is incorrect to refer to a group of more than two chiral molecules collectively as a set of enantiomers. Therefore the example of the 2,3-diaminobutanoic acid stereoisomers is in fact a case of confounding *chirality* with *enantiomerism*: the four molecules in question *are* chiral and related as stereoisomers but the majority of the stereochemical relationships among the four are not *enantiomeric*. Thus, such usage of *enantiomer* contradicts the definition of enantiomerism.

Racemic mixture designates the 1:1 mixture of the two enantiomers of a chiral substance and should not be applied to any other stereoisomeric mixture, chiral or achiral. However, the term is in fact often applied, entirely incorrectly, to other mixtures of stereoisomers. For example, the following mixtures, among others, have all been erroneously described as "racemic": (1) a mixture of diastereoisomers produced by esterifying a racemic carboxylic acid with a single-enantiomer alcohol (the two stereoisomers resulting from this reaction are diastereoisomers and not enantiomers, and therefore cannot be called "racemic"); (2) mixtures of *cis* and *trans* achiral stereoisomeric cyclic molecules; (3) a mixture of two diastereoisomeric racemates (i.e., four stereoisomers; such a mixture of *two racemates* cannot be called "racemic"); etc. [17].

Another term that needs to be addressed in the present context is *molecular asymmetry*. This expression is often employed to refer to *molecular chirality*, but such usage, in which "asymmetry" is equated with "chirality," is incorrect [9]. To put it succinctly: an asymmetric object is necessarily chiral, but a chiral object is not necessarily asymmetric. An object or molecule is asymmetric if it has no symmetry element other than the identity operation (*E* or *I*), i.e., belonging to the (trivial) point group C_1. Such a structure is necessarily incongruent with (i.e., not superposable on) its mirror image, that is, chiral. However, the presence in a structure of some symmetry, namely, one or more simple axes of symmetry (i.e., proper rotation axis, C_n, $n > 1$), does not preclude chirality. For example, the enantiomers of *trans*-1,2-dimethylcyclohexane are chiral but not asymmetric since they contain a C_2 axis of symmetry. This means that 180° rotation of the molecule around the axis results in the same molecule, superposed on the original (Fig. 3).

Thus an object or molecule may be chiral without being asymmetric, and therefore "asymmetry" and "chirality" are not synonyms and should not be conflated. Overall, "molecular asymmetry," when it is employed to refer specifically to the phenomenon of molecular chirality, should in fact be replaced with "molecular chirality" [9].

The synthesis of single-enantiomer substances is, naturally, an essential activity in stereochemistry and its various applications, and several approaches to such syntheses are used. Not surprisingly, a complex variety of terms have been introduced to refer to such reactions, e.g., "enantioselective synthesis (or reaction)," "enantiospecific synthesis," "asymmetric synthesis," etc. The application of such terminology has often been rather loose, and some authors have attempted to clarify and rationalize this language; however, the matter is indeed complicated and the reader is referred to its discussion in the literature [15, 23, 24].

Only a few examples of problematic usage could be provided in the above survey, but careful examination of the literature shows that the misuse of basic stereochemical language is widespread. It is recommended that, when questions arise concerning correct usage, the definitions and discussions of stereochemical nomenclature and terminology be consulted, including, but not limited to, some of the works cited above [9, 14, 15, 17, 18].

3 History

Why concern ourselves with the historical aspects of our science? Perhaps the most succinctly stated answer to this question came from Sir Hans Krebs, Nobel Laureate in Physiology or Medicine (1953): "Those ignorant of the historical development of science are not likely ever to understand fully the nature of science and scientific research." [25]. The history of molecular chirality is particularly rich in beautiful experiments and bold theories, and it appears worthwhile, therefore, in this introduction to the compendium, to peruse some of the pages of this history.

3.1 The Discovery of Molecular Chirality

Molecular chirality was discovered in 1848 by a young French chemist, Louis Pasteur (1822–1895) [26]. The foundations for his discovery were laid during the first half of the nineteenth century, primarily in France, and the reader is referred to the excellent and detailed review and discussion of the subject by Mauskopf [27]. *Hemihedrism* in crystals was an essential element in the story (*holohedral* crystals have the highest symmetry within their crystal class, while in *hemihedral* crystals the symmetry is reduced by the appearance of certain additional facets in only one-half the number required by the crystal system). Hemihedrism in quartz crystals was studied by René-Just Haüy (1743–1822), a French priest and

Fig. 4 Pasteur's official photograph as member of the *Académie française*. Reproduced from http://academie-francaise.fr/immortels/index.html, courtesy of the *Académie française*

crystallographer, in 1801, and François Arago (1786–1853), another French physicist, was the first to observe optical rotation by a substance, when he studied the effects of quartz crystals on polarized light. French physicist and astronomer Jean-Baptiste Biot (1774–1862) discovered in 1815 that a number of natural organic compounds rotate polarized light in the non-crystalline state, e.g., in the liquid or gaseous state or in solution. Among these compounds were camphor, turpentine, sucrose, and tartaric acid (TA). (+)-TA – from tartar deposits formed by the fermenting juice of grapes during the wine-making process – had been discovered by Carl Wilhelm Scheele (1742–1786), a Swedish pharmacist, in 1769, and Biot showed that the natural compound was optically active. Biot understood that optical rotation by substances in the non-crystalline state was due to some *molecular* property, but the basis of the phenomenon, molecular chirality, was discovered later by Pasteur (Fig. 4).

After earning a doctorate in 1847 with two dissertations, one in chemistry and one in physics, Pasteur focused his attention on questions of crystallography and optical rotation. He was familiar with the earlier work on quartz; moreover, he recognized that the appearance of hemihedral facets on quartz crystals rendered them chiral, i.e., the crystal habit (external morphology) was chiral, with some crystals displaying "right-handed" morphology while others were "left-handed," that is the two crystal types were enantiomorphous. This was a novel realization by Pasteur, since earlier investigators of quartz crystals (e.g., Haüy, Biot, Herschel), while fully familiar with the hemihedrism of quartz, had not explicitly recognized the chiral morphology of the crystals. Pasteur's recognition of the chirality of quartz crystals was helpful in his discovery of molecular chirality. He understood that the external chiral morphology of quartz crystals was due to a particular ordering of the molecules within the crystal and *not* to a property of the *individual molecules* of quartz [26].

In 1848 Pasteur examined the crystals of sodium ammonium tartrate (a salt of the natural (+)-TA) and found that they were hemihedral and had a chiral habit. Pasteur then examined the sodium ammonium salt of another, related, acid. That acid had been obtained ca. 1819 as an unexpected side-product during the production

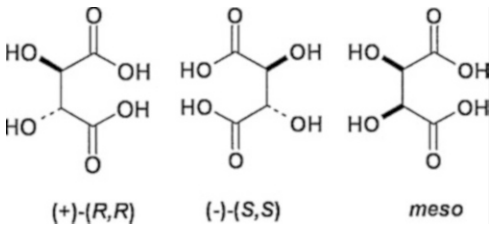

Fig. 5 (+)-, (−), and *meso*-tartaric acid

of (+)-TA from tartar at a chemical plant in the region of Alsace, in eastern France. The identity of the mysterious new acid was not clear and intrigued chemists. The eminent French chemist and physicist Louis Joseph Gay-Lussac (1778–1850) obtained a sample for study and showed it to have the same composition as "ordinary" (dextrorotatory) TA; he named it *racemic acid*, from the Latin *racemus*, i.e., cluster of grapes. Another name used for the compound was *paratartaric* acid (PTA). In most of its properties PTA was shown to be identical with the natural (+)-TA, but the two substances differed in crystal morphology, solubility, and in that PTA did not rotate polarized light [26].

Pasteur found that the sodium ammonium salt of PTA crystallized as a mechanical mixture (*conglomerate* in today's terminology) of two distinct crystal types that were hemihedral and enantiomorphous. He manually separated the two crystal types and examined their optical activity in solution separately (he was thoroughly familiar with Biot's work on optical rotation by natural organic compounds). The two PTA salts showed optical rotations equal in absolute magnitude (within experimental error) but opposite in direction. Furthermore, Pasteur found that the dextrorotatory salt was identical in all respects with the corresponding salt of natural (+)-TA. The free acids liberated from the two sodium ammonium salts of PTA had enantiomorphous crystal morphology and equal optical rotations in absolute value but opposite in direction. Pasteur concluded that PTA was the 1:1 combination of *dextro*- and *levo*-TA and that the molecules of TA are chiral, and he proposed that the optical activity of these substances in solution was the result of the chirality of their molecules (in this he recognized the difference between quartz and TA: unlike the quartz molecules, the TA molecules were chiral) [26]. He even proposed that a tetrahedral or helical arrangement of the atoms in chiral molecules may be the basis of their chirality, proposals we now know to be correct. Pasteur's discovery was all the more remarkable as the chemical structure of TA (Fig. 5) was not known at the time.

Concerning Pasteur's term for handedness, he did not use *chirality* since this term was coined, by Lord Kelvin in 1894, i.e., long after Pasteur had abandoned studies of molecular chirality. Instead, Pasteur adapted the little-used French term *dissymétrie* (dissymmetry) to the phenomenon that today we call chirality [17].

It should be mentioned here that in 1820, i.e., well before Pasteur, there was a theoretical suggestion that some molecules may lack symmetry. It came from Sir John Frederick William Herschel (1792–1871), an eminent English astronomer, physicist, and chemist. He proposed that such lack of symmetry may be the

explanation for Biot's observation (see above) that some substances are optically active in the non-crystalline state [17]. In 1827 Herschel repeated his suggestion, stating that such molecules "must be conceived as unsymmetrically constituted, i.e., as having a right and left side." This is, no doubt, a seed of the concept of molecular chirality. It must be recognized, however, that, insightful as it was, Herschel's proposal of "unsymmetrical molecules" was limited in scope and remained only a theoretical suggestion: he did not elaborate further on the subject and did not pursue any experimental studies on the phenomenon. It was in fact Pasteur (whether he had been aware of Herschel's ideas or not) who placed the concept of molecular chirality on a solid experimental foundation in a series of studies that demanded a great deal from him: the recognition of the fundamental problem of the sodium ammonium tartrate/paratartrate crystals, the design and execution of crucial and difficult experiments, exceptional powers of observation, thorough familiarity with the literature, and superior scientific intuition. Ultimately, based on his tartrate work, Pasteur was able to elaborate a fundamental chemical phenomenon that his eminent predecessors, i.e., Biot, Mitscherlich, de La Provostaye, Hankel, etc., all of whom had worked with tartrate crystals and had access to Herschel's publications, had failed to recognize. All in all, it is therefore not inaccurate to speak of "*Pasteur's discovery* of molecular chirality" [17].

Pasteur's preparation of (−)-TA in 1848 produced the first known example of the existence of *both* enantiomers of a chiral substance. In 1851 the isolation of (−)-camphor from a natural source by Chautard [28] created the second example [(+)-camphor had been known for a long time].

All in all, Pasteur's resolution of (±)-TA is considered among the most elegant experiments in the history of chemistry. Moreover, he made his discovery of molecular chirality at a time when little was known about chemical structure and atomic bonding.

3.2 The Asymmetric Carbon Atom

The next fundamental discovery in the history of molecular chirality occurred a quarter-century later, in 1874, when the Dutch and French chemists Jacobus Henricus van 't Hoff (1852–1911) [29] and Joseph Achille Lebel (1847–1930) [30], respectively, proposed, independently and nearly simultaneously, the asymmetric carbon atom as a basis for molecular chirality. As they explained, in such an atom the four substituents differ, and if their arrangement around the carbon is not planar, two non-superposable-mirror-image configurations are possible, i.e., chirality is introduced. Although the two publications differ in some respects, the fundamental conclusions reached by the two authors concerning the "asymmetric carbon atom" (van 't Hoff's term) as a basis for molecular chirality are similar. For example, they both referred to the "asymmetry" of an appropriately substituted carbon atom, and both proposed that the four valences of the saturated carbon atom were arranged in the form of a tetrahedron [29, 30].

The discovery of the asymmetric carbon atom finally provided the explanation for the existence of "optical isomers" and for the chiral nature of the molecules of optically active substances, including many naturally occurring substances. Initially the proposal received little attention from chemists but, eventually, the usefulness of the theory in explaining the known examples of "isomers" (and in predicting new cases) was recognized and the asymmetric atom gained influence and came to be generally accepted. Several detailed analyses of the history of the discovery of the asymmetric carbon atom have appeared [31, 32].

3.3 Biological Enantioselectivity

Molecular chirality has considerable importance in biology and therefore a brief review of the essential early discoveries in this domain is of interest. The first key observation was made by Pasteur himself in 1857. At the time, he was professor of chemistry and dean of the Faculty of Sciences at the University of Lille, an industrial region in northern France where agricultural and food industries had considerable economic significance and fermentation-based manufacturing, such as the production of ethanol from sugar beets and the production of beer, was of particular importance. On December 21st, 1857, Pasteur presented a communication to the *Académie des sciences* entitled "Memoir on Alcoholic Fermentation" which was published as a memoir in the proceedings of the *Académie*, the *Comptes rendus des séances de l'Académie des Sciences* (*Comptes rendus* henceforth) [33]. The memoir dealt with certain aspects of alcoholic fermentation, but near the end of the communication Pasteur said the following:

> Before concluding, I ask for the permission of the Academy to present results to which I attach great importance. I have discovered a means of fermenting tartaric acid which readily affects ordinary right tartaric acid but involves left tartaric acid very poorly or not at all. Now, a remarkable thing, predictable from the preceding fact, is that when paratartaric acid, formed by the combination, molecule for molecule, of the two tartaric acids, right and left, is subjected to the same method of fermentation, it is resolved into the right acid which is fermented and left acid which remains intact, in such a way that the best means of obtaining left tartaric acid I know of today is to resolve PTA by fermentation.

Approximately 3 months after that brief announcement, Pasteur presented to the *Académie* a communication devoted entirely to the subject of the fermentation of (±)-TA [34, 35]. He did not identify a specific microorganism in the memoir, although he referred to the organism as "yeast." He also described it as resembling the "lactic ferment," i.e., the microorganism he had identified as responsible for lactic fermentation. In his scientific biography of Pasteur, Duclaux suggested that the microorganism of the tartrate fermentation may have been a species of *Penicillium,* a fungal microorganism. In fact, in 1860 Pasteur reported in a brief note that *Penicillium glaucum,* a common mold, enantioselectively metabolized PTA in a manner very similar to the earlier fermentation: here too, (+)-TA was consumed and (−)-TA was left behind largely untouched. The nature of the products of the

fermentation of TA was also not addressed by Pasteur in his memoir of March, 1858, but he did mention that an earlier report in the literature identified *metacetonic acid* as a product of the fermentation of calcium (+)-tartrate. "Metacetonic acid" is an old name for propionic acid.

Pasteur's description of the enantioselective fermentation of PTA in the memoir of December, 1857, constitutes the first published observation of enantioselectivity in a biological process, and his finding was a key discovery that placed the foundation stone of the science of molecular chirality in biology.

As a result of the advances in organic chemistry during the second half of the nineteenth century, the chemical structures of many compounds became known, which in turn led to studies of the biological properties of many chiral substances. Since initially only in relatively few cases were both enantiomers available separately, at first only a small number of studies of enantioselectivity appeared (some of the investigations compared the activity of one of the enantiomers to that of the racemate). With time, however, the pace accelerated, and many studies were published on the role of molecular chirality in biology. Two general areas were addressed: (1) stereoselectivity in enzymatic reactions, as manifested in the metabolic fate or enzyme-catalyzed specific transformations of substances; (2) stereoselectivity in the physiological, pharmacological, or toxicological effects of a variety of biologically active compounds.

Concerning stereoselectivity in enzymatic activity, while a comprehensive review of the early work in this field would be beyond the scope of this chapter, the extensive and pioneering work on the role of stereochemistry in enzyme action by the eminent German chemist Emil Fischer (1852–1919) during ca. the last 2 decades of the nineteenth and early in the twentieth century should be mentioned here. Fischer's work in this domain has been amply chronicled [36], and only some relevant fundamental aspects will be discussed here. Fischer began his work on carbohydrates in 1884 and pioneered the synthesis of sugars and the determination of their structures and stereochemical relationships. Indeed, Fischer's work on the synthesis of sugars qualifies him as a pioneer of "asymmetric synthesis" [23, 36]. Fischer applied the fundamental concepts of van 't Hoff and Lebel concerning the asymmetric carbon atom and its role in stereochemistry, and his work in this regard was a powerful validation of the ideas of the two chemists. Fischer's work also benefited from the great advances in structural organic chemistry, valence theory, etc., achieved during the second half of the nineteenth century.

Fischer studied both natural and synthetic sugars, and demonstrated that the microbial fermentation (e.g., by beer yeast) and other enzymatic reactions of sugars displayed considerable stereoselectivity. He found both diastereoselectivity and enantioselectivity in the action of enzymes on sugars. For example, he showed that natural glucose, fructose, and galactose were readily fermented by yeast but their "optical antipodes" (an inaccurate term often used in the past to refer to enantiomeric molecules) were left unchanged. As for diastereoselectivity, he found, for example, that crude aqueous yeast extracts (which he named "invertin") hydrolyzed α-methyl-D-glucoside but not its diastereoisomer (epimer) β-methyl-D-glucoside, while a preparation obtained from almonds Fischer called "emulsin"

Fig. 6 Arnaldo Piutti in the laboratory at the age of ca. 40–50. Photograph and permission to reprint kindly provided by Dr. Claudia Piutti

hydrolyzed β-methyl-D-glucoside but not α-methyl-D-glucoside (the methyl-L-glucosides were entirely unaffected) [37]. Fischer also realized that "fermentation" by microorganisms is almost certainly the result of the action of enzymes within them, and his findings on the stereoselectivity of enzyme action prompted him to propose the famous lock-and-key model [37] to emphasize the requirement for geometric complementarity between enzyme and substrate for the reaction to occur. Fischer also made an important contribution to stereochemistry with his system of drawing stereochemically explicit and convenient structures using a convention now known as the Fischer projection [38].

Fischer was intrigued by nature's ability to synthesize sugars in single-enantiomer form and, as pointed out by Ramberg in his insightful analysis of Fischer's work on sugars, Fischer concluded that "asymmetric" chemical constituents within cells were responsible for this asymmetric synthesis, rather than external universal "dissymmetric forces" (e.g., sunlight or magnetism) believed by Pasteur to be the agents ultimately responsible for the single-enantiomer character of natural compounds [39].

Today it is generally agreed that Fischer's work was revolutionary. His groundbreaking achievements were recognized in 1902 with the Nobel Prize in chemistry for "the extraordinary services he has rendered by his work on sugar and purine syntheses." In the award address, Professor Hj. Théel, President of the Swedish Royal Academy of Sciences, specifically discussed the revolutionary importance of Fischer's work on sugars, their stereochemistry, and the nature of enzymes and their interactions with sugars, and emphasized the overall impact of Fischer's work on the essential connections of chemistry and biology (http://www.nobelprize.org/nobel_prizes/chemistry/laureates/1902/press.html).

Concerning the other major area of interest mentioned above, stereoselectivity in physiological, pharmacological, or toxicological effects was also studied. The first observation in this domain was made in 1886 by the Italian chemist Arnaldo Piutti (1857–1928) (Fig. 6), when he discovered enantioselectivity in what is considered

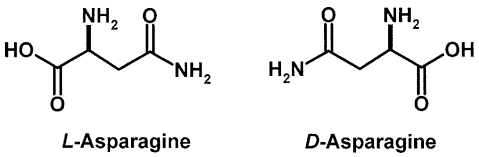

Fig. 7 The asparagine enantiomers

today receptor-mediated biological activity [40, 41]. Receptors are macromolecules "at the cell surface and within cells that mediate the effects of chemical messengers and hormones and the actions of many drugs in the body" [42]. The receptor concept was introduced at the dawn of the twentieth century, independently by the German physician and immunologist Paul Ehrlich (1854–1915) [43] and the British physiologist John Newport Langley (1852–1925) [44]. However, the concept of receptors was not widely accepted until the 1960s. More recently, the science of receptors has undergone an explosive growth and has assumed great importance in many areas of the biological sciences, including neuroscience, immunology, biochemistry, molecular biology, physiology, and pharmacology. Indeed, today receptors constitute one on the most intensively studied areas of biology.

Piutti completed his university education in chemistry at the University of Turin in 1879 and in 1881 moved to Florence to work with Ugo (Hugo) Schiff, an eminent professor of chemistry originally from Germany (he is mostly remembered today for "Schiff's bases" which he discovered). It was in 1886, while working in Schiff's laboratory, that Piutti made his discovery [40, 41], which concerned the amino acid asparagine. In 1886 L-asparagine had already been known for 80 years. "Ordinary asparagine," as it was often referred to, is today's L-asparagine (Fig. 7).

L-Asparagine (a non-essential amino acid) is thought to have been the first amino acid identified in natural sources and was first isolated in 1806 by the renowned French chemist and pharmacist Louis Nicolas Vauquelin (1763–1829) and his young assistant (and later a respected chemist and pharmacist in his own right) Pierre Jean Robiquet (1780–1840) [45]. They obtained the substance from the juice of the asparagus plant they indicated to be *Asparagus sativus*. Linn. (L-asparagine is now known to occur in the free state in many other plants as well, e.g., marshmallow, vetches, soybeans, and white lupino beans).

In the spring of 1885 Piutti assisted in the production on a large scale of ordinary asparagine in a factory producing the substance in Siena, Italy [40]. From 6,500 kg of germinated vetch, 20 kg of crude levorotatory asparagine was obtained. The mother liquors remaining after this operation deposited, with time and natural evaporation, a mixture of two *enantiomorphous* crystal types, one being L-asparagine and the other a new species. Piutti manually separated the two types of crystals and purified the material, obtaining in this manner 100 g of a new substance whose crystals were enantiomorphous with the crystal habit of natural asparagine. The optical rotation of the new substance was found to be equal in absolute magnitude and opposite in direction to that of natural (L) asparagine. In addition, the chemical properties and elemental composition of the new compound were the same as those of L-asparagine. No additional details on the isolation procedure are provided [40].

Even during the isolation and purification process leading to the new asparagine Piutti noticed that the mixture of the two asparagines tasted sweet. His newly isolated asparagine retained the sweet taste and in this differed drastically from L-asparagine, which was without taste. Piutti stated that other known amidated acids have a sweet taste, and, importantly, he pointed out that in other known examples of enantiomerically related substances the taste does not differ [40].

The chemical structure of asparagine was known in its major features at the time but not in all of its details. Specifically, the presence of the amino, carboxyl, and carboxamide groups was known, and it was understood that the carboxyl and carboxamide groups were separated by two saturated carbons. However, the position of the amino group was uncertain, i.e., it was not known whether the amino group is located α to the carboxyl group or α to the carboxamide function. Accordingly, Piutti asked the question whether the two asparagines (i.e., the "ordinary" form and the newly isolated compound) could be constitutional isomers, i.e., differing insofar as the position of the amino group is concerned, namely, that one of the two substances would have the structure $HO_2CCH(NH_2)CH_2CONH_2$ (an α-amino acid) while the other would correspond to $HO_2CCH_2CH(NH_2)CONH_2$.

Piutti settled the question of the exact structure of asparagine with an unequivocal synthesis that was imaginative and elegant for his time [46]. He showed that asparagine is in fact an alpha-amino acid (Fig. 7) and proved that the new asparagine he had isolated was the "inverse" (i.e., the mirror-image form, in molecular terms) of L-asparagine. Today his compound is known as D-asparagine (Fig. 7).

In summary, Piutti's discovery of a difference in the taste of D- and L-asparagine in 1886 was a milestone first observation of enantioselectivity at what is known today to be a biological (human) receptor (whose concept was first proposed 15 years after Piutti's discovery). The discovery was also the first observation of stereoselectivity of any kind in taste, the first finding of biological enantioselectivity in an organism higher than microorganisms, the first example of biological enantioselectivity in an effect other than enzyme action, and one of the earliest reports of the preparation of a D-amino acid. Piutti also proved the structure of asparagine with an elegant synthetic pathway. Overall, Piutti's investigations on asparagine addressed a series of challenging problems and were carried out with originality and imagination, and the result was a key discovery in the history of molecular chirality in biology. Today, stereoselectivity at biological receptors is recognized as an important aspect of ligand-receptor interactions and the phenomenon has substantial implications and consequences for the science and associated technologies, e.g., in new-drug development.

The first clear example of enantioselectivity in a pharmacological action proper was the demonstration by Cushny that (−)-hyoscyamine (Fig. 8) was ca. 12–20 times more potent than the *dextro* enantiomer in a variety of pharmacological effects, e.g., mydriasis in the cat, salivary secretion in the dog, and at cardiac myoneural junctions. Interestingly, (+)-hyoscyamine was the more potent enantiomer in CNS-excitatory effects [47]. Cushny also found that the enantiomers of epinephrine (adrenalin) differ significantly in their ability to increase blood pressure, the levorotatory form being 12–15 times more potent than (+)-(*S*)-epinephrine [48].

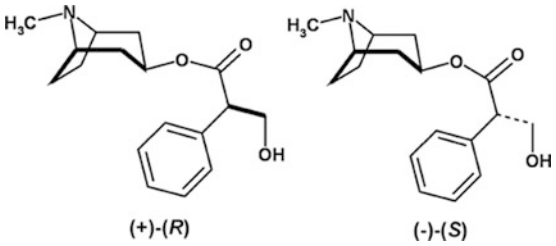

Fig. 8 The hyoscyamine enantiomers

Arthur Robertson Cushny (1866–1926), a Scottish pharmacologist, made important experimental contributions to the field of enantioselectivity in pharmacology; in 1926 he reviewed the studies of enantioselective pharmacology and enzyme action published during the previous ca. 40 years and provided a detailed and critical discussion of enantioselectivity in biology [49] that revealed a great deal of insight into the nature of molecular chirality and its biological implications. Cushny was a leading figure in the discovery of the role of chirality in biology, particularly in pharmacology.

4 Significance

The importance of molecular chirality for the chemical sciences hardly needs an explanation. An exceedingly large number of known substances are constituted of chiral molecules and represent an extraordinarily wide variety of chemical structures, and a discussion of the implications of the phenomenon for various branches of chemistry (e.g., analytical, synthetic, polymer) would be beyond the scope of the present chapter. As mentioned above, however, molecular chirality and enantiomerism also have considerable importance for biology, and their importance for pharmacotherapy and new-drug development constitutes one of the main driving forces behind the current intense interest in molecular chirality. Therefore, a brief discussion of this topic appears warranted.

It is widely recognized today that chirality is a fundamentally important modulator of the effects and properties of chiral substances in a variety of branches of biology and medicine, e.g., biochemistry, physiology, pharmacology, toxicology, clinical therapeutics, etc. Enantioselectivity has frequently been found in enzyme action, at biological receptors, at binding proteins, etc. [50–53]. Enantioselectivity in pharmacological effects, clinical efficacy, toxicity, metabolism, and pharmacokinetics of chiral drugs is a commonly observed phenomenon, and stereochemical factors are often of great importance in pharmacotherapy and drug discovery [52]. Beginning in the 1980s, a recognition began to emerge concerning the importance of stereochemistry, particularly chirality, in drug action and disposition (the somewhat provocative yet useful admonitions in this regard by Ariens [54, 55] were catalytic). These considerations led in turn to the appreciation that in

many cases the racemic form of a drug is biologically distinctly different from a single-enantiomer form, since the former contains both enantiomers (a large percentage of therapeutic agents on the market were racemic [55]).

Today it is generally believed that a single-enantiomer version of a therapeutic agent is likely to have advantages over the racemic or some other stereoisomeric mixture. For example, the pharmacology and toxicology profiles will be clearer for the single substance, the pharmacokinetics and the relationship between serum concentration and biological effects will be more readily interpretable, in some cases adverse effects or toxicity will be eliminated with the removal of the less-favorable stereoisomer, the dosage of the single-enantiomer drug may be lower than that of the stereoisomer mixture, reduced potential for complex drug interactions, etc. (However, a word of caution is in order here: in a few cases it has been shown that the racemic or some other mixture of the stereoisomers was a safer drug than a single-enantiomer form [56]. Thus, each case should be considered on its own merits).

The new awareness of the importance of chirality for drugs eventually resulted, in the 1990s, in guidelines issued by drug-regulatory authorities concerning the development of new drugs based on chiral molecules. Thus the US Food and Drug Administration (FDA) issued their guidelines in 1991 [57], and other countries issued such rules at around the same time. The new regulations thus introduced require that during the development of new chiral drugs the role and implications of molecular chirality in the pharmacological, therapeutic, and toxic effects of the drug candidates be taken into account. The impact of this change in the approach to chirality in new-drug development has been dramatic. For example, today the appearance of a new racemic drug on the market is a highly unlikely event (the significance of this change can be appreciated when we consider that a few years before the publication of the new FDA rules ca. 30% of all marketed drugs were racemic [55]). A justification for the introduction of a new racemic drug today concerns those cases where the drug is stereochemically labile [58], i.e., if there is an in vitro and/or in vivo change in stereoisomeric composition on a time scale sufficiently fast to be relevant during the shelf-life of the drug or during the therapeutic treatment. For example, in vivo inversion of one of the enantiomers to the other is commonly seen in the "profens," i.e., the 2-arylpropionic-acid-based non-steroidal anti-inflammatory agents (NSAIDs) [59].

The question may be asked: what were the factors that prompted this change in attitude toward the role of chirality in pharmacotherapy and new-drug development? In retrospect, it appears that advances in two chemical disciplines played a major role in focusing the attention on the importance of molecular chirality:

1. The considerable advances in the synthesis of single-enantiomer compounds during the last several decades of the twentieth century [60]. These improved methods of organic synthesis have allowed the preparation of a wide variety of single-enantiomer drugs and other substances. Needless to say, such synthetic methodologies are essential for the study and development of single-enantiomer drugs.

2. The advent, during the same period, of powerful methods for enantioselective analysis, i.e., the detection and quantification of enantiomerically related substances in the presence of each other, particularly via enantioselective chromatography (the present compendium is in fact a testimonial to these advances). The new chromatographic analytical methods have allowed the convenient, rapid, precise, and accurate determination of the enantiomer composition or enantiopurity of chiral substances, even in cases of trace contamination of single enantiomers with the opposite (enantiomeric) form. Such analytical capability is essential in a variety of settings, e.g., in the development of synthetic methods, in assuring stereochemical purity during pharmacological testing, in studies of the pharmacokinetics and metabolism of chiral substances, etc. (An important additional advantage of some of the chromatographic enantioseparations is that in the (semi)preparative mode they may rapidly provide sufficient amounts of the individual enantiomers for prompt initial pharmacological and toxicological evaluation, without the need to resort to synthetic methods to obtain them, methods which are often challenging and time-consuming.)

Acknowledgments Helpful information from the following individuals (listed in alphabetical order) is gratefully acknowledged: Prof. Pedro Cintas (University of Extremadura, Spain); Prof. Mark M. Green (New York University, USA); Prof. Andrew J. Hutt (University of Hertfordshire, UK). The author is deeply indebted to the Piutti family, Dr. Claudia Piutti (Nerviano Medical Sciences, Nerviano, Italy), great-granddaughter of Arnaldo Piutti; Pietro Piutti (of Conegliano, Italy), grandson of Arnaldo Piutti; and Pietro's spouse Caterina (née Rovetto) for providing Arnaldo's photograph and permission to reproduce it. The author is grateful to John Wiley & Sons, Inc., for permission to use text from some of his previously published articles [9, 17, 20, 35, 41].

References

1. Eliel EL, Wilen SH (1994) Stereochemistry of organic compounds. Wiley, New York, p 1194
2. Mislow K (1999) Molecular chirality. Top Stereochem 22:1–82
3. Eliel EL, Wilen SH (1994) Stereochemistry of organic compounds. Wiley, New York, p 1197
4. Eliel EL, Wilen SH (1994) Stereochemistry of organic compounds. Wiley, New York, p 1198
5. Anslyn EV, Dougherty DA (2006) Modern physical organic chemistry. University Science Books, Sausalito, pp 298–302
6. Anslyn EV, Dougherty DA (2006) Modern physical organic chemistry. University Science Books, Sausalito, p 300
7. Mislow K, Siegel J (1984) Stereoisomerism and local chirality. J Am Chem Soc 106:3319–3328
8. Anslyn EV, Dougherty DA (2006) Modern physical organic chemistry. University Science Books, Sausalito, p 301
9. Gal J (2011) Stereochemical vocabulary for structures that are chiral but not asymmetric: history, analysis, and proposal for a rational terminology. Chirality 23:647–659
10. Eliel EL, Wilen SH (1994) Stereochemistry of organic compounds. Wiley, New York
11. Anslyn EV, Dougherty DA (2006) Modern physical organic chemistry. University Science Books, Sausalito, pp 297–351

12. Carroll FA (1998) Perspectives on structure and mechanism in organic chemistry. Brooks/Cole Publishing Company, Pacific Grove, pp 58–118
13. Nicolaou KC, Boddy CNC, Siegel JS (2001) Does CIP nomenclature adequately handle multiple stereoelements? A case study of vancomycin and cognates. Angew Chem Int Ed 40:701–704
14. Davankov VA (1991) Should the terminology used in chirality be more precise? Chirality 3:442
15. Helmchen G (1997) Glossary of problematic terms in organic stereochemistry. Enantiomer 2:315–318
16. Bentley R (2010) Chiral: a confusing etymology. Chirality 22:1–2
17. Gal J (2011) Louis Pasteur, language, and molecular chirality–I. Background and dissymmetry. Chirality 23:1–16
18. Eliel EL (1997) Infelicitous stereochemical nomenclature. Chirality 9:428–430
19. Gal J (1998) Problems of stereochemical nomenclature and terminology. 1. The *homochiral* controversy. Its nature, origins, and a proposed solution. Enantiomer 3:263–273
20. Gal J (2007) Carl Friedrich Naumann and the introduction of *enantio* terminology: a review and analysis on the 150th anniversary. Chirality 19:89–98
21. Pifferi G, Perucca E (1995) The cost benefit ratio of enantiomeric drugs. Eur J Drug Metab Pharmacokinet 20:15–25
22. Han H, Yoon J, Janda KD (1998) An efficient asymmetric route to 2,3-diaminobutanoic acids. J Org Chem 63:2045–2048
23. Kagan H, Gopalaiah K (2011) Early history of asymmetric synthesis: who are the scientists who set up the basic principles and the first experiments? New J Chem 35:1933–1937
24. Eliel EL, Wilen SH (1994) Stereochemistry of organic compounds. Wiley, New York, p 1192
25. Krebs HA (1970) The history of the tricarboxylic acid cycle. Perspect Biol Med 14:154–170
26. Pasteur L (1922) Recherches sur la dissymétrie moléculaire des produits organiques naturels. In: Pasteur Vallery-Radot L (ed) Œuvres de Pasteur, vol 1. Masson et Cie, Paris, pp 314–344
27. Mauskopf SH (1976) Crystals and compounds: molecular structure and composition in nineteenth-century French science. Trans Am Phil Soc 66:5–80
28. Chautard J (1853) Mémoire sur l'acide camphorique gauche et sur le camphre gauche. Compt Rend Acad Sci 37:166–7
29. Van 't Hoff JH (1874) Sur le formules de structure dans l'espace. Arch Neerl 9:1–10
30. Lebel JA (1874) Sur les relations qui existent entre les formules atomiques des corps organiques et le pouvoir rotatoire de leurs dissolutions. Bul Soc Chim Paris 22:337–347
31. Ramberg PJ (2003) Chemical structure, spatial arrangement: the early history of stereochemistry 1874–1914. Ashgate Publishing Limited, Aldershot, pp 53–109
32. Ramsay OB (1981) Stereochemistry. Heyden, London, pp 81–97
33. Pasteur L (1857) Mémoire sur la fermentation alcoolique. C R Séances Acad Sci 45:1032–1036
34. Pasteur L (1858) Mémoire sur la fermentation de l'acide tartrique. C R Séances Acad Sci 46:615–618
35. Gal J (2008) The discovery of biological enantioselectivity: Louis Pasteur and the fermentation of tartaric acid – a review and analysis 150 years later. Chirality 20:5–19
36. Lichtenthaler FW (1992) Emil Fischer's proof of the configuration of sugars. A centennial tribute. Angew Chem Int Ed 31:1541–1546
37. Fischer E (1894) Einfluss der Konfiguration auf der Wirkung der Enzyme. Ber Dtsch Chem Ges 27:2985–2993
38. Fischer E (1891) Ueber die Configuration des Traubezuckers und seiner Isomeren Ber dtsch chem. Ges 24:1836–1845
39. Ramberg PJ (2003) Chemical structure, spatial arrangement: the early history of stereochemistry 1874–1914. Ashgate Publishing Limited, Aldershot, pp 243–276
40. Piutti A (1886) Ein neues Asparagin. Ber Dtsch Chem Ges 19:1691–1695

41. Gal J (2012) The discovery of stereoselectivity at biological receptors: Arnaldo Piutti and the taste of the asparagine enantiomers – history and analysis on the 125th anniversary. Chirality 24:959–976
42. Prüll C-R, Maehle A-H, Halliwell RF (2009) A short history of the drug receptor concept. Palgrave MacMillan, Basingstoke, p 1
43. Ehrlich P, Morgenroth J (1900) Ueber Haemolysine. Dritte Mittheilung. Berliner klin Wochenschrift 37:453–458
44. Langley JN (1905) On the reaction of cells and nerve-endings to certain poisons, chiefly as regards the reaction of striated muscle to nicotine and to curare. J Physiol 33:374–413
45. Vauquelin LN, Robiquet PJ (1806) La découverte d'un nouveau principe végétal dans le suc des asperges. Ann Chim 57:88–93
46. Piutti A (1888) Sintesi e costituzione delle asparagine. Gazz Chim Ital 18:457–472
47. Cushny AR (1920) On optical isomers. V Tropeines J Pharmacol 15:105–127
48. Cushny AR (1909) Further note on adrenalin isomers. J Physiol 38:259–262
49. Cushny AR (1926) Biological relations of optically isomeric substances. The Williams and Wilkins Company, Baltimore
50. Crossley R (1992) The relevance of chirality to the study of biological activity. Tetrahedron 48:8155–8178
51. Patel BK, Hutt AJ (2004) Stereoselectivity in drug action and disposition: an overview. In: Reddy IK, Mehvar R (eds) Chirality in drug design and development. Marcel Dekker, New York
52. Eichelbaum M, Testa B, Somogyi A (eds) (2003) Stereochemical aspects of drug action and disposition. Springer, Berlin
53. Ariëns EJ, Soudijn W, Timmermans PBMWM (eds) (1983) Stereochemistry and biological activity of drugs. Blackwell Scientific Publications, Oxford
54. Ariëns EJ (1984) Stereochemistry, a basis for sophisticated nonsense in pharmacokinetics and clinical pharmacology. Eur J Clin Pharmacol 26:663–668
55. Ariëns EJ, Wuis EW (1987) Bias in pharmacokinetics and clinical pharmacology. Clin Pharmacol Ther 42:361–363
56. Shah RR, Midgley JM, Branch SK (1998) Stereochemical origin of some clinically significant drug safety concerns: lessons for future drug development. Adverse Drug React Toxicol Rev 17:145–190
57. Anonymous (1992) Fed Reg 5(102):22249
58. Reist M, Testa B, Carrupt PA, Jung M, Schurig V (1995) Racemization, enantiomerization, diastereomerization, and epimerization – their meaning and pharmacological significance. Chirality 7:396–400
59. Caldwell J, Hutt AJ, Fournel-Gigleux S (1988) The metabolic chiral inversion and dispositional enantioselectivity of the 2-arylpropionic acids and their biological consequences. Biochem Pharmacol 37:105–114
60. Vogel P (2003) Recent advances in asymmetric organic synthesis: principles and examples. In: Eichelbaum M, Testa B, Somogyi A (eds) Stereochemical aspects of drug action and disposition. Springer, Berlin, pp 3–44

Top Curr Chem (2013) 340: 21–40
DOI: 10.1007/128_2013_454

Published online: 4 July 2013

Terms for the Quantitation of a Mixture of Stereoisomers

Volker Schurig

Abstract Various terms for the quantitation of a mixture of enantiomers and diastereomers are discussed.

Keywords Diastereomeric excess · Diastereomeric ratio · Enantiomeric composition · Enantiomeric excess · Enantiomeric fraction · Enantiomeric proportion · Enantiomeric ratio · Retention excess · Stereoselectivity factor

Contents

V. Schurig (✉)
Institute of Organic Chemistry, University of Tübingen, Auf der Morgenstelle 18, 72076 Tübingen, Germany
e-mail: volker.schurig@uni-tuebingen.de

1 Introduction

The enantiomeric proportion of macroscopic samples of chiral compounds requires its own descriptive adjectives [1]. The proposed terms should generally be applicable and suitable for two important borderline cases in enantiomeric analyses: (1) to establish the high enantiomeric purity status of natural compounds [2] and to determine minute amounts of enantiomeric impurities, e.g., in the evaluation of the enantioselectivity of enzymes and chiral catalysts in enantioselective syntheses and kinetic resolutions and (2) to determine low enantiomeric imbalances [3], e.g., minuscule deviations from truly racemic compositions in experiments devoted to the amplification of enantiomeric bias under prebiotic conditions.

The historical development of expressions for the quantitation of stereoisomeric proportions is outlined and recommendations for its contemporary use are presented. The stereoisomers are treated separately as enantiomers and diastereomers.

2 Enantiomers

Depending on whether a mixture of enantiomers is quantified by (1) spectroscopic or chromatographic methods, employing a nonracemic auxiliary compound, or by (2) chiroptical methods, different definitions have been used [4–10].

2.1 Nonchiroptical Methods

2.1.1 Enantiomeric Excess ee

Enantiomeric excess, ee, has been defined as the excess of one enantiomer over the other [1]. The expression ee was proposed in 1971 by Morrison and Mosher [5]:

$$\mathrm{ee} = (E_1 - E_2)/(E_1 + E_2), \tag{1}$$

where E_1 is the amount of the major enantiomer and E_2 is the amount of the minor enantiomer. The magnitude of the enantiomeric excess ee extends from ee = 0 for the racemic mixture to ee = 1 for pure E_1. The term ee is unequivocal, since it describes the relationship between two enantiomers in a mixture, as determined by whatever means are available [11]. Equation (1) was originally introduced by Raban and Mislow and was referred to as enantiomeric purity [4]. The incentive for the new definition arose from the assumption of numeric equality between optical rotation and enantiomeric proportion in nonracemic mixtures [4, 5]. Indeed it was stated that the value of the enantiomeric purity is identical with the value of the optical purity [4]. This statement is valid only when ideal conditions prevail in

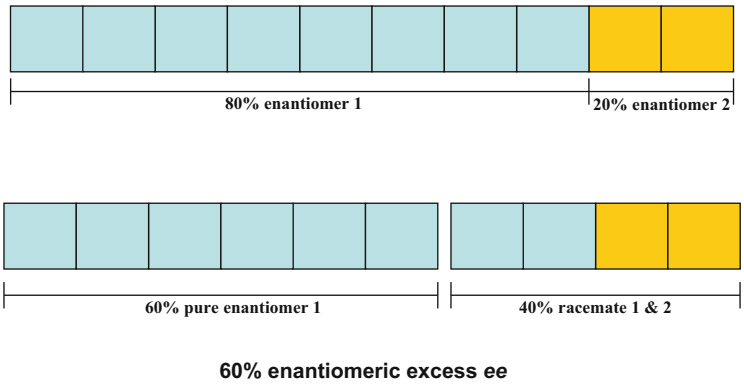

Fig. 1 Visualization of the definition of enantiomeric excess for ee = 60%

the determination of optical purity (see below). Moreover, the link to the criterion of purity in the terms enantiomeric purity and optical purity has subsequently been considered as unfortunate as it implies that the "impurity" is the racemic composition and not the minor enantiomer [11].

In practice, ee is often quoted as a percentage [1]:

$$\%\text{ee} = (E_1 - E_2)/(E_1 + E_2) \cdot 100 = \%E_1 - \%E_2. \tag{2}$$

The term ee has now correctly been defined as the excess of one enantiomer over the racemic composition in the mixture E_1 + E_2 [6, 12, 13]. Thus for a mixture of the proportion E_1:E_2 = 99:1, E_1 = 99% while ee = 98% and for a mixture enriched in one enantiomer, e.g., 80:20, E_1 = 80% but ee = 60% (Fig. 1).

When the mole or mass fractions x_{E1} and x_{E2} are used, the following simplified expressions apply because enantiomers possess the same molar mass and to due x_{E1} + x_{E2} = 1 [1]:

$$\text{ee} = x_{E1} - x_{E2} = 2x_{E1} - 1 = 1 - 2x_{E2} \tag{3}$$

The converse relations are [1]

$$x_{E1} = (1 + \text{ee})/2 \text{ and } x_{E2} = (1 - \text{ee})/2. \tag{4}$$

The expression *enantiomeric purity* was originally used as a synonym for ee [4]. However, the use of *enantiomeric purity* should be avoided as it has also been defined as mole fraction of the major enantiomer x_{E1} [4, 6] or simply as the percentage of one enantiomeric in a mixture [14, 15] (cf. the following section).

2.1.2 Enantiomeric Composition ec and Enantiomeric Fraction EF

The enantiomeric proportion of a sample may be described as the dimensionless mole ratio (or a mole percent of the major enantiomer) and this has been suggested the most generally useful way to describe the composition of all types of stereoisomeric mixtures [1]. The use of the mole fraction of the major enantiomer E_1 in a mixture, x_{E1}, was first suggested by Horeau (cf. footnote in [4]). It has been named *enantiomeric composition*, ec [8, 16]:

$$\text{ec} = x_{E1} = E_1/(E_1 + E_2). \tag{5}$$

The terms ec and ee are related as follows:

$$\text{ec} = \text{ee} + x_{E2} = (\text{ee} + 1)/2. \tag{6}$$

The *enantiomeric composition* of a sample has also been simply quoted as % E_1 and % E_2 [17].

More recently, the mole fraction of an enantiomer in a mixture is called *enantiomeric fraction* with the symbol EF_1 applying to the major enantiomer and EF_2 for the minor enantiomer [18–20]:

$$EF_1 = E_1/(E_1 + E_2) \text{ and } EF_2 = E_2/(E_1 + E_2). \tag{7}$$

The magnitude of the enantiomeric ratio EF extends from 0 to 1 with the value of 0.5 for the racemic mixture.

The enantiomeric ratio EF has now become the standard descriptor for chiral signatures of environmental samples [18]. The EF definition is superior because it provides meaningful representation of graphical data and is more easily employed in mathematical expressions of the fate of enantiomers in environmental compartments and for the investigation of enantioselective degradation processes [18] (Fig. 2).

2.1.3 Enantiomeric Ratio er and er_{inv}

The term *enantiomeric ratio*, er (ER or q), is defined as follows [8, 21–23]:

$$\text{er} = E_1/E_2, \tag{8}$$

where E_1 is the major enantiomer.

The magnitude of the enantiomeric ratio er extends from er = 1 for a racemic mixture to er = ∞ for pure E_1. Since er involves large numbers for the major enantiomer in high preponderance, the logarithmic scale, log er, extending from zero to infinity, has been proposed [24]. The terms er and ee are related as follows [8]:

$$\text{ee} = (\text{er} - 1)/(\text{er} + 1) \tag{9}$$

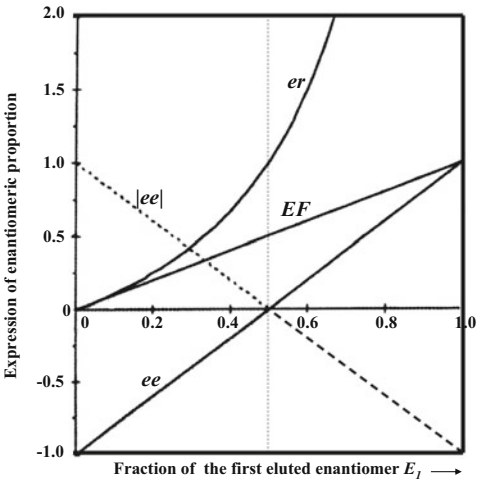

Fig. 2 Graphical representation of the various expressions for enantiomeric proportions plotted against the fraction of the first eluted enantiomer in enantioselective gas chromatography E_1 [19]. Reprinted with permission from [19], © Elsevier

and

$$\mathrm{er} = (1 + \mathrm{ee})/(1 - \mathrm{ee}). \tag{10}$$

The inverse definition of the enantiomeric ratio has also been considered [21, 22] and applied in practice [25]:

$$\mathrm{er_{inv}} = E_2/E_1 \tag{11}$$

$\mathrm{er_{inv}}$ and ee are related as follows:

$$\mathrm{er_{inv}} = (1 - \mathrm{ee})/(1 + \mathrm{ee}) \tag{12}$$

and

$$\mathrm{ee} = (\mathrm{er_{inv}} + 1)/(\mathrm{er_{inv}} - 1). \tag{13}$$

The magnitude of the inverse enantiomeric ratio $\mathrm{er_{inv}}$ extends from er = 0 for pure E_1 to $\mathrm{er_{inv}} = 1$ for a racemic mixture. Note that log $\mathrm{er_{inv}}$ is rendered negative.

2.1.4 Enantiomeric Ratio E and the Stereoselectivity Factor s in Kinetic Resolutions

A source of confusion associated with the term *enantiomeric ratio* has been addressed by Faber as the term is used in two different albeit related ways [26]. The enantiomeric ratio $\mathrm{er} = E_1/E_2$ is directly related to the ratio of the relative rate constants k_{E1}/k_{E2} in the conversion of prochiral substrates or in

meso-differentiating reactions whereby the ratio k_{E1}/k_{E2} is linked to the difference in the Gibbs free energy of activation of the diastereomeric transition states $\Delta\Delta G^{\#} = \Delta\Delta H^{\#} - T\Delta\Delta S^{\#} = -RT \ln er$. The ratio k_{E1}/k_{E2} is independent of the conversion of the reaction because the enantioselective transformations start with the same prochiral substrate S, i.e., $S \rightarrow E_1(k_{E1})$ and $S \rightarrow E_2(k_{E2})$. Therefore the ratio of the product enantiomers E_1 and E_2 will not change during the course of the reaction [26].

A more complicated situation arises in the realm of enzymatic kinetic resolution obeying Michaelis–Menton kinetics when the enantiomers E_1 and E_2 present in a sample are transformed at different rates to the enantiomeric products E'_1 and E'_2, i.e., $E_1 \rightarrow E'_1\,(k'_{E1})$ and $E_2 \rightarrow E'_2\,(k'_{E2})$. In the ideal case only E_1 is transformed to enantiopure E'_1 leaving enantiopure E_2 behind after 50% conversion c. In kinetic resolutions the rate of the reaction of E_1 and E_2 varies with the degree of conversion c since the ratio of the two enantiomers does not remain constant during the transformation. Furthermore, the enantiomeric excess of the substrates ee_S (E_1 and E_2) and of the products ee_P (E'_1 and E'_2) depends on the conversion c. Sih et al. arrived at a parameter describing the enantioselectivity of an irreversible enzymatic kinetic resolution devoid of product and substrate inhibition which is identical with the ratio of the rate constants (k'_{E1}/k'_{E2}) [27]. The parameter which remains constant during the kinetic resolution has been called the *enantiomeric ratio* E which is readily accessible from ee_S, ee_P, and c:

$$E = \ln[(1-c)(1-ee_S)]/\ln[(1-c)(1+ee_S)] = k'_{E1}/k'_{E2} \tag{14}$$

with

$$c = 1 - (E_1 + E_2)/(E^{\circ}{}_1 + E^{\circ}{}_2) \tag{15}$$

When the product arising from the kinetic resolution is itself chiral the following expression can also be used [27, 28]:

$$E = \ln[1 - c(1+ee_P)]/\ln[1 - c(1-ee_P)] \tag{16}$$

A non-enantioselective kinetic transformation has an E value of 1 whereas an E value above 20 is the minimum for an acceptable kinetic resolution [29]. The enantiomeric ratio E is identical to the *stereoselectivity factor* s in the realm of general kinetic resolutions of racemic mixtures defined by Kagan and Fiaud and the same equations apply [30]. E is linked to the difference in Gibbs free activation energy difference of the diastereomeric transition states, i.e., $\Delta\Delta G^{\#} = \Delta\Delta H^{\#} - T\Delta\Delta S^{\#} = -RT \ln E$. An E value of 100 corresponds to $\Delta\Delta G^{\#}$ of 2.7 kcal/mol at 25 °C.

Equation (14) is rendered imprecise at very low or very high conversions c and it is preferentially used in the range of ~40–60% conversion to provide a substantial amount of chemical yield of both the product and the remaining substrate [26].

For low or high conversions c an equation was proposed which requires only the knowledge of ee_S and ee_P, being readily accessible by enantioselective NMR and enantioselective chromatography, whereby the conversion term c is substituted by $ee_S/(ee_S + ee_P)$ [31]:

$$E = [\ln[ee_P(1 - ee_S)]/(ee_P + ee_S)]/[\ln[ee_P(1 + ee_S)]/(ee_P + ee_S)] \quad (17)$$

or in its rearranged form [29]

$$E = \ln[(1 - ee_S)/(1 + (ee_S/ee_P)]/\ln[(1 + ee_S)/(1 + (ee_S/ee_P)] \quad (18)$$

E values greater than 200 should be treated with caution since small variations of ee_P and ee_S will cause large differences in the E value [26]. Reliable data for ee_P and ee_S ($ee > 99\%$) can be measured, e.g., by enantioselective gas chromatography [32].

2.1.5 Naming of Enantiomers: Eutomers and Distomers

The definition of an *enantiomer* [33] as one of a pair of molecules which are mirror images of each other and are non-superposable does not explicitly reserve specific names for the two distinct entities of stereoisomers (Greek: $\varepsilon\nu\alpha\nu\tau\acute{\iota}o\varsigma$ = *opposite* and $\mu\varepsilon\rho o\xi$ = part). This leads to undesired expressions in the literature such as the "wanted enantiomer" for the major enantiomer E_1 and the "wrong enantiomer" or "enantiomeric impurity" for the minor enantiomer E_2 in a mixture of high ee or er.

In pharmacology and pharmacy specific names have been introduced for a pair of enantiomers when a given biological system displays enantioselectivity. The more active enantiomer is termed the *eutomer* (Eu) and the less active enantiomer is called the *distomer* (Dis). The use of the terms derived from Greek $\varepsilon\upsilon$ = good, $\delta\upsilon\xi$ = bad, and $\mu\varepsilon\rho o\xi$ = part was suggested by Lehmann et al. [34] in analogy to the designations of *eutopic* (well-fitting) complexes and *dystopic* (ill-fitting) complexes [35]. A homologous series of enantiomeric pairs consist of a *eutomeric series* and a *distomeric series*. For a given enantiomeric pair the *ratio* of their activities is termed the *eudismic ratio* and its logarithm is termed the *eudismic index* (E.I.) [34, 36]. A correlation between the eudismic potency ratio and the averaged human potency of the racemate for 14 different drugs was discovered by Pfeiffer [37]. The generalized *Pfeiffer's rule* states that in a series of chiral compounds the *eudismic ratio* increases with increasing potency of the *eutomer*.

The definitions ee, er, and ec are derived with E_1 being the major enantiomer in a mixture, i.e., $x_{E1} > 0.5$. Unfortunately, in selected cases there is a need to cover the entire range of $0 \leq x_{E1} \leq 1$. Situations invoking opposite enantioselectivities are frequently encompassed in enzymatic reactions or in pharmacokinetic and pharmacodynamic studies of chiral drugs whereby opposite enantiomers may be favoured

Table 1 Comparison of the various definitions for the quantitation of a mixture of enantiomers

Enantiomeric proportion	% ec (EF)	% ee	er	log er	ln er
50:50	50	0	1	0	0
51:49	51	2	1.041	0.017	0.04
99:1	99	98	99	2	4.6
99.9:0.1	99.9	99.8	999	3	6.9
99.99:0.01	99.99	99.98	9,999	4	9.2
0.01:99.99	0.01	−99.98	0.0001	−4	−9.2

case by case. The different and opposite percentages of the enantiomers E_1 and E_2 are reflected in the definitions as characteristic, and sometimes negative quantities (ee). In the literature the total range $0 \leq x_{E1} \leq 1$ has been treated simply as a percentage, i.e., % E_1 and % E_2 [17], or by their ratio er [38]. Indeed, in cases where no emphasis is given to one major enantiomer, i.e., each of the enantiomers may be in preponderance at specific conditions, ee is not a useful term. The definitions EF and er or ln er are more appropriate in this circumstance (Table 1).

2.2 Chiroptical Methods

Historically, "optically active" has often been used as synonym for "chiral" and to describe nonracemic mixtures of enantiomers. This expression suffers from the fact that it is linked to the determination of chiroptical properties which is gradually being discontinued in modern methodologies to quantify enantiomeric proportions. Moreover, enantiomerically pure samples need not be optically active at a given concentration, temperature, wavelength, and solvent [39].

The term *optical purity* op (or *p*) is defined as the ratio of the measured specific rotation $[\alpha]$ of an enantiomeric mixture, divided by the maximum specific rotation $[\alpha_{max}]$ of one enantiomer (E_1 or E_2 with ee = 1) [4, 39]:

$$\text{op} = [\alpha]/[\alpha_{max}], \tag{19}$$

where the sign of the specific rotation and its complicated CGS dimension is ignored for convenience. In practice, op is quoted as a percentage:

$$\%\,\text{op} = [\alpha]/[\alpha_{max}] \cdot 100. \tag{20}$$

The specific rotation of a mixture of enantiomers is equal to the specific rotation of the pure enantiomer times the optical purity. These relationships are illustrated in Table 2 for a chiral compound whose maximum specific rotation $[\alpha_{max}]$ is arbitrarily set to 150 [6]. Knowing % op from polarimetric measurements one can calculate % E_1 and % E_2 [8]:

$$\%\ E_1 = (100 + \text{op})/2 \quad \text{and} \quad \%\ E_2 = (100 - \text{op})/2. \tag{21}$$

Table 2 Relationship between % enantiomeric proportion, % optical purity p, and specific rotation $[\alpha]$ [6]

Enantiomeric proportion %	% Optical purity	$[\alpha]$
100:0	100	+150
75:25	50	+75
50:50	0	0
75:25	50	−75
0:100	100	−150

Whereas the optical purity op relates to experimental properties, i.e., the specific rotations $[\alpha]$ and $[\alpha_{max}]$, the enantiomeric excess ee describes the composition of a chiral substance without recourse to any physical measurement [4]. Traditionally, op has been used for the quantitation of enantiomers because polarimetry had been the only tool available until the more recent advent of spectroscopic and chromatographic methods. However, op is related to experimental properties whose precision and accuracy is often unsatisfactory [12, 39].

The terms "non-racemic," "optically pure," and "enantiomerically enriched" imply that the racemate constitutes the impurity [14]. Both the definitions of op and ee account for this notion. Historically, the use of op and ee was also preferred since its numerical value is identical under ideal conditions. Thus in the absence of self-associations of enantiomers in non-ideal solutions, the measured optical purity op is equivalent to the value of the true enantiomeric excess ee:

$$\text{op} = [\alpha]/[\alpha_{max}] \equiv (E_1 - E_2)/(E_1 + E_2) = \text{ee}. \tag{22}$$

However, it is important to note that the measured optical purity op of a sample is not linearly related to the true enantiomeric excess ee when non-ideal conditions prevail in concentrated solutions, i.e., when the enantiomers interact between themselves. Thus, the op may markedly deviate from the true ee if the enantiomers undergo molecular self-association to dimers and/or oligomers. The associates formed in solution will display their individual optical rotation and, depending on their concentration, contribute in a specific way to the overall specific rotation. The non-equivalence between op and ee has been experimentally demonstrated for 2-ethyl-2-methylbutanedioic acid in dichloromethane by Horeau (the "Horeau effect," Fig. 3) [40].

The mole fractions of x_{E1} and x_{E2} of enantiomers present in a mixture can be calculated from the measured op [8]:

$$x_{E1} = (1 + \text{op})/2 \tag{23}$$

and

$$x_{E2} = (1 - \text{op})/2. \tag{24}$$

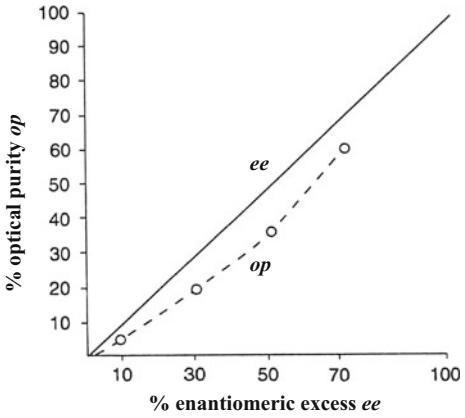

Fig. 3 Non-equivalence between optical purity % op and enantiomeric excess % ee for 2-ethyl-2-methylbutanedioic acid in dichloromethane [40]. Reprinted with permission from [40], © Elsevier

The prerequisite for determining op is a moderate-to-high value of the specific rotation of the sample permitting the correct determination of small differences of the op. Specific rotations may vary from very high values, e.g., for helicenes, to very low values, e.g., for unfunctionalized saturated hydrocarbons. The individual contributions of different elements of chirality (including induced chirality) in a molecule may also lead to an accidental cancellation of the optical activity. Another cause of apparent optical inactivity is the change of the sign of the ORD (optical rotatory dispersion) curve at a specific wavelength.

It has been remarked that measurements of optical rotations is assumed by many chemist to be a trivial experimental procedure because the basic instrument is relatively simple and adaptable in undergraduate laboratories [39]. The fact is, however, that optical rotations are not necessarily self-consistent because variations can occur with any of the parameters often assumed to be constant, i.e., temperature, concentration, wavelength, and solvent. In addition, parameters such as purity of the sample and solvent must be the same for the determination of $[\alpha]$ and $[\alpha_{max}]$. The maximum specific rotation $[\alpha_{max}]$ is not always known and it requires an independent proof of the 100% ee of the sample by a non-chiroptical method. The error due to the instrument reading becomes dramatic for samples with very low optical rotation and at nearly racemic compositions. The uncritical use of apparent values for $[\alpha_{max}]$ led to pitfalls in the optical purity determination of enantioselective transformations [7]. Thus the op of unreacted cycloolefin in the classical Brown kinetic resolution of 3-methylcyclopentene with (+)-diisopinocampheyl borane [41] was not 65% based on an erroneous experimental and theoretical value of $[\alpha_{max}]$ [42] but only 30% through evidence by enantioselective GC [43]. A serious source of error in determining op may arise from the concentration dependence of the specific rotation [39]. Examples are malic acid in water and 2-phenylpropanol in benzene [7]. Thus the op of hydratropaldehyde (2-phenylpropanal) obtained by hydroformylation of styrene had to be corrected from 95 to 73% when specific rotations were re-measured under identical conditions (solvent, concentration, temperature) [44].

The claim of enantiomeric bias via asymmetric synthesis in a rapidly spinning reaction vessel by employing the chiral gravitational field on Earth [45], later disputed on theoretical grounds [46], was solely based on minute (a few millidegrees) optical rotations. Values for op $> 97\%$ may be questionable unless experimental conditions are clearly stated and claims of op $= 100\%$ determined by polarimetry should be treated with the necessary caution.

The use of op has been gradually discontinued and the enantiomeric composition of a sample should only be linked to *optical purity* when exclusively chiroptical methods were employed. This applies, e.g., to chiroptical detectors in enantioselective liquid chromatography [47].

3 Selected Applications of the Terms ee, er, and ec (EF)

3.1 Enantiomeric Excess ee

Enantiomeric excess ee is compatible with the law of mixing (mixing of samples of different ee) and it is useful for calculating the corrected ee when auxiliary compounds with ee < 1 are used in enantioselective synthesis and catalysis [8]. When ee$^\circ$ refers to the maximum ee of the product with an enantiopure auxiliary, the expected ee_{prod} observed (in the absence of nonlinear effects) with an auxiliary of ee_{aux} is given by [8]

$$ee_{prod} = ee^\circ \cdot ee_{aux}. \tag{25}$$

In enantioselective chromatography the chiral selector employed is not always available in an enantiomerically pure form. However, the magnitude of the enantioseparation factor $\alpha = k_2/k_1$, i.e., the ratio of the retention factors of the enantiomers, critically depends on the enantiomeric excess ee of the chiral selector. The value of the maximum enantioseparation factor $\alpha^{ee=1}$ of a chiral selectand which can be attained on a sometimes elusive enantiomerically pure selector with ee $= 1$ can be extrapolated from the enantioseparation factor α measured on an enantiomerically impure selector as follows [48, 49]:

$$\alpha^{ee=1} = [(\alpha + 1)ee + (\alpha - 1)]/[(\alpha + 1)ee - (\alpha - 1)]. \tag{26}$$

An equation describing the drop of α with decreasing ee of a chiral selector can be obtained by rearranging (26) or can be derived de novo by independent considerations [50], including a virtual tandem column approach for which the definition of ee is mandatory [51, 52]:

$$\alpha^{obs} = \left[\alpha^{ee=1}(1 + ee) + (1 - ee)\right]/\left[\alpha^{ee=1}(1 - ee) + (1 + ee)\right]. \tag{27}$$

Thus an enantioseparation factor of $\alpha^{ee=1} = 100$ achieved on an enantiomerically pure selector (ee = 1) drops by more than half to $\alpha^{obs} = 49.75$ when the selector contains as little as 1% of an enantiomeric impurity (ee = 0.98) [50, 51, 53]! The large drop of the enantioseparation factor α of a racemic selectand with decreasing ee of the selector is due to the definition of selectivity as the ratio between retention factors with α resembling the term er. In order to get the same graphic relationship between ee of catalysts and ee of product enantiomers employed in enantioselective catalysis (Fig. 4), the definition *retention excess* re has been introduced in enantioselective chromatography [50, 52] where k_2 and k_1 are the retention factors of the second and first eluted enantiomers, respectively:

$$\text{re} = (k_2 - k_1)/(k_1 + k_2). \tag{28}$$

The retention excess re and the enantioseparation factor α are related to each other by the following expressions:

$$\text{re} = (\alpha - 1)/(\alpha + 1) \quad \text{or} \quad \alpha = (1 + \text{re})/(1 - \text{re}). \tag{29}$$

The unified linear correlation between ee of chiral catalysts in enantioselective catalysis and ee of selector in enantioselective chromatography toward ee of major product enantiomer and re of separated enantiomers, respectively is depicted in Fig. 4.

The term re has also been linked to an *enantioselectivity scale ESS* which defines the ability of an enantiopure chiral selector to produce a retention excess re for the enantioseparated selectands, i.e., re = ESS = 1 refers to 100% enantioselectivity with $\alpha = \infty$, whereas re = ESS = 0.5 refers to 50% enantioselectivity producing $\alpha = 3$ and re = ESS = 0 refers to nil enantioselectivity with $\alpha = 1$ [52]. The unified definition ESS applies both to a chiral catalyst in enantioselective catalysis and to a chiral selector in enantioselective chromatography (Fig. 4). For example, the major enantiomer with ee = 0.5 obtained by enantioselective catalysis (kinetic control) and the enantiomers with re = 0.5 separated by enantioselective chromatography (thermodynamic control) results either from enantiomerically pure auxiliaries with ee = 1 and ESS = 0.5 or from enantiomerically impure auxiliaries with ee = 0.5 and ESS = 1 (Fig. 4) [52].

3.2 Enantiomeric Composition ec and Enantiomeric Fraction EF

The enantiomeric fraction EF is based on a bounded additive scale that is linear and finite ranging from 0 to 1 and is symmetric about the equivalency value EF = 0.5 for the racemic composition (Fig. 2) [54]. DeGeus et al. argue that enantiomeric differences in a number of experimental data may either be overestimated for ER (er or q) values larger than unity or underestimated for ER values smaller than unity due to the nonlinear scale of the multiplicative ER definition (Fig. 2) leading to

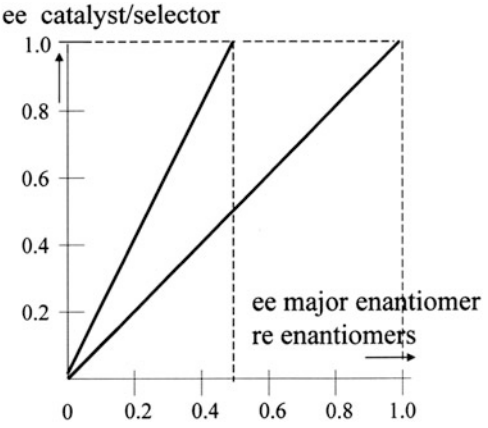

Fig. 4 Unified linear dependence of ee of chiral catalysts and ee of chiral selector with ee of major product enantiomer and re of selectand enantiomers for 50% and 100% enantioselectivity (ESS = 0.5 and ESS = 1), respectively [52]. Reprinted with permission from [52], © Elsevier

skewed data distributions, whereas the linearity of the EF scale (Fig. 2) causes changes to be numerically the same both above and below the 0.5 value for the racemic composition [19].

3.3 *Enantiomeric Ratio er and er_{inv}*

For the quantitative differentiation of enantiomers by enantioselective NMR and chromatography, the enantiomeric ratio er is directly obtained by peak integration of non-equivalent resonances in the NMR spectra and of enantioseparated peaks in the chromatograms. Thus cumbersome re-calculation in the ee scale is not required. The er is compatible with Hammett or Eyring relationships [8] and is a direct measure of the kinetic ratio k_{Re}/k_{Si} in enantiotopos- and enantiofacial-differentiating enantioselective reactions [8, 11, 21]. The Gibbs free energy difference of diastereomeric transition states is $\Delta\Delta G^{\#} = \Delta\Delta H^{\#} - T\Delta\Delta S^{\#} = -RT$ ln er. An er value of 99 corresponds to $\Delta\Delta G^{\#}$ of 2.7 kcal/mole at 25°C. Thus this rather small energy difference already produces enantiomers in the proportion of E_1:E_2 = 99:1. Selke et al. prefer the definition er for the comparison of two different asymmetric hydrogenations employing distinct catalysts by introducing the relative enantioselectivity factor Q [21, 22]. The following equation allows the calculation of the expected enantiomeric ratio er_2 of a de novo catalyst from Q and er_1 of the first catalyst:

$$er_2 = Q \cdot er_1. \tag{30}$$

The term er is the expression of choice in the realm of very high enantiomeric ratios since very large differences between the proportions of enantiomers are not properly represented by the ee definition close at unity. Thus, EF and er or ln er may eventually supersede the more traditional term ee.

In enantioselective chromatography, the enantiomer of opposite configuration has been used as an ideal internal standard for the quantitation of the target enantiomer in a mixture, provided that self-recognition of enantiomers in concentrated solutions is absent. The approach called *enantiomer labeling* [55] is intriguing because enantiomers possess identical non-chiroptical properties in an achiral environment and therefore the enantiomeric composition is not influenced by sample manipulation (isolation, derivatization, fractionation, storage), by chromatographic manipulations (dilution, partitioning, splitting, injection, detection), or by losses (thermal or catalytic decomposition and incomplete isolation). The inverse enantiomeric ratios er_{inv} of sample and standard are used by the "enantiomer labeling method" when sample and standard are not enantiomerically pure. The amount of the chiral component in a sample X after addition of the chiral standard is obtained as follows [55]:

$$X = m_S[(A_R - A_S \cdot er_{invS})(1 + er_{invR})/(A_S - A_R \cdot er_{invR})(1 + er_{invS})], \qquad (31)$$

Where A_R = peak area of the (*R*)-enantiomer after addition of the standard, A_S = peak area of the (*S*)-enantiomer after addition of the standard, er_{invR} = inverse enantiomeric ratio (*S*)/(*R*) of the sample, er_{invS} = inverse enantiomeric ratio (*R*)/(*S*) of the standard, m_S = amount of enantiomeric standard (*S*) added, and X = amount of the chiral component (as sum of its enantiomers) present in the sample.

4 Recommendations for the Quantitation of a Mixture of Enantiomers

The enantiomers present in unequal amounts in a mixture are called the *major enantiomer* E_1 and the *minor enantiomer* E_2.

The *enantiomeric excess* ee, *enantiomeric ratio* er or ln er, and *enantiomeric composition* ec *or* EF are useful terms for the quantitation of a mixture of enantiomers. Each term has its merits under special circumstances. The enantiomeric ratio er is the best descriptor for the result of enantioselection of enantiotopic faces or enantiotopic atoms or groups in a prochiral substrate. Enantioselectivity is reflected by the ratio of products since the relative rates of reaction determine the product ratio by kinetic control [11]. The recommendation to discontinue or prohibit the use of ee [11] is not justified.

For synthetic kinetic resolutions the stereoselectivity factor s is employed whereas for enzymatic kinetic resolutions the enantiomeric ratio E is used which must clearly be distinguished from the coequal term enantiomeric ratio er.

In studies on the fate of enantiomers in the environment or in biological matrices the term enantiomeric fraction EF should be used in lieu of the enantiomeric ratio previously expressed as the terms er and ER [54, 56] or er_{inv} [25].

Only % op is determined when chiroptical detectors are used in enantioselective liquid chromatography and % ee is equivalent to % op only in the absence of self-association of enantiomers.

For the sake of a unified terminology, the following expressions should be avoided, i.e., *enantiomeric yield* and *enantiomeric purity*, while the term *enantiomeric composition* must be correctly defined when applied, e.g., as a mole fraction of the major enantiomer x_{E1}.

It should be noted that the original proportions of the enantiomers in a sample may be altered by *accidental enrichment* during purifications, e.g., by crystallization or by chromatography [1, 12, 57]. Detailed information on sample preparation and analytical procedures are required when % ee = 100 (!) is claimed in enantioselective transformations.

The use of the term *homochiral* for % ee = 100 or, likewise, *heterochiral* for racemic (% ee = 0) should be discontinued [1, 58] since these terms have been reserved for other more concise meanings [59–61]. Eliel et al. proposed to use the expression "enantiomerically pure" (or the contraction "enantiopure") to describe enantiomerically homogeneous samples [62]. In accordance with common practice, the term *nonracemic* rather then *scalemic* [14, 16] is used as synonym of "enantiomerically enriched" and *enantiopure* rather than *holemic* [14] is used as synonym for "enantiomerically pure". As an alternative expression for the macroscopic single-enantiomeric composition the conceptual term *unichiral* has been proposed by Gal [63].

Optical purity op should only be referred to when non-chiroptical methods are not available for the quantitation of a mixture of enantiomers. The origin and reliability of $[\alpha]_{max}$, used for the calculation of op, should always be quoted.

Clearly, the prefix *optical* should never be used in connection with nonchiroptical methods (Sect. 2.1) and expressions such as *optical purity determination by NMR* or *optical resolution by chromatography* should be avoided.

Unfortunately, little attention has been focused in the literature on the nature and range of errors involved in the quantitation of a mixture of enantiomers. It is interesting to scrutinize how precision and accuracy will affect the definitions discussed herein. For example, ee is sensitive to an error in the percentage of the enantiomers, i.e., % (E_1:E_2 = 52 ± 1:48 ± 1) → % ee = 4 ± 2 [9]. De Geus et al. argue that relative standard deviations (RSD) derived from EF (ec)-based calculations are rendered only half as large as those obtained from er calculations [19]. Moreover, when for example a duplicate measurement is performed and the areas (in arbitrary units) are 12.5 and 10.0 in the first run, and 10.0 and 12.5 in the second, ERs of 12.5 and 0.80 results with the mean value of 1.02 instead of 1.00. The EFs calculated to 61% and 39% afford the correct mean value of 50% [19]. Applying parametric summary statistics, such as mean and standard deviation, to EF data is more appropriate because its additive scale provides data which are more symmetric than those obtained using the ER scale [19, 54].

5 Diastereomers

In analogy to the definitions for a mixture of enantiomers, the *diastereomeric excess* de:

$$\text{de} = D_1 - D_2/D_1 + D_2 \tag{32}$$

or the *diastereomeric ratio* dr (or q): [8]

$$\text{dr} = D_1/D_2 \tag{33}$$

have been used for the quantitation of a mixture of diastereomers in the case that only two isomers D_1 and D_2 are involved (this applies for epimers, anomers, and geometrical (*cis,trans*/*E,Z*/*syn,anti*/*endo,exo*)-isomers) where D_1 is the major diastereomer. Complications arise with the occurrence of stereoisomerism due to the presence of multiple stereogenic elements. Two distinct stereogenic elements in a molecule give rise to two diastereomers each forming a pair of enantiomers. When the stereoisomers are chiral and nonracemic, the definitions de and dr do not, a priori, differentiate between the proportions of the enantiomers, but treat them as the sum, i.e., $D_1 = E_1 + E_2$. Therefore, unless the proportions of all stereoisomers are preferably given as a percentage or as mole fraction, the mixture of enantiomers of each of the diastereomers must be quantified separately by ee or er.

Whereas dr is measured by spectroscopy or chromatography of diastereomers in an achiral environment, dr and er can be obtained simultaneously by employing enantioselective methods with appropriate chiral selectors.

When more than two diastereomers are involved, the term diastereoselectivity ds has been suggested as the mole fraction of diastereomer D_1 in a mixture of all diastereomers $\sum D_i$ [64]. In analogy to ec, this term is called *diastereomeric composition* dc

$$\text{dc} = x_{D1} = D_1/\Sigma D_i \tag{34}$$

The mole fraction of the major enantiomer x_{E1} of a chiral diastereomer D_i in a mixture of two or more diastereomers is given by

$$x^i_{E1} = \text{ec}^i \cdot \text{dc}^i. \tag{35}$$

The terms for diastereomers present in a mixture are summarized as follows:[9]

ee = enantiomeric excess
er = enantiomeric ratio
ec = enantiomeric composition
de = diastereomeric excess (for $\sum D_i = 2$)
dr = diastereomeric ratio (for $\sum D_i = 2$)
dc = diastereomeric composition (for $\sum D_i = 2$)

6 Recommendations for the Quantitation of a Mixture of Diastereomers

The use of the term *diastereomeric excess* % de is discouraged except for selected applications (see below). Seebach et al. argue that the commonly used % de is not a useful number because it is applicable to mixtures of two and only two diastereomers and because one has to convert it back to a diastereomeric ratio dr to arrive at a meaningful number (footnote 13 in [64]).

The term *diastereomeric ratio* dr or ln dr is useful for the quantitation of a mixture of two achiral or of two chiral (either racemic or enantiopure) diastereomers. When two or more chiral and nonracemic diastereomers *i* are present in a mixture, the proportions of the major diastereomer and major enantiomer are quantified by dc^i and ec^i. When all stereoisomers, i.e., diastereomers and enantiomers, are considered, their proportions are best quoted as mole fractions or percentages.

When the enantiomeric excess of a substrate $ee_{substrate}$ is determined via formation of diastereomers by achiral NMR spectroscopy or achiral chromatography the measured diastereomeric excess $de_{measured}$ must be corrected for the ee_{aux} of the auxiliary in case it is not enantiomerically pure [65]:

$$ee_{substrate} = de_{measured}/ee_{aux}. \tag{36}$$

Consider a substrate consisting of 90% E_1 and 10% E_2 ($ee_{substrate} = 0.80$) which is reacted with an auxiliary consisting of 95% E'_1 and 5% E'_2 ($ee_{aux} = 0.90$). Following quantitative derivatization four stereoisomers are present: $E_1E'_1 = 85.5\%$, $E_1E'_2 = 4.5\%$, $E_2E'_1 = 9.5\%$, and $E_2E'_2 = 0.5\%$. The mixture renders two signals or peaks of the diastereomers $E_1E'_1$ and $E_2E'_2$ (enantiomeric pair 1) and $E_1E'_2$ and $E_2E'_1$ (enantiomeric pair 2) with the proportion 86.0% and 14.0%, respectively, with $de_{measured} = 0.72$. The data is compatible with (36).

References

1. Eliel EL, Wilen SH, Mander LN (1994) Stereochemistry of organic compounds: determination of enantiomer and diastereomer composition. Wiley Interscience, New York, pp 214–295, Chapter 6 and 5
2. Koppenhoefer B, Muschalek V, Hummel M, Bayer E (1989) Determination of the enhancement of the enantiomeric purity during recrystallization of amino acids. J Chromatogr 477:139–145
3. Reiner C, Nicholson GJ, Nagel U, Schurig V (2007) Evaluation of enantioselective gas chromatography for the determination of minute deviations from racemic composition of α-amino acids with emphasis on tyrosine: accuracy and precision of the method. Chirality 19:401–414
4. Raban M, Mislow K (1967) Modern methods for the determination of optical purity. Top Stereochem 2:199–230
5. Morrison JD, Mosher HS (1971) Asymmetric organic reactions. Prentice Hall, Eaglewood Cliffs

6. Orchin M, Kaplan F, Macomber RS, Wilson RM, Zimmer H (1980) The vocabulary of organic chemistry. Wiley, New York, p 130
7. Schurig V (1985) Current methods for the determination of enantiomeric compositions (part 1): definitions, polarimetry. Kontakte (Darmstadt) 1:54–60
8. Kagan HB (1995) Is there a preferred expression for the composition of enantiomers? Recueil Trav Chim Pays-Bas 114(4–5):203–205
9. Schurig V (1996) Terms for the quantitation of a mixture of stereoisomers. Enantiomer 1(2):139–143
10. http://en.wikipedia.org/wiki/Enantiomeric_excess
11. Gawley RE (2005) Do the terms "% ee" and "% de" make sense as expressions of stereoisomer composition or stereoselectivity? J Org Chem 71:2411–2416
12. Schurig V, Lindner W (1995) Determination of enantiomeric purity by direct methods. In: Helmchen G, Hoffmann RW, Mulzer J, Schaumann E (eds) Stereoselective synthesis, vol E 21a, Houben-Weyl, methods of organic chemistry. Thieme, Stuttgart, New York, pp 147–192 (V.S.) & pp. 193–224 (W.L.)
13. Eliel EL, Wilen SH, Mander LN (1994) Stereochemistry of organic compounds. Wiley Interscience, New York, pp 1197–1198
14. Brewster JH (1992) Racemic, scalemic, holemic. Chem Eng News 70(2):3 (May 18)
15. Rautenstrauch V, Lindström M, Bourdin B, Currie J, Oliveros E (1993) Enantiomeric purities of (R)-camphors and (S)-camphors from the chiral pool and high enantiomeric purities in general. Helv Chim Acta 76(1):607–615
16. Rautenstrauch V, Mégard P, Bourdin B, Furrer A (1992) Treating the camphors with potassium in liquid-ammonia leads to a double Horeau duplication. J Am Chem Soc 114(4):1418–1428
17. Wistuba D, Nowotny H-P, Träger O, Schurig V (1989) Cytochrome P-450-catalyzed asymmetric epoxidation of simple prochiral and chiral aliphatic alkenes: species dependence and effect of enzyme induction on enantioselective oxirane formation. Chirality 1:127–136
18. Harner T, Wiberg K, Norstrom R (2000) Enantiomer fractions are preferred to enantiomer ratios for describing chiral signatures in environmental analysis. Environ Sci Technol 34(1):218–220
19. De Geus HJ, Wester PG, de Boer J, Brinkman UAT (2000) Enantiomer fractions instead of enantiomer ratios. Chemosphere 41(5):725–727
20. Hashim NH, Shafie S, Khan SJ (2010) Enantiomeric fraction as an indicator of pharmaceutical biotransformation during wastewater treatment and in the environment – a review. Environ Technol 31(12):1349–1370
21. Selke R, Facklam C, Foken H, Heller D (1993) Application of the term "relative enantioselectivity" as useful measure for comparison of chiral catalysts, demonstrated on asymmetric hydrogenation of amino acid precursors. Tetrahedr Asymm 4(3):369–382
22. Selke R (1997) Importance of the term "enantiomeric ratio" for comparison of chiral catalysts in prochiral substrate reactions. Enantiomer 2(5):415–419
23. Seebach D, Beck AK, Schmidt B, Wang YM (1994) Enantioselective and diastereoselective titanium-taddolate catalyzed addition of diethyl and bis(3-buten-1-yl) zinc to aldehydes – a full account with preparative details. Tetrahedron 50(15):4363–4384
24. Rautenstrauch V (1994) The 2 expressions of the Horeau principle, *n*th-order Horeau amplifications, and scales for the resulting very high enantiopurities. Bull Soc Chim Fr 131(5):515–524
25. Glausch A, Hahn J, Schurig V (1995) Enantioselective determination of chiral 2,2′,3,3′,4,6′-hexachloro-biphenyl (PCB 132) in human milk samples by multidimensional gas chromatography/electron capture detection and by mass spectrometry. Chemosphere 30:2079–2085
26. Faber K (1997) The "enantiomeric ratio" – beware of confusion! Enantiomer 2(5):411–414
27. Chen C-S, Fujimoto Y, Girdaukas G, Sih CJ (1982) Quantitative analyses of biochemical kinetic resolutions of enantiomers. J Am Chem Soc 104(25):7294–7299
28. Sih CJ, Wu S-H (1989) Resolution of enantiomers via biocatalysis. Top Stereochem 19:63–125

29. Bornscheuer UT, Kazlaukas RJ (1999) Hydrolases in organic synthesis. Wiley-VCH, Weinheim
30. Kagan HB, Fiaud JC (1988) Kinetic resolution. Top Stereochem 18:249–330
31. Rakels JLL, Straathof AJJ, Heijnen JJ (1993) A simple method to determine the enantiomeric ratio in enantioselective biocatalysis. Enyzme Microb Technol 15(12):1051–1056
32. Ghanem A, Schurig V (2003) Lipase-catalyzed access to enantiomerically pure (*R*)- and (*S*)-*trans*-4-phenyl-3-butene-2-ol. Tetrahedr Asymm 14:57–62
33. Gal J (2007) Carl Friedrich Naumann and the introduction of enantio terminology: a review and analysis on the 150th anniversary. Chirality 19(2):89–98
34. Lehmann FPA, Rodrigues De Miranda JF, Ariëns EJ (1976) Stereoselectivity and affinity in molecular pharmacology. In: Jucker E (ed) Progress research, vol 20. Birkhäuser, Basel, pp 101–142
35. Zeller EA, Banerjee R (1963) Eutopic and dystopic complexes of bovine lens amino peptidase. Invest Ophthalmol 2(5):519–519
36. Ariëns EJ (1984) Stereochemistry, a basis for sophisticated nonsense in pharmacokinetics and clinical pharmacology. Eur J Clin Pharmacol 26(6):663–668
37. Pfeiffer CC (1956) Optical isomerism and pharmacological action, a generalization. Science 124(3210):29–31
38. Rochat B, Amey M, Van Gelderen H, Testa P, Baumann P (1995) Determination of the enantiomers of citalopram, its demethylated and propionic-acid metabolites in human plasma by chiral HPLC. Chirality 7(6):389–395
39. Lyle GG, Lyle RE (1983) Polarimetry. In: Morrison JD (ed) Asymmetric synthesis, vol I, Analytical methods. Academic, New York, pp 13–27
40. Horeau A (1969) Interactions d'enantiomeres en solution; influence sur le pouvoir rotatoire: purete optique et purete enantiomerique. Tetrahedr Lett 10(36):3121–3124
41. Brown HC, Ayyangar NR, Zweifel G (1964) Hydroboration. XVIII. The reaction of diisopinocampheylborane with representative cis-acyclic, cyclic, and bicyclic olefins. A convenient synthesis of optically active alcohols and olefins of high optical purity and established configuration. J Am Chem Soc 86(3):397–403
42. Brewster H (1959) The optical activity of endocyclic olefins. J Am Chem Soc 81(20):5493–5500
43. Schurig V, Gil-Av E (1976/1977) Chromatographic resolution of chiral olefins. Specific rotation of 3-methylcyclopentene and related compounds. Israel J Chem 15:96–98
44. Consiglio G, Pino P, Flowers LI, Pittman CU (1983) Asymmetric hydroformylation of styrene by chiral platinum catalysts: a re-evaluation of the optical yields. J Chem Soc Chem Commun: 612–613
45. Edwards D, Cooper K, Dougherty RC (1980) Asymmetric synthesis in a confined vortex: gravitational fields can cause asymmetric synthesis. J Am Chem Soc 102(1):381–382 & 7618
46. Mead CA, Moscowitz A (1980) Some comments on the possibility of achieving asymmetric synthesis from achiral reactants in a rotating vessel. J Am Chem Soc 102(24):7301–7302
47. Schurig V (1995) Determination of enantiomeric purity by direct methods. In: Helmchen G, Hoffmann RW, Mulzer J, Schaumann E (eds) Stereoselective synthesis, vol E 21a, Houben-Weyl, methods of organic chemistry. Thieme, Stuttgart, New York, p 157, Chapter 3.1.3.7
48. Beitler U, Feibush B (1976) Interaction between asymmetric solutes and solvents: diamides derived from L-valine as stationary phases in gas–liquid partition chromatography. J Chromatogr 123(1):149–166
49. Schurig V, Bürkle W, Hintzer K, Weber R (1989) Evaluation of nickel(II) bis[α-(heptafluorobutanoyl)-terpeneketonates] as chiral stationary phases for the enantiomer separation of alkyl-substituted cyclic ethers by complexation chromatography. J Chromatogr 475:23–44
50. Levkin PA, Schurig V (2008) Apparent and true enantioselectivity of single- and binary-selector chiral stationary phases in gas chromatography. J Chromatogr A 1184(1–2):309–322

51. Pirkle WH, Welch CJ (1996) Some thoughts on the coupling of dissimilar chiral columns or the mixing of chiral stationary phases for the separation of enantiomers. J Chromatogr 731 (1–2):23–44
52. Schurig V (2009) Elaborate treatment of retention in chemoselective chromatography – retention increment approach and non-linear effects. J Chromatogr A 1216(10):1723–1736
53. Levkin PA, Maier NM, Schurig V, Lindner W (2010) Strong detrimental effect of a minute enantiomeric impurity of a chiral selector on the enantioselectivity factor. Angew Chem Int Ed 49(42):7742–7744
54. Ulrich EM, Helsel DR, Foreman WT (2003) Complications with using ratios for environmental data: comparing enantiomeric ratios (ERs) and enantiomeric fractions (EFs). Chemosphere 53(5):531–538
55. Frank H, Nicholson GJ, Bayer E (1978) Enantiomer labelling, a method for the quantitative analysis of amino acids. J Chromatogr 167:187–196
56. Vetter W, Schurig V (1997) Enantioselective determination of chiral organochlorine compounds in biota by gas chromatography on modified cyclodextrins. J Chromatogr A 774:143–175
57. Gil-Av E, Schurig V (1994) Resolution of non-racemic mixtures in achiral chromatographic systems: a model for the enantioselective effects observed. J Chromatogr A 666:519–525
58. Eliel EL, Wilen SH (1990) Misuse of homochiral. Chem Eng News 68(3):2 (September 10)
59. Ruch E (1972) Algebraic aspects of the chirality phenomenon in chemistry. Acc Chem Res 5(2):49–56
60. Schurig V (1977) Internal vs. external diastereotopism in homochiral *cis* vs. *trans* olefin metal π complexes. Tetrahedr Lett 18(45):3977–3980
61. Schurig V (1984) Stereoheterotopicity and stereoisomerism in heterochiral *cis* vs. *trans* olefin metal π complexes. Tetrahedr Lett 25(26):2739–2742
62. Eliel EL, Wilen SH, Mander LN (1994) Stereochemistry of organic compounds. Wiley Interscience, New York, p 215
63. Gal J (1998) Problems of stereochemical nomenclature and terminology. 1. The *homochiral* controversy. Its nature and origins, and a proposed solution. Enantiomer 3(3):263–273
64. Thaisrivongs S, Seebach D (1983) Diastereoselective benzyloxymercuration/demercuration of derivatives of γ-alkyl-δ-hydroxy-α, β-unsaturated esters. A new strategy for the synthesis of aldol-type products. J Am Chem Soc 105(25):7407–7413
65. Cawley A, Duxbury JP, Kee TP (1998) NMR determination of enantiopurity via chiral derivatisation. Tetrahedr Asymm 9:1947–1949

Top Curr Chem (2013) 340: 41–72
DOI: 10.1007/128_2013_439

Published online: 11 May 2013

Enantiomeric Differentiation by Synthetic Helical Polymers

Eiji Yashima, Hiroki Iida, and Yoshio Okamoto

Abstract Recent advances in the synthesis of helical polymers and their applications as chiral materials, in particular chiral stationary phases (CSPs), for high-performance liquid chromatography (HPLC) are reviewed with an emphasis on the key role of the helical conformations with one-handedness for the prominent chiral recognition of enantiomers. The historical background of artificial optically active helical polymers is also briefly described.

Keywords Chiral recognition · Chiral stationary phase · Enantioseparation · Helical macromolecules · Helix

Contents

E. Yashima (✉) and H. Iida
Department of Molecular Design and Engineering, Graduate School of Engineering, Nagoya University, Furo-cho, Chikusa-ku, Nagoya 464-8603, Japan
e-mail: yashima@apchem.nagoya-u.ac.jp

Y. Okamoto
Polymer Materials Research Center, College of Materials Science and Chemical Engineering, Harbin Engineering University, Harbin 150001, China

Nagoya University, Furo-cho, Chikusa-ku, Nagoya 464-8603, Japan

1 Introduction

Who prepared helical polymers for the first time? It may be a difficult question, but it may not be emphasized enough that in 1955 Natta discovered the isotactic polypropylene that formed a helical structure in the crystalline state when polymerized using the Ziegler–Natta catalyst [1]. Although the helical conformation of the polypropylene consists of a mixture of right- and left-handed helices and changes into a random conformation once dissolved in solvents due to the insufficient steric requirement of the side groups, this finding was a significant milestone, through which remarkable progress has been achieved in the field of synthetic helical polymers during the past three decades. At that time, however, there was almost no prospect for applications of these helical polymers.

The first innovative research was reported in 1979 [2]; Okamoto et al. developed a helical polymethacrylate synthesized by helix-sense-selective polymerization using an optically active initiator that showed an excellent chiral recognition ability for aromatic racemic compounds when used as a chiral stationary phase (CSP) for high-performance liquid chromatography (HPLC). Bulky ester groups introduced at the side groups force the polymer to maintain its helical conformation in solution. Since then, a number of optically active helical polymers have been prepared and applied as CSPs for HPLC. Importantly, prior to this discovery, Blaschke et al. prepared optically active polyacrylamides and polymethacrylamides by the radical polymerization of the corresponding monomers with chiral pendants, which resolved many racemates, particularly chiral drugs, in liquid chromatography (LC) to reveal the differences in the pharmacological and physiological behaviors of both drug enantiomers [3]. These results will be described in more detail below.

Nowadays it is recognized that thorough investigations of such pharmacological and physiological actions of both enantiomers of chiral drugs are essential before being commercialized. The separation of enantiomers using CSPs by HPLC is of key importance for determining their enantiomeric excess (ee) and also for obtaining pure enantiomers on analytical and industrial scales [4–14]. At present, many CSPs for HPLC that are commercially available involve small chiral molecule-based CSPs [15–20] and chiral polymer-based CSPs derived from polysaccharides [21–28], proteins [29–31], and synthetic helical polymers [3, 32, 33]. Among them, the helical polymer-based CSPs, particularly CSPs composed of synthetic helical polymers with a controlled helical sense, and cellulose and amylose derivatives [21–28], are particularly interesting because their chiral recognition abilities are dependent on their highly-ordered helical structures that are responsible for their powerful resolving abilities. Therefore, in this chapter we focus on the recent advances in the synthesis of helical polymers and their applications, mainly as CSPs for HPLC.

Synthetic Helical Polymers

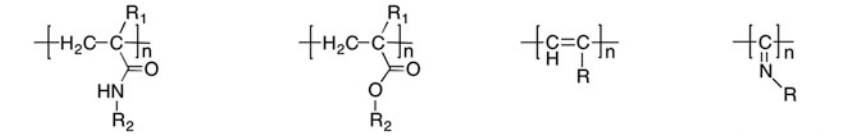

Natural Helical Polymers and Their Derivatives

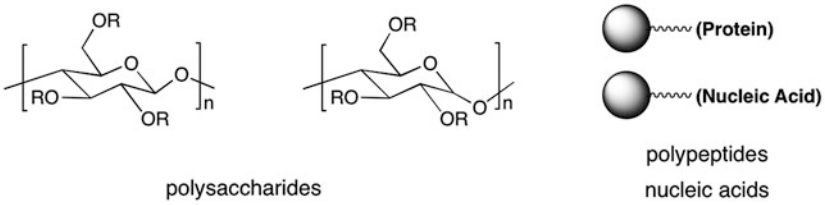

2 Chiral Recognition by Synthetic Helical Polymers

2.1 Poly(meth)acrylamides

Before the 1980s, Blaschke and coworkers systematically synthesized a series of optically active polyacrylamides and polymethacrylamides (**1**–**4**) by radical polymerization of the corresponding monomers, and investigated their chiral recognition abilities as CSPs for LC [3]. In those days, the chirality of drugs was often neglected, and many chiral drugs were put on the market as racemates. Blaschke et al. successfully resolved many chiral pharmaceutical compounds using optically active polyacrylamide gels on a preparative scale and investigated the differences in the pharmacological behaviors between the enantiomers. For example, (±)-thalidomide (**6**), which had been used as a hypnotic and sedative drug and caused a terrible tragedy due to its potent teratogenicity, was for the first time completely resolved into its enantiomers using their CSPs including **2** (Fig. 1). They reported that the teratogenic action was caused only by the *S* enantiomer, whereas the *R* enantiomer did not show any teratogenic behavior, even at high doses [34]. Although this result stirred controversy arising from the fact that each enantiomer readily racemizes at physiological pH or after injection into rabbits [35, 36], this study is of key importance even now, since legislative authorities have now recognized the importance of evaluating the different pharmacological behaviors of both enantiomers of a drug before marketing. Up to now, diverse optically active poly(meth)acrylamides involving **1**–**5** have been prepared for the development of more efficient CSPs with wide applicability. For example, **3** could resolve various racemates, such as **7**–**9**, and has been

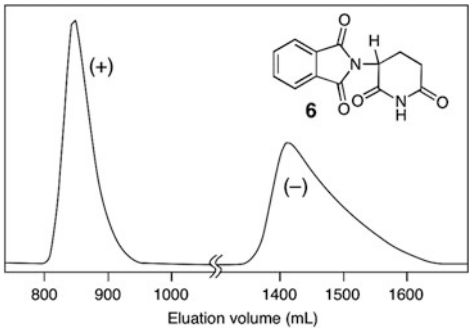

Fig. 1 Chromatographic resolution of **6** on **2**. Eluent: benzene/dioxane (8/2, v/v). (Reproduced with permission from [3]. Copyright 1980 Wiley-VCH)

commercialized under the trade name of Chiraspher (Merck) [37]. The structures of polymethacrylamides used as chiral packing materials remain unknown because most of the polymers were prepared by radical polymerization, thus mostly producing atactic polymers. However, Blaschke et al. found that the chiral recognition abilities of polymethacrylamides depend on the synthetic route. The polymers prepared by radical polymerization of the corresponding optically active methacrylamides showed much better chiral recognition than those prepared from poly(acryloyl chloride) followed by the reaction with chiral amines [3]. These results suggest that chiral recognition sites in the CSPs derived from the polymethacrylamides may be kinetically produced, implying a possible higher order structure, such as a helical conformation in part induced by the optically active pendant groups that may be formed during the polymerization process. Interestingly, it was also reported that the tacticity of polymethacrylamides is an important factor for their chiral recognition abilities [38].

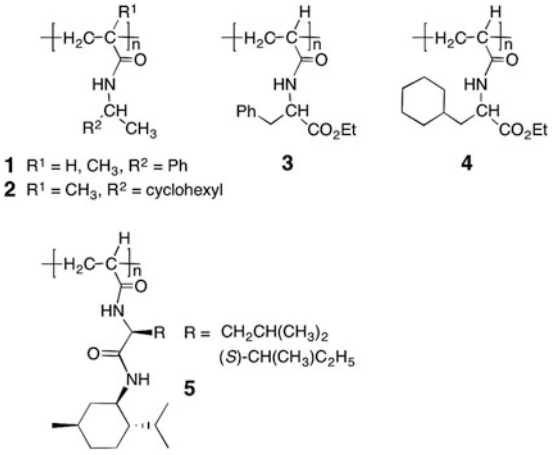

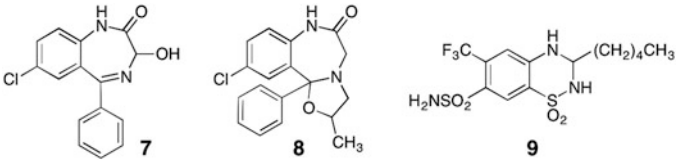

Poly(*N*-substituted maleimide)s bearing various optically active pendant groups, such as **10** and **11**, prepared by the anionic polymerization of the corresponding monomers with chiral catalysts or initiators often showed a relatively high optical rotation, probably due to a helical conformation with a preferential helical sense [39–42]. However, there is another possibility to explain the optical activity of the poly(*N*-substituted maleimide)s. In contrast to vinyl polymers prepared from 1-substituted and 1,1-disubstituted vinyl monomers, including poly(meth)acrylamides and polymethacrylates, poly(maleimide)s can be optically active due to truly chiral stereogenic centers in the main-chain when the polymerization produces one of two enantiomeric *trans* structures (**10** and **11**). The vinyl polymers, even if they possess highly stereoregular isotactic or syndiotactic structures, whose stereogenic centers in the main-chain are pseudoasymmetric because the whole polymer chain has a mirror plane, are optically inactive. The poly(*N*-substituted maleimide)s involving **11** were able to resolve enantiomers, such as 1,1′-bi-2-naphthol, when used as an HPLC packing material that was also commercialized.

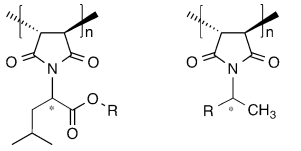

2.2 Polymethacrylates

Polymethacrylates with a one-handed helical structure belong to an important class of polymer-based CSPs. Okamoto et al. prepared the first helical vinyl polymer by helix-sense-selective polymerization of an achiral (prochiral) bulky methacrylate, i.e., triphenylmethyl methacrylate (TrMA), using chiral anionic initiators, such as *N,N*′-diphenylethylenediamine monolithium amide (DPEDA-Li) complexed with chiral ligands, such as (+)-2,3-dimethoxy-1,4-bis(dimethylamino) butane (DDB), giving a single-handed, fully isotactic helical polymer with a high optical rotation (PTrMA) (Fig. 2a) [2, 43]. The chiral ligand coordinating to the living propagating polymer end controls the main-chain configuration as well as the helical sense of the entire polymer chain, resulting from the bulky triphenylmethyl groups that

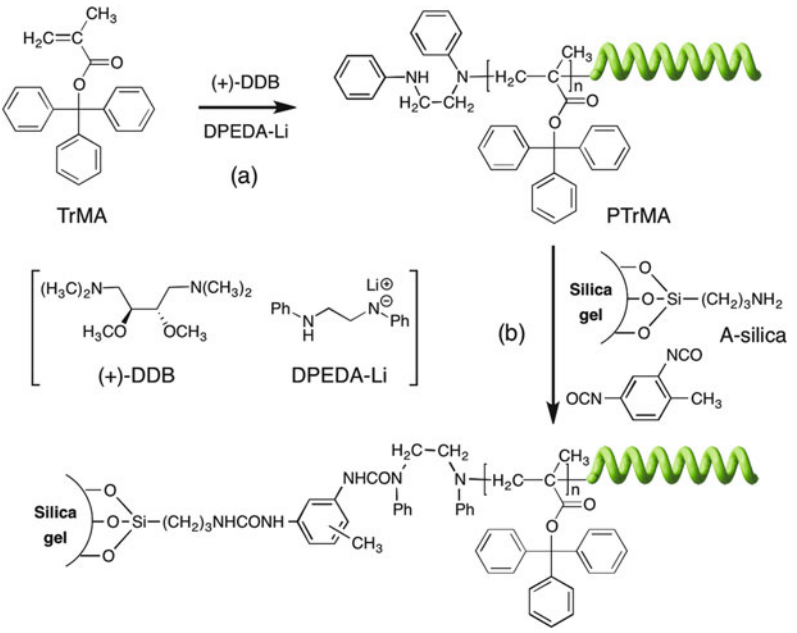

Fig. 2 (**a**) Helix-sense-selective polymerization of TrMA using chiral anionic initiators. (**b**) Preparation of PTrMA-immobilized CSP using A-silica and toluen-2,4-diyldiisocyanate

prevent the polymer from unfolding or racemization of the helical conformation kinetically formed during the polymerization process. The optically active helical PTrMA showed an excellent chiral recognition for a variety of racemic compounds when coated on a macroporous silica gel and used as a CSP for HPLC [44], and the PTrMA-based CSP has been commercialized (CHIRALPAK OT(+)). In particular, the PTrMA-based CSP is useful for the enantiomeric differentiation of stereochemically interesting aromatic racemates [45] including **12**–**18** [46–52], which are difficult to resolve by other CSPs or conventional methods. Polar eluents, such as methanol and a methanol–water mixture, are often used for better resolution, indicating that hydrophobic interactions between nonpolar groups of a solute and the side groups (triphenylmethyl groups) of PTrMA play an important role. It has been proposed that the triphenylmethyl pendant groups take a propeller-like chiral structure along the helically twisted polymer main-chain, which contributes to its quite high chiral recognition [53].

Figure 3 shows a chromatogram of the resolution of racemic 1,1′-bi-2-naphthol (**19**) on PTrMA, where the (+)-enantiomer elutes first, followed by the (−)-enantiomer at retention times of t_1 and t_2, respectively, showing complete baseline separation [44]. The results of the chromatographic differentiation of enantiomers can be evaluated using the following three parameters: retention factor k_1' [$= (t_1 - t_0)/t_0$], separation factor α [$= (t_2 - t_0)/(t_1 - t_0)$], and resolution factor R_S [$= 2(t_2 - t_1)/(w_1 + w_2)$], where t_0 is the dead time (retention time of a non-retained compound),

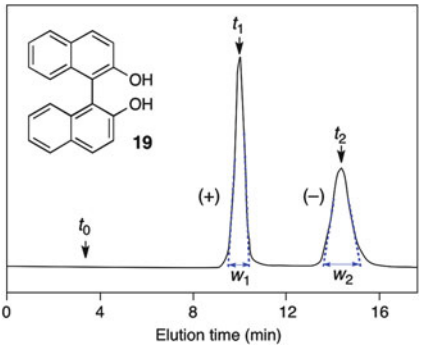

Fig. 3 Chromatographic resolution of **19** on PTrMA. Eluent: methanol. (Reproduced with permission from [44]. Copyright 1981 American Chemical Society)

and w_1 and w_2 are the bandwidths of the peaks. For a chromatographic enantioseparation, α is directly related to the chiral recognition ability of a CSP, and R_S reflects both the chiral recognition ability of a CSP and the column efficiency (theoretical plate number).

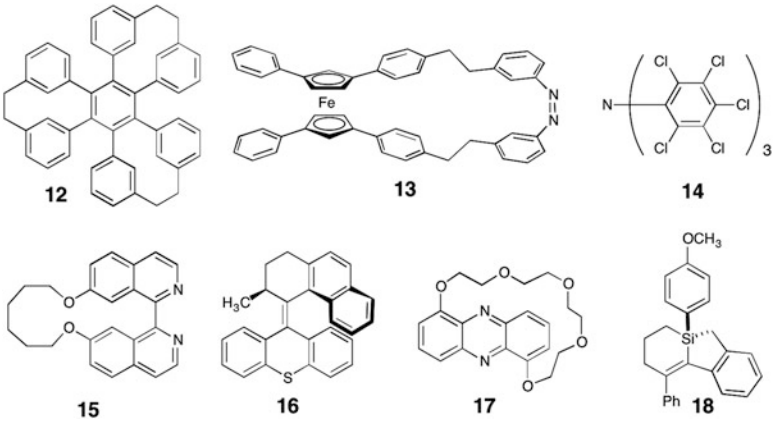

PTrMA is among the popular chiral polymer-based CSPs, but has a drawback that the triphenylmethyl ester groups are slowly solvolyzed in methanol when used as an eluent during HPLC separation, and the polymer gradually loses its helical conformation, resulting in a loss of its chiral recognition ability. Therefore, a one-handed helical PD2PyMA bearing diphenylpyridylmethyl groups as the pendants was prepared by the helix-sense-selective anionic polymerization to improve its durability, since the corresponding monomer is more robust against solvolysis than TrMA, providing a more practically useful CSP. In fact, the methanolysis of PD2PyMA-coated silica gel in methanol at 60°C was 16-fold slower than that of the PTrMA-coated one [54]. The PD2PyMA-based CSP exhibited a slightly lower resolution ability than that of the PTrMA-based CSP under the same chromatographic conditions, but several 1,1′-bi-2-naphthyl derivatives were better resolved on PD2PyMA than PTrMA [54].

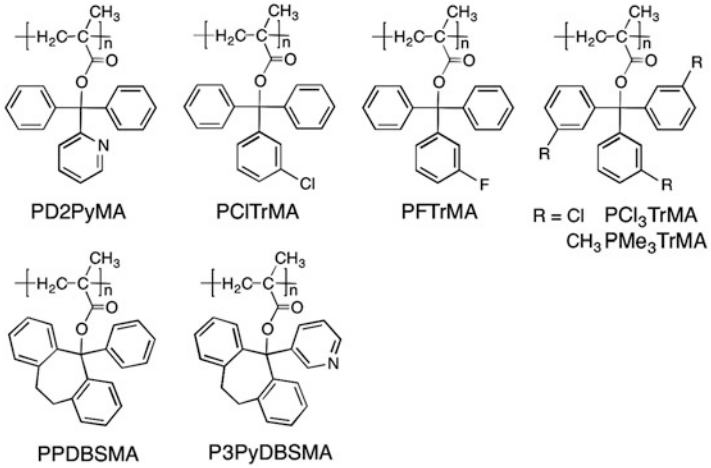

The related meta-halogen- and methyl-substituted optically active PTrMA-derivatives were also prepared and their chiral recognition abilities as CSPs were investigated [55, 56]. The chiral recognition abilities of PClTrMA and PFTrMA were slightly low in comparison to that of PTrMA, and PCl_3TrMA exhibited almost no resolving ability, although introduction of the electron-withdrawing halogen groups on the triphenylmethyl pendants makes the PTrMA derivatives robust against solvolysis of the ester groups. PMe_3TrMA also possessed a high chiral recognition ability, resolving some racemates more efficiently than PTrMA, but the introduction of such an electron-donating methyl group caused a decrease in durability. PPDBSMA and P3PyDBSMA bearing a dibenzosuberyl group as the pendant also had a higher durability against solvolysis compared to PTrMA, but their chiral recognition abilities were rather low [57].

Optically active PTrMA chemically bonded to silica gel was also prepared by the reaction of PTrMA bearing one DPEDA-derived $PhNHCH_2CH_2$- terminal group with 3-aminopropyl-silanized silica gel (A-silica) that were cross-linked using toluen-2,4-diyldiisocyanate (Fig. 2b). The resulting PTrMA-immobilized CSP exhibited a chiral recognition ability similar to that of the corresponding coated-type CSP when methanol was used as an eluent. Interestingly, the chemically bonded CSP partially resolved the racemic helical polymers composed of an equimolar mixture of right- and left-handed helices, such as PTrMA [58], PD2PyMA [59], and PPDBSMA [60], into the enantiomers with a single-handed helical conformation as shown in Fig. 4.

A unique approach to create a chiral cavity using helical polymers as a template has been reported based on a molecular imprinting method. Optically active single-handed helical P3PyDBSMA was used as a template and further cross-linked by radical copolymerization to produce a gel (Fig. 5) [61]. After removal of the template, the gel maintained its optical activity and preferentially adsorbed the P3PyDBSMA with the same helical sense used as the template. The gel also could recognize the chirality for some racemates, such as *trans*-stilbene oxide, and enantioselectively adsorbed one of the enantiomers, whereas the gel showed no

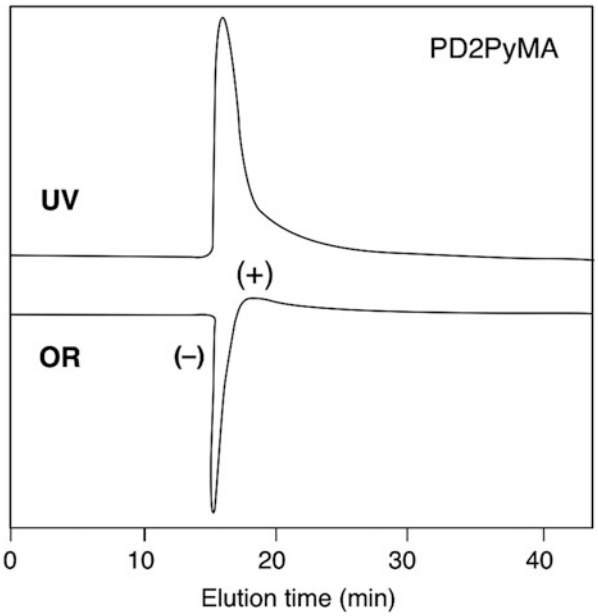

Fig. 4 Chromatographic resolution of racemic PD2PyMA on PTrMA. Eluent: $CHCl_3$. (Reproduced with permission from [59]. Copyright 1989 American Chemical Society)

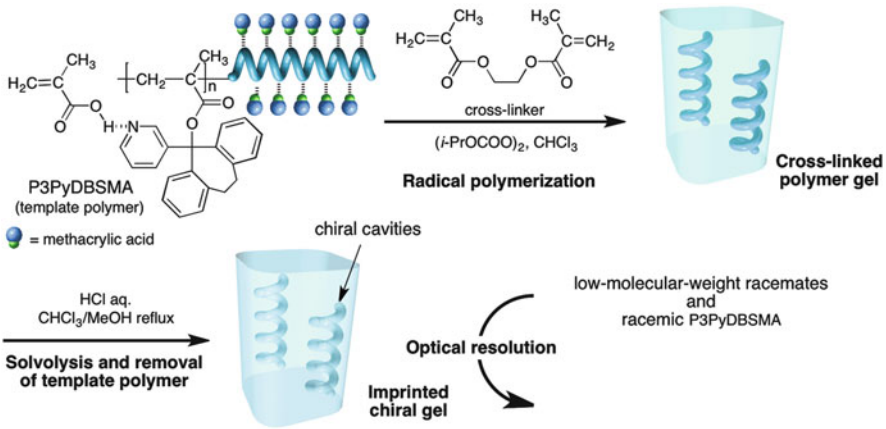

Fig. 5 Schematic illustrations of the chiral gel synthesis by a molecular imprinting method using a single-handed helical P3PyDBSMA as a template. After cross-linking of methacrylic acid using a cross-linker, P3PyDBSMA is removed to produce an imprinted chiral gel

chiral recognition toward *trans*-stilbene oxide before removal of the template, suggesting that the helical structure of the template is indeed "imprinted" [62, 63] in the gel and the observed resolution is most likely based on the chiral cavity imprinted in the gel.

2.3 Polyacetylenes

Since 1967, a large number of helical polyacetylenes with optical activities mediated by the enantiomerically pure pendants has been prepared mostly by the transition metal-catalyzed polymerization of optically active acetylenes. Among them, phenylacetylenes bearing enantiomerically pure pendant groups have the ability to be designed and synthesized, and readily polymerize using a rhodium catalyst, giving stereoregular (*cis-transoidal*) high molecular weight poly (phenylacetylene)s with an excess of a one-handed helical sense [64–68]. An optically active poly(phenylacetylene) bearing (*R*)-phenylethylcarbamoyl pendant groups **20a** was the first helical polyacetylene to have its chiral recognition ability evaluated as a CSP for HPLC after coating on a macroporous silica gel. The CSP efficiently resolved several racemates [69]. The precise control of the main-chain stereoregularity is essential for induction of a preferred-handed helical conformation and the resulting chiral recognition as well. This was revealed by the fact that a stereoirregular poly(phenylacetylene) with a chemical structure identical to **20a**, prepared by a different synthetic route, exhibited poor chiral recognition. A similar, but chemically bonded-type CSP **21** has also been prepared by the copolymerization of the corresponding chiral monomer with a rhodium catalyst in the presence of silica gel with phenylacetylene residues chemically bonded on a silica surface. The CSP completely resolved several racemates, including **23** (Fig. 6) [70]. Both the chemically and physically immobilized CSPs derived from **20b** also showed relatively high and similar chiral recognition ability to each other.

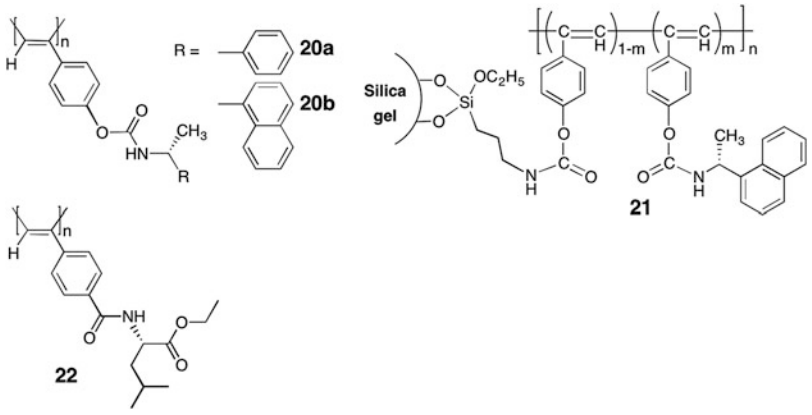

Cinchona alkaloids are naturally-occurring optically active compounds each consisting of two pseudoenantiomeric forms (diastereomers), such as cinchonidine (**Cd**)/cinchonine (**Cn**) and quinine (**Qn**)/quinidine (**Qd**). They have been extensively used not only as versatile chiral organocatalysts [71, 72] but also as CSPs after modification and being chemically bonded to silica gel. The cinchona alkaloid-derived CSPs showed powerful chiral recognition abilities for acidic racemates

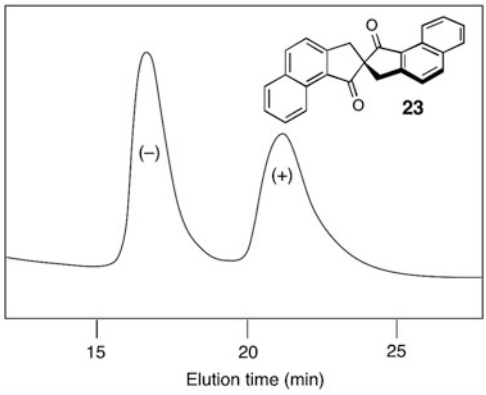

Fig. 6 Chromatographic resolution of **23** on **21**. Eluent: methanol. (Reproduced with permission from [70]. Copyright 1996 The Polymer Society of Korea)

under anion-exchange HPLC conditions [19], and some of them have been commercialized. A series of optically active helical poly(phenylacetylene)s bearing amino-functionalized cinchona alkaloid pendant groups connecting to the phenyl rings through an amide linkage were prepared with the expectation that the cinchona alkaloid pendants are capable of inducing a one-handed helical conformation of the polymers (Fig. 7a), so that the enantioselectivities would be further enhanced as compared to those of the cinchona alkaloids when used as chiral organocatalysts [73] and CSPs. The polymers were coated on a macroporous silica gel to obtain novel CSPs [74]. The circular dichroism (CD) spectral patterns between poly-**ACd** and poly-**ACn** (Fig. 7b) and also poly-**AQn** and poly-**AQd** were almost mirror images of each other due to their pseudoenantiomeric relationships, suggesting an opposite helical sense induced by the amide-linked cinchona alkaloid pendants. These helical polymers could resolve various racemic compounds into enantiomers including alcohols, diols, metal tris(acetylacetonato)s, and *N*-Boc-amino acids; in particular, poly-**ACd** and poly-**ACn** exhibited excellent chiral recognition abilities for the tested racemates (Fig. 8a). The reversed elution order was observed for racemates resolved on the pseudoenantiomeric poly-**ACd** and poly-**ACn** (Fig. 7c,d). In order to confirm the importance of the macromolecular helicity on the chiral recognition, *trans*-enriched poly-**ACn** (poly-**ACn′**) was prepared by grinding the *cis*-poly-**ACn**. Poly-**ACn′** showed a poor chiral recognition ability (Fig. 8b) because the polymer almost lost its helical conformation, resulting in the almost complete disappearance of the CD in the polymer backbone regions (Fig. 7b). These results clearly indicated that the chiral recognition ability was significantly influenced by the macromolecular helicity induced by the alkaloid pendants. Interestingly, these optically active helical polymers can be employed as an efficient polymeric organocatalyst for the asymmetric Henry reaction [73, 75]. Stereoregular poly(phenylacetylene)s bearing L-leucine ethyl ester side groups, such as **22**, also resolved some racemic compounds as CSPs for HPLC [76]. Interestingly, their resolving ability was significantly influenced by the solvents used for coating the polymer on the silica gel, because the helical conformations of poly(phenylacetylene)s are dynamic in nature, and the helical poly(phenylacetylene)s may take a different conformation, for example, an opposite helicity via inversion of helices, depending on the coating solvents.

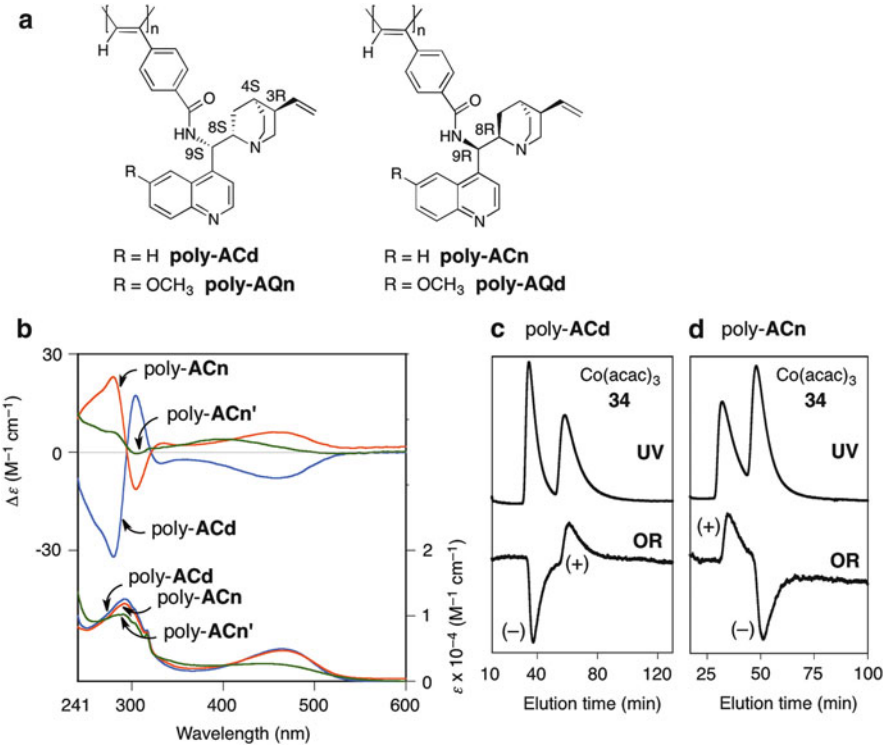

Fig. 7 (**a**) Structures of cinchona alkaloid-bound helical poly(phenylacetylene)s. (**b**) CD and absorption spectra of poly-**ACn**, poly-**ACd**, and poly-**ACn**′ measured in $CHCl_3$–CF_3CH_2OH (6:1, v/v) at 25 °C. (**c**,**d**) Chromatograms for the resolution of **34** on poly-**ACd** (**c**) and poly-**ACn** (**d**). Eluent: hexane-2-propanol (9:1, v/v). (Reproduced with permission from [74]. Copyright 2012 The Chemical Society of Japan)

Helical poly(phenylacetylene)s having chiral pinanyl groups (**37** and **38**) [77, 78] and hydrophilic *N*-(2-hydroxyethyl)aminomethyl groups, being capable of chelating to Cu^{2+} ion as the pendants (**39**) [79], have also been prepared and used as solid membranes for separating the enantiomers of amino acids through permeation. Helical polymer-based solid membranes have a significant potential and are attractive from the continuous and preparative standpoints for development of a practically useful new chiral separation method, but require further improvements in efficiency and enantioselectivity before practical use.

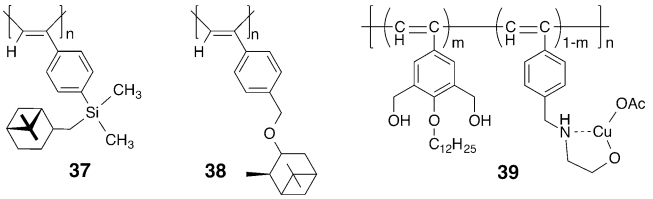

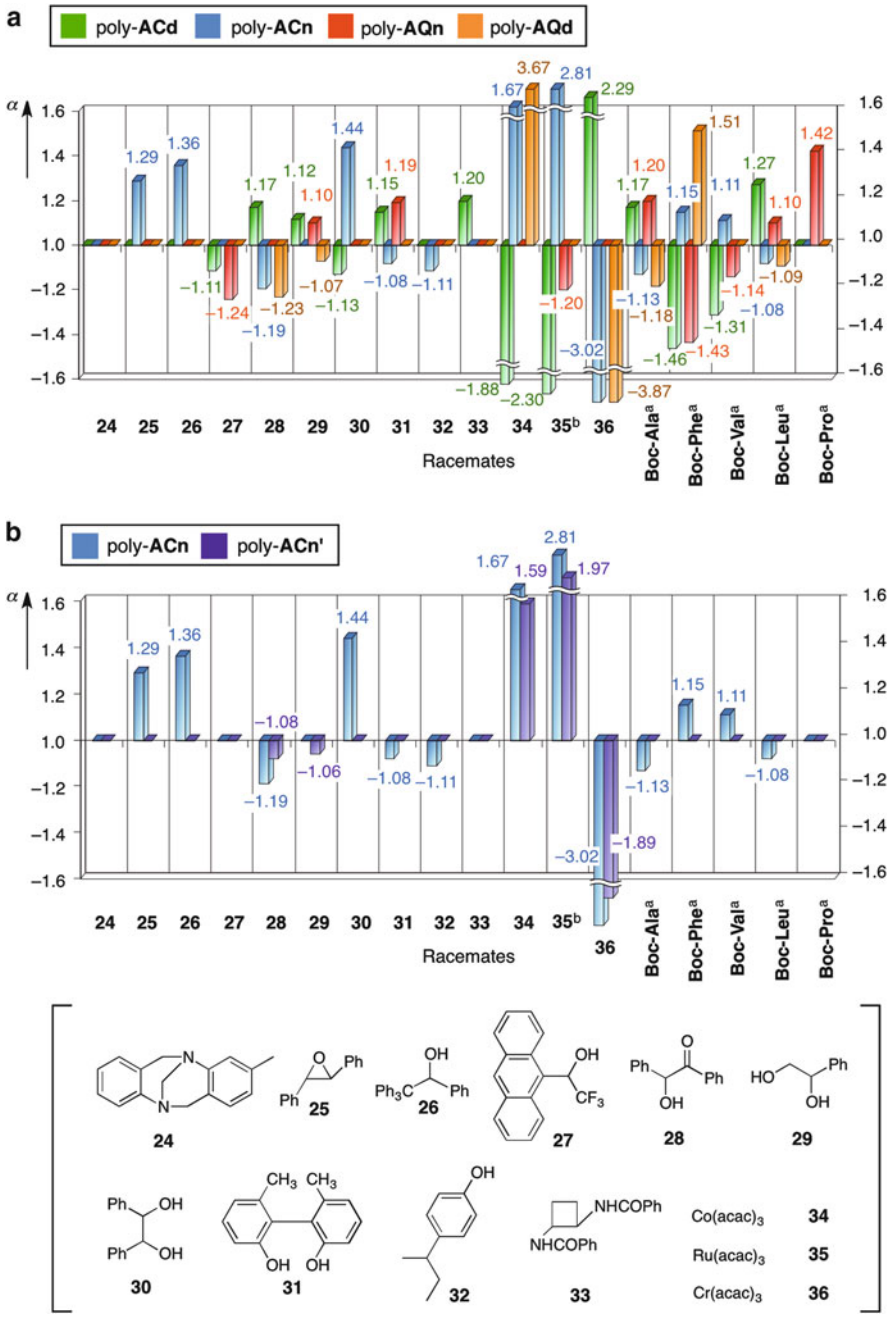

Fig. 8 Histograms of the separation factors (α) on poly-**ACd**, poly-**ACn**, poly-**AQn**, and poly-**AQd** (**a**) and poly-**ACn** and poly-**ACn′** (**b**). Eluent: hexane–2-propanol (9:1, v/v). The signs of the vertical axis (α value) represent the optical rotation of the first-eluted enantiomers. [a]Eluent: hexane–2-propanol (9:1, v/v) containing 2% acetic acid. [b]The signs of the vertical axis (α value) represent the CD detection (254 nm) of the first-eluted enantiomer

Optically active polyacetylene gels prepared by the copolymerization of L-lysine-derived *N*-propargylamides (**40a** and **40b**) with an achiral diacetylene or dipropargyl adipate as a cross-linker using a rhodium catalyst enantioselectively adsorbed *N*-benzyloxycarbonyl L-Ala derivatives and a chiral diol [80]. A similar gel derived from an optically active *N*-propargylamide (**41**) and a bifunctional achiral acetylene monomer also adsorbed one of the enantiomers of the racemic phenylethanol and benzoin [81].

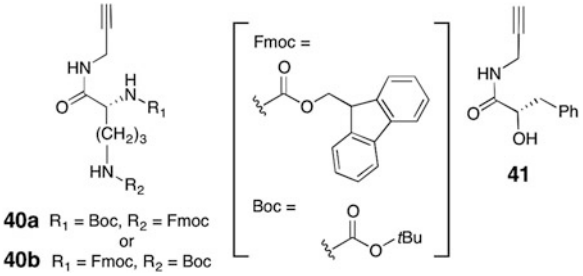

2.4 Polyisocyanides

Polyisocyanides with a bulky side group possess a stable helical conformation in solution as revealed by the direct resolution of poly(*tert*-butyl isocyanide) (**42**) into enantiomeric right- and left-handed helices by column chromatography using an optically active poly((−)-*sec*-butyl isocyanide) as a CSP [82]. This study clearly indicated the potential of helical polyisocyanides as CSPs. In fact, some racemates, such as $Co(acac)_3$ (**34**), were resolved in part when optically active **42** prepared by the helix-sense-selective polymerization was used as a CSP for HPLC [83]. As mentioned in Sect. 3.1, the 3,5-dimethylphenylcarbamates of cellulose and amylose are the most popular CSPs among the wide variety of commercially available CSPs. Accordingly, 3,5-dimethylphenylcarbamate-modified glucose- and galactose-carrying helical poly(phenyl isocyanide)s (**43**) have been prepared, and their chiral recognition abilities as CSPs for HPLC were evaluated [84]. The helical polyisocyanides completely or partially separated different types of racemates with functional groups depending on the stereostructure of the pendant sugar residues. Importantly, a non-helical vinyl polymer bearing the identical sugar units showed a lower chiral recognition, thus demonstrating the important role of the helical structures of **43**. Among the poly(phenyl isocyanide)-based CSPs, the galactose-carrying poly(phenyl isocyanide)s (**43c** and **43d**) showed a better resolving ability for broader racemates than those having the glucose-derived pendant groups (**43a** and **43b**).

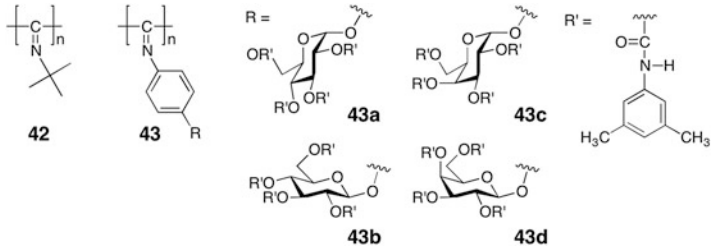

Helical polymers with a controlled helical sense can be readily synthesized by the polymerization of specific optically active monomers, such as substituted isocyanides and acetylenes as described in the previous sections. Chiral residues introduced in the monomers determine their helical senses. Recently, the unprecedented helix-sense-controlled living polymerization has been found for the polymerization of one enantiomer of phenyl isocyanide (L-**44**) bearing an L-alanine pendant with a long *n*-decyl chain through an amide linkage using the μ-ethynediyl Pt-Pd catalyst (**45**), which produced both diastereomeric right (*P*)- and left (*M*)-handed helical polyisocyanides with different molecular weights and narrow molecular weight distributions (*P*- and *M*-poly-**44**s, respectively) [85, 86]. Each single-handed, rodlike helical polyisocyanide stabilized by intramolecular hydrogen-bonding networks through the neighboring amide NH groups [87] was easily separated by solvent fractionation using acetone (Fig. 9a) [88]. Quite interestingly, the helical structures of the fractionated *M*- and *P*-poly-**44**s including helical pitch, helical sense (right- and left-handed helices), and excess handedness were for the first time visualized and determined by high resolution atomic force microscopy (AFM) (Fig. 9b,c) [88] when the polymers were deposited on a graphite substrate under organic solvent vapors. The fractionated single-handed helical polyisocyanides (*P*- and *M*-poly-**44**s) maintained their living features and can be used as an initiator for the further block copolymerizations of isocyanides [89]. This advantage was utilized to immobilize chemically these right- and left-handed helical polyisocyanides on silica gel and their chiral recognition abilities were investigated as CSPs for HPLC with anticipation that the *P*- and *M*-poly-**44**s having the same L-alanine residues as the pendants, but with the opposite polymer backbone helical conformation, could exhibit different chiral recognition abilities toward enantiomers, depending on their helical sense [90]. The CSP derived from the left-handed helical polyisocyanide (Si-*M*-BP(−)) successfully resolved racemates including a cyclic ether and dibenzamides, while the right-handed helical polyisocyanide-based CSP (Si-*P*-BP(+)) exhibited a rather complementary chiral recognition ability and specifically separated racemic metal acetylacetonate complexes, which could not be separated at all on the former CSP (Fig. 9d). Moreover, the reversed elution order was observed for some racemates resolved on the right- and left-handed helical polymer-based CSPs (Fig. 9e), thus indicating that the enantioselectivity and elution order of the enantiomers are significantly influenced by the helical sense of the polyisocyanides.

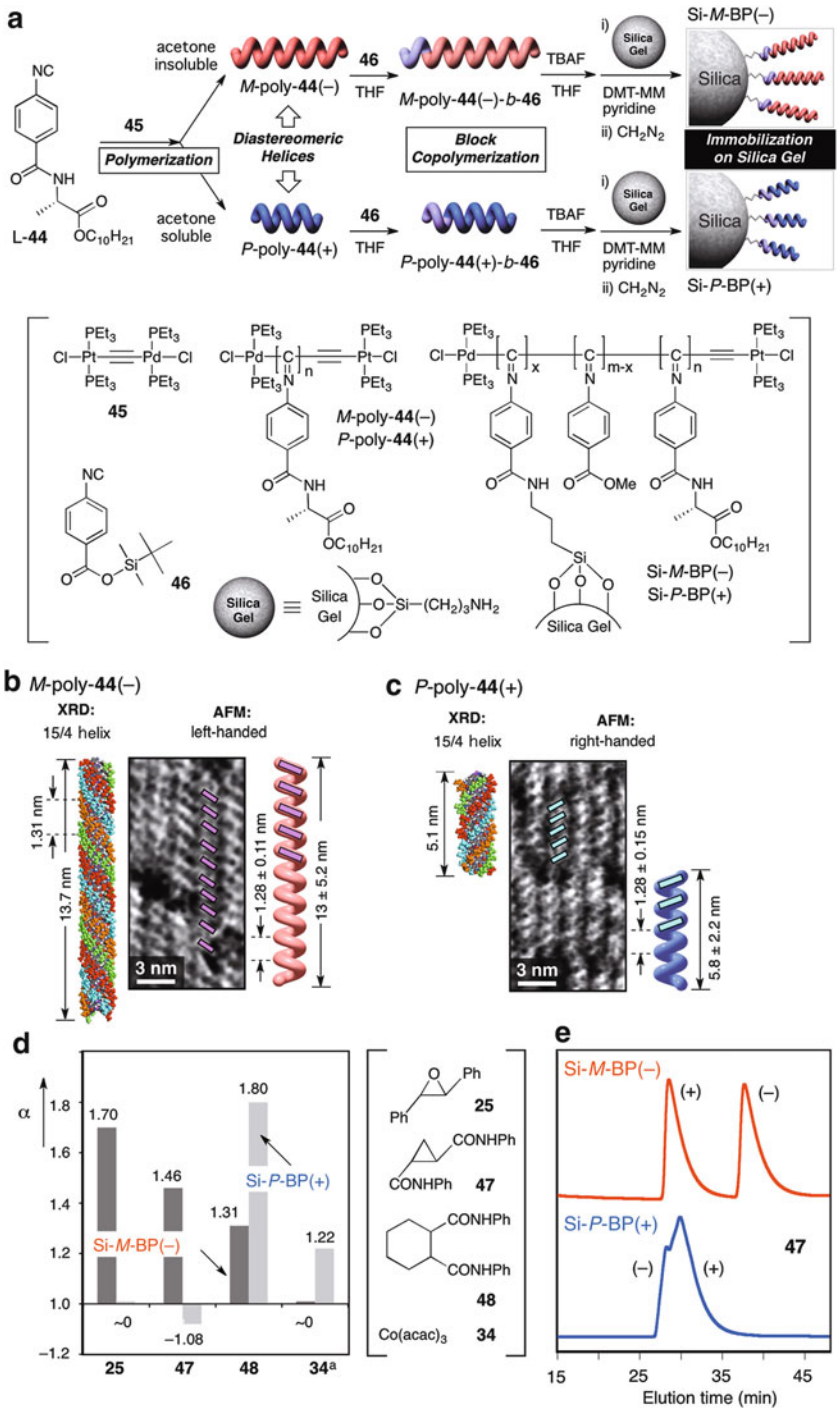

Fig. 9 (**a**) Synthesis of *M*-poly-**44**(−)-*b*-**46** and *P*-poly-**44**(+)-*b*-**46** and immobilization on silica gel. (**b**,**c**) AFM images of *M*-poly-**44**(−) (**b**) and *P*-poly-**44**(+) (**c**) on a highly oriented pyrolytic

When the left-handed helical polyisocyanide (*M*-poly-**44**(−)) was copolymerized with a bifunctional cross-linker (**49**), a unique optically active star polymer (*M*-poly-**44**(−)-*b*-**49**) was formed (Fig. 10a) and its star-shaped unique "spiny" architecture and its structure with individual helical arms including the number and length of the arms and its handedness have been directly visualized by high-resolution AFM (Fig. 10b) [91]. The star polymer (*M*-poly-**44**(−)-*b*-**49**) could discriminate the chirality of some racemates (**25**, **28**, and **50**) and a racemic helical polyisocyanide bearing no chiral pendants (poly-**51**), and enantioselectively adsorbed one of the enantiomers; the separation factors (α) calculated based on the enantioselective adsorption experiments were 1.81, 1.20, 1.45, and 1.14 respectively (Fig. 10c). Interestingly, the arm polyisocyanide (*M*-poly-**44**(−)) exhibited a poor chiral recognition ($\alpha = 1.03$) for poly-**51**. A confined chiral nano-space created in the star polymer through self-assembly of the helical arms may play a role in this helix-sense-selective adsorption of a large macromolecule.

Based on a facile method for constructing a helical polymer with a controlled helical sense via noncovalent bonding interactions, that is the "helicity induction and memory strategy" [66, 67, 92], discovered for the first time in poly(phenylacetylene)s [93] in 1999 and later in poly(phenyl isocyanide)s in 2004 [94–96], a series of optically active helical poly(phenyl isocyanide)s bearing achiral benzanilide pendant groups (poly(**53**–*co*-**54**-**Me**)s and poly-**55**) was prepared (Fig. 11a) [97]. The polymers possessing an optical activity solely due to the macromolecular helicity memory were chemically bonded to or coated on A-silica to prepare chiral packing materials for HPLC [97]. The CSPs resolved a variety of racemates; in particular, a right-handed helical poly(phenyl isocyanide) carrying achiral anilide pendants (*P*-poly-**55**(+)) showed an excellent resolving ability and completely or partially separated nine racemates into enantiomers, including a cyclic ether, amine, ketones, and metal acetylacetonate complexes, among the 12 racemates tested (Fig. 11b). The elution orders of the enantiomers were fully consistent with the helical senses of the polyisocyanides (*P* or *M*) as anticipated, because the optical activities of the polymers bearing achiral pendant groups result solely from the preferred-handed helical conformation with the macromolecular helicity memory.

Fig. 9 (continued) graphite (HOPG) substrate. Scale = 10 nm × 20 nm. Schematic representations of the left-handed helical *M*-poly-**44**(−) and right-handed helical *P*-poly-**44**(+) with periodic oblique stripes (*pink* and *blue lines*, respectively), which denote a one-handed helical array of the pendants and optimized 15/4 helical structures of *M*-poly-**44**(−) and *P*-poly-**44**(+) on the basis of X-ray structural analysis results, are also shown. (Reproduced with permission from [88]. Copyright 2008 American Chemical Society.) (**d**) Histograms of the separation factors (α) on Si-*M*-BP(−) and Si-*P*-BP(+). The signs of the vertical axis (α value) represent the optical rotation of the first-eluted enantiomers. Eluent: hexane–2-propanol (98:2, v/v). [a]Eluent: hexane–THF (98:2, v/v). The signs of the vertical axis (α value) represent the CD detection (254 nm) of the first-eluted enantiomer. (**e**) Chromatograms for the resolution of **47** on Si-*M*-BP(−) (*red lines*) and Si-*P*-BP(+) (*blue lines*). Eluent: hexane–2-propanol (98:2, v/v). (Reproduced with permission from [90]. Copyright 2011 The Royal Society of Chemistry)

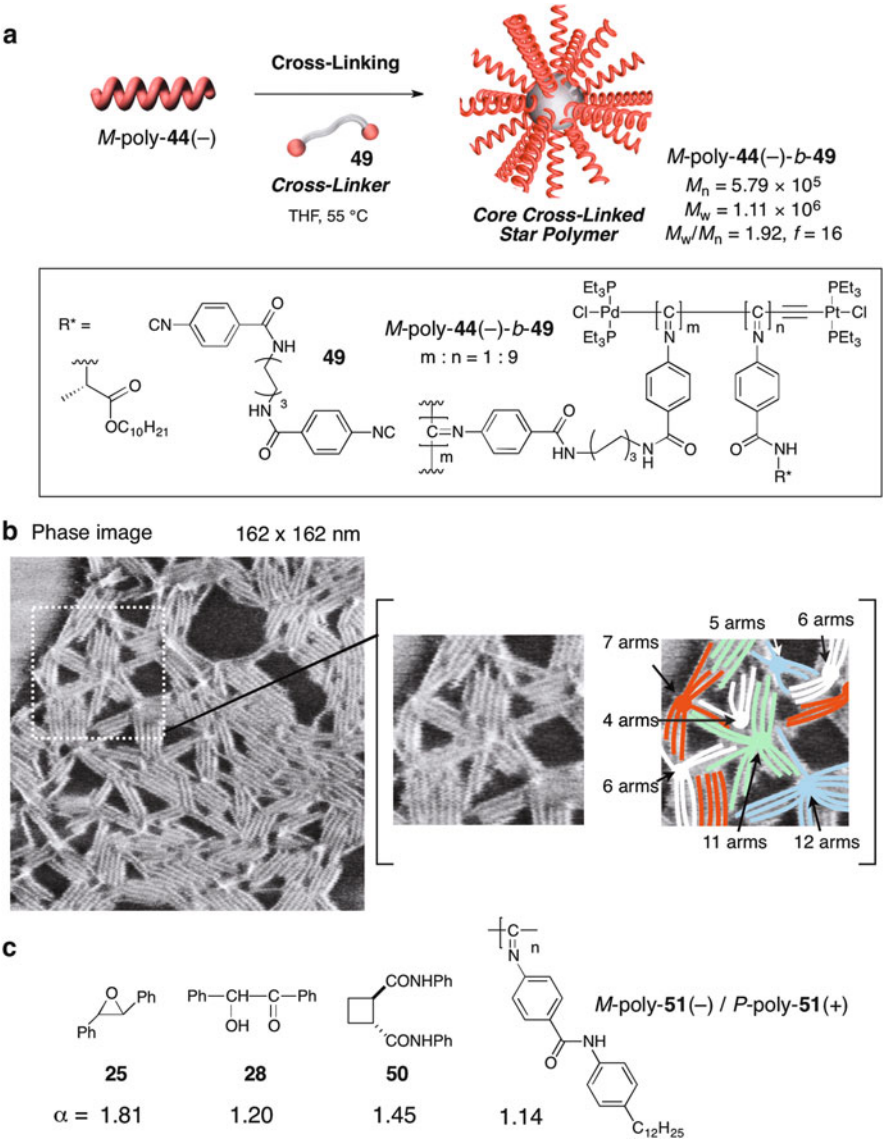

Fig. 10 (**a**) Synthesis of a star-shaped *M*-poly-**44**(−)-*b*-**49** with a cross-linker **49**. (**b**) AFM image (scale 162 nm × 162 nm) of 2D self-assembled *M*-poly-**44**(−)-*b*-**49** on HOPG. (**b**) Zoomed AFM image corresponding to the area indicated by a *white square*, and schematic representations of possible helix-bundle arrangements are also shown (*right*). Each molecule is indicated by different colors. (Reproduced with permission from [91]. Copyright 2011 American Chemical Society). (**c**) Results of enantioselective adsorption of racemic compounds (**25**, **28**, and **50**) and racemic helical polymer (poly-**51**) on *M*-poly-**44**(−)-*b*-**49**

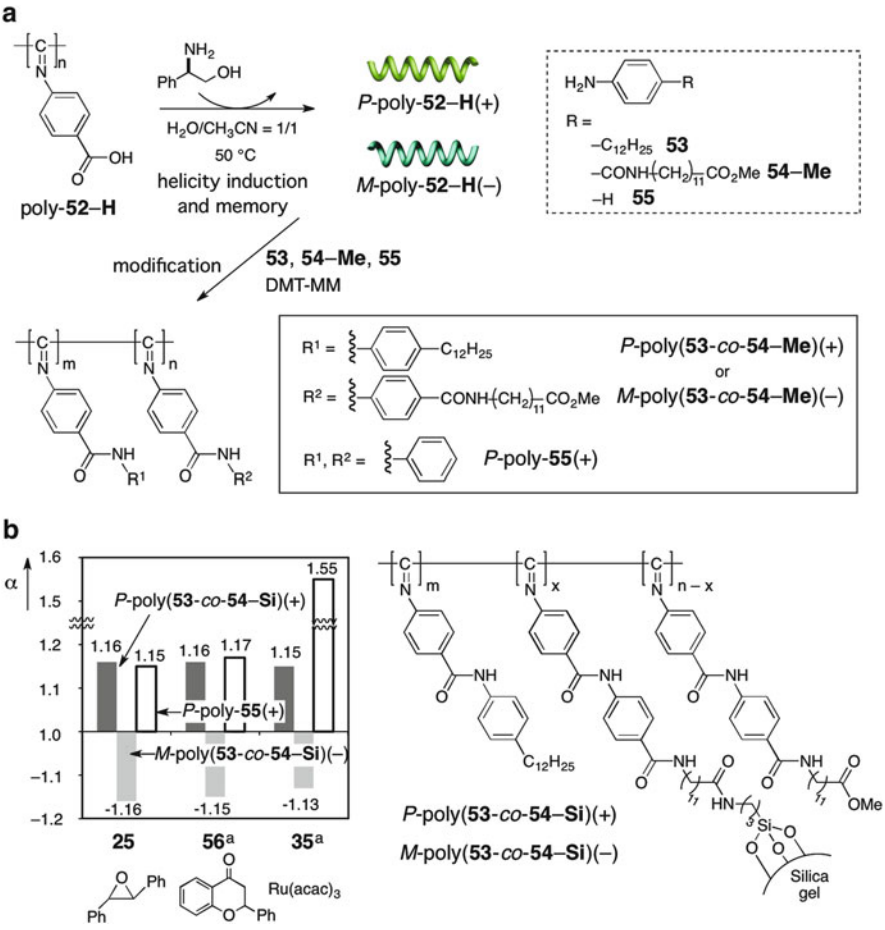

Fig. 11 (**a**) Synthesis of optically active helical poly(phenyl isocyanide)s bearing achiral benzanilide pendant groups (poly(**53**–*co*-**54**-**Me**)s and poly-**55**). (**b**) Histograms of the separation factors (α) on *P*-poly(**53**–*co*-**54**-**Si**)(+), *M*-poly(**53**–*co*-**54**-**Si**)(−), and *P*-poly-**55**(+). The signs of the vertical axis (α value) represent the optical rotation of the first-eluted enantiomers. Eluent: hexane–2-propanol (98:2, v/v). [a]The signs of the vertical axis (α value) represent the CD detection (254 nm) of the first-eluted enantiomer

2.5 *Other Synthetic Helical Polymers Showing Chiral Recognition*

An end-functionalized poly(4′-isocyanatobenzo-18-crown-6) (**57**) consists of achiral monomer units, but took a preferred-handed helical conformation induced by the optically active residue incorporated at the chain end as the initiator ("domino effect") [98], as supported by a rather intense CD induced by the chiral terminal group that appeared in the polymer backbone chromophore region. The polyisocyanate that

showed a chiral discrimination toward racemic amino acid derivatives, such as DL-**58** and the D-isomer, was enantioselectively extracted during the liquid–liquid extraction with **57**, whereas the corresponding unimer of **57** ($n = 1$) showed almost no enantioselectivity, indicating that a supramolecular helical array of achiral functional crown ether pendants with an excess screw-sense along the polymer backbone contributes to the present chiral recognition.

A stereoregular poly(phenylacetylene) bearing an analogous crown ether as the pendant (**59**) was quite sensitive to the chirality of the guest molecules, such as amino acids, and an almost one-handed helical conformation was induced in the entire polymer chain in the presence of 0.1 equiv. of L-Ala in acetonitrile [99]. The polymer showed an intense CD in the conjugated polymer backbone region even with 0.01 equiv. of L-Ala or 5% ee of Ala, indicating a remarkable chiral amplification with cooperative interactions in the pendant groups through noncovalent chiral interactions, and it could be applied to sense a tiny enantiomeric imbalance of specific guest molecules.

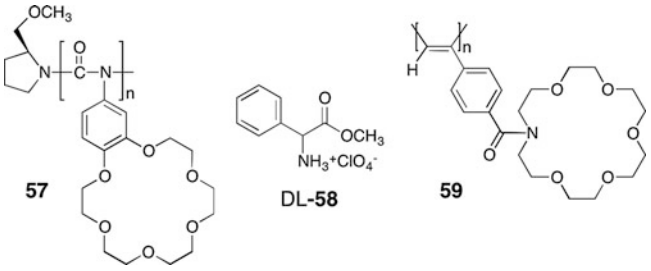

Poly(methyl methacrylate) (PMMA) constitutes a class of commodity plastics. When the polymer has a stereoregular syndiotactic (st) main-chain configuration, the st-PMMA forms a thermoreversible physical gel in aromatic solvents, such as toluene, due to a helical structure that possesses a sufficiently large cavity of ca. 1 nm, in which solvents are encapsulated [100]. Using an optically active alcohol, such as (*S*)- or (*R*)-1-phenylethanol (**60**) as the optically active additive in toluene, a preferred-handed helix can be induced in the st-PMMA backbone accompanied by gelation, and at the same time, fullerenes, such as C_{60}, C_{70}, and C_{84}, are encapsulated within its helical cavity to form a robust, processable peapod-like crystalline complex (Fig. 12a), as evidenced by the X-ray diffraction (XRD) profiles of the st-PMMA/C_{60} films and also by AFM and transmission electron microscopy (TEM) images of an st-PMMA/C_{60} film [101]. After complete removal of the optically active **60**, the st-PMMA–C_{60} complex gel showed vibrational circular dichroism (VCD) and CD signals in the PMMA IR and in the encapsulated C_{60} chromophore regions, respectively, although C_{60} itself is achiral, indicating that the macromolecular helicity of st-PMMA is memorized in the gel. The one-handed helical st-PMMA with a macromolecular helicity memory can recognize the size and chirality of fullerenes through an induced-fit mechanism. In fact, when an equimolar mixture of C_{60} and C_{70} in toluene was mixed with st-PMMA, C_{70} was

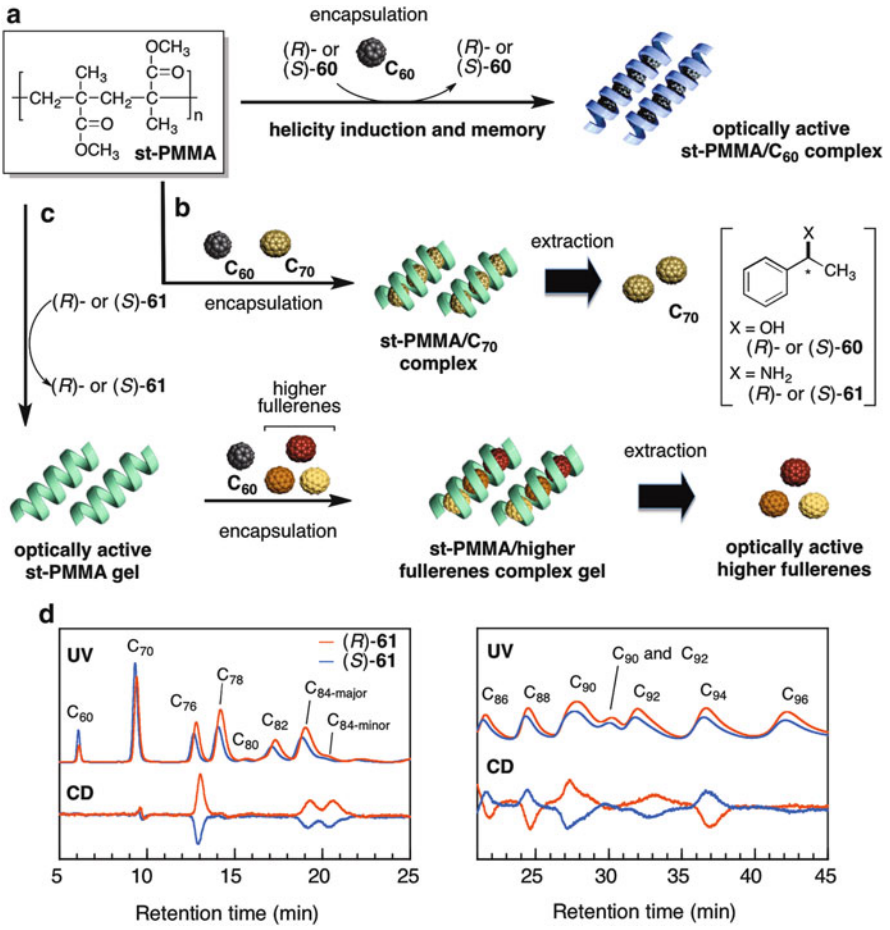

Fig. 12 (**a**) Schematic illustration of a helicity induction in st-PMMA in the presence of C_{60} with (*S*)- or (*R*)-**60**, and memory of the induced helicity after removal of **60**. (**b**) Schematic illustration of the preferential encapsulation of C_{70} over C_{60} by st-PMMA. (**c**) Selective extraction and resolution of higher fullerenes by helical st-PMMA with the induced helicity. (**d**) UV (356 nm, *top*) and CD (375 nm, *bottom*) detected HPLC chromatograms of the extracted fullerenes from carbon soot using optically active helical st-PMMAs prepared with (*R*)-**61** (*red lines*) and (*S*)-**61** (*blue lines*). (Reproduced with permission from [102]. Copyright 2010 American Chemical Society)

almost perfectly extracted with a selectivity of 99.8% (Fig. 12b) [102]. In addition, the optically active st-PMMA with an excess single-handed helix selectively extracted chiral higher fullerenes from carbon soot, and a series of optically active fullerenes (C_{76}, C_{84}, C_{86}, C_{88}, C_{90}, C_{92}, C_{94}, and C_{96}) were successfully extracted in one shot, as supported by the CD-detected HPLC chromatograms of the extract showing the apparent CDs (Fig. 12c,d) [102]. This strategy may provide a practical and valuable method for the size- and enantiomer-selective extraction of the elusive higher fullerenes.

3 Chiral Recognition Using Natural Helical Polymers and Their Derivatives

3.1 Polysaccharides

Polysaccharides, such as cellulose and amylose, are among the most abundant optically active biopolymers with perfect stereostructures, including stereogenic centers and tacticities. They have been used as chiral adsorbents since 1951 when Kotake resolved racemic amino acid derivatives by paper chromatography [103]. However, native cellulose and amylose are not effective as chiral packing materials for the separation of enantiomers, in particular for HPLC. Nowadays, more practically useful CSPs have been prepared by the modification of cellulose and amylose, and the tribenzoates of cellulose and trisphenylcarbamates of cellulose and amylose, having a one-handed helical conformation developed by Okamoto and the Daicel Corporation (Chart 1), have been recognized as the most widely used CSPs among more than 100 CSPs on the market, not only for analytical purposes, but also for the preparative scale separation of enantiomers including chiral drugs [5, 22–24, 27, 28, 104]. The detailed developments of these modified polysaccharide-based CSPs have been comprehensively reviewed elsewhere [5, 22–24, 27, 28, 104]. In this section, the most recent developments regarding the polysaccharide-based CSPs are briefly described.

The modified polysaccharide-based CSPs have been conventionally prepared by physically coating them on silica gel, while at present they are immobilized onto silica gel via chemical bonding, leading to ideal CSPs with a high durability against solvents, and some of them have been commercialized (Chart 2).

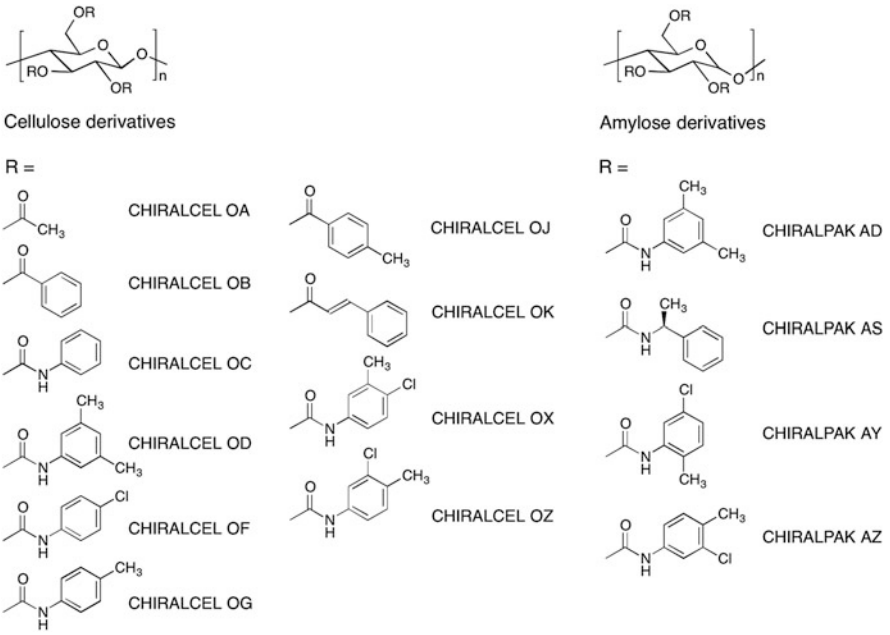

Chart 1

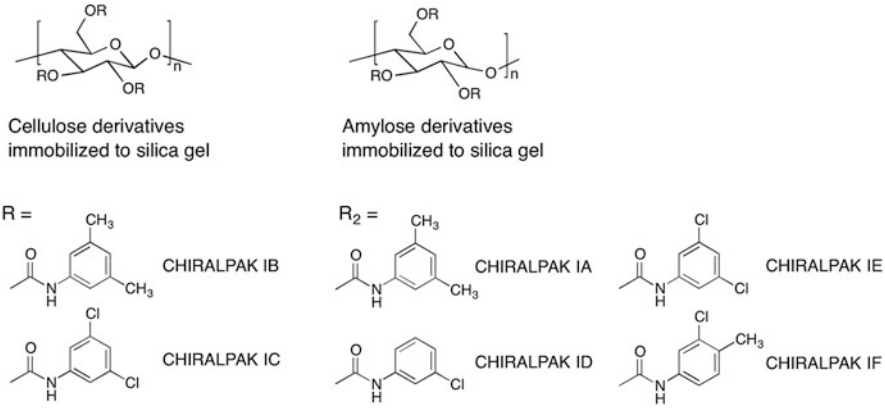

Chart 2

The first chemically bonded-type CSPs based on polysaccharide derivatives were reported in 1987; the cellulose trisphenylcarbamates were chemically linked with diisocyanates as a cross-linking reagent, which connect between the amino groups of the A-silica and the hydroxy groups of cellulose [105]. However, the resulting chemically bonded-type CSPs showed a low resolving ability, particularly when a large amount of cross-linking reagents was used, which may cause an alternation of the regular higher order structures, for example a helical conformation of the polysaccharide derivatives. Obviously, chemically bonding to silica gel at either end of the polysaccharide chains appears to be ideal, thus allowing the polysaccharides to maintain their ordered helical conformations even after immobilization.

To this end, amylose tris(3,5-dimethylphenylcarbamate) (CHIRALPAK AD) was chemically bonded to silica gel only at the reducing terminal residue of the amylose (Fig. 13a). Amylose, having the desired chain length with the reducing terminal residue, was readily prepared by the polymerization of the α-D-glucose 1-phosphate dipotassium salt with functionalized maltooligosaccharides using a phosphorylase isolated from potato. The amylose was then successfully bonded to silica gel only at the reducing terminus, followed by treatment with 3,5-dimethylphenyl isocyanate, to afford the chemically bonded-type CSP that exhibits an excellent resolving ability comparable to that of the coated-type CSP and high durability against solvents, such as THF and $CHCl_3$, and is commercially available (CHIRALPAK IA) [106]. Some racemates were more efficiently separated on this bonded-type CSP than on the coated-type CSP (CHIRALPAK AD) using $CHCl_3$ and THF as a component of the mobile phase (Fig. 14) [107].

This method is quite attractive, but only applicable to amylose derivatives, and hence a versatile method for immobilization of other polysaccharide derivatives has been developed. The radical copolymerization of vinyl residues introduced on the polysaccharide derivative with vinyl monomer-functionalized silica gel often afforded CSPs showing a slightly lower recognition ability [104, 108, 109]. To overcome this shortcoming, a polysaccharide derivative bearing a vinyl group was immobilized onto silica gel through radical copolymerization with a vinyl monomer

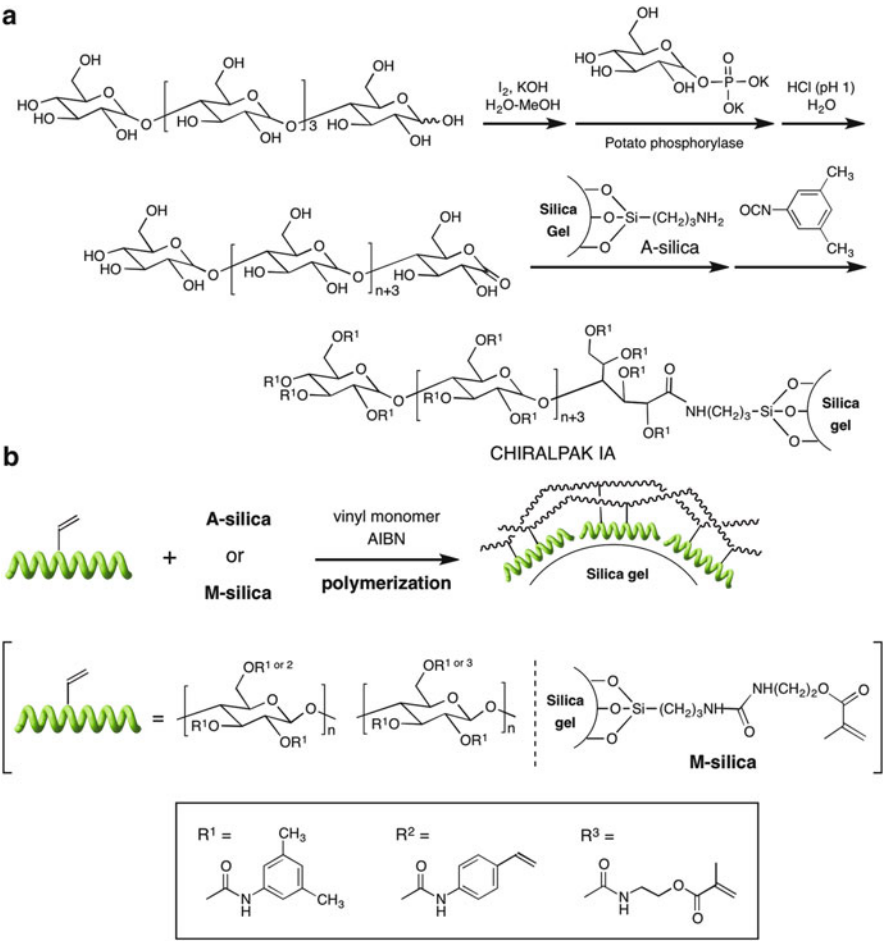

Fig. 13 (**a**) Immobilization of an amylose derivative onto silica gel only at the reducing terminal residue. (**b**) Immobilization of cellulose derivatives bearing a vinyl group onto silica gel by radical copolymerization with a vinyl monomer

[110–113]. After optimization of the immobilization conditions, such as the type and amount of the vinyl group introduced to the derivatives or the vinyl monomers, the chemically bonded-type cellulose-based CSPs showing a high recognition ability comparable to those of the coated ones were obtained (Fig. 13b).

Another efficient and more versatile immobilization method has been developed using a sol–gel condensation technique [114, 115]. The cellulose (**63**) and amylose (**64**) derivatives bearing 1−2% 3-(triethoxysilyl)propyl groups were coated on silica gel, which were then allowed to react with trimethylsilylchloride in the presence of water, resulting in the immobilization of the polysaccharides onto silica gel through intermolecular polycondensation with a low degree of cross-linking (Fig. 15). Therefore, the immobilized CSPs exhibited a high recognition ability similar to those of the conventional coated-type CSPs. This immobilization method

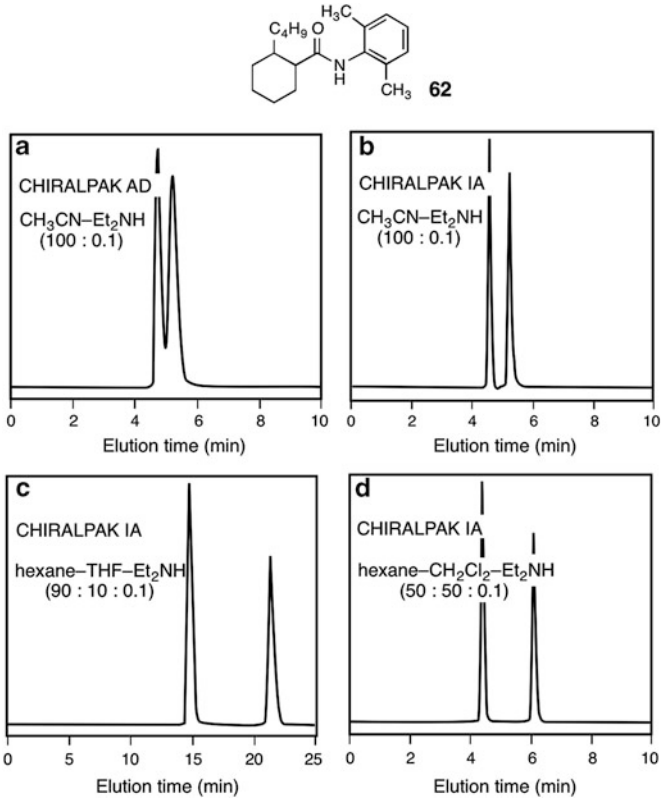

Fig. 14 Chromatograms for the resolution of **62** on CHIRALPAK AD (**a**) and CHIRALPAK IA (**b–d**). Eluent: CH_3CN–Et_2NH (100:0.1, v/v) (**a**,**b**), hexane–THF–Et_2NH (90:10:0.1, v/v) (**c**), hexane–CH_2Cl_2–Et_2NH (50:50:0.1, v/v) (**d**). (Reproduced with permission from [107]. Copyright 2005 Elsevier)

may be much better than others with respect to the simple and conventional processing and high immobilization efficiency, while retaining their high chiral recognition abilities, and can be used for other polysaccharide derivatives.

Amylose possesses a chiral hydrophobic cavity and is capable of forming inclusion complexes with specific small guest molecules [116] and polyrotaxanes with some polymers, such as carbon nanotubes that fit the cavity size in solution [117]. Recently, poly(*p*-phenylenevinylene) (PPV), an important π-conjugated luminescent polymer used as polymeric organic light-emitting diodes, was found to be encapsulated in amylose during the polymerization of its precursor monomer in an aqueous media, resulting in the luminescent amylose-PPV inclusion complex (APPV). The APPV is soluble in dimethyl sulfoxide (DMSO), and further modification of the hydroxy groups of the resulting amylose-PPV composite was possible [118]. Hence, a unique CSP composed of helical amylose tris(3,5-dimethylphenylcarbamate) (ADMPC) that encapsulates a rod-like PPV in its helical cavity (APPV-PC) has been prepared through a macromolecular reaction using the corresponding isocyanate (Fig. 16a) [119].

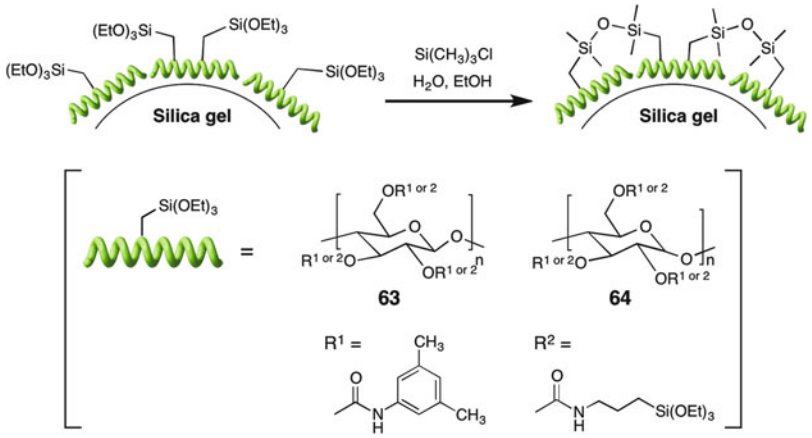

Fig. 15 Immobilization of polysaccharide derivatives bearing 3-(triethoxysilyl)propyl groups onto silica gel through the intermolecular polycondensation with a low degree of cross-linking

The CSP prepared from APPV-PC by coating on silica gel showed a remarkable chiral recognition ability for various racemates whose resolving ability was comparable to that of the commercially available amylose-based CSP (ADMPC, CHIRALPAK AD). Among the racemic compounds tested, the cyclic dibenzamide and dibenzanilide derivatives (**47** and **65**, respectively) were specifically resolved on APPV-PC ($\alpha = 3.17$ and 1.44, respectively) better than on ADMPC ($\alpha = 2.01$ and 1.08, respectively) as shown in Fig. 16b,c. The racemate **65** was partially separated on the ADMPC with the elution order of enantiomers such that the (+)-isomer eluted first followed by the (−)-isomer, whereas the reversed elution order was observed on the APPV-PC (Fig. 16c). The APPV-PC retains its helical inclusion structure after chemical modification of the hydroxy groups of the exterior amylose, and, therefore, its helical structure may be different from that of ADMPC, which results in the different chiral recognition abilities for several racemates.

3.2 Polypeptides and Nucleic Acids

Proteins and nucleic acids are fundamental to all living organisms and are optically active due to their inherent homo-chirality. Therefore it is quite natural to expect that proteins and nucleic acids may show chiral recognition abilities when used as CSPs. In fact, the first chiral separation of enantiomers using a protein-based CSP in liquid chromatography was reported in 1973 [120]. Since then, a variety of protein based-CSPs have been developed and some of them have been commercialized [29–31, 121]. Stereoselective monoclonal antibodies to D- and L-α-amino acids, raised against protein conjugates of *p*-amino-D- and L-phenylalanine, were immobilized on a chromatographic support, which could quite efficiently separate a

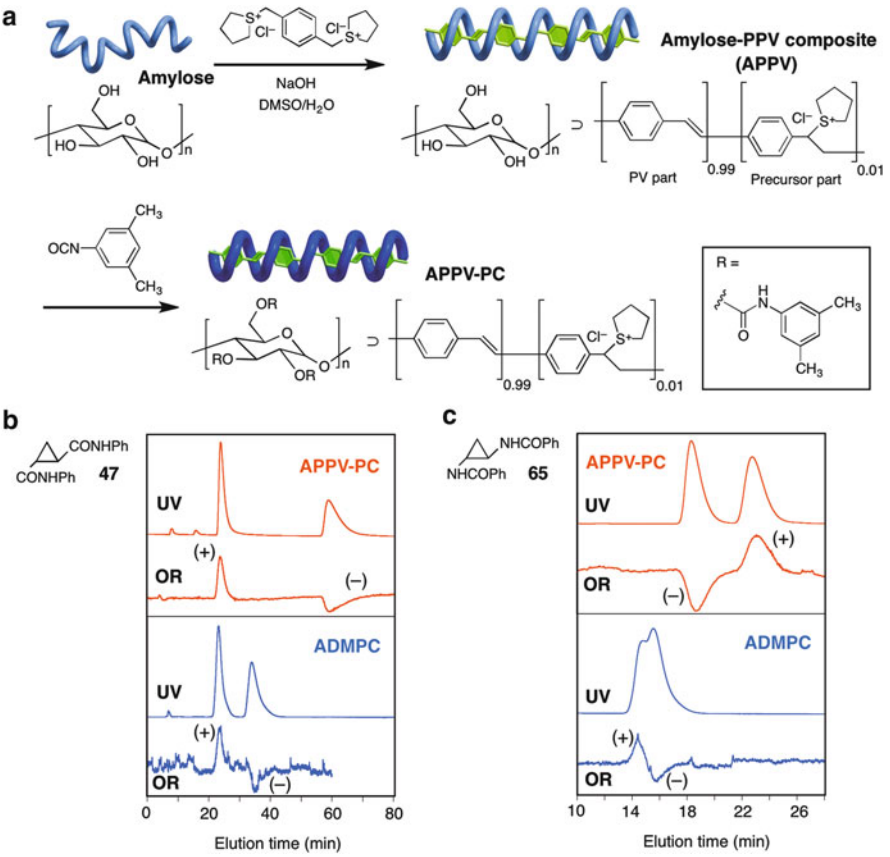

Fig. 16 (**a**) Schematic illustration of the synthesis of APPV and its derivative modified with 3,5-dimethylphenyl isocyanate (APPV-PC). The core PPV polymer contains approximately 1 mol% of the precursor units. (**b**,**c**) Chromatograms for the resolution of **47** (**b**) and **65** (**c**) on APPV-PC (column = 25 cm × 0.20 cm (i.d.), flow rate = 0.1 mL/min, *red lines*) and ADMPC (column = 25 cm × 0.46 cm (i.d.), flow rate = 0.5 mL/min, *blue lines*), respectively. Eluent: hexane-2-propanol (9:1, v/v). (Reproduced with permission from [119]. Copyright 2011 The Chemical Society of Japan)

number of amino acids into enantiomers with separation factors (α) up to 136 [122]. α-Helical polypeptides are a class of interesting synthetic helical polymers that also have potential as CSPs. Nevertheless, efficient CSPs with the same level of other helical polymer-based CSPs, including those based on helical poly(meth)acrylamides and polymethacrylates, and derivatized polysaccharides have not yet been developed. Initially, poly(L-glutamic acid) derivatives were immobilized on a cross-linked polystyrene gel to prepare the CSPs (**66a–c**) [123]. Among three CSPs, poly(N^5-benzyl-L-glutamine) with a right-handed helical conformation (**66c**) most effectively resolved racemic mandelic acid and the D-enantiomer was preferentially adsorbed. In contrast, poly(N^5-benzyl-D-glutamine)

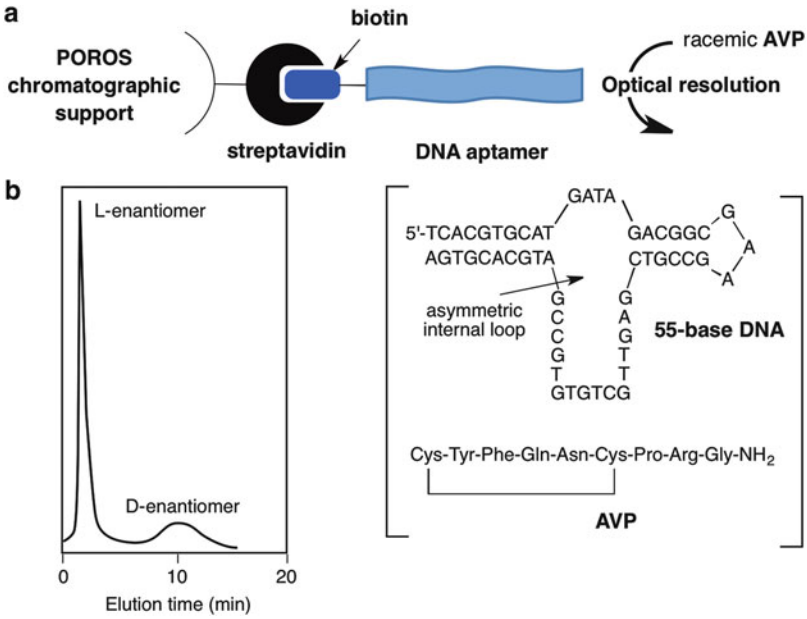

Fig. 17 (**a**) Schematic illustration of the immobilization of the DNA aptamer, and structures of the 55-base DNA aptamer and AVP. (**b**) Chromatographic resolution of racemic AVP on the DNA-based CSP. Eluent: 5 mM phosphate buffer containing 3 mM $MgCl_2$ (pH 6.0)

and poly(N^4-benzyl-L-asparagine), adopting the opposite left-handed helical conformation, showed an opposite enantioselectivity; the L-enantiomer preferentially adsorbed over the D-enantiomer, indicating an important effect of the helical structure on the chiral resolution. The dominant role of the helical structure and its handedness was also supported by the fact that the helical poly(N^5-benzyl-L-glutamine) (**66c**) with a longer main-chain (degree of polymerization (DP) = 18 or 11) exhibited a better separation factor ($\alpha = 1.08$) for mandelic acid than that of non-helical poly(N^5-benzyl-L-glutamine) with DP = 2 ($\alpha = 1.01$).

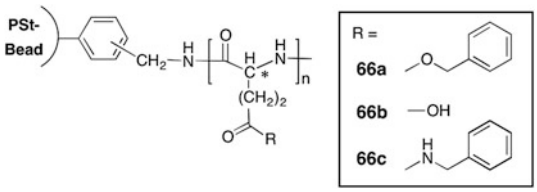

DNA and RNA aptamers have also been used as CSPs for HPLC [124–126]. For example, the 5′-biotinylated 55-base DNA aptamer, which is known to bind stereospecifically the (all-D)-enantiomer of an oligopeptide with a specific sequence (arginine-vasopressin, AVP), was immobilized on a streptavidin-bound chromatographic support through noncovalent biotin-streptavidin interactions (Fig. 17a). The resulting DNA-based CSP completely resolved a racemic mixture of

AVP into the enantiomers by HPLC (Fig. 17b) and the target D-peptide was more retained than the L-peptide [124]. This approach, including the use of RNA aptamers, has been extended to the separation of small chiral molecules, such as adenosine and tyrosinamide [125, 127].

4 Conclusion

As briefly described in this chapter, significant progress has been made in the synthesis of helical polymers over the past decade, which has significantly contributed to the development of novel polymer-based CSPs for efficiently differentiating enantiomers in HPLC. Apart from numerous synthetic variations in helical polymer syntheses, however, the rational design of synthetic helical polymers with a controlled helical sense from monomers via the polymerization process still remains a challenge. Among the commercially available CSPs, the cellulose- and amylose-based CSPs are the most frequently used CSPs and can resolve a wide range of racemates with a variety of functional groups on both analytical and preparative scales. Most importantly, the cellulose- and amylose-based CSPs belong to a class of helical polymers possessing a one-handed helical conformation after proper modification of the reactive hydroxy groups into esters and carbamates, which are also arranged into one-handed helical arrays along the polymer backbones, being responsible for their very high chiral recognition during diastereomeric interactions with each enantiomer. These structural features will provide a clue to the design and development of new helical polymers with a chiral resolving ability as high as those of the polysaccharide-based CSPs.

References

1. Natta G, Pino P, Corradini P, Danusso F, Mantica E, Mazzanti G, Moraglio G (1955) J Am Chem Soc 77:1708
2. Okamoto Y, Suzuki K, Ohta K, Hatada K, Yuki H (1979) J Am Chem Soc 101:4763
3. Blaschke G (1980) Angew Chem Int Ed 19:13
4. Maier NM, Franco P, Lindner W (2001) J Chromatogr A 906:3
5. Francotte ER (2001) J Chromatogr A 906:379
6. Andersson S, Allenmark SG (2002) J Biochem Biophys Methods 54:11
7. Roussel C, Rio AD, Pierrot-Sanders J, Piras P, Vanthuyne N (2004) J Chromatogr A 1037:311
8. Liu Y, Lantz AW, Armstrong DW (2004) J Liq Chromatogr Relat Technol 27:1121
9. Zhang Y, Wu DR, Wang-Iverson DB, Tymiak AA (2005) Drug Discov Today 10:571
10. Busch MA, Busch KW (2006) Chiral analysis. Elsevier, Amsterdam
11. Francotte E, Lindner W (2006) Chirality in drug research. Wiley-VCH Verlag GmbH & Co KGaA, Weinheim
12. Gübitz G, Schmid MG (2006) Mol Biotechnol 32:159
13. Subramanian G (2007) Chiral separation techniques: a practical approach. Wiley, Weinheim

14. Okamoto Y, Ikai T (2008) Chem Soc Rev 37:2593
15. Gasparrini F, Misiti D, Villani C (2001) J Chromatogr A 906:35
16. Ward TJ, Farris AB (2001) J Chromatogr A 906:73
17. Davankov VA (2003) J Chromatogr A 1000:891
18. Hyun MH (2005) Bull Korean Chem Soc 26:1153
19. Lämmerhofer M, Lindner W (2007) Adv Chromatogr 46:1
20. D'Acquarica I, Gasparrini F, Misiti D, Pierini M, Villani C (2008) Adv Chromatogr 46:109
21. Oguni K, Oda H, Ichida A (1995) J Chromatogr A 694:91
22. Yashima E, Yamamoto C, Okamoto Y (1998) Synlett 344
23. Okamoto Y, Yashima E (1998) Angew Chem Int Ed 37:1020
24. Yashima E (2001) J Chromatogr A 906:105
25. Tachibana K, Ohnishi A (2001) J Chromatogr A 906:127
26. Stringham RW (2006) Adv Chromatogr 44:257
27. Ikai T, Okamoto Y (2009) Chem Rev 109:6077
28. Okamoto Y, Ikai T, Shen J (2011) Israel J Chem 51:1096
29. Haginaka J (2001) J Chromatogr A 906:253
30. Millot MC (2003) J Chromatogr B 797:131
31. Haginaka J (2008) J Chromatogr B 875:12
32. Nakano T (2001) J Chromatogr A 906:205
33. Yamamoto C, Okamoto Y (2004) Bull Chem Soc Jpn 77:227
34. Blaschke G, Kraft HP, Fickentscher K, Kohler F (1979) Arzneimittel-Forschung/Drug Research 29:1640–1642
35. Müller GW (1997) ChemTech 27:21
36. Stinson SC (1994) Chem Eng News 72:38
37. Blaschke G, Bröker W, Fraenkel W (1986) Angew Chem Int Ed 25:830
38. Morioka K, Suito Y, Isobe Y, Habaue S, Okamoto Y (2003) J Polym Sci, Part A: Polym Chem 41:3354
39. Zhou H, Onimura K, Tsutsumi H, Oishi T (2001) Polym J 33:227
40. Onimura K, Zhang Y, Yagyu M, Oishi T (2004) J Polym Sci, Part A: Polym Chem 42:4682
41. Oishi T, Zhang Y, Fukushima T, Onimura K (2005) Polym J 37:453
42. Oishi T, Gao H, Nakamura T, Isobe Y, Onimura K (2007) Polym J 39:1047
43. Nakano T, Okamoto Y (2001) Chem Rev 101:4013
44. Okamoto Y, Honda S, Okamoto I, Yuki H, Murata S, Noyori R, Takaya H (1981) J Am Chem Soc 103:6971
45. Yuki H, Okamoto Y, Okamoto I (1980) J Am Chem Soc 102:6356
46. Kissener W, Vögtle F (1985) Angew Chem Int Ed 24:222
47. Muraoka T, Kinbara K, Kobayashi Y, Aida T (2003) J Am Chem Soc 125:5612
48. Okamoto Y, Yashima E, Hatada K, Mislow K (1984) J Org Chem 49:557
49. Dyker G, Stirner W, Henkel G, Schreiner PR (2008) Helv Chim Acta 91:904
50. Koumura N, Geertsema EM, van Gelder MB, Meetsma A, Feringa BL (2002) J Am Chem Soc 124:5037
51. Mateo Alonso A, Horcajada R, Groombridge HJ, Chudasama R, Motevalli M, Utley JHP, Wyatt PB (2005) Org Biomol Chem 3:2832
52. Shintani R, Moriya K, Hayashi T (2011) J Am Chem Soc 133:16440
53. Okamoto Y, Hatada K (1986) J Liq Chromatogr 9:369
54. Okamoto Y, Mohri H, Hatada K (1989) Polym J 21:439
55. Okamoto Y, Yashima E, Ishikura M, Hatada K (1987) Polym J 19:1183
56. Okamoto Y, Yashima E, Ishikura M, Hatada K (1988) Bull Chem Soc Jpn 61:255
57. Nakano T, Satoh Y, Okamoto Y (1998) Polym J 30:635
58. Okamoto Y, Mohri H, Nakamura M, Hatada K (1987) J Chem Soc Jpn 435
59. Okamoto Y, Mohri H, Nakano T, Hatada K (1989) J Am Chem Soc 111:5952
60. Nakano T, Shikisai Y, Okamoto Y (1996) Polym J 28:51
61. Nakano T, Satoh Y, Okamoto Y (2001) Macromolecules 34:2405

62. Haupt K, Mosbach K (2000) Chem Rev 100:2495
63. Wulff G (2002) Chem Rev 102:1
64. Yashima E, Maeda K, Nishimura T (2004) Chem Eur J 10:42
65. Shiotsuki M, Sanda F, Masuda T (2011) Polym Chem 2:1044
66. Yashima E, Maeda K (2008) Macromolecules 41:3
67. Yashima E, Maeda K, Furusho Y (2008) Acc Chem Res 41:1166
68. Liu J, Lam JWY, Tang BZ (2009) Chem Rev 109:5799
69. Yashima E, Huang S, Okamoto Y (1994) J Chem Soc, Chem Commun 1811
70. Yashima E, Matsushima T, Nimura T, Okamoto Y (1996) Korea Polym J 4:139
71. Marcelli T, Hiemstra H (2010) Synthesis 1229
72. Yeboah EMO, Yeboah SO, Singh GS (2011) Tetrahedron 67:1725
73. Tang Z, Iida H, Hu H-Y, Yashima E (2012) ACS Macro Lett 1:261
74. Naito Y, Tang Z, Iida H, Miyabe T, Yashima E (2012) Chem Lett 41:809
75. Miyake GM, Iida H, Hu H-Y, Tang Z, Chen EYX, Yashima E (2011) J Polym Sci, Part A: Polym Chem 49:5192
76. Zhang C, Liu F, Li Y, Shen X, Xu X, Sakai R, Satoh T, Kakuchi T, Okamoto Y (2013) J Polym Sci, Part A: Polym Chem 51:2271–2278
77. Aoki T, Kaneko T (2005) Polym J 37:717
78. Aoki T, Fukuda T, Shinohara KI, Kaneko T, Teraguchi M, Yagi M (2004) J Polym Sci, Part A: Polym Chem 42:4502
79. Hadano S, Teraguchi M, Kaneko T, Aoki T (2007) Chem Lett 36:220
80. Liu RY, Sanda F, Masuda T (2008) J Polym Sci, Part A: Polym Chem 46:4175
81. Sanda F, Fujii T, Tabei J, Shiotsuki M, Masuda T (2008) Macromol Chem Phys 209:112
82. Nolte RJM, Van Beijnen AJM, Drenth W (1974) J Am Chem Soc 96:5932
83. Yamagishi A, Tanaka I, Taniguchi M, Takahashi M (1994) J Chem Soc, Chem Commun 1113
84. Tsuchida A, Hasegawa T, Kobayashi K, Yamamoto C, Okamoto Y (2002) Bull Chem Soc Jpn 75:2681
85. Onitsuka K, Joh T, Takahashi S (1992) Angew Chem Int Ed 31:851
86. Takei F, Hayashi H, Onitsuka K, Kobayashi N, Takahashi S (2001) Angew Chem Int Ed 40:4092
87. Okoshi K, Nagai K, Kajitani T, Sakurai S-i, Yashima E (2008) Macromolecules 41:7752
88. Onouchi H, Okoshi K, Kajitani T, Sakurai S-i, Nagai K, Kumaki J, Onitsuka K, Yashima E (2008) J Am Chem Soc 130:229
89. Wu Z-Q, Nagai K, Banno M, Okoshi K, Onitsuka K, Yashima E (2009) J Am Chem Soc 131:6708
90. Tamura K, Miyabe T, Iida H, Yashima E (2011) Polym Chem 2:91
91. Miyabe T, Iida H, Banno M, Yamaguchi T, Yashima E (2011) Macromolecules 44:8687
92. Yashima E, Maeda K, Iida H, Furusho Y, Nagai K (2009) Chem Rev 109:6102
93. Yashima E, Maeda K, Okamoto Y (1999) Nature 399:449
94. Ishikawa M, Maeda K, Mitsutsuji Y, Yashima E (2004) J Am Chem Soc 126:732
95. Hase Y, Ishikawa M, Muraki R, Maeda K, Yashima E (2006) Macromolecules 39:6003
96. Hase Y, Nagai K, Iida H, Maeda K, Ochi N, Sawabe K, Sakajiri K, Okoshi K, Yashima E (2009) J Am Chem Soc 131:10719
97. Miyabe T, Iida H, Yashima E (2012) Chem Sci 3:863
98. Sakai R, Otsuka I, Satoh T, Kakuchi R, Kaga H, Kakuchi T (2006) J Polym Sci, Part A: Polym Chem 44:325
99. Nonokawa R, Yashima E (2003) J Am Chem Soc 125:1278
100. Kusuyama H, Yakase M, Higashihata Y, Tseng HT, Chatani Y, Tadokoro H (1982) Polymer 23:1256
101. Kawauchi T, Kumaki J, Kitaura A, Okoshi K, Kusanagi H, Kobayashi K, Sugai T, Shinohara H, Yashima E (2008) Angew Chem Int Ed 47:515

102. Kawauchi T, Kitaura A, Kawauchi M, Takeichi T, Kumaki J, Iida H, Yashima E (2010) J Am Chem Soc 132:12191
103. Kotake M, Sakan T, Nakamura N, Senoh S (1951) J Am Chem Soc 73:2973
104. Franco P, Senso A, Oliveros L, Minguillón C (2001) J Chromatogr A 906:155
105. Okamoto Y, Aburatani R, Miura S-I, Hatada K (1987) J Liq Chromatogr 10:1613
106. Enomoto N, Furukawa S, Ogasawara Y, Akano H, Kawamura Y, Yashima E, Okamoto Y (1996) Anal Chem 68:2798
107. Zhang T, Kientzy C, Franco P, Ohnishi A, Kagamihara Y, Kurosawa H (2005) J Chromatogr A 1075:65
108. Oliveros L, Lopez P, Minguillon C, Franco P (1995) J Liq Chromatogr 18:1521
109. Kimata K, Tsuboi R, Hosoya K, Tanaka N (1993) Anal Methods Instrum 1:23
110. Kubota T, Kusano T, Yamamoto C, Yashima E, Okamoto Y (2001) Chem Lett 724
111. Kubota T, Yamamoto C, Okamoto Y (2003) J Polym Sci, Part A: Polym Chem 41:3703
112. Kubota T, Yamamoto C, Okamoto Y (2004) J Polym Sci, Part A: Polym Chem 42:4704
113. Chen X-M, Yamamoto C, Okamoto Y (2006) J Chromatogr A 1104:62
114. Ikai T, Yamamoto C, Kamigaito M, Okamoto Y (2007) J Chromatogr A 1157:151
115. Ikai T, Yamamoto C, Kamigaito M, Okamoto Y (2006) Chem Lett 35:1250
116. Kubik S, Holler O, Steinert A, Tolksdorf M, Wulff G (1995) Macromol Symp 99:93
117. Star A, Steuerman DW, Heath JR, Stoddart JF (2002) Angew Chem Int Ed 41:2508
118. Ikeda M, Furusho Y, Okoshi K, Tanahara S, Maeda K, Nishino S, Mori T, Yashima E (2006) Angew Chem Int Ed 45:6491
119. Tamura K, Sam NSM, Ikai T, Okamoto Y, Yashima E (2011) Bull Chem Soc Jpn 84:741
120. Stewart KK, Doherty RF (1973) Proc Natl Acad Sci USA 70:2850
121. Allenmark SG, Andersson S (1994) J Chromatogr A 666:167
122. Hofstetter O, Lindstorm H, Hofstetter H (2002) Anal Chem 74:2119
123. Kiniwa H, Nishikaji T, Ogata N (1987) J Polym Sci, Part A: Polym Chem 25:2689
124. Michaud M, Jourdan E, Villet A, Ravel A, Grosset C, Peyrin E (2003) J Am Chem Soc 125:8672
125. Brumbt A, Ravelet C, Grosset C, Ravel A, Villet A, Peyrin E (2005) Anal Chem 77:1993
126. Ravelet C, Peyrin E (2006) J Sep Sci 29:1322
127. Michaud M, Jourdan E, Ravelet C, Villet A, Ravel A, Grosset C, Peyrin E (2004) Anal Chem 76:1015

Top Curr Chem (2013) 340: 73–106
DOI: 10.1007/128_2013_452

Published online: 14 June 2013

Chiral Supramolecular Selectors for Enantiomer Differentiation in Liquid Chromatography

Alessia Ciogli, Dorina Kotoni, Francesco Gasparrini, Marco Pierini, and Claudio Villani

Abstract Biochemical processes in living organisms rely on a plethora of molecular reactions and interactions involving chiral molecules, and these processes often show different responses to the enantiomers of exogenous or endogenous chemicals. The interaction of enantiomeric drugs with a target receptor is a paradigmatic example of chirality effects on general *biological* action and is directly related to the formation of a drug-receptor supramolecular complex. In particular the drug-receptor model can be used to explore the relation of chirality to at least three important issues encountered in supramolecular chemistry: complementarity, preorganization, and (enantio) selectivity. A detailed understanding of those factors governing enantioselectivity of biological receptors is facilitated by the study at molecular level of model systems with simplified structures that are amenable to physico-chemical investigations. Liquid chromatography on chiral stationary phases offers the opportunity to study enantioselective interactions between surface immobilized chiral selectors, viewed as minimalist mimics of macromolecular receptors, and a large set of chiral guests, under a variety of experimental conditions. Indeed, for a significant number of systems, close agreement has been found between retention data gathered by chromatography and association constants measured by spectroscopy in free solution. Chiral supramolecular selectors featuring highly preorganized, medium-sized macrocyclic structures are attractive in this context because they often afford high levels of enantioselectivity and yet have relatively low molecular complexity, thus facilitating the understanding of operative enantioselective recognition mechanisms from easily collected chromatographic data. In the present chapter we first illustrate the general principles of supramolecular chemistry and their integration into the design of liquid chromatographic systems, with particular focus on enantioselective variants based on chiral macrocyclic selectors of natural or synthetic origin. In the second part we discuss the elaboration of enantioselective recognition models from chromatographic data and

A. Ciogli, D. Kotoni, F. Gasparrini (✉), M. Pierini and C. Villani
Dipartimento di Chimica e Tecnologie del Farmaco, Sapienza Università di Roma,
P.le Aldo Moro 5, 00185 Rome, Italy
e-mail: francesco.gasparrini@uniroma1.it

how these models can be extended to and studied with non-chromatographic systems (free solution by nuclear magnetic resonance, gas phase by mass spectrometry).

Keywords Chirality · Enantioselective chromatography · Enantioselectivity · Macrocycles · Supramolecular chromatography · Supramolecular selectors

Contents

1 Introduction

Supramolecular chemistry has been defined as the "chemistry of molecular assemblies and of the intermolecular bond" [1], a definition that eventually transformed into the more informal expression "chemistry beyond the molecule." Supramolecular chemistry is often related to the non-covalent, reversible host–guest association, a process that leads to (usually) weakly bound and highly dynamic host–guest supramolecules.

In the broad sense, the host is generally considered as a large molecule, either natural or synthetic, featuring a cavity, a cleft, or a hole that is large enough to accommodate guest components. In addition, the host structure features an array of binding sites (a region capable of taking part in a non-covalent interaction) that *converge* in the complex. The guest structure may range from a simple inorganic ion to more complicated molecules having a *diverging* arrangement of binding sites in the complex.

Two additional factors contribute to the overall supramolecular association process in host–guest systems: *complementarity* and *preorganization*. In order to bind, a host must have binding sites that are of the correct electronic character (polarity, hydrogen bond donor/acceptor ability) to *complement* those of the guest. Stringent size and shape *complementarities* are also required for tight binding. The principle of complementarity has been summed up by Donald Cram: "To complex, hosts must have binding sites which cooperatively contact and attract binding sites of guests without generating internal strains or strong nonbonded repulsions" [2–6].

Complementarity alone, however, is not sufficient to drive host–guest association, because a certain degree of preorganization of the host is also required: the host is considered to be preorganized if it does not undergo a *significant* conformational change upon guest binding. Preorganized hosts are usually macrocycles frequently populating a single low energy conformation and this property contributes to lower the entropic cost to be paid during complexation of flexible, non preorganized hosts that have to adapt their shape to surround the guest and approach its binding sites. The original lock-and-key principle has thus progressed to include the notion of *induced fit* between a host and a guest molecule that interact in a flexible manner due to the conformational changes of the individual units to enhance complex stability (positive cooperativity).

In general, supramolecular chemistry concerns non-covalent bonding interactions. The term "non-covalent" encompasses a wide range of attractive and repulsive effects including ion–ion interactions, ion–dipole interactions, dipole–dipole interactions, hydrogen bonding, cation–π interactions, anion–π interactions, aromatic–aromatic interactions, and van der Waals forces. Solvation of the interacting partners is an additional key factor that regulates host–guest complexation equilibria. In non-polar solvents and in the gas phase, polar interactions are much more significant than in polar solvents. Polar solvents strongly compete for binding sites and in these solvents intrinsic host–guest interactions are accompanied by extensive desolvation of polar sites of the isolated species followed by resolvation upon complexation. Solvophobic forces related to removal of large molecular surfaces from the contact with *poor* solvents are also important when host and guest approach each other over extended surface areas.

One corollary to complementarity in host–guest association is selectivity, that is the ability to select a single guest out of a collection of structurally related components, and it can be related to guest size, shape, functionalities, or a combination of these features. Complexations of a single host with several guests of similar structure is frequently accompanied by large selectivities, i.e., one host–guest complex is much more stable than the others under a given set of experimental conditions. Since selectivity stems primarily from complementarity, it can in principle be incorporated by design into the host once the structure of the target guest is known. One particular case of selectivity is represented by enantioselectivity, the ability of a chiral host to distinguish between the enantiomers of a chiral guest: since enantiomers have the same size, shape, and functionalities, enantioselectivity must rely on subtle differences in the structure, energetics, and dynamics of the two diastereomeric host–guest complexes that can be generated starting from a single enantiomer of one component and the two enantiomers of the other. Several enantioselective hosts have been described in the past, all of them sharing some common structural features that are directly linked to their ability to bind guests with enantioselectivity: conformational homogeneity, presence of a cage-like structure endowed with interaction sites with high directionality [7].

2 Supramolecular Chromatography

Supramolecular host–guest association processes (and the theoretical principles behind them) can be conveniently adapted to and exploited in practical applications, where the molecular association and selective recognition events are translated into physical phenomena. Separation science is one field of theoretical and practical activity where supramolecular chemistry has found widespread application in the design of chromatographic systems, considering that selectivity is the prerequisite of any separation process [8–10]. Chromatographically derived association and selectivity data are easily collected under a variety of experimental conditions (solvent, temperature) for a large set of chemically diverse compounds, and these data can be used in concert with those gathered by spectroscopy to construct recognition models and refined chromatographic systems. The whole spectrum of discrimination abilities can be expressed in supramolecular chromatography, ranging from size and shape selectivity to enantioselectivity.

The following sections will illustrate several examples of enantioselective supramolecular systems that are relevant in the separation science scenario, together with a discussion of selected host–guest recognition models elaborated from experimental chromatographic and spectroscopic data and interpreted with the aid of molecular modeling techniques.

3 Chiral Supramolecular Selectors in Liquid Chromatography

A survey of the enantioselectivity shown by chiral supramolecular selectors in liquid chromatographic applications clearly indicates that they can be divided into two broad groups, according to the experimentally observed degree of enantiomer differentiation [11–14]. Supramolecular selectors like cyclodextrins and crown ethers afford low to medium enantiomer selectivities, that are in any case sufficient to obtain a complete separation in most liquid chromatographic systems, but do not reach those typically observed at receptorial level. Synthetic and naturally occurring macrocycles described in Sect. 4 are typical examples of chiral selectors able to distinguish guest enantiomers with receptor-like selectivities corresponding to differences in free energy of binding equal to or larger than 1.5 kcal mol^{-1} at room temperature. Receptor-like enantioselectivities are far beyond those required for analytical or preparative chromatographic separations; nevertheless, host–guest systems that display such large selectivities are of paramount relevance in that they can be further investigated by spectroscopic and computational techniques for the construction of recognition models that account for the observed discrimination, have predictive value, and are useful for the design of new selectors with improved or broadened recognition properties.

3.1 Cyclodextrins

Cyclodextrins (CDs) are toroid-shaped naturally occurring cyclic oligosaccharides originally described by Villiers in 1891 [15]. The most widely used CDs are composed of 6, 7, or 8 D-glucopyranosidic units (see Fig. 1), respectively named α-CD, β-CD, and γ-CD [17–19], although larger cyclodextrins containing 9–13 glucopyranosic units have been identified [20]. Cyclodextrins are derived from the enzymatic degradation of starch by cyclodextrin glycosyltransferase, an α-amylase found in various bacteria, such as *Bacillus* strains [21]. All the glucose units present in the cyclodextrin structure are in a chair conformation, as shown by Bender and Komiyama in 1978 [22], and are bound via α-(1,4) glycosidic linkage. Owing to the lack of free rotation about the α-(1,4) bonds, cyclodextrins are not perfectly cylindrical molecules but possess a three-dimensional architecture resembling a hollow torus (see Fig. 1). The primary 6-hydroxyl groups are located on the narrow rim of the torus, while the 2- and 3-hydroxyl secondary groups are located on the wider rim. The non-bonding electron pairs of the glycosidic oxygens bridges are directed towards the inner part of the torus, resulting in a high electron density area [17]. Given the position of the hydroxyl groups on the outer surface of the molecule, the outside is hydrophilic, while the internal cavity is relatively lipophilic and can form inclusion complexes. The most important property of CDs, in fact, is their ability to form host–guest complexes. In most cases, 1:1 complexes are formed, although 2:1, 1:2, and 2:2 host–guest complexes have been reported. In water, for example, appropriate guest molecules can easily replace the water molecules occupying the internal cavity of the torus, in a normally enthalpy-driven host–guest complexation [17]. The main interactions taking place between the guest and the CD are van der Waals and hydrophobic interactions, although steric factors and hydrogen bonding may also become important. In the case of modified CDs, where the hydroxyl groups have been derivatized with suitable functional groups further interactions can be observed (aromatic–aromatic interactions, ionic interactions). The diameter of the cyclodextrin cavity is a critical parameter in the complex formation: while the α-CD (cavity diameter between 4.7 and 5.3 Å) has limited applicability to only the smaller molecules, the β-CD (cavity diameter between 6.0 and 6.5 Å) and γ-CD (cavity diameter between 7.5 and 8.3 Å) have sufficient space for the incorporation of most pharmaceuticals, as well as chiral drugs (for a comprehensive study of the complexation thermodynamics of cyclodextrins see [23]). In particular, while the α-CD can accommodate only a single six-membered ring, the β-CD can incorporate larger rings (such as naphthalene or biphenyl) while the cavity of γ-CD is sufficient for the complexation of much larger molecules, such as substituted pyrenes. Given the high costs of γ-CD, however, β-cyclodextrin is the most used CD for applications in the pharmaceutical field, where cyclodextrins are extensively used as drug carriers to enhance solubility, bioavailability, stability, and reduce adverse effects [24]. Cyclodextrins, both naturally occurring and derivatized at the hydroxyl group, are also largely used in the cosmetic, textile, and food industries [25].

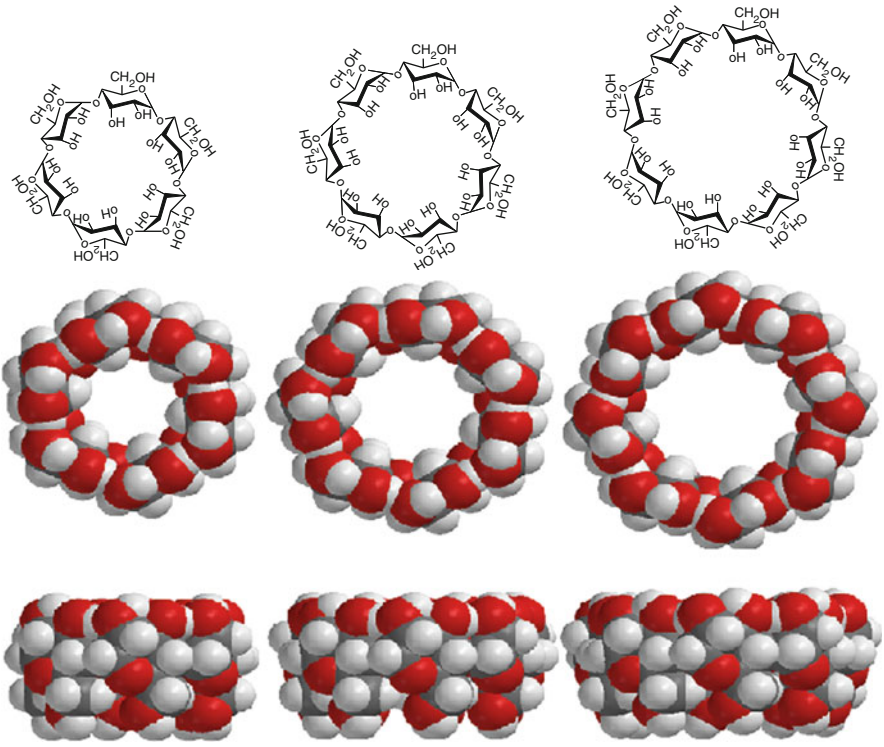

Fig. 1 Native α, β, and γ cyclodextrins (i.e., Cyclobond III, I, and II, respectively)

3.1.1 Supramolecular Chromatography and the Reciprocity Principle

The reciprocity principle in host–guest association has been followed in the early design and realization of supramolecular chromatographic devices. The reciprocity principle simply states that if a given host can bind a specific guest with large selectivity among a range of structurally related guests (one specific host–guest combination is much more stable than the others), then the most tightly bound guest can in principle be used to select the original host from a collection of molecules with similar structures. A special case of reciprocity is encountered in systems where a chiral molecule recognizes the enantiomers of a second chiral species: if a single enantiomer of the species A can distinguish the enantiomers of species B, then a single enantiomer of B will be able to distinguish the enantiomers of A. While this principle was elaborated and experimentally proved for bimolecular systems composed of small molecular components, recent works have demonstrated that it can be extended to supramolecular systems as well. When dealing with chromatographic systems in which one of the host–guest components is immobilized on a solid support, the reciprocity principle also extends to the position of the host or guest components: the intrinsic ability of the two species to

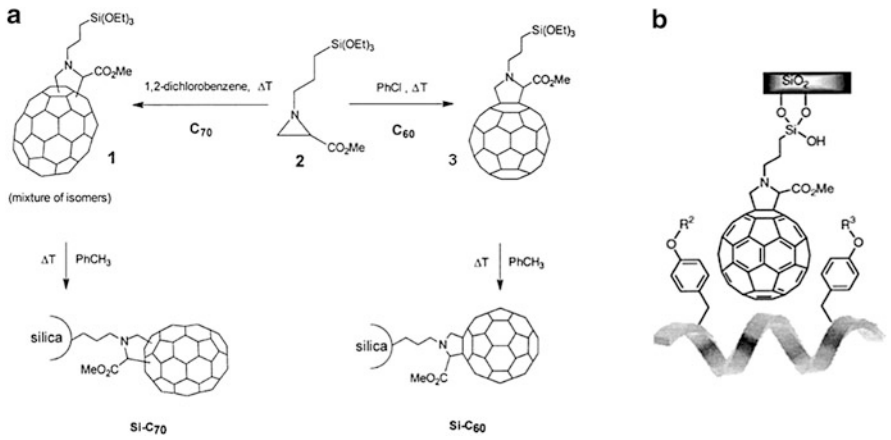

Fig. 2 (**a**) Synthesis of Si-C_{60} and Si-C_{70} fullerene stationary phases. (**b**) Schematic representation of Si-C_{60}/helical peptide complex as reported in [8, 26]

assemble into the supramolecular complex will be retained irrespective of their physical state, i.e., host–guest complex will form with almost unchanged stability and selectivity either when the host is surface-linked onto the solid support and the guest is present in free solution, or when the host and guest positions are reversed.

An early example of supramolecular chromatography design that uses the reciprocity principle was reported by Bianco et al. [8] and was later extended by Bogdanski et al. [9] A C_{60} fullerene stationary phase Si-C_{60} was prepared by surface immobilization of a fulleropyrrolidine onto silica gel microparticles via alkoxysilane chemistry (Fig. 2a). The known ability of C_{60} to complex with calix[8]arene (but not with calix[4]- and calix[6]-arenes) and with γ-cyclodextrin (but not with α- and β-cyclodextrins) was confirmed by chromatography on HPLC stationary phases packed with Si-C_{60}. In this particular case the positions of the host (the macrocycle) and guest (the C_{60} spheroid that is accommodated inside the macrocycle cavity) are reversed compared to other supramolecular chromatographic systems where the host is immobilized and the guests are in solution. To circumvent the ambiguity of the host–guest definition, associated in some way with the structural feature of the two partners rather than with their functioning in the particular physical device, the alternative terms selector–selectand are commonly used in chromatography to designate the molecular component that selects (selector, it is fixed to or incorporated into the stationary phase) the various species present in the system (selectands, they are dissolved in the mobile phase and are selectively retained). These terms were originally introduced by Mikeš and Boshart in analogy to the operator–operand terms used in cybernetics [27].

Chromatography on silica stationary phases covalently doped with fullerene derivatives facilitates the study of supramolecular associations in organic–aqueous media (in which the fullerenes nanostructures are insoluble) with biomolecules.

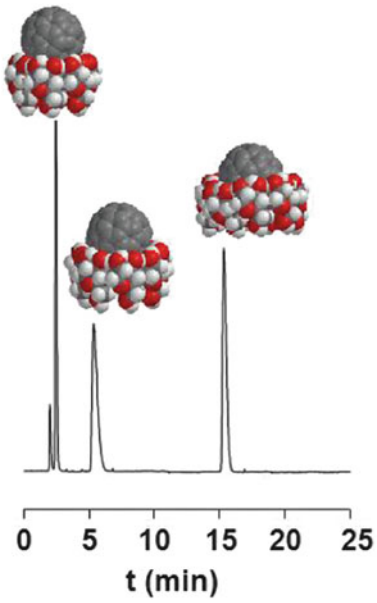

Fig. 3 Separation of α, β, and γ cyclodextrins on Si-C_{60} under reversed phase gradient elution. Structures on top of peaks are supramolecular cyclodextrin-C_{60} complexes obtained by molecular mechanics docking process (Amber* force field)

This was clearly proved by the effective separation of a mixture of α-, β-, and γ-cyclodextrins on Si-C_{60} under reversed phase conditions, with a clear preference of the immobilized fullerene for the larger eight-membered cyclic oligomer, whose cavity size nicely matches that of the C_{60} spheroid.

A similar approach using immobilized C_{60} on silica and aqueous mobile phases in liquid chromatography has been exploited to prove size-selectivity towards cyclodextrin congeners having from 6 to 25 glucose units. A remarkable preference for the 8-, 9-, and 10-membered cyclodextrin over the larger and smaller guests was demonstrated, thus confirming the original findings and showing unusually large increase in retention on passing from 11 to 10 units, and from 7 to 8 units (Fig. 3).

Additional selectivity and recognition ability in water-rich media was detected by immobilized C_{60} in Si-C_{60} for a series of designed peptides forming hydrophobic cavities as simplified models of more complex biological systems (enzymes and receptors). These peptides possess a high content of α-aminoisobutyric acid (Aib) that stabilizes 3_{10}- and α-helical structures, and are then suitable to contain the hydrophobic buckyball C_{60} (Fig. 2b) [26].

Inspection of retention and selectivity data for a set of calix[*n*]arenes congeners ($n = 4, 6, 8$) in organic solvents (toluene or dichloromethane in the presence of 0.5–2.0% of 2-propanol) confirmed the ability of Si-C_{60} to select cyclo-oligomeric guests according to the macroring size, and showed a marked preferential complexation with the larger calix[8]arene, in close analogy to earlier non-chromatographic experimental findings. Variable temperature chromatography of calix[6]- and calix[8]arenes on surface-linked fullerenes was used to extract thermodynamic data (enthalpy and entropy changes ΔH and ΔS of complexation) for the association

process between calix[*n*]arenes and either immobilized C_{60} or C_{70} (the latter prepared in analogy to Si-C_{60} via alkoxysilane fulleropyrrolidine) in different solvent systems: complexation equilibria were enthalpy dominated ($\Delta H = -7.4$ and -6.4 kcal mol^{-1} for calix[8]arene with C_{60} and C_{70}, respectively, in dichloromethane) and entropy opposed. The selectivity of the smaller calix[6]arene for the two immobilized fullerenes was solvent dependent, with C_{70} selected in CH_2Cl_2 and C_{60} in toluene [28]. In a related study, HPLC retention data collected on Si-C_{60} for a set of monotopic and ditopic aromatic tripodal receptors revealed that ditopic receptors have a greater affinity for the immobilized C_{60} spheroid as a result of extended π–π aromatic interactions. Comparison between LC retention data (collected using acetonitrile or acetonitrile/water mixture) and NMR experiments with free C_{60} (using low polarity solvents) showed that, with these particular receptors, highly polar solvents are required for the complexation to occur (solvophobic effect) [29].

Although the interaction takes place between chiral peptides or cyclodextrins with defined stereochemistry and the chiral fullerene-based stationary phases (in which the immobilized C_{60} derivative is chiral and racemic), the selectivities observed in these systems are driven by size and shape alone, and the same situation is present in the system comprising immobilized C_{60} and calix[*n*]arenes.

One of the most intriguing uses of cyclodextrins, however, has been in enantioselective chromatographic separations, where the chiral environment present at the hydrophobic cavity has been largely exploited for enantiomer differentiation in liquid chromatography and in capillary electrophoresis, as elucidated in a recent review by Scriba [14]. Since the introduction of the first CD-based CSP in 1984 by Armstrong and DeMond [30], a wide variety of stationary phases has been described, using both natural occurring and modified CDs. Both the architecture and the chemistry of cyclodextrins contribute to enantiomer differentiations, as interactions can take place either on the exterior or the interior surface of the cyclodextrin toroid. The parameters to determine whether an inclusion complex is formed or a superficial interaction prevails depend on the proper fit of the analyte in the cavity (shape and size of the analyte) and the mobile phase composition which can determine the type of interactions taking place. In reversed-phase mode inclusion complexes are necessary for enantiorecognition, although the entire molecule of the analyte does not have to fit inside the toroid cavity. Strong complex formation can, in fact, be obtained even with a partial fit of one of the two enantiomers in the cavity. To obtain chiral recognition in reversed-phase mode, besides the inclusion complex formation, it is also essential that the substituents on the stereogenic center of the guest molecule be near and interact with the secondary hydroxyl groups at the mouth of the CD cavity [31]. Surface interactions are, on the other hand, responsible for the enantioselective mechanism in polar organic mode and normal phase mode, as non-polar interactions between the analyte and the CD cavity are not observed due to the lack of water in the mobile phase. In polar organic mode, Chang et al. found that at least one polar group (hydroxyl, amide, secondary amine, etc.) must be present in the α- or β-position with respect to the stereogenic center of the analyte to observe H-bond formation and enantiorecognition [32]. Finally, in normal phase mode, interactions similar to those

described for Pirkle-CSPs prevail. Dipole interactions, π–π interactions between aromatic groups and hydrogen bonds with the amide dipoles present in the CSPs are the basis of the enantiorecognition mechanisms on CD-based CSPs [33].

A variety of techniques including NMR spectroscopy, mass spectrometry, thermodynamics, and X-ray crystallography, combined with capillary electrophoresis and HPLC studies, have been used to characterize the complexes formed [34, 35]. More recently, an important contribution has also been derived from molecular modeling, where chromatographic data have been interpreted and later predicted through theoretical studies [36–39]. Bikádi et al. predicted that the enantiodifferentiation of phenylazetidin derivatives would be better obtained on a permethylated β-CD CSP(PM-β-CD) than on the β-CD CSP [36], while Shi et al. investigated the direct resolution of methyl mandelate (MMA) on a permethylated β-CD CSP (PM-β-CD) with regards to organic modifier concentration and column temperature [37, 38]. Through quantum mechanics PM3 simulation they were able to predict the retention order of the enantiomers and provide an atomistic account of how the enantiodifferentiation takes place, with the main driving forces responsible for enantiorecognition being hydrophobic bonding interactions, dipole-dipole interactions, charge-transfer, and weak hydrogen bonding. Although the benzene ring of (*R*)-MMA was located horizontally on the wider edge of the PM-β-CD cavity, the aromatic ring of (*S*)-MMA was more deeply included in the hydrophobic cavity, thus leading to a higher retention of the (*S*)-MMA enantiomer (see Fig. 4 for energy-minimized structures). Thermodynamic calculations showed that the stabilization energy of the (*R*)-MMA/PM-β-CD complex is lower than that of the (*S*)-MMA/PM-β-CD complex. A cellular automata model was proposed by DeSoi et al. to predict enantiodifferentation on β-CD CSPs based on accepted chromatographic bonding forces between enantiomers and β-CD CSPs [39].

Although CD-based CSPs are largely used in enantioselective HPLC and account for about one-fourth of the direct enantiomeric separations reported in 2010–2011 [39], few significant enantiomeric differentiation in the complexation thermodynamics of enantiomeric guests with natural cyclodextrins are reported, probably because hydrophobic interactions and non-orienting van der Waals interactions prevail during the inclusion complex formation. Hosts with central chirality such as amino acids, carbohydrates, etc., are not rigorously fixed in the CD cavity and are thus not resolved with high α values as should be expected in the case of supramolecular chromatography. Appreciable differences in the thermodynamic quantities are observed with only a limited number of chiral guests, such as atropisomers of 1,1′-binaphthyl-2,2′-diyl hydrogen phosphate, which represent a good model for the CD supramolecular recognition mechanism, and with modified cyclodextrins which appear to enhance enantiomeric differentiation.

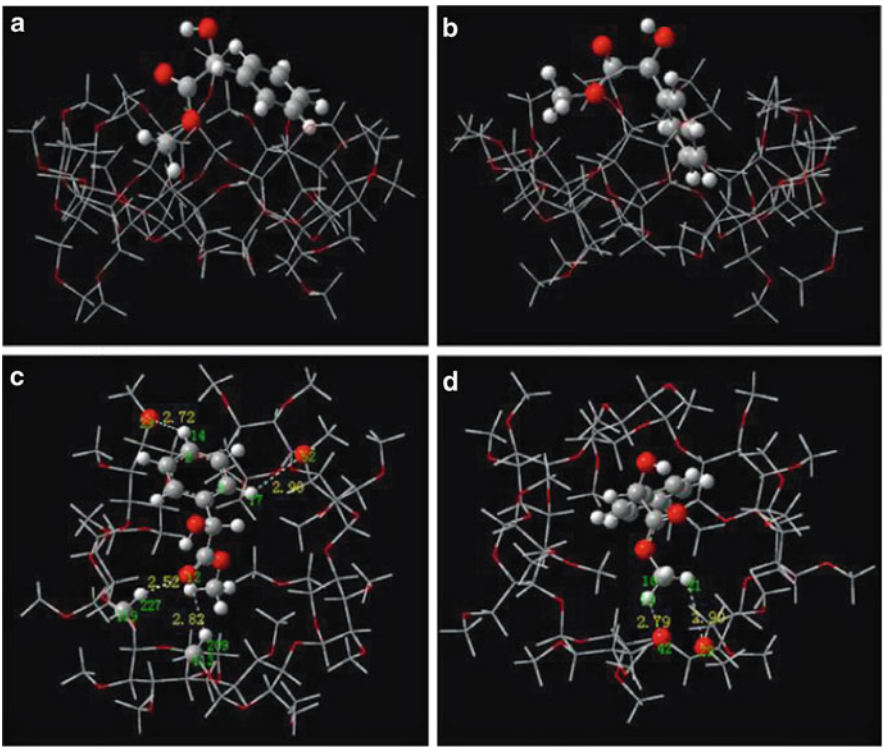

Fig. 4 Energy-minimized structures obtained by ONIOM calculations for the (*R*/*S*)-MMA/PM-β-CD complexes. (**a**) (*R*)-MMA/PM-β-CD seen from the side of the PM-β-CD wall. (**b**) (*S*)-MMA/PM-β-CD seen from the side of the PM-β-CD wall. (**c**) (*R*)-MMA/PM-β-CD seen from the wider edge of the PM-β-CD cavity. (**d**) (*S*)-MMA/PM-β-CD seen from the wider edge of the PM-β-CD cavity. The possible intermolecular hydrogen bonds are shown as a *dotted line*

3.2 Crown Ethers

Crown ethers are macrocyclic polyether compounds capable of selectively forming complexes with a variety of different cationic species. They were first introduced by Pedersen in 1967 [40, 41]. Crown ethers have been extensively used in the complexation of metal cations and ammonium cations, as the ether oxygen atoms present in the internal wall of the cavity are excellent electron donors [42, 43]. The ability of a crown ether molecule to complex with a cation is dependent upon the size of the hole formed by macrocyclic structure and, as a result, crown ethers of different sizes exhibit significantly different specificities for the complexation of cations. Chiral crown ethers are used in enantioselective chromatography following the incorporation of binaphthyl [44–47] or biphenanthryl units [48–50], tartaric acid derivatives, or carbohydrates. Aza crown ethers [51–53] and pyridine crown ethers [54] have also been described. These CSPs are essentially limited to the separation

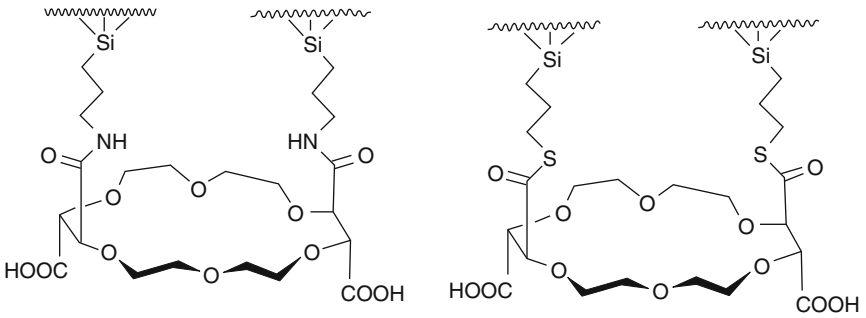

Fig. 5 Structures of (+)-(18-crown-6)-2,3,11,12-tetracarboxylic acid **1**, the previously reported **CSP 2** containing amido-linkages and the thioester-based **CSP 3**

of primary amines, although, as delineated by Scriba in a recent review [14], some exceptions have been reported. Huyn's 2005 review of the use of crown ether-based CSPs for HPLC [55] remains an excellent comprehensive reference. Recently, a crown ether-based chiral stationary phase containing thioester linkage was described by Cho et al. [56], prepared by bonding (+)-(18-crown-6)-2,3,11,12-tetracarboxylic acid (see Fig. 5) to mercaptopropyl silica gel. The enantiomeric recognition ability of the new CSP was found to be greater than that of the previously reported CSP containing amide linkages [57] in the resolution of various α-amino acids, racemic amines, and amino alcohols. The authors concluded that the new CSP is quite stable under acidic mobile phase conditions, indicating that the thioester linkage is useful as a tethering group. It was also shown that changing the bonding chemistry of the crown ether to the silica surface can influence the degree of enantioselectivity (quantitative difference) but not the elution order of the enantiomers. The same research team also demonstrated that free carboxylic acid functions in the crown ether structure are not necessary in the enantiorecognition mechanism [56].

Hirose et al. prepared a series of chiral pseudo crown ether selectors, having either a free phenolic or phenol ether group in the crown ring. After covalent grafting to aminopropyl silica particles, the CSPs showed high enantioselectivities for primary amines, amino alcohols, and amino acid derivatives [58–60].

The enantiorecognition mechanism involved in the differentiation of amino acid enantiomers on chiral stationary phases containing (+)-(18-crown-6)-2,3,11,12-tetracarboxyl acid has been extensively investigated through a variety of techniques, including NMR, ESI-MS, molecular modeling, and X-ray crystallography, and will not be further discussed in the present review.

4 Structure, Energetics, and Dynamics of Supramolecular Complexes Relevant to Enantioselective HPLC on Chiral Stationary Phases

While cyclodextrins and chiral crown ethers are typical examples of supramolecular hosts, the level of enantioselectivity they are able to generate when included in chromatographic systems is commonly modest and does not reach that displayed by natural receptors. In this section we describe several examples of synthetic and natural chiral hosts that afford large selectivities, corresponding to differences in free energy of binding for the two enantiomeric guests $-\Delta\Delta G_{R/S}^{\circ}$ larger than 1.5 kcal mol^{-1} (the subscripts *R*/*S*, here and in the following sections, do not indicate elution order or relative binding strengths, but simply indicate the two absolute configurations of the guest). In some cases the same chiral hosts are shown to select the enantiomeric guests with receptor-like selectivities not only when they are linked to a chromatographic support but also when they are in free solution or in the gas phase, suggesting that the key factors responsible for the observed selectivities can be largely ascribed to the host–guest interactions alone.

The occurrence of large enantiodifferentiation displayed by a chiral stationary phase (CSP) is grounded on some requirements which are related to at least five kind of factors:

1. Number and intensity of established selector-enantiomer interactions, both enantioselective and unspecific.
2. Extent of structural flexibility and symmetry characterizing the geometry of the chiral selector.
3. Purity of the chiral selector bonded to the chromatographic matrix.
4. Amount of chiral selector loaded on the chromatographic matrix.
5. Extent of unselective retention imparted by chromatographic matrix towards the enantiomers.

Inspection of these factors reveals that they can be split into those relevant to the peculiar structural properties of the selector operating the enantiomer differentiation (factors summarized in entries 1 and 2), and others more properly related to the manufacturing properties of the assembled chromatographic stationary phase, including the choice of the matrix used to accommodate the chemically bound chiral selector (factors from entries 3–5).

With reference to the first kind of factors, it is pertinent to stress the fundamental role played by the concomitant presence of geometric (i.e., size and shape) and binding sites complementarity between selector and interacting enantiomers (selectands).

Globally, the thermodynamic aspects of a host–guest interaction can be rationalized in terms of additive energetic contributions arising from the establishment of non-covalent forces between the species, distinguishable in (1) highly polar specific (H-bonds) and nonspecific (dipole–dipole and ionic) interactions, strongly energetic and long-range active, (2) dispersive forces (π–π, C–H···aromatic, dipole-stacking), short-range active and commonly established between any kind of molecular surfaces,

although especially facilitated by a high polarizability of the molecular frameworks involved in the contact, and (3) solvophobic forces, at short-range and of entropic origin, strongly active between apolar surfaces in the presence of a polar solvent, which heavily increase their strength on increasing of its permittivity. Importantly, many of the above interactions are multi-point (e.g., π–π, dipole-stacking) rather than single-point interactions (e.g., H-bonds, end-to-end dipole), so that the overall process of complexation will commonly be the result of the establishment of a network of elemental forces, some of which strongly depend on the orientation and/or distance between the interacting partners. Obviously the increasing number of favorable host–guest interactions has a direct impact on the retention time of selectands, but this is not a condition sufficient to also guarantee enantioselectivity, which instead requires the establishment of multiple interactions (at least three, according to the "three-point interaction model") involving in non-equivalent ways the two enantiomers. Typically, non-covalent interactions of the strongest type are those largely responsible for the retention of the guests, while short-range forces are mainly responsible for the enantiorecognition.

From the geometrical point of view, it is possible that the complementarity of the selector towards the selectand can already pre-exist in a rigid structure (often associated with macrocyclic frameworks) or, instead, can be established (most frequently, slightly improved) by suitable conformational changes driven by the progress of host–guest complexation (a mutual two-body conformational evolution commonly denoted as *induced fit*). Frequently, selectors endowed with rigid and quite large structure are associated with receptor-like discriminating behavior, which is typically characterized by really high enantioselectivities (i.e., α values greater than 15, with related $\Delta\Delta G_{R/S}^{\circ}$ close to -1.6 kcal mol^{-1}) but, by contrast, applicability limited to the separation of a rather narrow array of chiral selectands. In contrast, a residual flexibility of the selector structure makes much more probable the success of the enantiorecognition for a greater variety of compound classes, although, typically with reduced α factors. Relevant examples of CSPs manifesting receptor-like selectivities are based on compounds **S1–S11** surface bonded on silica particles, while brush-type (or Pirkle-type) CSPs, less selective but of wider applicability, are based on selectors like compounds **S12–S15** (Chart 1) [12, 61–67]. CSPs endowed with selectivity at receptorial level can be divided into two classes: (1) CSPs based on chemical structures taken from the natural pool, either in their pristine or chemically modified versions (vancomycin, norvancomycin, teicoplanin and its aglycon, ristocetin A, avoparcin, eremomycin glycopeptide macrocyclic antibiotics, or cyclodextrins in the α-, β-, or γ-forms) available in a single enantiomeric version [34, 67] and (2) CSPs based on completely synthetic receptors (e.g., chiral crown ethers, the tetramidic cyclic C_2-chiral selectors **S4–S7**, or the bowl-like C_3-chiral selectors **S10–S11**) available in both enantiomeric versions [55, 62, 66]. The reasons for which rigid structures can perform much more effective enantioseparations have an entropic origin. When in a partially flexible selector, a framework involved in the selective enantiorecognition is located on a portion of molecule that, to interact with the guest, must undergo an induced fit; after complexation the host structure within the

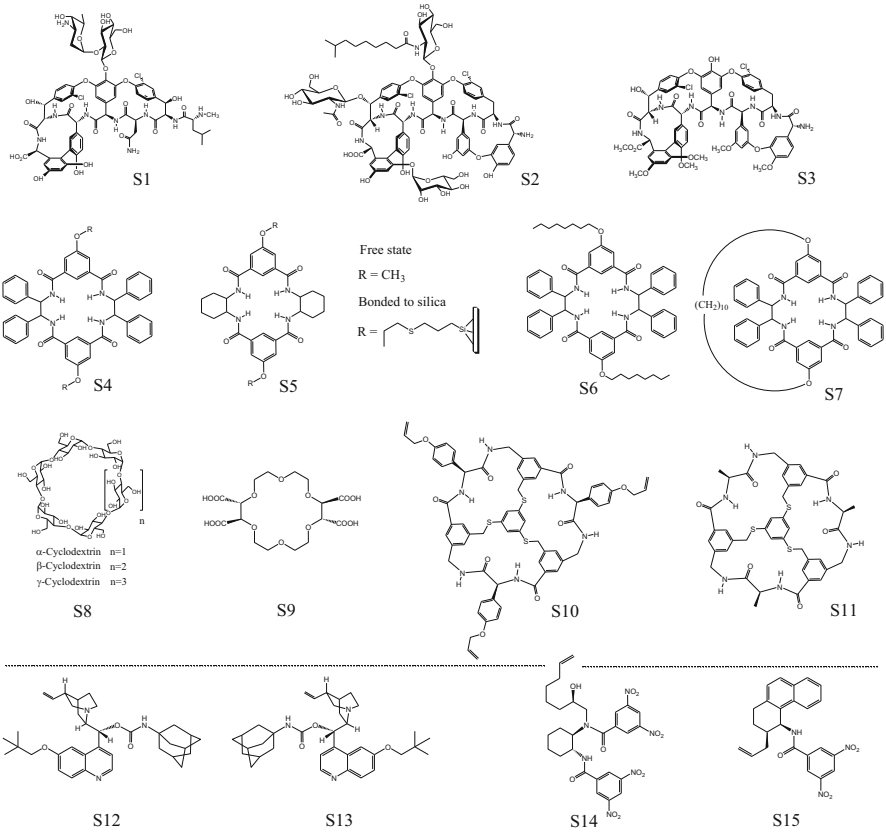

Chart 1 Overview selectors with receptor-like selectivity

resulting most stable supramolecular diastereomer will have lost more freedom degrees of internal rotational motions than its diastereomeric counterpart.

It was evaluated [68–70] that the entropy reduction related to the loss of free rotation around a single bond typically ranges from 3 to 5 cal mol^{-1} K^{-1}. On this basis, therefore, it can be directly assessed that at room temperature the hypothetical complete freezing of each single bond of the host will lead to an increase of the standard free energy variation in the range 0.9–1.5 kcal mol^{-1}, that is, a really significant amount. Such an effect is also expected to be more pronounced in the more stable diastereomeric complex (that in which the host suffered the greatest induced constraint to its original flexibility), leading to partial compensation of the differential enthalpic contribution favorable to the enantiodifferentiation. However, due to the non-covalent nature of the supramolecular interactions, as an effect of complexation, the true reduction of internal rotational motion must always be expected to be incomplete, so that the entropic effect will also never reach the limiting theoretical value.

4.1 Macrocyclic Tetramidic Synthetic Selectors

An interesting example relevant to the entropic effect just discussed is the really different enantiorecognition ability displayed by selectors **S4–S6** towards valine derivative **G1** (Chart 2) when they were employed as bonded to silica (HPLC measurements [66], selectors **S4–S5**), or instead as a free molecule (NMR spectroscopy determination [71], selector **S6**).

Conformational analysis of tetramidic cyclic mini-receptor **S6**, performed by ROESY experiments in free solution (also corroborated by molecular mechanics calculations on structure **S4**), showed that the molecule assumes a C_2-symmetrical "large" cone conformation (resembling a roof structure endowed with a convex and a concave surface both potentially active in establishing effective interaction with guest molecules), with the N–H and C═O bonds of all the amidic groups in *trans* disposition and defining planar frameworks lightly tilted out with respect to the planes containing the isophthalic rings (Fig. 6).

These same amidic moieties alternately point their N–H and C═O bonds inwards and outwards relative to the molecule. Very interestingly, at room temperature and in solution of either deuterated-DMSO or $CDCl_3$, thanks to suitable rotations around the bonds connecting each of the two isophthalic rings to a couple of the four amidic groups (i.e., Ar–C═O bonds), the roof structure of **S6** undergoes a fast flapping-wings movement, which leads to a rapid, continual, and mutual inversion of the convex surface of the molecule to the concave one, and vice versa. This NMR evidence, therefore, suggests scarce rigidity for free **S6** in solution. According to this picture, the enantiodifferentiation of racemic **G1** measured by NMR in $CDCl_3$ solution was quite modest, with $\Delta\Delta G_{R/S}^{\circ} = -0.2$ kcal mol^{-1}, corresponding to a hypothetical chromatographic enantioseparation factor α of only 1.4. The same enantiorecognition carried out by HPLC, with **S4** bonded to silica as the chiral selector, was instead performed with $\alpha = 158$ (i.e., $\Delta\Delta G_{R/S}^{\circ} = -3.0$ kcal mol^{-1}). Such macroscopic discrepancy in enantioselectivity may be reasonably explained by taking into account that receptor **S4** may undergo free and fast surface-flipping only in its free state, where the four C–Ar bonds between carbonyls and isophthalic moieties inside the two fragments O═C–Ar–C═O of the structure retain their rotational freedom and the above-mentioned detrimental entropy effect on α value can certainly be operative. In contrast, in its version as bonded selector of chromatographic CSP, the double covalent linkage of **S4** to silica (Fig. 7), as well as the possibility of its easy supramolecular interaction with the silanols groups on the surface of the matrix, certainly reduces (perhaps completely precludes) the freedom of flipping of the macrocycle, making the structure more rigid and therefore strongly reducing the unfavorable entropic contribution to the values of $\Delta\Delta G_{R/S}^{\circ}$.

In agreement with experimental evidence, molecular mechanics calculations based on a multi-conformational quasi-flexible molecular docking procedure [72, 73] indicated that, taking into account the couple of dominant diastereomeric adducts responsible for the enantiorecognition performed by **S4** on **G1** (structures **S4**(*R*,*R*,*R*,*R*):**G1**(*S*) hetero-chiral and **S4**(*R*,*R*,*R*,*R*):**G1**(*R*) homo-chiral reported in Fig. 8), only in the most stable of

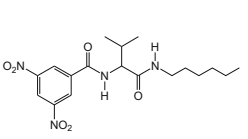

G1

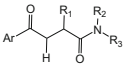

	Ar	R_1	R_2	R_3
G2	3,5- DNP	Me	hexyl	H
G3	3,5- DNP	Et	hexyl	H
G4	3,5- DNP	Pr	hexyl	H
G5	3,5- DNP	Bu	hexyl	H
G6	3,5- DNP	sBu	hexyl	H
G7	3,5- DNP	iBu	hexyl	H
G8	3,5- DNP	tBu	hexyl	H
G9	3,5- DNP	Ph	hexyl	H

	Ar	R_1	R_2	R_3
G10	3,5- DNP	Bn	hexyl	H
G11	3,5- DNP	Tio*	hexyl	H
G12	3,5- DNP	iPr	Et	Et
G13	3,5- DNP	iPr	tBu	H
G14	3,5- DNP	iPr	1-Adm*	H
G15	Ph	iBu	hexyl	H
G16	C_6F_5	iBu	hexyl	H
G17	1-naphthy	iBu	hexyl	H

Tio*= $MeSCH_2CH_2$
1-Adm* = 1-Adamantyl

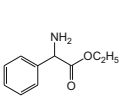

G18

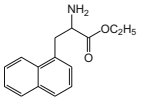

G19

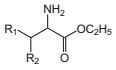

G20 (R_1 =R_2 =H)
G21 (R_1 =R_2 =CH_3)
G22 (R_1 = H ; R_2 = CH_3H_7)
G23 (R_1 = H; R_2 =C_2H_5)
G24 (R_1 = H; R_2 = OH)
G25 (R_1 = CH_3; R_2 =OH)

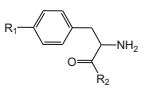

G26 (R_1 = H; R_2 = OH)
G27 (R_1 = H; R_2 = NH_2)
G28 (R_1 = H ; R_2 = OC_2H_5)
G29 (R_1 = F; R_2 = OC_2H_5)
G30 (R_1 = OCH_3; R_2 = OC_2H_5)

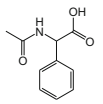

G31

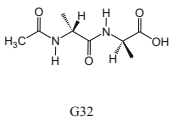

G32

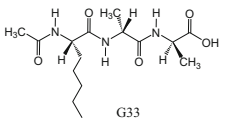

G33

G34

G35

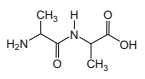

G36

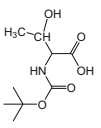

G37

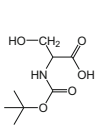

G38

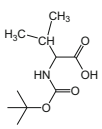

G39

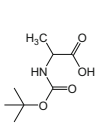

G40

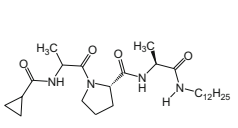

G41

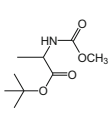

G42

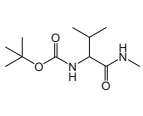

G43

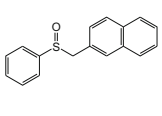

G44

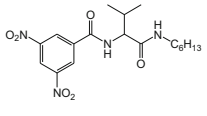

G45

Chart 2 Chiral selectands enantiodifferentiated by selectors shown in Chart 1

the two (that corresponding to the transient hetero-chiral diastereomer formed by the most retained enantiomer) does the selectand interact, via a couple of H-bonds, with both the framework-*wings* at the concave face of the host but just with one half of the selector structure (i.e., with a single *wing*) in the diastereomer formed by the less retained enantiomer, again at the concave surface (see Fig. 8). Beside the rigidity factor and the presence of functionalities strongly active in determining effective interactions with guests (i.e., the four amide groups), other properties of selectors **S4** and **S6** have to be stressed as relevant to the enantiorecognition mechanism. In fact, when the structure

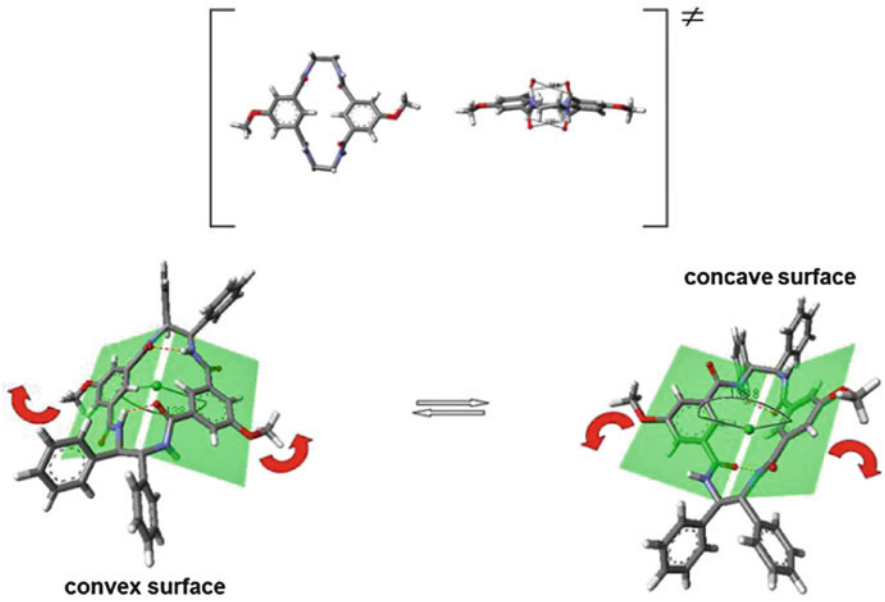

Fig. 6 Computed structure of selector **S4** (*bottom of figure*) and of the hypothetical transition state allowing the fast flipping in solution

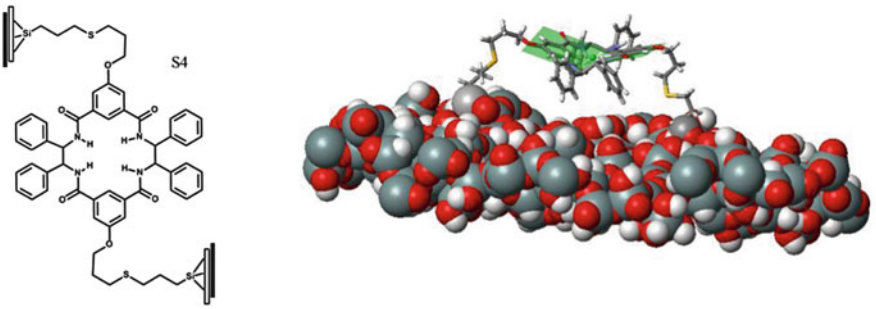

Fig. 7 Version of selector **S4** bonded to silica

of **S4** is deprived of the phenyl moieties bonded on the chiral carbon atoms, as was done by synthesizing the new selector **S5**, enantioselectivity α values for a wide number of chiral guests dramatically drop down (for the 17 different amino acid derivatives **G2–G17** in Chart 2 , showing enantioselectivities in excess of 100 on **S4** while α values were always smaller than 2 on **S5**), so indicating unambiguously the fundamental role played by these aromatic frameworks in the establishment of selective interactions in the form of dispersive forces and/or steric hindrance (i.e., forces of attractive and/or repulsive nature, respectively).

Further experiments [74–76], performed by mass spectrometry (MS) techniques (Fourier transform ion cyclotron resonance, FT-ICR, and collision-induced

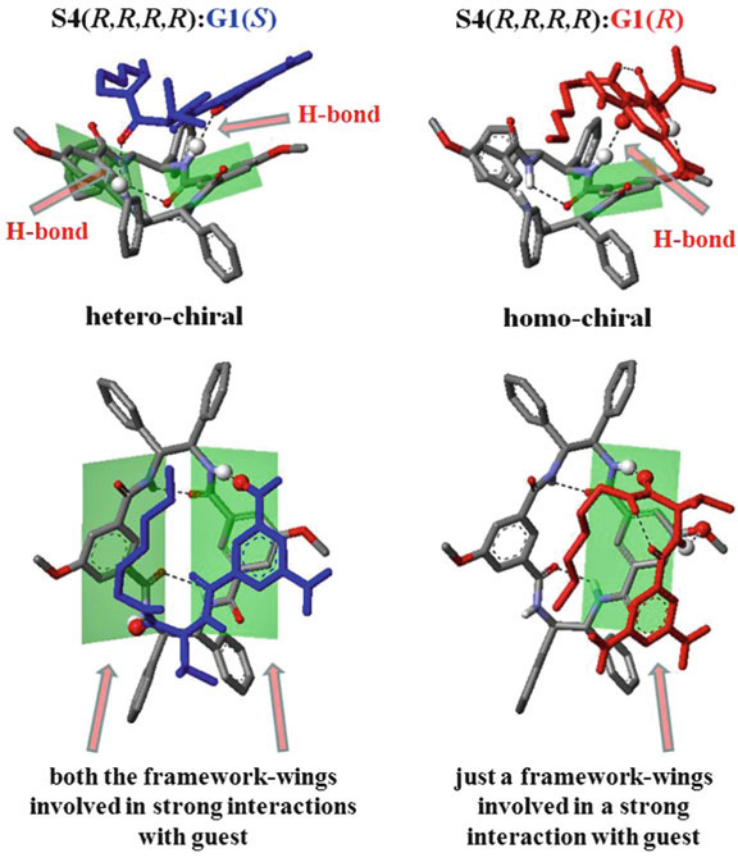

Fig. 8 Calculated most stable and representative homochiral and hetero-chiral adducts formed by selector **S4** and racemic guest **G1** (*red* and *blue* structures). Both the wings-frameworks of the hetero-chiral adduct are involved in H-bonds (pointed by *red arrows*) with the guest, whereas just one in the homo-chiral

dissociation, CID, methodologies) and focusing on analyzing the enantioselective behavior of **S4** in gas phase, confirmed the receptor-like ability of this tetramidic macrocycle in differentiating with high enantioselectivity suitably modified protonated α-amino acids (guests **G18–G30**, Chart 2, $\Delta\Delta G_{R/S}^{\circ}$ approaching the value of -1.8 kcal mol^{-1}). In these cases, however, theoretical molecular docking calculations showed that the supramolecular interactions take place on the convex surface of the host (Fig. 9).

An important point to note is that, with both FT-ICR and CID techniques, the enantioselectivity of receptor **S4** was studied by monitoring the dissociation of different pre-formed complexes of **S4** with the chiral guests **G** [75]: (1) the diastereomeric proton bound dimers [**S4**·H·**G**]$^+$ using the FT-ICR approach and (2) the diastereomeric proton bound trimers [(**S4**)$_2$·H·**G**]$^+$ using the CID approach.

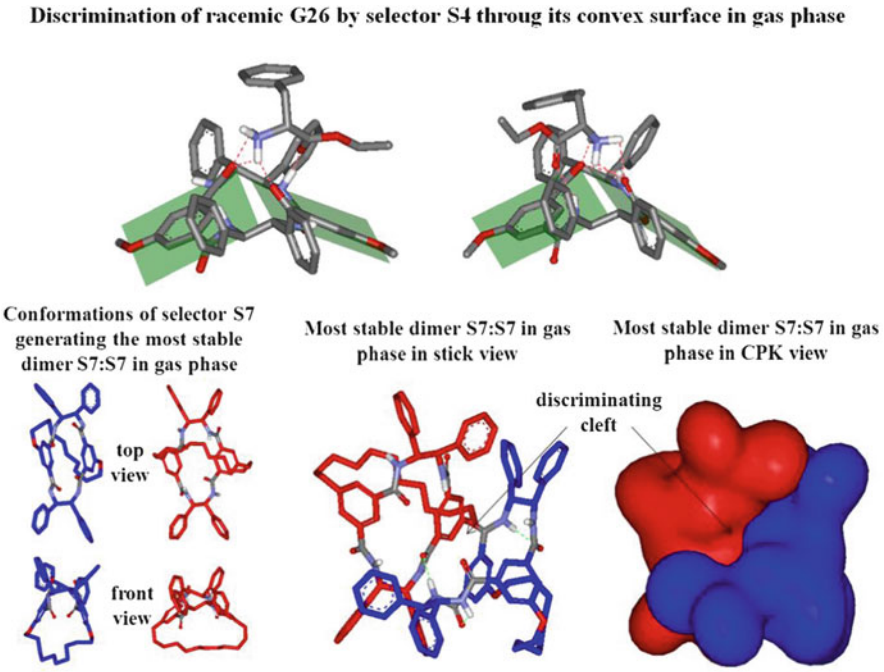

Fig. 9 Computed structures of transient diastereomers formed in gas phase between selector **S4** and the enantiomers of guest **G26** and stiff structure of the dimer **S7**:**S7** formed by selector **S7**

Within these complexes, **S4** is expected to have lost its original flexibility and is also expected to be rigidly held in a single conformation. Thus, the detrimental entropic effects observed in free solution are no longer operative here, as confirmed by the large enantioselectivity values experimentally observed.

Again, a significant improvement in enantioselectivity was observed in gas phase experiments in response to an increased stiffness of the selector **S4**, whose two isophthalic moieties were connected through an alkyl chain consisting of ten methylene groups (selector **S7**) [75, 77]. By FT-ICR-MS determinations, in its monomeric form receptor **S7** allowed the achievement of the really good enantioresolution factor $\Delta\Delta G_{R/S}^{\circ} = -2.0$ kcal mol^{-1} towards guest **G19**, which, however, increased to -2.6 kcal mol^{-1} with self-assembled **S7** that generates a largely constrained supramolecular dimer **S7**:**S7** (Fig. 9). Just this increase in stiffness, that arises from the particular and numerically limited conformational multiplicity of host **S7**, has been interpreted as the fourth "player" that, added to the classical three "players" of Davankov's model, may account for an enantioselectivity approaching that typical of biological receptors [77].

4.2 Glycopeptide Antibiotics

Enantioselectivities of similar high level are also expressed by the wide class of glycopeptide antibiotics, of which vancomycin (VA), **S1**, and teicoplanin (TE), **S2**, are very important and representative members [67]. The really determinant feature, common to the whole members of the class, is a heptapeptide core that extends itself along the main axis of the structure, and whose side chains are covalently joined to one other to form very rigid macrocycles. Looking at the cleft in its horizontal orientation (about 13–14 Å in length), the C-terminal group is placed on the left side, while the N-terminal to the right, with the numbering starting from the C-terminal amino acid (Fig. 10).

The rear wall and the ceiling defining the resulting ligand-binding cavity of the structure are just constituted by a biaryl ether framework departing from the second, fourth, and sixth amino acidic units of the peptide chain, while the left side of the cleft is closed by a biaryl moiety connected to the first and third amino acidic units. Thus, in VA-type antibiotics the right side of the active cleft is open and prone to allow a quite easy insertion of the chiral selectand to recognize. Instead, in TE-type antibiotics the right side of the cavity is closed by an additional biaryl ether moiety, departing from the side chains of the fifth and seventh amino acidic units of the heptapeptide core (Fig. 10). Sugar frameworks bonded at various positions of the macrocyclic cage (i.e., of the aglycone fragment) complete the pristine structure of such antibiotics. As pointed out by a really in-depth study [78], sugar frameworks are typically involved in controlling water solubility a and tendency to self-aggregation of these kinds of molecules, but they are not really important in modulating the enantiorecognition of chiral species. A typical example relevant to this evidence is the enantioresolution of *N*-acetylphenylglycine (*N*-APG, **G31**, Chart 2) performed by TE CSP, **S2**, and teicoplanin aglycone (TAG) CSP [67], **S3**. Indeed, the enantioseparation factor α obtained by TE CSP approaches the value of 64 ($\Delta\Delta G_{R/S}^{\circ} = -2.5$ kcal mol^{-1}), while that achieved through TAG CSP amounts to 82 ($\Delta\Delta G_{R/S}^{\circ} = -2.6$ kcal mol^{-1}), thus suggesting a virtual absence of participation of sugars in the discrimination process. However, numerous other enantioseparations in which the presence of native sugars caused a sensible reduction of α have been reported [78], indicating that probably their major effect is in hindering the approach of the guests to the cavity responsible for the enantiodifferentiation. Coherently with the example just reported, substrates of election for good enantiorecognition performed by TE-type or VA-type antibiotics are represented by amino acids, di- and tri-peptides, either pure or derivatized (especially as *N*-acetylated derivatives, **G31–G33**), with D-configured members showing larger bonding and retention. More specifically, a model of the enantiorecognition mechanism operated by TAG towards chiral amino acids as either independent units or incorporated into oligopeptide chains has been proposed [67] starting with molecular modelling studies based on multi-conformational molecular docking [72, 73] (Fig. 10). When the C-terminal group of the selectand is in the free carboxylate form and the amino function is derivatized as amide moiety, two patterns of interactions involved into the enantiodifferentiation may be identified: the first,

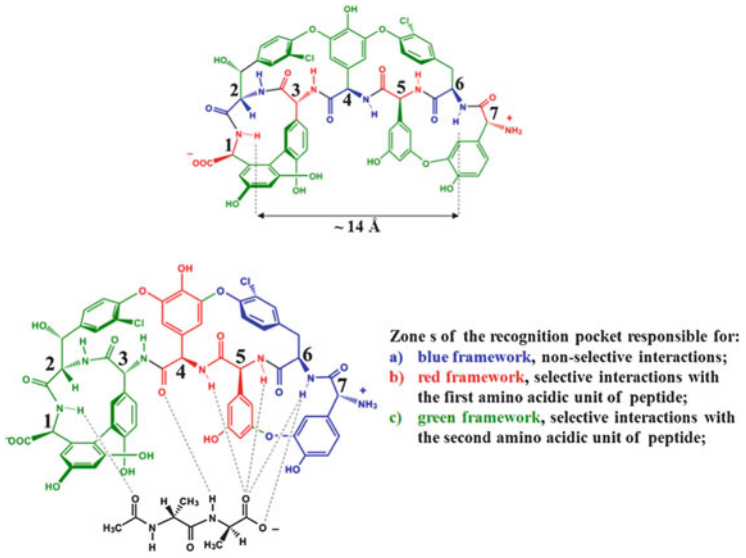

Fig. 10 Essential structure of the recognition pocket of TAG (selector **S3**) and mechanism of discrimination operated on peptides, as suggested by theoretical studies

energetically strong and non-selective, is responsible for binding and for the correct orientation of the selectand along the recognizing cleft; the second pattern is instead responsible for the enantioselectivity, and involves, as major partners, the N–H and carbonyl groups belonging to the first and fourth unit of the heptapeptide core, respectively (the N–H bond only in case of peptidic guests). The non-selective interactions mainly consist in H-bonds established among the carboxylate group of the guest and the three N–H bonds belonging to the fourth, fifth, and sixth amide groups of the heptapeptide chain. Nevertheless, dispersive forces involving the aromatic frameworks defining the cleft also contribute to both retention and differentiation of the enantiomers in a significant way. Thus, the recognition cleft (Fig. 10) can be schematically divided into two regions having different roles in controlling guest retention and enantioselectivity. One region, about 6 Å wide, extends from the N-terminal group towards the interior of the structure and controls the major contribution to retention. The other region extends from the central amino acid residue (4 in figure 10) towards the C-terminal group, and controls the enantioselective properties of the receptor. This region can recognize the stereoisomers of small amino acid derivatives and of acylated dipeptides, exploiting the outermost left region of the cleft to accommodate the larger guests. Coherently with the model described, the experimental enantioresolution of *N*-APG performed by TAG CSP ($\Delta\Delta G_{R/S}^{\circ} = -2.6$ kcal mol$_{-1}$) has been simulated and reproduced by docking procedure with an error of only 0.2 kcal mol^{-1} (the computed difference in free energy of binding was $\Delta\Delta G_{R/S}^{\circ} = -2.8$ kcal mol^{-1}). The experimental findings concerning the enantioresolution of underivatized amino acids proline (Pro, **G34**) and alanine (Ala, **G35**)

as well as that of the dipeptide alanyl-alanine (Ala-Ala, D,D/L,L forms **G36**) are also relevant to the above-mentioned discrimination mechanism [79]. The related α and $\Delta\Delta G_{R/S}^{\circ}$ values are as follows: Pro, $\alpha = 3.8$, $\Delta\Delta G_{R/S}^{\circ} = -0.79$ kcal mol^{-1}; Ala, $\alpha = 3.0$, $\Delta\Delta G_{R/S}^{\circ} = -0.65$ kcal mol^{-1}; Ala-Ala, $\alpha = 119$, $\Delta\Delta G_{R/S}^{\circ} = -2.83$ kcal mol^{-1}. By recalling that sugars have a negligible effect on the global context of the enantiodifferentiation mechanism (i.e., by assuming for TE CSP an association mechanism equivalent to that of TAG CSP), it can be seen that such results clearly match the above-mentioned enantioresolution model, with the expected strong increase of selectivity for the Ala-Ala dipeptide in response to the additional contribution to the enantiorecognition operating in this case (but not in that of Pro or Ala) by the end left zone of the receptor pocket.

4.3 C_3 Symmetric Macrocyclic Selector

Enantio- and diastereoselectivity factors of receptorial levels towards suitably derivatized amino acids (α values of 43.0, 35.3, 24.8, and 21.0 for **G37–G40**, threonine, valine, serine, and alanine derivatives, respectively) and oligopeptides (e.g., $\alpha = 21.0$ for D/L-Ala-L-Pro-L-Ala, **G41**) were also observed with the C_3-symmetric L-tyrosyl macrocycle **S10** [61–63] (Fig. 11). The large enantioselectivities are certainly connected to the presence in the selector structure of several functionalities able to establish multiple and effective hydrogen bonds (six amide groups) in the context of a strongly rigid bowl-like pocket. However, unlike glycopeptide antibiotics, in this case, the recognition ability is limited to the interaction with just one amino acidic unit of the guest, according to a quite general enantiodifferentiation mechanism that was proposed by a theoretical study, again based on molecular docking procedure [72, 73] (selector **S11** and guest **G42**, Fig. 11).

An interesting and peculiar aspect of receptors like **S4–S7** and **S10** is that they possess a proper axis of symmetry, which is certainly involved in modulating their retention ability. Indeed, there was in the past some disagreement about the role that symmetry can play in influencing the enantioselectivity of CSPs. This controversy originated from a preliminary interpretation given through statistical analysis of enantioresolutions performed on microcrystalline cellulose triacetate CSP of chiral guests having either C_2 or C_1 symmetry [80]. However, further successive determinations of α factors, aimed at shedding light on the matter, also corroborated by considerations relevant to the thermodynamic aspects involved by the process of enantio-discrimination [81], have clarified that "there is nothing inherent in C_n-symmetry which increases enantioselectivity," while it is expected that, for entropic reasons, the presence of a C_n proper axis of symmetry related to the structure of a chiral host will affect the retention according to an increase of its binding energy with the enantiomeric guests quantifiable as the amount RT × ln(n), n being the multiplicity of the axis of symmetry. Since the same increase applies with both enantiomers, it will not be able to affect per se the ratio between the corrected retention times of the enantiomers (i.e., α). Nevertheless, as is stressed below, under

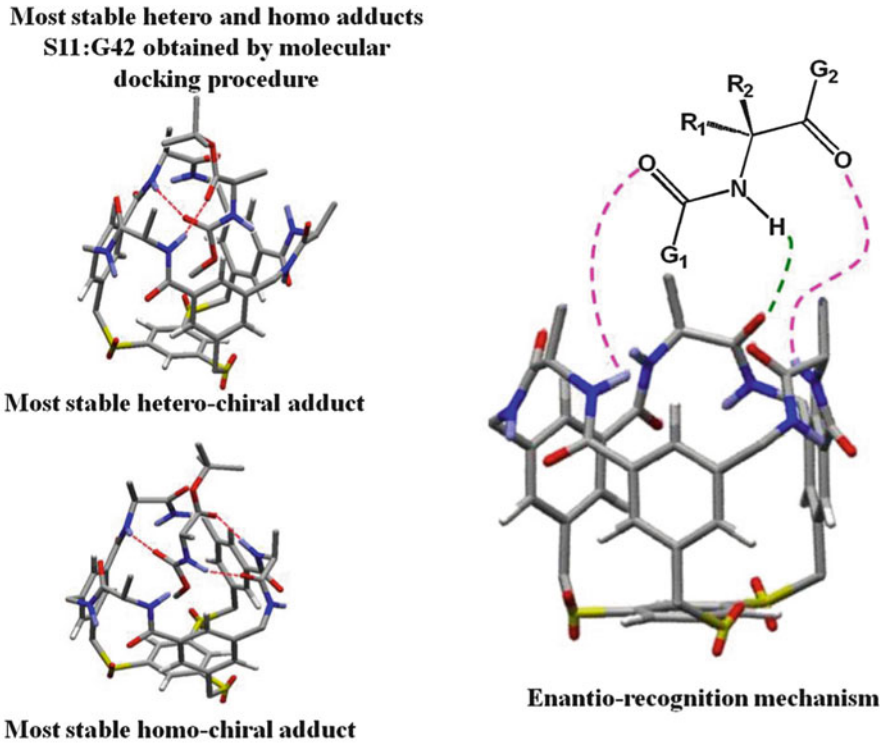

Fig. 11 Computed structures of the most stable and representative adducts formed between selector **S11** of C_3-symmetry and racemic of guest **G42** (*left side*). Generalization of the recognition mechanism proposed through docking studies (*right side*)

proper conditions the increase of retention could also have an indirect and positive effect on the apparent value of α.

4.4 Matrix Effects and Mixed Selectors

Beside the central and direct role played by the structural properties of the selector, other factors can influence the enantioselectivity that can be expressed by a chromatographic chiral stationary phase (CSP). Among these, determinants are the matrix chosen to host the selector in bonded form and the extent of loading and purity with which the same selector will be present in the final separation device. Recently [82, 83] these dependences have been incorporated in a simple mathematical formalization for the particular case of a chiral stationary phase containing binary-selectors:

$$\alpha_{\text{app}} = \frac{k'_0 + x_{\text{s1}} \cdot (K^{\text{s1}}_{R^*} \cdot C_{\text{s1}}) + x_{\text{s2}} \cdot (K^{\text{s2}}_{R^*} \cdot C_{\text{s2}})}{k'_0 + x_{\text{s1}} \cdot (K^{\text{s1}}_{S^*} \cdot C_{\text{s1}}) + x_{\text{s2}} \cdot (K^{\text{s2}}_{S^*} \cdot C_{\text{s2}})} \tag{1}$$

where α_{app} represents the enantioseparation factor directly calculable from the experimental chromatogram, and it can only approach the true value of α (that related to the only interaction selector–enantiomers, α_{true}), k'_0 is the non-selective retention factor expressed by the matrix towards both the enantiomers, $K^{s1}_{R^*}$, $K^{s1}_{S^*}$, $K^{s2}_{R^*}$, and $K^{s2}_{S^*}$ are the stability constants of complexes that enantiomers of relative configuration *R** and *S** formed with selectors s1 and s2, respectively, x_{s1} and x_{s2} represent the fraction of chromatographic phase containing selector s1 or s2 which contributes to the constitution of the whole CSP and, finally, C_{s1} and C_{s2} express the loading with which selectors s1 and s2 have been bonded to the phase. The products of type $K^{s1}_{E^*}$. C_{sn} are therefore amounts corresponding to the hypothetical retention factors, $k'_{E^*}sn$, with which enantiomers of relative configuration *E** (with *E** equal to *R** or *S**) would be eluted by the column containing only selector s*n*, without any non-selective contribution of matrix.

Starting from (1) a direct extension to the general case of multi-selector CSPs appears possible:

$$\alpha_{app} = \frac{k'_0 + \sum_i x_{si} \cdot (K^{s1}_{R^*} \cdot C_{si})}{k'_0 + \sum_i x_{si} \cdot (K^{s1}_{S^*} \cdot C_{si})} = \frac{k'_0 + \sum_i x_{si} \cdot k'^{si}_{R^*}}{k'_0 + \sum_i x_{si} \cdot k'^{si}_{S^*}} \tag{2}$$

By considering (2), it is evident that α_{app} can approach α_{true} if the contribution of k'_0 become negligible with respect to the cumulation of both selective and non-selective retention expressed by the selectors si bonded to the matrix.

Thus it may be concluded that the global retention of each enantiomer of relative configuration *E**, k'_{E^*}, can be expressed as a linear combination of contributions according to

$$k'_{E^*} = k'_0 + \sum_i k'^{si}_{E^*} \tag{3}$$

Consequently, at each k'_{E^*} value it is also possible to assign a percentage contribution coming from the matrix, $\%(k'_0/k'_{E^*})$, which will be analyzed below in order to highlight its detrimental effect on α_{app}.

The correctness of (1) was demonstrated by reproducing with high accuracy the α_{app} values determined by enantioresolution of *N*-3,5-dinitrobenzoyl α-amino acids (DNBAA) through a series of seven batches of CSPs, containing different molar fractions of adamantyl, neopentyl derivative of quinine (selector **S12**), and quinidine (selector **S13**) bonded on the same kind of matrix (a mercaptopropyl-modified silica gel) [83, 84]. Natural quinine and quinidine are diastereomers that show quasi pseudo-enantiomeric differentiation ability towards DNBAAs, so that in the quoted study they were used to mimic the case of non-racemic mixtures of a chiral selector bonded to silica as the discriminating tool, with the enantiomeric composition ranging from the pure enantiomer to the racemate. The relevant findings pointed out that, on increasing α_{true}, the α_{app} value drops much more rapidly as a function of loss of enantiomeric purity of selector. This behaviur is evident by looking at the

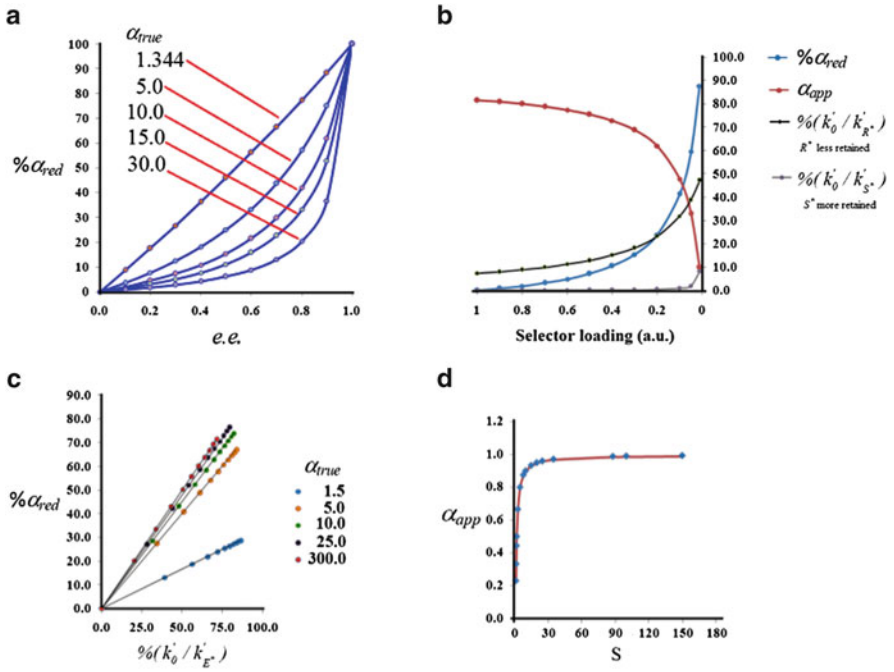

Fig. 12 Changes of α_{app} values as a function of enantiomeric excess of the chiral selector (**a**), extent of selector loading (**b**), non-selective contribution of matrix or selector to retention (**c** and **d**)

graph of Fig. 12a, where the percentage loss of enantioselectivity ($\%\alpha_{red}$) is plotted against the change of enantiomeric excess (e.e.) calculated by (2) for different values of α_{true}. By resorting to (2) it is also evident how the loading of chiral selector on the CSP affects the measurable value of α_{app} with respect to the relevant α_{true}.

The plot in Fig. 12b clearly shows that, as a consequence of a linear reduction of selector loading, the decrease of α_{app} is exponential. This is because, as the amount of selector decreases, the retention of the enantiomers is also reduced, so that the percentage of non-selective contribution afforded by the matrix to their retention (i.e., the $\%(k'_0/k'_{E^*})$ quantity) grows quickly. Again, through (2) it is possible to simulate in a realistic way how a progressive growth of $\%(k'_0/k'_{E^*})$ influences α_{app}. In Fig. 12c a relevant graph is presented in which increasing $\%(k'_0/k'_{E^*})$ values are plotted against the corresponding percentages of enantioresolution reduction, $\%\alpha_{red} = (\alpha_{true} - \alpha_{app})/\alpha_{true} \times 100$, which were calculated by (2) in the form limited to the presence of a single selector. The trend was also analyzed as a function of α_{true} (five values in the range from 1.5 to 300). Inspection of the graph shows that the dependence between $\%(k'_0/k'_{E^*})$ and $\%\alpha_{red}$ data is linear, with a slope (**S**, in the plot of Fig. 12d) that increase quickly for α_{true} varying from 1 to 25, while with a much slower progression for greater enantioselectivities, approaching unity as the limiting value (Fig. 12d).

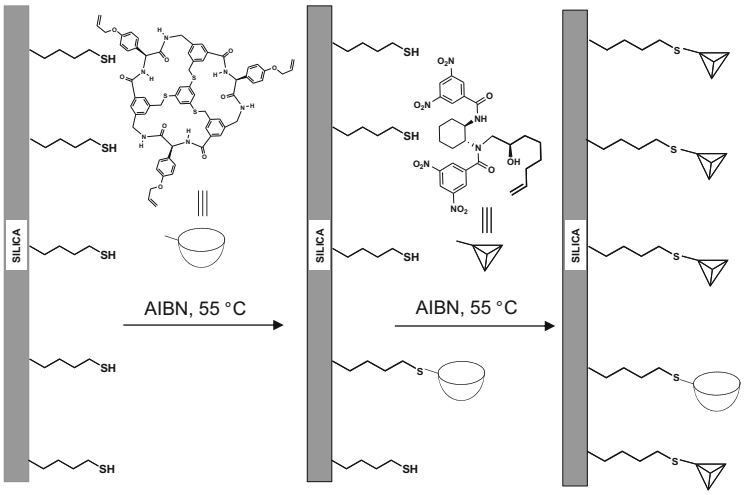

Fig. 13 Preparation of mixed-selector $CSP_{\mathbf{S10/S14}}$ through consecutive radical thiol-ene reactions of **S10** and **S14** with γ-mercaptopropyl silica gel

This means that, looking at all the factors responsible for the non-selective retention of the enantiomers (i.e., those leading to a growth of $\%(k'_0/k'_{E^*})$), either an increase due to a greater interaction with the matrix or a reduction due to a lesser unspecific interaction with the chiral selector, will lead to a detrimental reduction of α_{app}, with maximum impact achieved for α_{true} values greater than 25 (Fig. 12d).

A further important potentiality offered by (1) and its extended version (2) is the realistic simulation of the enantioselective behavior of CSPs bearing in bonded fashion two or more different chiral selectors (Fig. 13). Besides the considerations of the above example involving quinine and quinidine derivatives **S12** and **S13**, it is interesting to consider the new cases reported in Fig. 14a–d. These chromatograms were obtained by performing enantioseparations of some chiral species through the use of CSPs containing either the C_3-symmetric receptor **S10** ($CSP_{\mathbf{S10}}$) or the brush-type selector **S14**, the latter in the two enantiomeric (*R*,*R*,*R*) and (*S*,*S*,*S*) versions ($^{R}CSP_{\mathbf{S14}}$ and $^{S}CSP_{\mathbf{S14}}$), as well as the mixed-selector CSPs obtained by the sequential bonding of the two selectors in a 20:80 molar ratio ($^{R}CSP_{\mathbf{S10/S14}}$ and $^{S}CSP_{\mathbf{S10/S14}}$), respectively [62, 85]. In case 1, reported in Fig. 14a, chiral selector **S14** does not show any selectivity with regard to the analyzed valine derivative, **G43**, so that it acts as a non-selective retention agent. By contrast, the enantiomers of the same selectand are effectively recognized on $CSP_{\mathbf{S10}}$, with $\alpha = 35.3$. According to (1), for the resolution of chiral **G43**, performed through $^{R}CSP_{\mathbf{S10/S14}}$, an α_{app} value of 6.6 was assessed, against the experimental value of 7.7 (an error of only 0.1 kcal mol^{-1} on $\Delta\Delta G^{\circ}$). In a similar but opposite way, the chiral naphthylmethyl-phenyl-sulfoxide, **G44**, was effectively resolved by $^{R}CSP_{\mathbf{S14}}$ ($\alpha = 2.2$) but not by $CSP_{\mathbf{S10}}$ ($\alpha = 1.0$, Fig. 14b). The enantioresolution performed with $^{R}CSP_{\mathbf{S10/S14}}$ afforded $\alpha_{app} = 1.9$, in good agreement with the value $\alpha_{app} = 2.0$

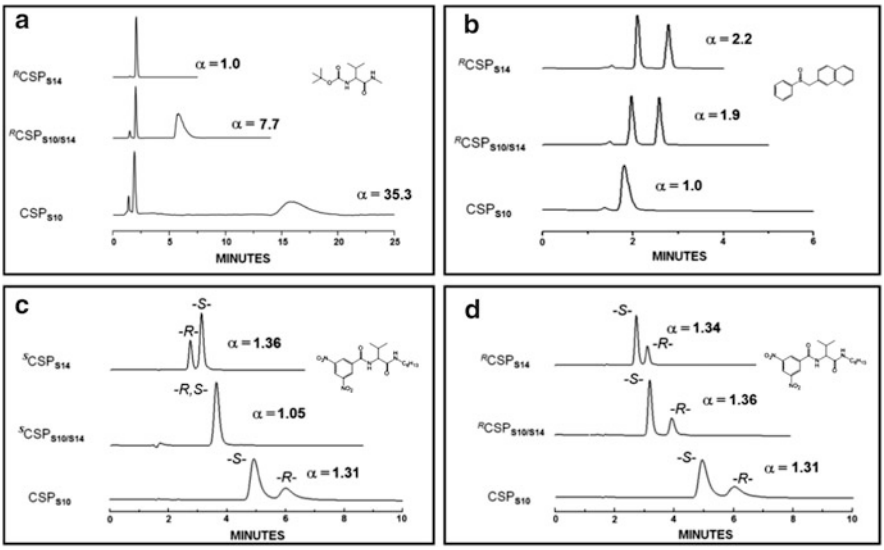

Fig. 14 Enantioseparations of some chiral species (**G43** in **a**, **G44** in **b**, **G45** in **c** and **d**) through use of CSPs containing the C_3-symmetric receptor **S10** ($CSP_{\mathbf{S10}}$), the brush-type selector **S14** in both its enantiomeric (*R*,*R*,*R*) and (*S*,*S*,*S*) versions ($^{R}CSP_{\mathbf{S14}}$ and $^{S}CSP_{\mathbf{S14}}$), and the mixed-selector CSPs ($^{R}CSP_{\mathbf{S10/S14}}$ and $^{S}CSP_{\mathbf{S10/S14}}$). In **c** and **d** are reported the cases of mismatching and matching of enantioselectivity, respectively, towards the valine derivative **G45**

assessed by (1) (an error of 0.03 kcal mol^{-1} on $\Delta\Delta G^{\circ}$). Finally, Fig. 14c, d refers to two examples of enantiorecognition in which the used $^{R}CSP_{\mathbf{S10/S14}}$ and $^{S}CSP_{\mathbf{S10/S14}}$ give rise to unprecedented cases of matching and mismatching of enantioselectivity towards valine derivative, **G45**, with protected carboxyl and amino terminal end groups. The example given in Fig. 14c presents the case of enantioselective mismatching, in which (***R***)-**G45** is eluted first on $^{S}CSP_{\mathbf{S14}}$ ($\alpha = 1.36$), while it is the second eluted enantiomer on $CSP_{\mathbf{S10}}$ ($\alpha = 1.31$). Instead, just as was predicted from (1) ($\alpha_{app} = 1.05$), the $^{S}CSP_{\mathbf{S10/S14}}$ was unable to perform the enantioresolution and gave an experimental enantioselectivity $\alpha = 1.0$. In contrast, Fig. 14d shows the case of enantioselective matching, in which (***R***)-**G45** is the second eluted enantiomer on $^{R}CSP_{\mathbf{S14}}$ ($\alpha = 1.34$), the same order of elution performed by $CSP_{\mathbf{S10}}$. Thus, in this case, through the mixed $^{R}CSP_{\mathbf{S10/S14}}$, **G45** was favorably resolved, although with a reduced retention, with a final experimental $\alpha_{app} = 1.36$ (virtually indistinguishable from that obtained through $^{R}CSP_{\mathbf{S14}}$), which was again correctly predicted by calculation ($\alpha_{app} = 1.33$).

5 Concluding Remarks

In the present chapter we first presented a brief introduction on supramolecular host–guest chemistry, with a general description of the structural features that control and modulate the ability of a given host to interact selectively with a range of guests. Incorporation of enantioselectivity in such systems, obtained by rational design as well as by inspiration from naturally occurring structures leads to chiral, enantiopure hosts that are able to bind the enantiomers of chiral guests with selectivities equalling or exceeding those observed for natural macromolecular receptors. Immobilization of synthetic or natural chiral macrocyclic selectors onto a chromatographic stationary phase opens the way to the field of enantioselective supramolecular chromatography, a particular area of investigation that combines the principles of supramolecular chemistry with the separation ability of modern chromatography. Liquid chromatography on stationary phases containing chiral supramolecular selectors affords enantioselectivity data for a large range of structurally diverse chiral guests, and these data are used to corroborate and to refine recognition models elaborated from spectroscopic investigations and computer simulations. Recognition models, in turn, are used to design improved supramolecular selectors and to rationalize enantioselectivities observed for the same hosts in different environments.

Some structural features that are responsible for high levels of enantioselectivity shown by chiral host–guest systems are clearly identified from the analysis of several chromatographic supramolecular systems: preorganization and conformational homogeneity and presence of binding sites with high directionality in the host, size and binding sites complementarity for the guest. These principles have been demonstrated with a series of chiral tetramidic macrocyclic hosts, assembled from isophthalic acid and C_2 symmetric 1,2-diamines: these hosts afford receptor-like enantioselectivities either towards the enantiomers of neutral amino acid derivatives when they are immobilized on chromatographic media or towards free amino acids and carboxy protected amino acids in the gas phase. Natural glycopeptide antibiotics like teicoplanin and vancomycin generate extreme enantioselectivities when they are covalently immobilized on chromatographic supports: enantiomeric guests resembling the D-Ala-D-Ala terminus of their natural ligand are strongly retained compared to the L-configured guests. Supramolecular associations between both synthetic and natural chiral hosts and their guests are investigated by computer simulations to unravel the structural determinants of affinity and selectivity.

The underlying chromatographic matrix and the enantiomeric purity of the chiral selector are additional factors that modulate enantioselectivity in supramolecular chromatography, with the latter aspect becoming increasingly important as selectivity approaches receptor-like levels. Chromatographic stationary phases containing mixed selectors with matched or mismatched selectivities are intriguing systems to investigate theoretically and experimentally mutual effects of multiple selectors on organized surfaces.

References

1. Lehn JM (1988) Supramolecular chemistry – scope and perspectives molecules, supermolecules, and molecular devices. Angew Chem Int Ed Engl 27:89–112
2. Cram DJ, Cram JM (1994) Container molecules and their guests. The Royal Society of Chemistry, Cambridge
3. Cram DJ (1986) Preorganization – from solvents to spherands. Angew Chem Int Ed Engl 25:1039–1057
4. Cram DJ (1988) The design of molecular hosts, guests, and their complexes. Angew Chem Int Ed Engl 27:1009–1020
5. Lehn JM (1993) Supramolecular chemistry. Science 260:1762–1763
6. Lehn JM (2002) Towards complex matter: supramolecular chemistry and self-organization. Proc Natl Acad Sci U S A 99:4763–4768
7. Ema T (2012) Synthetic macrocyclic receptors in chiral analysis and separation. J Incl Phenom Macrocycl Chem 74:41–55
8. Bianco A, Gasparrini F, Maggini M, Misiti D, Polese A, Prato M, Scorrano G, Toniolo C, Villani C (1997) Molecular recognition by a silica-bound fullerene derivative. J Am Chem Soc 119:7550–7554
9. Bogdanski A, Wistuba D, Larsen KL, Hartnagel U, Hirsch A, Schurig V (2010) Reciprocal principle of molecular recognition in supramolecular chromatography – highly selective analytical separation of cyclodextrin congeners on a silica-bonded [60]fullerene stationary phase. New J Chem 34:693–698
10. Schurig V (2012) Supramolecular chromatography. In: Schneider HJ (ed) Applications of supramolecular chemistry. CRC/Taylor & Francis Group, Boca Raton, pp 129–157
11. Gasparrini F, D'Acquarica I, Misiti D, Pierini M, Villani C (2003) Natural and totally synthetic receptors in the innovative design of HPLC chiral stationary phases. Pure Appl Chem 75: 407–412
12. Lämmerhofer M (2010) Chiral recognition by enantioselective liquid chromatography: mechanisms and modern chiral stationary phases. J Chromatogr A 1217:814–856
13. Cavazzini A, Pasti L, Massi A, Marchetti N, Dondi F (2011) Recent applications in chiral high performance liquid chromatography: a review. Anal Chim Acta 706:205–222
14. Scriba GKE (2012) Chiral recognition mechanisms in analytical separation sciences. Chromatographia 75:815–838
15. Villiers A (1891) Sur la transformation de la fécule en dextrine par le ferment butyrique. Compt Rend Fr Acad Sci 112:435–438
16. Schumacher DD, Mitchell CR, Xiao TL, Rozhkov RV, Larock RC, Armstrong DW (2003) Cyclodextrin-based liquid chromatographic enantiomeric separation of chiral dihydrofuro-coumarins, an emerging class of medicinal compounds. J Chromatogr A 1011:1037
17. Szejtli J (1998) Introduction and general overview of cyclodextrin chemistry. Chem Rev 98: 1743–1753
18. Szejtli J (2004) Past, present, and future of cyclodextrin research. Pure Appl Chem 76: 1825–1845
19. Szejtli J (2004) In encyclopedia of nanoscience and nanotechnology, vol 2. Marcel Dekker, New York, pp 283–384
20. Li S, Purdy WC (1992) Cyclodextrins and their applications in analytical chemistry. Chem Rev 92:1457–1470
21. Biwer A, Antranikian G, Heinzle E (2002) Enzymatic production of cyclodextrins. Appl Microbiol Biotechnol 59:609–617
22. Bender ML, Komiyama M (1978) Cyclodextrin chemistry-reactivity and structure, concepts in organic chemistry, vol 6. Springer, Berlin
23. Rekharsky MV, Inoue Y (1998) Complexation thermodynamics of cyclodextrins. Chem Rev 98:1875–1918

24. Brewster ME, Loftsson T (2007) Cyclodextrins as pharmaceutical stabilizers. Adv Drug Deliv Rev 59:645–666
25. Martin del Valle EM (2004) Cyclodextrins and their uses: a review. Proc Biochem 39: 1033–1046
26. Bianco A, Da Ros T, Prato M, Toniolo C (2001) Fullerene-based amino acids and peptides. J Pept Sci 7:208–219
27. Mikeš F, Boshart G, Gil-Av E (1976) Resolution of optical isomers by high-performance liquid chromatography, using coated and bonded chiral charge-transfer complexing agents as stationary phases. J Chromatogr 122:205–221
28. Gasparrini F, Misiti D, Della Negra F, Maggini M, Scorrano G, Villani C (2001) Molecular recognition of *p-tert*-butylcalixarenes by surface-linked fullerenes C_{60} and C_{70}. Tetrahedron 57:6997–7002
29. Dell'Anna G, Annunziata R, Benaglia M, Celentano G, Cozzi F, Francesconi O, Roelens S (2009) Aromatic tripodal receptors for (C_{60}-I_h)[5,6]fullerene. Org Biomol Chem 7:3871–3877
30. Armstrong DW, DeMond W (1984) Cyclodextrin bonded phases for the liquid chromatographic separation of optical, geometrical, and structural isomers. J Chromatogr Sci 22: 411–415
31. Han SM (1997) Direct enantiomeric separation by high performance liquid chromatography using cyclodextrins. Biomed Chromatogr 11:259–271
32. Chang SC, Reid GL III, Chen S, Chang CD, Armstrong DW (1993) Evaluation of a new polar-organic high-performance liquid chromatographic mobile phase for cyclodextrin-bonded chiral stationary phases. Trends Analyt Chem 12:144–153
33. Cachau C, Thienpont A, Soulard M-H, Fé1ix G (1997) Chromatographic properties in normal-mode HPLC of chiral stationary phases based on substituted β-cyclodextrins. Chromatographia 44:411–416
34. Dodziuk H, Kozinski W, Ejchart A (2004) NMR studies of chiral recognition by cyclodextrins. Chirality 16:90–105
35. Schneider H-J, Hacket F, Rüdiger V, Ikeda H (1998) NMR studies of cyclodextrins and cyclodextrin complexes. Chem Rev 98:1755–1786
36. Bikádi Z, Fodor G, Hazai I, Hári P, Szemán J, Szente L, Fülöp F, Péter A, Hazai E (2010) Molecular modeling of enantioseparation of phenylazetidin derivatives by cyclodextrins. Chromatographia 71:S21–S28
37. Shi JH, Ding ZJ, Hu Y (2011) Experimental and theoretical studies on the enantioseparation and chiral recognition of mandelate and cyclohexylmandelate on permethylated β-cyclodextrin chiral stationary phase. Chromatographia 74:319–325
38. Shi JH, Ding ZJ, Hu Y (2012) Theoretical study on chiral recognition mechanism of methyl mandelate enantiomers on permethylated β-cyclodextrin. J Mol Model 18:803–813
39. DeSoi D, Kier LB, Cheng C-K, Karnes HT (2012) A cellular automata model of enantiomer binding strengths to β-cyclodextrin. J Chromatogr A 1258:101–107
40. Pederson CJ (1967) Cyclic polyether and their complexes with metal salts. J Am Chem Soc 89:2495–2496
41. Pederson CJ (1967) Cyclic polyether and their complexes with metal salts. J Am Chem Soc 89:7017–7036
42. Izat RM, Terry RE, Haymore BL, Hansen LD, Dalley NK, Avondet AG, Christensen JJ (1976) Calorimetric titration study of the interaction of several uni- and bivalent cations with 15-crown-5, 18-crown-6, and two isomers of dicyclohexo-18-crown-6 in aqueous solution at 25 °C and $\mu = 0.1$. J Am Chem Soc 98:7620–7630
43. Gokel GW, Leevy WM, Weber ME (2004) Crown ethers: sensors for ions and molecular scaffolds for materials and biological models. Chem Rev 104:2723–2750
44. Kyba EP, Siegel MG, Sousa LR, Sogah GDY, Cram DJ (1973) Chiral, hinged, and functionalized multiheteromacrocycles. J Am Chem Soc 95:2691–2692
45. Kyba EP, Koga K, Sousa LR, Siegel MG, Cram DJ (1973) Chiral recognition in molecular complexing. J Am Chem Soc 95:2692–2693

46. Kyba EP, Timko JM, Kaplan LJ, de Jong F, Gokel GW, Cram DJ (1978) Host-guest complexation. 11. Survey of chiral recognition of amine and amino ester salts by dilocular bis dinaphthyl hosts. J Am Chem Soc 100:4555–4568
47. Lingenfelter DS, Helgeson RC, Cram DJ (1981) Host-guest complexation. 23. High chiral recognition of amino acid and ester guests by hosts containing one chiral element. J Org Chem 46:393–406
48. Yamamoto K, Noda K, Okamoto YJ (1985) Synthesis and chiral recognition of optically active crown ethers incorporating a 4,4-biphenanthryl moiety as the chiral centre. J Chem Soc Chem Commun 16:1065–1066
49. Yamamoto K, Kitsuki T, Okamoto Y (1986) Synthesis and chiral recognition of optically active crown ethers incorporating a 9,9′-biphenanthryl moiety as the chiral center. Bull Chem Soc Jpn 59:1269–1270
50. Yamamoto K, Yumioka H, Okamoto Y, Chikamatsu JH (1987) Synthesis and chiral recognition of an optically active bis-crown ether incorporating a diphenanthrylnaphthalene moiety as the chiral centre. J Chem Soc Chem Commun 3:168–169
51. Demirel N, Bulut Y (2003) Synthesis of chiral diaza 18-crown-6 ethers from chiral amines and molecular recognition of potassium and sodium salts of amino acids. Tetrahedron Asymmetry 14:2633–2637
52. Turgut Y, Hosgoren H (2003) Synthesis of chiral monoaza-15-crown-5 ethers from l-valinol and the enantiomeric recognition of chiral amines and their perchlorates salts. Tetrahedron Asymmetry 14:3815–3818
53. Gong Y, Xiang Y, Yue B, Xue G, Bradshaw JS, Lee HK, Lee ML (2003) Application of diaza-18-crown-6-capped β-cyclodextrin bonded silica particles as chiral stationary phases for ultrahigh pressure capillary liquid chromatography. J Chromatogr A 1002:63–70
54. Davidson RB, Bradshaw JS, Jones BA, Dalley KN, Christensen JJ, Izatt RM, Morin FG, Grant DM (1984) Enantiomeric recognition of organic ammonium salts by chiral crown ethers based on the pyridino-18-crown-6 structure. J Org Chem 49:353–357
55. Hyun MH (2005) Development and application of crown ether-based HPLC chiral stationary Phases. Bull Korean Chem Soc 26:1152–1163
56. Cho HS, Choi HJ, Hyun MH (2009) Preparation of a new crown ether-based chiral stationary phase containing thioester linkage for the liquid chromatographic separation of enantiomers. J Chromatogr A 1216:7446–7449
57. Hyun MH, Jin JS, Lee W (1998) Liquid chromatographic resolution of racemic amino acids and their derivatives on a new chiral stationary phase based on crown ether. J Chromatogr A 822:155–161
58. Hirose K, Nakamura T, Nishioka R, Ueshige T, Tobe Y (2003) Preparation and evaluation of novel chiral stationary phases covalently bound with chiral pseudo-18-crown-6 ethers. Tetrahedron Lett 44:1549–1551
59. Hirose K, Jin YZ, Nakamura T, Nishioka R, Ueshige T, Tobe Y (2005) Chiral stationary phase covalently bound with a chiral pseudo-18-crown-6 ether for enantiomer separation of amino compounds using a normal mobile phase. Chirality 17:142–148
60. Yongzhu J, Hirose K, Nakamura T, Nishioka R, Ueshige T, Tobe Y (2006) Preparation and evaluation of a chiral stationary phase covalently bound with a chiral pseudo-18-crown-6 ether having a phenolic hydroxy group for enantiomer separation of amino compounds. J Chromatogr A 1129:201–207
61. Hong J, Namgoong SN, Bernardi A, Still WC (1991) Highly selective binding of simple peptides by a C3 macrotricyclic receptor. J Am Chem Soc 113:5111–5112
62. Gasparrini F, Misiti D, Villani C, Borchardt A, Burger MT, Still WC (1995) Enantioselective recognition by a new chiral stationary phase at receptorial level. J Org Chem 60:4314–4315
63. Still WC (1996) Discovery of sequence-selective peptide binding by synthetic receptors using encoded combinatorial libraries. Acc Chem Res 29:155–163
64. Gasparrini F, Misiti D, Still WC, Villani C, Wennemers H (1997) Enantioselective and diastereoselective binding study of silica bound macrobicyclic receptors by HPLC. J Org Chem 62:8221–8224

65. Moberg C (1998) C3 symmetry in asymmetric catalysis and chiral recognition. Angew Chem Int Ed 37:248–268
66. Gasparrini F, Misiti D, Pierini M, Villani C (2002) A chiral A_2B_2 macrocyclic minireceptor with extreme enantioselectivity. Org Lett 4:3993–3996
67. D'Acquarica I, Gasparrini F, Misiti D, Pierini M, Villani C (2008) HPLC chiral stationary phases containing macrocyclic antibiotics: practical aspects and recognition mechanism. Adv Chromatogr 46:109–173
68. Page MI, Jencks WP (1971) Entropic contributions to rate accelerations in enzymic and intramolecular reactions and the chelate effect. Proc Natl Acad Sci U S A 68:1678–1683
69. Jencks WP (1981) On the attribution and additivity of binding energies. Proc Natl Acad Sci U S A 78:4046–4050
70. Benson SW (1967) Thermochemical kinetics, 2nd edn. Wiley, New York
71. Uccello-Barretta G, Balzano F, Martinelli J, Gasparrini F, Pierini M, Villani C (2011) NMR and computational investigations of the chiral discrimination processes involving a cyclic tetraamidic chiral selector. Eur J Org Chem 3738–3747
72. Alcaro S, Gasparrini F, Incani O, Mecucci S, Misiti D, Pierini M, Villani C (2000) A "quasi-flexible" automatic docking processing for studying stereoselective recognition mechanisms. Part 1. Protocol validation. J Comput Chem 21:515–530
73. Alcaro S, Gasparrini F, Incani O, Caglioti L, Pierini M, Villani C (2007) "Quasi flexible" automatic docking processing for studying stereoselective recognition mechanisms, part 2: prediction of $\Delta\Delta G$ of complexation and 1H-NMR NOE correlation. J Comput Chem 28: 1119–1128
74. Filippi A, Gasparrini F, Pierini M, Speranza M, Villani C (2005) Exceptional gas-phase enantioselectivity of chiral tetramide macrocycles. J Am Chem Soc 127:11912–11913
75. Gasparrini F, Pierini M, Villani C, Filippi A, Speranza M (2008) Induced-fit in the gas phase: conformational effects on the enantioselectivity of chiral tetra-amide macrocycles. J Am Chem Soc 130:522–534
76. Fraschetti C, Pierini M, Villani C, Gasparrini F, Levi Mortera S, Speranza M (2009) Towards enzyme-like enantioselectivity in the gas phase: conformational control of selectivity in chiral macrocyclic dimers. Chem Commun 36:5430–5432
77. Fraschetti C, Pierini M, Villani C, Gasparrini F, Levi Mortera S, Filippi A, Speranza M (2011) The "bridge" game: role of the fourth player in chiral recognition. Chem Eur J 17:3078–3081
78. Berthod A, Chen X, Kullman JP, Armstrong DW, Gasparrini F, D'Acquarica I, Villani C, Carotti A (2000) Role of the carbohydrate moieties in chiral recognition on teicoplanin-based LC stationary phases. Anal Chem 72:1767–1780
79. Cavazzini A, Pasti L, Dondi F, Finessi M, Costa V, Gasparrini F, Ciogli A, Bedani F (2009) Binding of dipeptides and amino acids to teicoplanin chiral stationary phase: apparent homogeneity of some heterogeneous systems. Anal Chem 81:6735–6743
80. Isaksson R, Wennerström H, Wennerström O (1998) Symmetry and chiral recognition; separation of enantiomers on triacetyl-cellulose columns. Tetrahedron 44:1697–1705
81. Pirkle WH, Liu Y, Welch CJ (1998) Does C_2 symmetry improve enantioselectivity? Enantiomer 3:477–483
82. Levkin PA, Schurig V (2008) Apparent and true enantioselectivity of single- and binary-selector chiral stationary phases in gas chromatography. J Chromatogr A 1184:309–322
83. Levkin PA, Maier NM, Schurig V, Lindner W (2010) Strong detrimental effect of a minute enantiomeric impurity of a chiral selector on the enantioselectivity factor. Angew Chem Int Ed 9:7742–7744
84. Levkin PA, Maier NM, Lindner W, Schurig V (2012) A practical method for the quantitative assessment of non-enantioselective versus enantioselective interactions encountered in liquid chromatography on brush-type chiral stationary phase. J Chromatogr A 1269:270–278
85. Gasparrini F (2012) Supramolecular chromatography: a blissful marriage of supramolecular chemistry and separation science. In: SAYCS 2012, 1–3 October 2012, Riccione, Italy

Top Curr Chem (2013) 340: 107–152
DOI: 10.1007/128_2013_441

Published online: 18 May 2013

Chiroptical Detectors for the Study of Unusual Phenomena in Chiral Chromatography

Nicolas Vanthuyne and Christian Roussel

Abstract Differentiation of enantiomers in chromatography requires specific detectors, based on polarimetry or circular dichroism. Their use is limited to chiral HPLC and SFC. We explain the operating principles of the different chiroptical detectors available and stress the influence of working wavelength and mobile phase on the output signal. Current and relevant applications of chiroptical detectors are absolute configuration assignment, measurement of enantiomeric excesses in complex mixtures and determination of elution order. We focus on the reversals of enantiomeric elution order, an important subject for the understanding of the chiral recognition mechanisms. We review the main parameters which can induce a reversal, show the usefulness of chiroptical detectors to easily identify reversals and emphasize the significance of the isoenantioselective temperature. The aim of this chapter is to highlight the valuable information provided by chiroptical detectors to study unusual behaviour in chiral HPLC and SFC, reversals of enantiomeric elution order and exchange phenomena as dynamic chromatography and self-disproportionation on achiral columns.

Keywords Absolute configuration assignment · Dynamic chromatography · Electronic circular dichroism · Isoenantioselective temperature · Polarimetry · Reversal of enantiomeric elution order · Self-disproportionation

Contents

N. Vanthuyne (✉) and C. Roussel
iSm2 CNRS, Aix Marseille University, 13397 Marseille Cedex 20, France
e-mail: nicolas.vanthuyne@univ-amu.fr; christian.roussel@univ-amu.fr

Abbrevations

1-PrOH	Propan-1-ol
2-PrOH	Propan-2-ol
AcOH	Acetic acid
CD	Electronic circular dichroism
CIP	Cahn–Ingold–Prelog priority rule
CSP	Chiral stationary phase
DEA	Diethylamine
ee	Enantiomeric excess
FA	Formic acid
HPLC	High performance liquid chromatography
k	Retention factor
L	Liter(s)
LED	Light-emitting diode
min	Minute(s)
MPLC	Medium pressure liquid chromatography
nd	Not determined
nm	Nanometer(s)
ORD	Optical rotatory dispersion
RI	Refractive index
SFC	Supercritical or subcritical fluid chromatography
SMB	Simulated moving bed
TFA	Trifluoroacetic acid
THF	Tetrahydrofuran
T_{iso}	Isoenantioselective temperature
UV	Ultraviolet
α	Enantioselectivity, ratio of retention factors for two enantiomers
β	Phase ratio, ratio of the volume of the mobile phase and stationary phase in the column
μg	Microgram
μL	Microliter

Chiral Stationary Phases

Chiral-AGP	α1-Acid glycoprotein
Chiralcel OB	Cellulose tris benzoate (Daicel)
Chiralcel OD	Cellulose tris(3,5-dimethylphenyl-carbamate) coated (Daicel)
Chiralcel OJ	Cellulose tris(4-methylbenzoate) (Daicel)
Chiralpak AD	Amylose tris(3,5-dimethylphenyl-carbamate) coated (Daicel)
Chiralpak AS	Amylose tris([(*S*)alpha-phenethyl]-carbamate) coated (Daicel)
Chiralpak IA	Amylose tris(3,5-dimethylphenyl-carbamate) immobilised (Daicel)
Chiralpak IB	Cellulose tris(3,5-dimethylphenyl-carbamate) immobilised (Daicel)
Chiralpak IC	Cellulose tris(3,5-dichlorophenyl-carbamate) immobilised (Daicel)
Chiralpak ID	Amylose tris(3-chlorophenyl-carbamate) immobilised (Daicel)
Lux-Cellulose-1	Cellulose tris(3,5-dimethylphenyl-carbamate) coated (Phenomenex)
Lux-Cellulose-2	Cellulose tris(3-chloro-4-methylphenyl-carbamate) coated (Phenomenex)
Lux-Cellulose-4	Cellulose tris(4-chloro-3-methylphenyl-carbamate) coated (Phenomenex)
Regispack	Amylose tris(3,5-dimethylphenyl-carbamate) coated (Regis Technologies)
Ultron ES-OVM	Ovomucoid protein bonded
(*S*,*S*)-Whelk-O1	(3*R*,4*S*)-4-(3,5-Dinitrobenzamido)-3-[3-(dimethylsilyloxy) propyl]-1,2,3,4-tetrahydrophenanthrene (Regis Technologies)

1 Introduction

Chiral chromatography is a powerful tool for enantiomer differentiation, on an analytical scale to determine the ee and on a preparative scale to obtain enantiopure molecules [1]. This chirotechnology is extensively used in various fields, such as drug discovery [2], agrochemicals, fragrances and functional materials. Many chiral stationary phases, with different chiral recognition mechanisms, are now available to separate chiral compounds [3, 4]. The understanding of the chiral recognition mechanisms, by the development of a chiral recognition model or by computational chemistry [5], requires knowledge of the absolute configuration of the eluted enantiomers.

From a practical point of view the control of the elution order is convenient, on an analytical scale, for the measurement of high ee by eluting the trace component

before the major enantiomer [6]. Indeed, the accuracy of this measurement is crucial to lower the limit of detection (LOD) and to validate chiral methods: interference from the tailing of the major enantiomer should be avoided when peaks are relatively broad, particularly on protein columns [7]. On a preparative scale, for batch separations (not with SMB), the best purity will be attained for the first eluted enantiomer compared to the second because of the tailing of the first eluted enantiomer occurring with high loading. The control of elution order is so important that original methods have been developed to reverse the enantiomeric elution order by altering the type of reagent used in the derivatization of amino-acids on vancomycin based CSP [8], or by using the temperature effect for enantiomeric pairs separated by chiral HPLC under a significant enthalpy-control [9].

So fundamental and practical reasons for the monitoring of the elution order during analysis by chiral chromatography exist. Some articles have already highlighted the need of well reported elution orders [10], detailed unusual effects [11] and reversals of enantiomeric elution order [12]. In this review we emphasize the use of chiroptical detectors to detect unusual phenomena, and particularly reversals of enantiomeric elution order. Thus we restrict our study to the field of chiral chromatography in which chiroptical detectors, polarimeters and circular dichroism detectors are operational: chiral HPLC and SFC (SFC in the sense of the term defined by Guiochon [13]).

2 Principle and Applications of Chiroptical Detection

2.1 Historical Background

Bench polarimeters were first adapted for use as chromatography detectors, working at low pressure. In 1976, Hesse and Hagel reported the first chromatogram obtained with a polarimetric detector [14]: a Perkin Elmer 141 was used to follow the elution of the 2-phenyl-cyclohexanone enantiomers at 436 nm on microcrystalline cellulose triacetate. In 1980, Drake, Gould and Mason published the first use of circular dichroism for detection in liquid chromatography on microcrystalline cellulose triacetate for pavine and Tröger's base [15]. These detectors were very useful in the early years of chiral chromatography, especially in the case of partial separations [16], occurring frequently at low pressure.

Cells improvements allowed the use of chiroptical detectors in HPLC. In different reviews, Mannschreck [17] and then other groups [18, 19] described their main applications and developments and prophesied their future widespread use.

2.2 *Operating Principle of Different Chiroptical Detectors*

2.2.1 Use of a Bench Polarimeter or Circular Dichroism Spectrometer

Circular dichroism spectrometers, able to measure the differential absorption of left and right circularly polarized light between 170 and 900 nm, or bench polarimeters, able to measure the angle of rotation caused by passing polarized light through an optically active substance at discrete wavelengths, usually the emission line of sodium or mercury lamps (589, 578, 546, 436 and 365 nm), can be used as chromatography detectors with suitable cells. Cell volume can be reduced to up to 40 μL in HPLC [20].

Differentiation of enantiomers during elution is possible with such a CD spectrometer [21] or a bench polarimeter [22]. Polarimeters usually have several available wavelengths and detect enantiomers even in the absence of chromophores. For example, a partial separation, not detected with a refractometer, was reported for heptachlor and chlordane on permethylated β-cyclodextrin [23]. CD spectrometers can also monitor partial separations at a chosen wavelength [24], and moreover allow the recording of CD spectra; in this case the flow has to be stopped [25].

2.2.2 Polarimetric and Circular Dichroism Detectors Dedicated to Chromatography

The only commercially available CD detector dedicated to chromatography, namely Jasco CD-2095, has many HPLC applications described in the literature, including SFC applications according to the supplier. Figure 1 shows typical chromatograms obtained with the CD-2095, by HPLC and by SFC: the sign and the area obtained depend on the chosen wavelength and on the nature of the eluent. The sign observed for (*S*)-(**1**) is (−) at 220 nm, (+) at 254 nm and gives no response at 300 nm (Fig. 1). Consequently, the wavelength must be given for each CD chromatogram.

Polarimetric detectors dedicated to HPLC were developed in the late 1980s. Some were used in the early 1990s but are no longer available, such as the Chiramonitor from Applied Chromatography Systems [26]. Nowadays, three polarimetric detectors for chromatography are on the market, differing in their operating mode and technical features: Chiralyser from IBZ Messtechnik (Germany) with an LED source and an operating wavelength at 426 nm, ALP from PDR (USA) with a laser source at 660 nm and OR-2090 (OR-1590 is an older model) from Jasco (Japan) with an Hg–Xe lamp, using wavelengths in the range 350–900 nm. Accordingly, the sign given by a Chiralyser is the sign of the eluted enantiomer at 426 nm in the eluent, the sign given by an ALP is the sign of the eluted enantiomer at 670 nm in the eluent, but the sign given by OR-2090 results from the addition of the optical rotation contributions at all wavelengths between 350 and 900 nm. For OR-2090 the contributions do not have the same weight and the main contributions come from the emission lines of the mercury lamp (365, 405, 436, 546 and 578 nm). OR-2090 has a multiple wavelength based operating mode, while Chiralyser and ALP are mono-wavelength based.

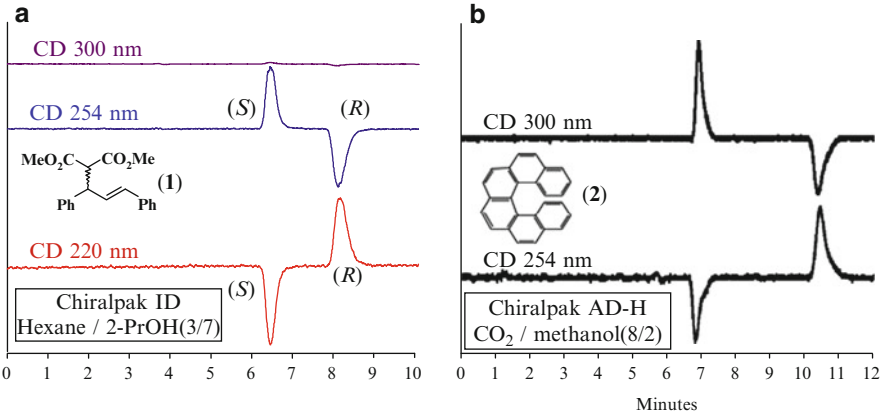

Fig. 1 CD chromatograms for (**a**) HPLC separation of (**1**) on Chiralpak ID, *n*-hexane/2-PrOH (3/7), 1 mL/min, 30°C, 4 μg injected, CD at 220, 254 and 300 nm from *bottom* to *top* and (**b**) SFC separation of [6]-helicene (**2**) on Chiralpak AD-H, CO_2/methanol (8/2), 4 mL/min, 40°C, outlet pressure = 120 bars

For compound **3**, the specific rotation is negative for the (a*R*) enantiomer on all the wavelengths, so the observed peak is negative on the polarimetric trace with OR-1590 (Fig. 2). In this case, the three commercial polarimetric detectors would have provided a negative sign. In the case of compound **4**, the ORD spectrum is more complex and less regular, with an anomalous curve with multiple Cotton effects (Fig. 2): the signal of the (*M*)-enantiomer is positive at 670 and 426 nm, but the sum of the different contributions in the range 350–900 nm gives a weak negative signal. The intensity and the sign given by a polarimetric detector depend on the operating mode of the model used. For (*M*)-**4** the three commercial polarimeters would give different signs: positive with ALP and Chiralyser and negative with Jasco detector.

2.2.3 Influence of the Mobile Phase

It is trivial to recall that the CD and above all ORD spectra depend on the solvent in which they are recorded, so that the intensity and the sign obtained with a chiroptical detector depend on the mobile phase used for chromatography. Comparisons of the sign from chiroptical detectors with data in another solvent should be carried out with caution and with a systematic check of the invariance of the sign.

Direct comparison with specific rotation are tempting but risky. For example, the sign given by a DIP-181C polarimeter, using an Hg lamp, is (−) for the (*R*)-enantiomer of 4-hydroxy-2-cyclopentenone in *n*-hexane/2-PrOH mixtures, but the sign in chloroform at 589 nm is (+) [28]. Driffield et al. wanted to choose a molecule with a large specific rotation to avoid sensitivity problems to prove the efficiency of a new polarimetric detector. This anticoagulant compound, warfarin, is

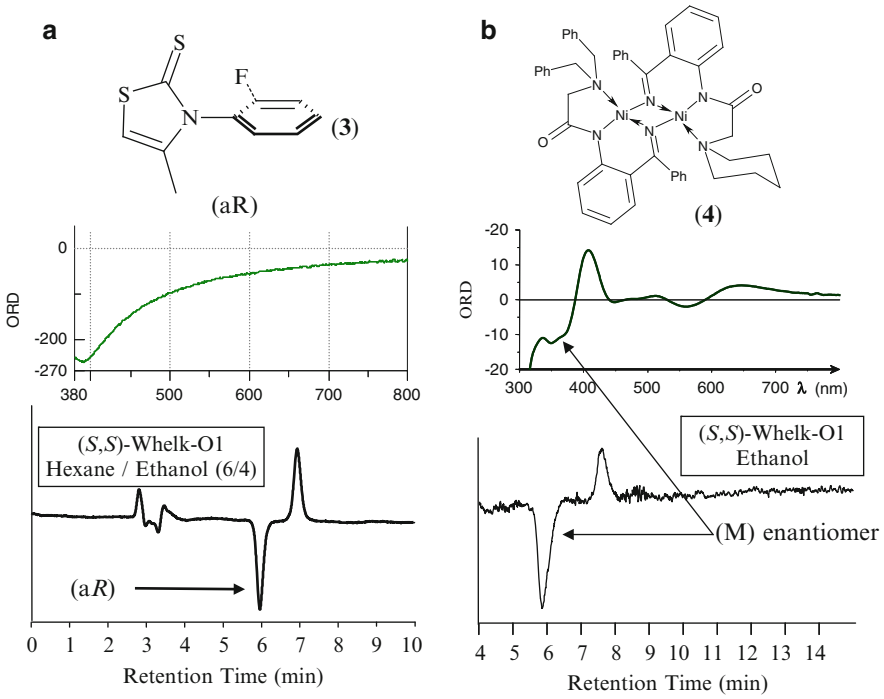

Fig. 2 ORD spectra and polarimetric traces (OR-1590) for (**a**) compound **3** on (*S*,*S*)-Whelk-O1, *n*-hexane/ethanol (6/4), 1 mL/min, 30°C and (**b**) compound **4** [27] on (*S*,*S*)-Whelk-O1, ethanol, 1 mL/min, 25°C

described with a specific rotation of −148 for the (*S*)-enantiomer in NaOH (0.5 N) [29], but the signal obtained at 635 nm is weak [30]. Indeed, the (*S*)-enantiomer has a specific rotation of +19 in 2-PrOH [29] and we have checked that (*S*)-warfarin has a low positive specific rotation at 635 nm in the eluent used (*n*-hexane/2-PrOH/AcOH 80/19.9/0.1). Moreover, the change in sign can lead to errors in the assignment of absolute configurations. Liu et al. asserted a high correlation between the magnitude and direction of the specific rotations of molecules at 675 nm and at the sodium D line [31], but also emphasized the influence of the mobile phase.

Unfortunately it is also possible to select a mobile phase in which there is no specific rotation: signals with opposite signs are observed with OR-1590 for (**5**) with 10% of ethanol, but these signals disappear with 40% of ethanol (Fig. 3b, c).

2.2.4 Case of Anomalous ORD

The type of ORD spectra, plain or anomalous, has little impact on the signal for the mono-wavelength based polarimetric detector. The specific rotation of a compound with an anomalous ORD spectrum may be zero or very low at the working wavelength, but the specific rotation of a compound with a plain curve ORD spectrum may

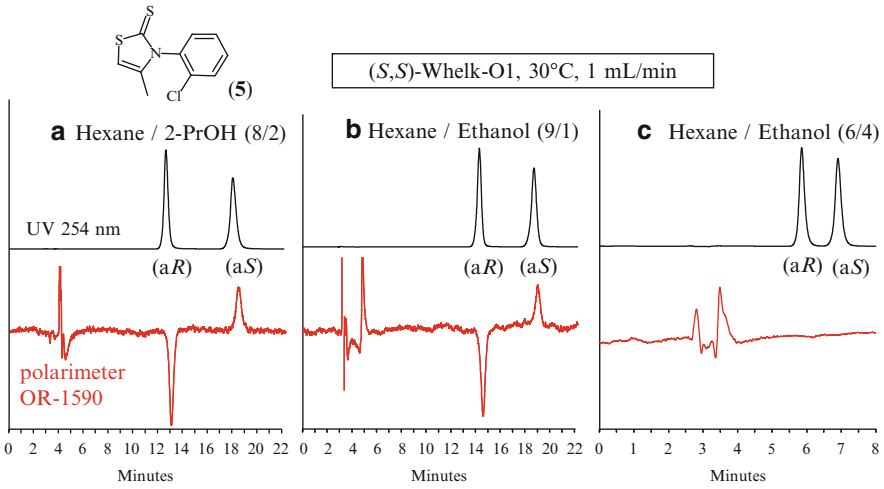

Fig. 3 UV chromatograms and polarimetric traces (OR-1590) for (**5**) on (*S*,*S*)-Whelk-O1, 30°C, 1 mL/min, with different mobile phases: (**a**) *n*-hexane/2-PrOH (8/2); (**b**) *n*-hexane/ethanol (9/1); (**c**) *n*-hexane/ethanol (6/4)

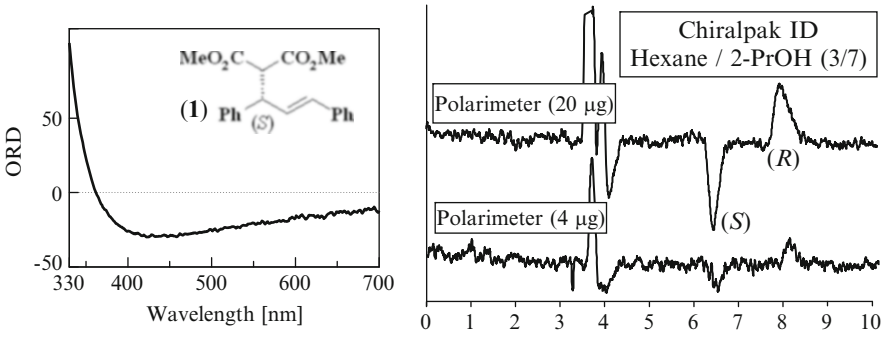

Fig. 4 ORD spectra, polarimetric traces (OR-1590) for (**1**) on Chiralpak ID, *n*-hexane/2-PrOH (3/7), 1 mL/min, 30°C, for injection of 4 and 20 µg

also be low. By using a multi-wavelength based polarimetric detector, a compound with an anomalous ORD often gives a poor signal, due to the compensation of positive and negative contributions of the specific rotation at the different wavelengths. Compound (**1**) shows an example of such behaviour: we need to increase the injected amount to 20 µg to observe a low intensity signal (Fig. 4). (*S*)-(**1**) gives a negative sign even if its specific rotation is strongly positive at wavelengths below 370 nm.

Optical filters can be used to select a part of the spectral domain and thus avoid the contributions of the low wavelengths. According to the specific rotation measured for (*S*)-warfarin (Table 1), this molecule is relevant to study both the influence of the working wavelengths and of the mobile phase.

Table 1 Specific rotation of (*S*)-warfarin reported at different wavelengths in various solvents for a concentration of 1 g/100 mL

	NaOH (0.5 N)	Ethanol	2-PrOH	Chloroform	Ethyl acetate
589 nm	−144	+8.4	+17	−19	+7.3
578 nm	−149	+9.0	+18	−20	+7.5
546 nm	−174	+9.5	+20	−24	+7.1
436 nm	−338	+5.3	+31	−52	−6.6
365 nm	nd	−51	+18	−133	−110

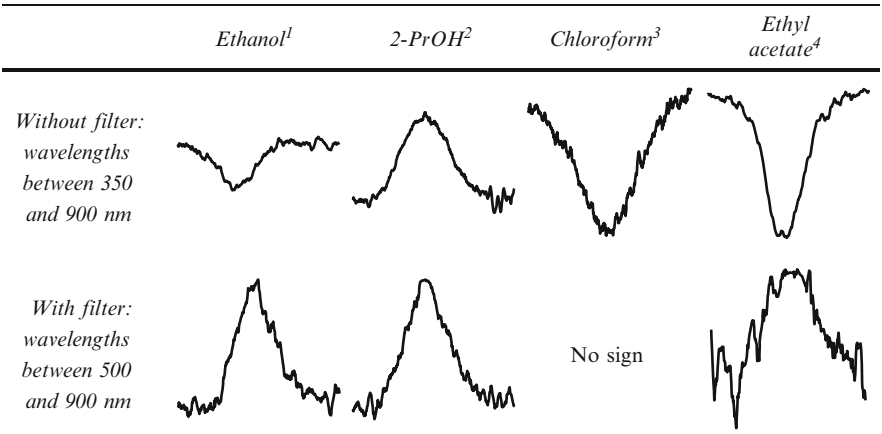

Fig. 5 Polarimetric traces (OR-1590, Chiralpak IC) obtained for (*S*)-warfarin depending on the mobile phase modifier and on the range of wavelengths used. (1) *n*-hexane/ethanol (7/3); (2) *n*-hexane/2-PrOH (1/1); (3) *n*-hexane/ethanol/chloroform (25/5/70); (4) *n*-hexane/ethyl acetate (1/1)

For instance, warfarin's specific rotations are too low in ethanol to be detected by mono-wavelength polarimetric detectors at analytical scale, but using a 350–900 nm range with multi-wavelengths polarimetric detector. Warfarin is still difficult to detect (Fig. 5), because the sign of its specific rotation changes in this range. The use of a sharp-cut filter to select the 500–900 nm range allows observation of a signal for (*S*)-warfarin by removing the highly negative contribution at low wavelengths.

Warfarin enantiomers have been separated on Chiralpak IC using different mobile phase modifiers with *n*-hexane, the (*R*)-warfarin being eluted first in each case. We could check that the sign of the (*S*)-warfarin given by the polarimetric detector changes with the chosen wavelength and modifier in accordance with the measured specific rotation. In ethanol its sign is (+) using the 500–900 nm range (with filter) but (−) using the 350–900 nm range (without filter), due to the strongly negative contribution below 400 nm. In 2-PrOH the specific rotation remains positive at all the wavelengths, so the sign given by the polarimetric detector is (+) in both cases. With chloroform and ethyl acetate as modifiers, the use of a sharp-cut filter cancels the strongest contributions to the signal between 350 and 500 nm and silences the signal. It follows that a polarimetric detector may provide a sign

either positive or negative depending on the wavelengths and the eluent used. This example also illustrates the need of a careful description of the conditions used to assign the sign of one enantiomer.

2.2.5 Artefacts

In addition to the chiroptical properties that clearly determine the response of the chiroptical detectors, other experimental parameters influence the signal. It is known that temperature affects the optical activity, while a rapid change in temperature in the laboratory may lead to a considerable drift of the baseline of the polarimetric detector (Fig. 7c). The overall performance of chiroptical detectors is good, but users should be aware that artefacts may appear for some molecules or in some conditions. In 1993, Däppen et al. [32] described the major problems encountered with polarimetric detectors. First, a signal is obtained for achiral 2-phenylethanol: this observation was explained by refractive index related effects generated by the eluted peaks. Second, distorted peak shapes in reversed phase were reported for samples with low ee or with small specific rotations, and nonlinear relationship between the area of the peaks and the ee. Such behaviour is also seen in Fig. 3a for (**5**), where the injection of a racemic mixture gives two peaks with equal areas in UV whereas on the polarimetric trace, the area of the second eluted peak is noticeably smaller than the first one. In 2008, similar observations were made and were explained by Sanchez et al. by refractive index artefacts [33].

For all the chiroptical detectors an injection peak may be present and sometimes quite intense, as a consequence of the difference in refractive index between the mobile phase and the solvent containing the injected sample.

The saturation of the detector results in a reflection of the portion of the peak beyond the saturation limit. This saturation limit depends mainly on the compound and on the wavelength, but not on the electric signal output from the detector. This saturation can be observed on only one peak (Fig. 6a) or on both enantiomers as for (**3**) (Fig. 6b). In this latter case, injection of 4 μg of *rac*-(**3**) led to a correct chromatogram, while injection of 10 μg led to the chromatogram displayed in Fig. 6b. In rare cases encountered in chiral HPLC, the CD detector provides the same sign for two enantiomers: a chromatogram with two negative peaks was reported for both enantiomers of 2-methyl-1-tetralone, separated on Chiralpak AD-RH with water/acetonitrile (6/4) and detected by CD at 230 nm [34]. We also encountered this case sometimes, as for atropisomers of (**6**) [35], which gave two positive peaks at 254 nm.

Artefacts can sometimes be avoided or reduced by adjusting the experimental parameters (amount injected, choice of wavelength, eluent, sample injection solvent) or the detector parameters (gain, cell size).

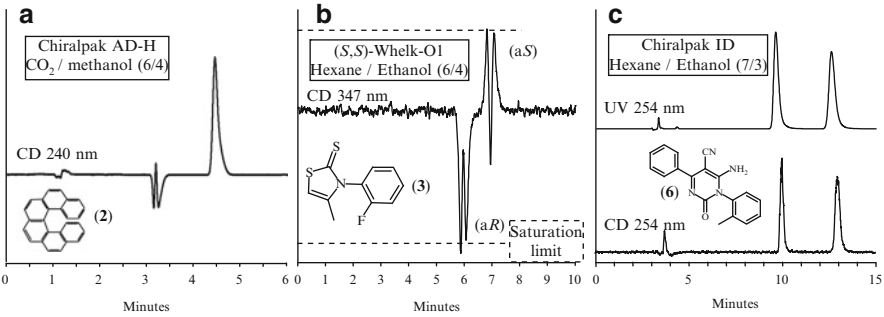

Fig. 6 CD chromatograms for (**a**) (**2**) on Chiralpak AD-H, CO_2/methanol (6/4), 3 mL/min, 40°C, outlet pressure = 120 bars, at 240 nm, (**b**) (**3**) on (*S*,*S*)-Whelk-O1, *n*-hexane/ethanol (6/4), 30°C, 1 mL/min, 10 µg injected, at 347 nm, and (**c**) (**6**) on Chiralpak ID, *n*-hexane/ethanol (7/3), 25°C, 1 mL/min, at 254 nm

2.2.6 Comparison of the Different Chiroptical Detectors

A direct comparison between the different chiroptical detectors for one or more molecules is not relevant, since each detector has a different principle or operating mode. For each detector, it is possible to find undetectable chiral molecules as well as very useful applications, so general conclusions cannot be drawn. However, generally speaking, a CD detector is more sensitive than most polarimetric detectors, but CD requires a chromophore in the chiral molecule. In the literature, discussions between polarimetric and CD detectors turn in favour of CD, considered to be more sensitive and having the advantage of the choice of the wavelength [34, 36]. Polarimetric detectors are nevertheless very helpful for molecules without chromophores [37] and have been proved to be sufficiently accurate detectors, for instance to determine an ee as high as 99.8% for mandelic acid with a detector ALP [38]. It is likely that the performance and sensitivity of chiroptical detectors will be further improved with recent advances in optics. Indeed, research to improve the sensibility of CD detectors is ongoing [39]. For polarimetric detectors, it would be interesting to be able to select the operating wavelength among several available ones displayed by the same instrument.

2.3 Assignment of Absolute Configuration

The contribution of chiral liquid chromatography to the determination of absolute configurations has already been reviewed [40]. We will recall the interest in the data provided by the chiroptical detectors in this approach and the precautions to be taken in order to not be misled.

2.3.1 From the Sign Given by a Chiroptical Detector

The correlation of the sign given by a chiroptical detector for one enantiomer with a reference value can be used to deduce its absolute configuration. This reference value may be found in the literature or predicted by a model or theoretical calculations.

In 1984, Salvadori et al. deduced the absolute configuration of a series of aryl-alkylcarbinols, binaphthol, *trans*-l,2-cyclohexanediol dibenzoate and 1-acenaphthenol benzoate by comparison of the sign of the CD detector and the sign predicted by semi-empirical methods, applying helicity rules and sector rules [21]. A correlation in a series of oxazepam analogs, the alcohol being replaced by acetate or isopropyl groups, was reported by Bertucci et al. [24], assuming that the (*S*)-enantiomers of these similar structures have a positive sign with a CD detector at 254 nm, because the isopropyl (*S*) analog has a positive CD at 260 nm. The safest way is to take as a reference the CD sign of the molecule analyzed in a given solvent at the wavelength used for analysis and verify that this sign is not changed by the eluent. This method was used to assign the absolute configuration of the naringenin enantiomers from the sign at 290 nm given by a CD detector [41].

A similar approach is possible with a polarimetric detector, being aware of the meaning of the sign obtained as outlined in the previous paragraphs. Indeed, a wrong configuration can be deduced, as in the case of Lao and Gan [42], who in 2012 studied the enantioselective degradation of warfarin in soils. They separated warfarin on a CSP with an *n*-hexane/2-PrOH/TFA (92/8/0.1) mobile phase; the sign of rotation of the resolved enantiomers was determined by an on-line ALP at 675 nm and an (*S*) configuration was assigned to the (−) sign. However, as we noted in Sect. 2.2.4, and checked, the (*S*)-enantiomer is (+) in this mobile phase. (*S*)-Warfarin is typically described with a (−) sign in the literature, in reference to the first reported specific rotation measured in NaOH (0.5 N) [29].

One of the advantages of the polarimetric detector is the ability to work with a very small amount of sample, less than 1 mg, and with mixtures. Thus, heterocyclic atropisomer absolute configurations have been determined by analysing mixtures obtained through a chemical interconversion method associated with chiroptical detection [43].

2.3.2 From On-line Circular Dichroism Spectra

An experimental CD spectrum can be recorded with CD detectors if the flow is stopped when a chiral molecule is in the cell. The first stopped-flow measurements were performed by Mannschreck in 1991 [44] and this technique is still used, particularly by Bringmann [45, 46]. With this method, the spectrum is obtained without having to collect the pure enantiomers and therefore it can be very useful for relatively unstable compounds. The use of electronic CD for the determination of absolute configuration is beyond the scope of this chapter, but has been recently reviewed by Bertucci and Tedesco [47].

2.4 Determination of Enantiomeric Excess

2.4.1 From a Partial Separation on a Chiral Stationary Phase

In the early years of chiral chromatography, CSPs were few and not very efficient, so overlapping peaks were often observed. Chiroptical detectors were then very useful to exploit these poor separations. Techniques for deconvolution of overlapping peaks have been used to determine ee from partial separations, and their accuracy was studied [48]. Nowadays, the performances of the numerous available chiral selectors allow baseline separation for all pairs of enantiomers if these are sufficiently stable. Deconvolution is therefore no longer useful in analytical chromatography to measure ee. However, the main interest remains in preparative separations [49] to collect enantiopure fractions [50]. Upon preparative separations, peak overlap is a consequence of high sample loading, and deconvolution of the chiroptical signal is a way to increase productivity [51].

2.4.2 On an Achiral Stationary Phase

On an achiral stationary phase, enantiomers are not differentiated: while the racemate gives no signal with chiroptical detection, an enantio-enriched sample provides a single peak (see self-disproportionation for exceptions), whose area is proportional to its optical purity. This method is similar to the direct use of polarimetry to measure optical purities, with the same requirements and drawbacks [52]. In the case of the Horeau effect [53], the optical purity is different from the ee due to nonlinear effects. The maximum specific rotation of the targeted compound must be known with certainty. Reference samples of known ee and a second method of detection giving the sum of the two enantiomers are required to make a calibration, i.e. to correlate the two areas obtained and ee. The first reports concerned the ee determination for permethrinic acid pentafluorobenzyl ester [54], epinephrine [55], pyrethroids [56] and amino-acids [57]. This type of dual detection as UV/CD or RI/polarimetry has limitations, especially when the chiroptical signal intensity is weak, and for the determination of high ee [58]. The method was proven to be less accurate than HPLC on CSP [59], but ees up to 99% have been determined for L-hexose during reaction monitoring using RI/polarimetry detections [60]. Sensitivity improvements of a CD detector by filter addition were used [61], but calibration and tests to validate the method are quite long compared to the development of a new method on a CSP. Articles with precise determination of ees on achiral columns have been written or sponsored by the suppliers of chiroptical detectors on particular cases. This method however does not in fact yield adequate sensitivity for pharmaceutical enantiomeric purity determinations [34].

The dual detection method has proven its interest and its efficiency in areas where the accuracy of the ee determination is not the main aim. For high-throughput analysis, the use of chromatography on achiral support with a chiroptical detector informs on the enantiopurity of the mixture components. Thus, high-throughput

screening of enantioselective catalysts [62] and investigations in organic reaction discovery by high-throughput experimentations [63] can be optimized. Obviously, care should be taken regarding the risks of overlapping peaks with other chiral components of the respective mixture such as catalysts, ligands or by-products and nonlinear responses of the chiroptical signal, owing to aggregation of some compounds. The same principle can be applied to the detection of conglomerates by chromatography on achiral support [64].

2.4.3 From Complex Mixtures

By definition, achiral molecules are not sensed by chiroptical detectors and it may be worthwhile to simplify an analysis by hiding all achiral products. Examples are described on achiral support, with the detection by polarimetric detector of sugars in human urine [18], and on CSPs, with the quantitation of the enantiomers of lorazepam in human plasma by CD detectors [65]. Chiral signatures in essential oils, i.e. polarimetric traces with peaks of the major chiral components, obtained with a polarimetric detector on a CSP, were recently proposed to study the enantiomeric diversity in essential oils [66].

2.5 Determination of Elution Order

The use of chiroptical detectors to determine enantiomeric elution order on CSPs seems quite easy by direct comparison of the observed signs, but the dependence of the signal on the experimental parameters should be kept in mind. True reversals of elution order are observed if the different analytical conditions do not affect the sign given by the chiroptical detector. Conversely, apparent reversals of elution order are observed when the observed sign is reversed with the analytical conditions for a given absolute configuration [67].

Direct comparison cannot be made for different compounds: even for analogs, CD spectra and specific rotation may change. For instance, by monitoring the enantiomeric elution order of fluoxetine, miconazole and analogs on Chiralcel OD with a CD detector at 280 nm and recording their CD spectrum, Cirilli et al. clearly explained that the apparent reversal of elution order established by on-line CD at 280 nm for the first eluted enantiomer, $(+)_{CD280}$-(*S*)-miconazole and $(-)_{CD280}$-(*S*) for analog, was only due to an inversion of the Cotton effect [68].

Using the same mobile phase, for the same compound and detector obviously, signs can be compared directly. In practice, many different mobile phases can now be screened with the widespread immobilised polysaccharide based CSPs and the sign may depend on the mobile phase modifier. The chiral HPLC separation of the enantiomers of 1-methyl-5-phenyl-5-propylbarbituric acid on Chiralpak IB monitored by a Chiralyser demonstrates that the (*R*)-enantiomer is (+) in *n*-hexane/2-PrOH (9/1) mixture but (−) in *n*-hexane/THF (9/1) [69]. So the effect of the mobile phases should always be tested [70], especially when the chiroptical signal is weak [37].

The reported examples emphasize how the deduction of the enantiomeric elution order, solely based on the sign of the chiroptical detector, could lead to mistaken conclusions. In case of doubt, the injection of a non-racemic mixture is required to confirm the enantiomeric elution order [71].

3 Reversal of Enantiomeric Elution Order

Elution order is difficult to control in chiral chromatography. Reversal of elution order can be obtained by switching the absolute configuration of the chiral selector, but it is only possible for molecular CSPs available in their two enantiomeric forms. The main objective of this section is to deal with unusual reversal of elution order, i.e. unexpected, astonishing and not easily explainable reversals.

3.1 Reversal of Enantiomeric Elution Order Due to the Chiral Stationary Phase

3.1.1 Case of Different Chiral Selector

It is obvious that different chiral selectors generate different recognition mechanisms and there is no reason why two different chiral selectors give the same elution order. However, study of the recent literature shows that the assignment of the absolute configurations from elution order by chromatography is sometimes incorrect because the authors did not compare the same CSPs, particularly in the area of asymmetric catalysis [72]. That is why we stress on this trivial point.

Reversals of elution order have been reported on molecular CSPs: for α-amino-esters from tyrosine based CSP to phenylglycine based CSP [73]; on cyclodextrins [74]; on glycopeptides: for dansyl-aminoacids, L-enantiomers are eluted first on vancomycin and teicoplanin, but second on ristocetin [75]; on polysaccharide esters: for *trans*-1,2-diphenylcyclopropane from triacetyl to tribenzoyl cellulose [22]; on polysaccharide carbamates: for naringenin from Chiralcel OD-H to Chiralpak AD-H [41]. Reversals of elution order from Chiralcel OD-H to Chiralpak AD-H, cellulose and amylose tris(3,5-dimethylphenyl)-carbamate, respectively, may occur [76], but it is not a general rule.

3.1.2 Case of CSP Based on Similar Chiral Selector

This section deals with CSPs prepared from chiral selectors similar in structure but with different packing: coating, bonding or immobilization on silica for instance.

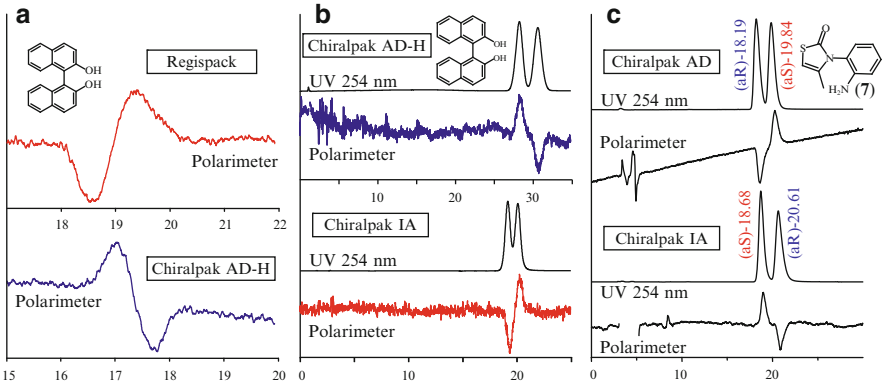

Fig. 7 Polarimetric traces (OR-1590): (**a**) for binaphthol, with *n*-hexane/2-PrOH (95/5), at 40°C, on Regispack at 2 mL/min and on Chiralpak AD-H at 3 mL/min; UV chromatograms and polarimetric traces (OR-1590); (**b**) for binaphthol on Chiralpak AD-H and on Chiralpak IA, with *n*-hexane/2-PrOH (95/5), at 1 mL/min and 25°C; (**c**) for (**7**) on Chiralpak AD and on Chiralpak IA, *n*-hexane/2-PrOH (9/1), 1 mL/min, 25°C

The quality of the silica has an impact on the performance of the column, but may also lead to a reversal of elution order. Nebivolol, a β-blocker, has opposite enantiomeric elution orders on Chiralpak AD and Chiralpak AD-RH, with 2-PrOH as mobile phase [77]. These two columns are based on the same amylose carbamate, but are coated on silica with different granulometry and hydrophobicity. According to the supplier, in reversed phase, the same chiral selector as found in the normal phase is coated on a hydrophobic high quality silica support. Influence of the silica has also been recently highlighted by a reversal of elution of the diastereomers, α- and β-thujone, on Whelk-01, depending on the characteristics of the silica used: spherical or Kromasil [66]. We have also found a reversal of elution order for binaphthol enantiomers on chiral columns coated with the same amylose carbamate chiral selector, namely Regispack and Chiralpak AD-H (Fig. 7a). The polarimetric trace shows the reversal unambiguously due to the silica characteristics, coating method of polysaccharide or packing process.

In the case of polysaccharide derivatives, the solvent used for the coating on silica plays a significant effect on the enantioselectivity of CSPs. Francotte showed that the enantiomeric elution order can be reversed depending on the solvating agent of the polymer used before its precipitation in *n*-hexane. For substituted 1-phenylethyl benzoates, elution orders were opposite using dichloromethane or nitrobenzene to dissolve cellulose tris(3-methylbenzoate) before coating [78].

The way the chiral selector is associated with silica is also an important parameter. Thus, Doyle et al. illustrated the difference between ionic and covalent CSP by a reversal of elution order on a poor separation ($\alpha = 1.03$ in both cases) of (3,5)-dinitrobenzoyl amide of 1-phenyl-2-aminopropane, on (*R*)-*N*-(3,5-dinitrobenzoyl)-phenylglycine ionically or covalently bonded. In the ionic column, the CSP is bound to the silica through an ion pair between the carboxylate of phenylglycine and the protonated nitrogen of the amino-propyl-silica [79].

Switching from a coated chiral selector to a bonded (or immobilised) chiral selector leads to change in chiral recognition mechanisms because the chiral selector has to be modified to be bonded on silica. A spacer (alkyl or other) has to be introduced on the initial chiral selector and alters its conformation, resulting in modification of the enantioselectivity. Rigorously, it is not the same chiral selector. Examples were given on glycopeptides CSP; dansyl aminoacids have opposite enantiomeric elution orders on a chemically bonded vancomycin column or on a CSP prepared by dynamic coating of a monolithic reversed-phase HPLC column with a vancomycin-derivative as chiral selector [80]. For polysaccharide, immobilised CSPs have been introduced for cellulose and amylose (3,5-dimethylphenyl)-carbamate. In the coated version (Chiralcel OD and Chiralpak AD), the substitution degree of cellulose or amylose is 3, while in the immobilised version (Chiralpak IB and IA) the substitution degree is lower than 3, because some hydroxy groups of the glucose units are not substituted by carbamate but used for the bonding to silica. So these chiral selectors are different, as proven by the reversal of elution order obtained for atropisomer (**7**) [81] and binaphthol between Chiralpak AD and Chiralpak IA. Using the same mobile phase, polarimetric detection shows clearly the different elution orders (Fig. 7b, c). Opposite elution orders have also been reported between Chiralpak IB and Chiralcel OD-H for ten barbiturates [69].

3.2 Reversal of Enantiomeric Elution Order Due to Experimental Parameters on the Same CSP

According to the literature, almost all chromatographic experimental parameters can induce a reversal of enantiomeric elution order. Several articles have dealt with the influence of a parameter for the separation of a particular compound on a given CSP. Recently, Chankvetadze has reported an impressive study with reversals of enantiomeric elution order for Fmoc-isoleucine on Lux-Cellulose-1, depending on the content of the polar organic modifier of the mobile phase, the temperature and, for the first time, the acidic modifier content in the mobile phase [82]. We present in this section the parameters that have led to the observation of reversals of enantiomeric elution order in literature.

3.2.1 Influence of Mobile Phase Modifier

The influence of the mobile phase modifier has been shown on protein based CSP when acetonitrile replaces an alcohol. Indeed, a change from 1-PrOH to acetonitrile leads to reversal of elution order for enantiomers of clevedipine and of its hydrolysed analog on a Chiral-AGP column [83]. In the same way, on Ultron ES-OVM, a change in organic modifier from ethanol to acetonitrile causes a reversal of elution order for the *cis*-(2*S*,4*S*) and *cis*-(2*R*,4*R*) enantiomers of the

ketal tosylate intermediate of azalanstat [84] and for propanolol propyl ester enantiomers [85]. For propanolol *n*-pentyl ester, the same enantiomeric elution order is observed using ethanol, 2-PrOH and acetonitrile, but use of methanol results in the opposite [85].

One example is also described on a molecular CSP, based on a dinitrobenzoyl-tyrosine derivative, the elution order of different dinitrobenzoyl amino-esters is reversed from the mixture *n*-hexane/ethanol (85/15) to *n*-hexane/chloroform (35/65) [73].

All other reported reversals of enantiomeric elution order with the mobile phase modifier concern polysaccharide based CSPs. On Chiralcel OB, 19 different alcohols in *n*-hexane were tested for the separation of methyl 2-phenoxypropanoate enantiomers, which gave the opposite elution order according to the authors; but this case may be doubtful because the elution order was monitored by the sign from a polarimetric detector without checking that the sign was not reversed by the change of mobile phase [86]. On another cellulose ester, Chiralcel OJ, pyriproxyfen enantiomers show both elution orders depending on the 14 alcohols used as modifier in *n*-hexane [87, 88]. The absence of alcohol in the mobile phase may also lead to elution order reversal, such as for *trans*-chlordane separated on Chiralcel OD in pure *n*-hexane or with 1% of 2-PrOH in *n*-hexane [37]. When the mobile phase modifier is changed from ethanol to 2-PrOH, by HPLC, the enantiomeric elution order is reversed for binaphthol on Chiralcel OD [89], for 3-(4-fluoro)phenyl-4-benzyl-2-morpholinone on Chiralpak AS [90], and on Chiralpak AD, for omeprazole (from 2-PrOH or 1-PrOH to methanol or acetonitrile too in this case) [71, 91], nebivolol (from 2-PrOH or butan-1-ol to methanol, ethanol or 1-PrOH too) [77], morpholine derivatives [90], *N*-[2-hydroxy-2-pyridin-3-yl-ethyl]-2-(4-nitrophenyl)acetamide and its amino analog [76] and linezolid [92]. In the case of "pineno" fused terpyridyl ligands [93], ethanol, 2-PrOH, 1-PrOH and *tert*-butanol give the elution order opposite to that given by 1-butanol, 1-pentanol or 1-hexanol. On home-made amylose tris-(3,5-dimethylphenyl)-carbamate, the alcoholic modifier changes the elution order for diniconzole, uniconazole, paclobutrazol and their analogs [70]. In normal phase HPLC, methanol can be used in a mixture with ethanol, so on Chiralpak AD the enantiomeric elution order for ibuprofen and mandelic acid can be reversed when the polar alcohol modifier in isohexane, 2-PrOH, is replaced by a mixture methanol/ethanol (2/1) [94]. By SFC, the reversal is obtained from 2-PrOH to methanol for omeprazole (from 2-PrOH to ethanol too) [71, 95], naproxen, ibuprofen and ketoprofen [96]. The reversals of elution order observed on Chiralpak AD can usually be reproduced on Chiralpak IA, its immobilised version, as for omeprazole [71]. The number of solvents usable on Chiralpak IA is much larger and increases the probability of observing reversals, switching from 2-PrOH to THF in *n*-hexane, or from 100% ethanol to 100% ethyl acetate for example [97].

Such reversals of enantiomeric elution order are illustrated in Fig. 12 for compound (**1**): on Chiralpak AD-H, by HPLC, with 50% of alcoholic modifier in *n*-hexane, (*S*)-(**1**) is eluted first with ethanol and second with 2-PrOH, but also 1-PrOH, butan-1-ol, butan-2-ol, *tert*-butanol, 3-methyl-1-butanol, 4-methyl-2-pentanol, while, by SFC, with 25% of co-solvent (*S*)-(**1**) is eluted first with

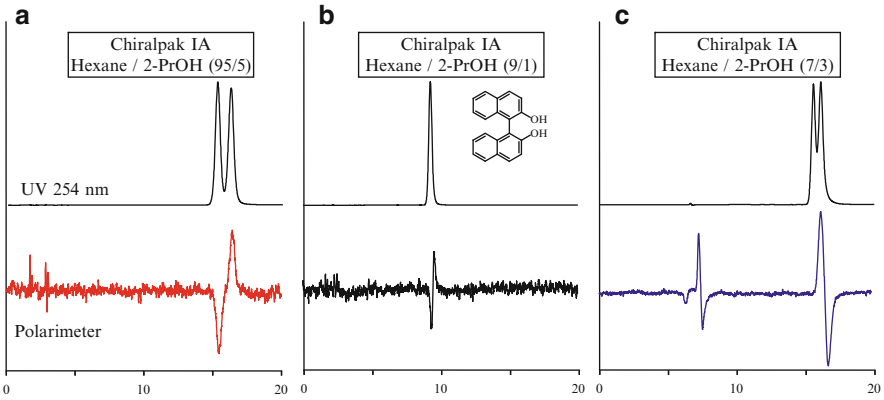

Fig. 8 UV and polarimetric traces (OR-1590) for binaphthol, on Chiralpak IA, at 35°C: (**a**) *n*-hexane/2-PrOH (95/5), at 2 mL/min; (**b**) *n*-hexane/2-PrOH (9/1), at 2 mL/min; (**c**) *n*-hexane/2-PrOH (7/3), at 0.5 mL/min

methanol and ethanol and second with 2-PrOH. A similar effect is observed for binaphthol, by SFC at 40°C with 20% of alcohol: (*R*)-binaphthol is eluted first with methanol and 2-PrOH and second with ethanol (Fig. 13). The steric bulk of the alcohols has often been cited to explain these reversals [87], but from all these examples it appears that there is no clear rule for predicting the influence of alcohols. A majority of described reversals occur on chiralpak AD but we cannot know whether this observation is due to a characteristic of this CSP or to its widespread use in laboratories.

The elution order may be affected by the proportion of organic modifier in the mobile phase. Some cases are reported in the literature: for amino acids dependent on the acetonitrile content of the eluent on copper(II)-D-penicillamine chiral stationary phase [98], for metoprolol analog with the 1-PrOH ratio on Chiralcel OD [99], for methyl *N*-Boc α-methyl (4-bromo)-phenylalaninate on Chiralpak AD from 20% ethanol in *n*-hexane to 1% ethanol [100] and on Chiralpak IA dependent on the 2-PrOH content for naproxen [101] and for binaphthol with 3-methyl-1-butanol [102] or with 2-PrOH (Fig. 8). In the latter case, the reversal of elution order is monitored by a polarimetric detector. (*R*)-Binaphthol, which gives a positive sign in the three mobile phases used, is eluted second with 5% of 2-PrOH and first with 30%. This type of reversal is not often observed because decreasing the ratio of organic modifier leads to very long retention times.

3.2.2 Influence of Mobile Phase Additives

Additives are sometimes added in the mobile phase to elute basic or acidic compounds. Acids, bases or both are mixed with the eluent in amounts ranging from 0.01 to 1 vol.%. Use of acid additives may affect the elution order; thus it is

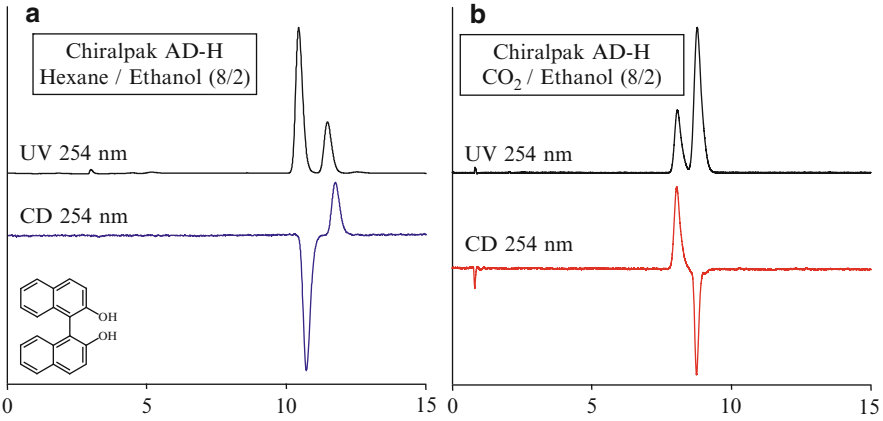

Fig. 9 UV and CD traces (CD-1595) at 254 nm for (*R*)-enriched solution of binaphthol, with 20% of ethanol, at 40°C, on Chiralpak AD-H: (**a**) by HPLC, *n*-hexane/ethanol (8/2), at 1 mL/min; (**b**) by SFC, CO_2/ethanol (8/2), 4 mL/min, outlet pressure = 120 bars

reversed for a metoprolol analog on Chiralcel OD when acetic acid (25 mM) is present [103]. In a few reported cases the nature and the ratio of these additives induce a reversal of enantiomeric elution order. On Lux-Cellulose-2 and Lux-Cellulose-4, (*R*)-ropivacaine is eluted before (*S*)-ropivacaine when using acetonitrile with 0.1% DEA and 0.1% formic acid (FA) as mobile phase, but the opposite elution order is obtained when formic acid is replaced by trifluoroacetic acid [104]. The formic acid ratio may also be an important parameter: on Lux-Cellulose-1, D-Fmoc-isoleucine is the first enantiomer eluted in *n*-hexane/2-PrOH (85/15) with 0.1% FA but the second with 0.5% FA [82]; on Lux-Cellulose-2 and Lux-Cellulose-4, with acetonitrile and 0.1% DEA as eluent, (*R*)-amlodipine eluted first with FA ratio lower than 0.02% and 0.035% respectively, but second at higher FA concentrations [105, 106], although this behaviour is not noted for other dihydropyridines tested. The influence of water contained in the eluent has also been pointed out on Chiralcel OD for a metoprolol analog: going from 0.2 to 1.6 g/L of water in *n*-hexane/2-PrOH (75/25) with DEA (10 mM) results in a reversal of enantiomeric elution order [99, 103].

3.2.3 Reversal Between SFC and HPLC

The apolar solvent may also affect the elution order, as illustrated by the reversal observed for binaphthol between SFC and HPLC techniques (Fig. 9): other experimental parameters being equal (temperature, percentage of alcohol), (*R*)-binaphthol is eluted first by HPLC with *n*-hexane and second by SFC with carbon dioxide.

3.2.4 Influence of the Injected Amount

On microcrystalline cellulose triacetate, two atropisomers, 3-(2-propylphenyl)-4-methyI-4-thiazolin-2-one and its thiazolinethione analog, show reversal of elution order when the amount of sample injected is increased from 2 to 16 mg [107], so that the enantiomer separation is lost for a given quantity. This is the only example described from analytical scale to preparative scale. Nowadays, this behaviour will be difficult to detect because the loading capacity studies are usually done gradually and stopped when the separation is lost. Compounds with such isotherms [108] are interesting for preparative purposes by sequential injections.

3.2.5 Influence of pH

On protein bonded CSPs, OVM and Chiral-AGP, the enantioselectivity of the separation of propanolol and its ester derivatives varies with the pH. It is possible to reverse the elution order by changing pH in the range 3–6.9 [109, 110]. Likewise, the enantiomeric elution order of mosapride and its main metabolite can be controled by the mobile phase pH on Chiral-AGP: pH was varied between 4.2 and 7.4 and the reversal of elution order occurred at 6.9 [111].

3.2.6 Influence of the Temperature

In chromatography on a chiral support, enantioselectivity α is related to the difference between the free energy of adsorption of both enantiomers, according to (1). The retention factors for each enantiomer, k_R and k_S, are dependent on enthalpy and entropy adsorptions on the chiral support, ΔH_R and ΔS_R for the (*R*)-enantiomer, as shown in (2).

Equation 1. Relationship between thermodynamic parameters for the adsorption process of enantiomers onto CSP and chromatographic parameters, β is the column phase ratio.

$$\Delta\Delta G = -\mathrm{RT}\ln\alpha, \tag{1}$$

$$\ln k_R = \frac{-\Delta H_R}{\mathrm{RT}} + \frac{\Delta S_R}{R} - \ln\beta, \tag{2}$$

$$T_{\mathrm{iso}} = \frac{\Delta H_R - \Delta H_S}{\Delta S_R - \Delta S_S}. \tag{3}$$

Accordingly, a temperature exists at which $\Delta\Delta G = 0$ ($k_R = k_S$). This temperature, called isoenantioselective temperature or isoelution temperature in older articles (T_{iso}, (3)) [112], was predicted by Davankov [113] and Schurig [114], and first observed [115, 116] and then studied in gas chromatography, mainly by Schurig

[117]. The Van't Hoff plot, i.e. the line obtained by plotting the natural logarithm of the retention factors against the reciprocal of temperature (in Kelvin), can be drawn for each enantiomer, after collecting data at different temperatures (Fig. 15). The relationship between ln k and $1/T$ is linear if ΔH and ΔS are temperature independent, if enantiomer retention results from a single associative mechanism [112] and if the experimental data are very accurate. The crossing of the lines obtained for both enantiomers should give the isoenantioselective temperature. However, if the temperature range is extended, T_{iso} predicted by such extrapolation may be inaccurate [118]. Moreover, linear plots seem difficult to observe in SFC [119], because ΔH is dependent on fluid density, and thus on temperature, because the critical temperature is crossed [120] or because of variation of the column phase ratio β [121]. If the surface of the chiral support is not homogeneous, this approach does not give a correct estimate of the thermodynamic parameters [122].

For each enantiomer separation it is possible to reverse the elution order beyond T_{iso}. As the temperature range used for chiral chromatography is usually narrow, between 10°C and 50°C, T_{iso} is often unreachable, but has been seen in some cases by the observation of isoelution and/or reversal of elution order. The first report in chiral chromatography by Pirkle in 1993 [123] dealt with the separation of *N*-(3,5-dinitro-benzoyl)-α-phenylethylamine enantiomers on a proline based molecular CSP: with *n*-hexane/2-PrOH (8-2) as mobile phase, (*R*)-enantiomer was first eluted at 30°C, but was second eluted at −25°C; T_{iso} is 0°C in this case. Pirkle has also shown the influence of the eluent, since T_{iso} is 25°C in *n*-hexane/ethanol (8/2), higher than 27°C in methanol/water (7/3) and lower than −25°C in *n*-hexane/dichloromethane (1/1). In one article, extreme experimental conditions were used in SFC, the temperature ranging between −10°C and 190°C with an outlet pressure of 300 bars, in order to observe reversal of enantiomeric elution order for two original molecules on Whelk-O1, with T_{iso} of 70°C and 150°C [120]. On the same molecular CSP, di-(3,5-dinitrophenyl)-carbamate of *trans*-1,2-cyclohexanediol and *trans*-1,2-cycloheptanediol have reversed elution order in the mobile phase chloroform/methanol (99/1) between 25°C and 85°C with T_{iso} around 65°C, but (*S*,*S*) enantiomer remains the first eluted in this temperature range with 15% of acetonitrile or 25% of ethyl acetate in chloroform [108]. For sotalol enantiomers, on an immobilized cellobiohydrolase Chiral-CBH, by increasing the temperature from 5°C to 40°C the retention time of the (*S*)-enantiomer rapidly decreases while the retention of the (*R*)-enantiomer is only slightly affected, resulting in a reversal with T_{iso} around 28°C [124]. On polysaccharide based CSP, reversals of enantiomeric elution order were reported for ketoprofen and naproxen by SFC on Chiralpak AD between −15°C and 30°C [96]; for binaphthol on Chiralpak IA between 10°C and 50°C [125]; for 1-(naphthylethylamino)methyl-2-naphthol analog on Lux-Cellulose-1 with $T_{iso} = 20$°C [126]; for Fmoc-isoleucine on Lux-Cellulose-1 with $T_{iso} = 20$°C [82]. The reversal of elution order for binaphthol on Chiralpak IA with *n*-hexane/2-PrOH (9/1) is illustrated in Fig. 10: at 15°C, (*R*)-binaphthol, which gives a positive sign with polarimetric detection, is first eluted; T_{iso} is reached at 30°C; at 60°C, (*R*)-binaphthol is eluted second.

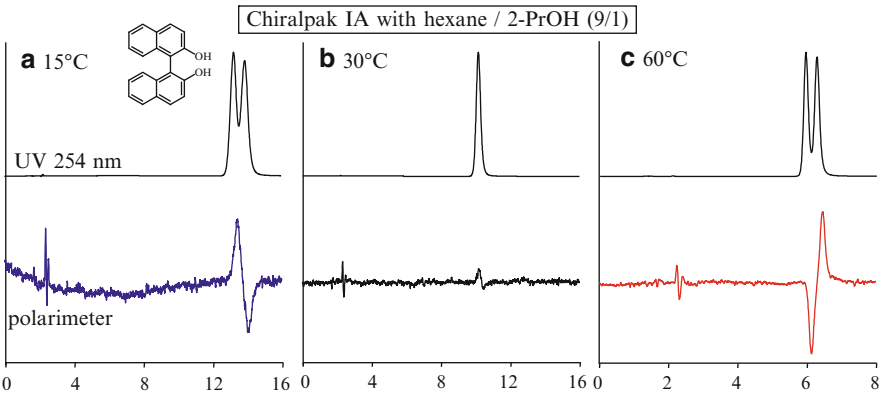

Fig. 10 UV at 254 nm and polarimetric traces (OR-1590) for binaphthol, on Chiralpak IA, *n*-hexane/2-PrOH (9/1), at 1 mL/min: (**a**) 15°C; (**b**) 30°C; (**c**) 60°C

3.2.7 Two-Dimensional Reversal of Enantiomeric Elution Order

The two main parameters prone to reverse an elution order on a given CSP are the temperature and the mobile phase. We have monitored with polarimetric detection the reversal of elution order of binaphthol enantiomers on Chiralpak IA, by varying the temperature from 15°C to 60°C and the content of 2-PrOH in the mobile phase from 5% to 30%. Polarimetric traces for this two-dimensional reversal of enantiomeric elution order are depicted in Fig. 11. For *n*-hexane/2-PrOH (8/2) mobile phase, (*R*)-binaphthol is eluted first until 40°C and second beyond 50°C. With increasing temperature, retention times decrease, the intensity of the polarimetric signal increasing at first because peaks are thinner, then decreasing because the separation is gradually lost. At T_{iso}, around 45°C, the signal is weak and above T_{iso}, the signal starts to increase again but with opposite elution order. So T_{iso} can be directly determined from the absence of polarimetric signal: 30°C with 10% of 2-PrOH, 45°C with 20% and around 52°C with 30%. Obviously, with a UV or RI detector, a single peak is obtained for both enantiomers between 30°C and 55°C; this range has been named "temperature-induced blind zone in chiral recognition, in which enantioseparation could not be obtained" by Weng and co-workers [101, 102, 125]. Obviously chiroptical detection reveals this so-called "blind zone" which does not exist anymore.

By SFC, a similar study was carried out by varying the temperature and the alcoholic co-solvent with an (*R*)-enriched solution of binaphthol to highlight the reversal of elution order and the isoenantioselective temperature. With 20% of co-solvent, $T_{iso} = 60$°C with methanol and 2-PrOH and $T_{iso} = 20$°C with ethanol, reversal of elution order is obtained at 40°C switching from methanol or 2-PrOH to ethanol (Fig. 14, lines a, c and e).

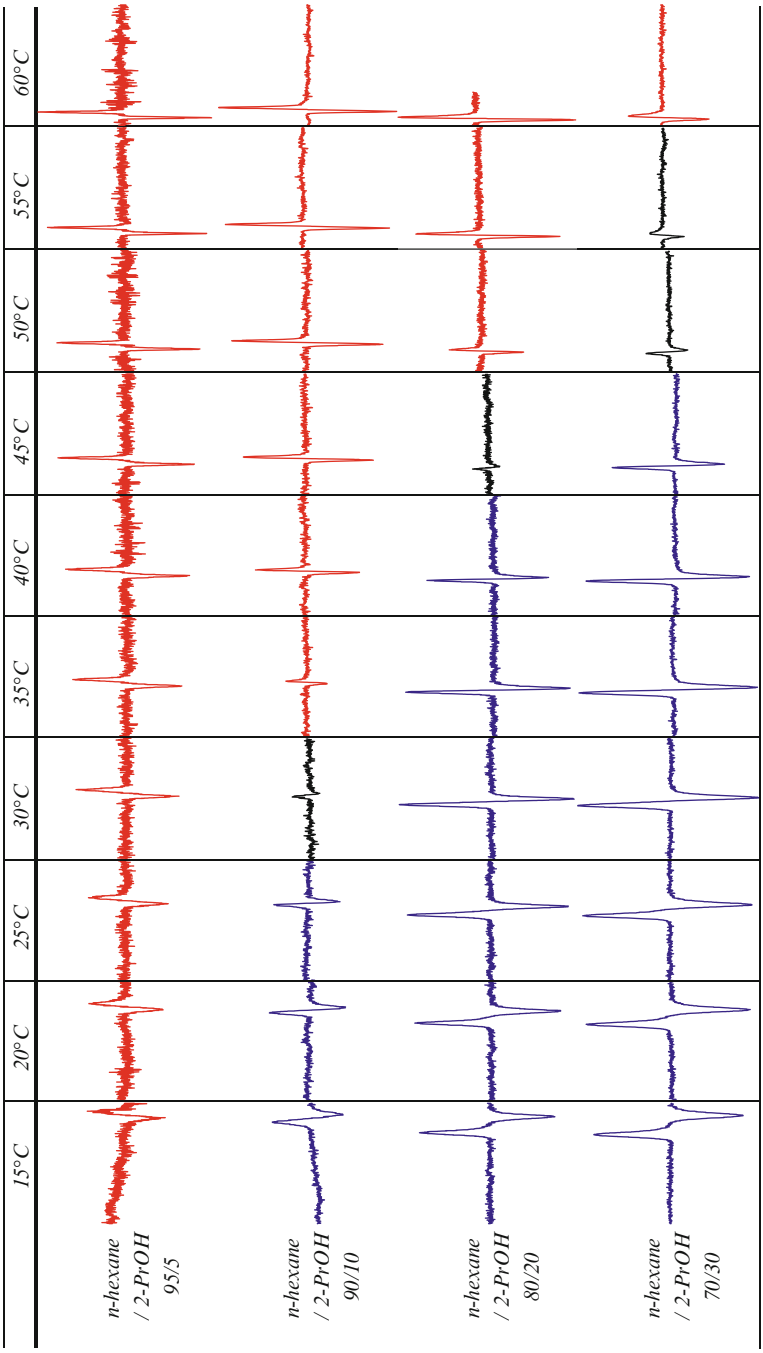

Fig. 11 Polarimetric traces (OR-1590) for binaphthol on Chiralpak IA at different temperatures and different percentages of 2-PrOH in the mobile phase; *blue*: (*R*)-enantiomer first eluted; *red*: (*S*)-enantiomer first eluted

3.3 Unusual Phenomena with Mixtures of Co-solvents

Reversed enantioselectivities ($k_{\text{second eluted enantiomer}}/k_{\text{first eluted enantiomer}}$) observed using different co-solvents or organic modifiers lead us to look at chromatographic behaviour in the case of co-solvent mixtures. Very few studies of the influence of co-solvent mixtures on the enantiorecognition have been published. This type of ternary mixtures of solvents, apart from acidic and basic additives, is sometimes described in the literature for improving the solubility of a compound in the mobile phase or to decrease retention times. Particularly, on immobilised polysaccharide CSPs, the addition of chloroform is often used to solubilize racemates in the mobile phase [127–129]. The absence of alcohol in the mobile phase can prevent the elution, so alcohol is often added, even in small amount (1–5%). In HPLC, immiscibility of methanol in *n*-hexane explains the reason why the addition of ethanol is required to obtain a unique phase.

On Chiralpak AD, reversals of elution order are observed for ibuprofen and for mandelic acid when 2-PrOH, the organic modifier in isohexane, is replaced by methanol/ethanol (2/1) [94]. The influence of methanol addition in *n*-hexane/2-PrOH mobile phase was discussed on Chiralpak AD [91]: for timoprazole, methanol addition increases the retention of the second enantiomer and, accordingly, enantioselectivity, while for omeprazole the addition of more than 4% of methanol reverses the elution order. In SFC, addition of 10% 2-PrOH in methanol co-solvent improves the enantioselectivity of omeprazole separation from 1.74 to 2.41 [71]. Again, on Chiralpak AD the reversal of elution order for nebivolol between ethanol and 2-PrOH was investigated by mixing both solvents in different proportions [77]: there is no correlation between the enantiomer retention times and the ratio of 2-PrOH in ethanol and the reversal of elution order is sudden, with 25% of 2-PrOH (*SSSR*)-nebivolol eluted first, but second with 20%. Addition of chloroform in *n*-hexane/ethanol (85/15) mobile phase for a dinitro-benzoyl amino-ester on a dinitro-benzoyl-tyrosine CSP reverses the elution order, but also decreases the retention times [73]. Thus, there are several possible behaviours when mixing several co-solvents or organic modifiers that are illustrated in several cases in the following paragraphs with mixtures of alcohols.

If we consider two different alcohols used as organic modifiers, leading to separation of enantiomers with identical elution order for a racemate on a given CSP, the expected behaviour when mixing these alcohols should be a separation with the same elution order. This is true for the chiral separation of binaphthol on Lux-cellulose-2; going from 20% ethanol to 20% 2-PrOH by addition of 5% of 2-PrOH results in a quite linear relationship between retention and ratio of 2-PrOH (Fig. 12a). However, unexpected behaviour can occur, leading to separation loss or separation with reversal of elution order. Examples are provided for binaphthol on Chiralpak AD-H by SFC (Fig. 14): at 40°C, with methanol and 2-PrOH alone, (*R*)-binaphthol is first eluted, but with an equal volume mixture of both alcohols, the separation is lost; at 50°C, a small separation exists with 100% methanol and 100% 2-PrOH, but with the mixture the opposite elution order is obtained. Improvement of enantioselectivity is possible, as for binaphthol on Chiralpak AD-H, with 20% of

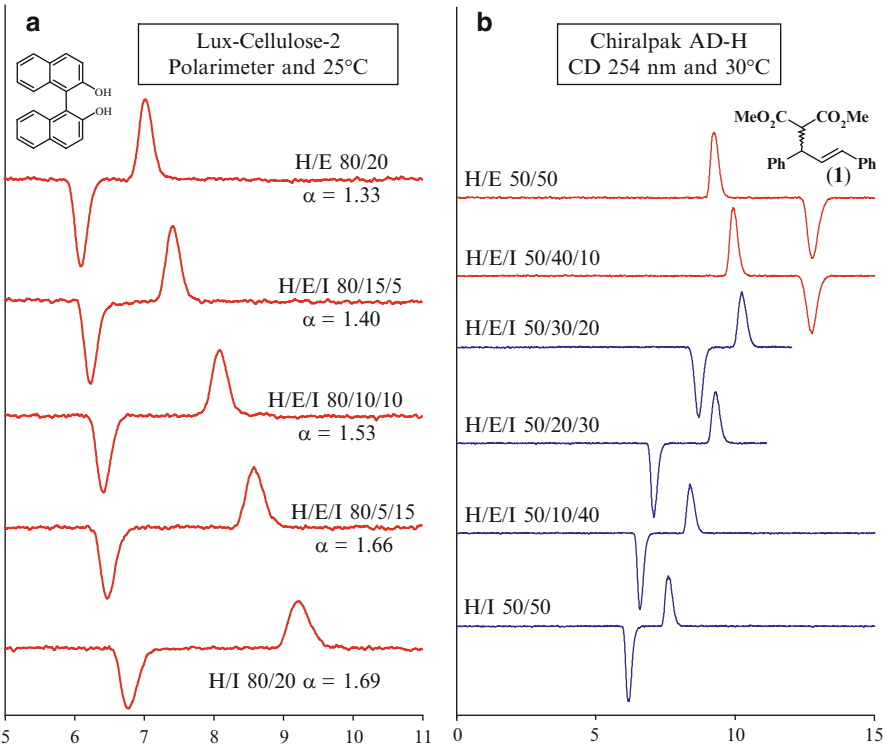

Fig. 12 Effects of mixtures of alcohols in *n*-hexane: (**a**) polarimetric traces (OR-1590) for binaphthol on Lux-Cellulose-2, 1 mL/min, at 25°C; (**b**) CD chromatograms (CD-1595) at 254 nm for (**1**), at 30°C, on Chiralpak AD-H; *H*: *n*-hexane, *E*: ethanol, *I*: 2-PrOH; *blue*: (*R*)-enantiomer first eluted; *red*: (*S*)-enantiomer first eluted

ethanol or 2-PrOH in *n*-hexane: enantioselectivity is 1.28 for both with the same elution order, but jumps to 1.70 with the mobile phase *n*-hexane/ethanol/2-PrOH (8/1/1) (Fig. 13b).

If we consider two different alcohols, giving no separation for a racemate on a given CSP, we do not expect a separation when mixing these alcohols. However, for binaphthol on Chiralpak AD-H by SFC at 60°C (Fig. 14) there is no separation with methanol and 2-PrOH, but enantiomers are separated with their mixture (1/1).

If we consider two different alcohols used as organic modifiers, leading to separation of enantiomers with opposite elution order for a racemate, the prediction on a given CSP is tricky. If enantioselectivities are reciprocal, one can assume that the separation will be lost with the mixture, as for binaphthol by SFC at 40°C (Fig. 14): methanol and ethanol result in the separations with similar enantioselectivities and opposite elution order, and there is no separation with methanol/ethanol (1/1). This first approximation, that the retention factor for an enantiomer using a mixture of solvents is proportional to the retention factor for this enantiomer in each pure solvent and molar ratio of each solvent, is not a rule. Only three articles report

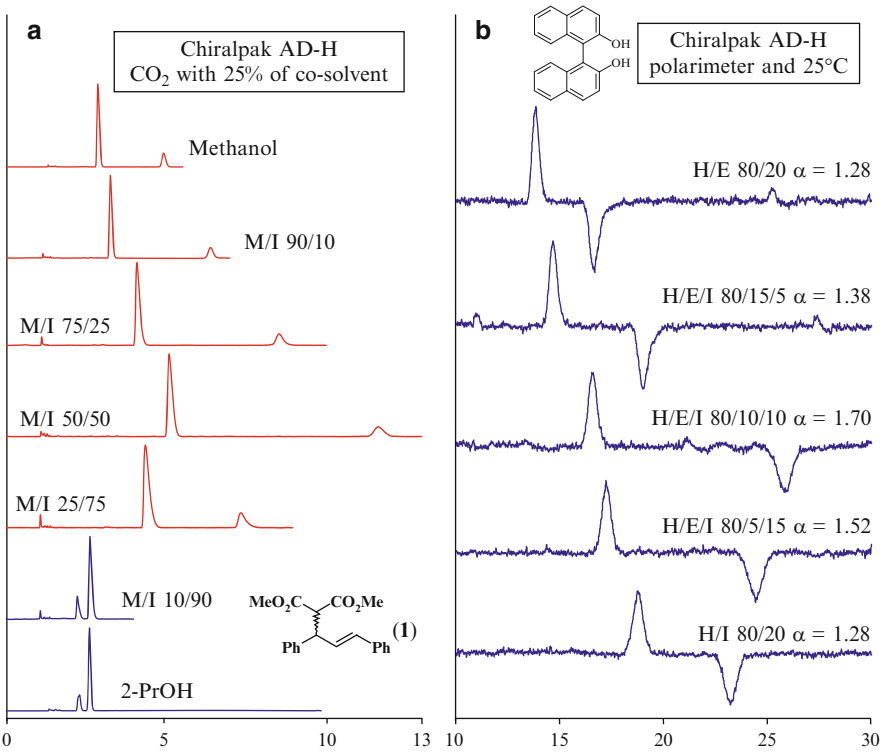

Fig. 13 Synergistic effects when mixing alcohols: (**a**) CD chromatograms (CD-1595) at 254 nm for (**1**) with mixtures of alcohol in *n*-hexane, at 30°C, on Chiralpak AD-H; (**b**) polarimetric traces (OR-1590) for binaphthol on Chiralpak AD-H, 1 mL/min, 25°C. *H*: *n*-hexane, *M*: methanol, *E*: ethanol, *I*: 2-PrOH; *blue*: (*R*)-enantiomer first eluted; *red*: (*S*)-enantiomer first eluted

the determination of the point of reversal of the elution order [73, 77, 91]. In each, the reversal is sudden, i.e. only a slight change in the mobile phase composition causes the reversal. Such behaviour is illustrated in Fig. 12b; enantioselectivities are quite similar when (*S*)-**1** is eluted first with 0–10% 2-PrOH, and (*R*)-**1** is eluted first with 20–50% 2-PrOH: the reversal is sudden between 10 and 20% 2-PrOH. In SFC, mixing methanol and 2-PrOH leads to a dramatic effect on retention for (*R*)-**1** and on enantioselectivity (Fig. 13a): retention time of (*R*)-**1** jumps from 2.3 min (2-PrOH) and 5.4 min (methanol) to 11.7 min (methanol/2-PrOH 1/1). This impressive and unusual improvement in enantioseparation of (**1**) kindles the interest in testing mixtures of modifiers in screening stategies.

The use of alcohol mixtures may induce linear, antagonist or synergistic effects on enantioselectivity. Even if these effects are not yet predictable, such unusual phenomena may be interesting for a better understanding of chiral recognition mechanisms.

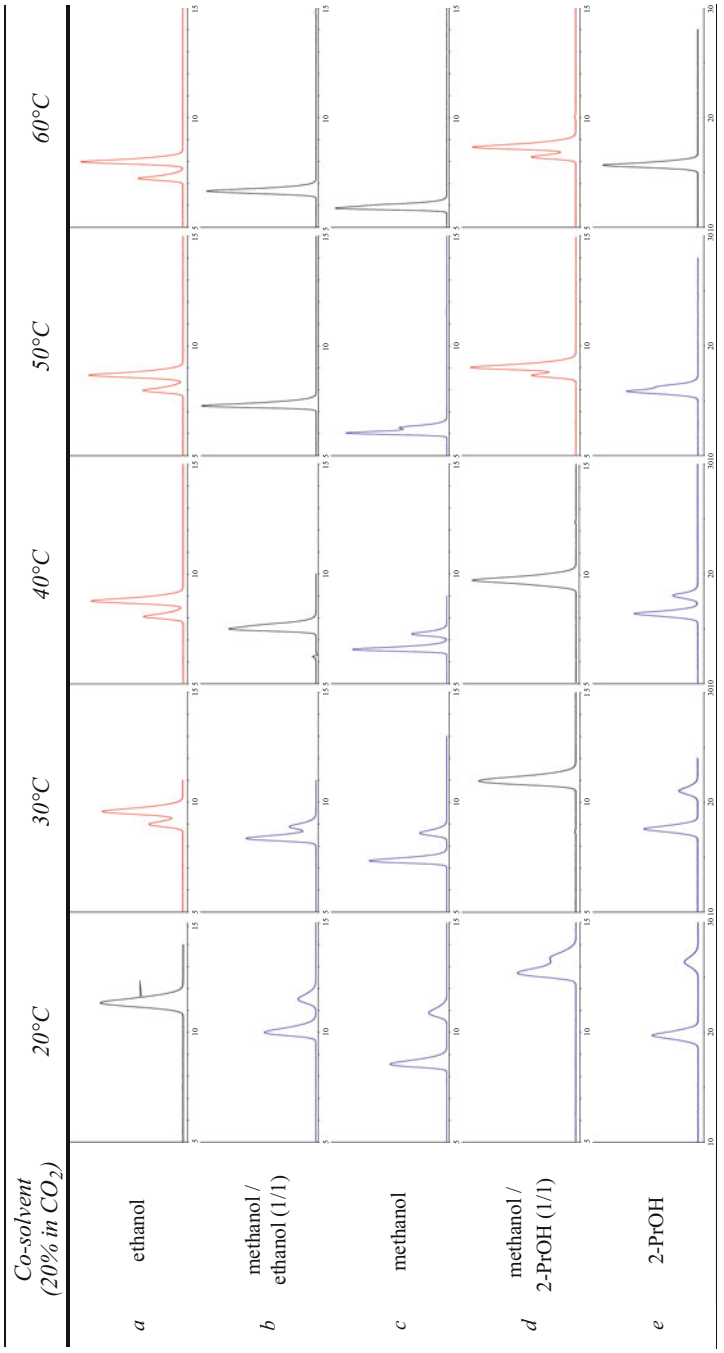

Fig. 14 UV chromatograms at 254 nm for (*R*)-enriched solution of binaphthol on Chiralpak AD-H, CO_2/co-solvent (8/2), 4 mL/min, outlet pressure = 120 bar, for different temperatures and co-solvents; *blue*: (*R*)-enantiomer first eluted; *red*: (*S*)-enantiomer first eluted

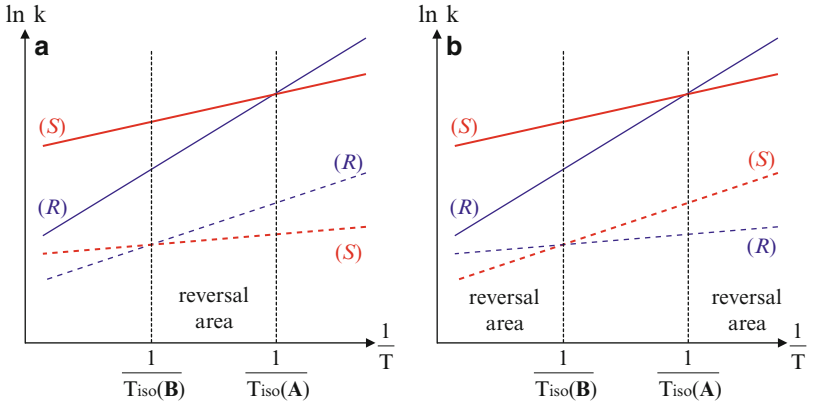

Fig. 15 Theoretical Van't Hoff plots for enantiomers (*blue* for the (*R*)-enantiomer and *red* for the (*S*)-enantiomer) separated on the same chiral selector, using two different chromatographic conditions **A** (*solid lines*) and **B** (*dashed lines*): (**a**) reversal of elution order between isoenantioselective temperatures; (**b**) identical elution order between isoenantioselective temperatures

3.4 Reversal of Enantiomeric Elution Order to Study Enantiorecognition Mechanisms

Authors who report reversals of elution order justify their observations by the complexity of the chiral recognition mechanisms, particularly on polysaccharide based CSPs, such as drastic conformational changes of the chiral selector, alteration of chiral cavities, steric effect of organic modifier and variety of binding sites. However, the observation of a reversal of enantiomeric elution order is not sufficient proof to invoke different binding sites and major modifications in the enantiorecognition mechanism or in the geometry of the diastereomeric complexes formed between enantiomers and CSP. Reversal of elution order should always be studied together with temperature dependence, and the isoenantioselective temperature should be estimated. Indeed, there are two main cases when a reversal is observed, when plotting ln k against $1/T$, assuming that ΔH and ΔS are temperature independent and that an isoenantioselective temperature exists. If we consider (*R*) and (*S*) enantiomers separated on the same chiral selector, using two different chromatographic conditions **A** and **B**, the lines ln k against $1/T$ (blue for the (*R*)-enantiomer and red for the (*S*)-enantiomer) can be drawn for each chromatographic conditions (solid lines for **A** and dashed lines for **B**). The lines for each enantiomer cross at the isoenantioselective temperature: T_{iso}(**A**) and T_{iso}(**B**) for the different chromatographic conditions (Fig. 15). **A** and **B** chromatographic conditions may differ by mobile phase (nature or content of the organic modifier, pH, water amount, ...) or by the preparation of the chiral selector (coating, immobilisation, packing, silica, ...). In Fig. 15a, elution orders are the same in the two chromatographic conditions at low and high temperature, but between $1/T_{iso}$(**A**) and $1/T_{iso}$(**B**), reversal of enantiomer elution order is observed. If the isoenantioselective temperatures are in an accessible range for

chiral HPLC or SFC (0–60°C), the reversal of elution order is experimentally reachable. We are unable, a priori, to determine whether the gap between T_{iso}(**A**) and T_{iso}(**B**) comes from a difference in chiral recognition mechanism, but we can assert that with T_{iso}(**A**) around ambient temperature it is quite easy to find conditions to reverse the elution order. This was done for binaphthol on Chiralpak AD-H and IA by changing temperature, mobile phase and column (immobilisation, supplier) in this section. The first example of multiple reversals of elution order, Fmoc-isoleucine on Lux-Cellulose-1 [82], is another example of the same behaviour with T_{iso}(**A**) = 22°C. Modifications of the chromatographic conditions lead to slight change in the solvation of the diastereomeric complexes, in conformations for the chiral selector or the solute, and so to a shift of the T_{iso}. In Fig. 15b, elution orders are different in the two chromatographic conditions at low and high temperature, but between $1/T_{iso}$(**A**) and $1/T_{iso}$(**B**) the same elution order can be observed. This is the case for compound (**1**) by HPLC on Chiralpak IA with *n*-hexane/2-PrOH (9/1); (*R*)-enantiomer is first eluted, T_{iso} is extrapolated to 160°C, and on replacing 2-PrOH by ethanol, (*S*)-enantiomer is first eluted and T_{iso} is extrapolated to 99°C, so the reversal is before both isoenantioselective temperatures. By SFC, on Chiralpak AD-H with 25% of co-solvent, the (*S*)-enantiomer is first eluted with methanol (T_{iso} around 105°C) and with methanol/2-PrOH (1/1) mixture (T_{iso} around 420°C), while the (*R*)-enantiomer is first eluted with 2-PrOH (no influence of temperature between 30°C and 55°C). In the case of compound (**1**) we can highlight two different chiral recognition mechanisms with 2-PrOH and with methanol or ethanol on Chiralpak IA and AD-H.

Estimation of the isoenantioselective temperature for a racemate on a CSP has three main points of interest. First, to optimize a chiral separation it is interesting to know whether the working temperature is above or below isoenantioselective temperature, because below T_{iso}, the higher the temperature the worse the enantioselectivity and above T_{iso}, the higher the temperature the better the enantioselectivity. Second, if T_{iso} is around ambient temperature, it will be quite easy to develop a method to reverse the elution order with accurate monitoring of the parameters. Third, the reproducibility of a chiral separation will vary from one laboratory to another if T_{iso} is around ambient temperature, particularly if the temperature is not controlled or if the CSPs are not strictly identical.

4 Chiroptical Detectors to Study Exchange Phenomena

An exchange phenomenon occurs during chromatography if analytes undergo a reversible reaction which alters their chirality (enantiomerisation, dimerisation . . .). Dynamic chiral chromatography allows the study of the interconversion of stereoisomers, while self-disproportionation is a consequence of homo- and heterodimers or oligomers formation in the mobile phase.

4.1 Dynamic Chiral Chromatography

Observation of the enantiomerisation of analytes during chromatography depends on the enantiomerisation rate constants. If the enantiomerisation is fast, with a barrier to enantiomerisation lower than 85 kJ/mol at 25°C, the enantiomers cannot be isolated and neither separated by chiral chromatography. If the enantiomerisation is slow, with a barrier to enantiomerisation higher than 105 kJ/mol at 25°C, the enantiomers can be baseline separated by chiral chromatography and isolated. For a barrier to enantiomerisation between 85 and 105 kJ/mol at 25°C, i.e. half-life between 43 s and 38 h at 25°C, it is possible to reveal enantiomerisation by selecting an adequate analysis temperature in order to obtain a half life on the order of a few minutes.

The typical chromatogram for racemate, subject to an interconversion process taking place inside the chiral column simultaneously with the chiral separation, shows a plateau between two peaks. Chiroptical detectors give opposite signs for the peaks and no signal for the plateau, as illustrated in Fig. 16 for the atropisomers (**8**) at 10°C. Each peak with a chiroptical sign corresponds to enantiomers which have not undergone any enantiomerisation in the column and the plateau corresponds to molecules which have undergone one or several enantiomerisations. At lower temperature the exchange would be slowed down and both peaks baseline separated. The plateau height increases and enantioselectivity decreases with temperature until coalescence of the two peaks (Fig. 16, at 35°C). The intensity of the chiroptical signal decreases with temperature because the amount of non-interconverted enantiomers decreases.

The first examples of dynamic chiral chromatography studies were performed by Schurig for gas chromatography [130] and by Mannschreck for liquid chromatography [131]. Such plateau chromatograms have been reported for different enantiomerisation mechanisms: rotation about a hindered bond for heterocyclic atropisomers [132], ring opening/ring closure for oxazepam [133] and torsion for helicenes [134]. The polarimetric [133, 134] and CD [135] detectors have been used to monitor dynamic chromatograms. Chiroptical detectors are useful to develop the analytical method to observe a suitable plateau, by varying CSP, mobile phase, temperature and flow-rate. Polarimetric signals have been deconvoluted [134] to estimate enantiomerisation rate constants. Indeed, the main interest of dynamic chromatography is to determine the barrier to enantiomerisation. Since the first estimation from the chromatogram profiles [134, 136], Trapp has developed a unified equation and software to calculate isomerisation rate constants [137–139] and the influence of the stationary phase on the enantiomerisation kinetic has been proven [140, 141]. For instance, the barrier to rotation of (**8**) was estimated at 85.3 kJ/mol in *n*-hexane/ethanol (8/2) from the UV chromatogram at 10°C.

Chiral dynamic chromatography is a versatile and now widespread tool [142–152] for studying the enantiomerisation or diastereomerisation processes in a domain of energies which was difficult or impossible to cover with dynamic NMR or classical thermal enantiomerisation kinetics. Thermal or catalyzed interchanges can thus be easily detected. In the field of dynamic stereochemistry [153], dynamic chromatography is a complementary method to dynamic NMR and classical kinetic thermal enantiomerisation, to determine the barrier to interconversion [154].

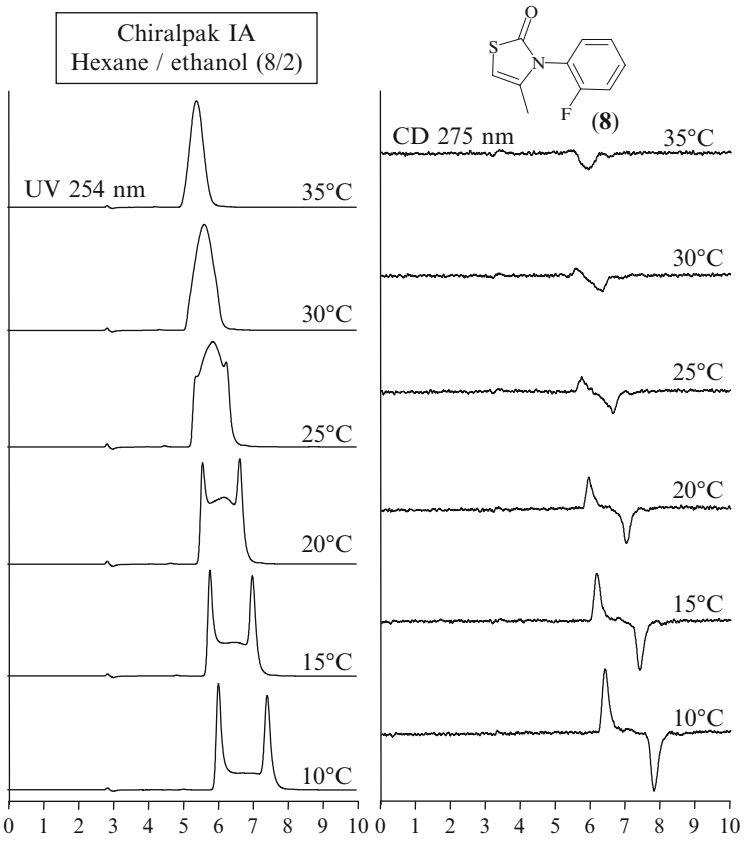

Fig. 16 UV (254 nm) and CD (275 nm) chromatograms (CD-1595) for (**8**), *n*-hexane/ethanol (8/2), 1 mL/min, on Chiralpak IA, for different temperatures

4.2 Self-Disproportionation

Enantiomers are eluted with the same retention times on achiral stationary phases. It is true when pure enantiomers are injected separately at the same concentration. Whatever the association state as homo-dimer or homo-oligomer of a pure enantiomer, the other enantiomer will produce exactly the same result. Chiroptical detection will show peaks with identical area and opposite sign. If the enantiomers in a racemic mixture behave strictly independently without the formation of associated states at a given concentration in an elution solvent, the retention of the racemate will be identical to those of the pure enantiomers. Interestingly, the injection of a racemic mixture might lead to different retention compared to the individual enantiomers. The origin of such a difference arises from the occurrence of both homo- and heterodimers (or higher order associations) when a racemate is involved. However, as expected, the composition of the mixture all along the elution peak of a racemate is strictly

composed of the racemic mixture without any enrichment whatever the type of associated states. In a racemate, a pair of enantiomeric homodimers can be formed in equal amount while heterodimers will correspond to a "meso" form. Heterodimers and homodimers are in a diastereomeric relationship and they may migrate differently on an achiral support. However, at each point of the chromatographic process the sample will be racemic due to the same migration of enantiomeric homodimers or to the occurrence of heterodimer composed of the two enantiomers. Chiroptical detection will be completely silent.

On the other hand, chromatography of a non-racemic mixture on an achiral stationary phase may lead to "self disproportionation of enantiomers" [155, 156], i.e. the enantiomeric composition of the elution peak of the mixture is not constant. One may find in the literature a handful of examples [157–170] which were recently reviewed [171, 172]. In general, a single peak is observed but the enantiomeric composition strongly varies all along the elution profile. In some extreme cases, the elution profile is composed of two distinguishable peaks without baseline separation; one shows a large increase of the ee while the other is approaching a racemic composition. Fractions with 99% ee were isolated from a mixture having an initial 40% ee on regular silica gel column [173]. In most of the reported cases the elution peak was divided into several successive fractions which were submitted to enantioselective chromatography to determine the enantiomeric excess at each point. It is thus possible to scan the actual self-disproportionation all along the peak.

On line chiroptical detection with a polarimetric or a CD detector is another way to scan the enantiomeric composition of the eluted peak. This method is perfectly suitable when HPLC columns are used but one can imagine that monitoring the output flow from MPLC is also possible. The principle is to have dual detection, e.g. UV and polarimeter or UV and CD. The use of a dual detection associating UV and polarimetry has been described in only one paper which dealt with the separation of binaphthol enantiomers through achiral chromatography [174]. We have reproduced the experiments performed on Lichrospher 100 NH_2 column eluted with chloroform. Figure 17 reports the chromatograms obtained with UV at 305 nm, CD detector at 300 nm and polarimeter for injection of 10 µL of a 2-mg/mL solution for (*R*), (*R*)-enriched and racemic binaphthol. It is clearly shown that the front of the peak is mostly composed of the pure (*R*) form while the tail is almost racemic. A signal probably due to an artefact is obtained for racemic binaphthol with chiroptical detections. The same behaviour is obtained with injection of 20 and 80 µL, but a single peak is observed for injection of 2 µL of the (*R*)-enriched sample.

The use of dual detection associating a UV or RI detector with a chiroptical detector is probably a very rapid way to spot the occurrence of self-disproportionating enantiomers during chromatography of a non-racemic mixture on achiral support. In case of disproportionation, the two signals will not have the same shape.

Modelling of chromatographic behaviour of non-racemic compounds under various conditions in achiral chromatography is generally done by simulation of elution profiles using UV detection [175–179]. Simultaneous simulation of the polarimeter or CD signals could provide a complementary useful and tutorial description of the phenomenon.

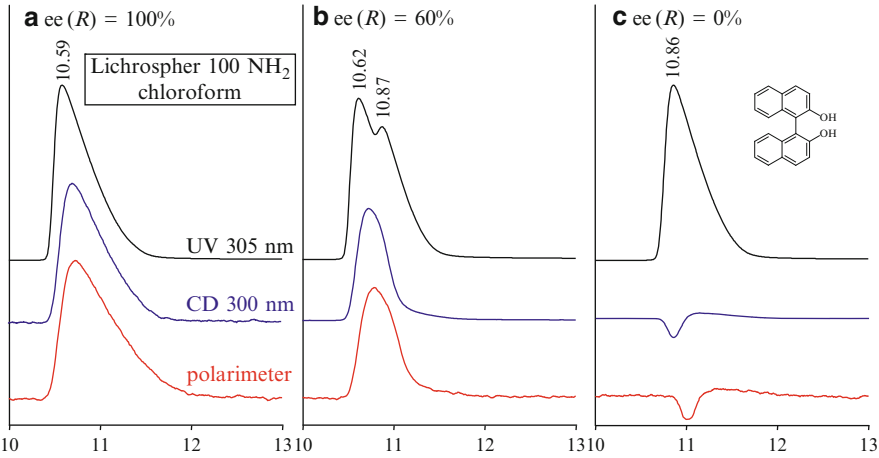

Fig. 17 UV (305 nm), CD (300 nm) and polarimetric chromatograms on Lichrospher 100 NH_2 (250 × 4 mm, 5 µm) eluted with chloroform, 1 mL/min, 25°C: (**a**) (*R*)-binaphthol; (**b**) (*R*)-enriched binaphthol; (**c**) racemic binaphthol

Chromatography of a non-racemic mixture on achiral stationary phases is a common post-reaction purification of most asymmetric catalysis media or resolution media before the determination of ee with the appropriate enantioselective chromatography on chiral stationary phases. It turns out that during the purification step particular attention shall be paid to collect the whole fraction of the non-racemic mixture in order to obtain a true evaluation of the ee. As shown above, the ratio of enantiomers may vary along the fraction containing the non-racemic mixture and thus different ees may be monitored for different zones of collection. Many more examples have probably been ignored during the chromatographic purifications of non-racemic mixtures issuing from chirotechnologies. Chiroptical detection can provide the answer.

5 Conclusion

Polarimetric and circular dichroism detectors are unique tools to differentiate enantiomers by chiral HPLC and SFC. However, the performances of these detectors depend on the chiroptical properties of the analytes: appropriate wavelength or range of wavelengths must be chosen to obtain a relevant output signal. The chiroptical sign given by the detector may serve to assign absolute configuration only after paying attention to the influence of the mobile phase on the sign. Reversals of enantiomeric elution order can thus be easily followed. These help in improving the knowledge of chiral recognition mechanisms. Many experimental parameters, such as temperature, mobile phase composition and column packing, may induce unusual and surprising

reversals. The temperature effect is thermodynamically explained and an isoenantioselective temperature exists in most cases, but is often difficult to reach in the working temperature range of chiral chromatography.

Reversals of enantiomeric elution order should not be systematically explained by different chiral recognition mechanisms involving diverse binding sites. Isoenantioselective temperature should be estimated to reveal a reversal due to a variation of this isoenantioselective temperature, caused by a slight modification in the energy of the diastereomeric complexes formed between enantiomers and the chiral selector.

Chiroptical detectors are essential to identify enantiomers in complex mixtures or during exchange phenomena where enantiomers and racemic peaks overlap while other detectors like UV or RI are inefficient in these cases. In particular, chiroptical detectors may provide very useful data for the understanding of a subject of growing interest, the self-disproportionation of enantiomers.

References

1. Francotte ER (2001) Enantioselective chromatography as a powerful alternative for the preparation of drug enantiomers. J Chromatogr A 906(1–2):379–397
2. Andersson S, Allenmark SG (2002) Preparative chiral chromatographic resolution of enantiomers in drug discovery. J Biochem Biophys Methods 54(1–3):11–23. doi:10.1016/s0165-022x(02)00126-4
3. Lämmerhofer M (2010) Chiral recognition by enantioselective liquid chromatography: mechanisms and modern chiral stationary phases. J Chromatogr A 1217(6):814–856. doi:10.1016/j.chroma.2009.10.022
4. Okamoto Y, Ikai T (2008) Chiral HPLC for efficient resolution of enantiomers. Chem Soc Rev 37(12):2593–2608. doi:10.1039/b808881k
5. Del Rio A (2009) Exploring enantioselective molecular recognition mechanisms with chemoinformatic techniques. J Sep Sci 32(10):1566–1584. doi:10.1002/jssc.200800693
6. Perry JA, Rateike JD, Szczerba TJ (1987) Eluting trace components before major constituents: I. Sensitivity enhancement in analytical determinations of optical purity. J Chromatogr 389(1):57–64. doi:10.1016/s0021-9673(01)94410-3
7. Zhou LL, Mao B, Ge ZH (2008) Comparative study of immobilized alpha 1 acid glycoprotein and ovomucoid protein stationary phases for the enantiomeric separation of pharmaceutical compounds. J Pharm Biomed Anal 46(5):898–906. doi:10.1016/j.jpba.2007.07.008
8. Chen S (2005) The factors that influence the elution order for the resolution of amino acids on vancomycin phase using the polar-organic mobile phases after their pre-column derivatization with electrophilic reagents. Biomed Chromatogr 19(6):426–433. doi:10.1002/bmc.501
9. Cirilli R, Ferretti R, Gallinella B, Zanitti L, La Torre F (2004) A new application of stopped-flow chiral HPLC: inversion of enantiomer elution order. J Chromatogr A 1061(1):27–34. doi:10.1016/j.cliroma.2004.11.001
10. Srinivas NR (2009) Reversal in elution order in liquid chromatography-compilation of experimental observations. Biomed Chromatogr 23(2):222–223. doi:10.1002/bmc.1116
11. Persson BA, Andersson S (2001) Unusual effects of separation conditions on chiral separations. J Chromatogr A 906(1–2):195–203. doi:10.1016/s0021-9673(00)00949-3
12. Okamoto M (2002) Reversal of elution order during the chiral separation in high performance liquid chromatography. J Pharm Biomed Anal 27(3–4):401–407. doi:10.1016/s0731-7085(01)00646-x

13. Guiochon G, Tarafder A (2011) Fundamental challenges and opportunities for preparative supercritical fluid chromatography. J Chromatogr A 1218(8):1037–1114
14. Hesse G, Hagel R (1976) Chromatographic resolution of racemates. Liebigs Ann Chem 6:996–1008
15. Drake AF, Gould JM, Mason SF (1980) Simultaneous monitoring of light-absorption and optical-activity in the liquid-chromatography of chiral substances. J Chromatogr 202 (2):239–245
16. Mannschreck A, Mintas M, Becher G, Stuhler G (1980) Liquid-chromatography of enantiomers: determination of enantiomeric purity in spite of extensive peak overlap. Angew Chem Int Ed 19(6):469–470
17. Mannschreck A, Andert D, Eiglsperger A, Gmahl E, Buchner H (1988) Chiroptical detection – novel possibilities of its application to enantiomers. Chromatographia 25(3):182–188. doi:10.1007/bf02316442
18. Lloyd DK, Goodall DM (1989) Polarimetric detection in high-performance liquid-chromatography. Chirality 1(4):251–264
19. Salvadori P, Bertucci C, Rosini C (1991) Circular-dichroism detection in hplc. Chirality 3(4):376–385
20. Cirilli R, Ferretti R, Gallinella B, Turchetto L, Bolasco A, Secci D, Chimenti P, Pierini M, Fares V, Befani O, La Torre F (2004) Enantiomers of C-5-chiral 1-acetyl-3,5-diphenyl-4,5-dihydro-(1H)-pyrazole derivatives: analytical and semipreparative HPLC separation, chiroptical properties, absolute configuration, and inhibitory activity against monoamine oxidase. Chirality 16(9):625–636. doi:10.1002/chir.20085
21. Salvadori P, Rosini C, Bertucci C (1984) Circular dichroic detection in the hplc of chiral molecules – direct determination of elution orders. J Org Chem 49(26):5050–5054
22. Rimbock KH, Kastner F, Mannschreck A (1986) Microcrystalline tribenzoylcellulose – a high-performance liquid-chromatographic sorbent for the separation of enantiomers. J Chromatogr 351(2):346–350
23. Mueller MD, Buser HR (1994) Identification of the (+)-enantiomers and (−)-enantiomers of chiral chlordane compounds using chiral high-performance liquid-chromatography chiroptical detection and chiral high-resolution gas-chromatography mass-spectrometry. Anal Chem 66(13):2155–2162
24. Bertucci C, Rosini C, Pini D, Salvadori P (1987) Chiral stationary phases and circular-dichroism detection in high-performance liquid-chromatography – determination of stereo-chemical purity of drugs. J Pharm Biomed Anal 5(2):171–176
25. Szokan G, Szarvas S, Majer Z, Szabo D, Kapovits I, Hollosi M (1999) On-line CD detection in chiral separation of spiro-lambda(4)-sulfanes. J Liq Chromatogr Relat Technol 22(7):993–1007. doi:10.1081/jlc-100101713
26. Okamoto M, Sato R, Nagano E, Nakazawa H (1991) Optical resolution and biological-activities of S-23121, a new cereal herbicide. Agric Biol Chem 55(12):3151–3153
27. Soloshonok VA, Ono T, Ueki H, Vanthuyne N, Balaban TS, Burck J, Fliegl H, Klopper W, Naubron JV, Bui TTT, Drake AF, Roussel C (2010) Ridge-tile-like chiral topology: synthesis, resolution, and complete chiroptical characterization of enantiomers of edge-sharing binuclear square planar complexes of Ni(II) bearing achiral ligands. J Am Chem Soc 132 (30):10477–10483
28. Okamoto Y, Aburatani R, Kawashima M, Hatada K, Okamura N (1986) Resolution of 4-hydroxy-2-cyclopentenone derivatives by hplc on cellulose triphenylcarbamate derivatives. Chem Lett 10:1767–1770
29. West BD, Preis S, Schroeder CH, Link KP (1961) Studies on the 4-hydroxycoumarins. The resolution and absolute configuration of warfarin. J Am Chem Soc 83(12):2676–2679. doi:10.1021/ja01473a020
30. Driffield M, Bergstrom ET, Goodall DM, Klute AS, Smith DK (2001) High-performance liquid chromatography applications of optical rotation detection with compensation for scattering and absorbance at the laser wavelength. J Chromatogr A 939(1–2):41–48. doi:10.1016/s0021-9673(01)01336-x

31. Liu YS, Yu T, Armstrong DW (1999) HPLC detection and evaluation of chiral compounds with a laser-based chiroptical detector. LCGC North Am 17(10):946–957
32. Däppen R, Voigt P, Maystre F, Bruno AE (1993) Aspects of quantitative-determinations with polarimetric detectors in liquid-chromatography. Anal Chim Acta 282(1):47–54. doi:10.1016/0003-2670(93)80350-t
33. Sanchez FG, Diaz AN, Lama IM (2008) Polarimetric detection in liquid chromatography: an approach to correct refractive index artefacts. J Liq Chromatogr Relat Technol 31(20):3115–3131. doi:10.1080/10826070802480057
34. Kott L, Holzheuer WB, Wong MM, Webster GK (2007) An evaluation of four commercial HPLC chiral detectors: a comparison of three polarimeters and a circular dichroism detector. J Pharm Biomed Anal 43(1):57–65. doi:10.1016/j.jpba.2006.06.015
35. Najahi E, Sudor J, Chabchoub F, Nepveu F, Zribi F, Duval R (2010) Synthesis of 6-amino-5-cyano-1,4-disubstituted-2(1H)-pyrimidinones via copper-(I)-catalyzed alkyne-azide "click chemistry" and their reactivity. Molecules 15(12):8841–8855
36. Mannschreck A (1992) Chiroptical detection during liquid-chromatography: 4. Applications to stereoanalysis and stereodynamics. Chirality 4(3):163–169. doi:10.1002/chir.530040306
37. Champion WL, Lee J, Garrison AW, DiMarco JC, Matabe A, Prickett KB (2004) Liquid chromatographic separation of the enantiomers of *trans*-chlordane, *cis*-chlordane, heptachlor, heptachlor epoxide and alpha-hexachlorocyclohexane with application to small-scale preparative separation. J Chromatogr A 1024(1–2):55–62. doi:10.1016/j.chroma.2003.10.026
38. Linder SW, Yanik GW, Bobbitt DR (2004) Evaluation of laser-based polarimetry for the determination of enantiomeric excess (ee) at the extremes of the ee scale. Microchem J 76(1–2):105–112
39. Nunes JA, Tong WG (2010) Wave-mixing circular dichroism detector for chiral liquid chromatography. Appl Spectrosc 64(1):46–51
40. Roussel C, Del Rio A, Pierrot-Sanders J, Piras P, Vanthuyne N (2004) Chiral liquid chromatography contribution to the determination of the absolute configuration of enantiomers. J Chromatogr A 1037(1–2):311–328. doi:10.1016/j.chroma.2004.01.065
41. Gaggeri R, Rossi D, Collina S, Mannucci B, Baierl M, Juza M (2011) Quick development of an analytical enantioselective high performance liquid chromatography separation and preparative scale-up for the flavonoid Naringenin. J Chromatogr A 1218(32):5414–5422
42. Lao WJ, Gan J (2012) Enantioselective degradation of warfarin in soils. Chirality 24(1):54–59. doi:10.1002/Chir.21023
43. Roussel C, Hart N, Bonnet B, Suteu C, Hirtopeanu A, Kravtsov VC, Luboradzki R, Vanthuyne N (2002) Contribution of chiral HPLC in tandem with polarimetric detection in the determination of absolute configuration by chemical interconversion method: example in 1-(thi)oxothiazolinyl-3-(thi)oxothiazolinyl toluene atropisomer series. Chirality 14(8):665–673. doi:10.1002/chir.10125
44. Brandl G, Kastner F, Mannschreck A, Nolting B, Andert K, Wetzel R (1991) Chiroptical detection during liquid-chromatography: 3. Nonstop acquisition of circular-dichroism spectra during liquid-chromatography. J Chromatogr 586(2):249–254. doi:10.1016/0021-9673(91)85128-3
45. Scher JM, Zapp J, Becker H, Kather N, Kolz J, Speicher A, Dreyer M, Maksimenka K, Bringmann G (2004) Optically active bisbibenzyls from Bazzania trilobata: isolation and stereochemical analysis by chromatographic, chiroptical, and computational methods. Tetrahedron 60(44):9877–9881. doi:10.1016/j.tet.2004.08.037
46. Bringmann G, Gulder TAM, Reichert M, Gulder T (2008) The online assignment of the absolute configuration of natural products: HPLC-CD in combination with quantum chemical CD calculations. Chirality 20(5):628–642
47. Bertucci C, Tedesco D (2012) Advantages of electronic circular dichroism detection for the stereochemical analysis and characterization of drugs and natural products by liquid chromatography. J Chromatogr A 1269:69–81

48. Holik M, Mannschreck A (2004) Determining enantiomeric excess from overlapping HPLC peaks: discussion of errors in the methods. Chemometrics Intell Lab Syst 72(2):153–160. doi:10.1016/j.chemolab.2004.01.0090
49. Edkins TJ, Meier PC, Shah RD, Bobbitt DR, Saranadasa H, Lodevico RD (2002) Quantitative analysis of incomplete HPLC resolution of enantiomers. Fit of polarimetric detection for D- and L-phenylalanine to a Gaussian function. Enantiomer 7(1):11–22. doi:10.1080/10242430210703
50. Brandl F, Pustet N, Mannschreck A (2001) Chiroptical detection during liquid chromatography 7 – the rotation angle/absorbance ratio of chiral molecules. Its possible use for on-line analysis during preparative separations of enantiomers. J Chromatogr A 909(2):147–154. doi:10.1016/s0021-9673(00)01105-5
51. Kiesswetter R, Brandl F, Kastner-Pustet N, Mannschreck A (2003) Chiroptical detection during liquid chromatography: deconvolution of overlapping peaks of enantiomers and its applications. Chirality 15:S40–S49. doi:10.1002/chir.10275
52. Schurig V (1995) Determination of enantiomeric purity by direct methods – overview, by chemical correlation, by polarimetry, by NMR-spectroscopy and by gas chromatography. In: Helmchen G, Hoffmann RW, Mulzer J, Schaumann E (eds) Stereoselective Synthesis, vol E21A. Houben-Weyl, Methods of organic chemistry. Thieme Stuttgart, New York, pp 147–192
53. Horeau A, Guette JP (1974) Diastereoisomeric interactions of antipodes in the liquid phase. Tetrahedron 30(13):1923–1931
54. Boehme W, Wagner G, Oehme U, Priesnitz U (1982) Spectrophotometric and polarimetric detectors in liquid-chromatography for the determination of enantiomer ratios in complex-mixtures. Anal Chem 54(4):709–711
55. Scott BS, Dunn DL (1985) High-performance liquid-chromatographic analysis of epinephrine enantiomers using a UV detector in series with an optical-activity detector. J Chromatogr 319(3):419–426
56. Meinard C, Bruneau P, Perronnet J (1985) High-performance liquid chromatograph coupled with 2 detectors – a UV spectrometer and a polarimeter – example in the field of pyrethroids – identification of enantiomers. J Chromatogr 349(1):109–116
57. Reitsma BH, Yeung ES (1986) High-performance liquid-chromatographic determination of enantiomeric ratios of amino-acids without chiral separation. J Chromatogr 362(3):353–362
58. Zukowski J, Tang YB, Berthod A, Armstrong DW (1992) Investigation of a circular-dichroism spectrophotometer as a liquid-chromatography detector for enantiomers – sensitivity, advantages and limitations. Anal Chim Acta 258(1):83–92. doi:10.1016/0003-2670(92)85200-p
59. Bossu E, Cotichini V, Gostoli G, Farina A (2001) Determination of optical purity by nonenantioselective LC using CD detection. J Pharm Biomed Anal 26(5–6):837–848. doi:10.1016/s0731-7085(01)00483-6
60. Shaw CJ, Huang AH, Zhang XN (2003) Quantitation and test of enantiomeric purity of the L-ketohexoses by liquid chromatography with dual refractive index and laser-based chiroptical detection. J Chromatogr A 987(1–2):439–443. doi:10.1016/s0021-9673(02)01413-9
61. Lorin M, Delepee R, Maurizot JC, Ribet JP, Morin P (2007) Sensitivity improvement of circular dichroism detection in HPLC by using a low-pass electronic noise filter: application to the enantiomeric determination purity of a basic drug. Chirality 19(2):106–113. doi:10.1002/chir.20352
62. Reetz MT, Kuhling KM, Hinrichs H, Deege A (2000) Circular dichroism as a detection method in the screening of enantioselective catalysts. Chirality 12(5–6):479–482
63. Welch CJ, Gong XY, Schafer W, Pratt EC, Brkovic T, Pirzada Z, Cuff JF, Kosjek B (2010) MISER chromatography (multiple injections in a single experimental run): the chromatogram is the graph. Tetrahedron Asymmetry 21(13–14):1674–1681. doi:10.1016/j.tetasy.2010.05.029

64. Roussel C, Vanthuyne N, Jobert JL, Loas AI, Tanase AE, Gherase D (2007) HPLC on chiral support with polarimetric detection: application to conglomerate discovery. Chirality 19(6):497–502. doi:10.1002/chir.20405
65. Kanazawa H, Kunito Y, Matsushima Y, Okubo S, Mashige F (2000) Stereospecific analysis of lorazepam in plasma by chiral column chromatography with a circular dichroism-based detector. J Chromatogr A 871(1–2):181–188. doi:10.1016/s0021-9673(99)01244-3
66. Dahmane EM, Aamouche A, Vanthuyne N, Jean M, Vanloot P, Taourirte M, Dupuy N, Roussel C (2013) Attempts to separate (−)-α-thujone, (+)-β-thujone epimers from camphor enantiomers by enantioselective HPLC with polarimetric detection. J Sep Sci 36(5):832–839
67. Roussel C, Vanthuyne N, Serradeil-Albalat M, Vallejos JC (2003) True or apparent reversal of elution order during chiral high-performance liquid chromatography monitored by a polarimetric detector under different mobile phase conditions. J Chromatogr A 995 (1–2):79–85. doi:10.1016/s0021-9673(03)00533-8
68. Cirilli R, Ferretti R, Gallinella B, La Torre F, La Regina G, Silvestri R (2005) Comparative study between the polysaccharide-based Chiralcel OJ and Chiralcel OD CSPs in chromatographic enantioseparation of imidazole analogues of fluoxetine and miconazole. J Sep Sci 28(7):627–634. doi:10.1002/jssc.200400102
69. Ghanem A (2006) True and false reversal of the elution order of barbiturates on a bonded cellulose-based chiral stationary phase. J Chromatogr A 1132(1–2):329–332. doi:10.1016/j.chroma.2006.09.043
70. Lv CG, Zhou ZQ (2011) Chiral HPLC separation and absolute configuration assignment of a series of new triazole compounds. J Sep Sci 34(4):363–370. doi:10.1002/jssc.201000762
71. Andersson S, Nelander H, Ohlen K (2007) Preparative chiral chromatography and chiroptical characterization of enantiomers of omeprazole and related benzimidazoles. Chirality 19(9):706–715. doi:10.1002/chir.20375
72. Ramillien M, Vanthuyne N, Jean M, Gherase D, Giorgi M, Naubron JV, Piras P, Roussel C (2012) Enantiomers of dimethyl [(2E)-1,3-diphenylprop-2-en-1-yl]propanedioate resulting from allylic alkylation reaction: elution order on major high-performance liquid chromatography chiral columns. J Chromatogr A 1269:82–93
73. Macaudiere P, Lienne M, Caude M, Rosset R, Tambute A (1989) Resolution of pi-acid racemates on pi-acid chiral stationary phases in normal-phase liquid and subcritical fluid chromatographic modes – a unique reversal of elution order on changing the nature of the achiral modifier. J Chromatogr 467(2):357–372. doi:10.1016/s0021-9673(01)93989-5
74. Stalcup AM, Chang SC, Armstrong DW (1991) Effect of the configuration of the substituents of derivatized beta-cyclodextrin bonded phases on enantioselectivity in normal-phase liquid-chromatography. J Chromatogr 540(1–2):113–128. doi:10.1016/s0021-9673(01)88802-6
75. Xiao TL, Zhang B, Lee JT, Hui F, Armstrong DW (2001) Reversal of enantiomeric elution order on macrocyclic glycopeptide chiral stationary phases. J Liq Chromatogr Relat Technol 24(17):2673–2684. doi:10.1081/jlc-100106094
76. Wang T, Chen YDW, Vailaya A (2000) Enantiomeric separation of some pharmaceutical intermediates and reversal of elution orders by high-performance liquid chromatography using cellulose and amylose tris(3,5-dimethylphenylcarbamate) derivatives as stationary phases. J Chromatogr A 902(2):345–355. doi:10.1016/s0021-9673(00)00862-1
77. Aboul-Enein HY, Ali I (2001) Studies on the effect of alcohols on the chiral discrimination mechanisms of amylose stationary phase on the enantioseparation of nebivolol by HPLC. J Biochem Biophys Methods 48(2):175–188. doi:10.1016/s0165-022x(01)00148-8
78. Francotte E, Zhang T (1995) Supramolecular effects in the chiral discrimination of meta-methylbenzoyl cellulose in high-performance liquid chromatography. J Chromatogr A 718(2):257–266
79. Doyle TD, Wainer IW (1984) A unique reversal of elution order during direct enantiomeric resolution of amide derivatives of 1-phenyl-2-aminopropane by high-performance liquid-chromatography on chiral stationary phases. J High Resolut Chromatogr Chromatogr Commun 7(1):38–40. doi:10.1002/jhrc.1240070107

80. Pittler E, Schmid MG (2010) Enantioseparation of dansyl amino acids by HPLC on a monolithic column dynamically coated with a vancomycin derivative. Biomed Chromatogr 24(11):1213–1219. doi:10.1002/bmc.1430
81. Vanthuyne N, Andreoli F, Fernandez S, Roman M, Roussel C (2005) Synthesis, chiral separation, barrier to rotation and absolute configuration of N-(O-functionalized-aryl)-4-alkyl-thiazolin-2-one and thiazoline-2-thione atropisomers. Lett Org Chem 2(5):433–443. doi:10.2174/1570178054405931
82. Chankvetadze L, Ghibradze N, Karchkhadze M, Peng L, Farkas T, Chankvetadze B (2011) Enantiomer elution order reversal of fluorenylmethoxycarbonyl-isoleucine in high-performance liquid chromatography by changing the mobile phase temperature and composition. J Chromatogr A 1218(37):6554–6560. doi:10.1016/j.chroma.2011.06.068
83. Karlsson A, Nystrom A (2001) Addition of organic modifiers to control retention order of enantiomers of dihydropyridines on chiral-AGP. Chromatographia 53(3–4):135–139
84. Alfredson TV, Towne R, Elliott M, Griffin B, Abubakari A, Dyson N, Kertesz DJ (1996) Enantioselectivity of azalanstat and its ketal tosylate intermediate in chiral high performance liquid chromatography separations. J Liq Chromatogr Relat Technol 19(10):1653–1668. doi:10.1080/10826079608005499
85. Haginaka J, Wakai J, Takahashi K, Yasuda H, Katagi T (1990) Chiral separation of propranolol and its ester derivatives on an ovomucoid-bonded silica – influence of pH, ionic-strength and organic modifier on retention, enantioselectivity and enantiomeric elution order. Chromatographia 29(11–12):587–592
86. Gaffney MH, Stiffin RM, Wainer IW (1989) The effect of alcoholic mobile phase modifiers on retention and stereoselectivity on a commercially available cellulose-based hplc chiral stationary phase – an unexpected reversal in enantiometric elution order. Chromatographia 27(1–2):15–18. doi:10.1007/bf02290397
87. Okamoto M, Nakazawa H (1991) Reversal of elution order during direct enantiomeric separation of pyriproxyfen on a cellulose-based chiral stationary phase. J Chromatogr 588(1–2):177–180. doi:10.1016/0021-9673(91)85020-g
88. Okamoto M, Nakazawa H (1991) Direct enantiomeric resolution of pyriproxyfen on a cellulose-based chiral stationary phase. A unique reversal of elution order on changing the nature of the mobile phase modifier. Anal Sci 7:147–150. doi:10.2116/analsci.7.Supple_147
89. Zhan FP, Yu GY, Yao BX, Guo XP, Liang T, Yu MG, Zeng QL, Weng W (2010) Solvent effect in the chromatographic enantioseparation of 1,1′-bi-2-naphthol on a polysaccharide-based chiral stationary phase. J Chromatogr A 1217(26):4278–4284. doi:10.1016/j.chroma.2010.04.016
90. Wang T, Chen YDW (1999) Application and comparison of derivatized cellulose and amylose chiral stationary phases for the separation of enantiomers of pharmaceutical compounds by high-performance liquid chromatography. J Chromatogr A 855(2):411–421. doi:10.1016/s0021-9673(99)00733-5
91. Balmer K, Persson BA, Lagerstrom PO (1994) Stereoselective effects in the separation of enantiomers of omeprazole and other substituted benzimidazoles on different chiral stationary phases. J Chromatogr A 660(1–2):269–273
92. Bielejewska A, Duszczyk K, Zukowski J (2005) HPLC separation of linezolid enantiomers using polysaccharide-based chiral stationary phases. Acta Chromatogr 15:183–191
93. Tatini R, Sadik O, Bernhard S, Abruna H (2005) Direct resolution of chiral “pineno” fused terpyridyl ligands on amylose based chiral stationary phase using long chain alcohol modifiers. Anal Chim Acta 534(2):193–198. doi:10.1016/j.aca.2004.11.032
94. Gyllenhaal O, Stefansson M (2008) Reversal of elution order for profen acid enantiomers in normal phase LC on Chiralpak AD. J Pharm Biomed Anal 46(5):860–863. doi:10.1016/j.jpba.2007.03.009
95. Toribio L, Alonso C, del Nozal MJ, Bernal JL, Jimenez JJ (2006) Enantiomeric separation of chiral sulfoxides by supercritical fluid chromatography. J Sep Sci 29(10):1363–1372. doi:10.1002/jssc.20060009

96. Gyllenhaal O, Stefansson M (2005) Reversal of elution order for profen acid enantiomers in packed-column SFC on Chiralpak AD. Chirality 17(5):257–265. doi:10.1002/chir.20160
97. Cirilli R, Ferretti R, Gallinella B, De Santis E, Zanitti L, La Torre F (2008) High-performance liquid chromatography enantioseparation of proton pump inhibitors using the immobilized amylose-based Chiralpak IA chiral stationary phase in normal-phase, polar organic and reversed-phase conditions. J Chromatogr A 1177(1):105–113. doi:10.1016/j.chroma.2007.11.027
98. Schlauch M, Volk FJ, Fondekar KP, Wede J, Frahm AW (2000) Enantiomeric and diastereomeric high-performance liquid chromatographic separation of cyclic beta-substituted alpha-amino acids on a copper(II)-D-penicillamine chiral stationary phase. J Chromatogr A 897(1–2):145–152. doi:10.1016/s0021-9673(00)00808-6
99. Balmer K, Lagerstrom PO, Persson BA, Schill G (1992) Reversed retention order and other stereoselective effects in the separation of amino-alcohols on chiralcel OD. J Chromatogr 592(1–2):331–337
100. Ma S, Shen S, Lee H, Eriksson M, Zeng X, Xu J, Fandrick K, Yee N, Senanayake C, Grinberg N (2009) Mechanistic studies on the chiral recognition of polysaccharide-based chiral stationary phases using liquid chromatography and vibrational circular dichroism reversal of elution order of N-substituted alpha-methyl phenylalanine esters. J Chromatogr A 1216(18):3784–3793. doi:10.1016/j.chroma.2009.02.046
101. Cui X, Liu GQ, Kang SS, Guo XP, Yao BX, Wen W, Zeng QL (2011) Unusual chromatographic enantioseparation behavior of naproxen on an immobilized polysaccharide-based chiral stationary phase. J Chromatogr A 1218(48):8718–8721. doi:10.1016/j.chroma.2011.10.014
102. Yao BX, Liu GQ, Kang SS, Xiang C, Huang B, Weng W, Zeng QL (2011) Reversal of elution order between enantiomers of binaphthol on an immobilized polysaccharide-based chiral stationary phase. Chromatographia 74(7–8):625–631. doi:10.1007/s10337-011-2104-5
103. Svensson S, Vessman J, Karlsson A (1999) Direct high-performance liquid chromatographic separations of metoprolol analogues on a chiralcel OD column using chemometrics. J Chromatogr A 839(1–2):23–39
104. Dossou KSS, Chiap P, Servais AC, Fillet M, Crommen J (2011) Development and validation of a LC method for the enantiomeric purity determination of S-ropivacaine in a pharmaceutical formulation using a recently commercialized cellulose-based chiral stationary phase and polar non-aqueous mobile phase. J Pharm Biomed Anal 54(4):687–693. doi:10.1016/j.jpba.2010.10.020
105. Dossou KSS, Edorh PA, Chiap P, Chankvetadze B, Servais AC, Fillet M, Crommen J (2011) Determination of enantiomeric purity of S-amlodipine by chiral LC with emphasis on reversal of enantiomer elution order. J Sep Sci 34(15):1772–1780. doi:10.1002/jssc.201100339
106. Jibuti G, Mskhiladze A, Takaishvili N, Karchkhadze M, Chankvetadze L, Farkas T, Chankvetadze B (2012) HPLC separation of dihydropyridine derivatives enantiomers with emphasis on elution order using polysaccharide-based chiral columns. J Sep Sci 35(19):2529–2537. doi:10.1002/jssc.201200443
107. Roussel C, Stein JL, Beauvais F, Chemlal A (1989) Example of the concentration-dependence of elution order in the resolution of enantiomers on microcrystalline triacetylcellulose chiral stationary phase. J Chromatogr 462:95–103
108. Golshanshirazi S, Guiochon G (1991) Use of the levan – vermeulen isotherm model for the calculation of elution band profiles in nonlinear chromatography. J Chromatogr 545(1):1–26. doi:10.1016/s0021-9673(01)88692-1
109. Haginaka J, Seyama C, Yasuda H, Takahashi K (1992) Investigation of enantioselectivity and enantiomeric elution order of propranolol and its ester derivatives on an ovomucoid-bonded column. J Chromatogr 598(1):67–72. doi:10.1016/0021-9673(92)85115-a
110. Haginaka J, Seyama C, Yasuda H, Takahashi K (1992) Retention, enantioselectivity and enantiomeric elution order of propranolol and its ester derivatives on an α1-acid glycoprotein-bonded column. Chromatographia 33(3–4):127–132. doi:10.1007/bf02275892

111. Karlsson A, Aspegren A (1998) The use of mobile phase pH and column temperature to reverse the retention order of enantiomers on chiral-AGP. Chromatographia 47(3–4):189–196. doi:10.1007/bf02466580
112. Gasparrini F, Marini F, Misiti D, Pierini M, Villani C (1999) Temperature dependent elution order of enantiomers on a two-armed receptor HPLC chiral stationary phase. Enantiomer 4(3–4):325–332
113. Kurganov AA, Zhuchkova LY, Davankov VA (1978) Stereoselectivity in bis(alpha amino acid) copper(II) complexes thermodynamics of N-benzylproline coordination to copper(II). J Inorg Nucl Chem 40(6):1081–1083
114. Schurig V (1984) Gas-chromatographic separation of enantiomers on optically-active metal-complex free stationary phases. Angew Chem Int Ed Engl 23(10):747–765
115. Schurig V, Ossig J, Link R (1989) Evidence for a temperature-dependent reversal of the enantioselectivity in complexation gas-chromatography on chiral phases. Angew Chem Int Ed Engl 28(2):194–196
116. Watabe K, Charles R, Gil-Av E (1989) Temperature-dependent inversion of elution sequence in the resolution of alpha-amino-acid enantiomers on chiral diamide selectors. Angew Chem Int Ed Engl 28(2):192–194
117. Jiang ZJ, Schurig V (2008) Existence of a low isoenantioselective temperature in complexation gas chromatography – profound change of enantioselectivity of a nickel(II) chiral selector either bonded to, or dissolved in, poly(dimethylsiloxane). J Chromatogr A 1186(1–2):262–270
118. Pirkle WH (1991) Unusual effect of temperature on the retention of enantiomers on a chiral column. J Chromatogr 558(1):1–6
119. West C, Bouet A, Routier S, Lesellier E (2012) Effects of mobile phase composition and temperature on the supercritical fluid chromatography enantioseparation of chiral fluoro-oxoindole-type compounds with chlorinated polysaccharide stationary phases. J Chromatogr A 1269:325–335. doi:10.1016/j.chroma.2012.09.078
120. Stringham RW, Blackwell JA (1996) "Entropically driven" chiral separations in supercritical fluid chromatography. Confirmation of isoelution temperature and reversal of elution order. Anal Chem 68(13):2179–2185. doi:10.1021/ac960029e
121. Chester TL, Coym JW (2003) Effect of phase ratio on van't Hoff analysis in reversed-phase liquid chromatography, and phase-ratio-independent estimation of transfer enthalpy. J Chromatogr A 1003(1–2):101–111
122. Fornstedt T, Sajonz P, Guiochon G (1997) Thermodynamic study of an unusual chiral separation. Propranolol enantiomers on an immobilized cellulase. J Am Chem Soc 119(6):1254–1264
123. Pirkle WH, Murray PG (1993) An instance of temperature-dependent elution order of enantiomers from a chiral brush-type HPLC column. J High Resolut Chromatogr 16(5):285–288
124. Fulde K, Fraham AW (1999) Temperature-induced inversion of elution order in the enantioseparation of sotalol on a cellobiohydrolase I-based stationary phase. J Chromatogr A 858(1):33–43
125. Yao B, Zhan F, Yu G, Chen Z, Fan W, Zeng X, Zeng Q, Weng W (2009) Temperature-induced inversion of elution order in the chromatographic enantioseparation of 1,1′-bi-2-naphthol on an immobilized polysaccharide-based chiral stationary phase. J Chromatogr A 1216(28):5429–5435. doi:10.1016/j.chroma.2009.05.032
126. Aranyi A, Ilisz I, Pataj Z, Szatmari I, Fulop F, Peter A (2011) High-performance liquid chromatographic enantioseparation of 1-(phenylethylamino)- or 1-(naphthylethylamino) methyl-2-naphthol analogs and a temperature-induced inversion of the elution sequence on polysaccharide-based chiral stationary phases. J Chromatogr A 1218(30):4869–4876. doi:10.1016/j.chroma.2011.01.027
127. Vachon J, Harthong S, Jeanneau E, Aronica C, Vanthuyne N, Roussel C, Dutasta JP (2011) Inherently chiral phosphonatocavitands as artificial chemo- and enantio-selective receptors of natural ammoniums. Org Biomol Chem 9(14):5086–5091. doi:10.1039/C1ob05194f

128. Vachon J, Harthong S, Dubessy B, Dutasta JP, Vanthuyne N, Roussel C, Naubron JV (2010) The absolute configuration of an inherently chiral phosphonatocavitand and its use toward the enantioselective recognition of L-adrenaline. Tetrahedron Asymmetry 21(11–12):1534–1541. doi:10.1016/j.tetasy.2010.03.028
129. Norel L, Rudolph M, Vanthuyne N, Williams JAG, Lescop C, Roussel C, Autschbach J, Crassous J, Reau R (2010) Metallahelicenes: easily accessible helicene derivatives with large and tunable chiroptical properties. Angew Chem Int Ed Engl 49(1):99–102. doi:10.1002/anie.200905099
130. Bürkle W, Karfunkel H, Schurig V (1984) Dynamic phenomena during enantiomer resolution by complexation gas-chromatography – a kinetic-study of enantiomerization. J Chromatogr 288(1):1–14
131. Eiglsperger A, Kastner F, Mannschreck A (1985) The enantiomers of *N,N*-dimethylthiobenzamides – chromatographic behavior and rotational barriers. J Mol Struct 126(Jan):421–432
132. Alkorta I, Elguero J, Roussel C, Vanthuyne N, Piras P (2012) Atropisomerism and axial chirality in heteroaromatic compounds. Adv Heterocycl Chem 105:1–188
133. Nishikawa T, Hayashi Y, Suzuki S, Kubo H, Ohtani H (1997) On-column enantiomerization of 3-hydroxybenzodiazepines during chiral liquid chromatography with optical rotation detection. J Chromatogr A 767(1–2):93–100. doi:10.1016/s0021-9673(96)01097-7
134. Mannschreck A, Kiessl L (1989) Chiroptical detection after liquid-chromatography: 2. Enantiomerization during HPLC on an optically-active sorbent – deconvolution of experimental chromatograms. Chromatographia 28(5–6):263–266. doi:10.1007/bf02260772
135. Gasparrini F, Lunazzi L, Misiti D, Villani C (1995) Organic stereochemistry and conformational-analysis from enantioselective chromatography and dynamic nuclear-magnetic-resonance measurements. Acc Chem Res 28(4):163–170. doi:10.1021/ar00052a001
136. Veciana J, Crespo MI (1991) Dynamic HPLC – a method for determining rate constants, energy barriers, and equilibrium-constants of molecular dynamic processes. Angew Chem Int Ed 30(1):74–76. doi:10.1002/anie.199100741
137. Trapp O, Schurig V (2002) Novel direct access to enantiomerization barriers from peak profiles in enantioselective dynamic chromatography: enantiomerization of dialkyl-1,3-allenedicarboxylates. Chirality 14(6):465–470
138. Trapp O (2006) Fast and precise access to enantiomerization rate constants in dynamic chromatography. Chirality 18(7):489–497
139. Trapp O (2008) A novel software tool for high throughput measurements of interconversion barriers: DCXplorer. J Chromatogr B 875(1):42–47
140. Cirilli R, Costi R, Di Santo R, La Torre F, Pierini M, Siani G (2009) Perturbing effects of chiral stationary phase on enantiomerization second-order rate constants determined by enantioselective dynamic high-performance liquid chromatography: a practical tool to quantify the accessible acid and basic catalytic sites bonded on chromatographic supports. Anal Chem 81(9):3560–3570. doi:10.1021/ac802212s
141. Maier F, Trapp O (2012) Effects of the stationary phase and the solvent on the stereodynamics of biphep ligands quantified by dynamic three-column HPLC. Angew Chem Int Ed Engl 51(12):2985–2988
142. Wolf C, Xu H (2007) Analysis of the stereodynamics of 2,2′-disubstituted biphenyls by dynamic chromatography. Tetrahedron Lett 48(39):6886–6889
143. Roussel C, Vanthuyne N, Shineva N, Bouchekara M, Djafri A (2008) Atropisomerism in the 2-arylimino-*N*-(2-aryl)-thiazoline series. Arkivoc (viii):28–41
144. Villani C, Gasparrini F, Pierini M, Mortera SL, D'Acquarica I, Ciogli A, Zappia G (2009) Dynamic HPLC of stereolabile iron(II) complexes on chiral stationary phases. Chirality 21(1):97–103
145. Bu X, Skrdla PJ, Dormer PG, Bereznitski Y (2010) Separation of triphenyl atropisomers of a pharmaceutical compound on a novel mixed mode stationary phase. A case study involving dynamic chromatography, dynamic NMR and molecular modeling. J Chromatogr A 1217(46):7255–7264

146. Cannazza G, Carrozzo MM, Battisti U, Braghiroli D, Parenti C, Troisi A, Troisi L (2010) Determination of kinetic parameters of enantiomerization of benzothiadiazines by DCXplorer. Chirality 22(9):789–797
147. Ciogli A, Bicker W, Lindner W (2010) Determination of enantiomerization barriers of hypericin and pseudohypericin by dynamic high-performance liquid chromatography on immobilized polysaccharide-type chiral stationary phases and off-column racemization experiments. Chirality 22(5):463–471
148. Lunazzi L, Mancinelli M, Mazzanti A, Pierini M (2010) Stereomutation of axially chiral aryl coumarins. J Org Chem 75(17):5927–5933
149. Uray G, Jahangir S, Fabian WMF (2010) On- and off column enantiomerization of 4,4′-bis-quinolin-2-ones: a comparison of Auto-, DHPLcy2k and DCXplorer calculated thermodynamic data generated by dynamic high performance liquid chromatography with theoretically calculated data. J Chromatogr A 1217(7):1017–1023
150. Kamuf M, Trapp O (2011) Stereodynamics of tetramezine. Chirality 23(2):113–117
151. Rotzler J, Gsellinger H, Neuburger M, Vonlanthen D, Haussinger D, Mayor M (2011) Racemisation dynamics of torsion angle restricted biphenyl push-pull cyclophanes. Org Biomol Chem 9(1):86–91
152. Rizzo S, Benincori T, Bonometti V, Cirilli R, Mussini PR, Pierini M, Pilati T, Sannicolo F (2013) Steric and electronic effects on the configurational stability of residual chiral phosphorus-centered three-bladed propellers: tris-aryl phosphanes. Chemistry 19(1):182–194
153. Wolf C (2008) Dynamic stereochemistry of chiral compounds: principles and applications. Roy Soc Chem. doi:10.1039/9781847558091-00006
154. Piron F, Vanthuyne N, Joulin B, Naubron JV, Cismas C, Terec A, Varga RA, Roussel C, Roncali J, Grosu I (2009) Synthesis, structural analysis, and chiral investigations of some atropisomers with ee-tetrahalogeno-1,3-butadiene core. J Org Chem 74(23):9062–9070
155. Soloshonok VA (2006) Remarkable amplification of the self-disproportionation of enantiomers on achiral-phase chromatography columns. Angew Chem Int Ed Engl 45(5):766–769
156. Soloshonok VA, Berbasov DO (2006) Self-disproportionation of enantiomers on achiral phase chromatography. One more example of fluorine's magic powers. Chim Oggi 24(3):44–47
157. Cundy KC, Crooks PA (1983) Unexpected phenomenon in the high-performance liquid-chromatographic analysis of racemic C-14-labeled nicotine – separation of enantiomers in a totally achiral system. J Chromatogr 281(Dec):17–33
158. Monde K, Harada N, Takasugi M, Kutschy P, Suchy M, Dzurilla M (2000) Enantiomeric excess of a cruciferous phytoalexin, spirobrassinin, and its enantiomeric enrichment in an achiral HPLC system. J Nat Prod 63(9):1312–1314
159. Suchy M, Kutschy P, Monde K, Goto H, Harada N, Takasugi M, Dzurilla M, Balentova E (2001) Synthesis, absolute configuration, and enantiomeric enrichment of a cruciferous oxindole phytoalexin, (S)-(−)-spirobrassinin, and its oxazoline analog. J Org Chem 66(11):3940–3947
160. Charles R, Gil-Av E (1984) Self-amplification of optical-activity by chromatography on an achiral adsorbent. J Chromatogr 298(3):516–520. doi:10.1016/s0021-9673(01)92750-5
161. Matusch R, Coors C (1989) Chromatographic-separation of the excess enantiomer under achiral conditions. Angew Chem Int Ed Engl 28(5):626–627. doi:10.1002/anie.198906261
162. Dobashi A, Motoyama Y, Kinoshita K, Hara S, Fukasaku N (1987) Self-induced chiral recognition in the association of enantiomeric mixtures on silica-gel chromatography. Anal Chem 59(17):2209–2211
163. Soloshonok VA, Berbasov DO (2006) Self-disproportionation of enantiomers of (R)-ethyl 3-(3,5-dinitrobenzamido)-4,4,4-trifluorobutanoate on achiral silica gel stationary phase. J Fluorine Chem 127(4–5):597–603
164. Tsai WL, Hermann K, Hug E, Rohde B, Dreiding AS (1985) Enantiomer-differentiation induced by an enantiomeric excess during chromatography with achiral phases. Helv Chim Acta 68(8):2238–2243. doi:10.1002/hlca.19850680818

165. Diter P, Taudien S, Samuel O, Kagan HB (1994) Enantiomeric enrichment of sulfoxides by preparative flash chromatography on an achiral phase. J Org Chem 59(2):370–373. doi:10.1021/jo00081a015
166. Nakajima M, Kanayama K, Miyoshi I, Hashimoto S (1995) Catalytic asymmetric synthesis of binaphthol derivatives by aerobic oxidative coupling of 3-hydroxy-2-naphthoates with chiral diamine-copper complex. Tetrahedron Lett 36(52):9519–9520. doi:10.1016/0040-4039(95)02063-2
167. Nakajima M, Miyoshi I, Kanayama K, Hashimoto S, Noji M, Koga K (1999) Enantioselective synthesis of binaphthol derivatives by oxidative coupling of naphthol derivatives catalyzed by chiral diamine copper complexes. J Org Chem 64(7):2264–2271. doi:10.1021/jo981808t
168. Takahashi M, Tanabe H, Nakamura T, Kuribara D, Yamazaki T, Kitagawa O (2010) Atropisomeric lactam chemistry: catalytic enantioselective synthesis, application to asymmetric enolate chemistry and synthesis of key intermediates for NET inhibitors. Tetrahedron 66(1):288–296
169. Takahata H, Takahashi S, Kouno S, Momose T (1998) Symmetry-assisted synthesis of C-2-symmetric trans-alpha, alpha′-bis(hydroxymethyl)pyrrolidine and -piperidine derivatives via double sharpless asymmetric dihydroxylation of alpha, omega-terminal dienes. J Org Chem 63(7):2224–2231
170. Tanaka K, Osuga H, Suzuki H, Shogase Y, Kitahara Y (1998) Synthesis, enzymic resolution and enantiomeric enhancement of bis(hydroxymethyl) 7 thiaheterohelicenes. J Chem Soc Perkin Trans 1(5):935–940. doi:10.1039/a707196e
171. Soloshonok VA, Roussel C, Kitagawa O, Sorochinsky AE (2012) Self-disproportionation of enantiomers via achiral chromatography: a warning and an extra dimension in optical purifications. Chem Soc Rev 41(11):4180–4188
172. Sorochinsky AE, Acena JL, Soloshonok VA (2013) Self-disproportionation of enantiomers of chiral, non-racemic fluoroorganic compounds: role of fluorine as enabling element. Synthesis 45(2):141–152
173. Ogawa S, Nishimine T, Tokunaga E, Nakamura S, Shibata N (2010) Self-disproportionation of enantiomers of heterocyclic compounds having a tertiary trifluoromethyl alcohol center on chromatography with a non-chiral system. J Fluorine Chem 131(4):521–524
174. Baciocchi R, Zenoni G, Mazzotti M, Morbidelli M (2002) Separation of binaphthol enantiomers through achiral chromatography. J Chromatogr A 944(1–2):225–240
175. Gil-Av E, Schurig V (1994) Resolution of non-racemic mixtures in achiral chromatographic systems – a model for the enantioselective effects observed. J Chromatogr A 666(1–2):519–525. doi:10.1016/0021-9673(94)80413-3
176. Trapp O, Schurig V (2010) Nonlinear effects in enantioselective chromatography: prediction of unusual elution profiles of enantiomers in non-racemic mixtures on an achiral stationary phase doped with small amounts of a chiral selector. Tetrahedron Asymmetry 21(11–12):1334–1340. doi:10.1016/j.tetasy.2010.04.027
177. Jung M, Schurig V (1992) Computer-simulation of 3 scenarios for the separation of nonracemic mixtures by chromatography on achiral stationary phases. J Chromatogr 605(2):161–166. doi:10.1016/0021-9673(92)85233-j
178. Baciocchi R, Mazzotti M, Morbidelli M (2004) General model for the achiral chromatography of enantiomers forming dimers: application to binaphthol. J Chromatogr A 1024(1–2):15–20. doi:10.1016/j.chroma.2003.10.071
179. Nicoud RM, Jaubert JN, Rupprecht I, Kinkel J (1996) Enantiomeric enrichment of non-racemic mixtures of binaphthol with non-chiral packings. Chirality 8(3):234–243. doi:10.1002/(sici)1520-636x(1996)8:3<234::aid-chir2>3.0.co;2-h

Top Curr Chem (2013) 340: 153–208
DOI: 10.1007/128_2013_440

Published online: 11 May 2013

Salient Features of Enantioselective Gas Chromatography: The Enantiomeric Differentiation of Chiral Inhalation Anesthetics as a Representative Methodological Case in Point

Volker Schurig

Abstract The enantiomeric differentiation of the volatile chiral inhalation anesthetics enflurane, isoflurane, and desflurane by analytical and preparative gas chromatography on various modified cyclodextrins is described. Very large enantioseparation factors α are obtained on the chiral selector octakis(3-*O*-butanoyl-2,6-di-*O*-pentyl)-γ-cyclodextrin (Lipodex E). The gas-chromatographically observed enantioselectivities are corroborated by NMR-spectroscopy using Lipodex E as chiral solvating agent and by various sensor devices using Lipodex E as sensitive chiral coating layer. The assignment of the absolute configuration of desflurane is clarified. Methods are described for the determination of the enantiomeric distribution of chiral inhalation anesthetics during narcosis in clinical trials. The quantitation of enantiomers in a sample by the method of enantiomeric labeling is outlined. Reliable thermodynamic parameters of enantioselectivity are determined by using the retention-increment R' approach for the enantiomeric differentiation of various chiral halocarbon selectands on diluted cyclodextrin selectors.

Keywords Absolute configuration · Chiral inhalation anesthetics · Enantiomer labeling · Enantioselective gas chromatography · Enantioselective sensors · Modified cyclodextrins · Retention-increment

Contents

V. Schurig (✉)
Institute of Organic Chemistry, University of Tübingen, Auf der Morgenstelle 18, 72076 Tübingen, Germany
e-mail: volker.schurig@uni-tuebingen.de

1 Introduction

There are a number of contemporary reviews available on the gas-chromatographic separation of enantiomers on chiral stationary phases (CSPs) [1–5]. In the present account, the various aspects of the technique will be illustrated via the gas-chromatographic analytical and preparative enantioseparation of the chiral volatile inhalation anesthetics *enflurane*, *isoflurane*, and *desflurane* on modified cyclodextrins.

The use of inhalation anesthetics allows patients to undergo medical treatment without distress and pain. They have changed the operating room from a chamber of horrors, where patients felt and noticed everything, to a place in which medical care is provided in a tranquil atmosphere [6]. Inhaled narcotics enter the brain and induce profound sleep, passive state, muscle relaxation, and analgesia. Anesthetics should have a rapid onset and a rapid recovery, returning the patient from a deep hypnotic sleep to an awakened state, i.e., to resume "street fitness" as rapidly as possible. At the same time the anesthetics should produce few or no side effects and exit the body essentially unchanged [6]. Diethyl ether was described by Valerius Cordus in the sixteenth century and its anesthetic properties were adopted in the same century by Paracelsus. In 1842, Crawford Long in Jefferson used diethyl ether as a surgical anesthetic [6, 7], while the dentist William T.G. Morton introduced it at Massachusetts General Hospital at Boston in 1846 [8] (Fig. 1).

The "fluorine revolution" [9] enabled the introduction of new anesthetics into medicinal practice such as enflurane (2-chloro-1,1,2-trifluoroethyl difluoromethyl ether = 2-chloro-1-(difluoromethoxy)-1,1,2-trifluoroethane), isoflurane (1-chloro-2,2,2-trifluoroethyl difluoromethyl ether = 2-chloro-2-(difluoromethoxy)-1,1,1-trifluoroethane), and desflurane (difluoromethyl-1,2,2,2-tetrafluoroethyl ether = 2-(difluoromethoxy)-1,1,1,2-tetrafluoroethane) (Fig. 2) [6, 7, 10]. Isoflurane is a structural isomer of enflurane and in desflurane the chlorine of isoflurane is

Fig. 1 Panel from a monument in Boston's Public Garden commemorating Morton's demonstration of diethyl ether's anesthetic use at Massachusetts General Hospital in 1846 (private photograph)

substituted by fluorine. Halothane (2-bromo-2-chloro-1,1,1-trifluoroethane) will not be treated here. The new achiral anesthetic sevoflurane (fluoromethyl-2,2,2-trifluoro-1-(trifluoromethyl)ethyl ether) = 1,1,1,3,3,3-hexafluoro-2-(fluoromethoxy)propane) [7] and its chiral decomposition product "compound B" (2-(fluoromethoxy)-3-methoxy-1,1,1,3,3-pentafluoropropane) will be addressed later on in this account.

As compared to diethyl ether, reduction in toxicity and flammability, resistance to peroxidation, reduction or absence of metabolic conversion, increase in volatility, and potency guided the design of modern haloethers for anesthesia. Yet the unintended introduction of a stereogenic center into the molecules and its impact on enantioselective biological action has totally been ignored from the outset. Although chiral inhalational anesthetics have been produced and administered as racemic mixtures up to now, in vivo and in vitro studies have suggested differences in their pharmacological properties notably for isoflurane [11, 12]. However, these differences appeared not as striking as to warrant actions by legislative authorities for the use of single enantiomers. Yet the study of enantioselective effects in

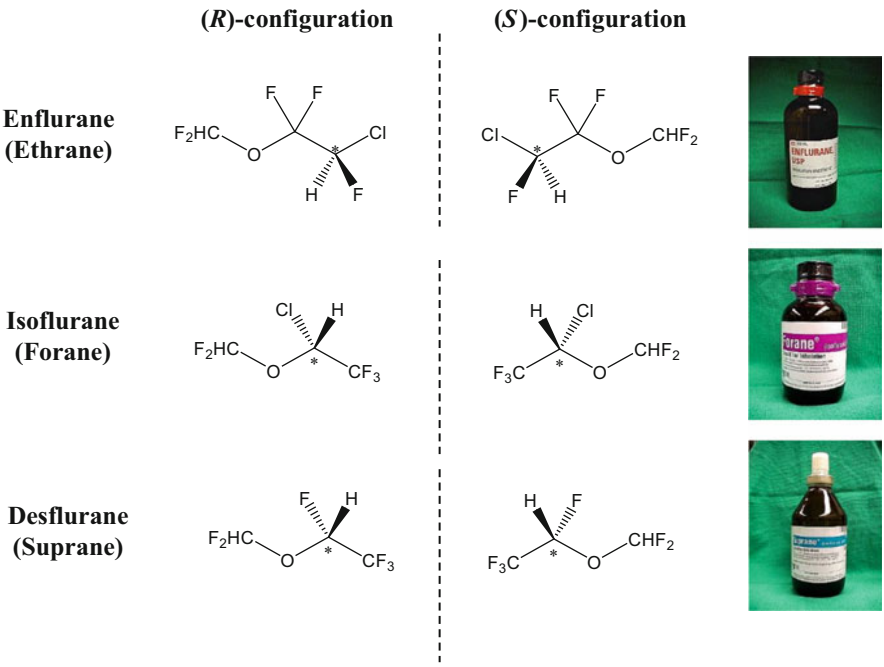

Fig. 2 Molecular structures of modern chiral inhalation anesthetics

pharmacokinetics and pharmacodynamics may help to unravel the still unknown pharmacological action of inhalation anesthetics. For this purpose, apart from enantioselective synthetic approaches [9], the development of analytical and preparative gas-chromatographic methodologies for the enantiomeric differentiation of enflurane, isoflurane, and desflurane became essential [12].

2 Analytical Gas-Chromatographic Enantioseparation of Enflurane, Isoflurane, and Desflurane

Owing to the lack of suitable functionalities, chiral haloethers are not amenable to gas-chromatographic enantioseparation via hydrogen-bonding CSPs [13] or by metal-complex containing CSPs [14]. However, with the advent of modified cyclodextrin CSPs, inclusion-type enantioselective GC became feasible and it soon emerged as an important tool for the enantioseparation of almost each class of chiral compounds [2, 15, 16]. Moreover, most chiral selectands are not required to be derivatized for effective enantiomeric differentiation on cyclodextrin-derived selectors. For gas-chromatographic enantioseparation using alkylated and/or acylated cyclodextrin (CD) derivatives, two different approaches have been developed. (1) In order to combine the enantioselectivity of modified cyclodextrins with the high efficiency encountered with silicone stationary phases, permethylated β-cyclodextrin was diluted

in semipolar polysiloxanes (e.g., OV-1701) and then coated on glass [17] or fused silica capillary columns [18]. Later on, permethylated β-cyclodextrin was chemically linked to an apolar polydimethylsiloxane backbone to improve column performance by yielding the CSP Chirasil-Dex [19]. The polymeric CSP can be immobilized via thermal surface bonding on the inner capillary wall and a single capillary column coated with Chirasil-Dex can be used in open-tubular enantioselective gas chromatography (*o*-GC), supercritical fluid chromatography (*o*-SFC), liquid chromatography (*o*-LC), and capillary electrochromatography (*o*-CEC) in a unified multichromatographic approach [20]. (2) Pentylated/acylated cyclodextrins are viscous liquids at room temperature and they can be used as undiluted CSPs coated on glass and fused silica columns [16, 21, 22]. In order to improve column performance, the pentylated/acylated cyclodextrins were later also diluted in polysiloxanes, e.g., octakis (3-*O*-butanoyl-2,6-di-*O*-pentyl)-γ-cyclodextrin (Lipodex E) in OV-1701 [23]. It has been demonstrated that the enantioseparation factor α is concentration-dependent when modified cyclodextrins are diluted in polysiloxanes and it is not increased after a threshold value of dilution [24]. Thus the diluted selector approach [17] nowadays represents the method of choice of enantioseparation by GC using modified CDs.

At the outset, isoflurane has been enantioseparated by Meinwald et al. on a 25-m fused silica capillary column coated with hexakis(2,3,6-tri-*O*-pentyl)-α-cyclodextrin (column A) and on a 25 m Pyrex glass capillary column coated with octakis(6-*O*-methyl-2,3-di-*O*-pentyl)-γ-cyclodextrin (column B) at 30°C [25] using the *undiluted selector approach* of König [16]. Whereas isoflurane has been enantioseparated on both columns, halothane could be enantioseparated only on column A and enflurane only on column B [25]. Shitangkoon et al. enantioseparated enflurane, isoflurane, and desflurane on 30 m × 0.25 mm i.d. fused silica capillary columns coated with 0.25 μm thick films of undiluted 2,6-di-*O*-pentyl-3-*O*-trifluoroacetylated α-, β-, and γ-cyclodextrins [26], a CSP comprising of synthetic mixtures of isomers and homologues [22]. Other commercially available pentylated and hydroxypropylated cyclodextrins (Cyclodex) were also used as CSPs [26]. In a subsequent study emerging from an industrial laboratory engaged in the production of fluorocarbon anesthetics, various CSPs were tested for racemic enflurane, isoflurane, and desflurane and related synthetic analogues [27]. Octakis(2,6-di-*O*-pentyl-3-*O*-trifluoroacetyl)-γ-cyclodextrin and octakis(3-*O*-butanoyl-2,6-di-*O*-pentyl)-γ-cyclodextrin (Lipodex E) were compared to probe the influence of substitution at the 3-position of the CDs, whereas hexakis(2,3,6-tri-*O*-pentyl)-α-cyclodextrin and heptakis(2,3,6-tri-*O*-pentyl)-β-cyclodextrin were tested to assess the role of the cavity size [27]. In few cases exceptionally high enantioseparation factors α were observed which could be correlated with the magnitude of chemical shift differences between ^{1}H- and ^{19}F-nuclei of the enantiomers in the presence of the modified cyclodextrins used as chiral solvating agents (CSA) in NMR spectroscopy [27]. It was therefore suggested that the simple and inexpensive NMR experiment could be used as predictive tool for proper CSP selection in enantioselective GC of fluoroethers employing CDs [27].

By the *diluted selector approach* of Schurig and Nowotny [17], octakis(3-*O*-butanoyl-2,6-di-*O*-pentyl)-γ-cyclodextrin (Lipodex E) [28] diluted to 40 wt% in

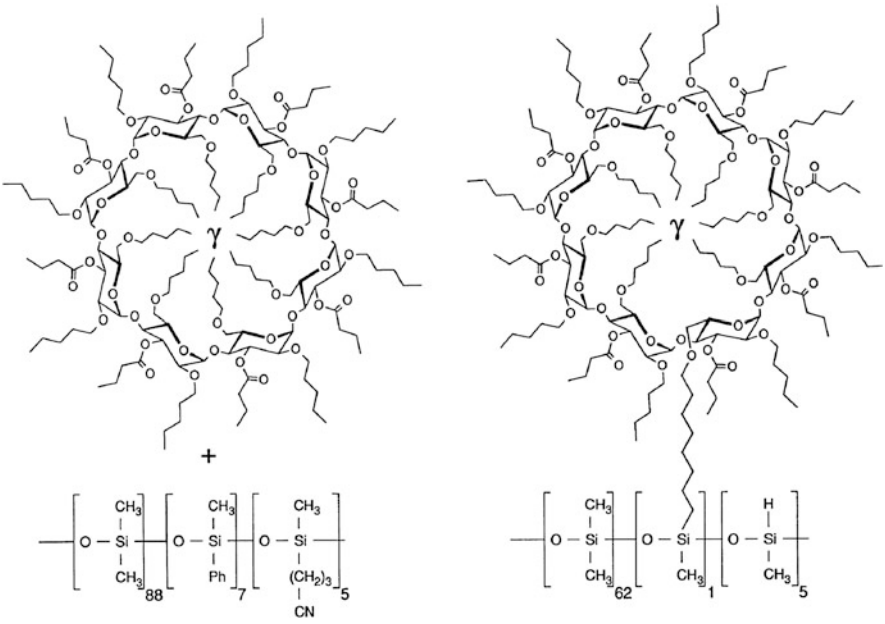

Fig. 3 *Left*: Octakis(3-*O*-butanoyl-2,6-di-*O*-pentyl)-γ-cyclodextrin (Lipodex E) [28] diluted in OV-1701 [31]. *Right*: Octakis(3-*O*-butanoyl-2,6-di-*O*-pentyl)-γ-cyclodextrin (Lipodex E) chemically linked via an octamethylene spacer to polydimethylsiloxane to yield Chirasil-γ-Dex [31, 32]

polysiloxane OV-1701 (5% cyanopropyl–7% phenyl-dimethylpolysiloxane) (Fig. 3, left) enantioseparated enflurane with $\alpha = 2.16$ and isoflurane with $\alpha = 1.36$ at 24°C (Fig. 4, left) [29]. Due to the large enantioseparation factors α observed, very fast enantioseparations within 30 s became feasible at elevated temperatures and higher carrier gas velocities (Fig. 4, right) [29]. For the enantiomeric analysis of enflurane by its enantioselective clathrate inclusion in tri-*o*-thymotide, a 25 m × 0.25 mm (i.d.) fused silica capillary column coated with 0.25 µm Chirasil-β-Dex [19] has been used at −1 to 7°C [30]. The simultaneous analytical enantioseparation of enflurane, isoflurane and desflurane in 2.5 min has been achieved on a 25 m × 0.25 mm (i.d.) fused silica capillary column coated with 0.5 µm octakis (3-*O*-butanoyl-2,6-di-*O*-pentyl)-γ-cyclodextrin (Lipodex E) in polysiloxane SE-54 and on a 10 m × 0.25 mm (i.d.) fused silica capillary column coated with immobilized Chirasil-γ-Dex (Fig. 5) [31]. In Chirasil-γ-Dex the selector octakis (3-*O*-butanoyl-2,6-di-*O*-pentyl)-γ-cyclodextrin (Lipodex E) [28] is chemically linked via a monooctamethylene spacer to polydimethylsiloxane at the 6-*O*- and/or 2-*O*-position of CD (Fig. 3, right) [32].

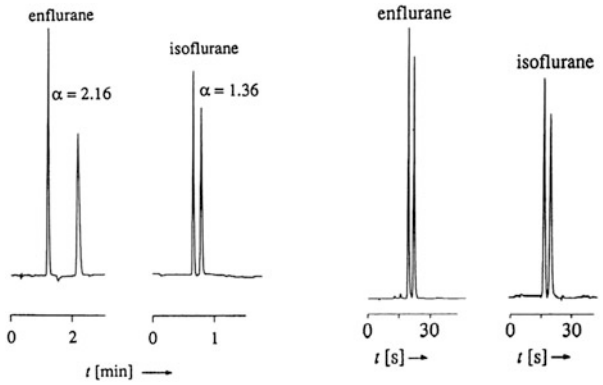

Fig. 4 *Left*: Analytical gas-chromatographic enantioseparation of enflurane and isoflurane. 6 m × 0.25 mm (i.d.) fused silica capillary column coated with 0.25 μm octakis(3-*O*-butanoyl-2,6-di-*O*-pentyl)-γ-cyclodextrin (Lipodex E) in OV-1701 (40 wt%) at 24°C and 45 cm/s dihydrogen [29]. *Right*: Rapid enantioseparation of enflurane at 60°C, 54 cm/s dihydrogen and isoflurane at 26°C, 100 cm/s dihydrogen [29]

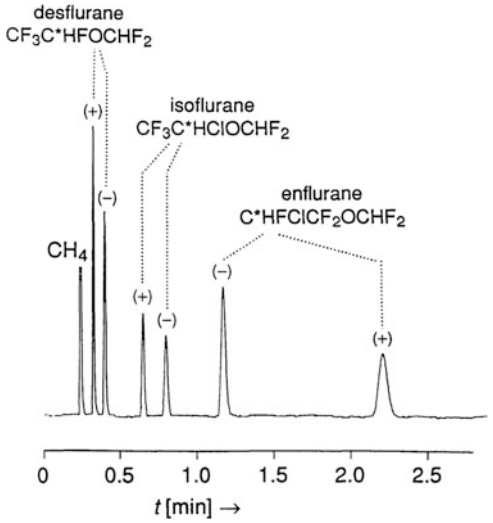

Fig. 5 Fast simultaneous gas-chromatographic enantioseparation of enflurane, isoflurane and desflurane. 10 m × 0.25 mm (i.d.) fused silica capillary column coated with 0.18 μm immobilized Chirasil-γ-Dex at 28°C and 40 cm/s dihydrogen [31]

3 Preparative Gas-Chromatographic Enantioseparation of Enflurane, Isoflurane, and Desflurane

The state-of-the-art of enantioselective preparative GC has been reviewed [33]. This method is restricted to thermally stable and volatile compounds. Due to the absence of liquid mobile phases as compared to LC, the recovery of the isolated enantiomers from the gaseous mobile phase is straightforward when aerosol and mist formation is prevented by using specially designed collection vessels [33]. The absence of an isolation problem of separated compound from the solvent is especially beneficial for volatile racemates like those of chiral inhalation anesthetics. However, preparative enantioselective GC does not match the overwhelming success of preparative enantioselective LC [34, 35]. The preparative GC method has only been successful for racemates exhibiting enantioseparation factors $\alpha > 1.5$ [33]. Preparative enantioselective chromatography relies on a compromise between three variables: (1) peak resolution (governed by enantioselectivity, efficiency and retention), (2) speed of enantioseparation, and (3) chiral column sample capacity. Any of two desired goals may only be achieved at the expense of the third. If a large sample throughput is required in a short time, resolution must be high. However, if resolution is insufficient, either the column load is limited or the time of enantioseparation is long [33].

Interestingly, in the early development of enantioselective GC, packed columns containing supported CSPs were employed for a hydrogen-bonding-type CSP [36], a metal-complexation-type CSP [37], and an inclusion-type CSP [38]. In complexation GC, semi-preparative enantioseparations at the milligram-scale have been reported for spiroketals (among them pheromones) [14, 39]. The preparative invertomer separation of 1-chloro-2,2-dimethylaziridine permitted the determination of chiroptical data, the absolute configuration, and the inversion barrier at the stereogenic nitrogen atom [40]. Large enantioseparation factors α were observed for the saturated hydrocarbons *cis*- and *trans*-pinane on a mixture of α-cyclodextrin and formamide impregnated on celite [38]. The preparative enantioseparation of camphene was subsequently realized on a packed column [41].

With the advent of alkylated/acylated CDs as versatile CSPs for analytical enantioseparations by GC (Sect. 2), their potential for semi-preparative enantioseparations of flavours, fragrances, and terpenoids was recognized. Micro-preparative enantioseparations by GC on modified cyclodextrins have been achieved on thick-film wide-bore fused silica capillary columns [42]. The enantiomers of 2 mg of racemic methyl jasmonate were enantioseparated within 80 min on a 1.8 m × 4 mm (i.d.) stainless steel column packed with 5 wt% heptakis(2,6-di-*O*-methyl-3-*O*-pentyl)-β-cyclodextrin in polysiloxane OV-1701 (1:1, w/w) coated onto Chromosorb W-HP (100–120 mesh) at 120°C and 0.4 bar helium [43]. The analytical and semi-preparative enantioseparation of all-anti-*trans*-perhydrotriphenylene on heptakis(2,3-di-*O*-acetyl-6-*O*-*tert*-butyldimethylsilyl)-β-cyclodextrin has also been described [44], demonstrating that even a rather nonvolatile racemate exhibiting a low enantioseparation factor α was amenable to semi-preparative enantioseparation by GC.

As human inhalation anesthetics enflurane, isoflurane, and desflurane exhibited unprecedented high enantioseparation factors α on octakis(3-*O*-butanoyl-2,6-di-*O*-pentyl)-γ-cyclodextrin (Lipodex E) (Fig. 5), their preparative enantioseparation represented an attractive target [33]. The availability of sufficient amounts of single enantiomers of the chiral haloethers was the prerequisite for medical trials and for the determination of chiroptical data and their absolute configurations. The absence of suitable functionalities precluded resolution of the racemates via diastereomers. The liquid phase chromatographic enantioseparation on CSPs is hampered by the difficulty in separating the volatile compounds from the liquid mobile phases. Enantioselective GC was therefore the method of choice [33]. Two approaches were advanced. (1) Racemic isoflurane was semi-preparatively enantioseparated on a 2 m × 10 mm (i.d.) stainless steel column containing 23.4 wt% of undiluted octakis(2,6-di-*O*-pentyl-3-*O*-trifluoroacetyl)-γ-cyclodextrin coated on Chromosorb W (AW, 80–100 mesh) using helium as carrier gas at 40°C [45, 46]. Employing a sampling interface between the column end and the fraction collector, the enantiomeric excess (ee) was detected online by an analytical enantioselective column. This set-up allowed the calculation of ee, recovery rate, and production rate. Racemic enflurane was enantioseparated on a 1 m × 10 mm (i.d.) stainless steel column containing 25.0 wt% of octakis(2,6-di-*O*-pentyl-3-*O*-trifluoroacetyl)-γ-cyclodextrin using dihydrogen as carrier gas at 40°C [46]. Up to 24 mg of the first eluted enantiomers with ee ~ 100% could be obtained when 75 mg of the racemate was injected whereas only 6 mg of the second eluted enantiomer with ee ~ 100% was obtained upon injecting 20 mg of the racemate in the optimized system. Higher production rates could only be obtained by sacrificing the enantiomeric excess (ee) [46]. (2) Whereas the above described endeavor utilized an undiluted CD selector, the dilution of modified CDs in semipolar polysiloxanes, previously applied successfully in analytical enantioselective GC [17], also proved useful for packed columns in a conventional GC apparatus (Fig. 6). Thus 30 μL (47 mg) racemic enflurane was enantioseparated in 45 min at 26°C into the first eluted (*R*)-enantiomer and at 50°C into the second eluted (*S*)-enantiomer on a 4 m × 7 mm (i.d.) glass column containing 95 g Lipodex E diluted in SE-54 (dimethyl-phenyl(5%)-polysiloxane) (10 wt%) and coated onto Chromosorb P (AW, DMCS, 80–100 mesh) (20 wt%) (Fig. 7, left) [29, 47]. A chemical purity of at least 99.9% and an enantiomeric excess (ee) of at least 99.8% were achieved for both enflurane enantiomers. The eluates from the column were split 1:1,500 (Fig. 6) between a flame-ionization detector and a cold-trap cooled with dry ice/acetone or liquid dinitrogen. Although the separation of the enantiomers from the carrier gas helium is straightforward, some mist formation during collection reduced the amount of recovered enantiomers (~12 mg each). An overloading study is depicted in Fig. 7, right [29].

Repetitive injections allowed the collection of 250 mg each of enflurane enantiomers of ee = 99.8% daily. By using the same procedure, only 6 mg of racemic isoflurane could be baseline enantioseparated isothermally at 26°C in 28 min [29]. However, with isothermal runs, repetitive injections in close succession and at short intervals were possible (Fig. 8) [29].

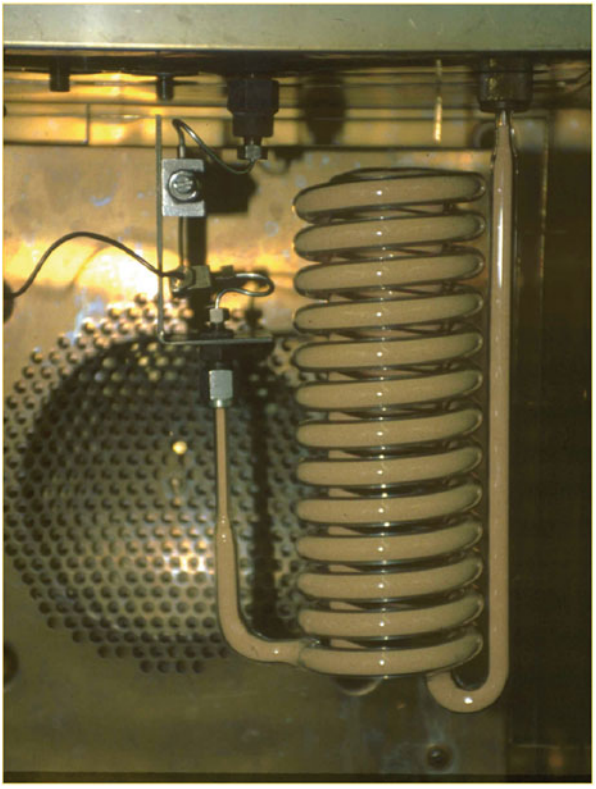

Fig. 6 Instrumental set-up of enantioselective preparative GC in a conventional apparatus (Carlo-Erba, HRGC 5300). The home-made packed 4 m × 7 mm i.d. glass column consisted of a modified condenser of a discarded rotary evaporator [33]

The above-described set-up was insufficient for large scale preparative enantioseparations of isoflurane and desflurane. Therefore an up-scaled column design was employed [48]. A packed 1 m × 24 mm (i.d.) stainless steel column filled with Chromosorb P (AW-DMCS, 80–100 mesh) which was coated with 20.3 wt% of the mixture of 10.6 wt% octakis(3-*O*-butanoyl-2,6-di-*O*-pentyl)-γ-cyclodextrin (Lipodex E) in polysiloxane SE-54, was installed in an automated Hupe & Busch preparative GC (built in the 1960s). It required the synthesis of 500 g CSP consisting of 10.75 g unpurified Lipodex E and 90.5 g SE-54 coated onto 400 g Chromosorb P. Unpurified Lipodex E contains under- and over-pentylated species and, interestingly, the crude selector showed a higher enantioseparation factor α for isoflurane (from 1.3 to 1.6 at 30°C) but reduced values for desflurane and enflurane. Here 300 mg of the single enantiomers of isoflurane were obtained daily with 130 automated repetitive injections isothermally at room temperature (Fig. 9) [48, 49]. The very high enantiomeric excess of both isoflurane enantiomers (ee = 99.8%) was determined by analytical enantioselective GC (Fig. 10). Desflurane could only be enantioseparated under overlapping conditions and recycling or discharging the middle fractions [48].

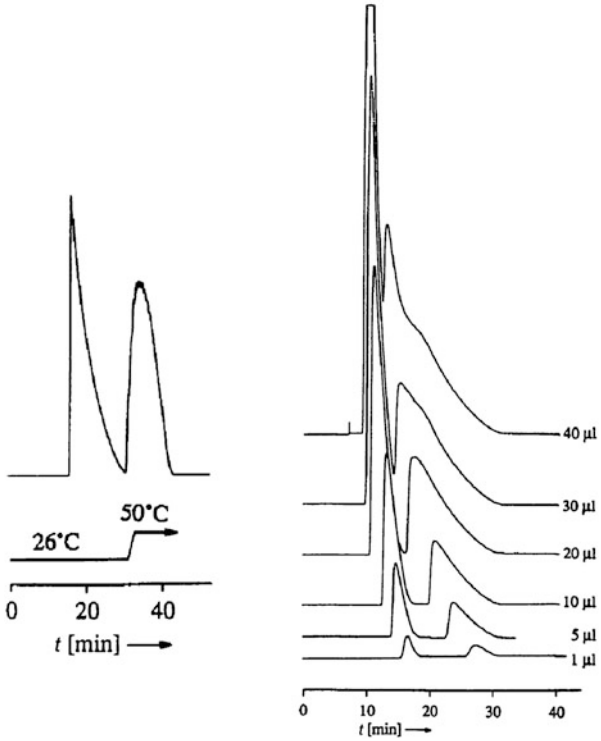

Fig. 7 *Left*: Temperature-programmed semi-preparative gas-chromatographic enantioseparation of enflurane. 4 m × 7 mm (i.d.) glass column filled with 95 g Chromosorb P-AW-DMCS coated with 20.3 wt% Lipodex E in SE-54 (10 wt%). Injected amount: 30 µL, 8.4 cm/s helium. *Right*: Overloading experiment (1–40 µL of racemic enflurane) at 40°C and 8.4 cm/s helium [29]

Then 500 mg of the first eluted enantiomer (ee = 91%) and 450 mg of the second eluted enantiomer (ee only 68%) were obtained daily. This amount was drastically reduced when higher ee values were required.

With the availability of pure enantiomers of the inhalation anesthetics with ee ~ 99.8% (corresponding to 0.1% of enantiomeric impurity; for enantiomers of isoflurane, cf. Fig. 9, right), various topics could be investigated: (1) in olfaction the enantiomers of isoflurane possessed a different odor [27], (2) the absolute configurations of (+)-isoflurane and (+)-desflurane were determined by cryoscopic X-ray crystallography (Sect. 5), (3) biological trials showed only small differences in the MAC values of isoflurane enantiomers in rodents [12, 50], (4) the use of single isoflurane enantiomers as novel chiral additive to the mobile phase in GC did not exhibit any enantiomeric differentiation for a host of tested racemates [51], (5) single enantiomers of enflurane, isoflurane, and desflurane were used as analytes for enantioselective sensor devices (Sect. 4), (6) single enflurane enantiomers were employed for NMR studies with CDs used as CSAs (Sect. 10), and (7) single isoflurane enantiomers were required for the enantiomer labelling method (Sect. 7).

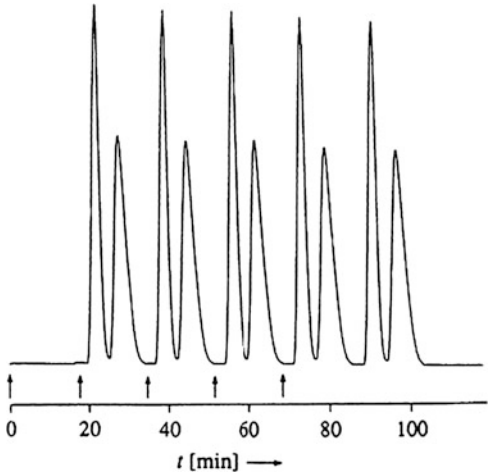

Fig. 8 Semi-preparative gas-chromatographic enantioseparation of racemic isoflurane with repetitive injections of 4 µL during one run. 4 m × 7 mm (i.d.) glass column filled with 95 g Chromosorb P-AW-DMCS (80–100 mesh) coated with 20.3 wt% Lipodex E in SE-54 (10.0 wt%) at 26°C and 8.4 cm/s helium [29]

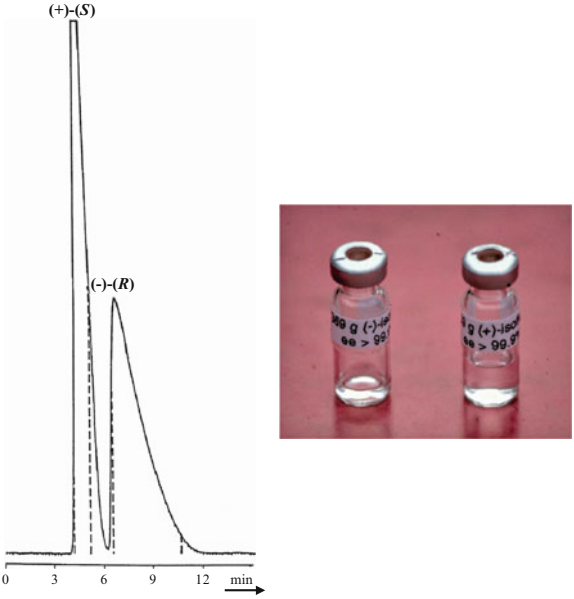

Fig. 9 *Left*: Preparative gas-chromatographic enantioseparation of isoflurane. 1 m × 24 mm (i.d.) steel column filled with 450 g Chromosorb P-AW-DMCS (80–100 mesh) coated with 20.3 wt% of unpurified Lipodex E in SE-54 (10.6 wt%) at 27°C and 1 bar dinitrogen [48]. *Right*: isolated single enantiomers of isoflurane with ee = 99.9%

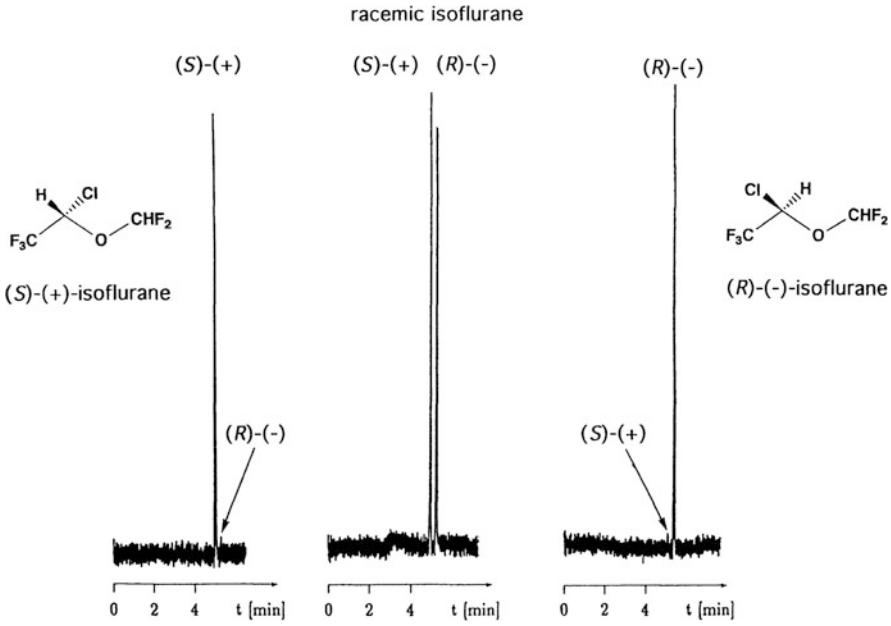

Fig. 10 Proof of the very high ee of isoflurane enantiomers. 25 m × 0.25 mm (i.d.) fused silica capillary column coated with 0.5 μm octakis(3-*O*-butanoyl-2,6-di-*O*-pentyl)-γ-cyclodextrin (Lipodex E) in SE-54 (10 wt%) at 26°C and 1.1 bar helium (courtesy, Dr. M. Juza)

In an attempt to scale-up the discontinuous preparative GC approach by a continuous enantioseparation of inhalation anesthetics, the simulated moving bed (SMB) technology has been employed in enantioselective GC, adapting the previous findings obtained in the batch-wise processes described above. Preliminary studies included enflurane [52, 53] and isoflurane [54], which were enantioseparated on unpurified octakis(3-*O*-butanoyl-2,6-di-*O*-pentyl)-γ-cyclodextrin (Lipodex E) diluted in polysiloxane SE-54 and coated on Chromosorb P (AW, DMCS, 80–100 mesh). An optimized version of the enantioselective SMB unit later on consisted of eight 80 cm × 15 mm (i.d.) stainless steel columns assembled in a home-made SMB-GC unit (Fig. 11) operated at 35°C. Each column with an adsorption bed volume of 140 mL contained 20% unpurified Lipodex E diluted in SE-54 and coated on Chromosorb A (NAW, 20–30 mesh) (17 wt%). Under carefully optimized conditions the SMB-GC pilot unit furnished a total of 20 g of each single enantiomers of enflurane with an averaged ee of 96.6% with dinitrogen as carrier gas [55]. This set-up represented the first gas-chromatographic SMB-GC pilot plant for preparative enantioseparations.

In enantioselective GC-SMB, the required continuous counter-current flow of the fluid and of the solid adsorbent ("moving bed chromatography") is simulated by periodically switching the different inlets and outlets in the eight-column-array (Fig. 11). The preparative enantioseparation of enflurane by SMB and pressure swing adsorption (PSA) was theoretically investigated by dynamic simulations [56]

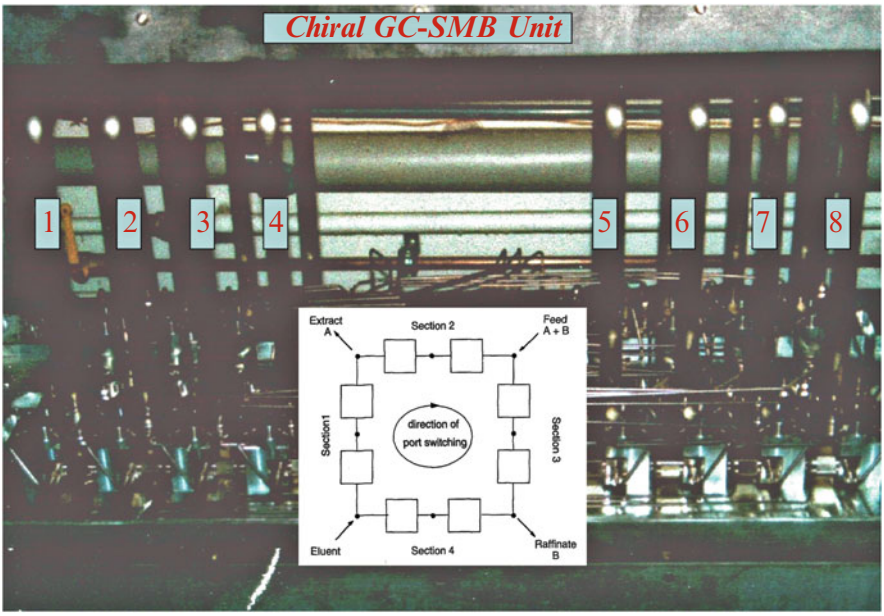

Fig. 11 An enantioselective GC-SMB-plant. (Courtesy Prof. M. Morbidelli, ETH, Zürich) containing eight columns. *Inserted*: schematic principle of SMB [55]

based on model parameters reported in previous experimental investigations [55]. A key difference between the enantioselective liquid and gas phase SMB is the strong influence of the pressure drop on the flow rate in the latter approach and the limited solubility of the feed in the gas phase which in turn results in limited productivities [57].

4 Enantioselective Sensor Devices for Inhalation Anesthetics

The gas-chromatographically obtained single enantiomers of enflurane, isoflurane, and desflurane were used for enantioselective trials using a chiral quartz microbalance sensor system [58, 59]. The quartz crystal was coated with octakis(3-*O*-butanoyl-2,6-di-*O*-pentyl)-γ-cyclodextrin (Lipodex E) diluted in polysiloxane SE-54. A schematic representation of the thickness-shear mode resonator (TSMR) employed is shown in Fig. 12, top.

Upon exposure of the TSMR to single enantiomers of enflurane, the sorption of analyte molecules by the cyclodextrin coating leads to a change in the oscillating mass which in turn causes a shift of the operating frequency. As depicted in Fig. 12, middle, representative experiments consisted of the alternating exposure of the coated TSMR to sample vapour (in ppm) and dry synthetic air, respectively. In addition to the chiral sensor, an achiral reference device coated with pure SE-54 (devoid of enantiomeric

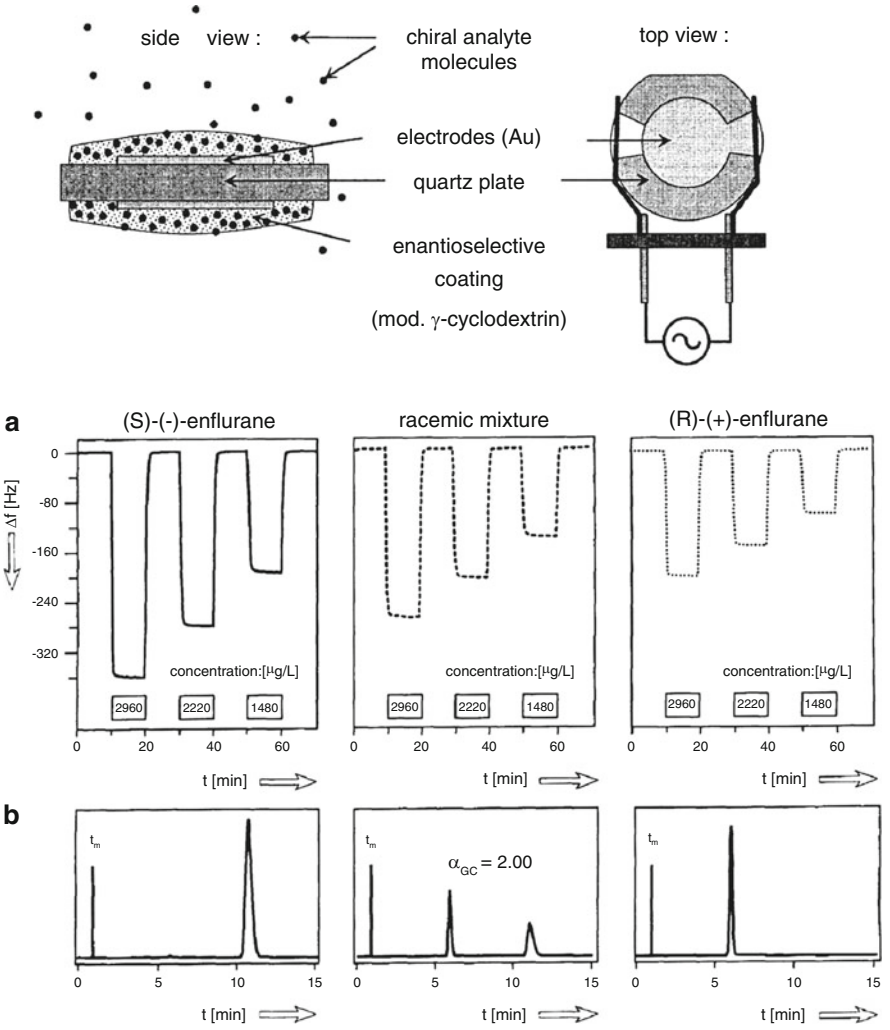

Fig. 12 *Top*: Principle of the enantioselective TMSR sensor. *Bottom*: Comparison of enantioselective TMSR sensor device (**a**) and enantioselective GC (**b**) for single enantiomers of enflurane and its racemic mixture exposed to 50 wt% Lipodex E in SE-54. The sensor responses upon alternate exposure to enantiomer-loaded to pure synthetic air are given in Hz, the analyte concentration in µg/L. The GC retention times obtained with a 25 m × 0.25 mm (i.d.) capillary column are displayed in min [58, 59]

differentiation) was used for the purpose of artefact adjustment including fluctuating gas phase concentrations and analyte contaminations. The sensor responses upon the exposure to the single enflurane enantiomers showed an unprecedented frequency difference and the observed enantioseparation factor α agreed well with that of the gas-chromatographic experiment. Similar results were obtained for the enantiomers of isoflurane and desflurane [60] (cf. also Fig. 15 in [61]). The sensor experiment and the

gas-chromatographic set-up displayed the same sign and magnitude of enantioselectivity (Fig. 13). As the recognition step in the case of a gas sensor involves just one theoretical plate while GC enantioseparation arises from some thousands of subsequent absorption-desorption-steps in single theoretical plates, the suitability of TSMR for enantiomer discrimination was far from being obvious at the outset of the experiments [58–60].

5 Determination of Absolute Configurations in Enantioselective GC

The assignment of absolute configurations [62] of minute amounts of chiral compounds is an important task in trace enantiomeric analysis. *By direct evidence*, absolute configurations can be determined by enantioselective GC (free of chiroptical evidence) via the simultaneous injection of a reference compound with an established stereochemistry. *By indirect evidence*, it is tempting to correlate the absolute configuration of the enantiomers of structurally related compounds (congeners, homologues) with their order of elution from a given CSP in enantioselective GC. Indeed, on L-valine diamide selectors, the derivatized L-enantiomers of all proteinogenic α-amino acids were found to elute as the second peak [4]. By coincidence, the same elution order was also observed for Chirasil-γ-Dex (Lipodex E, comprised of D-glucose moieties, anchored to polydimethylsiloxane [32], Fig. 3, right), except for proline and threonine where the L-enantiomers eluted first [63]. In enantioselective complexation GC, a rather consistent correlation between absolute configuration and elution order of 2-alkyl- and 2,3-dialkyl-substituted oxiranes on metal(II)-bis(perfluoroacyl-(1*R*)-camphorates), was found, leading to the formulation of a quadrant rule [14]. However, striking exceptions to the rule were also noted for structurally related racemates. Thus, *trans*-(2*S*,3*S*)-dimethyloxirane (a "hard" donor selectand) and *trans*-(2*R*,3*R*)-dimethylthiirane (a "soft" donor selectand) were both eluted as the second peak on nickel(II) bis(3-heptafluorobutanoyl-(1*R*)-camphorate) despite their opposite configurations, whereas (*R*)-methyloxirane and (*S*)-methylthiirane showed the expected opposite elution order on the same selector [64]. (*S*)-2-*Methyl*-tetrahydrofuran was eluted as the first peak while (*S*)-2-*ethyl*-tetrahydrofuran was eluted as the second peak from nickel(II) bis(3-heptafluorobutanoyl-(1*R*)-camphorate) [65]. These examples vividly showed that predictions of absolute configuration from retention behavior for homologues or structurally related compounds may be ambiguous. Moreover, the temperature-dependent reversal of the elution order may obscure assignments of absolute configurations by enantioselective chromatography as the result of enthalpy–entropy compensation (Sect. 8) within an extended temperature-range of operation. Thus, isopropyloxirane as compared to other alkyloxiranes exhibited the remarkably low $T_{iso} = 64°C$ on nickel(II) bis(3-heptafluorobutanoyl-10-ethylidene-(1*S*)-camphorate) [66]. Thus peak inversion occurs above T_{iso}, and a non-consistent elution order would result between isopropyloxirane and other

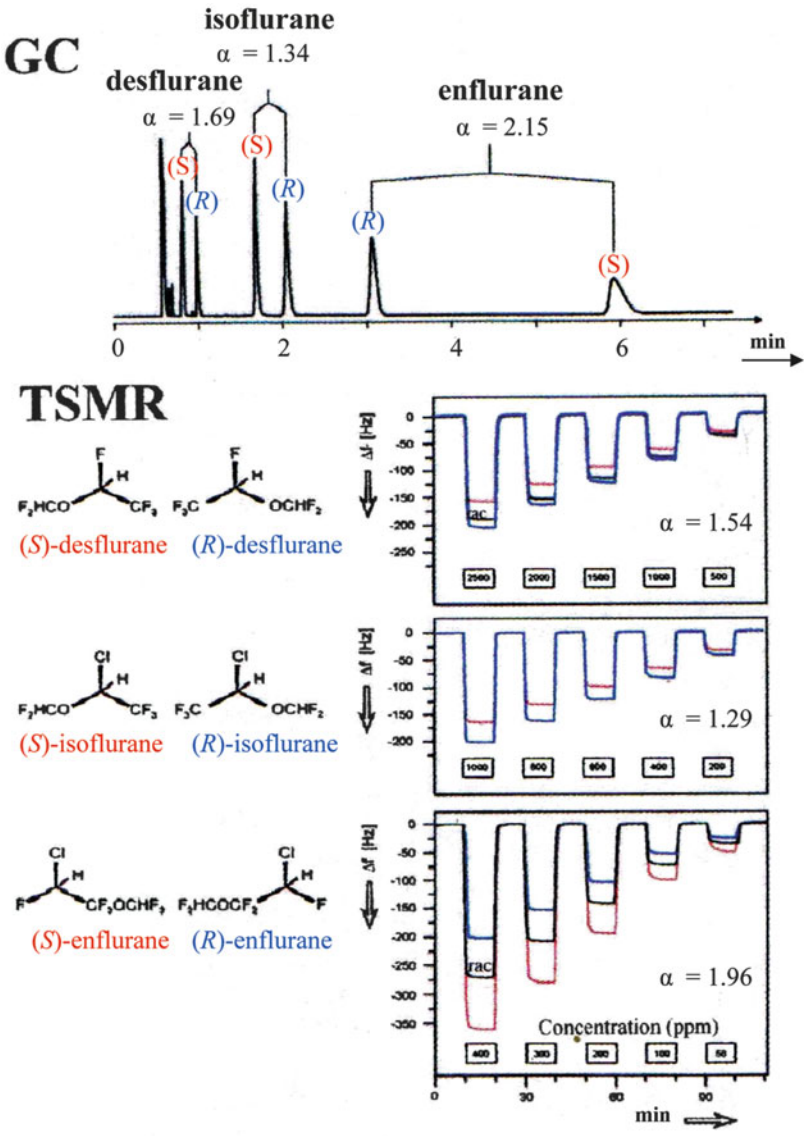

Fig. 13 *Top*: Analytical gas-chromatographic enantioseparation of desflurane, isoflurane and enflurane (structures see *bottom*, *left*). 25 m × 0.25 mm (i.d.) fused silica capillary column coated with 0.5 μm octakis(3-*O*-butanoyl-2,6-di-*O*-pentyl)-γ-cyclodextrin (Lipodex E) in SE-54 (10 wt%,) at 26°C and 1.1 bar helium [48]. *Bottom*, *right*: Sensor responses of a quartz thickness-shear mode resonator (TSMR) coated with Lipodex E in SE-54 (50 wt%) in Hz for μg/L amounts of single enantiomers and its racemic mixture of desflurane, isoflurane and enflurane, depicted as an overlay of strongly and weakly interacting enantiomers and, in between, for the racemate (the latter except for isoflurane) [61]

homologues alkyloxiranes with identical absolute configuration at elevated temperatures in the GC experiment on simple thermodynamic grounds.

Some confusion existed previously in the assignment of the absolute configurations of isoflurane vs desflurane. The two molecules differ only by chlorine vs fluorine at the stereogenic carbon atom (Fig. 2). The enantiomers of isoflurane and desflurane were isolated by preparative enantioselective GC on the γ-cyclodextrin CSP Lipodex E (Sect. 3) and the dextrorotatory enantiomers (+)-isoflurane and (+)-desflurane were eluted before the levorotatory enantiomers (–)-isoflurane and (–)-desflurane [31] (optical rotations refer to the sodium-*D*-line at 20°C). Thermodynamic considerations using the retention-increment R' approach (Sect. 8) supported the reasonable assumption that the enantiomers of isoflurane and desflurane with the same configuration possess the same sign of optical rotation and the same elution order on Lipodex E [31].

The assignment of absolute configuration to dextro- and levorotatory isoflurane and desflurane was carried out by vibrational circular dichroism (VCD) spectra [67]. Thus the recorded spectrum of (+)-isoflurane in CCl_4 was compared with the theoretical spectra calculated by ab initio methods for different conformers of (*R*)- and (*S*)-isoflurane [68]. The theoretical VCD spectrum obtained as the sum of those for the two lowest energy conformers with (*S*)-configuration was found to match well with the experimental VCD spectrum for (+)-isoflurane. Therefore it was concluded that (+)-isoflurane had the (*S*)-configuration and hence (–)-isoflurane had the (*R*)-configuration [68]. However, in order to approximate better the experimental and theoretical VCD spectra, different ratios of the two conformers were applied. Moreover, the influence of the solvent on the VCD spectra was not considered. An analogous study with desflurane implied that (+)-desflurane had the (*R*)-configuration and hence (–)-desflurane had the (*S*)-configuration [69]. The surprising reversal of the sign of optical rotation vs absolute configuration (i.e., (+)-(*S*)- isoflurane vs (–)-(*S*)-desflurane) was also in contradiction to other consequences resulting from the assignment by VCD. The preparative conversion of (–)-isoflurane to (+)-desflurane (likely an S_{N2} process) would proceed with retention of configuration whereas the decarboxylation of a desflurane precursor would proceed with inversion of configuration; cf. references in [31, 70] (Fig. 14, left). Interestingly, single crystals obtained under cryogenic conditions of (+)-isoflurane and (+)-desflurane, which were previously isolated by preparative enantioselective GC (Sect. 3) [31], allowed the assignment of absolute configuration by anomalous X-ray crystal structural analysis at −180°C. Dextrorotatory isoflurane and desflurane were both found to possess (*S*)-configuration, thus confirming the VCD assignment (+)-(*S*)-isoflurane, but revising the VCD assignment of (+)-(*R*)-desflurane to (+)-(*S*)-desflurane [70]. Although the revised X-ray assignment of (+)-(*S*)-desflurane was still not unambiguous due to the small spatial differences between hydrogen and fluorine atoms and an unfavorable Flack parameter [70], it was in agreement with the general reaction stereochemistry of S_{N2} reactions proceeding with Walden inversion of configuration and decarboxylations at a stereogenic center proceeding with retention of configuration [71] (Fig. 14, right). The preliminary assignment of absolute configuration by VCD to (+)-(*R*)-desflurane has later been revised to (–)-(*R*)-desflurane and had been explained as arising from a wrongly labeled specimen [72, 73]. An extensive theoretical VCD

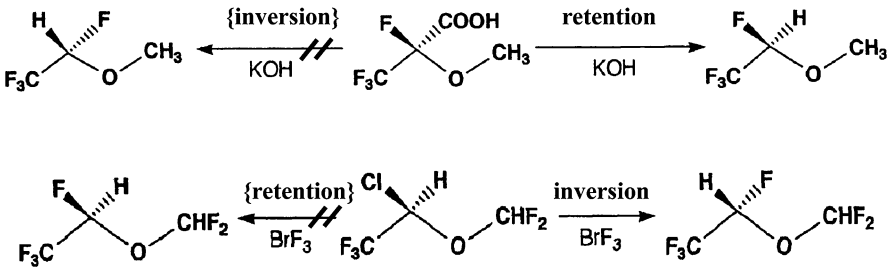

Fig. 14 Revised stereochemical course of chemical reactions relevant to the preparation of enantiomeric inhalation anesthetics. *Top*: Decarboxylation. *Bottom*: S_{N2}-substitution

study of isoflurane and desflurane has subsequently been advanced by Biedermann et al. [74].

Based on the previous VCD configurative assignment of (+)-(*S*)-desflurane, the decarboxylation of a desflurane precursor was described to proceed with inversion of configuration (Fig. 14, left, top) [75, 76] (despite some reservation; cf. footnote in [28] in [76]) but has later been corrected as proceeding with retention of configuration [77] (Fig. 14, right, top). Thus the gas-chromatographic elution order of isoflurane and desflurane enantiomers on Lipodex E is consistent with their absolute configurations [31, 70]. Furthermore, the magnitude of NMR shifts of protons of isoflurane and desflurane enantiomers in the presence of Lipodex E is compatible with their absolute configurations [70] and the frequency shifts of isoflurane and desflurane enantiomers on a quartz sensor coated with Lipodex E are also in line with their absolute configurations (Sect. 4) [58]. The enantiomers of isoflurane and desflurane are identified and differentiated by their chiroptical properties, i.e., the sign of optical rotation and circular dichroism. General methods for the assignment of absolute configuration of dextro- and levorotatory enantiomers rely on VCD and anomalous X-ray methodologies. The present elaboration shows that different approaches finally contribute to the clarification of a difficult research topic and that enantioselective chromatography plays an important role in it [62].

In the US patent 5,114,714 of May 19, 1992 it is claimed that (*R*)-isoflurane and (*R*)-desflurane (essentially free of the (*S*)-enantiomers), while inducing and maintaining anesthesia, are insufficient to cause adverse effects associated with the (*R*,*S*)-racemates [78]. In a follow-up US patent 5,114,715 of May 19, 1992 it is claimed that (*S*)-isoflurane and (*S*)-desflurane (essentially free of the (*R*)-enantiomers), while inducing and maintaining anesthesia, are insufficient to cause adverse effects associated with the (*R*,*S*)-racemates [79]. The two patents are identical in the wording except for the interchanged stereochemical descriptors (*R*) and (*S*) (Fig. 15). The "enantiomeric" patents are entirely devoid of physical characterizations and pharmacological data of the compounds claimed. No experimental details on the enantioselective preparation of the (*R*)- vs (*S*)-enantiomers are given. The identification of the enantiomers by their absolute configuration is also missing. Although no supporting details were disclosed, the two patents imply that either the (*R*)- or the (*S*)-enantiomers of isoflurane and desflurane do not possess adverse effects as

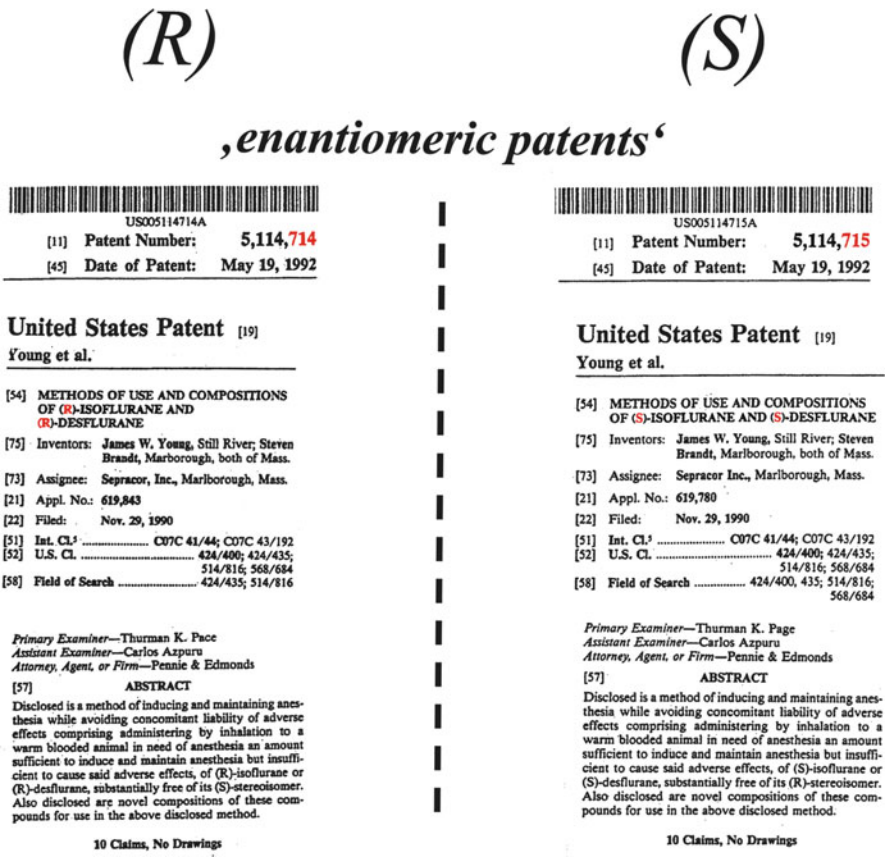

Fig. 15 "Enantiomeric" US patents 5,114,714 [78] and 5,114,715 [79] of May 19, 1992, claiming that (*R*)-isoflurane and (*R*)-desflurane (first patent) and (*S*)-isoflurane and (*S*)-desflurane (second patent) while inducing and maintaining anesthesia do not cause adverse effects associated with the (*R*,*S*)-racemates of isoflurane and desflurane

compared to the racemic composition in which (*R*)- and (*S*)-enantiomers are present. Unfortunately, the (*R*)- and (*S*)-enantiomers were not identified by their sign of optical rotation and the incertitude in the assignment of absolute configuration of desflurane could only be resolved later on (see above).

6 In Vivo Studies of the Enantiomeric Distribution of Administered Isoflurane and Desflurane in Humans After Anesthesia

Due to the availability of enantiomeric differentiation of isoflurane by chiral GC (Sect. 2), a small preponderance of the (+)-(*S*)-enantiomer over the (–)-(*R*)-enantiomer could readily be demonstrated for the first time in blood samples collected

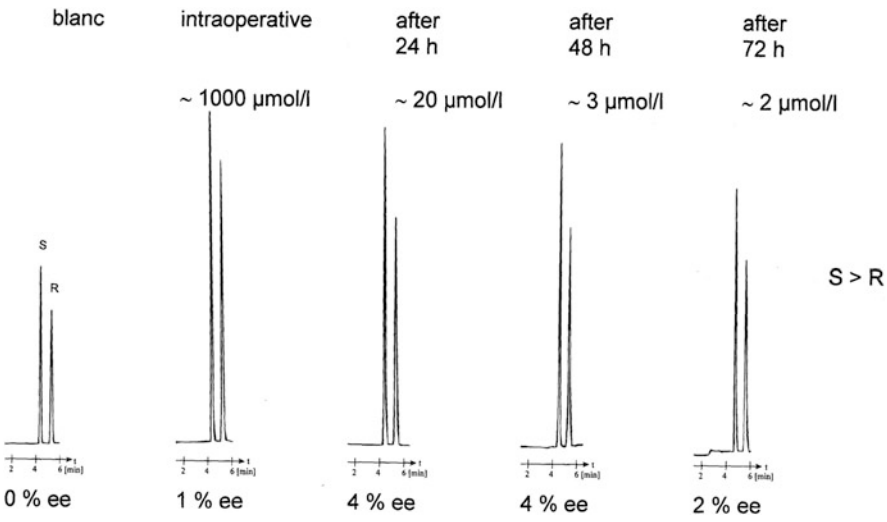

Fig. 16 Deviation from the 1:1 ratio of racemic isoflurane ((*S*) > (*R*)) during anesthesia in a single patient. 30 m × 0.25 mm (i.d.) fused-silica capillary column coated with 0.28 µm octakis (3-*O*-butanoyl-2,6-di-*O*-*n*-pentyl)-γ-cyclodextrin (Lipodex E) in PS 255 (30 wt%) at 28–29°C and 1.62 bar dihydrogen [80]

during anesthesia with racemic isoflurane in a routine surgery via a self-experiment (V.S. in 1997, Fig. 16) [80]. This finding was subsequently confirmed in a small group of patients undergoing eye surgery (Fig. 17) [81]. The highest enantiomeric bias of 51.8% (+)-(*S*)-isoflurane (ee = 3.6%) was observed after 1 day (1,440 min). This result initiated a comprehensive clinical study to detect differences in the pharmacokinetics of isoflurane enantiomers in humans involving a group of 41 volunteers (of whom 25 were females) who underwent anesthesia maintained with racemic isoflurane [82, 83].

Isoflurane enantiomers were analyzed in blood samples drawn before induction, at onset of anesthesia, after tracheal extubation, and daily for up to eight postoperative days by venous puncture. The following procedure was employed [82]. Blood samples were treated with the anticoagulant EDTA to prevent coagulation and 1 mL of the blood plasma was placed into 2-mL GC headspace vials and stored at −18°C. Prior to analysis, the sample vials were equilibrated for 10 min at 50°C at a preheating station before injection. A multipurpose sampler (Gerstel® MPS) was used for the headspace GC–MS analysis and it was combined with a cold injection system (Gerstel® CIS 3) for cold-trapping, enrichment, and cryo-focusing of the analyte (Gerstel, Mülheim an der Ruhr, Germany). The enantiomeric ratio of isoflurane was determined on a 30 m × 0.25 mm fused silica capillary column coated with 0.28 µm (film thickness) octakis(3-*O*-butanoyl-2,6-di-*O*-*n*-pentyl)-γ-cyclodextrin (Lipodex E) [28, 31] which was diluted in poly(vinylmethylsiloxane) PS 255 (30 wt%). The enantiomers were detected in the selected ion monitoring mode (GC–MS-SIM) with the ions 117 and 149 *m*/*z*. Thus interference of co-eluted volatiles (e.g., acetone, 2-propanol and, occasionally, ethanol!) was excluded (Fig. 18) [82]. Upon anesthesia, approximately

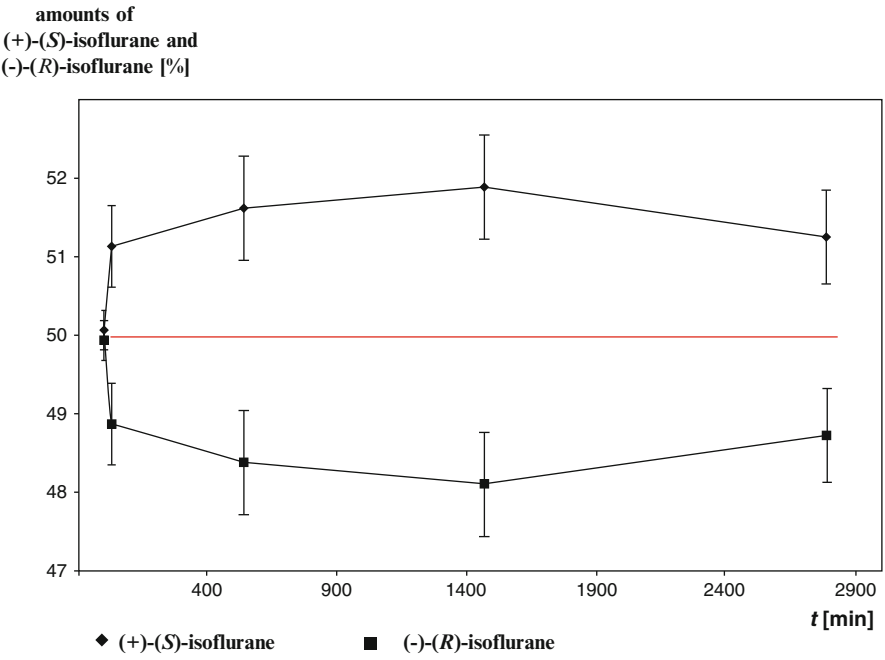

Fig. 17 Enrichment of (+)-(*S*)-isoflurane (first eluted enantiomer) in blood samples taken during and after eye surgery under narcosis with racemic isoflurane (mean of 36 measurements) [81]

1.2 vol.% of racemic isoflurane were added to the gas mixture of N_2O and O_2 (70:30, v/v) yielding blood concentrations of approximately 0.5 µmol/mL or ~0.1 g/L, which was well amenable to FID-detection of the anesthetic.

An enrichment of (+)-(*S*)-isoflurane was found in all blood samples drawn after anesthesia [82, 83] in agreement with the former studies (Figs. 16 and 17) [80, 81]. The highest level between 52% and 54% as opposed to 50% for the racemic form was reached on day 2 for most of the volunteers. Blood samples drawn after several days of anesthesia showed isoflurane concentrations below 1 nmol/mL blood (Sect. 7). It was therefore necessary to increase sensitivity by optimizing the headspace GC/MS method. The mass selective detector was used in the SIM mode (Fig. 18) with two monitored ions 117 and 149 *m*/*z* (Fig. 19) [82].

In a follow-up study, patients were categorized according to body mass index, duration of anesthesia, and pre-existing lung disease. None of these factors had any significant influence on the shift toward accumulation of (+)-(*S*)-isoflurane, although in obese patients the preponderance of the (+)-(*S*)-enantiomer exceeded that in non-obese patients [83]. Quite unexpectedly, and due to the extraordinary sensitivity of the GC set-up, isoflurane enantiomers were already present in blood samples which were drawn pre-operatively before the actual onset of anesthesia as the result of the omnipresence of traces of isoflurane in the operating room and/or contamination of medical instrumentation with minute amounts of isoflurane [80, 81].

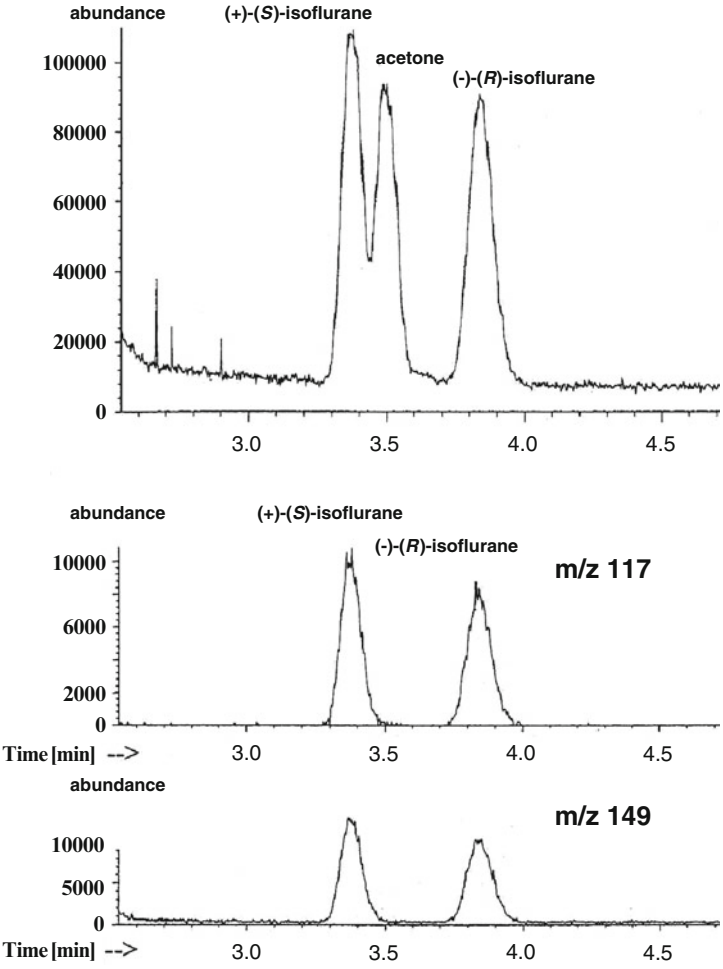

Fig. 18 *Top*: Total ion chromatogram (scan 40–200 m/z). *Bottom*: ion chromatogram by headspace GC/MS of a blood sample obtained at onset of isoflurane anesthesia [82]

The data obtained rely on the conditions that the distribution of the enantiomers in the headspace is not biased by the presence of enantiomeric constituents in the liquid (e.g., chiral proteins) and that the ionization of isoflurane enantiomers is not affected by the presence of co-eluted contaminants (e.g., acetone). Consequently, after each of 21–30 sample measurements (corresponding to samples of three patients), quality control experiments were performed with blank blood samples spiked by variable amounts of racemic isoflurane which gave the expected unbiased 1:1 ratio of the enantiomers within experimental error. The controls were analyzed in series with the patient specimens to exclude any deleterious effect (e.g., memory effects) of the analytical method [82]. In addition, the integration parameters (slope-test) were optimized [80, 82] which constitutes an essential requirement

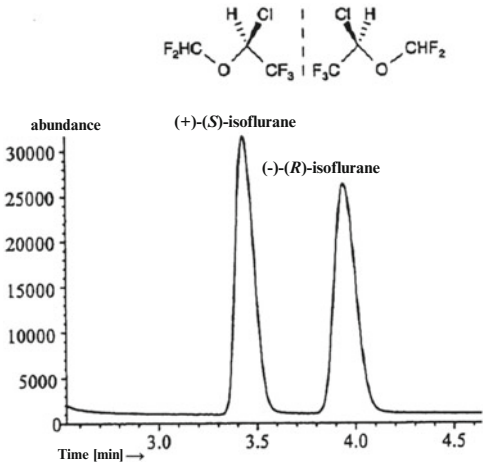

Fig. 19 Isoflurane analysis of a blood sample by GC/MS/SIM (117 and 149 *m/z*). 30 m × 0.25 mm (i.d.) fused-silica capillary column, retention gap 1.5 m, coated with 0.28 μm octakis(3-*O*-butanoyl-2,6-di-*O*-*n*-pentyl)-γ-cyclodextrin (Lipodex E) [28, 31] in PS 255 (30 wt%) at 33°C and 60 kPa helium [82]

when true 1:1 ratios of racemic mixtures, and small deviations therefrom, are quantified with high precision [84]. The mean enantiomeric enrichment (52.1 ± 0.1%) of (+)-(*S*)-isoflurane observed in vivo in the clinical study on day 2 as compared with the racemic isoflurane controls (50.0 ± 0.1%) was considered to be statistically significant [82]. The observed enrichment of (+)-(*S*)-isoflurane is important in view of the fact that isoflurane is subject to little (maximum 0.2%) or no biotransformation [85]. The distribution of volatile chlorofluoroethers into different tissues depends on uptake and arterial concentration, perfusion of the tissue, and the partition coefficient into the different compartments (blood plasma, interstitial fluid, fat tissue, intra- and transcellular fluid). The two enantiomers of the vaporized racemate may have different pharmacokinetic properties during uptake and redistribution. Enantioselective partitioning between gas and liquid may already occur in the lung, somewhat reminiscent of the principle of enantioselective gas chromatography! It has been concluded previously that anesthetics act on membranes rather than on lipids whereby isoflurane was shown to activate potassium channels (which silence the cell via hyperpolarization) whereby the (+)-(*S*)-enantiomer was about twice as effective as the (–)-(*R*)-enantiomer [86, 87].

The same methodology has been used to determine the enantiomeric ratio of isoflurane in urine samples collected from patients undergoing anesthesia. Comparable to blood samples, in urine samples isoflurane enantiomers could be determined up to 9 days after surgery [88, 89]. Yet in contrast to blood, in urine (–)-(*R*)-isoflurane was enriched to a low degree (up to 51.3%) [88].

In analogy to the isoflurane study, the time-dependent distribution of desflurane enantiomers in the blood and urine of five patients undergoing general anesthesia

with racemic desflurane was scrutinized [90]. EDTA-treated blood samples were drawn immediately after tracheal extubation. In the following 3 days, 1-mL blood and urine samples were collected and transferred in 2-mL GC-headspace vials. In all blood samples, an enrichment of (+)-(*S*)-desflurane (up to 53.6%) was found, whereas in urine (–)-(*R*)-desflurane (up to 52.9%) was abundant. For controls in which blood and urine samples were spiked with racemic desflurane, the expected 1:1 ratio within experimental error was found. The enantiomeric enrichment in the samples of the patients was appreciably higher than the standard deviation of the control measurements.

As isoflurane possesses a negligible metabolic rate (<0.2%) in humans [85], it is mostly eliminated via respiration in the course of anesthesia. Isoflurane could be detected in breath even 23 days after surgery [88]. The percentage of isoflurane enantiomers in human breath, although the anesthetic is administered as a racemate, varied significantly with the time of exhalation [91, 92]. Breath samples were collected using a 1-L-tedlar bag and were then transferred onto a freshly conditioned thermodesorption tube filled with Tenax®. Analysis was performed by direct thermodesorption-GC–MS (Gerstel® TDS 2) combined with the cold injection system (Gerstel® CIS 3). Any remaining water on the adsorbent was removed by a stream of helium at a TDS temperature of 20°C. Thermodesorption was achieved by raising the temperature to 220°C at a rate of 60°C/min and then keeping it there for 10 min. The temperature of the CIS was held at −150°C to cryo-focus the components efficiently and then heated to 250°C at a rate of 12°C/s. Isoflurane enantiomers in breath were quantified up to 19 days after surgery [91, 92]. During the early postoperative phase, (+)-(*S*)-isoflurane was slightly enriched (50.5% at day 3) whereas up to 5 days after surgery a noticeable excess of (–)-(*R*)-isoflurane (51.8% at day 19) was observed [91].

In view of the existing, but low, bias of isoflurane enantiomers during human anesthesia, and because the minimum alveolar concentrations (MACs necessary to prevent movement in response to a painful stimulus in rats) differ only minimally for isoflurane enantiomers [50], the use of single enantiomers of isoflurane, as insinuated in two consecutive patents (Sect. 5) [78, 79], is clearly unwarranted. Besides, enantioselective syntheses or preparative chromatographic enantioseparations of excessive amounts of chiral inhalation anesthetics would appear to be unrealistic and cumbersome. The findings also show that enantiomers do not always display striking differences in a biological chiral environment.

7 Quantitation of Enantiomers in a Sample by the Method of Enantiomer Labeling

The enantiomer of opposite configuration represents an ideal internal standard for the quantitation of the target enantiomer in a mixture. This has first been established in chiral α-amino acid analysis. Thus the amount of an L-amino acid in a sample has been extrapolated from the change of the enantiomeric ratio after addition of a *known*

amount of the oppositely configurated D-amino acid (or the DL-racemate) employed as an internal label. This method was first conceived by Bonner [93, 94] via referring to the use of an *enantiomer marker*. The approach, which was subsequently termed *enantiomer labeling* [95–97], is intriguing because enantiomers possess identical (non-chiroptical) properties in an achiral environment and therefore the enantiomeric composition is not influenced by sample manipulation (isolation, derivatization, fractionation, storage) or by chromatographic manipulations (dilution, partitioning, splitting, injection, detection). Not even thermal or catalytic decomposition, losses, or incomplete isolation will obscure the analytical result. Thus the added enantiomer serves as an overall internal standard through the whole analytical procedure. The method relies on the absence of self-recognition between enantiomers, undergoing molecular association (e.g., dimerization), in concentrated nonracemic mixtures (the *EE*-effect) [98]. However, such nonlinear effects in enantioselective chromatography [99] constitute a rather rare phenomenon and can probably be totally ignored in diluted systems.

The amount of a particular enantiomer (X_a) present in the sample is calculated from the ratio of the peak areas of the (*R*)-enantiomer (A_R) and the enantiomeric (*S*)-label (A_S) multiplied by the amount of the (*S*)-label (m_S) added as the internal standard [95]:

$$X_a = m_S \cdot \left(\frac{A_R}{A_S}\right). \tag{1}$$

Substance specific calibration factors *f* need not be considered by the enantiomer labeling method [95]. The method of enantiomer labeling can also be used for chiral compounds in samples and standards possessing only incomplete enantiomeric purities even including racemic compositions. The method only requires the precise knowledge of the enantiomeric ratios of the sample and the standard which are readily accessible by the same enantioselective GC method. The amount of the chiral component in a sample after addition of the chiral standard can be obtained as follows [95]:

$$X_i = m_S \cdot \left[\frac{(A_R - A_S \cdot C_S)(1 + C_R)}{(A_S - A_R \cdot C_R)(1 + C_S)}\right], \tag{2}$$

where A_R is the peak area of the (*R*)-enantiomer after addition of the standard, A_S is the peak area of the (*S*)-enantiomer after addition of the standard, C_R is the enantiomeric ratio (*S*)/(*R*) of the sample, C_S is the enantiomeric ratio (*R*)/(*S*) of the standard, m_S is the amount of enantiomeric standard (*S*) added, and X_i is the amount of the chiral component *i* (as sum of its enantiomers) present in the sample.

The amount of a racemate ((*S*)+(*R*)) present in a complex matrix can also be quantitatively determined via the enantiomer labeling method when a known amount of a single enantiomer ((*S*) or (*R*)) is added to the sample and the change of the peak areas is determined by enantioselective GC.

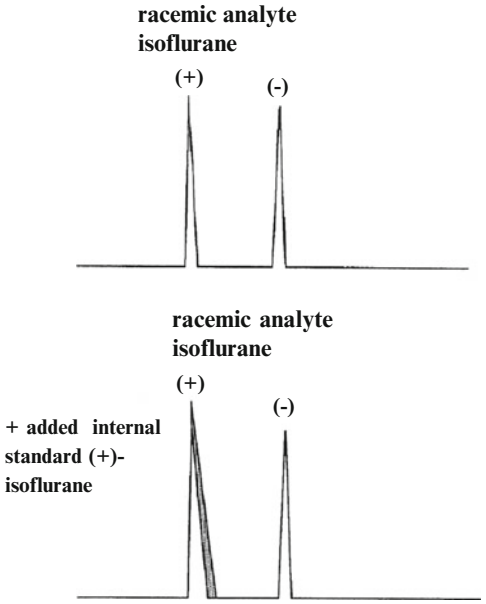

Fig. 20 Schematic chromatograms for enantiomeric labeling. *Top*: first analysis: enantioseparation of isoflurane in a sample. First and second peak: isoflurane enantiomers. *Bottom*: second analysis: enantioseparation of isoflurane in a sample after addition of the enantiomerically pure internal standard (+)-(*S*)-isoflurane. First peak: isoflurane enantiomer spiked with a known amount of the pure (+)-(*S*)-enantiomer (in practice the shaded peak will merge with the unshaded peak thereby enhancing the overall peak height). Second peak: non-labelled isoflurane enantiomer [81]

The quantitative determination of the inhalation anesthetic isoflurane in blood samples during and after surgery has been performed by enantioselective headspace GC–MS (Sect. 6), employing enantiopure (+)-(*S*)-isoflurane obtained by preparative GC (Sect. 3, Fig. 9, right) [48] as an internal standard [80, 81]. The method of enantiomer labeling requires two measurements on the enantioselective GC set-up (Fig. 20).

For quantitation, (3) has been used [81]:

$$P_{\text{isoflurane}} = \frac{W_{\text{standard}}}{W_{\text{sample}}} \cdot \frac{1}{\frac{A_{i,2}A_{k,1}}{A_{i,1}A_{k,2}} - 1}, \tag{3}$$

where $P_{\text{isoflurane}}$ is the percentage amount of each single enantiomer contained in the blood sample prior to the addition of the enantiopure standard (+)-(*S*)-isoflurane, W_{standard} is the weight of the internal standard of (+)-(*S*)-isoflurane solution added to the blood sample and being eluted as the first peak, W_{sample} is the weight of the blood sample in the headspace vial, $A_{i,1}$ and $A_{i,2}$ are the peak areas obtained for the first eluted enantiomer in the first measurement (before addition of the standard solution) and the second measurement (after addition of the standard solution), and

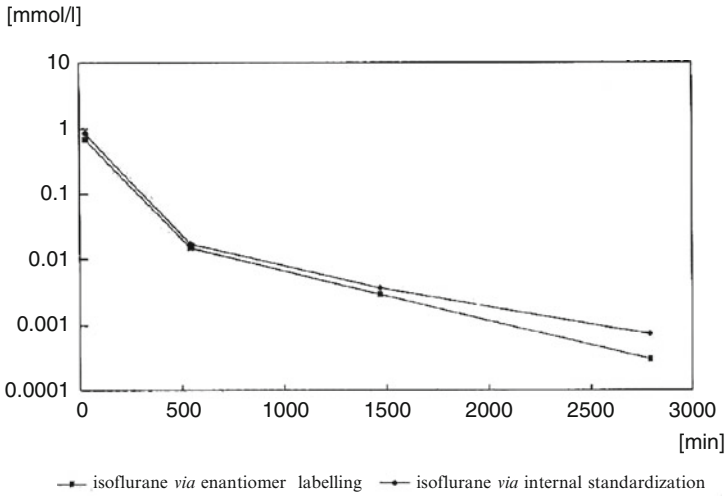

Fig. 21 Elimination of isoflurane in blood samples determined by enantiomer labeling and internal standardization [81]

$A_{k,1}$ and $A_{k,2}$ are the peak areas of the second eluted enantiomer in the first and second measurement.

The equation compensates for all errors caused by different injection volumes in the first and second measurement. The following procedure was used. Approximately 4 mL of blood specimens of patients undergoing eye surgery were collected before, during, and after surgery every 12 h for 3 days and stored after addition of citrate buffer at −20°C in vials sealed with silicon septa. A stock solution of a concentration of 0.80 μm/g of (+)-(*S*)-isoflurane in Ringer's solution was employed. Thus 1 g standard solution contained 0.15 mg (+)-isoflurane standard (molecular weight = 184.5 g/mol). For headspace GC analysis, 1 mL blood samples were transferred into 12-mL vials, sealed and equilibrated at 27°C for 30 min. The first analysis was performed prior to, and the second analysis after, addition of the stock solution containing (+)-(*S*)-isoflurane. Between 20 and 100 μL of the headspace were injected. Cryo-focusing was carried out to avoid band broadening (Sect. 6). The isoflurane enantiomers were then determined by enantioselective GC–MS (SIM) (Sect. 6). The elimination profile of isoflurane is depicted in Fig. 21. Isoflurane is washed out in blood samples in the range of 1,000–1 nmol/mL within 2 days after narcosis. In an independent study involving five patients undergoing general surgery under isoflurane anesthesia and employing the enantiomer labeling method by using (2), the isoflurane concentration decreased rapidly from ~500 nmol/mL blood sample (mean) directly after onset of anesthesia to ~0.5 nmol/mL (mean) 8 days after anesthesia (Table 1) [82].

The high volatility and the low gas–liquid partition coefficient (concentration in the liquid vs concentration in the solvent [100]) of isoflurane may cause analytical difficulties during the determination of its concentration in liquids. Apart from the problematic preparation of the standards at the concentrations in the therapeutic

Table 1 Isoflurane concentration (both enantiomers) in blood samples of five patients [82]

	Days after anesthesia								
Patient[a]	0	1	2	3	4	5	6	7	8
1	247.8	7.5	3.5	1.6	0.7	0.6	n.q.[b]	n.q.[b]	0.2
2	609.9	31.8	10.6	5.9	3.9	3.6	1.8	1.6	0.9
3	498.9	20.0	8.2	3.1	2.0	1.5	0.2	0.7	0.4
4	254.4	22.8	11.8	6.2	4.6	4.9	2.4	2.2	0.7
5	303.4	24.5	23.5	13.6	10.2	7.9	2.5	2.6	0.8

[a]Values are in nmol/mL blood
[b]Not quantified

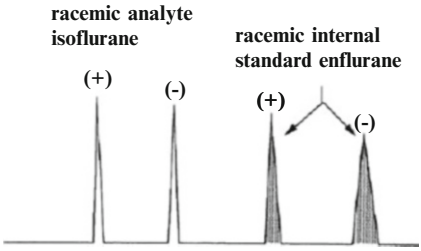

Fig. 22 Schematic chromatograms for internal standardization. First and second peak: isoflurane enantiomers; third and forth peak: known amount of internal standard racemic enflurane [81]

range (~1 mmol/L), any step in the storage and transfer of the standard which exposes the liquid to the gas phase will introduce an error via partitioning of enflurane from the liquid to the gas phase. Therefore the enantiomer labeling method is the method of choice as the internal standard possesses identical properties in complex mixtures.

The enantiomer labeling method was also compared with the common internal standard method (Fig. 22) [81]. As internal standard the racemic anesthetic enflurane (Fig. 2) has been selected. Isomeric enflurane possesses the same molecular weight as isoflurane. The method of internal standardization (Fig. 22) requires only a single measurement on the enantioselective GC set-up in contrast to the enantiomer labeling method (Fig. 20).

For quantitation, (4) has been used [81]:

$$P_{\text{isoflurane}} = \frac{W_{\text{standard}}}{W_{\text{sample}}} \cdot f_{\text{rr}} \cdot \frac{A_{\text{isoflurane}}}{A_{\text{standard}}}, \tag{4}$$

where $P_{\text{isoflurane}}$ is the percentage amount of each single enantiomer of isoflurane contained in the blood sample, W_{standard} is the weight of the internal standard of racemic enflurane solution added to the blood sample being eluted as two peaks, f_{rr} is the dimensionless relative response factor determined separately, and $A_{\text{isoflurane}}$ and $A_{\text{enflurane}}$ are the peak areas obtained for the two compounds.

Equation (4) can be used for the quantitation of either enantiomer of isoflurane by either enantiomer of enflurane. The total amount of isoflurane in the blood sample corresponds to the sum of both enantiomers. Since racemic enflurane is resolved into two peaks, it represents a twin standard molecule, i.e., double-checking of the analytical result is feasible in the case where the second eluted

peak of enflurane is not unduly broadened (Fig. 22). Figure 21 shows a small discrepancy when the two methods for the quantitation of isoflurane in blood samples were employed [81].

8 The Retention-Increment R' Approach and Thermodynamic Parameters of Enantiomeric Differentiation by GC

The gas-chromatographic enantiomeric differentiation is governed by thermodynamics and requires a *fast* and *reversible* 1:1 association equilibrium of the injected selectand enantiomers D and L and the enantiopure selector A present in the CSP. Different stabilities of the transient diastereomeric association complexes AD and AL are the prerequisite of gas-chromatographic enantiomeric differentiation. The true thermodynamic enantioseparation factor α^{assoc} is defined as the ratio of the association constants $K_{\text{D}}^{\text{assoc}}$ and $K_{\text{L}}^{\text{assoc}}$ of the energetically distinct diastereomeric complexes AD and AL according to $\text{A} + \text{D} \rightleftharpoons \text{AD}\,(K_{\text{D}}^{\text{assoc}})$ and $\text{A} + \text{L} \rightleftharpoons \text{AL}\,(K_{\text{L}}^{\text{assoc}})$, whereby D is arbitrarily eluted after L from the GC column [101]:

$$\alpha^{\text{true}} = \frac{K_{\text{D}}^{\text{assoc}}}{K_{\text{L}}^{\text{assoc}}}. \tag{5}$$

Thus, α^{true} quantifies the *true enantioselectivity* imparted by the enantiopure and undiluted selector A on the selectand enantiomers D and L. As shown for the gas-chromatographic enantioseparation of enflurane, isoflurane, and desflurane, (5) applies to the undiluted CD selector [26]. However, in contemporary enantioselective GC, chiral selectors (amino acid derivatives, metal complexes, or modified cyclodextrins) are either diluted in, or chemically bonded to, polysiloxanes used as achiral solvent matrix S. In the case of a diluted selector A present in S, the apparent enantioseparation factor α^{app} is defined as the ratio of the retention factors k_{D} and k_{L} of the selectand enantiomers D and L observed on the total CSP (A in S) [101]:

$$\alpha^{\text{app}} = \frac{k_{\text{D}}}{k_{\text{L}}}, \tag{6}$$

α^{app} being customarily used as a practical measure of enantioselectivity. However, when the selector A is diluted in an achiral solvent S, the retention factors k_{D} and k_{L} of the enantiomers D and L are determined (1) by non-enantioselective contributions to retention which arise from the achiral solvent S and which are identical for the enantiomers and (2) by the different enantioselective contribution to retention due the distinct diastereomeric molecular association of the enantiomers D and L with the chiral selector A. Due to the presence of an achiral matrix in the total CSP, i.e., the solvent S containing the chiral selector A, α^{app} is always lower than α^{true}.

In order to obtain data on the true thermodynamics of enantiomeric recognition by (5), the achiral contributions to retention must be separated from the chiral contribution to retention via the retention-increment R' approach [102]. The method requires the determination of retention data of the enantiomers D and L (1) on a reference column containing only the pure solvent S and (2) on a column containing the selector A diluted in, or chemically bonded to, the solvent S.

In the reference column, the enantiomers D and L are distributed between the mobile gas phase and the stationary phase containing the solvent S and the general equation of chromatography applies (k = retention factor, K_c = distribution constant, β = mobile phase over stationary phase volume ratio, t_R = total retention time, t'_R = adjusted retention time, t_M = unretained-peak holdup time with $t'_R = t_R - t_M$; the circle above the parameters refers to the reference column):

$$k^\circ = \frac{t'^\circ_R}{t^\circ_M} = \left(\frac{t^\circ_R}{t^\circ_M}\right) - 1 = \frac{K^\circ_c}{\beta^\circ}, \tag{7}$$

k° being identical for the enantiomers D and L on the achiral solvent S. If a chiral selector A, which interacts with the enantiomers, is diluted in the solvent S, enantioselectivity is introduced into the separation process according to the different diastereomeric association constants K_D^{assoc} and K_L^{assoc}. For each enantiomer, a distinct retention-increment R' is observed. It can be calculated from the retention factor k of the enantiomer measured on the enantioselective column containing A in S:

$$k = \frac{t'_R}{t_M} = \left(\frac{t_R}{t_M}\right) - 1 = \frac{K_c}{\beta}, \tag{8}$$

and the retention factor k° of the same enantiomer measured on the reference column containing only the solvent S (7). With $K_c = K^\circ_c + K^\circ_c\, K^{assoc} - a_A$ and $\beta^\circ = \beta$, the following equation for the retention-increment R' has been derived (K^{assoc} = association constant and a_A = activity of A in S) [66]:

$$R' = \left(\frac{k}{k^\circ}\right) - 1 = K^{assoc} \cdot a_A. \tag{9}$$

The retention-increment R' quantifies the increase of retention due to the association of each single enantiomer D and L with A in S. Equation (9) requires that the holdup times, t°_M and t_M, and the phase ratios, β° and β, of the reference column (S) and the enantioselective column (A in S) are identical. Column dimensions as well as the amount of solvent S in both columns must also be the same. In order to become independent of all column parameters, relative retentions r ($r = k/k_{ref} = t'_R/t'_{Rref}$) and r° ($r^\circ = k^\circ/k^\circ_{ref} = t'^\circ_R/t'^\circ_{Rref}$), correlated to an *inert reference standard*, have been used in practice [66, 102, 103]. Equation (9) can thus be rewritten as

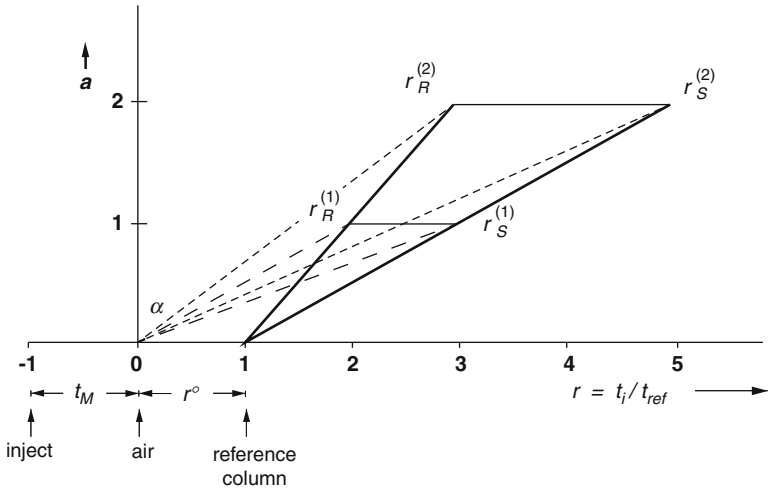

Fig. 23 Schematic representation of the distinction between (1) the non-enantioselective contribution to the relative retention of r°, and (2) the enantioselective contribution to the retention of the enantiomers (*R*) and (*S*), $r_i - r^\circ$, leading to a constancy of the retention-increment ratio R'_S/R'_R as required by (11). t_M and r° were arbitrarily set at unity, and the ratio R'_S/R'_R was arbitrarily set 2:1 [104]

$$R' = \left(\frac{r}{r^\circ}\right) - 1 = K^{\text{assoc}} \cdot a_A. \tag{10}$$

Thus, for the enantiomers D and L, irrespective of a_A, the ratio $K_D^{\text{assoc}}/K_L^{\text{assoc}}$ is directly related to the ratio of the retention-increments R'_D/R'_L which is readily accessible from the relative retentions r_D, r_L, and r°, and the true enantioselectivity $-\Delta_{D,L}\Delta G^{\text{true}}$ in diluted selector systems is then obtained as follows:

$$\begin{aligned} -\Delta_{D,L}\Delta G^{\text{true}} &= -\Delta_{D,L}\Delta H^{\text{true}} + T\Delta_{D,L}\Delta S^{\text{true}} = \text{RT ln}\, a^{\text{true}} \\ &= \text{RT ln}\left(\frac{K_D^{\text{assoc}}}{K_L^{\text{assoc}}}\right) = \text{RT ln}\left(\frac{R'_D}{R'_L}\right) = \text{RT ln}\left(\frac{r_D - r^\circ}{r_L - r^\circ}\right). \end{aligned} \tag{11}$$

Equation (11) links the true enantioselectivity $-\Delta_{D,L}\Delta G^{\text{true}}$ (and the enthalpic and entropic parameters $\Delta_{D,L}\Delta H^{\text{true}}$ and $\Delta_{D,L}\Delta S^{\text{true}}$ via the Gibbs–Helmholtz equation) with the individual retention-increments R' of the enantiomers D and L. From a thermodynamic point of view the distinction between α^{app} and α^{true} is mandatory. A schematic representation of the inherent differences between r° and r underscoring the differences between RT ln α^{true} and RT ln α^{app} is depicted in Fig. 23 [102, 104].

It follows from (11) that the expression $-\Delta_{D,L}\Delta G$ {=} RT ln α^{app}, linking enantioselectivity with the apparent enantioseparation factor being frequently used in the literature, is inappropriate when diluted selectors A are employed in enantioselective GC.

For α^{app} the new (12) is obtained by substituting k_D and k_L in (6) via the expression of (9):

$$a^{app} = \frac{K_D^{assoc} a_A + 1}{K_L{}^{assoc} a_A + 1} = \frac{R_D' + 1}{R_L' + 1} \tag{12}$$

Thus α^{app} approaches α^{true} of (5) only when the association constants K^{assoc} and/or the activity a_A of A in S are high, resulting in $R' >> 1$ [24], or when non-enantioselective contributions to retention are negligible, i.e., $r^\circ \sim 0$ (Fig. 23). Moreover α^{true}, and hence the true enantioselectivity $-\Delta_{D,L}\Delta G^{true} = RT \ln \alpha^{true}$, is independent of the activity a_A (or concentration c_A at high dilution) of A in S, whereas α^{app} is concentration-dependent due a mixed retention mechanism [24, 101]. However, a concentration-dependence is not compatible with a true thermodynamic quantity. The retention-increment R' approach has also been applied for binary selector systems, i.e., diluted mixed CSPs containing two different chiral selectors [101].

The differentiation of apparent and true enantioselectivity in enantioseparations was at first employed in enantioselective complexation GC employing metal chelate CSPs [103] and was later extended to enantioselective inclusion GC utilizing modified cyclodextrin selectors [24, 104, 105]. The distinction between non-enantioselective and enantioselective interactions has also been adopted in enantioselective LC [106–108].

It should be recognized that the enantioselectivity, as expressed by $-\Delta_{D,L}\Delta G^{true}$, is only determined by the *ratio* of the association constants of the selectand enantiomer and the chiral selector, $RT \ln(K_D^{assoc}/K_L^{assoc})$, regardless of whether the average associations of the selectand enantiomers D and L and the selector A, $-\Delta G = RT \ln K^{assoc}$, are weak, intermediate, or strong. Thus, high enantioselectivities are often observed at quite low retention-increments R' (due to weak molecular association) while only low enantioselectivities may arise despite high retention-increments R' (due to strong molecular association). Consequently, the value of a virtual enantiorecognition factor $\chi = -\Delta_{D,L}\Delta G/-\Delta G$ is unpredictable and varies at random [109]. The enantioselectivity is usually pronounced when the selectand/selector interaction is impaired by steric congestion.

The Gibbs–Helmholtz parameters $-\Delta_{D,L}\Delta H$ and $\Delta_{D,L}\Delta S$ of the thermodynamic enantioselectivity are readily accessible by linear van't Hoff plots when measurements are performed at different temperatures T according to

$$R \ln\left(\frac{R_D'}{R_L'}\right) = \frac{-\Delta_{D,L}\Delta G}{T} = \frac{-\Delta_{D,L}\Delta H}{T} + \Delta_{D,L}\Delta S. \tag{13}$$

According to the Gibbs–Helmholtz equation (11), the true enantioselectivity $-\Delta_{D,L}\Delta G$ is governed by an enthalpy term $-\Delta_{D,L}\Delta H$ and an entropy term $\Delta_{D,L}\Delta S$, where the latter term is linked with the temperature T. For a 1:1 association equilibrium both quantities oppose each other in determining $-\Delta_{D,L}\Delta G$. Thus *enthalpy/entropy compensation* arises due to the fact that the more tightly bonded

complex ($-\Delta H_D > -\Delta H_L$) is more ordered ($\Delta S_D < \Delta S_L$). Since the entropy term increases with temperature T, an *isoenantioselective temperature* will be reached at the compensation temperature $T_{iso} = \Delta_{D,L}\Delta H/\Delta_{D,L}\Delta S$ at which $\Delta_{D,L}\Delta G$ is rendered zero (i.e., absence of enantioselectivity), since $K_D^{assoc} = K_L^{assoc}$. Peak coalescence (no enantioseparation) takes place at T_{iso} [110]. Above T_{iso} enantioseparation commences with inversed elution order. Below T_{iso} enantioseparation is governed by the predominant enthalpic contribution to enantiorecognition, whereas above T_{iso} it is governed by the predominant entropic contribution ($\Delta S_D < \Delta S_L$) to enantiorecognition with the stronger bonded enantiomer D ($-\Delta H_D > -\Delta H_L$) bizzarrely eluted as the first peak. Whereas the sign of the enantioselectivity changes at T_{iso}, the association constants K_D^{assoc} and K_L^{assoc} between the selectand enantiomers D and L and selector A steadily decrease with increasing temperature T. The existence of an isoenantioselective temperature T_{iso} in enantioselective GC has been observed independently in hydrogen-bonding equilibria [111, 112] and in metal complexation equilibria [113, 114] whereby the intriguing peak reversal for the enantiomers below and above T_{iso} was clearly evident in the gas-chromatograms. A report of a peak reversal for the enantiomers of methyl lactate on a modified cyclodextrin selector (Lipodex E) [115] could not be ascertained [112] while a temperature-induced reversal of the elution order has been observed for the enantiomers of *N*-trifluoroacetyl-α-amino acid ethyl esters on the selector Chirasil-Dex [112]. Thus the derivatives of valine and leucine showed a peak reversal on Chirasil-Dex below and above $T_{iso} = 70°$ and only a single peak was observed at the coalescence temperature. For the isoleucine derivative the isoenantioselective temperature was as low as $T_{iso} = 30°$ [112]. A different enthalpy/entropy compensation approach based on the plot of ln R' vs ΔH for the second eluted enantiomer has also been described [105].

Enthalpy/entropy compensation must be considered for molecular modeling studies whereby the importance of entropy changes should be taken into account. Most gas-chromatographic enantioseparations on modified cyclodextrins are governed by the enthalpy term of the Gibbs–Helmholtz equation. Consequently, enantioselectivity increases by reducing the elution temperature. This will be illustrated in the GC enantioseparation of halocarbons on CDs in the following sections. As nonvolatile racemates usually require a high elution temperature, it is advisable to use short columns (1–10 m × 0.25 mm i.d.). The loss of efficiency arising from the smaller theoretical plate number N of a short column is often overcompensated by the gain of enantioselectivity below T_{iso}, due to an increased enantioseparation factor α^{true} at the lower elution temperature.

9 Determination of Thermodynamic Parameters of the Enantioselectivity of Enflurane, Isoflurane, and Desflurane on Diluted Lipodex E

The pronounced enantioselectivity between the haloethers enflurane, isoflurane, and desflurane on Lipodex E diluted in SE 54 allows quantitative enantioseparations within 2.5 min (Fig. 5) [31]. The apparent enantioseparation factor α^{app} strongly increases in the order: isoflurane < desflurane < enflurane and the observed $\alpha^{app} > 2.0$ for enflurane can still be increased to $\alpha^{app} = 2.7$ at 0°C. In order to get thermodynamic data on the true enantioselectivity by the retention-increment R' approach (Sect. 8), three columns were used. The reference column (50 m × 0.25 mm i.d.) was coated statically with pure polysiloxane (polydimethylsiloxane SE 54 containing 5% phenyl, and 1% vinyl, CP polarity index 8) while the enantioselective columns (25 m × 0.25 mm i.d.) were coated statically with ~5% and ~10 wt% Lipodex E in polysiloxane SE 54. The stationary phase film thicknesses were 0.5 μm. The haloethers, methane (as holdup time marker) and the reference standards (*n*-pentane, *n*-hexane, *n*-heptane, or diethylether) were mixed in headspace vials and were split-injected (1:100). Highly precise data for the true enantioselectivity $-\Delta_{DL}\Delta G^{true}$ were obtained [104] irrespective of the choice of the reference standards (C5–C7, diethylether) and the concentration of the selector in the polysiloxane (5% vs 10%), thus underlining the validity of (11) and the need to separate rigorously achiral from chiral contributions to retention in (10) via the concept of the retention-increment R'. The true enantioselectivity $-\Delta_{DL}\Delta G^{true}{}_{303}$ at 30°C is 2.0 (0.02) kJ/mol for enflurane, 0.9 (0.03) kJ/mol for isoflurane and 1.55 (0.03) kJ/mol for desflurane obtained on the column with 10% selector concentration and as mean value for all reference standards used. Temperature-dependent data for the true enantioselectivity $-\Delta_{DL}\Delta G^{true}$ obtained at five temperatures between 0 and 60°C and measured at both concentrations of the selector (5 wt% and 10 wt%) and four reference standards furnished the following mean thermodynamic parameters via the strictly linear van't Hoff plots according to (13) [104]:

$$\text{enflurane}:$$
$$-\Delta_{DL}\Delta H^{true} = 7.2(0.2)\ \text{kJ/mol}$$
$$\Delta_{DL}\Delta S^{true} = -17.2(0.6)\ \text{J/mol K}$$
$$T_{iso} = 420(40)\text{K},$$

$$\text{isoflurane}:$$
$$-\Delta_{DL}\Delta H^{true} = 4.1(0.2)\ \text{kJ/mol}$$
$$\Delta_{DL}\Delta S^{true} = -10.6(0.5)\ \text{J/mol K}$$
$$T_{iso} = 390(60)\text{K},$$

$$\text{desflurane}:$$
$$-\Delta_{DL}\Delta H^{true} = 9.4(0.6)\ \text{kJ/mol}$$
$$\Delta_{DL}\Delta S^{true} = -25.7(2.1)\text{J/mol K}$$
$$T_{iso} = 365(40)\ \text{K}.$$

The highest enantioselectivity $-\Delta_{DL}\Delta G$ was found for enflurane whereas the largest quantities for $-\Delta_{DL}\Delta H$ and $\Delta_{DL}\Delta S$ were observed for desflurane. When comparing isoflurane and desflurane, substitution of chlorine by fluorine leads to more than a doubling of the thermodynamic quantities. The large enthalpy term for desflurane implies that temperatures as low as possible should be employed for enantioseparation and that $-\Delta_{DL}\Delta G$ of desflurane will exceed that of enflurane below −15°C [104]. The ratio between $-\Delta_{DL}\Delta H$ and $\Delta_{DL}\Delta S$ is not constant, furnishing different values of T_{iso} for enflurane, isoflurane, and desflurane. The high volatility of the haloethers precluded the experimental verification of the existence of T_{iso} above 100°C.

For $2 \times 3 \times 4 \times 6 = 144$ measurements, involving the two enantiomers of three haloethers related to four references standards at six temperatures, all ratios of the retention-increments R' for the two columns 1 and 2, containing different concentrations of the selector A (~5% vs ~10%), were identical, i.e., ${R'_L}^{(2)}/{R'_L}^{(1)} = {R'_D}^{(2)}/{R'_D}^{(1)} = {a_A}^{(2)}/{a_A}^{(1)} = 1.64 \pm 0.04$. According to (9) the constant factor directly reflected the true activity ratio ${a_A}^{(2)}/{a_A}^{(1)}$ of the two columns 1 and 2, their absolute values being unknown. By the known activity ratio and the measured sets of relative retentions $r^{(1)}$ and $r^{(2)}$, the r° values of all three haloethers expected for the reference column were graphically extrapolated (or calculated via (14), Sect. 11) and a reasonably good agreement (0.5–18% standard deviation) indicated that r° values can even be assessed without resorting to a reference column [104]. The results also confirmed the validity of the retention-increment R' approach to distinguish enantioselective and non-enantioselective contributions to retention in chiral GC (Fig. 23) [104].

The enantioselectivity $-\Delta_{DL}\Delta G^{true}$ for enflurane and Lipodex E has been corroborated by ^{1}H-NMR spectroscopy employing the modified cyclodextrin selector as CSA in d_{12}-cyclohexane for enantiomeric differentiation [31, 116]. It was observed that the proton resonance absorptions of (*S*)-enflurane were shifted more downfield than those of (*R*)-enflurane in the presence of Lipodex E. Likewise (*S*)-enflurane is eluted well after (*R*)-enflurane on Lipodex E in the GC experiment. A ratio of the association constants $K_S^{assoc}/K_R^{assoc} = 2.25$ was found as mean value for the α- and β-proton of enflurane in d_{12}-cyclohexane in the presence of Lipodex E yielding $-\Delta_{SR}\Delta G_{298} = 2.00$ kJ/mol [116]. This value compares well with the GC data of $-\Delta_{SR}\Delta G_{298} = 2.08$ kJ/mol in SE-54 at 25°C [104] whereby the absolute association constants K^{assoc} of the GC and NMR experiments differed by a factor of 5 due to different experimental conditions of the two methods. Notwithstanding, the result confirms the synergism between enantioselective NMR spectroscopy and enantioselective GC.

For an undiluted selector, thermodynamic parameters can be directly obtained from the equation RT ln $\alpha = -\Delta_{D,L}\Delta G$ (Sect. 8). Temperature-dependent measurements in the range 35–50°C gave the following averaged enantioselectivity data for the haloethers enantioseparated by GC on octakis(2,6-di-*O*-pentyl-3-*O*-trifluoroacetyl)-γ-cyclodextrin [26]:

$$\text{enflurane}: -\Delta_{DL}\Delta H = 4.51\ \text{kJ/mol},\ \Delta_{DL}\Delta S = -10.9\ \text{J/mol K}$$
$$\text{isoflurane}: -\Delta_{DL}\Delta H = 6.09\ \text{kJ/mol},\ \Delta_{DL}\Delta S = -15.7\ \text{J/mol K}$$
$$\text{desflurane}: -\Delta_{DL}\Delta H = 3.79\ \text{kJ/mol},\ \Delta_{DL}\Delta S = -9.4\ \text{J/mol K}.$$

The isoenantioselective temperatures T_{iso} were estimated at around 400 K (~125°C) but could not be verified experimentally. All thermodynamic data represent only average values owing to a range of interactions between the anesthetics and the cyclodextrin selectors as the CSP octakis(2,6-di-*O*-pentyl-3-*O*-trifluoroacetyl)-γ-cyclodextrin employed was comprised of a mixture of isomers and homologues [26].

10 ^{1}H-NMR NOE Difference Spectroscopy of Enflurane and Lipodex E

Intermolecular ^{1}H-NMR-nuclear Overhauser effect (NOE) investigations were performed to obtain insights into the molecular complexes formed by the stronger interacting (*R*)-enantiomer of enflurane and octakis(3-*O*-butanoyl-2,6-di-*O*-pentyl)-γ-cyclodextrin (Lipodex E) [116]. A negative NOE intensity change for the H-α- and H-β-proton signals of (*R*)-enflurane was detected upon irradiation of the inner protons H-3 and H-5 of Lipodex E while no NOE intensity changes were observed upon irradiation of the corresponding outer protons H-1, H-2, H-4, H-6A, H-6B, or either of the diastereotopic butanoyl protons of Lipodex E (Fig. 24). Analogous results were obtained for (*S*)-enflurane and Lipodex E. Thus it was concluded that both enflurane enantiomers are clearly located inside the cyclodextrin cavity. Internal and external contributions to enantiomeric differentiation involving cyclodextrins have been discussed previously [5] and the total absence of molecular inclusion is manifested by the efficient enantioseparation capability of modified linear dextrins ("acyclodextrins") [117]. The established inclusion properties of Lipodex E for haloethers have been ascribed to internal dipole–dipole interactions and hydrogen-bonding involving acidic H-α- and H-β-protons of enflurane [116]. Precise molecular modeling studies have been elusive thus far.

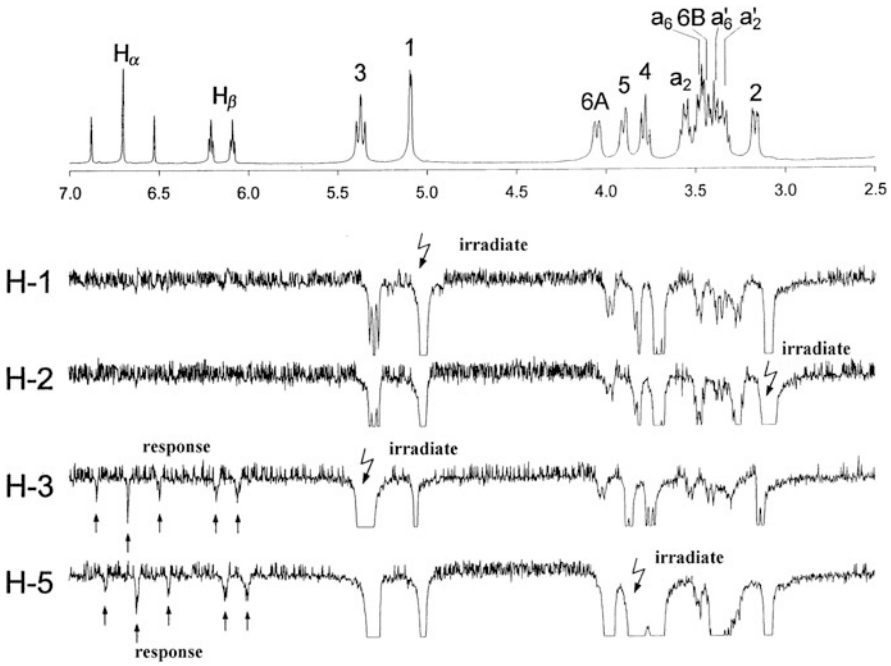

Fig. 24 400 MHz ^{1}H-NMR NOE difference spectra of 0.078 M (*R*)-enflurane in the presence of 0.013 M of the CSA Lipodex E in d_{12}-cyclohexane [116]. *Top*: Spectrum of enflurane at 6–7 ppm and spectrum of Lipodex E at 3.0–5.5 ppm. *Bottom*: Irradiation of external cyclodextrin H-1 and H-2 (no response) and of internal cyclodextrin protons H-3 and H-5 (with response)

11 An Extraordinary Enantiomeric Differentiation Between "Compound B" and Lipodex E

Enantiomeric differentiations by GC employing modified cyclodextrins are usually characterized by low enantioselectivities [2, 16]. Yet, due to the high resolving power of capillary GC, very low enantioseparation factors of $1.01 < \alpha < 1.10$ are sufficient for quantitative analytical enantioseparations in a short time. However, for an understanding of chromatographic enantioselectivity [118, 119], small values of α are detrimental to reliable mechanistic studies of enantiorecognition [105, 120], e.g., by molecular modeling calculations involving cyclodextrins [119, 121–123]. Low enantioselectivities are also totally inappropriate for predictions of the elution order of enantiomers on modified cyclodextrins (Sect. 5). The correlation of the elution order and configuration of the separated enantiomers may further be obscured by the possibility of peak reversals due to enthalpy-entropy compensation (Sect. 8), thus requiring extended temperature-dependent studies. High values of $\alpha > 1.5$ are only rarely encountered for selectand enantiomers in enantioselective GC employing modified cyclodextrin selectors. Yet unexpected large enantioseparation factors α has been observed with enflurane,

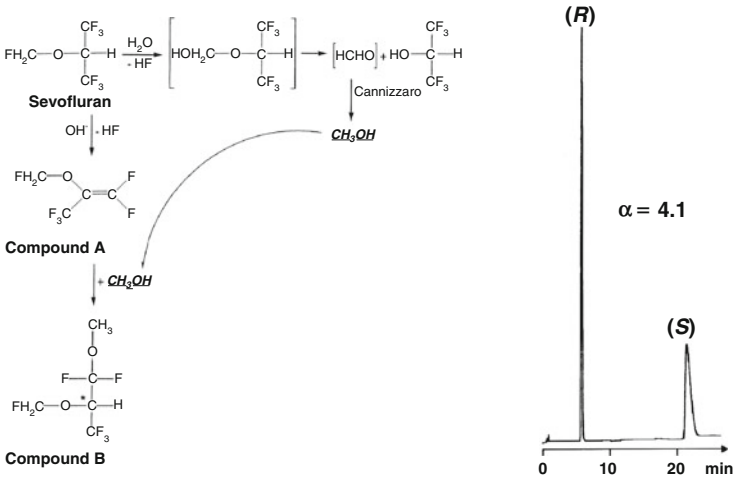

Fig. 25 *Left*: Decomposition products of sevoflurane in an alkaline environment [129]. *Right*: Analytical gas-chromatographic enantioseparation of "compound B." 10 m × 0.25 mm (i.d.) fused silica capillary column coated with 0.25 μm heptakis(2,3-di-*O*-acetyl-6-*O*-*tert*-butyldimethylsilyl)-β-cyclodextrin in PS 86 (~15% diphenyl, ~85% dimethyl-PS, 20 wt%) at 30°C and 1.25 bar dihydrogen [129]

isoflurane, and desflurane (Sect. 2). This observation is in line with a general trend of favourable enantioselectivities occurring with halogenated chiral compounds and modified cyclodextrins. Even the smallest five-atomic halocarbons bromochlorofluoromethane and chlorofluoroiodomethane can be resolved by enantioselective inclusion GC (Sect. 12).

Methyl 2-chloropropanoate has been enantioseparated on undiluted heptakis (3-*O*-acetyl-2,6-di-*O*-pentyl)-β-cyclodextrin (Lipodex D) [124] with $\alpha = 2.02$ corresponding to $-\Delta_{S,R}\Delta G = 2.1$ kJ/mol at 60°C, whereby the (*S*)-enantiomer is eluted after the (*R*)-enantiomer, and NMR studies and molecular dynamics calculations were carried out for this efficient enantioselective system [125, 126]. Methyl 2-chloropropanoate was also enantioseparated on octakis(3-*O*-butanoyl-2,6-di-*O*-pentyl)-γ-cyclodextrin (Lipodex E) with $\alpha = 2.27$ corresponding to $-\Delta_{S,R}\Delta G = 2.34$ kJ/mol, $-\Delta_{S,R}\Delta H = 13.8$ kJ/mol, and $-\Delta_{S,R}\Delta S = 33.5$ J/mol K at 70°C [127]. The enantioseparation of methyl 2-chloropropanoate on undiluted heptakis(2,6-di-*O*-pentyl-3-*O*-trifluoroacetyl)-β-cyclodextrin at 50°C gave the following thermodynamic data: $-\Delta_{S,R}\Delta G = 3.01$ kJ/mol, $-\Delta_{S,R}\Delta H = 13.4$ kJ/mol, $-\Delta_{S,R}\Delta S = 31.4$ J/mol K, and $T_{iso} = 150$°C [128]. All thermodynamic data refer to true values since the selectors were used in the undiluted form (Sect. 8).

The enantioseparation of "compound B" (2-(fluoromethoxy)-3-methoxy-1,1,1,3,3-pentafluoropropane) (Fig. 25, left) on modified CDs exhibited the highest enantioseparation factor α ever observed in enantioselective GC [129]. This unexpected result implies that one enantiomer undergoes a strong molecular association, whereas the other enantiomer does not. The very high GC enantioseparation factors α for "compound B" on modified CDs have been found by mere chance as the target

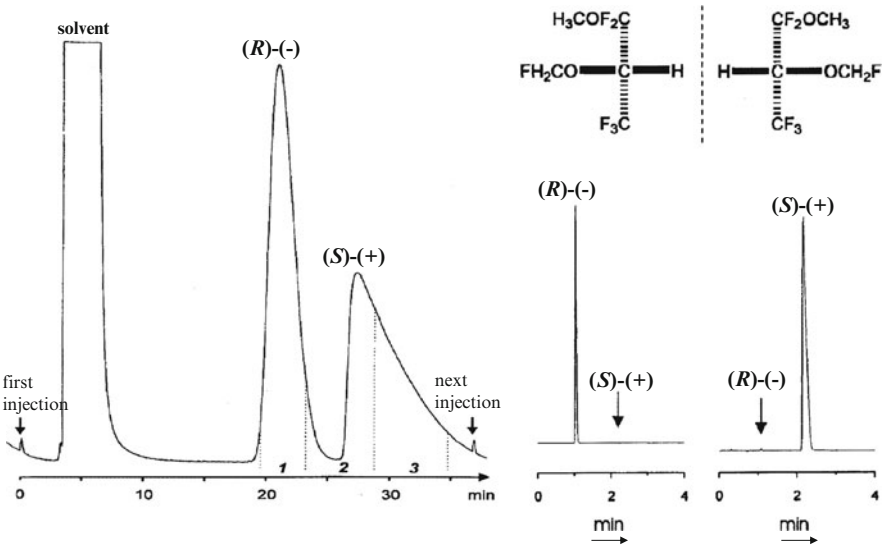

Fig. 26 *Left*: Preparative gas-chromatographic enantioseparation of "compound B" dissolved in diethylether. 1 m × 18 mm (i.d.) stainless steel column packed with Chromosorb P-AW-DMCS (80–100 mesh) coated with 19.1 wt% of heptakis(2,3-di-*O*-acetyl-6-*O*-*tert*-butyldimethylsilyl)-β-cyclodextrin in PS 86 (15.2 wt%) at 70°C and 1.4 bar dinitrogen. The *dotted lines* indicate the three fractions collected [129]. *Right*: Gas-chromatographic determination of the high enantiomeric excess (ee) of the isolated single enantiomers (conditions as in Fig. 25, *right*) [129]

compound represents just a minor chiral decomposition product of the achiral new generation anesthetic sevoflurane (1,1,1,3,3,3-hexafluoro-2-(fluoromethoxy)propane) (Fig. 25, left) [130]. Since volatile anesthetics are recycled during anesthesia in re-breathing units, the exhaled carbon dioxide is trapped with soda lime. In the alkaline environment, methanol is formed by a Cannizzaro reaction from formaldehyde which is the result of hydrolysis of sevoflurane. Methanol is then added to the double bond of "compound A" which is generated by hydroformic acid abstraction from sevoflurane by soda lime (Fig. 25, left). The perfluorodiether "compound B" represents a chiral molecule. It has been analytically enantioseparated on heptakis(2,3-di-*O*-acetyl-6-*O*-*tert*-butyldimethylsilyl)-β-cyclodextrin [131] diluted in polysiloxane PS 86 (~15% diphenyl, ~85% dimethyl-PS, 20 wt%), exhibiting the large enantioseparation factor $\alpha = 4.1$ at 30°C (Fig. 25, right) [129]. The high enantioselectivity allowed the isolation of the enantiomers of "compound B" by preparative GC (Sect. 3) and the subsequent determination of their specific rotation by polarimetry and their absolute configurations both by anomalous X-ray diffraction [129] and by VCD [132]. Thus in ten repetitive runs under the conditions detailed in Fig. 26 (left), a total of 275 mg of the first eluted enantiomer were collected as first fraction with ee $> 99.9\%$ and 73 mg of the second eluted enantiomer as third fraction with ee $> 99.7\%$, whereby the middle fraction was not discarded but re-injected [129]. The high enantiomeric excess (ee) of both enantiomers has been determined analytically (Fig. 26, right). By X-ray evidence, the levorotatory enantiomer had the (–)-(*R*)-configuration while the dextrorotatory

enantiomer had the (+)-(*S*)-configuration. The elution order of the enantiomers of "compound B" on heptakis(2,3-di-*O*-acetyl-6-*O*-*tert*-butyldimethylsilyl)-β-cyclodextrin is (*S*) after (*R*) [129]. In order to gain information on the origin of enantiomeric differentiation, ^{1}H- and ^{19}F-NMR-spectroscopic studies have been performed whereby heptakis(2,3-di-*O*-acetyl-6-*O*-*tert*-butyldimethylsilyl)-β-cyclodextrin has been employed as a CSA for inducing chemical shift anisochrony of the externally enantiotopic nuclei of racemic "compound B" in d_{12}-cyclohexane as solvent [133]. Experiments with single enantiomers of "compound B" obtained by preparative GC revealed larger chemical shifts of the protons of the (*S*)-enantiomer as compared to the (*R*)-enantiomer by ^{1}H-NMR in the presence of the cyclodextrin selector in agreement with the GC experiment where (*S*) is eluted later than (*R*) [129]. A ratio of the association constants $K_S^{\text{assoc}}/K_R^{\text{assoc}} = 1.5$ was found as mean value for the α- and β-proton of enflurane in d_{12}-cyclohexane in the presence of the cyclodextrin selector yielding $-\Delta_{SR}\Delta G_{298} = 1.00$ kJ/mol. This value is lower than expected from the GC experiment exhibiting $\alpha = 4.1$ at 30°C corresponding to $-\Delta_{SR}\Delta G_{303} = 3.5$ kJ/mol [129]. Also by ^{19}F-NMR spectroscopy a large anisochrony was observed whereby the fluorine resonances of the (*S*)-enantiomer were shifted more downfield than those of the (*R*)-enantiomer [133]. In order to elucidate the association mechanisms of the complexes formed in solution, intermolecular rotating-frame Overhauser effect spectroscopy (1D- and 2D-ROESY) was performed with equimolar solutions of racemic "compound B" and heptakis(2,3-di-*O*-acetyl-6-*O*-*tert*-butyldimethylsilyl)-β-cyclodextrin in d_{12}-cyclohexane [133]. The results implied that the CH_3O-group of "compound B" is included at the wider opening of the cyclodextrin cavity whereas the CH_2F- and CF_3-groups interact with the external acetyl and silyl groups of the cyclodextrin used as CSA [133]. Thus the important role of the functional groups on the cyclodextrin rim and the occurrence of partial molecular inclusion in the enantiomeric differentiation mechanism were established.

The largest enantioseparation factor of $\alpha = 10.6$ at 26°C ever observed in enantioselective GC has been detected for "compound B" on octakis(3-*O*-butanoyl-2,6-di-*O*-pentyl)-γ-cyclodextrin (Lipodex E) [28] diluted in polysiloxane PS 255 (Fig. 27, left) [134].

The described finding was the result of mere serendipity rather than rational design as the structural requirements for efficient enantiomeric differentiation involving haloethers and modified cyclodextrins are currently unknown. This is also borne out by the unexpected observation that the enantioseparation factor drops to $\alpha = 2.1$ on heptakis(3-*O*-butanoyl-2,6-di-*O*-pentyl)-β-cyclodextrin and to $\alpha = 1.0$ (no enantioselectivity at all!) on hexakis(3-*O*-butanoyl-2,6-di-*O*-pentyl)-α-cyclodextrin [134]. This unusual dependence of enantioselectivity on the cavity size of CDs in enantioselective inclusion GC warrants an explanation and it may also be of interest to test the δ-CD congener of Lipodex E for the enantiomeric differentiation of "compound B" by GC and NMR in the future. One tentative explanation for the exclusive versatility of Lipodex E based on γ-cyclodextrin for the enantioseparation of many racemates in general [28], and of "compound B" in particular [134], may be associated with self-inclusion of *n*-pentyl groups into the cavity of the

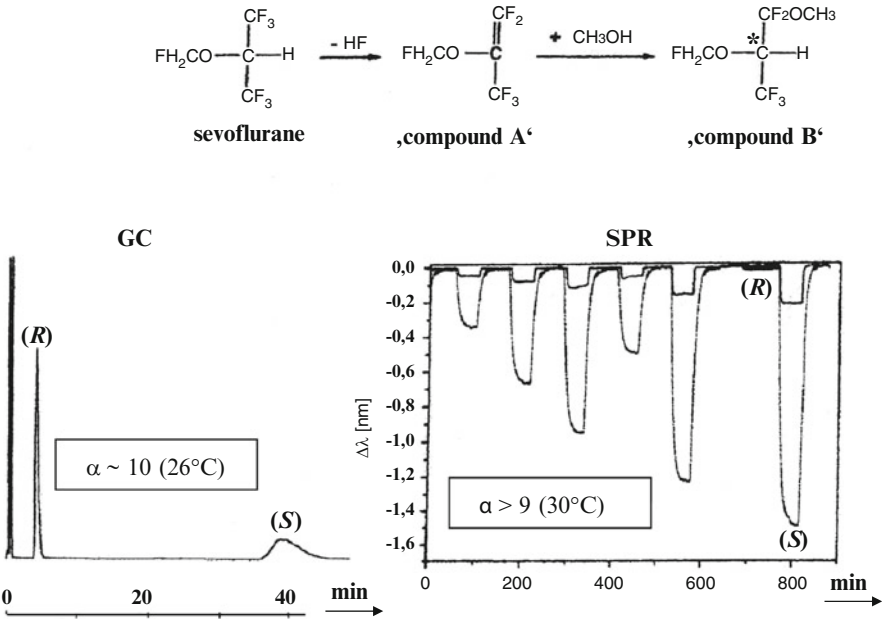

Fig. 27 *Left*: Analytical gas-chromatographic enantioseparation of "compound B." 5 m × 0.25 mm (i.d.) fused silica capillary column coated with 0.28 μm octakis(3-*O*-butanoyl-2,6-di-*O*-*n*-pentyl)-γ-cyclodextrin (Lipodex E) in PS 225 (30 wt%), 26°C, 1.12 bar dihydrogen [134]. *Right*: Stepwise enantioselective surface plasmon resonance (SPR) signals with Lipodex E as sensor coating on exposure to single enantiomers of "compound B" in a concentration range between 0 and 140 μg/L at 30°C [141]

selector followed by competitive displacement by the selectand. A clue to this proposal, i.e., self-inclusion of one 6-*O*-pentyl group into Lipodex E, has been obtained by NMR measurements and molecular dynamics (MD) calculations [135]. The molecular associations of single enantiomers of "compound B" obtained by preparative GC and octakis(3-*O*-butanoyl-2,6-di-*O*-pentyl)-γ-cyclodextrin (Lipodex E) and heptakis(3-*O*-butanoyl-2,6-di-*O*-pentyl)-β-cyclodextrin were also studied by ^{19}F-NMR spectroscopy in apolar d_{12}-cyclohexane [136]. Association constants of the interaction of the two enantiomers of "compound B" with Lipodex E and its β-cyclodextrin analogue were determined by NMR chemical shift titration and showed large differences in agreement with the GC results. Heteronuclear NOE measurements proved that inclusion complex formation takes place with "compound B" located inside the cavity of the cyclodextrin moiety. The study could not rationalize the striking difference in enantioselectivity between the β-CD and its γ-CD congener observed by enantioselective GC.

A comprehensive thermodynamic study has been performed for the enantiomeric differentiation of "compound B" by Lipodex E diluted in polysiloxane PS 255 (30 wt%) which exhibited the unexpectedly high enantioseparation factor α of 10.6 at 26°C [134]. Since the selector was diluted in the polysiloxane solvent S, the retention-increment R' method (Sect. 8) has been employed. The use of (9) in

comparing the retention factors k of the enantiomers on the reference column and the enantioselective column would require identical column dimensions and coating parameters. In order to overcome this obstacle, relative retentions $r = t'_R/t'_{Rref}$ were used according to (10) in which the adjusted retention time t'_R (= total retention time t_R minus unretained-peak holdup time t_M) of the enantiomers was related to an inert reference standard. For α-amino-acid selectors and metal-complex selectors, *n*-alkanes have been used as reference standards as they undergo neither hydrogen-bonding nor complexation with transition metal ions [112, 114]. However, in the case of cyclodextrin selectors, minor molecular association with *n*-alkanes has been detected [24]. This is also corroborated by the observation that chiral branched alkanes, devoid of any functionality, can be enantioseparated on modified cyclodextrins by GC [137, 138]. A theoretical treatment of the retention-increment R' approach has been put forward for *n*-alkane reference standards which undergo a definite, albeit negligible, interaction with modified cyclodextrins [24]. Indeed, *n*-alkanes could previously not be used as reliable reference standards in a thermodynamic study of derivatized amino acids and modified cyclodextrins [112]. However, due to the very large retention factors k involved for "compound B" and Lipodex E, the use of *n*-alkanes as references standards was straightforward [134]. Three columns were used in the study. The reference column (30 m × 0.25 mm i.d.) was coated statically with pure polysiloxane PS 255 while the enantioselective columns (10 m × 0.25 mm i.d.) were coated statically with 0.5 μm Lipodex E in polysiloxane PS 255 (5 wt% and 10 wt%). "Compound B," methane (as holdup time marker), and the *n*-alkanes (the reference standards *n*-pentane, *n*-hexane, *n*-heptane, and *n*-octane) were split-injected together (1:100). Highly precise data for the true enantioselectivity $-\Delta_{SR}\Delta G^{true}$ (the (*S*)-enantiomer is eluted after the (*R*)-enantiomer) were obtained [134] irrespective of the choice of the reference standards (C5–C8) and the concentration of the selector in the polysiloxane (5 wt% vs 10 wt%), thus underlining the validity of (10) and the need to separate rigorously achiral from chiral contributions to retention via the concept of the retention-increment R' (Fig. 23). The measured value of $-\Delta_{SR}\Delta G^{true}_{303} = 5.7\ (0.05)$ kJ/mol (at 30°C) is very large and beyond the estimated intrinsic error of molecular modeling calculations [139].

The question arose why the (*S*)-enantiomer of "compound B" underwent an unprecedented high molecular interaction with the γ-cyclodextrin selector vis-à-vis the negligible interaction of the (*R*)-enantiomer and why this strong bias is lost for the corresponding α-cyclodextrin selector (see above). GC temperature-dependent data for the true enantioselectivity $-\Delta_{SR}\Delta G^{true}$ obtained at 11 temperatures between 30°C and 80°C and measured at both concentrations of the selector (5 wt% and 10 wt%) furnished the following thermodynamic parameters via the strictly linear van't Hoff plots according to (13) [134]:

$$\begin{aligned} -\Delta_{SR}\Delta H^{true} &= 20.1(0.64)\ \text{kJ/mol} \\ \Delta_{SR}\Delta S^{true} &= -47.4(2.0)\text{J/mol K} \\ T_{iso} &= 424(30)\ \text{K}. \end{aligned}$$

These data represent the highest figures ever found in enantioselective GC. The high value of T_{iso} (~150°C) prevented its experimental verification, i.e., peak coalescence and inversion of the elution order [134]. All thermodynamic data were obtained from the ratio of the retention-increments R'_S/R'_R according to (11) and were independent of the concentration (5 wt% and 10 wt%) of the selector A in the polysiloxane S for both columns. Indeed, with the retention-increment R' approach (Sect. 8) only the enantioselective contribution to retention of the selector A is quantified and $-\Delta_{SR}\Delta G^{true}{}_{303}$ does not refer to the total CSP (i.e., A in S). Therefore only the ratio of the retention-increments R'_S/R'_R and not the ratio of retention factors k_S/k_R is appropriate to quantify the true enantioselectivity for diluted CSPs (Fig. 23).

Enantiomers cannot be distinguished on the reference column containing the achiral solvent matrix S. Therefore $r^\circ{}_i$ is identical for the enantiomers (*S*) and (*R*) of "compound B." $r^\circ{}_i$ need not be determined separately but can be extrapolated from two sets of data of the relative retention, r_i, for the (*S*)- and (*R*)-enantiomers at two (arbitrary) activities a_i of the CD selector A in the solvent S of the columns (1) and (2) as a consequence of the following expression [140]:

$$r^\circ = \frac{\left(r_S{}^{(1)} r_R{}^{(2)} - r_R{}^{(1)} r_S{}^{(2)}\right)}{\left(r_S{}^{(1)} + r_R{}^{(2)}\right) - \left(r_R{}^{(1)} + r_S{}^{(2)}\right)} \quad . \tag{14}$$

This expression, which directly follows the theorem of intersecting lines of Thales (Fig. 23), can be used to assess the non-enantioselective contributions to retention when r° is not readily accessible due to the unavailability of the solvent S to prepare a reference column (e.g., for Chirasil-type CSPs). It is enough to collect retention data from two columns of different activities (or concentrations in dilute systems) of the selector A in S. Thus values for r° of "compound E" on Lipodex E were calculated using two columns coated with Lipodex E in polysiloxane PS 255 (5 wt% and 10 wt%) with four reference *n*-alkanes standards (C5–C8) at 11 temperatures and a satisfactory agreement between measured and extrapolated values of r° were obtained [134]. This finding reinforced the validity of the retention-increment R' approach which relies on some experimental conditions, i.e., use of traces of the selectand (10^{-8} g) to guarantee a true 1:1 association equilibrium and the presence of a dilute solution of the selector A in the solvent S (typically 0.05–0.1 molal). The method has also been adopted in enantioselective LC in order to separate achiral and chiral contributions to retention [108].

The highly enantioselective supramolecular selectand-selectant system "compound B" and Lipodex E has been selected as a versatile model system to study the enantiomeric differentiation of enantioselective sensor devices based on quartz thickness shear mode resonators (TSMR), surface acoustic wave sensors, surface plasmon resonance (SPR) (Fig. 27, right), and reflectometric interference spectroscopy [141]. For all enantioselective sensor devices the (*S*)-enantiomer of "compound B" showed the stronger interaction with Lipodex E as was found in enantioselective GC. Based on the distinction between enantioselective and non-enantioselective

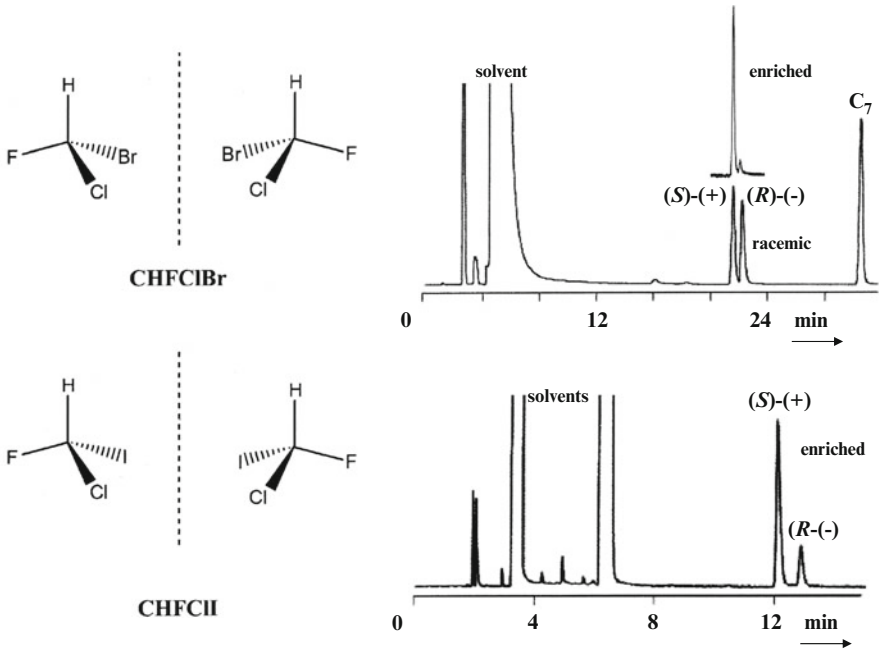

Fig. 28 *Left*: Enantiomers of C*HFClBr and C*HFClI. *Right*, *top*: Analytical gas-chromatographic enantioseparation of racemic and enantiomerically enriched C*HFClBr. 40 m × 0.25 mm (i.d.) fused silica capillary column coated with 0.25 μm immobilized Chirasil-γ-Dex at −20°C and 100 kPa dihydrogen [147]. *Right*, *bottom*: Analytical gas-chromatographic enantioseparation of enantiomerically enriched C*HFClI. 40 m × 0.25 mm (i.d.) fused silica capillary column coated with 0.25 μm immobilized Chirasil-γ-Dex at 15°C and 100 kPa dihydrogen [145]

interactions (see above), thermodynamic association constants of the single enantiomers of "compound B" with Lipodex E were determined by a quartz TSMR and by surface plasmon resonance at 30°C and the observed enantioselectivity $-\Delta_{SR}\Delta G^{\text{true}}{}_{303} = 5.7$ kJ/mol (TSMR) and $-\Delta_{SR}\Delta G^{\text{true}}_{303} = 5.9$ kJ/mol (SPR) [141] agreed well with that determined by enantioselective GC, i.e., $-\Delta_{SR}\Delta G^{\text{true}}_{303} = 5.7$ kJ/mol [134].

12 Analytical Gas-Chromatographic Enantioseparation of Bromochlorofluoromethane and of Chlorofluoroiodomethane

Enflurane possesses a stereogenic center at a carbon atom which is substituted by three different atoms (Fig. 2). When the organic ether residue in enflurane is replaced by either bromine or iodine, the smallest penta-atomic (non-isotopically labelled) chiral molecules, i.e., the enantiomers of bromochlorofluoromethane, C*HFClBr, and chlorofluoroiodomethane, C*HClFI, are obtained (Fig. 28, left)

(incidentally, the smallest hypothetical isotopically labelled chiral molecule is $C^{*1}H^2H^3HX$ (X = halogen) which is not considered here).

Theoretically, true enantiomers are based on the non-superposability of matter and antimatter. Earthbound chiral D and L molecules, e.g., proteinogenic 2-amino acids, which both possess negative charged electrons, are actually diastereomers (quasi-enantiomers) and not true enantiomers as the charge is not mirrored. The resulting parity violation energy difference (PVED) of the weak force between enantiomers is often linked with the evolution of homochirality on primordial Earth [142–144]. The penta-atomic chiral halomethanes C*HFClBr and C*HClFI containing heavy atoms represent ideal target molecules for spectroscopic PVED measurements [143]. However, the search for subtle differences in the ultrahigh infrared spectra of the right- and left-handed tri(hetero)halogenomethanes requires the availability of large amounts of single enantiomers. Preparative access to the enantiomers of C*HFClBr and C*HClFI relies on the decarboxylation (with retention of configuration [70, 71], Fig. 14, right) of the corresponding pre-resolved tri(hetero)halogenoacetic acids [143, 145]. However, only incomplete enantiomeric excesses ee have been obtained thus far. Also the direct preparative GC enantioseparation is as yet elusive. However, following a preliminary report on the GC enantioseparation of C*HFClBr by König [16], the quantitative analytical enantioseparation of C*HFClBr and C*HFClI has systematically been explored on Chirasil-γ-Dex (octakis(3-*O*-butanoyl-2,6-di-*O*-*n*-pentyl)-γ-cyclodextrin linked to poly(dimethylsiloxane)) [51, 145–147]. The Chirasil-γ-Dex CSP [32] exhibits the advantages inherent to polysiloxanes in GC, i.e., high resolution, inertness, and susceptibility to high and low GC operating temperatures. The CSP can even be used under cryoscopic conditions without loss of column efficiency down to −20°C which was required for the quantitative enantioseparation of C*HFClBr (Fig. 28, top right) whereas C*HFClI could be enantioseparated at 15°C (Fig. 28, bottom right). The analytical tool allowed the determination of the enantiomer excess ee of the tri(hetero)halogenomethanes obtained by decarboxylation of enantiomerically enriched tri(hetero)halogenoacetic acids (Fig. 28, bottom right) [145]. The (+)-(*S*)- and (–)-(*R*) configurations of C*HFClI and C*HFClBr were assigned by quantum mechanical calculations [145, 148].

The following thermodynamic data of enantioselectivity (Sect. 8) were obtained for the tri(hetero)halogenomethanes and Chirasil-γ-Dex [147] (D and L denote enantiomers irrespective of the true absolute configurations):

$$C * HFClBr:$$
$$\Delta_{D,L}\Delta H = -0.46\ \text{kJ/mol}$$
$$\Delta_{D,L}\Delta S = -1.37\ \text{J/mol K}$$
$$T_{iso} = 336\ \text{K},$$

$$C * HFClI:$$
$$\Delta_{D,L}\Delta H = -1.52 \text{ kJ/mol}$$
$$\Delta_{D,L}\Delta S = -4.57 \text{ J/mol K}$$
$$T_{iso} = 333 \text{ K}.$$

Thus the enantioselectivity difference of the haloethers on the CSP as expressed by thermodynamic data is threefold for the iodo compound. However, the linearity of the plot of $\Delta_{D,L}\Delta H$ vs $\Delta_{D,L}\Delta S$ is indicative of a compensation effect [105] and infers an identical inclusion mechanism. Moreover, the low isoenantioselective temperature T_{iso} (~60°C), which is due to a strong entropic contribution to enantiomeric differentiation, implies that very low temperatures are beneficial to increase enantioselectivity [147] and that cryogenic temperatures are required for any attempted preparative enantioseparation of tri(hetero)halogenomethanes on Chirasil-γ-Dex as a prerequisite of PVED measurements. Unfortunately, the reversal of the elution order above T_{iso} [111–114] could not be verified as the retention times were too short at ambient temperatures. The mechanistic rationalization of enantioselectivity between the smallest chiral molecules and a modified γ-cyclodextrin with the largest molecular cavity ($\alpha < \beta < \gamma$) remains a challenge for the future.

References

1. He L, Beesley TE (2005) Applications of enantiomeric gas chromatography: a review. J Liq Chromatogr Rel Techn 28:1075–1114
2. Schurig V (2010) Use of derivatized cyclodextrins as chiral selectors for the separation of enantiomers by gas chromatography. Ann Pharmaceut Française 68:82–98
3. Schurig V (2011) Separation of enantiomers by gas chromatography on chiral stationary phases. In: Ahuja S (ed) Chiral separation methods for pharmaceutical and biotechnological products, Chap. 9. Wiley, Hoboken, pp 251–297
4. Schurig V (2011) Gas-chromatographic enantioseparation of derivatized α-amino acids on chiral stationary phases - past and present. J Chromatogr B 879:3122–3140
5. Beesley T, Majors RE (2011) The state of the art in chiral gas chromatography. LC. GC North America 29:642–651 & LC x GC Europe (May 1, 2012) 232–243
6. Halpern DF (1989) Inhalation anesthetics – the new generation. CHEMTECH 305–308
7. Halpern DF (1993) Recent developments in fluorine substituted volatile anesthetics. In: Filler R et al. (eds) Organofluorine compounds in medicinal chemistry and biomedical applications. Elsevier Science Publishers B.V., pp 101–133
8. Zbinden A, Thomson D (1992) Inhalationsanästhetika: Pharmakokinetik. In: Doenicke A, Kettler D, List WF, Tarnow J, Thomson D (eds) Anästhesiologie. Springer, Berlin, Kapitel 2.4, p 116
9. Halpern DF (1994) Volatile anaesthetics for the 21st century. In: Banks RE, Lowe KC (eds) Fluorine in medicine in the 21st century, Paper 15. Rapra Technology, UMIST Manchester, pp 1–8
10. Halpern DF (1994) Fluorinated inhalation anesthetics. In: Banks RE et al. (eds) Organofluorine chemistry: principles and commercial applications, Chap. 25. Plenum, New York, 1994, pp 543–554

11. Franks NP, Dickinson R, Lieb WR (1994) Effects of isoflurane enantiomers on general anaesthetic target sites. In: Banks RE, Lowe KC (eds) Fluorine in medicine in the 21st century, Rapra Technology, UMIST Manchester, Paper 16, pp 1–7
12. Aboul-Enein HY, Bojarski J, Szymura-Oleksiak J (2000) The impact of chirality of the fluorinated volatile inhalation anaesthetics on their clinical applications. Biomed Chromatogr 14:213–218
13. Schurig V (1984) Gas chromatographic separation of enantiomers on optically active metal-complex-free stationary phases. Angew Chem Int Ed 23:747–765
14. Schurig V (1988) Enantiomer analysis by complexation gas chromatography – scope, merits and limitations. J Chromatogr 441:135–153
15. Schurig V, Nowotny H-P (1990) Gas chromatographic separation of enantiomers on cyclodextrin derivatives. Angew Chem Int Ed 29:939–957
16. König WA (1992) Gas chromatographic enantiomer separation with modified cyclodextrins. Hüthig, Heidelberg
17. Schurig V, Nowotny H-P (1988) Separation of enantiomers on diluted permethylated β-cyclodextrin by high-resolution gas chromatography. J Chromatogr 441:155–163
18. Schurig V, Jung M, Schmalzing D, Schleimer M, Duvekot J, Buyten JC, Peene JA, Mussche P (1990) CGS enantiomer separation on diluted cyclodextrin derivatives coated on fused silica columns. J High Resolut Chromatogr 13:470–474
19. Schurig V, Schmalzing D, Mühleck U, Jung M, Schleimer M, Mussche P, Duvekot C, Buyten JC (1990) Gas chromatographic enantiomer separation on polysiloxane-anchored permethyl-β-cyclodextrin (Chirasil-Dex). J High Resolut Chromatogr 13:713–718
20. Schurig V, Jung M, Mayer S, Negura S, Fluck M, Jakubetz H (1994) Toward unified enantioselective chromatography with a single capillary column coated with Chirasil-Dex. Angew Chem Int Ed 33:2222–2223
21. Armstrong DW, Li W-Y, Stalcup AM, Secor HV, Izac RR, Seeman JI (1990) Capillary gas-chromatographic separation of enantiomers with stable dipentyl α-cyclodextrin derivatized, β-cyclodextrin derivatized and γ-cyclodextrin derivatized stationary phases. Anal Chem Acta 234:365–380
22. Li W-Y, Jin L, Armstrong DW (1990) 2,6-Di-O-pentyl-3-O-trifluoroacetyl cyclodextrin liquid stationary phases for capillary gas chromatographic separation of enantiomers. J Chromatogr 509:303–324
23. Hardt I, König WA (1993) Diluted versus undiluted cyclodextrins derivatives in capillary gas chromatography and the effect of linear carrier gas velocity, column temperature, and length on enantiomer separation. J Microcol Sep 5:35–40
24. Jung M, Schmalzing D, Schurig V (1991) Theoretical approach to the gas chromatographic separation of enantiomers on dissolved cyclodextrin derivatives. J Chromatogr 552:43–57
25. Meinwald J, Thompson WR, Pearson DL, König WA, Runge T, Francke W (1991) Inhalational anesthetics stereochemistry: optical resolution of halothane, enflurane, and isoflurane. Science 251:560–561
26. Shitangkoon A, Staerk DU, Vigh G (1993) Gas-chromatographic separation of the enantiomers of volatile fluoroether anesthetics using derivatized cyclodextrins stationary phases, Part 1. J Chromatogr A 657:387–394
27. Ramig K, Krishnaswami A, Rozov LA (1996) Chiral interactions of the fluoroether anesthetics desflurane, isoflurane, enflurane, and analogues with modified cyclodextrins studied by capillary gas chromatography and nuclear magnetic resonance spectroscopy: a simple method for column-suitability screening. Tetrahedron 52:319–330
28. König WA, Krebber R, Mischnick P (1989) Cyclodextrins as chiral stationary phases in capillary gas chromatography, Part V: Octakis(3-*O*-butyryl-2,6-di-*O*-pentyl)-γ-cyclodextrin. J High Resolut Chromatogr 12:732–738
29. Schurig V, Grosenick H (1994) Preparative enantiomer separation of enflurane and isoflurane by inclusion chromatography. J Chromatogr A 666:617–625

30. Gnaim JM, Schurig V, Grosenick H, Green BS (1995) Partial preparative resolution of the inhalation anesthetic enflurane using clathrate inclusion complexes. Tetrahedron Asymmetry 6:1499–1502
31. Schurig V, Grosenick H, Juza M (1995) Enantiomer separation of chiral inhalation anesthetics (enflurane, isoflurane and desflurane) by gas chromatography on a γ-cyclodextrin derivative. Recl Trav Chim Pays-Bas 114:211–219
32. Grosenick H, Schurig V (1997) Enantioelective capillary gas chromatography and capillary supercritical fluid chromatography on an immobilized γ-cyclodextrin derivative. J Chromatogr A 761:181–193
33. Schurig V (2004) Preparative-scale separation of enantiomers on chiral stationary phases by gas chromatography. In: Toda F (ed) Enantiomer separation: fundamentals and practical methods. Kluwer, Dordrecht, pp 267–300
34. Yamamoto C, Okamoto Y (2004) Practical resolution of enantiomers by high-performance liquid chromatography. In: Toda F (ed) Enantiomer separation: fundamentals and practical methods, Kluwer, Dordrecht, pp 301–322
35. Francotte ER (2001) Enantioselective chromatography as a powerful alternative for the preparation of drug enantiomers. J Chromatogr A 906:379–397
36. Gil-Av E, Feibush B (1967) Resolution of enantiomers by gas liquid chromatography with optically active stationary phases. Separation on packed columns. Tetrahedron Lett 35:3345–3347
37. Golding BT, Sellars PJ, Wong AK (1977) Resolution of racemic epoxides on g.l.c. columns containing optically active lanthanoid complexes. J Chem Soc Chem Commun 570–571
38. Kościelski T, Sybilska D, Jurczak J (1983) Separation of α- and β-pinene into enantiomers in gas-liquid chromatography systems via α-cyclodextrin inclusion complexes. J Chromatogr 280:131–134
39. Schurig V (1987) Semi-preparative enantiomer separation of 1,6-dioxaspiro[4.4]nonanes by complexation gas chromatography. Naturwissenschaften 74:190–191
40. Schurig V, Leyrer U (1990) Semi-preparative enantiomer separation of 1-chloro-2,2-dimethylaziridine by complexation gas chromatography – absolute configuration and barrier of inversion. Tetrahedron Asymmetry 1:865–868
41. Lindström M, Norin T, Roeraade J (1990) Gas chromatographic separation of monoterpene hydrocarbon enantiomers on α-cyclodextrin. J Chromatogr 513:315–320
42. Bicchi C, Balbo C, D'Amato A, Manzin V, Schreier P, Rozenblum A, Brunerie P (1998) Cyclodextrin derivatives in GC separation of racemic mixtures of volatiles – Part XIV: Some applications of thick-film wide-bore columns for enantiomer GC micropreparation. J High Resolut Chromatogr 21:103–106
43. Hardt I, König WA (1994) Preparative enantiomer separation with modified cyclodextrins as chiral stationary phases. J Chromatogr 666:611–615
44. Schürch S, Saxer A, Claude S, Tabacchi R, Trusch B, Hulliger J (2001) Semi-preparative gas chromatographic separation of *all-trans*-perhydrotriphenylene enantiomers on a chiral cyclodextrin stationary phase. J Chromatogr 905:175–182
45. Staerk DU, Shitangkoon A, Vigh G (1994) Gas chromatographic separation of the enantiomers of volatile fluoroether anesthetics by derivatized cyclodextrins. II. Preparative-scale separations for isoflurane. J Chromatogr A 663:79–85
46. Staerk DU, Shitangkoon A, Vigh G (1994) Gas chromatographic separation of the enantiomers of volatile fluoroether anesthetics by derivatized cyclodextrins. III. Preparative-scale separations for enflurane. J Chromatogr A 667:133–140
47. Schurig H, Grosenick BS (1993) Green, Preparative enantiomer separation of the anesthetic enflurane by gas inclusion chromatography. Angew Chem Int Ed 32:1662–1663
48. Juza M, Braun E, Schurig V (1997) Preparative enantiomer separation of the inhalation anesthetics enflurane, isoflurane and desflurane by gas chromatography on a derivatized γ-cyclodextrin stationary phase. J Chromatogr A 769:119–127

49. Schurig V, Grosenick H, Juza M (June 1998) The chiral inhalation anesthetics enflurane, isoflurane and desflurane. Chimica Oggi (Chem Today) 16:40–44
50. Eger EI II, Koblin DD, Laster MJ, Schurig V, Juza M, Ionescu P, Gong D (1997) Minimum alveolar anesthetic concentration values for the enantiomers of isoflurane differ minimally. Anesth Analg 85:188–192
51. Schurig V, Czesla H (2001) Miniaturization of enantioselective gas chromatography. Enantiomer 6:107–128
52. Juza M, Di Giovanni O, Biressi G, Schurig V, Mazzotti M, Morbidelli M (1998) Continuous enantiomer separation of the volatile inhalation anesthetic enflurane with a gas chromatographic simulated moving bed unit. J Chromatogr A 813:333–347
53. Biressi G, Quattrini F, Juza M, Mazzotti M, Schurig V, Morbidelli M (2000) Gas chromatographic simulated moving bed separation of the enantiomers of the inhalation anesthetic enflurane. Chem Engineer Sci 55:4537–4547
54. Biressi G, Rajendran G, Mazzotti M, Morbidelli M (2002) The GC-SMB separation of the enantiomers of isoflurane. Sep Sci Technol 37:2529–2543
55. Biressi G, Mazzotti M, Morbidelli M (2002) Experimental investigation of the behavior of gas phase simulated moving beds. J Chromatogr A 957:211–225
56. Bentley J, Huang Q, Kawajiri Y, Eic M, Seidel-Morgenstern A (2011) Optimizing the separation of gaseous enantiomers by simulated moving bed and pressure swing adsorption. Adsorpt J Int Adsorpt Soc 17:159–170
57. Rajendran A, Paredes G, Mazzotti M (2009) Simulated moving bed chromatography for the separation of enantiomers. J Chromatogr A 1216:709–738
58. Bodenhöfer K, Hierlemann A, Juza M, Schurig V, Göpel W (1997) Chiral discrimination of inhalation anesthetics and methyl propionates by thickness shear mode resonators: new insights into the mechanisms of enantioselectivity by cyclodextrins. Anal Chem 69: 4017–4031
59. Bodenhöfer K, Hierlemann A, Göpel W, Juza M, Gross B, Schurig V (June 1998) Efficient gas sensor mediated enantiomer discrimination of 2-substituted methyl propionates and chiral inhalation anesthetics on a modified cyclodextrin. Chimica Oggi (Chem Today) 16:56–58
60. Hierlemann A, Bodenhöfer K, Juza M, Gross B, Schurig V, Göpel W (1999) Enantioselective monitoring of chiral inhalation anesthetics by simple gas sensors. Sens Mater 11:209–218
61. Schurig V (2005) Contribution to the theory and practice of the chromatographic separation of enantiomers. Chirality 17:S205–S226
62. Roussel C, Del Rio A, Pierrot-Sanders J, Piras P, Vanthuyne N (2004) Chiral liquid chromatography contribution to the determination of the absolute configuration of enantiomers. J Chromatogr A 1037:311–328
63. Schurig V, Juza M, Preschel M, Nicholson GJ, Bayer E (1999) Gas-chromatographic enantiomer separation of proteinogenic amino acid derivatives: comparison of Chirasil-Val and Chirasil-γ-Dex used as chiral stationary phases. Enantiomer 4:297–303
64. Schurig V, Bürkle W (1982) Extending the scope of enantiomer resolution by complexation gas chromatography. J Amer Chem Soc 104:7573–7580
65. Keinan K, Seth KK, Lamed R (1986) Organic synthesis with enzymes. 3. TBADH-catalyzed reduction of chloro ketones. Total synthesis of (+)-(S, S)-(cis-6-methyltetrahydropyran-2-yl) acetic acid: a civet constituent. J Amer Chem Soc 108:3474–3480
66. Schurig V (2002) Review – practice and theory of enantioselective complexation gas chromatography. J Chromatogr A 965:315–356
67. Polavarapu PL (2012) Molecular structure determination using chiroptical spectroscopy: where we may go wrong? Chirality 24:909–920
68. Polavarapu PL, Cholli AL, Vernice G (1992) Absolute configuration of isoflurane. J Am Chem Soc 114:10953–10955
69. Polavarapu PL, Cholli AL, Vernice G (1993) Determination of absolute configurations and predominant conformations of general inhalation anesthetics: desflurane. J Pharmaceut Sci 82:791–793

70. Schurig V, Juza M, Green BS, Horakh J, Simon A (1996) Absolute configuration of the inhalation anesthetics isoflurane and desflurane. Angew Chem Int Ed Engl 35:1680–1682
71. Ramig K, Lavinda O, Szalda DJ (2012) The highly stereoselective decarboxylation of (+)-bromo-1-chloro-2,2,2-trifluoropropanoic acid to give (+)-1-bromo-1-chloro-2,2,2-trifluoroethane [(+)-halothane] with retention of configuration. Tetrahedron Asymmetry 23:201–204
72. Polavarapu PL, Cholli AL, Vernice G (1997) Determination of absolute configurations and predominant conformations of general inhalation anesthetics: desflurane (vol 82, pg 791, 1993). J Pharmaceut Sci 86:267
73. Polavarapu PL, Zhao CX, Cholli AL, Vernice GG (1999) Vibrational circular dichroism, absolute configuration, and predominant conformations of volatile anesthetics: desflurane. J Phys Chem 103:6127–6132
74. Biedermann PU, Cheeseman JR, Frisch MJ, Schurig V, Gutman I, Agranat I (1999) Conformational spaces and absolute configurations of chiral fluorinated inhalation anaesthetics. A theoretical study. J Org Chem 64:3878–3884
75. Ramig K, Brockunier L, Rafalko PW, Rozov LA (1995) Carbon–carbon bond cleavage with inversion of configuration: conversion of (*R*)-(+)-1-methoxytetrafluoropropionic acid to (*S*)-(−)-1,2,2,2-tetrafluoroethyl methyl ether. Angew Chem Int Ed 34:222–223
76. Rozov LA, Rafalko PW, Evans SM, Brockunier L, Ramig K (1995) Asymmetric synthesis of the volatile anesthetic 1,2,2,2-tetrafluoroethyl chlorofluoromethyl ether using a stereospecific decarboxylation of unusual stereochemical outcome. J Org Chem 60:1319–1325
77. Rozov LA, Rafalko PW, Evans SM, Bockunier L, Ramig K (1995) Asymmetric synthesis of the volatile anesthetic 1,2,2,2-tetrafluoroethyl chlorofluoromethyl ether using a stereospecific decarboxylation of unusual stereochemical outcome, correction. J Org Chem 62:6094
78. Young JW, Brandt S (1992) Methods of use and compositions of (R)-isoflurane and (R)-desflurane. US patent 5,114,714, 19 May 1992
79. Young JW, Brandt S (1992) Methods of use and compositions of (S)-isoflurane and (S)-desflurane. US patent 5,114,715, 19 May 1992
80. Schmidt R (1997) R/S-Isofluran. Enantiomeranalytik mittels Headspace-Gaschromatographie in Patientenblutproben. Diploma thesis, University of Tübingen
81. Juza M, Jakubetz H, Hettesheimer H, Schurig V (1999) Quantitative determination of isoflurane enantiomers in blood samples during and after surgery via headspace gas chromatography-mass spectrometry. J Chromatogr B 735:93–102
82. Schmidt R, Wahl HG, Häberle H, Dieterich H-J, Schurig V (1999) Headspace gas chromatography – mass spectrometry analysis of isoflurane enantiomers in blood samples after anesthesia with the racemic mixture. Chirality 11:206–211
83. Haeberle HA, Wahl HG, Jakubetz H, Krause H, Schmidt R, Schurig V, Dieterich H-J (2002) Accumulation of S(+)-enantiomer in human beings after general anaesthesia with isoflurane racemate. Eur J Anaesthes 19:641–646
84. Reiner C, Nicholson GJ, Nagel U, Schurig V (2007) Evaluation of enantioselective gas chromatography for the determination of minute deviations from racemic compositions of α-amino acids with emphasis on tyrosine: accuracy and precision of the method. Chirality 19:401–414
85. Holaday DA, Fiserova-Bergerova V, Latto IP, Zumbiel MA (1975) Resistance of isoflurane to biotransformation in man. Anesthesiology 43:325–332
86. Franks NP, Lieb WR (1991) Stereospecific effects of inhalational general anesthetic optical isomers on nerve ion channels. Science 254:427–430
87. Franks NP, Lieb WR (1994) Molecular and cellular mechanisms of general anaesthesia. Nature 367:607–614
88. Wahl HG, Günkinger T, Aigner GC, Schmidt R, Häberle H, Schurig V, Liebich HM, Luft D, Dieterich HJ (2000) GC-MS analysis of isoflurane enantiomers in human breath, plasma and urine. In: Proceedings of 23rd international symposium on capillary chromatography, 2000. Riva del Garda, Italy

89. Wahl HG, Schmidt R (2000) Analyse von Isofluran-Enantiomeren in Blut. Urin und Atem, GIT Labor-Fachzeitschrift 44:412–416
90. Schmidt R, Hadjidimos M, Wahl HG, Schurig V (2000) Enantiomer separation of desflurane in human blood and urine samples by headspace GC/MS. In: Proceedings of 23rd international symposium on capillary chromatography, 2000. Riva del Garda, Italy
91. Aigner GC (2003) Relationsanalyse von Isofluran-Enantiomeren in der Exspirationsluft während der postoperativen Phase. Ph.D. thesis, University of Tübingen
92. Haeberle HA, Wahl HG, Aigner G, Unertl K, Dieterich H-J (2004) Release of S(+) enantiomers in breath samples after anaesthesia with isoflurane racemate. Eur J Anaesthes 21:144–150
93. Bonner WA (1973) Enantiomeric markers in the quantitative gas chromatographic analysis of optical isomers. Application to the estimation of amino acid degradation. J Chromatogr Sci 11:101–104
94. Blair NE, Bonner WA (1980) Quantitative determination of D $\neq$ L mixtures of optical enantiomers by gas chromatography. J Chromatogr 198:185–187
95. Frank H, Nicholson GJ, Bayer E (1978) Enantiomer labelling, a method for the quantitative analysis of amino acids. J Chromatogr 167:187–196
96. Frank H, Rettenmeier A, Weicker H, Nicholson GJ, Bayer E (1980) A new gas chromatographic method for determination of amino acid levels in human serum. Clinica Chim Acta 105:201–211
97. Bayer E, Frank H, Gerhardt J, Nicholson G (1987) Capillary gas chromatographic analysis of amino acids by enantiomer labelling. J Assoc Off Anal Chem 70:234–240
98. Tsai W-L, Hermann K, Hug E, Rohde B, Dreiding AS (1985) Enantiomer-differentiation induced by an enantiomeric excess during chromatography with achiral phases. Helv Chim Acta 68:2238–2243
99. Trapp O, Schurig V (2010) Nonlinear effects in enantioselective chromatography: prediction of unusual elution profiles of enantiomers in non-racemic mixtures on an achiral stationary phase doped with small amounts of a chiral selector. Tetrahedron Asymmetry 21:1334–1340
100. Rohrschneider L (1973) Solvent characterization by gas-liquid partition coefficients of selected solutes. Anal Chem 45:1241–1247
101. Levkin PA, Schurig V (2008) Apparent and true enantioselectivity of single- and binary-selector chiral stationary phases in gas chromatography. J Chromatogr A 1184:309–322
102. Schurig V (2009) Review: Elaborate treatment of retention in chemoselective chromatography – the retention increment approach and non-linear effects. J Chromatogr A 1216: 1723–1736
103. Schurig V, Weber R (1981) Manganese(II)-bis(3-heptafluorobutyryl-1*R*-camphorate): a versatile agent for the resolution of racemic cyclic ethers by complexation gas chromatography. J Chromatogr 217:51–70
104. Schurig V, Juza M (1997) Approach to the thermodynamics of enantiomer separation by gas chromatography – enantioselectivity between the chiral inhalation anesthetics enflurane, isoflurane and desflurane and a diluted γ-cyclodextrin derivative. J Chromatogr A 757: 119–135
105. McGachy NT, Grinberg N, Variankaval N (2005) Thermodynamic study of *N*-trifluoroacetyl-*O*-alkyl nipecotic acid ester enantiomers on diluted permethylated β-cyclodextrin stationary phase. J Chromatogr A 1064:193–204
106. Allenmark S (1993) Chiral discrimination by albumin: a mechanistic study of liquid chromatographic optical resolution of nonaromatic carboxylic acids. Chirality 5:295–299
107. Götmar G, Fornstedt T, Guiochon G (2000) Apparent and true enantioselectivity in enantioseparations. Chirality 12:558–564
108. Levkin P, Maier NM, Lindner W, Schurig V (2012) A practical method for the quantitative assessment of non-enantioselective *versus* enantioselective interactions encountered in liquid chromatography on a brush-type chiral stationary phase. J Chromatogr A 1269:270–278

109. Schurig V, Bürkle W, Hintzer K, Weber R (1989) Evaluation of nickel(II) bis[α-(heptafluorobutanoyl)-terpeneketonates] as chiral stationary phases for the enantiomer separation of alkyl-substituted cyclic ethers by complexation chromatography. J Chromatogr 475:23–44
110. Schurig V (1998) Peak coalescence phenomena in enantioselective chromatography. Chirality 10:140–146
111. Watabe K, Charles R, Gil-Av E (1989) Temperature dependent inversion of elution sequence in the resolution of α-amino acid enantiomers on chiral diamide selectors. Angew Chem Int Ed 28:192–194
112. Levkin PA, Levkina A, Czesla H, Schurig V (2007) Temperature-induced inversion of the elution order of enantiomers in gas chromatography: *N*-ethoxycarbonyl propylamides and *N*-trifluoroacetyl ethyl esters of α-amino acids on Chirasil-Val-C_{11} and Chirasil-Dex stationary phases. Anal Chem 79:4401–4409
113. Schurig V, Ossig J, Link R (1989) Evidence for a temperature dependent reversal of the enantioselectivity in complexation gas chromatography on chiral phases. Angew Chem Int Ed 28:194–196
114. Jiang Z, Schurig V (2008) Existence of a low isoenantioselective temperature in complexation gas chromatography. Profound change of enantioselectivity of a nickel(II) chiral selector either bonded to, or dissolved in, poly(dimethylsiloxane). J Chromatogr A 1186:262–270
115. König WA, Icheln D, Hardt I (1991) Unusual retention behaviour of methyl lactate and methyl 2-hydroxybutyrate enantiomers on a modified cyclodextrin. J High Resolut Chromatogr 14:694–695
116. Grosenick H, Juza M, Klein J, Schurig V (1996) NMR spectroscopic investigation of the enantioselective complexation between the inhalation anesthetics enflurane and isoflurane and a γ-cyclodextrin derivative. Enantiomer 1:337–349
117. Sicoli G, Pertici F, Jiang Z, Jicsinszky L, Schurig V (2007) Gas-chromatographic approach to probe the absence of molecular inclusion in enantioseparations by carbohydrates. Investigation of linear dextrins ("acyclodextrins") as novel chiral stationary phases. Chirality 19:391–400
118. Lämmerhofer M (2010) Chiral recognition by enantioselective liquid chromatography: mechanisms and modern chiral stationary phases. J Chromatogr A 1217:814–856
119. Scriba GKE (2012) Chiral recognition mechanisms in analytical separation sciences. Chromatographia 75:815–838
120. Pirkle WH, Pochapsky TC (1989) Considerations of chiral recognition relevant to the liquid chromatographic separation of enantiomers. Chem Rev 89:347–362
121. Lipkowitz KB (1998) Application of computational chemistry to the study of cyclodextrins. Chem Rev 98:1829–1873
122. Dodziuk H, Lukin O (2000) Dependence of the average energy between the 1: 2 complexes of enantiomeric α-pinenes with α-cyclodextrin on the length of dynamic simulation. Chem Phys Lett 327:18–22
123. Dodziuk H, Lukin O, Nowiński KS (2000) Molecular mechanics calculations of molecular and chiral recognition by cyclodextrins. Is it reliable? The selective complexation of decalins by β-cyclodextrin. J Mol Struct (Theochem) 503:221–230
124. König WA, Lutz S, Wenz G, van der Bey E (1988) Cyclodextrins as chiral stationary phases in capillary gas chromatography. Part II: heptakis(3-*O*-acetyl-2,6-di-*O*-pentyl)-β-cyclodextrin. J High Resolut Chromatogr 11:506–509
125. Köhler JEH, Hohla M, Richters M, König WA (1992) Cyclodextrin derivatives as chiral selectors – investigation of the interaction with (R, S)-methyl-2-chloropropionate by enantioselective gas-chromatography, NMR-spectroscopy, and molecular-dynamics simulation. Angew Chem Int Ed 31:319–320
126. Köhler JEH, Hohla M, Richters M, König WA (1994) A molecular-dynamics simulation of the complex formation methyl (*R*)/(*S*)-2-chloropropionate and heptakis(3-*O*-acetyl-2,6-di-*O*-pentyl)-β-cyclodextrin. Chem Ber 127:119–126

127. Koen de Vries N, Coussens B, Meier RJ, Heemels G (1992) The separation of enantiomers on modified cyclodextrin columns: measurements and molecular modeling. J High Resolut Chromatogr 15:499–504
128. Berthod A, Li W, Armstrong DW (1992) Multiple enantioselective retention mechanisms on derivatized cyclodextrin gas chromatographic chiral stationary phases. Anal Chem 64: 873–879
129. Schmidt R, Roeder M, Oeckler O, Simon A, Schurig V (2000) Separation and absolute configuration of the enantiomers of a degradation product of the new inhalation anesthetic sevoflurane. Chirality 12:751–755
130. Huang CL, Venturella VS, Cholli AL, Venutolo FM, Silbermann AT, Vernice GG (1989) Detailed investigation of fluoromethyl-1,1,1,3,3,3-hexafluoro-2-propyl ether (sevoflurane) and its degradation products. 1. Synthesis of fluorinated, soda lime induced degradation products. J Fluorine Chem 45:239–253
131. Dietrich A, Maas B, Karl V, Kreis P, Lehmann D, Weber B, Mosandl A (1992) Stereoisomeric flavor compounds. LV. Stereodifferentiation of some chiral volatiles on heptakis (2,3-di-*O*-acetyl-6-*O*-*tert*-butyldimethylsilyl)-β-cyclodextrin. J High Resolut Chromatogr 15:176–179
132. Wang F, Polavarapu PL, Schurig V, Schmidt R (2002) Absolute configuration and conformational analysis of a degradation product of inhalation anaesthetic sevoflurane: a vibrational circular dichroism study. Chirality 14:618–624
133. Uccello-Baretta G, Sicoli G, Balzano F, Schurig V, Salvadori P (2006) Highly efficient NMR enantiodiscrimination of 1,1,1,3,3-pentafluoro-2-(fluoromethoxy)-3-methoxypropane, a chiral degradation product of sevoflurane, by heptakis(2,3-di-*O*-acetyl-6-*O*-*tert*-butyldimethylsilyl)-ß-cyclodextrin. Tetrahedron Asymmetry 17:2504–2510
134. Schurig V, Schmidt R (2003) Extraordinary chiral discrimination in inclusion gas chromatography. Thermodynamics of enantioselectivity between a racemic perfluorodiether and a modified γ-cyclodextrin. J Chromatogr A 1000:311–324
135. Mele A, Raffaini G, Ganazzoli F, Juza M, Schurig V (2003) Macrocycle conformation and self-inclusion phenomena in octakis(3-O-butanoyl-2,6-di-O-pentyl)-γ-cyclodextrin (Lipodex E) by NMR spectroscopy and molecular dynamics. Carbohydr Res 338:625–635
136. Bogdanski A, Larsen KL, Wimmer R (2008) Structural and thermodynamic investigation of an unusual enantiomeric separation: Lipodex E and compound B. Tetrahedron 64:1257–1262
137. Sicoli G, Kreidler D, Czesla H, Hopf H, Schurig V (2009) Gas chromatographic enantioseparation of unfunctionalized chiral alkanes: a challenge in separation science (overview, state of the art, and perspectives). Chirality 21:183–198
138. Schurig V, Kreidler D (2013) Gas-chromatographic enantioseparation of unfunctionalized chiral hydrocarbons: an overview. In: Scriba GKE (ed) Chiral separations, methods and protocols, 2nd edn. Chap. 3. Humana, Springer, New York, pp 45–67
139. Francotte E (1997) Enantioselective chromatography: an essential and versatile tool for the analytical and preparative separation of enantiomers. Chimia 51:717–725
140. Schurig V, Link R (1988) Recent developments in enantiomer separation by complexation gas chromatograpy. In: Stevenson D, Wilson ID (eds) Chiral separations. Plenum, New York, pp 91–114
141. Kieser B, Fietzek C, Schmidt R, Belge G, Weimar U, Schurig V, Gauglitz G (2002) Use of a modified cyclodextrin host for the enantioselective detection of a halogenated diether as chiral guest via optical and electrical transducers. Anal Chem 74:3005–3012
142. Quack M (2002) How important is parity violation for molecular and biomolecular chirality? Angew Chem Int Ed 41:4618–4630
143. Darquie B et al (2010) Progress toward the first observation of parity violation in chiral molecules by high-resolution laser spectroscopy. Chirality 22:870–884
144. Barron LD (2012) From cosmic chirality to protein structure: Lord Kelvin's legacy. Chirality 24:879–893

145. Crassous J, Jiang Z, Schurig V, Polavarapu P (2004) Preparation of (+)-chlorofluoroiodomethane, determination of its enantiomeric excess and its absolute configuration. Tetrahedron Asymmetry 15:1995–2001
146. Grosenick H, Schurig V, Costante J, Collet A (1995) Gas chromatographic enantiomer separation of bromochlorofluoromethane. Tetrahedron Asymmetry 6:87–88
147. Jiang Z, Crassous J, Schurig V (2005) Gas-chromatographic separation of tri(hetero) halogenomethane enantiomers. Chirality 17:488–493
148. Costante-Crassous J, Marrone TJ, Briggs JM, McCammon JA, Collet A (1997) Absolute configuration of bromochlorofluoromethane from molecular dynamics simulation of its enantioselective complexation by cryptophane-C. J Am Chem Soc 119:3818–3823

Top Curr Chem (2013) 340: 209–276
DOI: 10.1007/128_2013_438

Published online: 11 May 2013

Differentiation of Enantiomers by Capillary Electrophoresis

Gerhard K. E. Scriba

Abstract Capillary electrophoresis (CE) has matured to one of the major liquid phase enantiodifferentiation techniques since the first report in 1985. This can be primarily attributed to the flexibility as well as the various modes available including electrokinetic chromatography (EKC), micellar electrokinetic chromatography (MEKC), and microemulsion electrokinetic chromatography (MEEKC). In contrast to chromatographic techniques, the chiral selector is mobile in the background electrolyte. Furthermore, a large variety of chiral selectors are available that can be easily combined in the same separation system. In addition, the migration order of the enantiomers can be adjusted by a number of approaches. In CE enantiodifferentiations the separation principle is comparable to chromatography while the principle of the movement of the analytes in the capillary is based on electrophoretic phenomena. The present chapter will focus on mechanistic aspects of CE enantioseparations including enantiomer migration order and the current understanding of selector–selectand structures. Selected examples of the basic enantioseparation modes EKC, MEKC, and MEEKC will be discussed.

Keywords Capillary electrophoresis · Chiral selector · Electrokinetic chromatography · Enantiodifferentiation · Enantiomer migration order · Micellar electrokinetic chromatography · Microemulsion electrokinetic chromatography · Mobility model · Selector–selectand complex

Contents

G.K.E. Scriba (✉)
Department of Pharmaceutical/Medicinal Chemistry, Friedrich Schiller University Jena, Philosophenweg 14, 07743 Jena, Germany
e-mail: gerhard.scriba@uni-jena.de

Abbreviations

CD	Cyclodextrin
Dns	Dansyl
EKC	Electrokinetic chromatography
EOF	Electroosmotic flow
id	Inner diameter
MEKC	Micellar electrokinetic chromatography
MEEKC	Microemulsion electrokinetic chromatography
(+)-18C6H4	(+)-(18-Crown-6)-2,3,11,12-tetracarboxylic acid

"*What can more resemble my hand or my ear, and be more equal in all points, than its image in a mirror? And yet, I cannot put such a hand as is seen in the mirror in the place of its original*." As stated by Immanuel Kant in 1783 in his discourse on metaphysics [1], a chiral object and its mirror image, although looking alike, are nevertheless incongruent. This epistemological analysis of a philosopher is also true in nature with regard to the interaction of chiral compounds with chiral biological targets which makes the differentiation of enantiomers a fundamental natural phenomenon. Chiral molecules play important parts in many aspects of life sciences, medical sciences, synthetic chemistry, food chemistry, as well as many other fields. Consequently, analytical techniques capable of differentiating stereoisomers, specifically enantiomers, are required. Chromatographic and electromigration techniques are currently most often applied due to the fact that these techniques separate not only enantiomers but also diastereomers and other chemically related compounds. For analytical enantioseparations, high-performance liquid chromatography (HPLC) and capillary electrophoresis (CE) are most often employed for non-volatile analytes while gas chromatography (GC) is preferably applied in the case of volatile analytes.

In capillary electrophoretic separation techniques analyses are performed in narrow bore capillaries exploiting the electrophoretic mobilities of charged molecules upon

the application of high electric field strength. Typically, the chiral selector is added to the background electrolyte in contrast to chromatography where the selector is bound to the stationary phase in most cases. Thus, in CE the chiral selector represents a so-called pseudostationary phase that may possess its own electrophoretic mobility. Combined with the different modes of CE including electrokinetic chromatography (EKC), micellar electrokinetic chromatography (MEKC), and, more recently, microemulsion electrokinetic chromatography (MEEKC), a multitude of separation scenarios can be realized contributing to the high flexibility of CE. Finally, the small quantities of samples, chemicals, and (if any) organic solvents render CE as an environmentally friendly and cost-effective technique.

This chapter discusses the current understanding of CE enantioseparations and will highlight examples in EKC, MEKC, and MEEKC. Capillary electrochromatography (CEC), which is considered a hybrid technique combining the separation principles of CE and HPLC, will not be considered here.

1 Historical Development of CE Enantioseparations

The first publication of an (achiral) CE analysis is often considered to be the paper by Jorgenson and Lukacs analyzing dansyl (Dns)-amino acids and other analytes in 75 μm inner diameter (id) fused-silica capillaries which was published in 1981 [2]. Approximately 4 years later the first CE enantioseparation was reported by Gassmann et al. who separated Dns-amino acids in the presence of a copper (II)–histidine complex as chiral selector [3]. It took until the late 1980s until further enantioseparations by CE were reported, including the paper by Cohen et al. using copper(II)–*N*,*N*-didecyl-L-alanine as chiral selector in a SDS micellar system in 1987 [4], or cyclodextrins (CDs) as chiral selectors in separations employing capillary isotachophoresis reported by Smolkova-Keulemansova and coworkers in 1988/1889 [5–7] and in capillary gel electrophoresis as demonstrated by Guttman et al. in 1988 [8]. The use of CDs in EKC was systematically addressed by Fanali in 1989 [9]. In this year several groups also reported the use of chiral micelles for analytical enantioseparations in MEKC. Terabe's group employed bile salt micelles for enantioseparations of Dns-amino acids [10, 11] while Dobashi et al. demonstrated the feasibility of *N*-dodecanoyl-L-valine as chiral surfactant for the separation of the enantiomers of amino acid derivatives [12, 13]. Since then many groups have focused on CE enantioseparations developing many chiral selectors and numerous applications so that CE can be considered a mature and reliable technique for analytical enantioseparations. This is also reflected in many review articles including recent publications [14–22] as well as monographs [23, 24]. Furthermore, special issues dedicated to enantioseparations by CE are regularly published by journals such as Journal of Chromatography A, Electrophoresis, Journal of Separation Science, Journal of Pharmaceutical and Biomedical Analysis, and others.

2 Fundamentals of CE Enantioseparations

CE can be regarded as an automated version of conventional (planar) electrophoresis. Separations are carried out in capillaries with an inner diameter (id) of 20–100 μm so that dissipation of Joule heat is very effective, allowing the application of high voltages up to 30 kV. The small diameters make CE a miniaturized technique requiring only small amounts of chemicals, solvents, and samples. The capillaries are manufactured from fused silica so that detection modes such as UV- or laser-induced fluorescence detection are typically carried out by on-column detection but hyphenation to a mass spectrometer is nowadays also routine. Therefore, staining techniques as in conventional electrophoresis are not required. The output of commercial instruments resembles a conventional chromatogram and can be integrated for quantitative analyses. While gel electrophoresis can only be applied to large molecules, CE allows the separation of small molecules including stereoisomers as well as the analysis of large molecules such as proteins or DNA and even whole cells.

In electrophoresis the mobility of an analyte is determined by the electrophoretic mobility of a particle, μ_{ep}, as a function of charge, q, and size of the analyte represented by the radius, r, for a spherical particle according to

$$\mu_{ep} = \frac{q}{6\pi\eta r}, \tag{1}$$

where η is the viscosity of the background electrolyte. In the case of acidic or basic analytes, the charge is a function of the pH of the electrolyte solution. In addition, the charged surface of the capillary results in the electroosmotic flow (EOF) as a general mass flow. The EOF creates a plug-like flow profile as compared to the parabolic flow profile of pressure driven chromatographic techniques rendering CE a high resolution technique. The mobility of the EOF is described by

$$\mu_{EOF} = \frac{\varepsilon\zeta}{4\pi\eta}, \tag{2}$$

where ε is the permittivity of the electrolyte solution and ζ is the zeta-potential resulting from the negatively charged capillary surface due to pH-dependent dissociation of the silanol groups.

The effective mobility of a solute is the sum of both electrophoretic forces, μ_{ep} and μ_{EOF}, according to

$$\mu_{eff} = \mu_{ep} + \mu_{EOF}. \tag{3}$$

As in chromatography, CE enantioseparations can be divided into indirect and direct methods. In the indirect approach the analyte enantiomers are derivatized with an enantiopure reagent to form a pair of diastereomers via covalent bonds. The diastereomers can be subsequently separated, in principle, under achiral conditions.

Direct methods refer to the separation of enantiomers in a chiral environment. This requires the presence of a chiral selector that is added to the background electrolyte. The separation is based on the formation of transient diastereomeric complexes in a thermodynamic equilibrium. This is identical with the situation in chromatographic techniques so that the stereospecific recognition of the analyte enantiomers by a chiral selector represents a chromatographic phenomenon [25]. The fact that the selector is mobile in CE compared to chromatography (a so-called "pseudo-stationary phase") is not a fundamental difference between the techniques. For this reason, enantioseparations by CE are also referred to as EKC. The transport of the analyte and/or the analyte–selector complex to the detector is achieved by electrokinetic phenomena. Thus, enantioseparations in CE contain a chromatographic and an electrophoretic component.

Many mathematical models have been proposed to describe the influence of the main parameters of a CE separation such as the concentration of the chiral selector, pH, EOF, nature of the background electrolyte co-ion and organic solvent additives. Most models assume a 1:1 complexation between the enantiomers and the chiral complexation agent although equations describing multiple complexation equilibria have been developed [26–28]. The analyte as well as the chiral selector may be neutral, anionic, cationic, or zwitterionic. In addition to buffer additives (other than the chiral selector) and the nature of the capillary wall (coated or uncoated), which may both affect the EOF, the charge of the solute and the chiral selector determine the mechanism and direction of the migration in CE. Therefore, the nature of the chiral additive contributes not only to the separation selectivity but also, in the case of charged selectors, to the migration direction and magnitude.

The theoretical models may be divided into "mobility difference models" where a separation is expressed as the difference between the effective mobilities of the enantiomers and "selectivity models" that use the separation selectivity α expressed as the ratio between either the effective mobilities of the enantiomers or the complexation constants as a measure of the separation. Only a few models required for the basic understanding of the separation mechanism will be briefly discussed. Further models have been summarized, for example, in [15, 20, 29, 30].

The development of the initial mobility difference model is attributed to Wren and Rowe [31] although the principal equation was derived earlier by Stepanova and Stepanov [32]. Assuming 1:1 complexation, the formation of transient diastereomeric complexes of the enantiomers R and S with a chiral selector, C, is characterized by the complexation constants K_R and K_S:

$$R + C \rightarrow RC \quad K_R = \frac{[RC]}{[R][C]}, \tag{4}$$

$$S + C \rightarrow SC \quad K_S = \frac{[SC]}{[S][C]}.$$

Generally, the effective mobility of an analyte, μ_{eff}, i.e., the apparent mobility corrected for the mobility of the EOF, is the sum of the electrophoretic mobilities of all different species in which the analyte may exist weighted by the mole fraction φ of the respective species

$$\mu_{\text{eff}} = \sum_n \varphi^n \cdot \mu^n, \tag{5}$$

where n is the number of the species present under the experimental conditions. Assuming that for a given chiral separation the enantiomers exist only in a complexed and non-complexed form, (5) becomes for the R-enantiomer

$$\mu^R_{\text{eff}} = f \cdot \mu_f + (1 - f)\mu^R_{\text{cplx}}, \tag{6}$$

where μ_{f} is the mobility of the free enantiomer, μ^R_{eff} is the mobility of the analyte–selector complex, and f is the fraction of the non-complexed species. Considering the complexation constant, K, and the concentration of the selector, $[C]$, the effective mobility of the R-enantiomer may be expressed as

$$\mu^R_{\text{eff}} = \frac{\mu_f + \mu^R_{\text{cplx}} K_R[C]}{1 + K_R[C]}. \tag{7}$$

Thus, the effective mobility of an analyte, μ_{eff}, interacting with a chiral selector is a function of the mobility of the free analyte, μ_{f}, the (limiting) mobility of the analyte–selector complex, μ_{cplx}, the complexation constant, K, (also referred to as binding constant or distribution constant), and the concentration of the chiral selector [31].

An enantioseparation is observed when the effective mobilities of the enantiomers differ, i.e.,

$$\Delta\mu = \mu^R_{\text{eff}} - \mu^S_{\text{eff}} = \frac{\mu_f + \mu^R_{\text{cplx}} K_R[C]}{1 + K_R[C]} - \frac{\mu_f + \mu^S_{\text{cplx}} K_S[C]}{1 + K_S[C]}. \tag{8}$$

The chromatographic enantioselective mechanism (also referred to as the thermodynamic mechanism) is the result of different affinities of the enantiomers towards the chiral selector reflected in differences in the complexation constants, i.e., $K_R \neq K_S$. The electrophoretic enantioselective mechanism is due to differences in the limiting mobilities of the enantiomer–selector complexes, i.e., $\mu^R_{\text{eff}} \neq \mu^S_{\text{eff}}$, caused, for example, by differences in the hydrodynamic radii of the complexes due to a "better fit" of one of the enantiomers. Both mechanisms can contribute simultaneously but the chromatographic mechanism is typically the predominant mechanism because the hydrodynamic radii of the two enantiomer–selector complexes do not differ

significantly and the effective charges of the two complexes are identical. In the case of equal complex mobilities ($\mu^R_{\text{cplx}} = \mu^S_{\text{cplx}} = \mu_{\text{cplx}}$) (8) may be rewritten as [25]

$$\Delta\mu = \frac{[C](\mu_f - \mu_{\text{cplx}})(K_R - K_S)}{1 + [C](K_R + K_S) + K_R K_S [C]^2}. \tag{9}$$

However, it has been clearly shown, that enantioseparations in CE are possible, even in the case of equal complexation constants, i.e., by the electrophoretic enantioselective mechanism based solely on mobility differences of the transient diastereomeric complexes [33]. In the case of equal complexation constants ($K_R = K_S = K$) (8) can be transformed to [25]

$$\Delta\mu = \frac{K[C]\,(\mu^R_{\text{cplx}} - \mu^S_{\text{cplx}})}{1 + K[C]}. \tag{10}$$

This separation mechanism is not possible in the case of immobilized selectors such as in chromatography. Examples for CE enantioseparations with essentially equal binding constants of the enantiomers based on different limiting mobilities of the complexes have been described [33–35].

Although frequently applied to investigating migration phenomena, the model of Wren and Rowe has the disadvantage that it does not account for the protonation equilibrium of the analyte in its free and complexed form. The latter may lead to different charge densities of the complexes at a given pH of the background electrolyte based on a complexation-induced pK_a shift resulting in different limiting mobilities of the diastereomeric selector–enantiomer complexes [36]. Analyte protonation equilibrium was included by Vigh and coworkers in a series of papers [37–39]. For example, for a weakly acidic compound the effective mobility, μ_{eff}, of an enantiomer can be expressed as [37]

$$\mu^R_{\text{eff}} = \frac{\mu^0_- + \mu^0_{\text{RCD}^-} K_{\text{RCD}^-}[C]}{1 + K_{\text{RCD}^-}[C] + \frac{[\text{H}_3\text{O}^+]}{K_a}(1 + K_{\text{HRCD}}[C])}, \tag{11}$$

where μ^0_- is the mobility of the fully deprotonated free analyte, $\mu^0_{\text{RCD}^-}$ is the mobility of the complex between the fully deprotonated species and the chiral selector, K_a is the dissociation constant of the analyte, K_{RCD^-} and K_{HRCD} are the complexation constants of the dissociated and non-dissociated species, $[\text{H}_3\text{O}^+]$ is the hydronium ion concentration of the buffer, and $[C]$ is the concentration of the chiral selector. Assuming identical dissociation constants of the analyte enantiomers the following selectivity model is obtained to characterize the enantioseparation:

$$\alpha = \frac{\mu^R_{\text{eff}}}{\mu^S_{\text{eff}}} = \frac{1 + \frac{\mu^0_{\text{RCD}^-}}{\mu^0_-} K_{\text{RCD}^-}[C]}{1 + \frac{\mu^0_{\text{SCD}^-}}{\mu^0_-} K_{\text{SCD}^-}[C]} \cdot \frac{1 + K_{\text{SCD}^-}[C] + \frac{[\text{H}_3\text{O}^+]}{K_a}(1 + K_{\text{HSCD}}[C])}{1 + K_{\text{RCD}^-}[C] + \frac{[\text{H}_3\text{O}^+]}{K_a}(1 + K_{\text{HRCD}}[C])}. \tag{12}$$

Subsequently, the so-called "chiral charged resolving agent migration model" (CHARM) for the permanently charged chiral selectors was developed including the mobility of the chiral selector [40]. The effective mobility of the *R* enantiomer is given by

$$\mu_{\text{eff}}^{R} = \frac{\mu_f + \mu_{\text{RCD}} K_{\text{RCD}}[\text{CD}] + K[\text{H}_3\text{O}^+](\mu_{\text{HR}} + \mu_{\text{HRCD}} K_{\text{HRCD}}[\text{CD}])}{1 + K_{\text{RCD}}[\text{CD}] + K[\text{H}_3\text{O}^+](1 + K_{\text{HRCD}}[\text{CD}])}. \tag{13}$$

Again the selectivity ratio of the effective mobilities of the enantiomers was applied to characterize an enantioseparation. Depending on the dissociation behavior of the analytes, the model was subdivided into forms for non-electrolytes, strong electrolytes, and weak electrolytes. The migration order of the enantiomers depends on the K and μ values. The model was eventually extended, introducing a binding selectivity term, a size selectivity term representing the mobility ratio of the transient diastereomeric complexes, and parameter for the effect of the complexation on the analyte mobility [41].

Dubsky et al. have developed a theoretical model based on the model by Wren and Rowe to rationalize the often observed superior enantioselectivity of randomly substituted chiral selectors compared to single isomer selectors [42, 43]. The randomly substituted CD was treated as a mixture of a (large) number of defined chiral selectors with different substitution patterns. In this system the effective mobility can be described by an equation formally identical to the equation used for a single selector system, i.e.,

$$\mu_i^{\text{eff}} = \frac{\mu_f + \mu_i^{\text{over}} K_i^{\text{over}} c_{\text{cs}}^{\text{tot}}}{1 + K_i^{\text{over}} c_{\text{cs}}^{\text{tot}}}, \tag{14}$$

where μ_{f} is the mobility of the free analyte, $c_{\text{cs}}^{\text{tot}}$ is the total concentration of the mixture of chiral selectors, i.e., the CDs with different substitution patterns. K_i^{over}, and μ_i^{over} are the overall (apparent) complexation constants and the overall (apparent) limiting mobilities of the complexes, respectively. K_i^{over} is defined by

$$K_i^{\text{over}} = \sum_q \chi^q K_i^q, \tag{15}$$

where χ^q is the molar fraction of the qth CD substitution isomer in the mixture and K_i^q the individual apparent complexation constants of the analyte with the q$^{\text{th}}$ CD isomer. Thus, the overall complexation constant of a multiple isomer CD system is the weighted sum of all individual constants with the mol fractions of the individual CDs as the weights. μ_i^{over} is described by

$$\mu_i^{\text{over}} = \frac{\sum_q \chi^q K_i^q \mu_i^q}{K_i^{\text{over}}}. \tag{16}$$

Equation 16 illustrates that the overall limiting mobility of an enantiomer interacting with a mixture of selector isomers is no longer an independent physicochemical (electrophoretic) property but depends on the distribution of the enantiomer between chiral and achiral environments represented by the complexation constant, K_i^{over}. Thus, μ_i^{over} becomes an apparent parameter influenced by the chromatographic as well as electrophoretic mechanisms so that the overall limiting mobilities of two enantiomers, μ_1^{over} and μ_2^{over}, may substantially differ even in the case of equal individual mobilities for every q^{th} CD in the isomer mixture, i.e., $\mu_1^q = \mu_2^q$. Therefore, even if enantiomers are separated solely on the chromatographic basis using one or another single isomer CD of the mixture an additional electrophoretic separation mechanism may appear if the two CDs are combined. This is even more likely when a mixture of many individual CD isomers is used as is the case in randomly substituted CDs. The theory has been experimentally proven for the enantioseparation of lorazepam using heptakis(6-*O*-sulfo)-β-CD as a single isomer selector and randomly sulfated β-CD as a mixture of multiple isomers [43]. The difference between the effective mobilities of the enantiomers as shown in Fig. 1 increases with increasing concentrations of randomly sulfated β-CD while remaining almost constant in the case of the single isomer CD. The enantioselectivity of the selectors expressed as the ratio of the binding constants, K_i^{over}, is similar for both selectors (1.29 vs 1.32 for the single isomer CD and the multiple isomer CD, respectively) despite the fact that heptakis (6-*O*-sulfo)-β-CD forms stronger complexes compared to randomly sulfated β-CD. However, there is a large difference between the apparent limiting mobilities, μ_i^{over}, for the enantiomers in the case of the multiple isomer CE while the values are practically identical in the case of heptakis(6-*O*-sulfo)-β-CD (Fig. 1). Thus, the enantioseparation with the single isomer CD is largely governed by the (thermodynamic) enantioselectivity of the selector, the electrophoretic enantioselective mechanism (complex mobility) significantly affecting the (increased) enantioseparation observed for the multiple isomer selector represented by randomly sulfated β-CD.

As described in this section, significant differences exist between enantioseparations in pressure-driven chromatographic systems and systems based on electrophoretic phenomena, although the general enantioselective recognition mechanism (i.e., the complexation of the analyte enantiomers by a chiral selector) is the same in both techniques. One striking example is the above-mentioned fact that enantioseparations are possible even if there is no stereoselective recognition of the enantiomers by the selector which can be attributed to the fact that the diastereomeric selector–selectand complexes are mobile and may differ in their respective mobilities.

3 Enantiomer Migration Order

3.1 Techniques for Enantiomer Migration Order Reversal

One of the most striking features of CE is the fact that the enantiomer migration order may be adjusted relatively easily by variation of the experimental conditions.

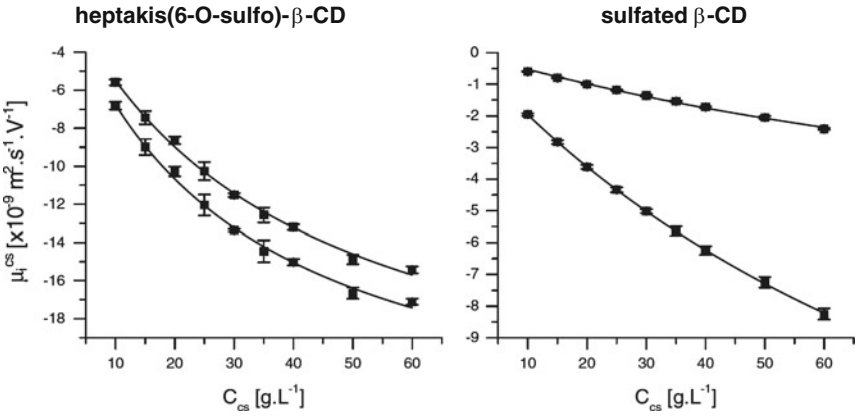

	1st enantiomer [x 10^{-3} L/g]	2nd enantiomer [x 10^{-9} $m^2V^{-1}s^{-1}$]
K_i^{over}	28.1 ± 1.8	36.1 ± 2.3
$\mu_i^{cs(over)}$	– 25.0 ± 0.8	– 25.5 ± 0.7

	1st enantiomer [x 10^{-3} L/g]	2nd enantiomer [x 10^{-9} $m^2V^{-1}s^{-1}$]
K_i^{over}	7.1 ± 1.1	9.4 ± 0.2
$\mu_i^{cs(over)}$	– 7.9 ± 0.9	– 22.8 ± 0.3

Fig. 1 Effective mobility of the enantiomers of lorazepam using heptakis(6-*O*-sulfo)-β-CD (*left*) and randomly sulfated β-CD (*right*) as chiral selectors in a 50 mM tris-tricine buffer, pH 8.11, using an applied voltage of 15 kV. The complexation constants and complex mobilities obtained from curve fitting according to (11) are also presented. (Reproduced with permission of Wiley from [42] © 2010)

For the determination of the enantiomeric excess (ee) the minor enantiomer has to be determined in the presence of a large amount of the other enantiomer. Based on the requirements by the regulatory authorities the excess of one enantiomer may be 1,000-fold. As peak tailing and peak fronting can be observed in CE it may be feasible to determine the minor enantiomer in front of a tailing peak of the main component or after a large fronting peak. Most chiral selectors used in CE are available only in one stereoisomeric form so that reversal of the enantiomer migration order often cannot be achieved by switching to the other enantiomer of the selector. Therefore, other phenomena must be exploited in such cases.

Considering the mobility difference models mentioned above, reversal of the enantiomer migration order is observed when the algebraic sign of the difference of the effective mobilities of enantiomers 1 and 2, $\Delta\mu = \mu_{eff1} - \mu_{eff2}$, or the terms $(K_1 - K_2)$ or $(\mu_f - \mu_{cplx})$ is reversed [44]. In a selectivity model [e.g., (12)], opposite migration order is observed when $\alpha = \mu_{eff1}/\mu_{eff2} > 0$ or < 0. Because the chromatographic principle reflected in the complexation of the solutes as well as the electrophoretic principles affect the effective mobilities of the enantiomers, the following mechanisms can affect the enantiomer migration order [44, 45]:

1. The strength of the complexation of the enantiomers by the selector.
2. The direction and magnitude of the EOF.
3. The direction and magnitude of the mobility of the free analyte.

4. The direction and magnitude of the mobility of the chiral selector.
5. The direction and magnitude of the mobility of the diastereomeric selector–enantiomer complexes.

Combinations may apply. Various scenarios are also possible due to the fact that detection in CE can be performed at the cathodic end (normal polarity of the applied voltage) as well as the anodic end of the capillary (reversed polarity of the applied voltage) so that cathodic as well as anodic mobility can be exploited. Different techniques have been utilized in order to reverse the migration order of enantiomers based on the general phenomena listed above. They are schematically summarized in Fig. 2 considering certain combinations of experimental conditions. However, other combinations than the depicted ones may also apply leading to comparable effects so that the current discussion of mechanisms leading to opposite enantiomer migration order cannot be comprehensive.

The first mechanism is the most obvious. Two chiral selectors possess opposite complexation selectivity toward the enantiomers of an analyte, i.e., enantiomer 1 is bound more strongly than enantiomer 2 by one selector but more weakly than enantiomer 2 by the other selector. If the overall migration direction is not altered by the exchange of the selector this will result in opposite enantiomer migration order. In the case of a positively charged analyte that is detected at the cathode the more weakly complexed analyte migrates first (Fig. 2a). In contrast, analyzing a negatively charged solute with an electrophoretic mobility towards the anode that is carried to the detector at the cathodic end of the capillary (Fig. 2b), the more strongly complexed stereoisomer will migrate first because the more weakly complexed enantiomer possesses a relatively higher mobility towards the anode. Examples of opposite chiral recognition include separations applying the enantiomers of a selector such as in the case of the synthetic polymeric micelles possessing either L- or D-valine as head group [46], in a ligand exchange system when switching the chiral chelator D-penicillamine to L-penicillamine [47], chiral surfactants based on β-L-glucose or β-D-glucose [48], or using the enantiomers of a chiral crown ether as selector [49]. Different complexation selectivities have also been observed for CDs as a group of chiral selectors available in only one configuration. In this case different complexes were formed depending on the size of the CD cavity, the CD derivative, the substitution pattern, or the position of the substituents (see also discussion on complex structures below) as summarized in [44, 45]. Recent examples include [50–57]. Opposite enantiomer migration order of analytes has also been found in the presence of CD derivatives with identical substituents but different substitution patterns [58, 59]. Furthermore, opposite stereoselective recognition of enantiomers by CDs has been observed depending on the charge of the analyte. Thus, one enantiomer is preferentially complexed in the charged form while the other enantiomer is complexed more strongly when the analyte is uncharged. This behavior has been reported for amphoteric compounds such as amino acid derivatives [36] or small peptides [35, 60, 61] (see also Sect. 3.2). Interestingly, the stereoselective recognition can also be affected by the nature of the background electrolyte. Thus, opposite migration order has been

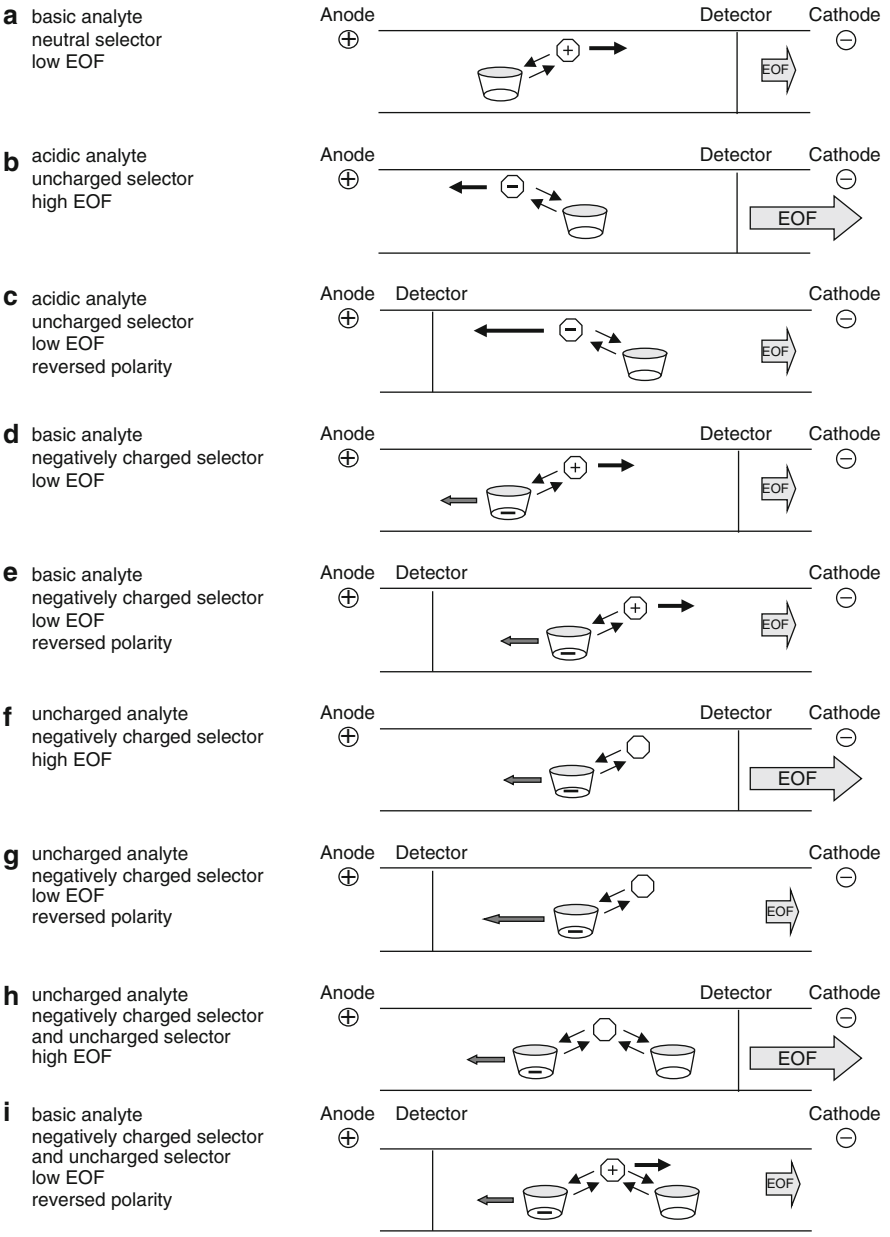

Fig. 2 Schematic representation of migration modes in capillary electrophoresis enantioseparations. The octagon represents the analyte with a possible charge indicated where appropriate. The *basket* represents the chiral selector. A charged selector is indicated by the additional *minus sign*. The *arrows* represent the electrophoretic mobility of analyte and selector, respectively. The net mobility in the different scenarios is always directed towards the detector

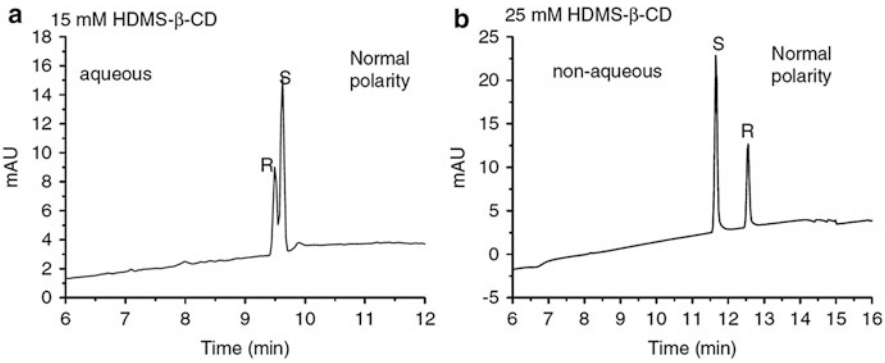

Fig. 3 Enantioseparation of propranolol using heptakis(2,3-di-*O*-methyl-6-*O*-sulfo)-β-CD as chiral selector in (**a**) 100 mM phosphoric acid adjusted to pH 3 by the addition of triethanolamine and (**b**) 10 mM ammonium formate/0.75 M formic acid in methanol. Other experimental conditions: 40/48.5 cm, 50 μm id fused-silica capillary, 15°C, 25 kV, UV detection at 230 nm. (Reproduced with permission of Wiley from [62] © 2010)

observed for propranolol using sulfated cyclodextrins as selectors in aqueous and non-aqueous electrolyte solutions [62–64] as shown for propranolol in the presence of heptakis(2,3-di-*O*-methyl-6-*O*-sulfo)-β-CD (Fig. 3) as a consequence of different complexes between analyte and the CD in an aqueous buffer and a methanolic electrolyte (see also Sect. 4.1). Finally, reversal of the migration order in case of different selector structures has been found in other modes such as MEKC using sugar-based surfactants [48] (Fig. 4) or in ligand-exchange CE using different chelating agents [65, 66].

The EOF is a non-stereoselective force affecting all components of a given separation system in the same way. Many methods are available to increase, decrease, eliminate, or reverse the direction of the EOF by modification of the capillary wall. Elimination or reversal of the EOF can result in opposite migration order under otherwise identical experimental conditions. The enantioselectivity of the chiral selector towards the analyte remains unchanged under both experimental set-ups. For example, opposite migration order of the enantiomers of an anionic compound using an uncharged selector can be observed comparing the situation at a low velocity of the EOF (Fig. 2c) to the situation at a high EOF (Fig. 2b). This has been illustrated for 1,1′-binaphthyl-2,2′-diyl hydrogen phosphate using β-CD as chiral selector in a fused-silica capillary (Fig. 5) [67]. At a low pH the EOF is essentially suppressed so that the negatively charged analytes migrate towards the anode applying reversed polarity of the voltage. Consequently, the more weakly complexed (*R*)-(−)-enantiomer is detected first due to a higher overall mobility. Increasing the pH of the background electrolyte to pH 6.5 results in a significant increase in the EOF so that the analytes are now detected at the cathode (normal polarity of the voltage). Because the more strongly bound (*S*)-(+)-enantiomer displayed an overall lower mobility towards the anode it is now detected first at the cathodic end of the capillary. Opposite migration order can also be observed when comparing bare fused-silica capillaries with a cathodic EOF with capillaries

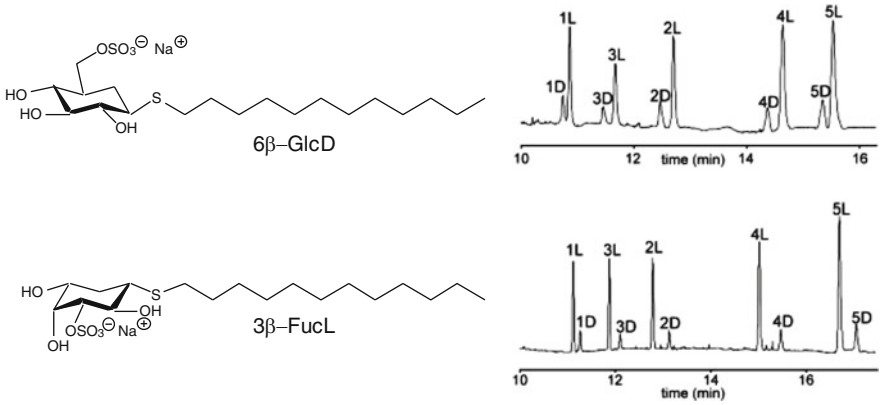

Fig. 4 Enantioseparation of Dns-amino acids (D/L ration 1:3) in MEKC using (*top*) sodium *n*-dodecyl 1-thio-β-D-glucopyranoside 6-hydrogen sulfate (6β-GlcD) and (*bottom*) sodium *n*-dodecyl 1-thio-β-L-fucopyranoside 3-hydrogen sulfate (3β-FucL) as chiral selector. Experimental conditions: 56/64.5 cm, 50 µm id fused-silica capillary, 50 mM phosphate buffer, pH 6.5, containing 30 mM of the surfactant, 25°C, 20 kV, UV detection at 215 nm. Peak assignment: (*1*) Dns-Val, (*2*) Dns-Leu, (*3*) Dns-Met, (*4*) Dns-Phe, (*5*) Dns-Trp. (Reproduced with permission of Wiley from [48] © 2008)

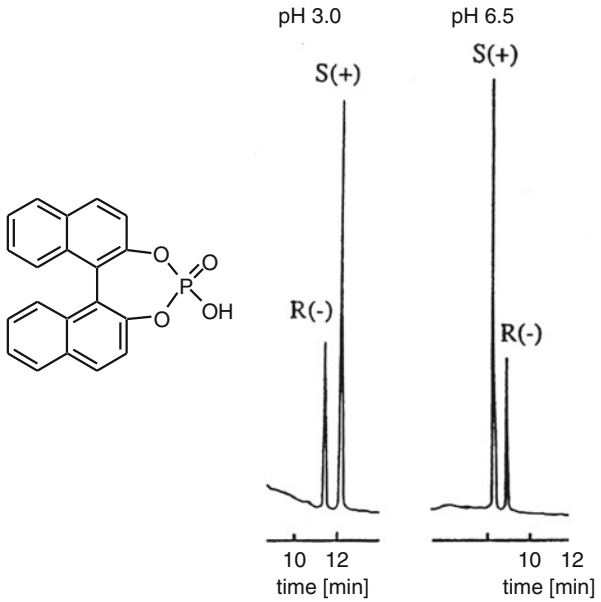

Fig. 5 Enantioseparation of 1,1′-binaphthyl-2,2′-diyl hydrogen phosphate (*S*/*R* ratio 2:1) using 2.5 mg/mL β-CD as chiral selector in 50 mM phosphate buffer (**a**) pH 3.0 and negative polarity of the applied voltage (−400 V/cm), and (**b**) pH 6.5 and normal polarity of the applied voltage (+400 V/cm). Experimental conditions: 50/60 cm, 50 µm id fused-silica capillary, 20°C, UV detection at 210 nm. (Reproduced with permission of Elsevier from [67] © 1996)

coated with positively charged compounds, resulting in an anodic EOF. Examples can be found in [68–70].

Analyte mobility may also be exploited for a reversal of the enantiomer migration order if the analyte can be analyzed as anionic and cationic species. In a fused-silica capillary the direction of the EOF and the mobility of a cationic analyte are both towards the cathode while they are in the opposite direction in the case of an anionic analyte. If the stereoselective recognition of the selector towards the analyte enantiomers remains unchanged whether the cation or the anion is complexed, reversal of the migration order will result. Thus, at a given pH of the background electrolyte the more strongly complexed enantiomer migrates second when analyzing the cationic form due to a lower effective mobility (Fig. 2a). In contrast, when analyzed as anionic species at a higher pH the more weakly complexed enantiomer exhibits a higher mobility towards the anode so that the more strongly complexed analyte is carried faster to the cathode by the EOF (Fig. 2b) resulting in opposite migration order compared to the analysis of the cationic form of the analyte. Examples can be found in [36, 71, 72].

Exploiting the mobility of the chiral selector for a reversal of the enantiomer migration order can be performed in two ways, using either permanently charged chiral selectors or selectors that can exist in either a charged or an uncharged form depending on the pH of the background electrolyte and exhibit identical chiral recognition towards the analyte enantiomers independent of the charge of the selector. A general advantage of charged selectors is the fact that uncharged analytes may also be separated. The situation of a permanently charged selector will be discussed first. For example, using a negatively charged complexation agent (possessing an electrophoretic anodic mobility) for the enantioseparation of a cationic compound, the more weakly complexed enantiomer will be detected first at the cathodic end of the capillary at a low selector concentration (Fig. 2d). At a high concentration the carrier ability of the charged selector can be exploited detecting the analyte at the anode. Thus, upon reversal of the polarity of the applied voltage the more strongly complexed analyte will be transported faster to the detector at the anodic end of the capillary resulting in a reversal of the enantiomer migration order (Fig. 2e). The same scenario would result with the combination of an uncharged analyte and a negatively charged selector. At low selector concentrations the more weakly complexed enantiomer is detected first at the cathode if a sufficiently high EOF exists (Fig. 2f), while under reversed polarity of the applied voltage exploiting the carrier ability of the selector the more strongly bound enantiomer will be detected first at the anodic end of the capillary (Fig. 2g). An example is the simultaneous separation of isomers and enantiomers of the dipeptide α/β-Asp-PheOMe in a pH 5.25 background electrolyte in the presence of carboxymethyl-β-CD (Fig. 6) [73]. At pH 5.25 the peptides are essentially uncharged while the CD is negatively charged. In addition, the inner wall of the capillary was coated with polyacrylamide in order to eliminate the EOF when using the CD as a carrier. Thus, at the low CD concentration the migration order is obtained as shown in Fig. 6a. The migration order of each enantiomeric pair is opposite at high concentrations of carboxymethyl-β-CD under reversed polarity of

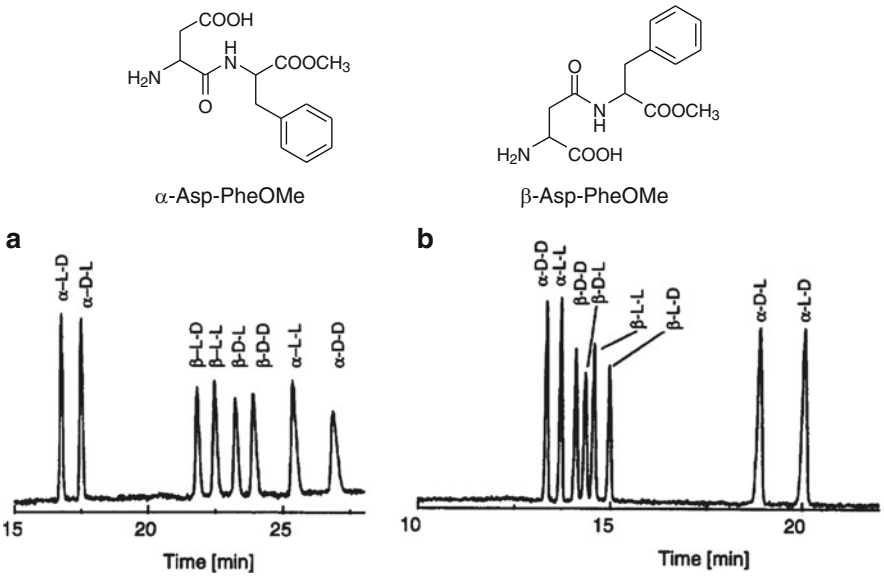

Fig. 6 Separation of enantiomers of the α/β-isomers of Asp-PheOMe under (**a**) normal polarity of the applied voltage (detection at the cathode) and (**b**) exploiting the carrier ability of the selector under reversed polarity of the applied voltage (detection at the anode). Experimental conditions: (**a**) 40/47 cm, 50 μm id fused-silica capillary, 50 mM sodium phosphate buffer, pH 5.25, 15 mg/mL carboxymethyl-β-CD, +20 kV, 20°C, UV detection at 215 nm and (**b**) 40/47 cm, 50 μm id polyacrylamide-coated capillary, 50 mM sodium phosphate buffer, pH 5.25, 60 mg/mL carboxymethyl-β-CD, −20 kV, 20°C, UV detection at 215 nm. (Reproduced with permission of Elsevier from [73] © 1998)

the applied voltage (Fig. 6b). Other examples can be found in [74–78] including the use of positively charged selectors [79, 80]. In the case of selectors possessing functional groups such as carboxylic acids or amines which are charged as a function of the pH of the background electrolyte, the selectors may be used as either neutral complexation agent without a self-mobility or as a charged compound with an electrophoretic self-mobility. If the chiral recognition towards the enantiomers does not change with the charge of the chiral selector, opposite migration order will be observed when detecting the enantiomers at the anode (reversed polarity of the voltage) as compared to the detection at the cathode (normal polarity of the voltage). The combinations are schematically illustrated for a positively charged analyte in Fig. 2a (uncharged form of the selector) and Fig. 2e (charged form of the selector). Examples of enantioseparations based on this principle or migration order reversal have been described in [81, 82].

Another technique applies a combination of chiral selectors. In this mode the selectors have to possess opposite chiral recognition towards the analyte enantiomers [83] or different mobilities in case the chiral recognition is the same but occurs with a different magnitude [84]. In the first case the migration order is a function of the CD used at a higher concentration in the binary mixture. This

mechanism is essentially the same as using the individual selector alone as discussed above as first option of a reversal of the enantiomer migration order. In the second scenario typically a charged and an uncharged selector are combined. The migration order of the enantiomers in the absence of the uncharged selector results from the analyte complexation by the charged complexation agent depending on whether the analyte itself is charged or uncharged and whether detection is subsequently carried out at the anodic or the cathodic end of the capillary. For example, when using a negatively charged selector for the separation of a neutral analyte detecting at the cathode, the more weakly complexed enantiomer will migrate first because it is carried to the detector by the EOF while the analyte–selector complex migrates towards the anode (Fig. 2f). Adding an uncharged selector with the same chiral recognition but stronger analyte complexation compared to the charged selector competition between the selectors for the analyte enantiomers results in a lower overall binding of the more strongly complexed enantiomer by the negatively charged selector. As a consequence, the complex between the neutral selector and the more strongly bound enantiomer is carried to the detector at the cathode by the EOF faster than the more weakly bound enantiomer (Fig. 2h) and reversal of the enantiomer migration order results. This has been shown for the separation of the enantiomers (*R*,*R*)- and (*S*,*S*)-hydroxybenzoin (the compound also exists as a mesoform) (Fig. 7) [85]. In a fused-silica capillary using a phosphate buffer, pH 9.0, as background electrolyte, the (*S*,*S*)-configured enantiomer migrates before the (*R*,*R*)-enantiomer in the presence of sulfated β-CD as chiral selector. Upon addition of increasing amounts of neutral β-CD co-migration is first observed followed by enantioseparation with reversed migration order, i.e., (*R*,*R*)-hydroxybenzoin before (*S*,*S*)-hydroxybenzoin. Interestingly the migration order of the enantiomers of the related substances benzoin or benzoin methyl ether is not affected by the addition of β-CD (Fig. 7). Another example of enantiomer migration order reversal of a neutral analyte as a function of a binary selector system is reported in [84]. A similar observation has also been made for protonated analytes in combination with negatively charged sulfated β-CD under reversed polarity of the applied voltage and detection at the anodic end of the capillary [86, 87] as schematically illustrated in Fig. 2i. In this set-up the more strongly complexed enantiomer is detected first when only working with the negatively charged selector. Adding an uncharged selector, with the same chiral recognition but stronger analyte complexation compared to the charged selector competition between the selectors for the analyte enantiomers, results in a lower overall binding of the more strongly complexed enantiomer by the negatively charged selector. As a consequence, the more weakly bound enantiomer is less retarded by the uncharged selector increasing its binding by the charged selector so that it now reaches the detector at the anode first. The combination of a CD with a polymeric chiral surfactant can also result in the reversal of the migration order of enantiomers [88].

It has also been shown that achiral additives in a system containing a chiral selector can affect the enantiomer migration order. Thus, it has been observed that addition of an achiral surfactant above the critical micelle concentration reversed the

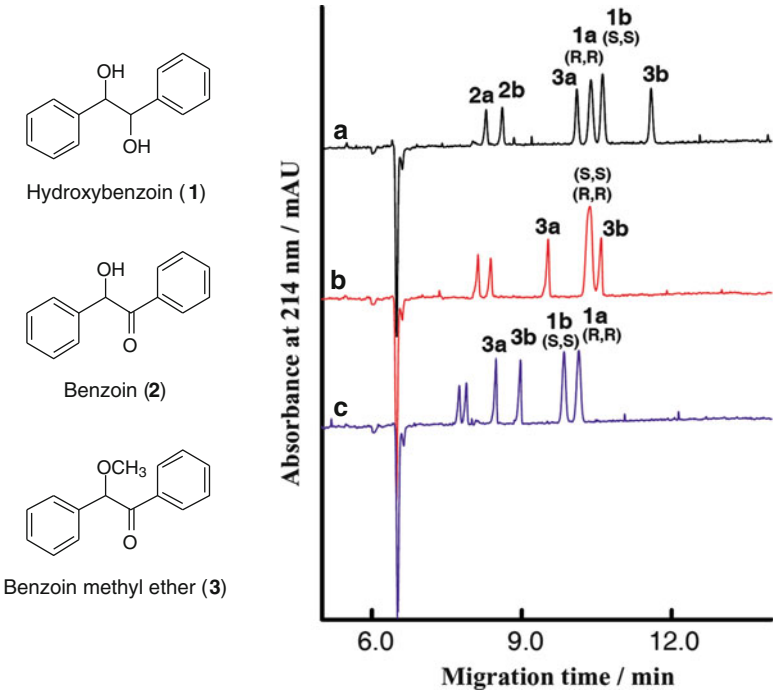

Fig. 7 Enantiomer migration order of benzoin derivatives in the presence of 3.5% (w/v) sulfated β-CD as a function of the addition of β-CD: (*A*) no addition, (*B*) 0.3 mM β-CD, and (*C*) 0.9 mM β-CD. Experimental conditions: 50/57 cm, 50 μm id fused-silica capillary, 50 mM borate buffer, pH 9.0, 25°C, 20 kV, UV detection at 214 nm. Peak assignment: (*1*) hydroxybenzoin, (*2*) benzoin, (*3*) benzoin methyl ether. (Reproduced with permission of Elsevier from [85] © 2004)

migration order of the enantiomers of amino acids in chiral ligand exchange [89] or in the presence of vancomycin as chiral selector [90]. The effects may be explained by a change of the electrophoretic mobility of the selector upon interaction with the micelles or by a preferred partitioning of the more weakly complexed enantiomer into the micelles which will migrate with the micelles in the opposite direction compared to the situation in the absence of the micelles. Furthermore, the same effect has been observed in an MEKC system containing γ-CD upon addition of 2-propanol [91]. A switch of the enantioselectivity of the complexation in the presence of organic solvents may be considered as the underlying mechanism.

Finally, complex mobility may be the reason for a reversal of the enantiomer migration order. This mechanism applies when the phenomenon is observed as a function of the concentration of the chiral selector or the pH of the background electrolyte. Of course, the mobility of the selector–selectand complex is also exploited in several cases above, especially in the case of charged chiral selectors in combination with the application of opposite polarity of the applied voltage. However, the present case refers to the situation when reversal of the migration order is observed without altering the polarity of the voltage but just upon increasing the selector

concentration. Moreover, the phenomenon has also been observed for uncharged selectors. In the present scenario the reversal is due to an increasing influence of the enantiomer–selector complex mobilities compared to the mobility of the free analyte. As can be concluded from (8), the enantiomer migration order will not depend on the concentration of a chiral selector if both, the enantioselective affinity and the limiting mobilities of the diastereomeric complexes act in the same direction. Thus, assuming a protonated analyte and a neutral selector, the (*S*)-enantiomer will be detected before the (*R*)-enantiomer independent of the selector concentration if $K_R > K_S$ and $\mu^R_{\mathrm{cplx}} < \mu^S_{\mathrm{cplx}}$ and, in addition, the EOF does not affect the migration order. However, if $\mu^R_{\mathrm{cplx}} > \mu^S_{\mathrm{cplx}}$ and $K_R > K_S$, the enantiomer migration order may be either $S > R$ or $R > S$ depending on the magnitude of the differences of the binding constants and the mobilities of the complexes. Generally speaking, at low selector concentration a relatively low molar fraction of the analyte is complexed. Consequently, the migration order of the enantiomers is determined by their magnitude of complexation by the selector so that the more strongly complexed enantiomer migrates second because it is retarded relative to the more weakly bound enantiomer. At high selector concentrations both enantiomers are bound to a significant extent so that the migration order is determined by the mobilities of the transient diastereomeric complexes. In many cases the diastereomeric complexes possess equal mobilities so that deterioration of the enantioseparation is observed at high selector concentrations. However, in the case where the mobilities of the transient diastereomeric differ and the complex of the more strongly bound enantiomer has the higher mobility, reversal of the migration order will be observed. The mechanism was described first by Schmitt and Engelhardt in 1993 for Dns-Phe as analyte and hydroxypropyl-β-CD as selector [92]. Recent publications on this topic include [34, 93–97]. A recent example is illustrated in Fig. 8 for the separation of the enantiomers of ketoconazole in a phosphate buffer, pH 3.0, using hydroxypropyl-β-CD as chiral selector [34]. Upon increasing the CD concentration, co-migration of the peaks and subsequent reversed enantiomer migration order were observed. The behavior could be rationalized based on the apparent complexation constants, K, and the limiting mobilities of the analyte–CD complexes, μ_{cplx}, also compiled in Fig. 8. Ketoconazole is a weak base so that the compound is protonated at pH 3 and migrates towards the cathode. At low CD concentrations the more weakly complexed (2*R*,4*S*)-enantiomer migrates first. However, the tighter complex between hydroxypropyl-β-CD and the (2*S*,4*R*)-enantiomer possesses the higher electrophoretic mobility of $3.85 \pm 0.08 \times 10^{-9}\ \mathrm{m^2\ V^{-1}\ s^{-1}}$ compared to the complex of the (2*R*,4*S*)-enantiomer ($3.65 \pm 0.09 \times 10^{-9}\ \mathrm{m^2\ V^{-1}\ s^{-1}}$). Thus, when increasing the CD concentration the molar fraction of complexed analyte also increases so that the mobilities of the complexes become more and more dominant. In the present case complex mobility and stereoselectivity of the CD counteract each other. As a consequence, co-migration of the enantiomers results at first and, subsequently, an enantioseparation but with opposite migration order of the enantiomers as compared to low selector concentrations. At high CD concentrations the complex mobilities determine the migration order of the enantiomers so that the (2*S*,4*R*)-enantiomer is now detected first.

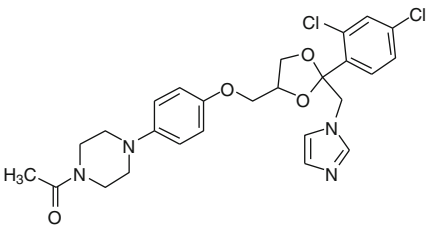

Enantiomer	K [M^{-1}]	μ_{cplx} [$m^2V^{-1}s^{-1}$ x 10^{-9}]
2R,4S	427 ± 11	3.65 ± 0.09
2S,4R	456 ± 9	3.85 ± 0.08

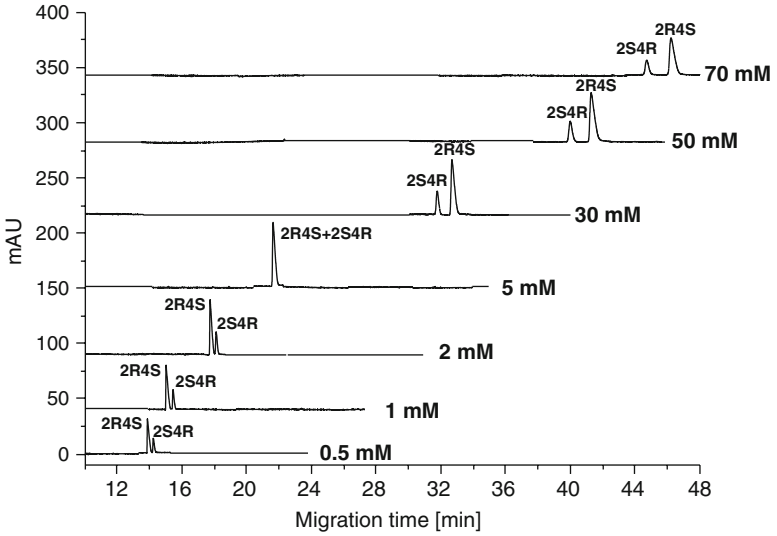

Fig. 8 Migration order of the enantiomers of ketoconazole as a function of the concentration of hydroxypropyl-β-CD as chiral selector as well as complexation constants and mobilities of the analyte–CD complexes. Experimental conditions: 56/64.5 cm, 50 μm id fused-silica capillary, 100 mM sodium phosphate buffer, pH 3.0, 15°C, 30 kV, UV detection at 200 nm. (Electropherograms reproduced with permission of Wiley from [34] © 2009)

The higher mobility of the complex of the more strongly bound enantiomer may be explained by an increased charged density resulting from a smaller size of the complex formed between the selector and the more tightly bound enantiomer as compared to the more weakly complexed enantiomer. Another phenomenon translating into a higher charge density of the stronger complex is the complexation-induced pK_a shift. A reversal of the enantiomer migration order was observed when increasing the pH of the background electrolyte in a rather narrow pH range for Dns-amino acids [36, 98] and small peptides [35, 60, 61, 80, 82, 99–101] in the range of pH = pK_a ± 2 using neutral or charged CD derivatives as chiral selectors.

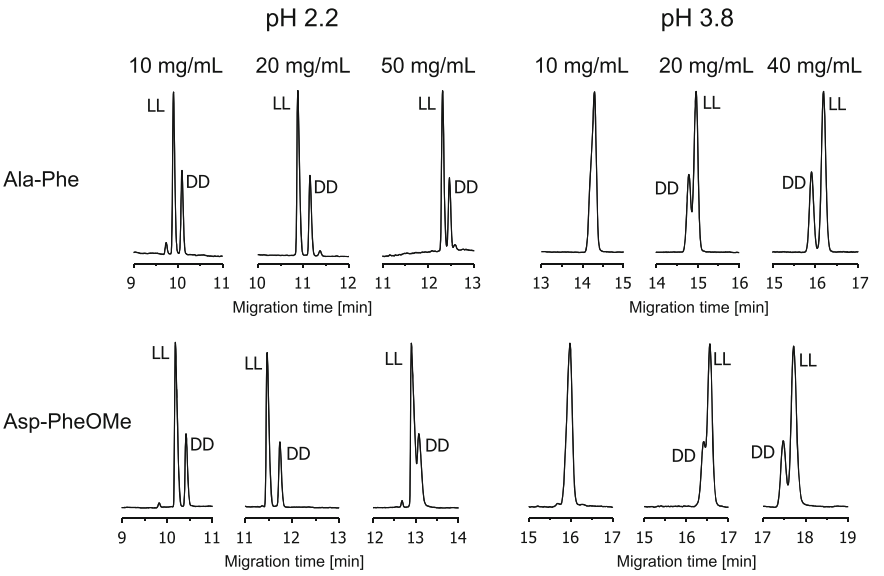

Peptide	$\mu_{H_2A^+}$ [10^{-9} $m^2s^{-1}V^{-1}$]	$\mu_{CD\text{-}H_2A^+}$ [10^{-9} $m^2s^{-1}V^{-1}$]	K_+ [M^{-1}]	K_n [M^{-1}]	pK_a	$pK_{a/cplx}$
L-Ala-L-Phe	17.9 ± 0.1	7.6 ± 0.6	34 ± 4	22 ± 4	3.26 ± 0.01	3.45 ± 0.04
D-Ala-D-Phe	17.9 ± 0.1	7.5 ± 0.5	42 ± 5	23 ± 4	3.26 ± 0.01	3.53 ± 0.04
L-Asp-L-PheOMe	17.0 ± 0.1	8.5 ± 0.3	63 ± 6	78 ± 4	3.16 ± 0.01	3.07 ± 0.02
D-Asp-D-PheOMe	17.0 ± 0.1	8.5 ± 0.3	79 ± 7	81 ± 4	3.16 ± 0.01	3.15 ± 0.02

Fig. 9 pH-dependent reversal of the migration order of the enantiomers of Ala-Phe and Asp-PheOMe using β-CD as chiral selector as well as mobilities, binding constants and pK_a values of the free analytes and the respective complexes. Experimental conditions: 50/57 cm, 50 mm id fused-silica capillary, 50 mM sodium phosphate buffer containing 2 M urea, 20°C, 25 kV, UV detection at 214 nm. (Electropherograms reproduced with permission of Wiley from [102] © 2010)

This phenomenon was attributed to a change of the pK_a value of the analyte upon complexation by the selector. If the pK_a is shifted towards higher values, the complex of the more strongly bound enantiomer has a higher overall charge compared to the complex of the more weakly bound enantiomer. The increasing contribution of the complex mobilities counteracts the enantioselectivity of the chiral selector represented by the complexation constants leading to a reversal of the enantiomer migration order at high concentrations of the selector. A recent example is the analysis of the LL- and DD-stereoisomers of the dipeptides Ala-Phe and Asp-PheOMe using β-CD as chiral selector [102]. At pH 2.2 the LL-enantiomers migrated before the DD-stereoisomers while reversed migration order was observed at pH 3.8 (Fig. 9). Complexation constants of the protonated form, K_+, and the neutral (zwitterionic) species of the peptide enantiomers, K_n, the mobilities of the

free analyte, $\mu_{H_2A^+}$, and the enantiomer–selector complexes, $\mu_{CD-H_2A^+}$, as well as the pK_a values of the complexes p$K_{a/cplx}$ can analyzed in order to rationalize the observed migration behavior. At pH 2,2 (about 1 unit below the pK_a value of the peptides), the peptides are essentially positively charged and the migration behavior is governed by the complexation constants, K_+, i.e., the selectivity of β-CD towards the protonated species. Thus, the LL-enantiomers migrate before the DD-stereoisomers. After an initial improvement of the resolution upon increasing the CD concentration, the separation deteriorated because of the increasing influence of the complex mobilities $\mu_{CD-H_2A^+}$ which are essentially equal. Furthermore, an enantioselective complexation-induced pK_a shift was found, with the higher shift of the more strongly complexed DD-enantiomers. This results in a shift of the equilibrium in favor of the protonated form of the complex at pH values close to the pK_a of the analytes. Consequently, the mobility of the complex becomes greater than the mobility of the free analyte at this specific pH value. Because the complexation constants of the neutral peptide, K_n, are essentially equal the enantiomer migration order is dominated by complex mobility. Thus, the enantiomer displaying the higher complex mobility migrates first. In the present case this applies to the DD-enantiomers, i.e., reversal of the enantiomer migration order is observed. Moreover, the resolution increases at higher CD concentrations because the friction of the complexed analyte is also increased. Similar pH-dependent reversal of the enantiomer migration order was also observed in the case of Dns-amino acids [36, 98] and other small peptides [35, 61, 80, 82, 99].

Enantiomer migration order reversal as a function of the selector concentration has also recently been described in chiral ligand exchange CE with the Cu(II)-D-quinic acid system as selector for the enantioseparation of tartaric acid in a pH 5.0 background electrolyte [103]. Keeping the concentration of Cu(II) constant at 10 mM, reversal of the enantiomer migration order was observed upon increasing the concentration of D-quinic acid from 10 to 120 mM. The same effect was observed when keeping the D-quinic acid concentration constant at 15 mM and increasing the concentration of Cu(II) from 1 to 10 mM. Subsequent spectroscopic studies proved the assumption that D-quinate acts as a bidentate ligand coordinated through the carboxylate oxygen and the C-1 hydroxyl group so that the formation of 1:1, 1:2 and 1:3 Cu(II)–D-quinate complexes is possible depending on the concentration ratio [104]. Furthermore, it was concluded from circular dichroism spectra that the 1:1 Cu(II)–D-quinate complex had a coordination selectivity for D-tartrate while the 1:2 Cu(II)–D-quinate complex displayed selectivity for L-tartrate. Thus, complexes with different stoichiometries and selectivities are formed depending on the Cu(II) D-quinic acid ratio leading to opposite enantiomer migration order. Therefore, this scenario resembles more the first situation discussed in this section where enantiomer migration order reversal is due to different selectors with different stereoselectivities rather than a reversal based on different mobilities of the selector–selectand complexes.

3.2 Theoretical Model of Enantiomer Migration Order Reversal

The dependence of the enantiomer migration order on selector concentration and pH of the background electrolyte appeared especially intriguing and has been the subject for theoretical models in order to rationalize and predict reversal of the enantiomer migration. A mathematical approach developed for a weak base and a neutral chiral selector considered the protonation equilibria of the free base and the analyte–selector complex as well as the complexation equilibria between the protonated and neutral species of the analyte with the selector [105, 106]. The effective mobility of an analyte, μ_{eff}, can be described as

$$\mu_{\text{eff}} = \frac{\mu_{\text{HB}^+} + \mu_{\text{HB}^+\text{C}} \cdot K_+ \cdot [C]}{1 + K_+ \cdot [C]} \cdot \frac{1}{1 + 10^{\text{pH} - \left(\text{p}K_\text{a} + \log \frac{1 + K_+ \cdot [C]}{1 + K_n \cdot [C]}\right)}}, \tag{17}$$

expressing μ_{eff} as a function the selector concentration, $[C]$, the pH of the background electrolyte, the pK_a value of the analyte, the binding constants of the protonated and neutral species, K_+ and K_n, and the mobilities of the protonated free species and the corresponding complex, μ_{HB^+} and $\mu_{\text{HB}^+\text{C}}$, respectively. The separation selectivity, S, is expressed as

$$\begin{aligned} S &= \frac{\mu_{\text{eff1}}}{\mu_{\text{eff2}}} \\ &= \frac{(\mu_{\text{HB}^+} + \mu_{\text{HB}^+\text{CD1}} \cdot K_{+1} \cdot [\text{CD}]) \cdot (10^{\text{p}K_\text{a}} \cdot (1 + K_{+2} \cdot [\text{CD}]) + 10^{\text{pH}} \cdot (1 + K_{n2} \cdot [\text{CD}]))}{(\mu_{\text{HB}^+} + \mu_{\text{HB}^+\text{CD2}} \cdot K_{+2} \cdot [\text{CD}]) \cdot (10^{\text{p}K_\text{a}} \cdot (1 + K_{+1} \cdot [\text{CD}]) + 10^{\text{pH}} \cdot (1 + K_{n1} \cdot [\text{CD}]))}. \end{aligned} \tag{18}$$

According to (18) a separation results from $\mu_{\text{eff1}} \neq \mu_{\text{eff2}}$ which is achieved when the enantiomers differ in the binding constants of the protonated species ($K_{+1} \neq K_{+2}$), the neutral species ($K_{\text{n1}} \neq K_{\text{n2}}$), and/or the mobilities of the two enantiomer–selector complexes ($\mu_{\text{HB}^+\text{C1}} \neq \mu_{\text{HB}^+\text{C2}}$).

Buffer pH and CD concentration are experimental variables. In a typical experiment one of them is set at a constant value so that (17) can be simplified. At a constant CD concentration μ_{eff} transforms to $\mu_{\text{eff/CD}}$:

$$\mu_{\text{eff/CD}} = \frac{\mu_{+/\text{CD}}}{1 + 10^{(\text{pH} - \text{p}K_{\text{a/CD}})}}, \tag{19}$$

where $\mu_{+/\text{CD}}$ is the effective mobility of the fully protonated analyte and p$K_{\text{a/CD}}$ is the pK_a value, both at the fixed CD concentration. $\mu_{+/\text{CD}}$ is described by

$$\mu_{+/\mathrm{CD}} = \frac{\mu_{\mathrm{HB}^+} + \mu_{\mathrm{HB}^+\mathrm{CD}} \cdot K_+ \cdot [\mathrm{CD}]}{1 + K_+ \cdot [\mathrm{CD}]}, \tag{20}$$

and $\mathrm{p}K_{\mathrm{a/CD}}$ by

$$\mathrm{p}K_{\mathrm{a/CD}} = \mathrm{p}K_{\mathrm{a}} + \log \frac{1 + K_+ \cdot [\mathrm{CD}]}{1 + K_n \cdot [\mathrm{CD}]}. \tag{21}$$

In the absence of a selector, μ_{f} is expressed by

$$\mu_f = \frac{\mu_{\mathrm{HB}^+}}{1 + 10^{(\mathrm{pH}-\mathrm{p}K_{\mathrm{a}})}}. \tag{22}$$

At an infinitely high CD concentration the complex mobility can be described by

$$\mu_c = \frac{\mu_{\mathrm{HB}^+\mathrm{CD}}}{1 + 10^{(\mathrm{pH}-\mathrm{p}K_{\mathrm{a/c}})}}, \tag{23}$$

where $\mathrm{p}K_{\mathrm{a/c}}$ is the $\mathrm{p}K_{\mathrm{a}}$ value of the diastereomeric analyte–CD complex and a function of the $\mathrm{p}K_{\mathrm{a}}$ of the free analyte and the complexation constants K_+ and K_n according to

$$\mathrm{p}K_{\mathrm{a/c}} = \mathrm{p}K_{\mathrm{a}} + \log \frac{K_+}{K_n}, \tag{24}$$

where $\mathrm{p}K_{\mathrm{a/c}}$ is the limiting value of $\mathrm{p}K_{\mathrm{a/CD}}$ for $[\mathrm{CD}] \rightarrow \infty$ according to (21) and is referred to as the complexation-induced $\mathrm{p}K_{\mathrm{a}}$ shift. At constant pH (17) can be simplified to (7). K is the apparent complexation constant defined by

$$K = \frac{K_+ + K_n \cdot 10^{(\mathrm{pH}-\mathrm{p}K_{\mathrm{a}})}}{1 + 10^{(\mathrm{pH}-\mathrm{p}K_{\mathrm{a}})}}, \tag{25}$$

where K_+, K_n, μ_{HB^+}, and $\mu_{\mathrm{HB}^+\mathrm{CD}}$ are pH-independent parameters while K, μ_{f}, and μ_{c} are pH-dependent parameters.

A systematic classification of enantiomer migration order as a function of selector concentration [CD] and buffer pH specifically considering the $\mathrm{p}K_{\mathrm{a}}$ of the analyte can be constructed as a 3D plot of the selectivity S possessing four corner points with low/high [CD] and low/high pH (Fig. 10) [105]. In each corner point the selectivity can be described as a function of the complexation equilibria between the charged and electroneutral species of the basic analyte and the selector as well as the mobility of the free analyte and the limiting mobility of the analyte–selector complexes. Depending on the conditions, only one or several of these factors will affect the selectivity. Therefore, at constant pH or selector concentration the selectivity (and with it the enantiomer migration order) parallel to the edges of the surface plot can be concluded. Knowing the selectivity in the corner points one

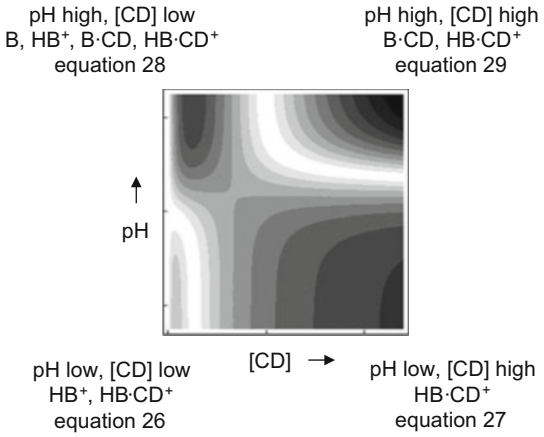

Fig. 10 Schematic representation of a 3D contour plot illustrating the low/high pH and low/high selector concentration conditions at the corner points. (Adapted with permission of Elsevier from [20] © 2011)

can deduce whether a selectivity change, i.e., reversal of the enantiomer migration order, occurs along the plot upon changing either pH or [CD].

In the mathematical treatment "low" and "high" pH with regard to analyte pK_a are defined as pH $\rightarrow -\infty$ and pH $\rightarrow +\infty$, respectively, meaning that the analyte is essentially fully protonated at "low" pH while it is basically completely deprotonated, i.e., neutral, at "high" pH. [CD] is defined between 0 (low) and $+\infty$ (high). At infinite [CD] essentially only the analyte–CD complexes exist. At [CD] = 0 enantioseparation is not possible, so that for mathematical treatment an infinitesimal CD concentration is assumed where selectivity S is derived from the first derivative $\delta S/\delta$[CD] at [CD] = 0. For $\delta S/\delta$[CD] < 0 S becomes < 1, for $\delta S/\delta$[CD] $= 0$ S becomes equal to 1, and for $\delta S/\delta$[CD] > 0 S becomes > 1.

At the vertex 1 with pH $\rightarrow -\infty$ and infinitesimal [CD] (pH low, [CD] low) basically only the non-complexed fully protonated analyte is present so that

$$\frac{\delta S}{\delta[\mathrm{CD}]} = \frac{\mu_{\mathrm{HB}^+} \cdot (-K_{+1} + K_{+2}) + \mu_{\mathrm{HB}^+\mathrm{CD1}} \cdot K_{+1} - \mu_{\mathrm{HB}^+\mathrm{CD2}} \cdot K_{+2}}{\mu_{\mathrm{HB}^+}}. \tag{26}$$

Therefore, complex mobilities and binding constants of the protonated analytes determine selectivity S and enantiomer migration order.

At the corner point 2 at pH $\rightarrow -\infty$ and [CD] $\rightarrow +\infty$ (pH low, [CD] high) essentially only the protonated analyte–CD complex exists, so that S is solely a function of the complex mobilities according to

$$S = \frac{\mu_{\mathrm{HB}^+\mathrm{CD1}}}{\mu_{\mathrm{HB}^+\mathrm{CD2}}}. \tag{27}$$

At the vertex 3 at pH $\rightarrow +\infty$ and infinitesimal [CD] (pH high, [CD] low) the analyte exists mainly in the neutral free form so that

$$\frac{\delta S}{\delta[\mathrm{CD}]} = \frac{\mu_{\mathrm{HB}^+} \cdot (-K_{n1} + K_{n2}) + \mu_{\mathrm{HB}^+\mathrm{CD1}} \cdot K_{+1} - \mu_{\mathrm{HB}^+\mathrm{CD2}} \cdot K_{+2}}{\mu_{\mathrm{HB}^+}}. \tag{28}$$

Here, S depends on the ratio of the affinity constants of the protonated analyte, K_{+1}/K_{+2}, relative to the ratio of binding constants of the neutral species, K_{n1}/K_{n2}, as well as on the dimensions of the affinity constants K_+ relative to K_n.

Finally, at the corner point 4 with pH $\rightarrow +\infty$ and [CD] $\rightarrow +\infty$ (pH high, [CD] high) the neutral, fully complexed species predominates resulting in

$$S = \frac{\mu_{\mathrm{HB}^+\mathrm{CD1}}}{\mu_{\mathrm{HB}^+\mathrm{CD2}}} \cdot \frac{K_{+1} \cdot K_{n2}}{K_{+2} \cdot K_{n1}}. \tag{29}$$

The coexisting protonated and neutral forms of the analytes are essentially complexed so that the selectivity is a function of complex mobilities as well as the binding constants of the protonated and neutral species.

Depending on the complexation constants and the complex mobilities, 15 different scenarios were classified mathematically with regard to the selectivity at the 4 corner points as summarized in Table 1 [106]. The model identifies four basic mechanisms leading to the inversion of the enantiomer migration order of a weak base in the presence of a neutral chiral selector, three in a pH-dependent manner and one as a function of the selector concentration. Further mechanisms for a reversal of the enantiomer migration order such as the use of selectors with opposite stereoselective recognition of the analyte enantiomers are not described by the model and were not considered.

A pH-dependent reversal of the enantiomer migration order is described by parallels between the corner points 1 and 3 (low [CD]) or 2 and 4 (high [CD]) of the selectivity plot (Fig. 10). It may be observed due to (1) inversion of the complex mobilities caused by an enantioselective pK_a shift, (2) inversion of the ratio of the mobilities of the analyte–selector complex and the free analyte due to a significant complexation-induced pK_a shift to a higher value, and (3) opposite chiral recognition of the protonated and the effectively electroneutral forms of the analyte by the chiral selector.

Mechanism 1 refers to the effects between the second and fourth corner points at high selector concentration. Comparing (27) and (29) it is clear that the migration order is affected by the ratio of the complexation constants $K_{+1}K_{n2}/K_{+2}K_{n1}$. Because the ratio K_+/K_n affects the protonation equilibrium of the complex [(24)] this relationship can be expressed as the difference of the pK_a values of the diastereomeric analyte enantiomer–CD complexes by $10^{\mathrm{p}K\mathrm{a/c1}-\mathrm{p}K\mathrm{a/c2}}$. Thus, the higher the ratio K_+/K_n, i.e., the more preferred the protonated form is complexed compared to the neutral species, the higher the resulting pK_a shift. Because only the protonated species contributes to the effective mobilities, the enantiomer with the higher complexation-induced pK_a

Table 1 Systematic classification of the separation selectivity with regard to the enantiomer migration order as derived from (26) to (29) in the area around the four corner points of the selectivity plot as defined by the extremes of pH and [CD][a]

	Selectivity				Enantiomer migration order reversal			
	Low pH		High pH		pH-dependent		[CD]-dependent	
Case	High [CD] (27)	Low [CD] (26)	High [CD] (29)	Low [CD] (28)	High [CD] (27–29)	Low [CD] (26–28)	Low pH (26–27)	High pH (28–29)
I	$S = 1$	$S = 1$	$S < 1$	$S < 1$	–	–	–	–
II		$S < 1$	$S = 1$	$S \leq 1$	–	–	–	–
III				$S > 1$	–	+	–	–
IV			$S < 1$	$S \leq 1$	–	–	–	–
V				$S > 1$	–	+	–	+
VI			$S > 1$	$S \leq 1$	–	–	–	+
VII				$S > 1$	–	+	–	–
VIII	$S < 1$	$S \leq 1$	$S \leq 1$	$S \leq 1$	–	–	–	–
IX				$S > 1$	–	+	–	+
X			$S > 1$	$S \leq 1$	+	–	–	+
XI				$S > 1$	+	+	–	–
XII		$S > 1$	$S \leq 1$	$S \leq 1$	–	+	+	–
XIII				$S > 1$	–	–	+	+
XIV			$S > 1$	$S \leq 1$	+	+	+	+
XV				$S > 1$	+	–	+	–

[a]A pH-dependent and selector-dependent reversal of the enantiomer migration order under the appropriate conditions is indicated by "+". For example, in the case of IX, selectivities at low pH/low [CD] and low pH/high [CD] show the same ratio compared to 1 so that no selector-dependent migration order reversal is observed as indicated by "−" in the (26–27) transition column on the right hand side of the table. In contrast, selectivities at low [CD]/low pH and low [CD]/high pH have opposite ratios which results in a pH-dependent enantiomer migration order reversal indicated by "+" in the (26–28) transition column.
(Adapted with permission of The American Chemical Society from [106] © 2010)

shift exhibits the higher pH-dependent mobility in the pH range close to the pK_a value of the analyte. An enantioselective pK_a shift can also result in a reversal of the enantiomer migration order at low selector concentration. This is observed when the difference between the complexation constants is rather small compared to the complex mobilities. A pH-dependent change in the ratio K_+/K_n is always associated with an enantioselective pK_a shift. Therefore, at low pH the affinity constants may dominate the migration order while at high pH complex mobilities will determine the order so that a reversal may be observed.

In contrast, mechanism 2, i.e., reversal of the enantiomer migration order due to a significant pK_a shift, will only be observed at low selector concentrations. The pK_a shift may be stereoselective but this must not necessarily be the case. The situation is described between the first [(26)] and third corner point [(28)] in the selectivity plot (Fig. 10). In this scenario the complexation constants dominate the enantiomer migration order and the conditions have to be fulfilled by both enantiomers. The ratio of the electrophoretic mobilities of the free species, μ_f, and the complex, μ_c,

can be reversed. At low pH, all species are essentially fully charged so that the pH-dependent mobilities μ_f and μ_c can be approximately described by the pH-independent parameters μ_{HB^+} and μ_{HB^+CD}, with $\mu_{HB^+} > \mu_{HB^+CD}$ due to the larger hydrodynamic radius of the complex. Upon increasing the buffer pH, μ_f and μ_c described by (22) and (23) are also affected by the respective protonation equilibria pK_a and $pK_{a/c}$. At low pH the ratio μ_c/μ_f can be described by μ_{HB^+CD}/μ_{HB^+} while at high pH it is described by $\mu_{HB^+CD}K_+/\mu_{HB^+}K_n$. Subsequently, reversal of the migration order will be observed when K_+/K_n exceeds μ_{HB^+}/μ_{HB^+CD}. At low pH when μ_f is higher compared to μ_c the enantiomer exhibiting the higher complexation constant migrates last while at a sufficiently high pH the more strongly complexed enantiomer migrates first when μ_c exceeds μ_f.

Probably the most obvious mechanism resulting in a pH-dependent reversal of the enantiomer migration order is mechanism 3 which is based on opposite stereoselective recognition of the analyte enantiomers as protonated and neutral species by a selector. This will lead to an inversion of the enantiomer migration order at low selector concentrations. In addition, opposite stereoselective recognition of the charged and uncharged forms will also result in differences in the K_+/K_n ratios of the enantiomers which will translate into enantioselective complexation-induced pK_a shifts (mechanism 1). Therefore a pH-dependent reversal of EMO will most likely also be observed at high selector concentrations as a function of both mechanisms. The pH-dependent reversal of the enantiomer migration order at low selector concentrations in the (27 → 29) transition column can be caused by all three mechanisms in cases VII, IX, XI, and XII, while only mechanism 2 leads to the migration order reversal in cases III, V, and XIV.

Selector concentration-dependent reversal of the enantiomer migration order can be observed at low and high pH, i.e., along the parallels to the corner points 1 and 2 (low pH) or 3 and 4 (high pH) of the selectivity plot (Fig. 10). Typically, the mobility of the free analyte, μ_f, exceeds the mobility of the complex, μ_c, due to its smaller size resulting in a higher charge density. Thus, for $\mu_c < \mu_f$ and $\mu_{c1} < \mu_{c2}$ the migration order is reversed when the affinity constant ratio K_2/K_1 exceeds $(\mu_f - \mu_{c1})/(\mu_f - \mu_{c2})$. Thus, inversion can be observed when the complex of the more strongly bound enantiomer also exhibits the higher complex mobility. The respective enantiomer will migrate last at low selector concentrations when the migration order is determined by the complexation constants but first at high selector concentrations when complex mobilities dominate. This mechanism can occur at high and low pH. At high pH where $\mu_c < \mu_f$ selector concentration-dependent reversal of the enantiomer migration order can also be observed when the more strongly complexed enantiomer possesses the lower complex mobility. In this case the ratio K_1/K_2 exceeds $(\mu_{c2} - \mu_f)/(\mu_{c1} - \mu_f)$.

The mechanism described for $\mu_c < \mu_f$ applies to all cases of selector-dependent reversal of the enantiomer migration order at low pH as indicated in (26) and (27), and the transition column in Table 1, and at high pH in the (28–29) column in cases VI, X, and XIII. The situation described for $\mu_c < \mu_f$ causes reversed migration order at high pH for cases V and XIV. In case IX both mechanisms can apply.

As an example of the pH dependent reversal of the enantiomer migration order illustrating the model, the enantioseparations of the LL- and DD-enantiomers of

Ala-Tyr and Asp-PheOMe using 2,6-dimethyl-β-CD as chiral selector were selected [105]. While Ala-Tyr displayed a pH-dependent inversion of the migration order of the enantiomers, Asp-PheOMe did not (Fig. 11a). At pH 2.2, the LL-enantiomer of Ala-Tyr migrated first with the enantioseparations deteriorating at higher concentrations. At pH 3.0, no separations were observed, while at pH 3.8, selectivity initially increased with increasing CD concentrations, quickly reaching a plateau. At pH 3.8 D-Ala-D-Tyr migrated before L-Ala-L-Tyr. The experimentally determined pH-independent parameters, μ_{HB^+}, μ_{HB^+CD}, K_+, and K_n, as well as pK_a and p$K_{a/c}$, are summarized in Table 2 and were used to calculate the selectivity curves shown in Fig. 11b. At pH 2.2 and 3.0 the curves also predicted a selector concentration-dependent reversal of the migration order that was not experimentally observed, probably due to the low resolution counteracted by diffusion phenomena. The separation behavior of Ala-Tyr could be rationalized based on these data. D-Ala-D-Tyr is complexed more strongly by the CD than the LL-enantiomer over the entire pH range. K_+ values are about ninefold higher than the K_n values, resulting in a pK_a shift of almost one unit (Table 2). Therefore, a reversal of the mobility ratio of the peptide–CD complex and the free analyte results when increasing the buffer pH in the vicinity of the pK_a of the peptide. At low selector concentrations, the more strongly complexed DD-enantiomer migrates more slowly than L-Ala-L-Tyr at pH 2.2 when the protonated form dominates and first when the pH is raised to pH 3.8. The deteriorating effect of increased selector concentrations at pH 2.2 is caused by the increasing influence of μ_{HB^+CD}, which differs only slightly between the enantiomers if at all. At pH 3.0, no separation is observed as the mobilities of the free from and the analyte–CD complexes differ only slightly.

A pH-dependent reversal of the enantiomer migration order was not observed for Asp-PheOMe in the presence of 2,6-dimethyl-β-CD, as can easily be rationalized from the pH-independent complexation constants and mobilities listed in Table 2; the separation selectivity is shown in Fig. 11b. Only a minor non-enantioselective pK_a shift and essentially identical $\mu_{HB^+\times CD}$ values were found for the enantiomers. The migration behavior of the Asp-PheOMe enantiomers can be rationalized using the complexation and mobility data. D-Asp-D-PheOMe is complexed more strongly than the LL-enantiomer in both, the protonated as well as the zwitterionic species. As μ_{HB^+CD} and pK_a values of both enantiomers are identical, the pH-dependent complex mobilities, μ_c, of both enantiomers are essentially equal in the pH range close to the pK_a of the analyte. Moreover, the mobility of the free analyte always exceeds μ_c due to the minor pK_a shift. Thus, the LL-enantiomer always migrates in front of the DD-isomer independent of the buffer pH. Due to the slightly weaker interaction of the zwitterionic form with the CD, the ratio of the mobilities of free and complexed analytes decreases upon increasing the buffer pH, resulting in a deteriorated separation selectivity at higher pH values.

The theoretical model has also been used to analyze the effect of pH on complex formation between β-CD and the migration order of the enantiomers of the dipeptides Ala-Phe, Ala-Tyr, and Asp-PheOMe [102].

Gas and coworkers recently developed the software Simul 5 Complex that allows the simulation of analyte separation by CE including the effects of complexation

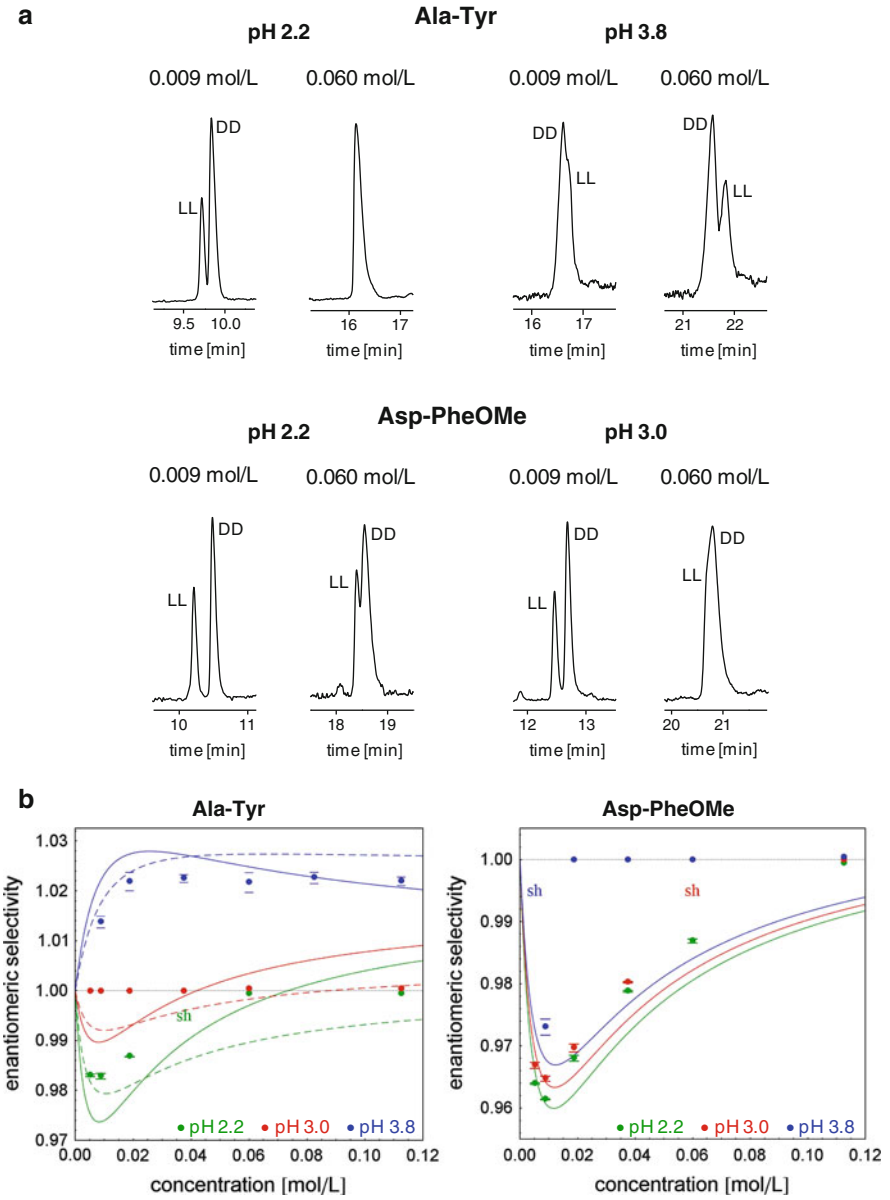

Fig. 11 (**a**) Electropherograms of the separation of the LL- and DD-enantiomers of Ala-Tyr and Asp-PheOMe using 2,6-dimethyl-β-CD as chiral selector. Experimental conditions: 40/50.2 cm, 50 μm id fused-silica capillary, 20°C, 25 kV, UV detection at 214 nm, pH 2.2: 60 mM sodium phosphate buffer, pH 3.0: 40 mM sodium phosphate buffer, pH 3.8: 30 mM sodium aspartate buffer. (**b**) Selectivity plots as a function of the CD concentration at pH 2.2 (*green*), 3.0 (*red*), and 3.8 (*blue*). The *symbols* represent the experimentally determined values, *sh* indicates a shoulder. (Adapted with permission of The American Chemical Society from [105] © 2009)

Table 2 Apparent mobilities and equilibrium constants describing the complexation of the LL- and DD-enantiomers of the Ala-Tyr and Asp-PheOMe by 2,6-dimethyl-β-CD as chiral selector

	Ala-Tyr		Asp-PheOMe	
Parameter	DD	LL	DD	LL
μ_{HB^+} (10^{-9} m^2 s^{-1} V^{-1})	15.88 ± 0.07		15.66 ± 0.08	
$\mu_{HB\cdot CD^+}$ (10^{-9} m^2 s^{-1} V^{-1})	6.68 ± 0.06	6.55 ± 0.06	5.89 ± 0.09	5.84 ± 0.10
K_+ (L/mol)	165 ± 7	139 ± 6	141 ± 6	116 ± 5
K_n (L/mol)	18.5 ± 1.5	15.0 ± 1.5	114 ± 7	94 ± 6
pK_a	3.12 ± 0.01		2.99 ± 0.01	
p$K_{a/c}$	4.07 ± 0.03	4.08 ± 0.03	3.08 ± 0.02	3.08 ± 0.02

Data reproduced with permission of The American Chemical Society from [105] © 2009

equilibria [107–109]. The program is based on separation selectivity analogous to (18) and can handle neutral and charged analytes as well as selectors. It also considers electromigration dispersion caused by the complexation. One of the examples used for the verification of the software was the above-mentioned enantioseparation of the LL- and DD-enantiomers of Ala-Tyr using 2,6-dimethyl-β-CD as chiral selector. The 3D plot of the selectivity as a function of the pH of the background electrolyte and CD concentration as well as the calculated electropherograms at pH 1.91 and 4.51 are shown in Fig. 12 [109]. They are in excellent agreement with the experimental data shown in Fig. 11. At low pH (pH 1.91 in the simulation and pH 2.2 in the experiments described in [105]) the enantiomers can be separated at low CD concentrations and the separation deteriorates when increasing the selector concentration. At high pH (pH 3.8 in the experiments vs pH 4.51 in the simulations) only partial separation of the enantiomers was observed. The simulations revealed electromigration dispersion as one of the main reasons for the poor enantioseparation at these pH values.

The simulation also demonstrated an interesting fact. At pH values higher than the pK_a of the analyte, the effective mobilities of the enantiomers increase with increasing selector concentrations because the complexation constants of the neutral forms are smaller compared to the charged species (Table 2). As the mole fraction of the charged complexed forms increase with increasing selector concentrations, the effective mobilities also increase. Therefore it was concluded that a pH value must exist where the effective mobilities of the enantiomers are independent of the CD concentration. As can be concluded from Fig. 12a, this pH value is between 3 and 4; the exact values were 3.393 for the LL-enantiomer and 3.405 for L-Ala-L-Tyr [109].

4 Chiral Selectors and Selector-Analyte Complex Structures

Many structurally diverse chiral compounds have been investigated as chiral selectors in CE including CDs, macrocyclic glycopeptide antibiotics, proteins, crown ethers, chiral ligand-exchangers, chiral ionic liquids, and chiral surfactants derived from

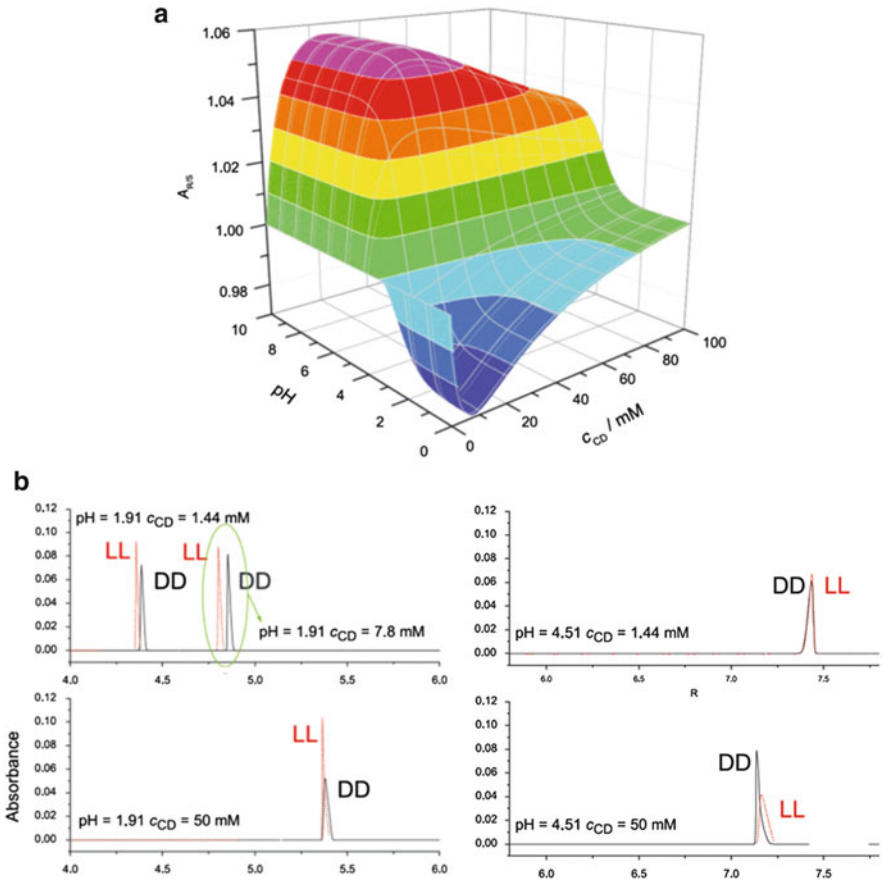

Fig. 12 Modeling of the enantioseparation of Ala-Tyr using 2,6-dimethyl-β-CD as chiral selector by Simul 5 Complex. (**a**) 3D contour plot of the separation selectivity as a function of the pH of the background electrolyte and the concentration of the chiral selector and (**b**) calculated electropherograms at pH 1.91 and pH 4.51 at CD concentrations of 1.44 and 50 mM. The *black solid line* represents D-Ala-D-Tyr while the *red dashed line* represents L-Ala-L-Tyr. (Adapted with permission of Wiley from [109] © 2012)

steroids, amino acids, tartaric acid, or glycosides [23, 24, 110]. Depending on the chiral selector and the analyte enantiomers, formation of the diastereomeric selector–selectand complexes is driven by several types of interactions including ionic interactions, ion-dipole or dipole-dipole interactions, hydrogen bonds, van der Waals interactions, or π–π interactions. Ionic interactions are strong and may be primarily involved in the "initial" contact because of their long range nature. However, they may not be stereoselective because both enantiomers are able to establish such interactions in contrast to short range interactions such as hydrogen bonds or π–π interactions. For an enantioseparation at least one interaction between selector and the analyte enantiomers has to be stereoselective. Finally, selector–selectand interactions

may be attractive or repulsive and at least one attractive interaction must exist in order to allow the formation of one of the two possible diastereomeric complexes. The following part will briefly highlight the most frequently applied chiral selectors and the current understanding of their chiral recognition mechanisms. A comprehensive summary of the chiral recognition mechanisms of chiral selectors can be found in [111–114].

Besides structure-separation studies, varying either the structure of the analytes or the selectors, spectroscopic techniques including UV spectroscopy, fluorimetry, Fourier transformation and attenuated total reflectance IR spectroscopy, NMR spectroscopy as well as circular dichroism and vibrational circular dichroism (VCD) spectroscopy have been employed. Especially NMR techniques, including nuclear Overhauser effect (NOE) and rotating-frame Overhauser enhancement spectroscopy (ROESY), have the advantage of allowing conclusions about the spatial proximity of atoms or substitutents [115–119]. The structure of the selectand–selector complex in the solid state can be obtained by X-ray crystallography while molecular modeling is very useful for the illustration of selector–selectand complexes [120]. Finally, chemoinformatic methods have also been applied [121].

4.1 Cyclodextrins

CDs are by far the most often applied chiral selectors in CE as documented in many reviews [122–129]. This is due to their UV-transparency as well as enantiodifferentiation ability towards compounds with a broad structural variety and commercial availability. Numerous separation scenarios can be realized.

CDs are cyclic oligosaccharides composed of α(1 → 4) linked D-glucose molecules. The most important CDs are α-CD, β-CD, and γ-CD consisting of 6, 7, and 8 glucose units, respectively, which form a hollow torus with a lipophilic cavity and a hydrophilic outside. The wider rim is formed by the secondary 2- and 3-hydroxyl groups of the glucose molecules while the primary 6-hydroxyl groups form the primary rim. The top (secondary rim) and bottom (primary rim) diameters of the cavities of the CDs are approximately 5.3 and 4.7 Å in the case of α-CD, 6.5 and 6.0 Å for β-CD, and 8.3 and 7.5 Å for γ-CD [130]. The hydroxyl groups can be derivatized yielding a large variety of CD derivatives containing uncharged or charged substituents (Table 3). Native CDs and CD derivatives have been used for enantioseparations in EKC employing aqueous and non-aqueous background electrolytes as well as in MEKC and MEEKC.

Numerous techniques including thermodynamics, mass spectrometry, X-ray crystallography, molecular modeling, and especially NMR spectroscopy [115–117] have contributed to the current understanding of the structures of CD–analyte complexes. The 1:1 complexes are generally assumed but complexes with other stoichiometry such as 2:1, 2:2, or higher order equilibria also exist. Complexation often involves inclusion of lipophilic parts of the analytes into the CD cavity displacing solvent molecules (in most cases water) from the cavity [130]. Hydrophobic and van der Waals interactions are believed to be primarily involved but hydrogen bonding

Table 3 Examples of commercially available CDs

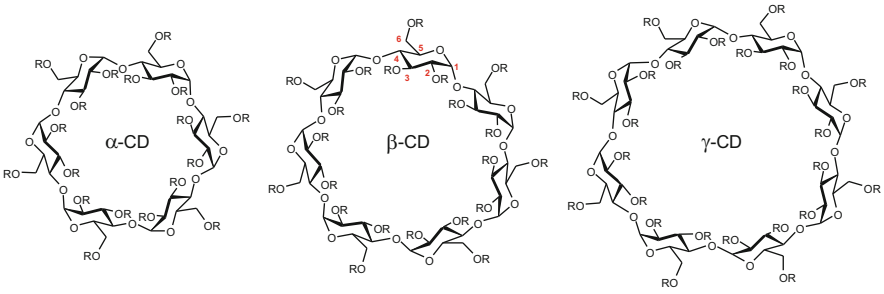

Derivative	Substituents
Native CDs	
α-CD	H
β-CD	H
γ-CD	H
Neutral CDs	
Methyl-α-CD	CH_3, randomly substituted
Methyl-β-CD	CH_3, randomly substituted
Heptakis-2,6-dimethyl-β-CD	CH_3 in positions 2 and 6
Heptakis-2,3,6-trimethyl-β-CD	CH_3 in positions 2, 3 and 6
Hydroxypropyl-α-CD	CH_2–CH_2–CH_2–OH, randomly substituted
Hydroxypropyl-β-CD	CH_2–CH_2–CH_2–OH, randomly substituted
Hydroxypropyl-γ-CD	CH_2–CH_2–CH_2–OH, randomly substituted
Negatively charged CDs	
Carboxymethyl-β-CD	CH_2–COONa, randomly substituted
Sulfated α-CD	SO_3Na, randomly substituted
Sulfated β-CD	SO_3Na, randomly substituted
Sulfated γ-CD	SO_3Na, randomly substituted
Sulfobutyl-β-CD	CH_2–CH_2–CH_2–CH_2–SO_3Na, randomly substituted
Heptakis-6-sulfo-β-CD	SO_3Na in position 6
Heptakis-(2,3-diacetyl-6-sulfo)-β-CD	CH_3CO in positions 2 and 3, SO_3Na in position 6
Heptakis-(2,3-methyl-6-sulfo)-β-CD	CH_3 in positions 2 and 3, SO_3Na in position 6
Positively charged CDs	
2-Hydroxy-3-trimethylammoniopropyl-β-CD	CH_2–CH(OH)–CH_2–$N(CH_3)_3Cl$, randomly substituted
6-Monodeoxy-6-monoamino-β-CD	NH_2 instead of one 6-OH group

with the glucose hydroxyl groups and steric factors also contribute. In the case of CD derivatives, interactions with the substituents also have to be considered, such as ionic interactions for CDs containing charged substituents. The increased strength of the complexation based on ionic interactions between oppositely charged analytes and CDs often allows the use of very low selector concentrations. Depending on the analyte, the inclusion into the cavity can occur from the narrow primary side or the wider secondary side. For example, opposite enantiomer migration order of the enantiomers of ephedrine was observed using β-CD as compared to α-CD and the negatively charged heptakis(2,3-di-*O*-acetyl-6-*O*-sulfo)-β-CD as chiral selectors in an

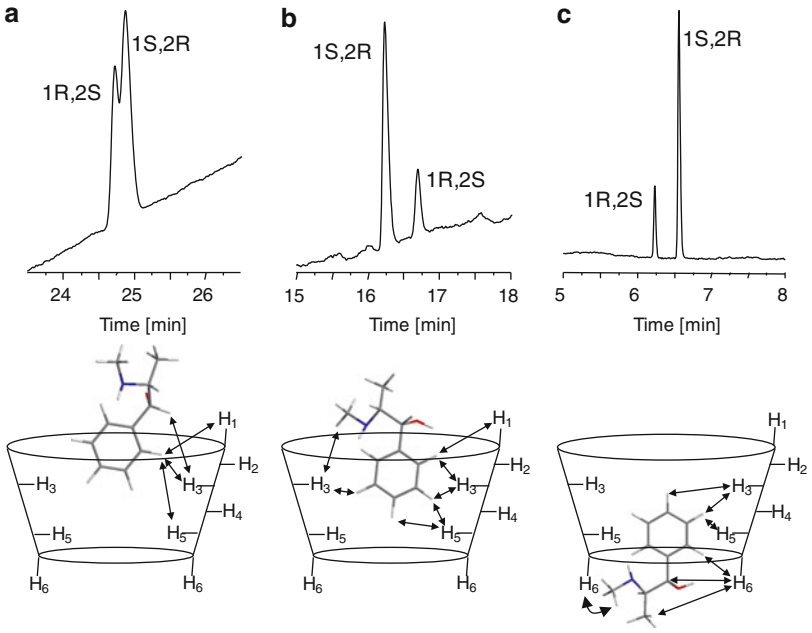

Fig. 13 Separation of the enantiomers of ephedrine in 200 mM sodium phosphate buffer, pH 2.5, as background electrolyte (*top*) and schematic structures of the cyclodextrin–ephedrine complexes as derived from ROESY measurements (*bottom*). The *arrows* indicate the NOE observed upon irradiation of the respective protons. (**a**) α-CD, (**b**) β-CD, and (**c**) heptakis(2,3-di-*O*-acetyl-6-*O*-sulfo)-β-CD. (Reproduced with permission of Wiley from [52] © 2011)

acidic background electrolyte (Fig. 13) [52]. As derived from subsequent NMR studies, the aromatic ring of ephedrine was included only partially into the cavity of α-CD from the secondary wider opening (Fig. 13a), while it penetrated β-CD more deeply also from the secondary side (Fig. 13b). In contrast, the compound entered heptakis(2,3-di-*O*-acetyl-6-*O*-sulfo)-β-CD from the narrower, primary side (Fig. 13c). Thus, the enantiomer migration order cannot be established from the structures of the complexes and, furthermore, small differences such as the depth of inclusion may result in opposite migration order as shown for α-CD and β-CD. The negatively charged derivative heptakis(2,3-di-*O*-acetyl-6-*O*-sulfo)-β-CD led to the same migration order as compared to α-CD under otherwise identical experimental conditions, i.e., a migration order opposite to the order observed for the underivatized native analogue β-CD. However, the structure of the analyte–CD complex was entirely different from the native CDs because the aromatic moiety was inserted into the cavity from the narrower primary side. Similar observations were made for the related analyte norephedrine [53]. Another example for the formation of inclusion complexes either via the wider or the narrower opening is the interaction between propranolol and β-CD or heptakis(6-*O*-sulfo)-β-CD where inclusion of the naphthyl ring occurs from the secondary side in the case of β-CD and from the narrow primary side in the case of heptakis(6-*O*-sulfo)-β-CD [131]. Furthermore, different moieties of a molecule may

interact with different CDs as shown for the combination of clenbuterol with β-CD and heptakis(2,3-di-*O*-acetyl)-β-CD, respectively [132]. The phenyl ring of the drug enters β-CD through the wider opening while the *tert*-butyl moiety of the compound is included in the cavity of heptakis(2,3-di-*O*-acetyl)-β-CD, also from the wider side. Opposite enantiomer migration order was observed. Different complex structures and, consequently, different migration order were also found for ketoprofen and 2,3,6-trimethyl derivatives of α-CD, β-CD, and γ-CD [54].

It has also been demonstrated that inclusion complexation is not a prerequisite for CD-mediated enantioseparations. Thus, effective resolution of the enantiomers propranolol [62] and bupivacaine [64] in the presence of heptakis(2,3-di-*O*-acetyl-6-*O*-sulfo)-β-CD as chiral selector were noted in CE experiments while no apparent interaction with the cavity of the CDs could be observed by NMR in the respective studies. Similar results were found for talinolol and heptakis(2,3-di-*O*-methyl-6-*O*-sulfo)-β-CD in aqueous background electrolytes as well as heptakis(2,3-di-*O*-acetyl-6-*O*-sulfo)-β-CD in non-aqueous electrolyte solutions [56]. Moreover, the structure of the complex can depend on the nature of the background electrolyte as demonstrated for propranolol and sulfated β-CD derivatives in aqueous and non-aqueous buffers [62]. Thus, inclusion of the aliphatic side chain of propranolol into the cavity of heptakis(2,3-di-*O*-acetyl-6-*O*-sulfo)-β-CD from the wider opening occurred in a non-aqueous background electrolyte while only an external complex was formed between propranolol and the CD in aqueous buffers. In the case of heptakis(2,3-di-*O*-methyl-6-*O*-sulfo)-β-CD, the opposite behavior was observed, i.e., an inclusion complex in aqueous electrolyte solutions and an external complex in a methanol-based background electrolyte. Moreover, the naphthyl moiety was enclosed via the narrower rim into the cavity of heptakis(2,3-di-*O*-methyl-6-*O*-sulfo)-β-CD. In the case of heptakis(2,3-di-*O*-methyl-6-*O*-sulfo)-β-CD, opposite enantiomer migration order was observed in aqueous and non-aqueous background electrolytes which could be rationalized based on the complex structures under the respective conditions. Only a few studies also reported spectroscopic proof of structural differences between the diastereomeric complexes. Enantioselective peak splitting due to non-equivalence of the complexation-induced chemical shifts for the propranolol enantiomers in the presence of heptakis(2,3-di-*O*-acetyl-6-*O*-sulfo)-β-CD was observed in aqueous as well as non-aqueous solutions, clearly indicating different complex geometries in the case of the aqueous solutions where an inclusion complex is apparently not formed [63]. With regard to the inclusion complex formed in non-aqueous electrolytes, (*S*)-propranolol apparently formed a tighter complex as the side chain of the molecule was inserted deeper into the CD cavity compared to the (*R*)-enantiomer. The data obtained from NMR measurements were supported by a molecular modeling study [64]. A higher interaction energy was calculated for the complex between heptakis-(2,3-di-*O*-acetyl-6-*O*-sulfo)-β-CD and (*S*)-propranolol than for the respective complex with (*R*)-propranolol, indicating the formation of a stronger complex in the case of the (*S*)-enantiomer. The modeling structures of the complexes are shown in Fig. 14. In accordance with the NMR data [63], the side chain of the (*S*)-enantiomer deeply penetrates the CD cavity through the wider secondary side. An electrostatic interaction appears to exist between the

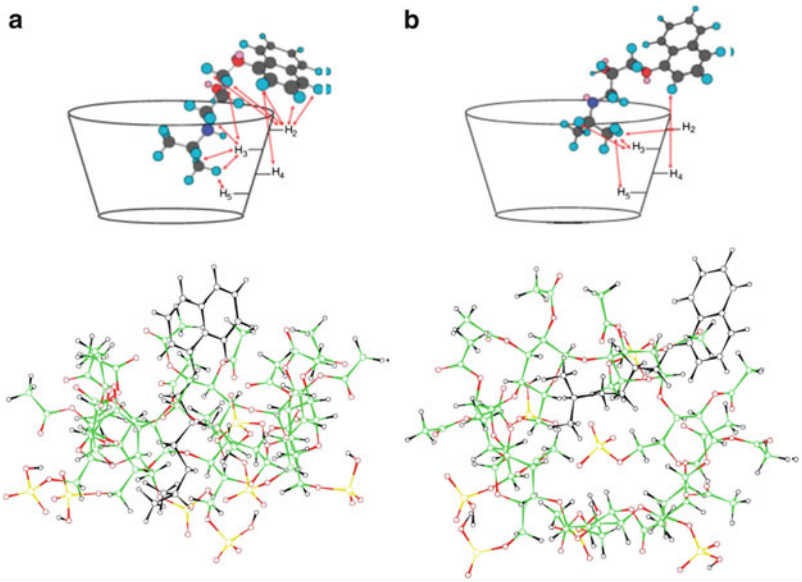

Fig. 14 Structures of the complexes of (*S*)-propranolol (**a**) and (*R*)-propranolol (**b**) with heptakis (2,3-di-*O*-acetyl-6-*O*-sulfo)-β-CD. *Top*: Schematic structures as derived from ROESY experiments. The *arrows* indicate the NOE observed upon irradiation of the respective protons. *Bottom*: Molecular modeling structure of the complexes. The atoms of propranolol are shown in *black*, the carbon, hydrogen, oxygen, and sulfur atoms are colored in *green*, *black*, *red*, and *yellow*, respectively. (Top structures reproduced with permission of Wiley from [63] © 2011; bottom structures reproduced with permission of Elsevier from [64] © 2012)

extended side chain and the sulfate groups located at the primary rim of the CD. In the case of the (*R*)-enantiomer, the side chain enters the cavity less deeply. Stereoselective complexation of the dipeptides Ala-Phe and Ala-Tyr by β-CD and sulfated derivatives was also derived from NMR studies [133, 134].

Finally, buffer additives can also affect the structure of the analyte–CD complex. Thus, it was shown by NMR measurements and molecular modeling that the enantiomers of the dipeptide Ala-Tyr in the protonated state penetrated deeper into the cavity of β-CD in the presence of urea compared to in the absence of urea [133]. This resulted in higher peak resolution in β-CD-mediated CE enantioseparations in the presence of urea in the background electrolyte. Another example is the complex between β-CD and naproxen when adding 1,2-dibromoethane [135]. In the presence of 1,2-dibromoethane naproxen enters the CD cavity from the wider secondary side while inclusion from the narrower primary side of β-CD occurs in the absence of 1,2-dibromoethane.

Summarizing, substantial structural differences between the analyte–CD complexes as derived from NMR spectroscopy or molecular modeling can rationalize the migration behavior observed in CE experiments. However, minor differences in complex structure (such as depth of insertion into the cavity) may also affect the chiral recognition of selectors towards analyte enantiomers which is translated into opposite enantiomer migration order in CE. In other cases entirely different types of

complexes had no apparent effect on the migration behavior. Therefore, significant differences in the enantiomer–CD complex structures do not appear to be a prerequisite in order to observe reversed enantiomer migration order in CE.

4.2 Macrocyclic Antibiotics

Macrocyclic glycopeptides are also called macrocyclic antibiotics due to their medical applications. The most important representatives used as chiral selectors in CE are vancomycin, ristocetin, teicoplanin, and the teicoplanin aglycone. The common structural feature of this class of compounds is a heptapeptide as a set of interconnected macrocylces each composed of two aromatic rings and a peptide sequence. Vancomycin contains three macrocycles while teicoplanin and ristocetin A are composed of four. The macrocycles form a three-dimensional, C-shaped basket-like structure with the carbohydrate moieties positioned at the surface. Due to the presence of ionizable groups, such as a carboxylic acid group or amino groups, a large number of interactions between analyte molecules and the glycopeptides antibiotics are possible, including hydrogen bonds, π–π, dipole–dipole, and ionic interactions depending on the experimental conditions [136]. The detailed recognition mechanism on a molecular basis has not been studied in detail yet. Mechanisms deduced from structure-separation studies using various classes of analytes were examined. However, detailed NMR studies or X-ray crystallographic studies with respect to chiral separations have not been published to date except for vancomycin and small ligands such as D-lactic acid, *N*-acetyl-Ala or *N*-acetyl Gly [137], or vancomycin with the tripeptide ligand N_{α},N_{ω}-diacetyl-L-Lys-D-Ala-D-Ala [138] as shown in Fig. 15, as well as the glycopeptide balhimycin and D-Ala-D-Ala [139]. A molecular docking has been performed for macrocyclic antibiotic selectors and chiral xanthone analytes [140]. The application of macrocyclic glycopeptides as chiral selectors in CE has been summarized [11, 141, 142].

4.3 Crown Ethers

Chiral crown ethers form complexes with protonated primary amines so that their use is essentially limited to this group of analytes, although some exceptions have been reported. In CE only (+)-(18-crown-6)-2,3,11,12-tetracarboxylic acid [(+)-18C6H4] has been employed as summarized in [143, 144]. Complex formation is due to hydrogen bonds between the protonated amino group and oxygen atoms of the crown ether. For chiral recognition (+)-18C6H4 adopts an asymmetric C1-type conformation exhibiting a bowl-like shape with the N–H and Cα-H protons of the amino acid interacting with the oxygen atoms of the ring system as well as the carboxylate groups [145]. This asymmetric C1-type shape is assumed to result from a conformational sequence of successive rotations in the macrocycle which appear to be promoted by protons. The diastereomeric complexes between the analyte enantiomers and

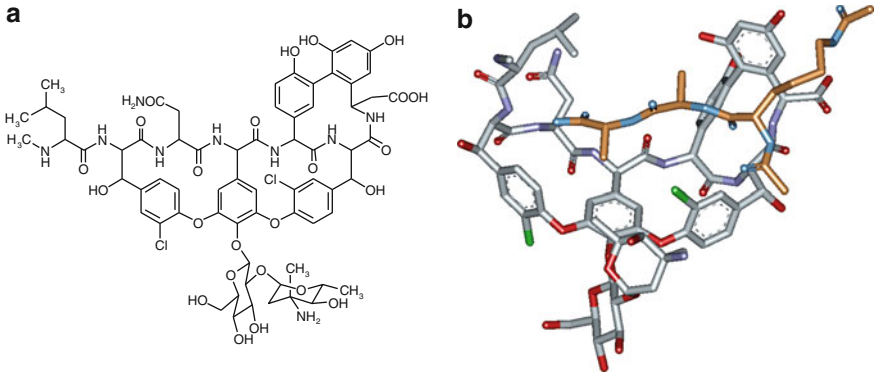

Fig. 15 Structure of vancomycin (**a**) and X-ray crystal structure of the complex of vancomycin with N_{α},N_{ω}-diacetyl-L-Lys-D-Ala-D-Ala (**b**). Vancomycin is shown in *gray* and the ligand in *orange*. Oxygen, nitrogen, and chlorine atoms are colored in *red*, *blue* (ligand) or *violet* (vancomycin), and *green*, respectively. The X-ray structure image was generated with the Accelrys Discovery Studio Visualizer 2.5 software from the coordinates deposited in the Brookhaven Protein Data Bank (www.rcbs.org/pdb, file 1FVM)

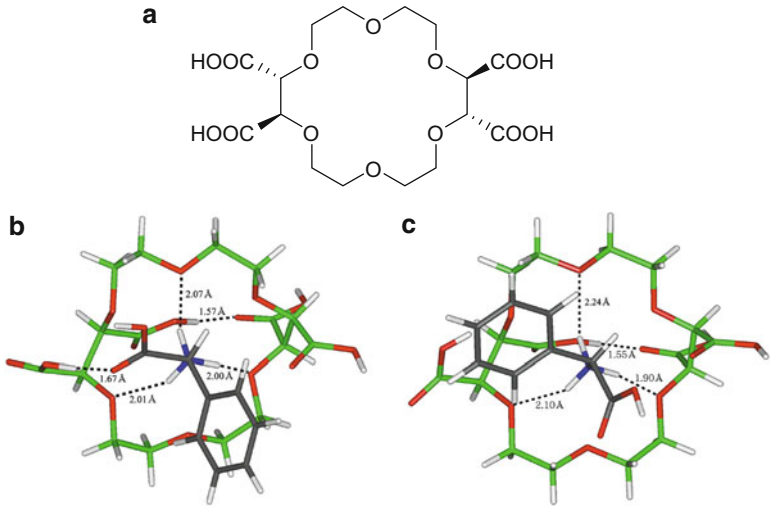

Fig. 16 Structure of (+)-(18-crown-6)-2,3,11,12-tetracarboxylic acid (**a**) and modeling structures of the complexes of the crown ether with protonated D-phenylglycine (**b**) and L-phenylglycine (**c**). The modeling structures were generated from NOE and molecular dynamics calculations. Hydrogen bonds are shown as *dotted lines*. (**a** and **b** reproduced with permission of The Royal Society of Chemistry from [146] © 2001)

(+)-18C6H4 displayed differences. For example, as demonstrated for phenylglycine, the more strongly complexed D-enantiomer exhibited a more favorable complex geometry and an additional hydrogen bond compared to the more weakly bound L-enantiomer as derived from NMR and molecular modeling (Fig. 16) [146]. A slightly different

structure of the more weakly bound L-phenylglycine featuring two hydrogen bonds with ring oxygen atoms and one with a carboxylic acid group has also been derived [147]. Further examples of differences in the structures of complexes between (+)-18C6H4 and amino acid enantiomers have been reported [148–150].

4.4 Ligand Exchange

Chiral ligand exchange was the first principle applied in CE for analyte enantioseparations [3]. This technique is based on the formation of ternary chelate complexes between ligands and a central metal atom. Amino acid derivatives are most frequently employed as chelating agents although D-quinic acid, D-gluconic acid, D-saccharic acid, or L-threonic acid have also been used as complexation agents [151]. The metal ions include divalent metal ions such as Cu^{2+}, Zn^{2+}, or Ni^{2+}. Enantioseparation by ligand exchange is restricted to analytes with two or three electron-donating groups such as amino acids, hydroxy acids, amino alcohols, or diols. In addition, borate can serve as central ion in a CE ligand exchange system in combination with diols as ligands for the separation of the enantiomers dihydroxy analytes [152]. Applications of ligand exchange for CE enantioseparations have been summarized, for example, in [151–154].

Ligand exchange is based on the reversible coordination of a chiral analyte into the sphere of a metal ion which is complexed with an enantiopure chelator, resulting in a selectand–metal ion–selector complex. The resulting diastereomeric chelates possess different thermodynamic formation ratios or stabilities. It is assumed that ternary complexes with a 1:1:1 stoichiometry are formed, although complexes with other stoichiometries such as 1:2:1 have also been reported for the system D-quinic acid–Cu(II)-tartrate depending on the configuration of the tartrate analyte [104]. Moreover, it should be kept in mind that the ligand exchange process does not necessarily has to be ascribed to the ligand in the Me–$(ligand)_2$ complex but can also occur by exchange with water molecules that complete for the coordination sphere of the metal ion, i.e., the Me–ligand–$(H_2O)_2$ complex [155, 156]. In addition, the ternary complex between selector, central ion, and analyte is uncharged and therefore does not possess an electrophoretic mobility in CE in contrast to the binary complex $[Me–analyte]^+$ [156]. Consequently, the different stabilities of the diastereomeric complexes result in a different distribution of charged species (free analyte and binary complexes) of the enantiomers. It has also been demonstrated that the ionization status of the analyte ligand may affect the stability of the diastereomeric mixed complexes. Thus, different stereoselectivities of complex formation have been observed whether the analyte enantiomers are charged or uncharged [157, 158]. The structures of the diastereomeric ternary complexes L-Pro–Cu(II)–L/D-Thr are shown in Fig. 17 as an example [159].

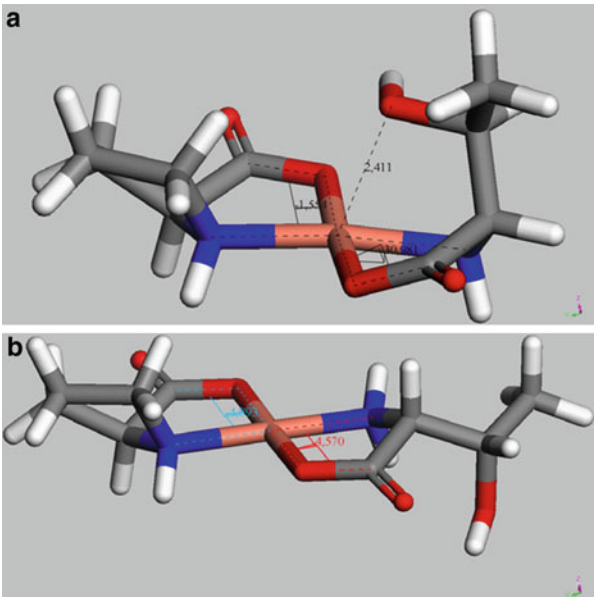

Fig. 17 Molecular modeling structure of the ternary L-proline–Cu(II)–threonine complex containing (**a**) L-threonine and (**b**) D-threonine. (Reproduced with permission of Elsevier from [159] © 2010)

4.5 Chiral Surfactants

Chiral micelles are formed from monomeric chiral surfactants in aqueous solution at concentrations above the critical micelle concentration. Furthermore, polymeric micelles (molecular micelles) have been developed [46, 160] in order to overcome the disadvantages of "classical" micelles such as the dynamic equilibrium between the surfactant monomers in the aqueous phase and the micelles. Polymeric micelles are obtained by polymerization of suitably functionalized surfactants via the hydrophobic tails. Chiral surfactants with a large structural variety are available including bile acid derivatives or surfactants derived from amino acids or carbohydrates (Fig. 18a). Molecular micelles are based on surfactants derived from amino acids or dipeptides (Fig. 18b). Reviews on the application of chiral micelles in enantioseparations can be found, for example, in [161, 162].

The chiral recognition process for chiral micelles has been less frequently addressed, probably due to the complex and dynamic structure of micelles that are difficult to assess by spectroscopic techniques. Compared to the (*R*)-enantiomer, the (*S*)-enantiomer of 1,1′-binaphthyl-2,2′-diyl hydrogen phosphate (BNDHP) appeared to interact more strongly with micelles formed by sodium cholate as derived from NMR experiments in accordance with the elution order in MEKC [163]. The naphthyl moieties are inserted into the micelle, leading to a discrimination of the analyte enantiomers.

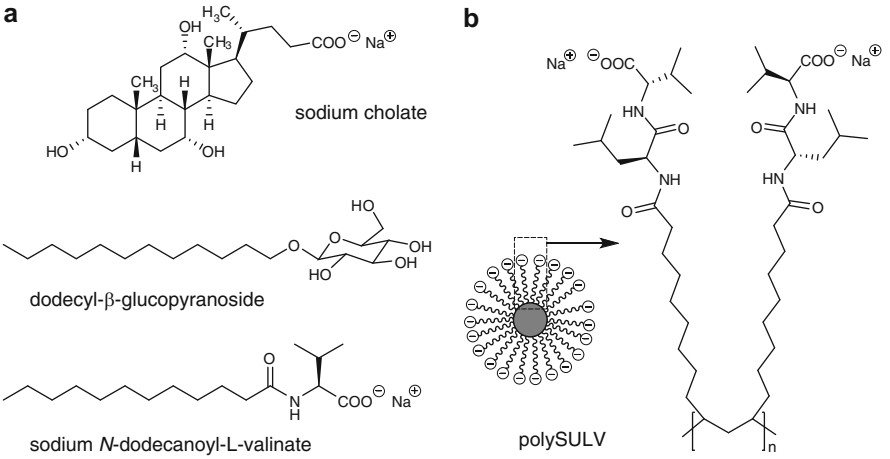

Fig. 18 Structures of chiral surfactants (**a**) and schematic representation of a chiral polymeric micelle of poly(sodium *N*-undecanoyl-L-leucyl-L-valinate (**b**)

Dipeptide-based surfactants seem to adopt a folded conformation in aqueous solutions, creating a chiral pocket into which analytes can be accommodated. In the case of BNDHP, the N-terminal amino acid of the dipeptide head group appears to be the primary site of chiral recognition in monomeric [164] as well as polymeric surfactants [165, 166]. As a consequence, the configuration of the amino acid also affected the elution order of the BNDHP enantiomers. In the case of an L-configured amino acid (*R*)-BNDHP was complexed more strongly and eluted faster in MEKC experiments [167]. When the configuration of the "inner" amino acid was changed to the D-configuration the elution order was reversed with the (*S*)-enantiomer of BNDHP eluting first. The stereochemistry of the C-terminal amino acid did not affect the enantiomer elution order of BNDHP. It did, however, influence the magnitude of the chiral resolution. Tröger's base and propranolol bind to the chiral pocket of the molecular micelle in a mode comparable to BNDHP while Dns-amino acids appeared to interact primarily with the C-terminal amino acid of poly(*N*-undecanoyl-L-leucine-L-valine) [166]. Molecular micelles obtained from surfactants containing a single amino acid as polar head group also created a chiral pocket which was able to adopt BNDHP [168].

4.6 Miscellaneous Selectors

Apart from the more often applied chiral selectors discussed above, many types of complex forming agents have been evaluated as chiral selectors in CE [14–16, 20, 23, 110]. However, in most cases only proof of concept, i.e., the application to enantioseparations, has been reported and only mechanistic studies for a few further groups of selectors were performed.

While being the most successful chiral selectors in HPLC, polysaccharide have not been frequently used as chiral selectors in CE, although successful applications have been reported such as [169–174]. Based on the fact that CE enantioseparations using native amylose as chiral selector deteriorated upon increasing the capillary temperature from 25°C to 60°C in the case of analytes with a molecular size smaller than 0.78 nm while chiral separations of larger analytes was not affected by temperature, it has been concluded that the chiral recognition of amylose possesses a helical and an ahelical component [175]. Addition of iodine, which is known to be included in the helices of polysaccharides, led to the same observation. Thus, small molecules appear to be stereoselectively included into helical groves of amylose while the stereoselective complexation of larger molecules appears to occur via other interactions.

Cyclofructans (CFs) are cyclic oligosaccharides composed of β(2 → 1) linked D-fructofuranose units. Derivatives containing 6 (CF6) or 7 (CF7) fructose units have been employed in separation sciences to date. These CFs possess a disk-type structure, the inner core having the structure of a crown ether. In the case of CF6 the fructose units are arranged in a spiral array around the 18-crown-6 core with alternating "inward" and "outward" orientation [176] so that three of the OH groups in position 3 of the fructofuranose moieties point towards the inner core blocking its access due to hydrogen bonding [177]. As a consequence, only poor or no enantioseparations have been observed using native CF6 in CE [178] due to the limited interaction possibilities with analytes. In contrast, sulfated CF6 proved to be an effective chiral selector in CE enantioseparations [178].

The stereoselective interaction of proteins with chiral compounds is a well-known phenomenon in nature. Consequently, proteins have been used as chiral selectors in separation sciences including CE [179, 180]. However, the fact that proteins tend to adsorb to the capillary inner surface somewhat limits their applications as chiral selectors in CE, often necessitating special measures such as coating of the capillary wall. Due to the complexity of the protein selectors a number of molecular interactions including hydrogen bonds, π–π, dipole, and ionic interactions contribute to the complexation of the analyte enantiomers.

Chiral ionic liquids have been recently introduced as chiral selectors in CE. Ionic liquids are salts that are liquid at or close to room temperature. Either the cation or the anion or both may be chiral [181]. Due to their high aqueous solubility chiral ionic liquids have been used as chiral background electrolyte or chiral selector in CE [182, 183] including MEKC [184] and ligand exchange [185, 186]. Ionic and ion-pair interactions between analyte and selector predominate in the case of these selectors. Enantiomeric differentiation by chiral ionic liquids has been demonstrated by spectroscopic techniques [187, 188] but the structures of the complexes formed between ionic liquids and the analyte enantiomers are currently unknown.

Aptamers are single stranded RNA or DNA oligonucleotides which are obtained by the iterative process of systematic evolution of ligands by exponential enrichment (SELEX) [189] which act as target-specific chiral selectors binding one enantiomer with high enantioselectivity. Aptamers possess a complex three-dimensional shape

containing structural motifs including stems, loops, bulges, hairpins, triplexes, or quadruplexes, and can bind a large variety of target compounds with an affinity, specificity, and selectivity comparable to antibodies. Complexation of the target molecules occurs via an adaptive conformational change of the aptamer in a so-called induced-fit process which results in a tight aptamer–solute complex with maximal complementarity between the aptamer and the preferred enantiomer [190–192]. The other enantiomer forms less stabilizing contacts yielding a lower binding affinity. Depending on the structure and functional groups of the target molecules, hydrogen bonding, electrostatic interactions, stacking interactions, or hydrophobic interactions contribute to this process. According to a molecular modeling study, the aptamer folds from a relatively disordered structure into a defined binding pocket encapsulating the target molecule [193]. For a summary of the use of aptamers in separation sciences see [194].

5 Modes of CE Enantioseparation: Selected Examples

As stated above, in CE enantioseparations the chiral selector is added to the background electrolyte performing as a mobile, pseudostationary phase. As in chromatography, chiral recognition is due to stereoselective interactions between the analyte enantiomers and the chiral selector while transport to the detector is achieved by electrokinetic phenomena. Differences in the formation equilibria of the diastereomeric complexes between the chiral selector and the analyte enantiomers and/or differences in the mobilities of the diastereomeric complexes result in enantioseparations (see Sect. 2). Combined with the different modes of CE, many separation scenarios can be envisioned. CE has been applied to the determination of the enantiomers including the enantiomeric composition of compounds in chemical, pharmaceutical, forensic, or environmental analysis, as well as bioanalysis. Many assays displayed enantioselectivity and chemoselectivity allowing the simultaneous analysis of chiral as well as achiral impurities in drug substances. The most frequently employed CE enantioseparation modes, i.e., EKC, MEKC, and MEEKC, will be briefly addressed.

5.1 Electrokinetic Chromatography

The EKC mode is the most often applied technique for CE enantioseparations as documented by numerous publications, many reviews [14–22] or monographs [23, 24]. The term EKC describes a system with a chiral selector in a background electrolyte without the presence of a further pseudostationary phase such as micelles or a microemulsion. It is often (incorrectly) also referred to as chiral CE. The selector may be charged, thus exhibiting an electrophoretic self-mobility allowing the enantioseparation of neutral analytes, or uncharged so that it is transported with the EOF. This enables many separation scenarios, some of which are schematically shown in Fig. 2. Many structurally diverse compounds have been utilized as chiral

selectors in CE including CDs, macrocyclic glycopeptide antibiotics, proteins, crown ethers, chiral ligand-exchangers, chiral ionic liquids, aptamers as well as chiral surfactants derived from steroids, amino acids, tartaric acid or glycosides [14, 16, 23, 24, 110]. When evaluating a specific chiral selector, the compound is typically investigated with regard to its enantioseparation ability towards a certain class of analytes. Conversely, the identification of the most suitable selector for a given class of analytes from a large library of potential selectors may also be applied by screening the entire library with subsequent deconvolution as described for cyclic peptides [195, 196]. The identification of selectors via combinatorial strategies has also been applied to the development of aptamer selectors [197].

Although some selectors appear to be limited to a certain group of analytes, for example chiral crown ethers for the enantioseparation of primary amines, there is no general rule for the application of certain selectors. Thus the choice of a specific selector currently depends on the experience and/or preferences of the analyst. Due to the large variety of derivatives as well as commercial availability, CDs are by far the most often applied chiral selectors in CE [110, 122–129]. Consequently, general strategies for screening approaches utilizing CDs have been published in order to find generalized starting conditions without excessive testing of a large number of CDs. Many analysts prefer negatively charged CDs as they can be used for charged and uncharged compounds [198–200]. At low pH, basic analytes are protonated and migrate to the cathode while the negatively charged CDs migrate to the anode. Neutral compounds interacting with the negatively charged CDs are transported to the anode and can be detected upon reversing the polarity of the applied voltage. Most acidic analytes are protonated at low pH and behave as neutral compounds. Strategies for dual CD systems have also been published [201, 202]. In these systems, both chiral selectors may cooperate in a synergistic manner or counteract each other. An improvement in separation selectivity compared to the use of a single selector is observed when both selectors display opposite affinity towards the analyte enantiomers. Alternatively, increased selectivity also occurs if one CD accelerates the analyte while the other either decelerates it or has no effect on the analyte mobility [203]. Analogous effects may be achieved if one of the selectors is immobilized on the inner wall of the capillary [204, 205].

As discussed above, opposite enantiomer migration order may be observed when switching from one CD to another. Moreover, pure single isomers of CD derivatives are not necessarily required for successful enantioseparations. In fact, many enantioseparations have been achieved using randomly substituted derivatives [43]. However, randomly substituted CDs are a mixture of isomers differing in their degree of substitution, i.e., the number and position of the substituents. Therefore, randomly substituted CDs from various suppliers may differ in this respect and differences may even be observed from batch to batch for a given CD from the same supplier. Literature examples clearly demonstrate that the source of the CD and the degree of substitution may affect the enantioseparation of one compound while this may have no effect for another analyte [206–208]. In addition, it cannot be predicted whether a higher or lower degree of substitution of a given CD results in a better enantioseparation.

Most CE enantioseparations were achieved in aqueous background electrolytes. However, it has been shown that nonaqueous conditions employing organic solvents for electrolyte preparation may be a valuable alternative. Organic solvents possess advantages in terms of higher dissolution of lipophilic analytes, increased stability of water-sensitive analytes, and shift of analyte pK_a or analyte–selector complexation equilibria, among others [209]. Consequently, many successful CE enantioseparations in nonaqueous background electrolytes have been reported [210].

The fact that the chiral selector is dissolved in the background electrolyte is often considered an advantage in terms of the ease of changing the experimental conditions, including the type of the chiral selector. However, this may become a disadvantage when CE is hyphenated with a mass spectrometer. Most selectors are not volatile and contaminate the ion source of the mass spectrometer when entering it. Two strategies have been implemented in order to prevent the entrance of the selector into the ion source [211–213]. The first called the counter migration technique exploits the self-mobility of a chiral selector migrating in the opposite direction of the mass spectrometer. The capillary is initially filled with the background electrolyte containing the chiral selector. Upon application of the separation voltage the analytes migrate towards the mass spectrometer while the selector migrates in the opposite direction. Interaction between analyte and selector results in the enantioseparation. This method is limited to charged chiral selectors. The second approach is the partial filling technique. In this case, only part of the capillary is filled with the background electrolyte containing the selector while the remainder contains a selector-free electrolyte. The experimental conditions have to be chosen in such a way that the analytes migrating through the zone containing the chiral selector have to exhibit a higher velocity towards the mass spectrometer compared to the selector zone so that the analytes reach the mass spectrometer before the selector can enter the ion source. Careful control of the EOF is required. Successful enantioseparations with mass spectrometric detection have been reported applying both approaches [211–213]. It has also been shown that background electrolytes with low concentrations of the chiral selector may be used in CE hyphenated to mass spectrometry without significant loss of sensitivity despite the entrance of the selector into the ion source [214].

A well-known phenomenon in CE is the fact that the peak area in CE depends on the migration velocity of the compounds and, subsequently, the area ratio of the enantiomers of a racemic compound differs from 1:1. This may be compensated by using the corrected peak area by dividing the peak area by the analyte migration time. It has also been shown that complexation of the enantiomers by a chiral selector may result in different detector responses for the individual enantiomers. As demonstrated for the hypnotic drug zopiclone, the drug–β-CD complex displays higher fluorescence intensity as compared to the non-complexed drug [215]. Consequently, in a CE enantioseparation using laser-induced fluorescence detection the more strongly complexed second migrating enantiomer of zopiclone possessed a significantly larger peak area than the faster migrating first enantiomer. This was explained by the fact that the slower migrating enantiomer passes the detector with a higher molar fraction in the complexed form compared to the faster migrating

enantiomer. Although different detector response of enantiomers does not appear to be a common phenomenon, especially when using UV detection, it should be kept in mind that analyte complexation may alter the spectroscopic properties of the compounds and, consequently, affect analyte quantitation.

The aim of any method development for an analytical separation is to obtain an assay allowing the separation of the analytes in a short period of time. Apart from the physicochemical characteristics of the analytes, experimental factors such as type and concentration of the chiral selector, type, pH, and concentration of the background electrolyte, as well as additives such as organic solvents or surfactants, applied voltage, or capillary temperature, and capillary rinsing procedures affect enantioseparations in CE. All these factors have to be optimized and properly validated. The univariate approach, i.e., optimizing one variable at a time while keeping all other variables constant, results in a large number of experiments. Typically, this approach only leads to a local optimum of the conditions. Therefore, chemometric methods have been increasingly used in order to find the global optimal conditions of the experimental variables [216–219]. In such approaches, the variables which significantly affect a separation are first identified by an experimental design and subsequently optimized using another type of design. Testing of the robustness of the analytical method can also be addressed by chemometrics. General practical considerations for obtaining a robust CE method can be found in [220].

An example illustrating the stereoselectivity and chemoselectivity of CE is the separation of the etomidate exhibiting (*R*)-configuration from its (*S*)-enantiomer as well as the related substances metomidate and etomidate acid (Fig. 19) [221]. All analytes could be detected at the cathodic end of the capillary using a 100 mM phosphate buffer, pH 2.1, as background electrolyte (Fig. 19a). The enantiomers of etomidate and metomidate could be separated using 30 mg/mL β-CD while the enantiomers of the acid comigrated under these conditions (Fig. 19b). Addition of 30 mg/mL α-CD only resulted in poor separation of the enantiomers of etomidate (Fig. 19c). However, α-CD also led to an increased resolution between metomidate and etomidate. Exploiting the carrier ability of sulfated β-CD and reversing the polarity of the applied voltage, i.e., detecting the analytes at the anodic end of the capillary, resulted in the separation of all enantiomers with large resolution values, R_S, at a concentration of 20 mg/mL of the CD (Fig. 19d). However, when overloading the system by injecting high concentrations of etomidate in order to achieve the required sensitivity for the detection of the impurities at the 0.1% level, peak splitting and peak distortion were observed. Finally, the combination of 30 mg/mL α-CD and 4.6 mg/mL sulfated β-CD allowed the determination of all potential impurities of the drug in the presence of a large excess of etomidate (Fig. 19e). The system allows the separation of all enantiomers (Fig. 19f) but the peak of the (*S*)-enantiomer of metomidate is "covered" by the peak of etomidate when high concentrations of the drug are injected (Fig. 19e). In the present case this was considered insignificant as (*S*)-metomidate is a very unlikely impurity of etomidate. In the dual CD system the enantioselectivity is achieved by sulfated

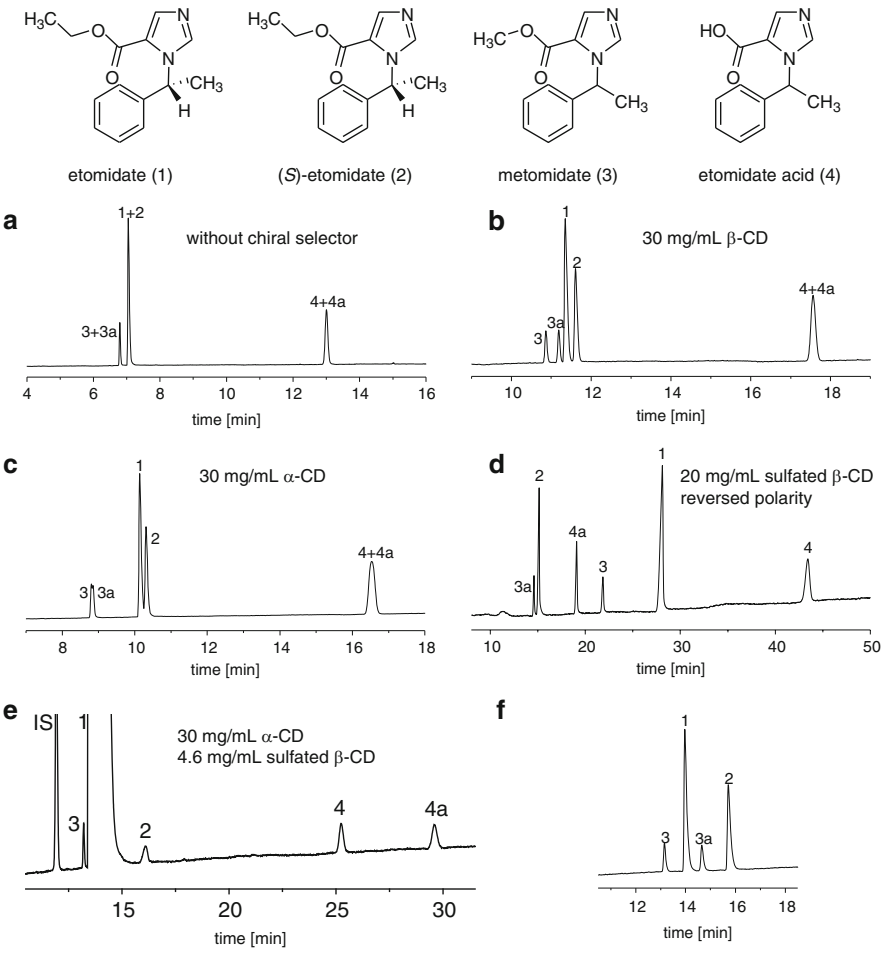

Fig. 19 Simultaneous separation of the enantiomers of etomidate, metomidate, and etomidate acid (**a**) in the absence of a chiral selector and in the presence of (**b**) β-CD, (**c**) α-CD, (**d**) sulfated β-CD and (**e**, **f**) a combination of α-CD and sulfated β-CD. Experimental conditions: 50.2/40 cm, 50 μm id fused-silica capillary, 100 mM sodium phosphate buffer, pH 2.1, 20°C, 20 kV. Peak assignment: (*1*) etomidate, (*2*) (*S*)-etomidate, (*3*) (*R*)-metomidate, (*3a*) (*S*)-metomidate, (*4*) (*R*) etomidate acid, (*4a*) (*S*)-etomidate acid. Sample concentration in (**e**): 5.4 mg/mL etomidate containing approximately 40–80 μg/mL of the related substances. (Adapted with permission of Wiley from [221] © 2006)

β-CD while α-CD contributes to the chemoselectivity of the system by assisting the separation of etomidate and metomidate. The CE assay was subsequently validated and applied to the simultaneous analysis of etomidate with regard to the stereochemical purity as well as related substances. Concentrations of the impurities as low as 0.01% could be detected with the CE method [221].

5.2 Micellar Electrokinetic Chromatography

MEKC has been introduced as a method allowing the analysis of uncharged compounds [10–13] but the technique is equally suitable for charged analytes. MEKC enantioseparations can be carried out using two basic systems. The first mode employs a chiral surfactant used in concentrations above the critical micelle concentration. These surfactants comprise bile salts or charged or neutral compounds derived from glucopyranosides or *N*-acylamino acids surfactants [222]. Mixed micelles composed of chiral and achiral surfactants have also been used. The separation mechanism using chiral micelles is based on the stereoselective interaction of the analyte enantiomers with the selector upon partitioning between the aqueous and the micellar phases.

A further development is the introduction of polymeric surfactants (polymeric micelles) by the groups of Warner [46] and Dobashi [160]. These are obtained by polymerization of the hydrocarbon chain of *N*-acyl amino acids or *N*-alkyloxycarbonyl derivatives of amino acids or dipeptides. The polymeric micelles overcome the limitations caused by the dynamic nature of conventional micelles and instability upon addition of higher concentrations of organic solvents. Furthermore, lower Joule heating is observed for polymeric micelles as compared to micelles formed from monomeric surfactants. Limitations of the polymeric micelles may be the presence of impurities originating from the polymerization process or slow mass transfer kinetics in the case of a high polydispersity of the polymers. Comparison of the separation selectivity of amino acid-based chiral surfactants and their polymeric analogs revealed a significant influence of steric effects as well as the orientation and charge of the headgroup [223–225].

In the second approach achiral micelles are combined with a chiral selector. A frequently employed combination is the use of SDS as surfactant combined with cyclodextrins. Also termed CD-modified MEKC, this system is based on several equilibria, i.e., the partitioning of the analyte between the (achiral) micelles and the aqueous phase as well as the stereoselective complexation of the enantiomers by the selector. Furthermore, distribution of the CD–analyte complexes into the micelles may be considered as well as the binding of the enantiomers by CDs associated with the micelles. The latter may differ from the complexation between CD and analyte in the aqueous phase. Furthermore, it has been shown by CE, spectroscopic techniques and molecular modeling that the hydrocarbon chain of SDS can be incorporated into the cavity of CDs, thereby modulating the binding affinity towards the analyte molecules [226–228]. Although not yet experimentally proven, the incorporation of surfactants other than SDS into the cavity of CDs can be expected. Conversely, CDs may affect the micellization of surfactants [226, 227], emphasizing the importance of a profound understanding of the interactions between surfactants and CDs in order to design proper separation systems.

Both modes, i.e., MEKC using chiral micelles and CD-modified MEKC, have been successfully applied to the enantioseparations of many basic, acidic, or neutral compounds [222]. An interesting characteristic of the polymeric micelles is their

compatibility with MS detection [211, 229]. MEKC employing monomeric chiral surfactants or achiral surfactants combined with CDs is not suitable for this purpose. Major concerns are signal suppression, poor volatility, interactions between surfactant and analytes, as well as the production of interfering background ions. The use of polymeric micelles has several advantages. First, as they do not possess a critical micelle concentration they may be used at relatively low concentrations in the background electrolyte, minimizing the deteriorating effects on the MS detection. Second, as the molecular organization of polymeric micelles is not affected by organic solvents, a high content of organic solvent may be used in the background electrolyte. Third, they do not interfere in the low molecular mass range due to their high molecular mass. Finally, their low surface activity provides a stable electrospray and consequently less suppression of the analyte signal. MEKC enantioseparations with MS detection using polymeric micelles has been reported for a number of structurally diverse analytes [230–232]. A recent illustrative example of MEKC-MS is the stereoselective analysis of warfarin and its metabolite hydroxywarfarin in serum samples [233]. The simultaneous separation of the drug and five hydroxylated metabolites upon optimization of the background electrolyte is shown in Fig. 20a. Except for 8-hydroxywarfarin, all enantiomers could be separated in the presence of 25 mM poly(sodium *N*-undecenoyl-L-leucyl-L-valinate) in an ammonium acetate buffer containing 15 vol.% methanol. Tandem mass spectrometry allowed limits of detection between 0.5 and 3 ng/mL depending on the analyte. The assay allowed the stereoselective analysis of plasma samples from patients (Fig. 20b) and the sensitive determination of metabolites that were apparently not detected in previous studies, illustrating the fact that MEKC-electrospray ionization-tandem mass spectrometry employing polymeric micelles is well suited to the bioanalysis with MS detection. Moreover, differences between the stereoselective metabolism of subjects possessing a mutant of the cytochrome enzyme CYP2C9 could be identified (Fig. 20b) [233].

5.3 Microemulsion Electrokinetic Chromatography

MEEKC was introduced in 1991 [234] and can be regarded as analogous to MEKC using microemulsion droplets as pseudostationary phase as compared to micelles in MEKC. The microemulsion is formed by a water immiscible organic liquid stabilized by a surfactant and a co-surfactant. The droplets of the microemulsion are typically charged due to the use of a negatively charged surfactant so that they migrate towards the anode. There has been much debate about both techniques with regard to enhanced stability, solubilization capacity, or higher mass transfer efficiency of the microemulsion vs the micelles. However, the literature published to date suggests that the answer regarding the superior separation mode may be analyte dependent, especially in the light of solvent-modified MEKC. Recent work on the achiral separation of steroids comparing MEEKC and MEKC with the addition of 1-butanol yielded comparable results with regard to separation performance [235].

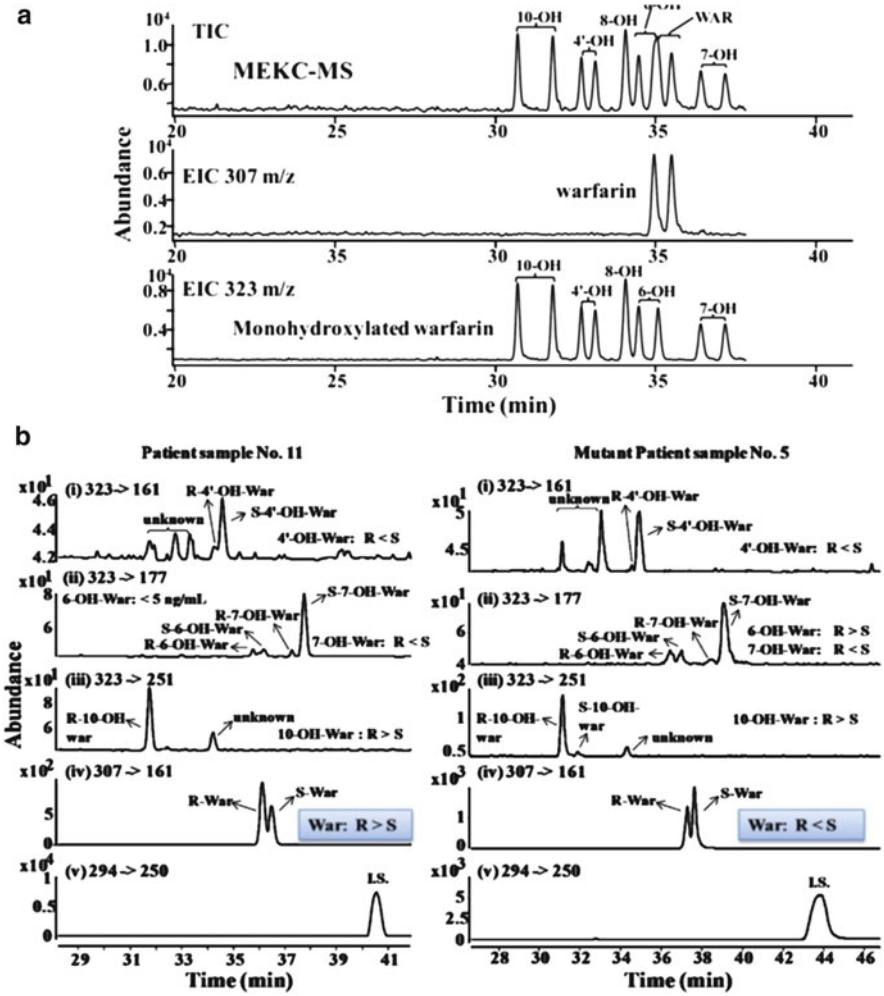

Fig. 20 MEKC-MS analysis of warfarin and its hydroxylated metabolites. (**a**) Analysis of standards showing the total ion chromatogram (TIC), the mass trace m/z 307 representing warfarin and the mass trace m/z 323 of the hydroxy metabolites. (**b**) Tandem MS extracted ion chromatograms of plasma samples. Patient sample 5 represents a subject with polymorphism of cytochrome CYP2C9. Experimental conditions: 118 cm, 50 μm id fused-silica capillary, 25 mM poly(sodium *N*-undecenoyl-L-leucyl-L-valinate) in 25 mM ammonium acetate, pH 5.0, containing 15 vol.% methanol, 30 kV. Spray chamber parameters: nebulizer pressure: 4 psi, drying gas temp.: 200°C, drying gas flow: 6 L/min, capillary voltage: −3,000 V, fragmentor voltage: 91 V. (Reproduced with permission of Elsevier from [233] © 2013)

For MEEKC enantioseparations, two general approaches have been realized. The first employs chiral components forming the microemulsion. For example, *N*-dodecoxycarbonyl-L-valine was used as chiral surfactant [236–238], chiral alkanols such as (2*R*)-pentanol or (2*R*)-hexanol as chiral co-surfactants [239], or

chiral oil phases such as dibutyl L-tartrate [240, 241]. Combinations of two [242–244] or three [245] chiral components have also been employed. Interestingly, effective separations of the enantiomers of β-blockers have also been obtained using a neutral microemulsion composed of Tween 20 and dibutyl L-tartrate in a sodium tetraborate buffer [246]. The mechanism of the enantioseparations using a chiral oil droplet is based on the partitioning equilibria of the analyte enantiomers between the aqueous phase and the chiral oil phase.

The second approach uses an achiral microemulsion in combination with a chiral selector such as a CD. In this case the microemulsion is composed of a water-immiscible organic solvent such as *n*-hexane, *n*-heptane, or ethyl acetate, a surfactant such as SDS, and a co-surfactant such as 1-butanol or 1-octanol. As chiral selectors, neutral [247] as well as negatively charged CD derivatives [248–251] have been employed. In these systems two equilibria have to be considered – the partitioning of the analyte between the aqueous phase and the lipid phase as well as the stereospecific complexation of the enantiomers by the CDs. The partitioning of the diastereomeric enantiomer–CD complexes may, in principle, also take place. It has been shown by NMR and molecular modeling that SDS used for the preparation of the microemulsion can also form complexes with CDs, modulating the interaction between the selector and analyte enantiomers [228].

In this context it is interesting to note that the way of preparation of the microemulsion, specifically the time of the addition of the chiral selector, may affect the performance of the separation system. Thus, a MEEKC method allowing the simultaneous separation of the enantiomers of amphetamine, i.e., dexamphetamine and levoamphetamine, as well as related substances was developed using a microemulsion composed of 1.5 wt% SDS, 0.5 wt% ethyl acetate, 3.5 wt% 1-butanol, 2.5 wt% 2-propanol, and 92 wt% 50 mM sodium phosphate buffer, pH 3.0, containing 5.5 wt% sulfated β-CD [251]. Superior separation of the amphetamine enantiomers and the related substances phenylacetone *E*-oxime and (1*S*,2*S*)-(+)-norpseudoephedrine was observed when sulfated β-CD was added to the phosphate buffer prior to the preparation of the microemulsion by sonication (Fig. 21a) as compared to addition of the chiral selector after preparation of the microemulsion (Fig. 21b). At present, the origin of the phenomenon is not clear. It may be speculated that it is due either to inclusion of SDS or other components of the microemulsion into the cavity of the CD or to association of the CD with the microemulsion droplets during the preparation. In any case, such effects have to be considered when developing methods for routine analysis. For recent reviews on MEEKC, including the use for enantioseparations, see, for example, [252, 253].

6 Concluding Remarks

Within the 30 years since its introduction CE has developed into a mature technique for the analysis of a large variety of analytes. Theoretical knowledge and understanding of the underlying mechanisms of CE separations has been compiled. Due to the different separation mechanisms, HPLC and CE are complimentary techniques where each has its own advantages and disadvantages so that the user

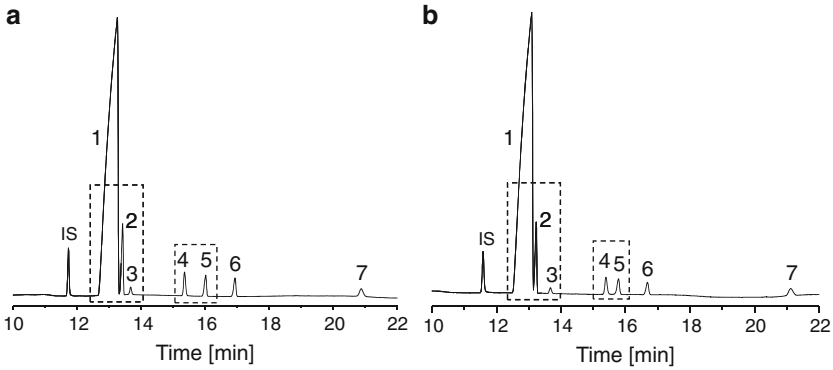

Fig. 21 Effect of the preparation of the microemulsion background electrolyte on analyte separation. (**a**) Addition of sulfated β-CD prior to the phosphate buffer preparation of the microemulsion by sonication and (**b**) addition of sulfated β-CD after preparation of the microemulsion. Experimental conditions: 50.2/40 cm, 50 μm id fused-silica capillary, 20°C, −14 kV, UV detection at 200 nm; background electrolyte: 1.5 wt% SDS, 0.5 wt% ethyl acetate, 3.5 wt% 1-butanol, 2.5 wt% 2-propanol, and 92 wt% 50 mM sodium phosphate buffer, pH 3.0, containing 5.5 wt% sulfated β-CD. Peak assignment: (IS) internal standard, (*1*) dexamphetamine, (*2*) levoamphetamine, (*3*) phenylacetone *Z*-oxime, (*4*) phenylacetone *E*-oxime, (*5*) (1*S*,2*S*)-(+)-norpseudoephedrine, (*6*) (1*R*,2*S*)-(−)-norephedrine, (*7*) phenylacetone. (Reproduced with permission of Wiley from [251] © 2010)

may have to choose between both techniques for a certain separation problem. CE offers many modes, chiral selectors, and migration options, making it a highly flexible and versatile technique. However, this flexibility may also be the reason why CE is often considered a less robust technique compared to HPLC. Consequently, CE is less accepted for routine analysis and sometimes referred to as an "academic" technique. This may be due to the fact that most analytical chemists are trained in chromatography and not in CE, so that the basic understanding of CE may not be as widespread as of chromatography. For example, the fused-silica capillary surface is often considered inert which does not apply. The ionization state of silanol groups on the surface generates the EOF. Therefore, understanding of the influencing factors and the EOF, which includes all rinsing steps and, consequently, properly controlling the EOF is the key to a successful method. In fact, it has been shown that properly validated CE methods perform as well as HPLC methods with regard to precision and robustness.

Another often mentioned fact is the relatively low UV-detection sensitivity of CE compared to HPLC because detection is performed on column which results in a low optical path length. Besides using specific capillaries with extended optical path lengths (bubble cells or Z-cells), detection modes other than UV may be employed such as laser-induced fluorescence or mass spectrometric detection. Moreover, on-column sample stacking techniques based on electrophoretic phenomena have been developed, resulting in an up to 1,000-fold increase in sensitivity as summarized, for example, in [254–257].

CE methods have been included in the documentation submitted to regulatory authorities such as the US Food and Drug Administration (FDA) or the European Medicines Agency (EMA). Furthermore, CE has been implemented in the draft guidance for industry of the FDA [258, 259] as well as in monographs of the United States Pharmacopeia (USP) and the European Pharmacopoeia (Ph. Eur.) [259, 260]. Within the pharmaceutical industry CE has seen an increase in recent years, especially in the biotechnological sector. This may be primarily due to the use of well defined commercial kits for specific applications such as CE-gel electrophoresis or capillary isoelectric focusing for biomolecules [260]. In the author's opinion, CE is also an excellent technique for small molecule analysis, especially for enantioseparations if such methods are properly validated. This has been shown in some of the examples discussed above where the simultaneous analysis of the stereochemical purity of a drug and of its related substances has been demonstrated, for example in [208, 221, 251], as well as the implementation of CE enantioseparation methods in international pharmacopeias. Further acceptance of CE, especially for routine analysis, will require trained laboratory staff with a profound understanding of the technique. CE is not just "like HPLC in capillaries" but a technique based on different phenomena compared to chromatography.

References

1. Kant I (1783) Prolegomena zu einer jeden künftigen Metaphysik die als Wissenschaft wird auftreten können. English translation: Hatfield G (1997) Prolegomena to any future metaphysics that will be able to come forward as science. Cambridge University Press, New York
2. Jorgenson JW, Lukacs KA (1981) Free zone capillary electrophoresis in open-tubular glass capillaries. Anal Chem 53:1298–1302
3. Gassmann E, Kuo JE, Zare R (1985) Electrokinetic separation of chiral compounds. Science 230:813–814
4. Cohen AS, Paulus A, Karger BL (1987) High-performance capillary electrophoresis using open tubes and gels. Chromatographia 24:15–24
5. Snopek J, Jelinek I, Smolkova-Keulemansova E (1988) Use of cyclodextrins in isotachophoresis: IV. The influence of cyclodextrins on the chiral resolution of ephedrine alkaloid enantiomers. J Chromatogr 438:211–218
6. Snopek J, Jelinek I, Smolkova-Keulemansova E (1988) Use of cyclodextrins in isotachophoresis: V. The separation of ketotifen and its polar intermediate enantiomers. J Chromatogr 439:386–392
7. Jelinek I, Dohnal J, Snopek J, Smolkova-Keulemansova E (1989) Use of cyclodextrins in isotachophoresis: VII. Resolution of structurally related and chiral phenothiazines. J Chromatogr 464:139–147
8. Guttman A, Paulus A, Cohen AS, Grinberg N, Karger BL (1988) Use of complexing agents for selective separation in high-performance capillary electrophoresis: chiral resolution via cyclodextrins incorporated within polyacrylamide gel columns. J Chromatogr 448:41–53
9. Fanali S (1989) Separation of optical isomers by capillary zone electrophoresis based on host-guest complexation with cyclodextrins. J Chromatogr 474:441–446
10. Terabe S (1989) Electrokinetic chromatography: an interface between electrophoresis and chromatography. Trends Anal Chem 8:129–134
11. Terabe S, Shibata M, Miyashita Y (1989) Chiral separation by electrokinetic chromatography with bile salt micelles. J Chromatogr 480:403–411

12. Dobashi A, Ono T, Hara S (1989) Optical resolution of enantiomers with chiral mixed micelles by electrokinetic chromatography. Anal Chem 61:1984–1986
13. Dobashi A, Ono T, Hara S, Yamaguchi J (1989) Enantioselective hydrophobic entanglement of enantiomeric solutes with chiral functionalized micelles by electrokinetic chromatography. J Chromatogr 480:413–420
14. Van Eeckhaut A, Michotte Y (2006) Chiral separations by capillary electrophoresis: recent developments and applications. Electrophoresis 27:2880–2895
15. Chankvetadze B (2007) Enantioseparations by using capillary electrophoretic technique. J Chromatogr A 1168:45–70
16. Gübitz G, Schmid MG (2008) Chiral separation by capillary electromigration techniques. J Chromatogr A 1204:140–156
17. Mikus P, Marakova K (2009) Advanced CE for chiral analysis of drugs, metabolites and biomarkers in biological samples. Electrophoresis 30:2773–2802
18. Preinstorfer B, Lämmerhofer M, Lindner W (2009) Advances in enantioselective separations using electromigration capillary techniques. Electrophoresis 30:100–132
19. Caslavska J, Thormann W (2011) Stereoselective determination of drugs and metabolites in body fluids, tissues and microsomal preparations by capillary electrophoresis (2000–2010). J Chromatogr A 1218:588–601
20. Scriba GKE (2011) Fundamental aspects of chiral electromigration techniques and application in pharmaceutical and biomedical analysis. J Pharm Biomed Anal 55:688–701
21. Scriba GKE (2011) Chiral electromigration techniques in pharmaceutical and biomedical analysis. Bioanal Rev 3:95–114
22. Lu H, Chen G (2011) Recent advances of enantioseparations in capillary electrophoresis and capillary electrochromatography. Anal Methods 3:488–508
23. Chankvetadze B (1997) Capillary electrophoresis in chiral analysis. Wiley, Chichester
24. Van Eeckhaut A, Michotte Y (eds) (2010) Chiral separations by capillary electrophoresis. CRC, Boca Raton
25. Chankvetadze B (1997) Separation selectivity in chiral capillary electrophoresis with charged selectors. J Chromatogr A 792:269–295
26. Sänger-van de Griend CE, Gröningsson K, Arvidsson T (1997) Enantiomeric separation of a tetrapeptide with cyclodextrin extension of the model for chiral capillary electrophoresis by complex formation of one enantiomer molecule with more than one chiral selector molecules. J Chromatogr A 782:271–279
27. Bowser MT, Kranack AR, Chen DDY (1998) Properties of multivariate binding isotherms in capillary electrophoresis. Anal Chem 70:1076–1084
28. Bowser MT, Chen DDY (1998) Higher order equilibria and their effect on analyte migration behavior in capillary electrophoresis. Anal Chem 70:3261–3270
29. Scriba GKE (2002) Selected fundamental aspects of chiral electromigration techniques and their application to pharmaceutical and biomedical analysis. J Pharm Biomed Anal 27: 373–399
30. Rizzi A (2001) Fundamental aspects of chiral separations by capillary electrophoresis. Electrophoresis 22:3079–3106
31. Wren SAC, Rowe RC (1992) Theoretical aspects of chiral separation in capillary electrophoresis. I. Initial evaluation of a model. J Chromatogr A 603:235–241
32. Stepanova ND, Stepanov AV (1969) Influence of temperature on the effectiveness of the electromigration separation of calcium and strontium in citric acid solutions. Zh Prikl Khimii (Russ J Appl Chem Engl Ed) 42:1670–1673
33. Chankvetadze B, Lindner W, Scriba GKE (2004) Enantiomer separations in capillary electrophoresis in the case of equal binding constants of the enantiomer with a chiral selector: commentary on the feasibility of the concept. Anal Chem 76:4256–4260
34. Lomsadze K, Martinez-Giron AB, Castro-Puyana M, Chankvetadze L, Crego AL, Salgado A, Marina ML, Chankvetadze B (2009) About the role of enantioselective selector-selectand

interactions and the mobilities of diastereomeric associates in enantiomer separations using CE. Electrophoresis 30:2803–2811
35. Süß F, Sänger-van de Griend CE, Scriba GKE (2003) Migration order of dipeptides and tripeptide enantiomers in the presence of single isomer and randomly sulfated cyclodextrins as a function of pH. Electrophoresis 24:1069–1076
36. Rizzi AM, Kremser L (1999) pK_a shift-associated effects in enantioseparations by cyclodextrin-mediated capillary zone electrophoresis. Electrophoresis 20:2715–2722
37. Rawjee YY, Staerk DU, Vigh G (1993) Capillary electrophoretic chiral separations with cyclodextrin additives: I. acids: chiral selectivity as a function of pH and the concentration of β-cyclodextrin for fenoprofen and ibuprofen. J Chromatogr 635:291–306
38. Rawjee YY, Williams RL, Vigh G (1993) Capillary electrophoretic chiral separations using β-cyclodextrin as resolving agent II. Bases: chiral selectivity as a function of pH and the concentration of β-cyclodextrin. J Chromatogr A 652:233–245
39. Rawjee YY, Williams RL, Vigh G (1994) Capillary electrophoretic chiral separations using cyclodextrin additives: III. Peak resolution surfaces for ibuprofen and homatropine as a function of the pH and the concentration of β-cyclodextrin. J Chromatogr 680:599–607
40. Williams BA, Vigh G (1977) A dry look at CHARM (charged resolving agent migration) model of enantiomer separations by capillary electrophoresis. J Chromatogr A 777:295–309
41. Zhu W, Vigh G (2000) Experimental verification of a predicted, hitherto unseen separations electivity pattern in the nonaqueous capillary electrophoretic separation of weak base enantiomers by oktakis (2,3-diacetyl-6-sulfato)-γ-cyclodextrin. Electrophoresis 21: 2016–2024
42. Dubsky P, Svobodova J, Gas B (2008) Model of CE enantioseparation systems with a mixture of chiral selectors. Part I. Theory of migration and interconversion. J Chromatogr B 875: 30–34
43. Dubsky P, Svobodova J, Tesarova E, Gas B (2010) Enhanced selectivity in CZE multi chiral selector enantioseparation systems: proposed separation mechanism. Electrophoresis 31: 1435–1441
44. Chankvetadze B, Schulte G, Blaschke G (1997) Nature and design of enantiomer migration order in chiral capillary electrophoresis. Enantiomer 2:157–179
45. Chankvetadze B (2002) Enantiomer migration order in chiral capillary electrophoresis. Electrophoresis 23:4022–4035
46. Wang J, Warner IM (1994) Chiral separations using micellar electrokinetic capillary chromatography and a polymerized chiral micelle. Anal Chem 66:3773–3776
47. Zheng Z, Lin J, Qu F, Hobo T (2003) Chiral separation with ligand-exchange micellar electrokinetic chromatography using a D-penicillamine-copper(II) ternary complex as chiral selector. Electrophoresis 24:4221–4226
48. Tano C, Son SH, Furukawa J, Furuike T, Sakairi N (2008) Dodecyl thioglycopyranoside sulfates: novel sugar-based surfactants for enantiomeric separations by micellar electrokinetic capillary chromatography. Electrophoresis 29:2869–2875
49. Lee W, La S, Choi Y, Kim KR (2003) Chiral discrimination of aromatic amino acids by capillary electrophoresis in (+)- and (−)-(18-crown-6)-2,3,11,12-tetracarboxylic acid selector modes. Bull Korean Chem Soc 24:1232–1234
50. Vaccher MP, Lipka E, Bonte JP, Foulon C, Groossens JF, Vaccher C (2005) Enantiomeric analysis of baclofen by capillary zone electrophoresis, using highly sulfated cyclodextrins: inclusion ionization constant pK_a determination. Electrophoresis 26:2974–2983
51. Lipka E, Charton J, Vaccher MP, Folly-Klan M, Bonte JP, Vaccher C (2009) Enantioseparation of chiral benzimidazole derivatives by electrokinetic chromatography using sulfated cyclodextrins. J Sep Sci 32:1907–1915
52. Dominguez Vega E, Lomsadze K, Chankvetadze L, Salgado A, Scriba GKE, Calvo E, López JA, Crego AL, Marina ML, Chankvetadze B (2011) Separation of enantiomers of ephedrine by capillary electrophoresis using cyclodextrins as chiral selectors: comparative CE, NMR and high resolution MS studies. Electrophoresis 32:2640–2647

53. Lomsadze K, Domínguez Vega E, Salgado A, Crego AL, Scriba GKE, Marina ML, Chankvetadze B (2012) Separation of enantiomers of norephedrine by capillary electrophoresis using cyclodextrins as chiral selectors: comparative CE and NMR studies. Electrophoresis 33:1637–1647
54. Samakashvili S, Salgado A, Scriba GKE, Chankvetadze B (2013) Comparative enantioseparation of ketoprofen with trimethylated α-, β- and γ-cyclodextrin in capillary electrophoresis and study of related selector-selectand interactions using nuclear magnetic resonance spectroscopy. Chirality 25:79–88
55. Chankvetadze B, Burjanadze N, Breitkreutz J, Bergander K, Bergenthal D, Kataeva O, Fröhlich R, Luftmann H, Blaschke G (2002) Mechanistic study of the opposite migration order of the enantiomers of ketamine with α- and β-cyclodextrin in capillary electrophoresis. J Sep Sci 25:1155–1166
56. Chankvetadze L, Servais AC, Fillet M, Salgado A, Crommen J, Chankvetadze B (2012) Comparative enantioseparation of talinolol in aqueous and non-aqueous capillary electrophoresis and study of related selector-selectand interactions by nuclear magnetic resonance spectroscopy. J Chromatogr A 1267:206–216
57. Süß F, Poppitz W, Sänger-van de Griend CE, Scriba GKE (2001) Influence of the amino acid sequence and nature of the cyclodextrin on the separation of small peptide enantiomers by capillary electrophoresis using randomly substituted and single isomer sulfated and sulfonated cyclodextrins. Electrophoresis 22:2416–2423
58. Fillet M, Chankvetadze B, Crommen J, Blaschke G (1999) Designed combination of chiral selectors for adjustment of enantioseparation selectivity in capillary electrophoresis. Electrophoresis 20:2691–2697
59. Scriba GKE (2003) Recent advances in enantioseparations of peptides by capillary electrophoresis. Electrophoresis 24:4063–4077
60. Li J, Waldron KC (1999) Estimation of the pH-independent binding constants of alanylphenylalanine and leucylphenylalanine stereoisomers with β-cyclodextrin in the presence of urea. Electrophoresis 20:171–179
61. Sabbah S, Süß F, Scriba GKE (2001) pH-dependence of complexation constants and complex mobility in capillary electrophoresis separations of dipeptide enantiomers. Electrophoresis 22:3163–3170
62. Servais AC, Rousseau A, Fillet M, Lomsadze K, Salgado A, Crommen J, Chankvetadze B (2010) Separation of propranolol enantiomers by CE using sulfated β-CD derivatives in aqueous and non-aqueous electrolytes; comparative CE and NMR study. Electrophoresis 31:1467–1474
63. Lomsadze K, Salgado A, Calvo E, Antonio Lopez J, Chankvetadze B (2011) Comparative NMR and MS studies on the mechanism of enantioseparation of propranolol with hepatakis (2,3-diacetyl-6-sulfo)-β-cyclodextrin in capillary electrophoresis with aqueous and non-aqueous electrolytes. Electrophoresis 32:1156–1163
64. Servais AC, Rousseau A, Dive G, Frederich M, Crommen J, Fillet M (2012) Combination of capillary electrophoresis, molecular modelling and nuclear magnetic resonance to study the interaction mechanisms between single-isomer anionic cyclodextrin derivatives and basic drug enantiomers in a methanolic background electrolyte. J Chromatogr A 1232:59–64
65. Qi L, Yang G (2009) Enantioseparation of dansyl amino acids by ligand-exchange capillary electrophoresis with zinc(II)-L-phenylalaninamide complex. J Sep Sci 32:3209–3214
66. Chen Z, Niitsuma M, Nakagama T, Uchiyama K, Hobo T (2002) Enantioseparations of dansyl amino acids by capillary electrophoresis using Cu(II) complexes with L-amino acylamides as chiral selectors in electrolytes. J Sep Sci 25:1197–1201
67. Chankvetadze B, Schulte G, Blaschke G (1996) Reversal of enantiomer elution order in capillary electrophoresis using charged and neutral cyclodextrins. J Chromatogr A 732: 183–187
68. Schmitt T, Engelhardt H (1995) Optimization of enantiomeric separations in capillary electrophoresis by reversal of the migration order and using different derivatized cyclodextrins. J Chromatogr A 697:561–570

69. Chankvetadze B, Schulte G, Blaschke G (1997) Selected applications of capillaries with dynamic or permanent anodal electroosmotic flow in chiral separations by capillary electrophoresis. J Pharm Biomed Anal 15:1577–1584
70. Knob R, Maier V, Ranc V, Znaleziona J, Sevcik J (2010) Dopa and tyrosine enantiomers migration order reversal using uncoated and polypyrrole-coated capillaries. Glob J Anal Chem 1:228–232
71. Werner A, Nassauer T, Kiechle P, Erni F (1994) Chiral separation by capillary zone electrophoresis of an optically active drug and amino acids by host-guest complexation with cyclodextrins. J Chromatogr A 666:375–379
72. Baumy P, Morin P, Dreux M, Viaud MC, Boye S, Gullmant G (1995) Determination of β-cyclodextrin inclusion complex constants for 3,4-dihydro-2*H*-1-benzopyran enantiomers by capillary electrophoresis. J Chromatogr A 707:311–325
73. Sabah S, Scriba GKE (1998) Electrophoretic stereoisomer separation of aspartyl dipeptides and tripeptides in untreated fused-silica and polyacrylamide-coated capillaries using charged cyclodextrins. J Chromatogr A 822:137–145
74. Liu L, Nussbaum MA (1995) Control of enantiomer migration order in capillary electrophoresis separations using sulfobutyl ether beta-cyclodextrin. J Pharm Biomed Anal 14: 65–72
75. Tamisier-Karolak SL, Stenber MA, Bommart A (1999) Enantioseparation of β-blockers with two chiral centers by capillary electrophoresis using sulfated β-cyclodextrins. Electrophoresis 20:2656–2663
76. Lin CE, Cheng HT, Fang IJ, Liu YD, Kuo CM, Lin WY, Lin CH (2006) Strategies for enantioseparations of catecholamines and structurally related compounds by capillary zone electrophoresis using sulfated β-cyclodextrins as chiral selectors. Electrophoresis 27: 3443–3451
77. Rudaz S, Geiser L, Sourverain S, Prat J, Veuthey JL (2005) Rapid stereoselective separations of amphetamine derivatives with highly sulphated γ-cyclodextrin. Electrophoresis 26: 3910–3920
78. Ha PTT, Van Schepdael A, Hauta-Aho T, Roets E, Hoogmartens J (2002) Simultaneous determination of DOPA and carbidopa enantiomers by capillary zone electrophoresis. Electrophoresis 23:3404–3409
79. Schulte G, Chankvetadze B, Blaschke G (1997) Enantioseparation in capillary electrophoresis using 2-hydroxypropyltrimethylammonium salt of β-cyclodextrin as chiral selector. J Chromatogr A 771:259–266
80. Süß F, Poppitz W, Scriba GKE (2002) Separation of dipeptide and tripeptide enantiomers in capillary electrophoresis by the cationic cyclodextrin derivative 2-hydroxypropyltrimethylammonium-β-cyclodextrin and by neutral β-cyclodextrin derivatives at alkaline pH. J Sep Sci 25:1147–1154
81. Schmitt T, Engelhardt H (1993) Charged and uncharged cyclodextrins as chiral selectors in capillary electrophoresis. Chromatographia 37:475–481
82. Sabbah S, Scriba GKE (2001) Separation of dipeptide and tripeptide enantiomers in capillary electrophoresis using carboxymethyl-β-cyclodextrin and succinyl-β-cyclodextrin: influence of the amino acid sequence, nature of the cyclodextrin and pH. Electrophoresis 22:1385–1393
83. Zhu X, Ding Y, Lin B, Jakob A, Koppenhöfer B (2000) Transient state of chiral recognition in a binary mixture of cyclodextrins in capillary electrophoresis. J Chromatogr A 888:241–250
84. Calvet C, Cuberes R, Perez-Maseda C, Frigola J (2002) Enantioseparation of novel COX-2 anti-inflammatory drugs by capillary electrophoresis using single and dual cyclodextrin systems. Electrophoresis 23:1702–1708
85. Lin CE, Lin SL, Liao WS, Liu YC (2004) Enantioseparation of benzoins and enantiomer migration reversal of hydrobenzoin in capillary zone electrophoresis with dual cyclodextrin systems and borate complexation. J Chromatogr A 1032:227–235

86. Lin CE, Liao WS, Cheng HT, Kuo CM, Liu YC (2005) Enantioseparation of phenothiazines in cyclodextrin-modified capillary zone electrophoresis using sulfated cyclodextrins as chiral selectors. Electrophoresis 26:3869–3877
87. Liao WS, Lin CH, Chen CY, Kuo CM, Liu YC, Wu JC, Lin CE (2007) Enantioseparation of phenothiazines in CD-modified CZE using single isomer sulfated CD as a chiral selector. Electrophoresis 28:3922–3929
88. Valle BC, Billot FH, Shamsi SA, Zhu Y, Powe AM, Warner IM (2004) Combination of cyclodextrins and polymeric surfactants for chiral separations. Electrophoresis 25:743–752
89. Lin JM, Hobo T (2001) Inspection of the reversal of enantiomer migration order in ligand exchange micellar electrokinetic capillary chromatography. Biomed Chromatogr 15:207–211
90. Rundlett KL, Armstrong DW (1995) Effect of micelles and mixed micelles on efficiency and selectivity of antibiotic-based capillary electrophoretic enantioseparations. Anal Chem 67: 2088–2095
91. Wan H, Engstrom A, Blomberg E (1996) Direct chiral separation of amino acids derivatized with 2-(9-anthryl)ethyl chloroformate by capillary electrophoresis using cyclodextrins as chiral selectors. Effect of organic modifiers on resolution and enantiomeric elution order. J Chromatogr A 731:283–292
92. Schmitt T, Engelhardt H (1993) Derivatized cyclodextrins for the separation of enantiomers in capillary electrophoresis. J High Resolut Chromatogr 16:525–529
93. Lin CE, Liao WS, Chen KH (2003) Enantioseparation of phenothiazines in cyclodextrin-modified capillary zone electrophoresis: reversal of migration order. Electrophoresis 24:3139–3146
94. Zhu H, Wu E, Chen J, Yang YS, Kang W, Choi JK, Lee W, Kang JS (2011) Reverse migration order of sibutramine enantiomers as a function of cyclodextrin concentration in capillary electrophoresis. J Pharm Biomed Anal 54:1007–1012
95. Krajian H, Mofaddel N, Villemin D, Desbene PL (2009) A new example of reversal of the order of migration of enantiomers, as a function of cyclodextrin concentration and pH, by cyclodextrin-modified capillary zone electrophoresis: enantioseparation of 6,6′-dibromo-1,1′-binaphthyl-2,2′-diol. Anal Bioanal Chem 394:2193–2201
96. Castro-Puyana M, Crego AL, Marina ML, Garcia-Ruiz C (2007) Enantioselective separation of azole compounds by EKC. Reversal of migration order of enantiomers with CD concentration. Electrophoresis 28:2667–2674
97. Mofaddel N, Krajian H, Villemin D, Desbene PL (2009) Enantioseparation of binaphthol and its monoderivatives by cyclodextrin-modified capillary zone electrophoresis: a mathematical approach. Talanta 78:631–637
98. Wren SAC (1997) Mobility measurements on dansylated amino acids. J Chromatogr A 768: 153–159
99. Sabbah S, Scriba GKE (1999) pH-dependent reversal of the chiral recognition of an aspartyl tripeptide by carboxymethyl-β-cyclodextrin. J Chromatogr A 833:261–266
100. Sabbah S, Scriba GKE (2000) Influence of the structure of cyclodextrins and amino acid sequence of dipeptides and tripeptides on the pH-dependent reversal of the migration order in capillary electrophoresis. J Chromatogr A 894:267–272
101. Sungthong B, Ivanyi R, Bunz SC, Neusüß C, Scriba GKE (2010) CE-MS characterization of negatively charged α-, β- and γ-CD derivatives and their application to the separation of dipeptide and tripeptide enantiomers by CE. Electrophoresis 31:1498–1505
102. Terekhova IV, Hammitzsch-Wiedemann M, Shi J, Sungthong B, Scriba GKE (2010) Investigation of the pH-dependent complex formation between β-cyclodextrin and dipeptides enantiomers by capillary electrophoresis and calorimetry. J Sep Sci 33:2499–2505
103. Kodama S, Aizawa S, Taga A, Yamashita T, Kemmei T, Suzuki KHY, Yamamoto A (2010) Metal(II)-ligand molar ratio dependence of enantioseparation of tartaric acid by ligand exchange CE with Cu(II) and Ni(II)-D-quinic acid systems. Electrophoresis 31:1051–1054
104. Aizawa S, Kodama S (2012) Mechanism of change in enantiomer migration order of enantioseparation of tartaric acid by ligand exchange capillary electrophoresis with Cu(II) and Ni(II)-D-quinic acid systems. Electrophoresis 33:523–527

105. Hammitzsch-Wiedemann M, Scriba GKE (2009) Mathematical approach by a selectivity model for rationalization of pH- and selector concentration-dependent reversal of the enantiomer migration order in capillary electrophoresis. Anal Chem 81:8765–8773
106. Hammitzsch-Wiedemann M, Scriba GKE (2010) Mathematical approach by a selectivity model for rationalization of pH- and selector concentration-dependent reversal of the enantiomer migration order in capillary electrophoresis – correction. Anal Chem 82:6744
107. Hruska V, Benes M, Svobodova J, Zuskova I, Gas B (2012) Simulation of the effects of complex-formation equilibria in capillary electrophoresis: I. Mathematical model. Electrophoresis 33:938–947
108. Svobodova J, Benes M, Hruska V, Uselova K, Gas B (2012) Simulation of the effects of complex-formation equilibria in capillary electrophoresis: II. Experimental verification. Electrophoresis 33:948–957
109. Svobodova J, Benes M, Dubsky P, Vigh G, Gas B (2012) Simulation of the effects of complex-formation equilibria in electrophoresis: III. Simultaneous effects of chiral selector concentration and background electrolyte pH. Electrophoresis 33:3012–3020
110. Tsioupi DA, Stefan-van Staden RI, Kapnissi-Christodoulou CP (2013) Chiral selectors in CE: recent developments and applications. Electrophoresis 34:178–204
111. Lämmerhofer M (2010) Chiral recognition by enantioselective chromatography: mechanisms and modern chiral stationary phases. J Chromatogr A 1217:814–856
112. Scriba GKE (2011) Chiral recognition mechanisms in analytical separation sciences. Chromatographia 75:815–838
113. Scriba GKE (2013) Chiral recognition in separation science: an overview. In: Scriba GKE (ed) Chiral separations, methods and protocols, vol 970, 2nd edn, Methods in molecular biology. Humana, New York, pp 1–27
114. Berthod A (ed) (2010) Chiral recognition in separation methods. Springer, Heidelberg
115. Schneider HJ, Hacket F, Rüdiger V (1998) NMR studies of cyclodextrins and cyclodextrin complexes. Chem Rev 98:1755–1785
116. Dodziuk H, Kozinski W, Ejchart A (2004) NMR studies of chiral recognition by cyclodextrins. Chirality 16:90–105
117. Chankvetadze B (2004) Combined approach using capillary electrophoresis and NMR spectroscopy for an understanding of enantioselective recognition mechanisms by cyclodextrins. Chem Soc Rev 33:337–347
118. Morris KF, Froberg AL, Becker BA, Almeida VK, Tarus J, Larive CK (2005) Using NMR to develop insights into electrokinetic chromatography. Anal Chem 77:254A–263A
119. Uccello-Barretta G, Vanni L, Balzano F (2010) Nuclear magnetic resonance approaches to the rationalization of chromatographic enantiorecognition processes. J Chromatogr A 1217: 928–940
120. Lipkowitz KB (2001) Atomistic modeling of enantioselection in chromatography. J Chromatogr A 906:417–442
121. Del Rio A (2009) Exploring enantioselective molecular recognition mechanisms with chemoinformatic techniques. J Sep Sci 32:1566–1584
122. Fanali S (2000) Enantioselective determination by capillary electrophoresis with cyclodextrins as chiral selectors. J Chromatogr A 875:89–122
123. Fanali S (2009) Chiral separations by CE employing CDs. Electrophoresis 30:S203–S210
124. Chankvetadze B (2009) Separation of enantiomers with charged chiral selectors in CE. Electrophoresis 30:S211–S221
125. Scriba GKE (2008) Cyclodextrins in capillary electrophoresis – recent developments and applications. J Sep Sci 31:1991–2001
126. Scriba GKE, Altria K (2009) Using cyclodextrins to achieve chiral and non-chiral separations in capillary electrophoresis. LC GC Eur 22:420–430
127. Juvancz Z, Kendrovics RB, Ivanyi R (2008) The role of cyclodextrins in chiral capillary electrophoresis. Electrophoresis 29:1701–1712
128. Schmitt U, Branch SK, Holzgrabe U (2002) Chiral separations by cyclodextrin-modified capillary electrophoresis – determination of the enantiomeric excess. J Sep Sci 25:959–974

129. Gübitz G, Schmid MG (2010) Cyclodextrin-mediated chiral separations. In: Van Eeckhaut A, Michotte Y (eds) Chiral separations by capillary electrophoresis, vol 100, Chromatogr science series. CRC, Boca Raton, pp 47–85
130. Rekharsky MV, Inoue Y (1998) Complexation thermodynamics of cyclodextrins. Chem Rev 98:1875–1917
131. Servais AC, Rousseau A, Fillet M, Lomsadze K, Salgado A, Crommen J, Chankvetadze B (2010) Capillary electrophoretic and nuclear magnetic resonance studies on the opposite affinity pattern of propranolol enantiomers towards various cyclodextrins. J Sep Sci 33: 1617–1624
132. Chankvetadze B, Lomsadze K, Burjanadze N, Breitkreutz J, Pintore G, Chessa M, Bergander K, Blaschke K (2003) Comparative enantioseparations with native β-cyclodextrin, randomly acetylated β-cyclodextrin and heptakis-(2,3-di-O-acetyl)-β-cyclodextrin in capillary electrophoresis. Electrophoresis 24:1083–1091
133. Waibel B, Schreiber J, Meier C, Hammitzsch M, Baumann K, Scriba GKE, Holzgrabe U (2007) Comparison of cyclodextrin-dipeptide inclusion complexes in the absence and presence of urea by means of capillary electrophoresis, nuclear magnetic resonance and molecular modeling. Eur J Org Chem 2921–2930
134. Kahle C, Deubner R, Schollmayer C, Schreiber J, Baumann K, Holzgrabe U (2005) NMR spectroscopic and molecular modeling studies on cyclodextrin-dipeptide inclusion complexes. Eur J Org Chem 1578–1589
135. Wei Y, Wang S, Chao J, Wang S, Cong C, Shuang S, Paau MC, Choi MMF (2011) An evidence for the chiral discrimination of naproxen enantiomers: a combined experimental and theoretical study. J Phys Chem C 115:4033–4040
136. Berthod A (2009) Chiral recognition mechanisms with macrocyclic glycopeptides selectors. Chirality 21:167–175
137. Loll PJ, Kaplan J, Selinsky BS, Axelson PH (1999) Vancomycin binding to low-affinity ligands: delineating a minimum set of interactions necessary for high-affinity binding. J Med Chem 42:4714–4719
138. Loll PJ, Derhovanessian A, Shapovalov MV, Kaplan J, Yang L, Axelson PH (2009) Vancomycin forms ligand-mediated supramolecular complexes. J Mol Biol 385:200–211
139. Lehmann C, Bunkoczi G, Vertesy L, Sheldrick GM (2002) Structures of glycopeptide antibiotics with peptides that model bacterial cell-wall precursors. J Mol Biol 318:723–732
140. Fernandes C, Tiritan ME, Cass Q, Kairys V, Fernandes MX, Pinto M (2012) Enantioseparation and chiral recognition mechanism of new chiral derivatives of xanthones on macrocyclic antibiotic stationary phases. J Chromatogr A 1241:60–68
141. Desiderio C, Fanali S (1998) Chiral analysis by capillary electrophoresis using antibiotics as chiral selectors. J Chromatogr A 807:37–56
142. Prokhorova A, Shapovalova EN, Shpigun OA (2010) Chiral analysis of pharmaceuticals by capillary electrophoresis using antibiotics as chiral selectors. J Pharm Biomed Anal 53: 1170–1179
143. Kuhn R (1999) Enantiomeric separations by capillary electrophoresis using a crown ether as chiral selector. Electrophoresis 20:2605–2613
144. Elbashir AA, Aboul-Enein HY (2010) Application of crown ethers as buffer additives in capillary electrophoresis. Curr Pharm Anal 6:101–113
145. Nagata H, Nishi H, Kamagauchi M, Ishida T (2008) Guest-dependent conformation of 18-crown-6 tetracarboxylic acid: relation to chiral separation of racemic amino acids. Chirality 20:820–827
146. Bang E, Jung JW, Lee W, Lee DW, Lee W (2001) Chiral recognition of (18-crown-6)-tetracarboxylic acid as a chiral selector determined by NMR spectroscopy. J Chem Soc Perkin Trans 2:1685–1692
147. Gerbaux P, De Winter J, Cornil D, Ravicini K, Pesesse G, Cornil J, Flammang R (2008) Noncovalent interactions between ([18]crown-6)tetracarboxylic acid and amino acids. Chem Eur J 14:11039–11049
148. Nagata H, Nishi H, Kamagauchi M, Ishida T (2004) Structural scaffold of 18-crown-6 tetracarboxylic acid for optical resolution of chiral amino acid: X-ray crystal analyses and

energy calculations of complexes of D- and L-isomers of tyrosine, isoleucine, methionine and phenylglycine. Org Biomol Chem 2:3470–3475
149. Nagata H, Nishi H, Kamagauchi M, Ishida T (2006) Structural scaffold of 18-crown-6 tetracarboxylic acid for optical resolution of chiral amino acid: X-ray crystal analyses of complexes of D- and L-isomers of serine and glutamic acid. Chem Pharm Bull 54:452–457
150. Nagata H, Machida Y, Nishi H, Kamagauchi M, Minoura K, Ishida T (2009) Structural requirement for chiral recognition of amino acid by (18-crown-6)-tetracarboxylic acid: binding analysis in solution and solid states. Bull Chem Soc Jpn 82:219–229
151. Schmid MG, Gübitz G (2011) Enantioseparation by chromatographic and electromigration techniques using ligand-exchange as chiral separation principle. Anal Bioanal Chem 400: 2305–2316
152. Aizawa S, Yamamoto A, Kodama S (2006) Mechanism of enantioseparation of DL-pantothenic acid in ligand exchange capillary electrophoresis using a diol-borate system. Electrophoresis 27:880–886
153. Schmid MG (2012) Chiral metal-ion complexes for enantioseparation by capillary electrophoresis and capillary electrochromatography: a selective review. J Chromatogr A 1267: 10–16
154. Zhang H, Qi L, Mao L, Chen Y (2012) Chiral separation using capillary electromigration techniques based on ligand exchange principle. J Sep Sci 35:1236–1248
155. Chen Z, Uchiyama K, Hobo T (2000) Estimation of formation constants of ternary Cu(II) complexes with mixed amino acid enantiomers based on ligand exchange by capillary electrophoresis. Anal Sci 16:837–841
156. Maccarrone G, Contino A, Cucinotta V (2012) The study of solution equilibria in chiral capillary electrophoresis by the ligand-exchange mechanism. Trends Anal Chem 32:133–153
157. Cucinotta V, Giuffrida A, Maccarrone G, Messina M, Puglisi A, Rizzarelli E, Vecchio G (2005) Coordination properties of 3-functionalized β-cyclodextrins. Thermodynamic stereoselectivity of copper(II) complexes on the A,B-diamino derivative and its exploitation in LECE. Dalton Trans 2731–2736
158. Shtyrlin VG, Zyavkina YI, Gilyazetdinov EM, Burkharov MS, Krutikov AA, Garipov RR, Mukhtarov AS, Zakharov AV (2012) Complex formation, chemical exchange, species structure, and stereoselective effects in the copper(II)-L/DL-histidine systems. Dalton Trans 41:1216–1228
159. Mofaddel N, Adoubel AA, Morin CJ, Desbene PL, Dupas G (2010) Molecular modeling of complexes between two amino acids and copper(II): correlation with ligand exchange capillary electrophoresis. J Mol Struct 975:220–226
160. Dobashi A, Hamada M, Dobashi Y, Yamaguchi J (1995) Enantiomeric separation with sodium dodecanoyl-L-amino acidate micelles and poly(sodium (10-undecenoyl)-L-valinate) by electrokinetic chromatography. Anal Chem 67:3011–3017
161. Dey J, Ghosh A (2010) Chiral separations by micellar electrokinetic chromatography. In: Van Eeckhaut A, Michotte Y (eds) Chiral separations by capillary electrophoresis. CRC, Boca Raton, pp 195–234
162. Yarabe HH, Billot E, Warner IM (2000) Enantiomeric separations by use of polymeric surfactant electrokinetic chromatography. J Chromatogr A 875:179–206
163. Hebling CM, Thompson LE, Eckenroad KW, Manley GA, Fry RA, Mueller KT, Strein TG, Rovnyak D (2008) Sodium cholate aggregation and chiral recognition of the probe molecule (R,S)-1,1´-binaphthyl-2.2´-dihydrogenphosphate (BNDHP) observed by ^{1}H and ^{31}P NMR spectroscopy. Langmuir 24:13866–13874
164. Rugutt JK, Billot E, Warner IM (2000) NMR study of the interaction of monomeric and polymeric chiral surfactants with (R)- and (S)-1,1′-binaphthyl-2-2′-diyl hydrogen phosphate. Langmuir 16:3022–3029
165. Kingsbury SA, Ducommun CJ, Zahakaylo BM, Dickinson EH, Morris KF (2010) NMR characterization of (S)-1,1′-binaphthyl-2-2′-diyl hydrogen phosphate binding to chiral molecular micelles. Magn Reson Chem 48:184–191

166. Morris KF, Becker BA, Valle BC, Warner IM, Larive CK (2006) Use of NMR binding interaction mapping techniques to examine interactions of chiral molecules with molecular micelles. J Phys Chem B 110:17359–17369
167. Valle BC, Morris KF, Fletcher KA, Fernand V, Sword DM, Eldridge S, Larive CK, Warner IM (2007) Understanding chiral molecular micelle separations using steady-state fluorescence anisotropy, capillary electrophoresis, and NMR. Langmuir 23:425–435
168. Yarabe HH, Rugutt JK, McCarroll ME, Warner IM (2000) Capillary electrophoretic separation of binaphthyl enantiomers with two polymeric chiral surfactants: ^{1}H-nuclear magnetic resonance and fluorescence spectroscopy study. Electrophoresis 21:2025–2032
169. Kano K, Minami K, Horiguchi K, Ishimura T, Kodera M (1995) Ability of non-cyclic oligosaccharides to form molecular complexes and its use for chiral separation by capillary zone electrophoresis. J Chromatogr A 694:307–313
170. Nishi M, Izumoto S, Nakamura K, Nakai H, Sato T (1996) Dextran and dextrin as chiral selectors in capillary zone electrophoresis. Chromatographia 42:617–630
171. Chen J, Du Y, Zhu F, Chen B (2010) Glycogen: a novel branched polysaccharide chiral selector in CE. Electrophoresis 31:1044–1050
172. Chankvetadze B, Saito M, Yashima E, Okamoto Y (1998) Enantioseparation of atropisomeric 1,1′-binaphthyl-2,2′-diyl hydrogen phosphate in capillary electrophoresis by using di- and oligosaccharides as chiral selectors: di- and oligosaccharide chiral selectors in capillary electrophoresis. Chirality 10:134–139
173. Du X, Taga A, Suzuki S, Liu W, Honda S (2002) Effect of structure modification of chondroitin sulfate C on its enantioselectivity to basic drugs in capillary electrophoresis. J Chromatogr A 947:287–299
174. Nojavon S, Fakhar AR (2011) Chiral separation and quantitation of cetirizine and hydroxzine by maltodextrin-mediated CE in human plasma: effect of zwitterionic property of cetirizine on enantioseparation. Electrophoresis 32:764–771
175. Wei W, Guo B, Lin JM (2009) Helical- and ahelical-dependent chiral recognition mechanism is capillary electrophoresis using amylose as the selector. Electrophoresis 30:1380–1387
176. Sawada M, Tanaka T, Takai Y, Hanafusa T, Taniguchi T, Kawamura M, Uchiyama T (1991) The crystal structure of cycloinulohexaose produced from inulin by cycloinulo-oligosacchride fructanotransferase. Carbohydr Res 217:7–17
177. Immel S, Schmitt GE, Lichtenthaler FW (1998) Cyclofructans with six to ten β-(1→2)-linked fructofuranose units: geometries, electrostatic profiles, lipophilicity patterns, and potential for inclusion complexation. Carbohydr Res 313:91–105
178. Jiang C, Tong M, Breitbach ZS, Armstrong DW (2009) Synthesis and examination of sulfated cyclofructans as a novel class of chiral selectors in CE. Electrophoresis 30:3897–3909
179. Haginaka J (2010) Chiral separations using proteins and peptides as chiral selectors. In: Van Eeckhaut A, Michotte Y (eds) Chiral separations by capillary electrophoresis. CRC, Boca Raton, pp 139–161
180. Haginaka J (2011) Mechanistic aspects of chiral recognition on protein-based stationary phases. In: Grushka E (ed) Advances in chromatography, vol 49. CRC, Boca Raton, pp 37–69
181. Bica K, Gaertner P (2008) Applications of chiral ionic liquids. Eur J Org Chem 3235–3250
182. Francois Y, Varenne A, Juillerat E, Villemin D, Gareil P (2007) Evaluation of chiral ionic liquids as additive to cyclodextrins for enantiomeric separations by capillary electrophoresis. J Chromatogr A 1155:134–141
183. Tran CD, Mejac I (2008) Chiral ionic liquids for enantioseparations of pharmaceutical products by capillary electrophoresis. J Chromatogr A 1204:204–209
184. Rizvi SAA, Shamsi SA (2006) Synthesis, characterization, and application of chiral ionic liquids and their polymers in micellar electrokinetic chromatography. Anal Chem 78: 7061–7069
185. Liu Q, Wu K, Tang F, Yao L, Yang F, Nie Z, Yao S (2009) Amino acid ionic liquids as chiral ligands in ligand-exchange chiral separations. Chem Eur J 15:9889–9896

186. Bi W, Tian M, Row KH (2011) Chiral separation and determination of ofloxacin enantiomers by ionic liquid-assisted ligand-exchange chromatography. Analyst 136:379–387
187. De Rooy A, Li M, Bwambok DK, El-Zahab B, Challa S, Warner IM (2011) Ephedrinium-based protic chiral ionic liquids for enantiomeric recognition. Chirality 23:54–62
188. Kroupa DM, Brown CJ, Heckman LM, Hopkins TA (2012) Chiroptical study of chiral discrimination by amino acid based ionic liquids. J Phys Chem B 116:4952–4958
189. Ellington AD, Szostak JW (1990) In vitro selection of RNA molecules that bind specific ligands. Nature 346:818–822
190. Patel DJ, Suri AK, Jiang F, Jiang L, Fan P, Kumar RA, Nonin S (1997) Structure, recognition and adaptive binding in RNA aptamer complexes. J Mol Biol 272:645–664
191. Hermann T, Patel DJ (2000) Adaptive recognition by nucleic acid aptamers. Science 287: 820–825
192. Yang X, Bing T, Mei H, Fang C, Cao Z, Shangguan D (2011) Characterization and application of a DNA aptamer binding to L-tryptophan. Analyst 36:577–585
193. Bishop GR, Ren J, Polander BC, Jeanfreau BD, Trent JO, Chaires JB (2007) Energetic basis of molecular recognition in a DNA aptamer. Biophys Chem 126:165–175
194. Peyrin E (2009) Nucleic acid aptamer molecular recognition principles and application in liquid chromatography and capillary electrophoresis. J Sep Sci 32:1531–1536
195. Jung G, Hofstetter H, Feiertag S, Stoll D, Hofstetter O, Wiesmüller KH, Schurig V (1996) Cyclopeptide libraries as new chiral selectors in capillary electrophoresis. Angew Chem Int Ed Engl 35:2148–2150
196. Chiari M, Desperati V, Manera E, Longhi R (1998) Combinatorial synthesis of highly selective cyclohexapeptides for separation of amino acid enantiomers by capillary electrophoresis. Anal Chem 70:4967–4973
197. Ravelet C, Peyrin E (2006) Recent developments in the HPLC enantiomeric separation using chiral selectors identified by a combinatorial strategy. J Sep Sci 29:1322–1331
198. Evans CE, Stalcup AM (2003) Comprehensive strategy for chiral separations using sulfated cyclodextrins in capillary electrophoresis. Chirality 15:709–723
199. Jimidar IM, van Ael W, van Nyen P, Peeters M, Redlich D, de Smet M (2004) A screening strategy for the development of enantiomeric separation method in capillary electrophoresis. Electrophoresis 25:2772–2785
200. Ates H, Mangelings D, Vander Heyen Y (2008) Fast generic chiral separation strategies using electrophoretic and liquid chromatographic techniques. J Pharm Biomed Anal 48:288–294
201. Nhujak T, Sastravaha C, Palanuvej C, Petsom A (2005) Chiral separation in capillary electrophoresis using dual neutral cyclodextrins: theoretical models of electrophoretic mobility difference and separation selectivity. Electrophoresis 26:3814–3823
202. Matthijs N, Van Hemelryck S, Maftouh M, Luc Massart D, Vander Heyden Y (2004) Electrophoretic separation strategy for chiral pharmaceuticals using highly sulfated and neutral cyclodextrins based dual selector systems. Anal Chim Acta 525:247–263
203. Fillet M, Hubert P, Crommen J (2000) Enantiomeric separations of drugs using mixtures of charged and neutral cyclodextrins. J Chromatogr A 875:123–135
204. Jakubetz H, Juza M, Schurig V (1998) Dual chiral recognitions system involving cyclodextrin derivatives in capillary electrophoresis. Part 2. Enhancement of enantioselectivity. Electrophoresis 19:738–744
205. Mayer S, Schleimer M, Schurig V (1994) Dual chiral recognition system involving cyclodextrin derivatives in capillary electrophoresis. J Microcolumn Sep 6:42–48
206. Skanchy DJ, Xie GH, Tait RJ, Luna E, Demarest C, Stobaugh JF (1999) Application of sulfobutylether-β-cyclodextrin with specific degrees of substitution for the enantioseparation of pharmaceutical mixtures by capillary electrophoresis. Electrophoresis 20:2638–2649
207. Sänger-van de Griend CE, Gröningsson K (1996) Validation of a capillary electrophoresis method for the enantiomeric purity testing of ropivacaine, a new local anaesthetic compound. J Pharm Biomed Anal 14:295–304
208. Wongwan S, Hammitzsch-Wiedemann M, Scriba GKE (2009) Determination of related substances of levodopa including the R-enantiomer by CE. Electrophoresis 30:3891–3896
209. Kenndler E (2009) Organic solvents in CE. Electrophoresis 30:S101–S111

210. Lämmerhofer M (2005) Chiral separations by capillary electromigration techniques in non-aqueous media. I. Enantioselective nonaqueous capillary electrophoresis. J Chromatogr A 1068:3–30
211. Shamsi SA (2002) Chiral capillary electrophoresis-mass spectrometry: modes and applications. Electrophoresis 23:4036–4051
212. Somsen GW, Mol R, de Jong GJ (2010) On-line coupling of electrokinetic chromatography and mass spectrometry. J Chromatogr A 1217:3978–3991
213. Simo C, Garcia-Canas V, Cifuentes A (2010) Chiral CE-MS. Electrophoresis 31:1442–1456
214. Sheppard RL, Tong X, Cai J, Henion JD (1995) Chiral separation and detection of terbutaline and ephedrine by capillary electrophoresis coupled with ion spray mass spectrometry. Anal Chem 67:2054–2058
215. Hempel G, Blaschke G (1996) Enantioselective determination of zopiclone and its metabolites in urine by capillary electrophoresis. J Chromatogr B 675:139–146
216. Jimidar MI, van Ael W, de Smet M (2004) Optimization of enantiomeric separations in capillary electrophoresis by applying a design of experiments approach. J Capill Electrophor Microchip Technol 9:13–21
217. Hanrahan G, Montes R, Gomez FA (2008) Chemometric experimental design based optimization techniques in capillary electrophoresis: a critical review of modern applications. Anal Bioanal Chem 390:169–179
218. Hanrahan G, Gomez FA (eds) (2010) Chemometric methods in capillary electrophoresis. Wiley, Hoboken
219. Dejaegher S, Mangelings E, Vander Heyden Y (2013) In: Scriba GKE (ed) Chiral separations, methods and protocols, vol 970, 2nd edn, Methods in molecular biology. Humana, New York, pp 409–427
220. Sänger-van de Griend CE (2008) General considerations to improve performance of CE methods. In: Ahuja S, Jimidar IM (eds) Capillary electrophoresis methods for pharmaceutical analysis. Academic, London, pp 123–144
221. Hammitzsch M, Rao RN, Scriba GKE (2006) Development and validation of a robust capillary electrophoresis method for impurity profiling of etomidate including the determination of the chiral purity using a dual cyclodextrin system. Electrophoresis 27:4334–4344
222. Dey J, Ghosch A (2008) Chiral separations by micellar electrokinetic chromatography. In: Van Eekhaut A, Michotte Y (eds) Chiral separations by capillary electrophoresis. CRC, Boca Raton, pp 195–234
223. Billot FH, Billot EJ, Warner IM (2001) Comparison of monomeric and polymeric amino acid based surfactants for chiral separations. J Chromatogr A 922:329–338
224. Thibodeaux SJ, Billot EJ, Torres E, Valle BC, Warner IM (2003) Enantiomeric separations using polymeric L-glutamate surfactant derivatives: effect of increasing steric factors. Electrophoresis 24:1077–1082
225. Thibodeaux SJ, Billot EJ, Warner IM (2002) Enantiomeric separation using poly(L-valine) and poly(L-leucine) surfactants: investigation of steric factors near the chiral center. J Chromatogr A 966:179–186
226. Lin CE, Huang HC, Chen HW (2001) A capillary electrophoresis study on the influence of β-cyclodextrin on the critical micelle concentration of sodium dodecyl sulfate. J Chromatogr A 917:297–310
227. Bendazzoli C, Mileo E, Lucarini M, Olmo S, Cavrini C, Gotti R (2010) Capillary electrophoretic study on the interaction between sodium dodecyl sulfate and neutral cyclodextrins. Microchim Acta 171:23–31
228. Melani F, Giannini I, Pasquini B, Orlandini S, Pinzauti S, Furlanetto S (2011) Evaluation of the separation mechanism of electrokinetic chromatography with a microemulsion and cyclodextrins using NMR and molecular modeling. Electrophoresis 32:3062–3069
229. Shamsi SA (2001) Micellar electrokinetic chromatography-mass spectrometry using a polymerized chiral surfactant. Anal Chem 73:5103–5108

230. Hou J, Rizvi SAA, Zheng J, Shamsi SA (2006) Application of polymeric surfactants in micellar electrokinetic chromatography-electrospray ionization mass spectrometry of benzodiazepines and benoxazocine chiral drugs. Electrophoresis 27:1263–1275
231. Hou J, Zheng J, Rizvi SAA, Shamsi SA (2007) Simultaneous chiral separation and determination of ephedrine alkaloids by MEKC-ESI-MS using polymeric surfactants: method development. Electrophoresis 28:1352–1363
232. Rizvi SAA, Zheng J, Apkarian RP, Dublin SN, Shamsi SA (2007) Polymeric amino acid surfactants: a class of versatile chiral selectors for micellar electrokinetic chromatography (MEKC) and MEKC-MS. Anal Chem 79:879–898
233. Wang X, Hou J, Jann M, Hon YY, Shamsi SA (2013) Development of a chiral micellar electrokinetic chromatography-tandem mass spectrometry assay for simultaneous analysis of warfarin and hydroxywarfarin metabolites: application to the analysis of patients serum samples. J Chromatogr A 1271:207–216
234. Watari H (1991) Microemulsion capillary electrophoresis. Chem Lett 20:391–394
235. Cao Y, Ni X, Sheng J (2011) Comparison of microstructures of microemulsion and swollen micelle in electrokinetic chromatography. J Chromatogr A 1218:2598–2603
236. Mertzman MD, Foley JP (2004) Effect of oil substitution on chiral microemulsion electrokinetic chromatography. Electrophoresis 25:723–732
237. Pascoe R, Foley JP (2002) Rapid separation of pharmaceutical enantiomers using electrokinetic chromatography with a novel chiral microemulsion. Analyst 127:710–714
238. Mertzman MD, Foley JP (2005) Temperature effects on chiral microemulsion electrokinetic chromatography employing the chiral surfactant dodecylcarbonylvaline. J Chromatogr A 1073:181–189
239. Zheng ZX, Lin JM, Chan WH, Lee AWM, Huie CW (2004) Separation of enantiomers in microemulsion electrokinetic chromatography using chiral alcohols as cosurfactants. Electrophoresis 25:3263–3269
240. Aiken JH, Huie CW (1993) Use of a microemulsion system to incorporate a lipophilic chiral selector in electrokinetic capillary chromatography. Chromatographia 35:448–450
241. Hu SQ, Chen YL, Zhu HD, Shi HJ, Ayn N, Chen XG (2010) Effect of molecular structure of tartrates on chiral recognition of tartrate-boric acid complex chiral selectors in chiral microemulsion electrokinetic chromatography. J Chromatogr A 1217:5529–5535
242. Kahle KA, Foley JP (2006) Chiral microemulsion electrokinetic chromatography with two chiral components: improved separations via synergies between a chiral surfactant and a chiral cosurfactant. Electrophoresis 27:896–904
243. Kahle KA, Foley JP (2007) Two-chiral-component microemulsion electrokinetic chromatography – chiral surfactant and chiral oil: part 1. Dibutyl tartrate. Electrophoresis 28:1723–1734
244. Kahle KA, Foley JP (2007) Two-chiral-component microemulsion electrokinetic chromatography—chiral surfactant and chiral oil: part 2. Diethyl tartrate. Electrophoresis 28:2644–2657
245. Kahle KA, Foley JP (2007) Influence of microemulsion chirality on chromatographic figures of merit in EKC: results with novel three-chiral component microemulsions and comparison with one- and two-chiral-component microemulsions. Electrophoresis 28:3024–3040
246. Hu SQ, Lü WJ, Ma YH, Dong LJ, Chen XG (2013) Chiral separation of β-blockers by MEEKC using neutral microemulsion: analysis of separation mechanism and further elucidation of resolution equation. Electrophoresis 34:260–268
247. Chu BL, Guo BY, Wang Z, Lin JM (2008) Enantioseparation of esbiothrin by cyclodextrin-modified microemulsion and micellar electrokinetic chromatography. J Sep Sci 31: 3911–3920
248. Bitar Y, Holzgrabe U (2007) Enantioseparation of chiral tropa alkaloids by means of cyclodextrin-modified microemulsion electrokinetic chromatography. Electrophoresis 28: 2693–2700
249. Borst C, Holzgrabe U (2008) Enantioseparation of dopa and related compounds by cyclodextrin-modified microemulsion electrokinetic chromatography. J Chromatogr A 1204:191–196

250. Borst C, Holzgrabe U (2010) Comparison of chiral electrophoretic separation methods for phenylethylamines and application on impurity analysis. J Pharm Biomed Anal 53: 1201–1209
251. Wongwan S, Scriba GKE (2010) Impurity profiling of dexamphetamine sulfate by cyclodextrin-modified microemulsion electrokinetic chromatography. Electrophoresis 31: 3006–3011
252. Yu L, Chu K, Ye H, Liu X, Yu L, Xu X, Chen G (2012) Recent advances in microemulsion electrokinetic chromatography. Trends Anal Chem 34:140–151
253. Ryan R, Altria K, McEvoy E, Donegan S, Power J (2013) A review of developments in the methodology and application of microemulsion electrokinetic chromatography. Electrophoresis 34:159–177
254. Wen Y, Li J, Ma J, Chen L (2012) Recent advances in enrichment techniques for trace analysis in capillary electrophoresis. Electrophoresis 33:2933–2952
255. Mala Z, Gebauer P, Bocek P (2011) Contemporary sample stacking in analytical electrophoresis. Electrophoresis 32:116–126
256. Mikus P, Marakova K (2010) Chiral capillary electrophoresis with on-line sample preparation. Curr Pharm Anal 6:76–100
257. Garcia-Ruiz C, Marina ML (2006) Sensitive chiral analysis by capillary electrophoresis. Electrophoresis 27:195–212
258. Guidance for Industry, Analytical Procedures and Methods Validation, Chemistry Manufacturing and Controls Documentation, Draft Guidance, FDA (2000) http://www.fda.gov/downloads/Drugs/. . ./Guidances/ucm122858.pdf
259. Muijselaar PG (2008) Overview of current regulatory guidance. In: Ahuja S, Jimidar MI (eds) Capillary electrophoresis methods for pharmaceutical analysis, Separation science and technology. Academic, London, pp 145–169
260. Sänger-van de Griend CE (2012) Revival of capillary electrophoresis techniques in the pharmaceutical industry. LC GC N Am 30:954–971

Index